


7-26-2016

# Can Skeletal Morphology Support New Molecular Phylogenies of Antedonidae (Crinoidea: Comatulida)?

Brenna Hays

Nova Southeastern University, [bkhays816@gmail.com](mailto:bkhays816@gmail.com)

Follow this and additional works at: [https://nsuworks.nova.edu/occ\\_stuetd](https://nsuworks.nova.edu/occ_stuetd)

 Part of the [Marine Biology Commons](#), and the [Oceanography and Atmospheric Sciences and Meteorology Commons](#)

## Share Feedback About This Item

---

### NSUWorks Citation

Brenna Hays. 2016. *Can Skeletal Morphology Support New Molecular Phylogenies of Antedonidae (Crinoidea: Comatulida)?*. Master's thesis. Nova Southeastern University. Retrieved from NSUWorks, . (424)  
[https://nsuworks.nova.edu/occ\\_stuetd/424](https://nsuworks.nova.edu/occ_stuetd/424).

This Thesis is brought to you by the HCNSO Student Work at NSUWorks. It has been accepted for inclusion in HCNSO Student Theses and Dissertations by an authorized administrator of NSUWorks. For more information, please contact [nsuworks@nova.edu](mailto:nsuworks@nova.edu).

HALMOS COLLEGE OF NATURAL SCIENCES AND OCEANOGRAPHY

Can skeletal morphology support new molecular phylogenies of Antedonidae  
(Crinoidea: Comatulida)?

By

Brenna Hays

Submitted to the Faculty of  
Halmos College of Natural Sciences and Oceanography  
in partial fulfillment of the requirements for  
the degree of Master of Science with a specialty in:

Marine Biology

Nova Southeastern University

August 30, 2016

## Abstract

Antedonidae (Crinoidea: Comatulida) is the largest of extant crinoid families; it currently includes ~155 accepted species in 50 genera and accounts for ~23% of extant crinoid species (~29% of feather stars) and 27% of genera. Molecular phylogenies have returned the family as polyphyletic, with several clades scattered among non-antedonid sister groups (Hemery 2011, Hemery et al. 2013, Rouse et al. in prep.). Traditional morphological characteristics are thus inadequate for reconstructing relationships among taxa. SEM imaging was used in an effort to discover new diagnostic features that will support the molecular data, focusing on skeletal ossicles within the calyx, specifically the radial ossicles, as they are least likely to be affected by their hydrodynamic environment. Geometric morphometric analysis and landmark software were used to systematically compare equivalent skeletal parts among antedonid and non-antedonid sister taxa to identify likely homologies and homoplasies. Principal Component Analysis (PCA/BGPCA) and Procrustes ANOVAs were used for visualizing and testing variances within and between taxonomic and molecular groups. Linear Discriminant Analysis (LDA) was used with leave-one-out cross validation (LOOCV) to identify any misclassifications based on morphological similarities. UPGMA Hierarchical clustering models using both Procrustes and Mahalanobis distances were produced for comparison, and inter-landmark measurements were compared between species in search for possible intra-radial character states. Results yielded significant variation of radial morphology within the family Antedonidae with significant effects by depth range, taxonomic classification, and phylogenetic forces. All species with a radial height to width (H:W) ratio <1.0 were restricted to the shallower depths (0-200m) and notable morphological similarities were seen within both molecular clades and taxonomic subfamilies (Antedoninae and Thysanometrinae excepted). Regional affects were seen within the subfamily Antedoninae, as the Atlantic antedonines differed significantly from the Pacific antedonines, both in overall radial appearance and in H:W ratio. These results, with limited variation within molecular clades, give at least rudimentary support to recent molecular phylogenetics and promote further morphological studies of this nature that will strengthen our understanding of extant crinoid phylogeny (Bull et al. 1993, Littlewood et al. 1997, Hemery 2011, Rouse et al. 2013, Roux et al. 2013).

Keywords: crinoid, Antedonidae, morphometrics, morphology, Comatulida, Crinoidea

## Acknowledgements

I would like to give special recognition to my main advisor, Dr. Charles Messing, for taking me under his wing, giving me invaluable opportunities both in the lab and in the field, and teaching me the tools necessary to become a successful invertebrate taxonomist. Your trust in me throughout this project has led me to become a more decisive and confident scientist, and for that, I thank you.

Additional recognition goes to Dr. Lenaig Hemery for her constant support and advice over the past year. You calmed me when I had doubts, and helped me solve the many problems that arose during this project. You will forever be a friend and mentor to me.

Final recognitions go my third committee member, Dr. Greg Rouse, and to the authors and contributors of the Morphomet forum who were so quick and vigilant with their responses to my many statistical questions. Specifically, Dr. Miriam Zelditch, Dr. Michael Collyer, Dr. Andrea Cardini. I would not have been able to accomplish what I did without your help.

<http://www.morphometrics.org/home/morphmet>

I. Introduction	
A. Background	1
B. Morphology-based classification	1
C. Molecular-based phylogenies	5
II. Objectives	13
III. Materials and Methods	
A. Specimens	15
B. SEM imaging	19
C. Landmarking	19
D. Additional factors	24
E. Statistical Analysis	30
IV. Test of the feasibility	
A. Results	34
i. Camera placement variability	34
ii. Landmark placement variability	36
B. Discussion	41
V. Using geometric morphometrics to discriminate crinoids	
A. Results	41
i. Intra-individual variability	41
ii. Intra-specific variability	42
iii. Intra-generic variability	55
a. <i>Antedon</i> spp	55
b. <i>Dorometra</i> spp	58
c. <i>Florometra</i> spp	58
d. <i>Isometra</i> spp	58
iv. Intra-subfamily variability	59
a. Antedoninae	59
b. Bathymetrinae	65
c. Heliometrinae	65
d. Isometrinae	69
e. Perometrinae	69
f. Thysanometrinae	71
g. <i>Antedonidae incertae sedis</i>	71
v. Intra-clade variability	74
a. Clade M (and other tree equivalents)	74
b. Clade N (and other tree equivalents)	76
c. Clade O (and other tree equivalents)	76
d. Clade P (and other tree equivalents)	77
e. Clade ‘unnamed’ (and other tree equivalents)	81
vi. Variation among all species	83
vii. Misclassifications through LOOCV	89

B. Discussion	89
i. Scenario 1 versus Scenario 2	92
VI. Application for crinoid classification	
A. Results	93
i. UPGMA Hierarchical clustering	93
ii. Inter-landmark measurements	100
a. Clade O taxa	100
b. Clade N taxa	102
c. Clade P taxa	103
d. Clade M taxa	104
e. Clade ‘unnamed’ taxa	105
f. Cladistic outliers	107
g. Taxa not included in the molecular phylogenies	108
iii. Character states in the phenograms and phylogenies	110
a. Character states in the phenograms	111
b. Character states in the phylogenies	114
B. Discussion	116
i. Scenario 1 versus Scenario 2	116
ii. Identities of uncertain species	117
a. <i>Antedon</i> c.f. <i>incommoda</i>	117
b. <i>Antedon parviflora</i> groups	119
1. <i>Antedon parviflora</i> B&E	119
2. <i>Antedon parviflora</i> C&D	120
3. <i>Antedon</i> c.f. <i>parviflora</i>	122
c. <i>Dorometra</i> c.f. <i>briseis</i>	122
d. <i>Antedon</i> c.f. <i>loveni</i>	123
e. Summary of reassigned taxa	123
iii. Comparing morphological relatives to phylogenies	124
a. Clade M (and equivalents)	124
b. Clade N (and equivalents)	127
c. Clade O (and equivalents)	127
d. Clade P (and equivalents)	131
e. Clade ‘unnamed’ (and equivalents)	132
iv. Visual comparisons of SEM images to phylogenies	135
v. Taxonomic revisions	135
VII. General discussion	
A. Study limitations / pros & cons	139
B. Future morphological focus	142
C. Conclusions	143
VIII. Appendices	
A. Appendix A	145
B. Appendix B	222
IX. References	260

Figures (in text)	Page #
Fig. 1: Lateral view of the proximal portion of an antedonid	3
Fig. 2A: Crinoid phylogeny (BI) from Hemery 2011	7
Fig. 2B-F: Close-up view of the 5 antedonid clades from Hemery 2011	8
Fig. 3: Antedonid portion of phylogeny from Hemery et al. 2013	9
Fig. 4: Antedonid portion of phylogeny from Rouse et al. in prep	11
Fig. 5: Articular facet view of radial ossicle with anatomy labels	14
Fig. 6: Digitized image example ( <i>F. asperrima</i> ) with 28 homologous landmarks	20
Fig. 7: Image of radial height and width measurement for <i>Florometra asperrima</i>	26
Fig. 8: Image of arm and syzygy diameter measurement for <i>Psathyrometra</i> sp.	27
Fig. 9: Image of inter-landmark measurements taken for <i>Antedon bifida bifida</i>	33
Fig. 10: Results of the camera placement error tests	35
Fig. 11: Results of landmark placement error for <i>C. hagenii</i> specimen C	37
Fig. 12: Results of landmark placement error for <i>C. hagenii</i> specimen D	38
Fig. 13: Results of landmark placement error for <i>D. briseis</i> specimen A	39
Fig. 14A-C: Superimposed configurations for all landmark placement bouts	40
Fig. 15A: Scenario 1 results of intra-species variation for <i>Antedon bifida bifida</i>	43
Fig. 15B: Scenario 2 results of intra-species variation for <i>Antedon bifida bifida</i>	44
Fig. 16: Scenario 2 results of intra-species variation for <i>Antedon loveni</i>	45
Fig. 17: Scenario 2 results of intra-species variation for <i>A. parviflora</i> groups	47
Fig. 18: Scenario 2 results of intra-species variation for <i>Anthometrina adriani</i>	48
Fig. 19: Scenario 2 results of intra-species variation for <i>Coccometra hagenii</i>	49
Fig. 20: Scenario 2 results of intra-species variation for <i>Dorometra briseis</i>	51
Fig. 21A: Scenario 1 results of intra-species variation for <i>Florometra asperrima</i>	52
Fig. 21B: Scenario 2 results of intra-species variation for <i>Florometra asperrima</i>	53
Fig. 22: Scenario 2 results of intra-species variation for <i>Hybometra senta</i>	54
Fig. 23A: Scenario 2 results of intra-genus variation for <i>Antedon</i> spp.	56
Fig. 23B-C: Scenario 2 results of intra-genus variation for <i>Antedon</i> spp cont'd	57
Fig. 24A: Scenario 2 results of intra-subfamily variation for Antedoninae	61
Fig. 24B-C: Scenario 2 results of intra-subfamily var. for Antedoninae cont'd	62
Fig. 24D: Scenario 2 results of intra-subfamily variation for Antedoninae cont'd	63
Fig. 25: Scenario 2 results of intra-subfamily variation for Bathymetrinae	67
Fig. 26: Scenario 2 results of intra-subfamily variation for Heliometrinae	68
Fig. 27: Scenario 2 results of intra-subfamily variation for Perometrinae	70
Fig. 28: Scenario 2 results of intra-subfamily variation for Thysanometrinae	72
Fig. 29: Scenario 2 results of intra-subfamily variation for Antedonidae <i>i.s.</i>	73
Fig. 30: Scenario 2 results of intra-clade variation for clade M	75
Fig. 31: Scenario 2 results of intra-clade variation for clade N	78
Fig. 32: Scenario 2 results of intra-clade variation for clade O	79
Fig. 33: Scenario 2 results of intra-clade variation for clade P	80
Fig. 34A: Scenario 2 results of intra-clade variation for clade 'unnamed'	82
Fig. 34B: Scenario 2 results of intra-clade variation for clade 'unnamed' cont'd	83
Fig. 35A: Scenario 2 results of variation between all species	86
Fig. 35B-C: Scenario 2 results of variation between all species cont'd	87
Fig. 35D-E: Scenario 2 results of variation between all species cont'd	88
Fig. 36: Procrustes distance UPGMA phenogram - scenario 1	96

Fig. 37: Procrustes distance UPGMA phenogram - scenario 2	97
Fig. 38: Mahalanobis distance UPGMA phenogram - scenario 1	98
Fig. 39: Mahalanobis distance UPGMA phenogram - scenario 2	99
Fig. 40: Procrustes distance UPGMA phenogram with specific rr - scenario 2	112
Fig. 41: Antedonid portion of Rouse et al. in prep. Phylogeny with radial ratios	113
Fig. 42A-C: Visual comparisons of <i>Antedon</i> c.f. <i>incommoda</i> , <i>Perometra diomedea</i> , and <i>Antedon serrata</i>	118
Fig. 43A-B: Visual comparisons of <i>Antedon parviflora</i> B&E & <i>Antedon serrata</i>	120
Fig. 44A-B: Visual comparisons of <i>A. parviflora</i> C&D & <i>Dorometra briseis</i>	121
Fig. 45A-B: Visual comparisons of <i>A. c.f. parviflora</i> & <i>Dorometra</i> c.f. <i>briseis</i>	123
Fig. 46: Visual comparisons of SEM images with clade M	126
Fig. 47: Visual comparisons of SEM images with clade N	129
Fig. 48: Visual comparisons of SEM images with clade O	130
Fig. 49: Visual comparisons of SEM images with clade 'unnamed'	134

---

Figures (in Appendix) Page #

Appendix A:

Fig. A1: Results of intra-individual variation for <i>Antedon</i> c.f. <i>parviflora</i> F	160
Fig. A2: Results of intra-individual variation for <i>Antedon bifida bifida</i> E	161
Fig. A3: Results of intra-individual variation for <i>Antedon hupferi</i> B	162
Fig. A4: Results of intra-individual variation for <i>Antedon loveni</i> A	163
Fig. A5: Results of intra-individual variation for <i>Antedon mediterranea</i> D	164
Fig. A6: Results of intra-individual variation for <i>Anthometrina adriani</i> A	165
Fig. A7: Results of intra-individual variation for <i>Aporometra occidentalis</i> B	166
Fig. A8: Results of intra-individual variation for <i>Coccometra hagenii</i> D	167
Fig. A9: Results of intra-individual variation for <i>Coccometra hagenii</i> F	168
Fig. A10: Results of intra-individual variation for <i>Comatonia cristata</i> B	169
Fig. A11: Results of intra-individual variation for <i>Ctenantedon kinziei</i> D	170
Fig. A12: Results of intra-individual variation for <i>Dorometra</i> c.f. <i>briseis</i> C	171
Fig. A13: Results of intra-individual variation for <i>Dorometra parvicirra</i> B	172
Fig. A14: Results of intra-individual variation for <i>Florometra asperrima</i> A	173
Fig. A15: Results of intra-individual variation for <i>Hathrometra tenella</i> A	174
Fig. A16: Results of intra-individual variation for <i>Tropiometra carinata</i> D	175
Fig. A17: Results of intra-individual variation for <i>Trichometra cubensis</i> E	176
Fig. A18: Results of intra-individual variation for <i>Tonrometra spinulifera</i> E	177
Fig. A19: Results of intra-individual variation for <i>Thysanometra tenelloides</i> D	178
Fig. A20: Results of intra-individual variation for <i>Thaumatometra tenuis</i> B	179
Fig. A21: Scenario 1 results of intra-species variation for <i>Antedon loveni</i> groups	180
Fig. A22: Scenario 1 results of intra-species variation for <i>A. parviflora</i> groups	181
Fig. A23: Scenario 1 results of intra-species variation for <i>Anthometrina adriani</i>	182
Fig. A24: Scenario 1 results of intra-species variation for <i>Coccometra hagenii</i>	183
Fig. A25: Scenario 1 results of intra-species variation for <i>Dorometra briseis</i>	184
Fig. A26: Scenario 1 results of intra-species variation for <i>Hybometra senta</i>	185
Fig. A27A: SC1 results of intra-genus variation for <i>Antedon</i> spp.	186
Fig. A27B-C: SC1 results of intra-genus variation for <i>Antedon</i> spp. cont'd	187
Fig. A28A: SC1 results of intra-genus variation for <i>Dorometra</i> spp.	188



Fig. A28B: SC2 results of intra-genus variation for <i>Dorometra</i> spp.	189
Fig. A29A: SC1 results of intra-genus variation for <i>Florometra</i> spp.	190
Fig. A29B: SC2 results of intra-genus variation for <i>Florometra</i> spp.	191
Fig. A30A: SC1 results of intra-genus variation for <i>Isometra</i> spp.	192
Fig. A30B: SC2 results of intra-genus variation for <i>Isometra</i> spp.	193
Fig. A31A: Scenario 1 results of intra-subfamily variation for Antedoninae	194
Fig. A31B-C: Scenario 1 results of intra-subfamily var. for Antedoninae cont'd	195
Fig. A31D: Scenario 1 results of intra-subfamily var. for Antedoninae cont'd	196
Fig. A32: Scenario 1 results of intra-subfamily variation for Bathymetrinae	197
Fig. A33: Scenario 1 results of intra-subfamily variation for Heliometrinae	198
Fig. A34: Scenario 1 results of intra-subfamily variation for Perometrinae	199
Fig. A35: Scenario 1 results of intra-subfamily variation for Thysanometrinae	200
Fig. A36: Scenario 1 results of intra-subfamily variation for <i>A. incertae sedis</i>	201
Fig. A37: Scenario 1 results of intra-clade variation for clade M	202
Fig. A38: Scenario 1 results of intra-clade variation for clade N	203
Fig. A39: Scenario 1 results of intra-clade variation for clade O	204
Fig. A40: Scenario 1 results of intra-clade variation for clade P	205
Fig. A41A: Scenario 1 results of intra-clade variation for clade 'unnamed'	206
Fig. A41B: Scenario 1 results of intra-clade variation for clade 'unnamed' cont'd	207
Fig. A42A: Scenario 1 results of variation between all species	208
Fig. A42B-C: Scenario 1 results of variation between all species cont'd	209
Fig. A42D-E: Scenario 1 results of variation between all species cont'd	210
Fig. A43: Scenario 1 Procrustes distance UPGMA phenogram w/ specific rr	222

#### Appendix B:

Fig. B1: SEM images of <i>Antedon</i> c.f. <i>incommoda</i>	223
Fig. B2: SEM images of <i>Antedon</i> c.f. <i>loveni</i>	224
Fig. B3: SEM images of <i>Antedon</i> c.f. <i>parviflora</i>	225
Fig. B4: SEM images of <i>Anthometrina adriani</i>	226
Fig. B5: SEM images of <i>Andrometra psyche</i>	227
Fig. B6: SEM images of <i>Antedon bifida bifida</i>	228
Fig. B7: SEM images of <i>Antedon hupferi</i>	229
Fig. B8: SEM images of <i>Antedon loveni</i>	230
Fig. B9: SEM images of <i>Antedon mediterranea</i>	231
Fig. B10: SEM images of <i>Antedon petasus</i>	232
Fig. B11: SEM images of <i>Antedon parviflora</i> B&E	233
Fig. B12: SEM images of <i>Antedon parviflora</i> C&D	233
Fig. B13: SEM images of <i>Antedon serrata</i>	234
Fig. B14: SEM images of <i>Aporometra occidentalis</i>	235
Fig. B15: SEM image of <i>Balanometra balanoides</i>	236
Fig. B16: SEM images of <i>Coccometra hagenii</i>	237
Fig. B17: SEM images of <i>Comatonia cristata</i>	238
Fig. B18: SEM images of <i>Ctenantedon kinziei</i>	239
Fig. B19: SEM images of <i>Dorometra</i> c.f. <i>briseis</i>	240
Fig. B20: SEM images of <i>Dorometra briseis</i>	241
Fig. B21: SEM images of <i>Dorometra parvicirra</i>	242

Fig. B22: SEM images of <i>Erythrometra rubra</i>	243
Fig. B23: SEM images of <i>Florometra asperrima</i>	244
Fig. B24: SEM images of <i>Florometra serratissima</i>	245
Fig. B25: SEM images of <i>Hathrometra tenella</i>	246
Fig. B26: SEM images of <i>Hybometra senta</i>	247
Fig. B27: SEM images of <i>Hypalometra defecta</i>	248
Fig. B28: SEM images of <i>Isometra graminea</i>	249
Fig. B29: SEM image of <i>Isometra vivipara</i>	250
Fig. B30: SEM images of <i>Iridometra adrestine</i>	250
Fig. B31: SEM images of <i>Notocrinus virilis</i>	251
Fig. B32: SEM images of <i>Perometra diomedea</i>	252
Fig. B33: SEM images of <i>Poliometra proluxa</i>	253
Fig. B34: SEM images of <i>Promachocrinus kerguelensis</i>	254
Fig. B35: SEM images of <i>Psathyrometra</i> sp.	255
Fig. B36: SEM images of <i>Thaumatometra tenuis</i>	256
Fig. B37: SEM images of <i>Thysanometra tenelloides</i>	257
Fig. B38: SEM images of <i>Tonrometra spinulifera</i>	258
Fig. B39: SEM images of <i>Trichometra cubensis</i>	259
Fig. B40: SEM images of <i>Tropiometra carinata</i>	260

<u>Tables (in text)</u>	<u>Page #</u>
Table 1: Specimens and museum sources	16
Table 2: Landmark point table (Bookstein 1991)	21
Equation 1: Percent of lost data equation	22
Table 3: Landmark point table revised for scenario 1	23
Table 4: Landmark point table revised for scenario 2	24
Table 5: Comprehensive list of species with factor information	28-29
Table 6: Inter-landmark measurement descriptions	33
Table 7: Closest morphological relatives table	95

<u>Tables (in Appendix)</u>	<u>Page #</u>
Table A1: Radial, centrodorsal, & syzygy measurement table for all ossicles	146-154
Table A2: Inter-landmark measurements after standardization	155-159
Table A3: Cross validation table - scenario 1	211
Table A4: Cross validation table - scenario 2	212
Table A5: Procrustes distances table - scenario 1	213
Table A6: Procrustes distances table - scenario 2	214
Table A7: Mahalanobis distances table - scenario 1	215
Table A8: Mahalanobis distances table - scenario 2	216
Table A9: Inter-landmark measurement ratio table	217-221

## I. Introduction

### A. *Background*

Family Antedonidae is included within order Comatulida (superfamily Antedonoidea) (Clark & Clark 1967, Pawson 2007, Hess & Messing 2011), the most diverse group of extant crinoids. The order is currently diagnosed on the basis of a postlarval stalk with synarthrial articulations (Hess & Messing 2011), but this may be a plesiomorphy. Most Comatulida, including antedonids, lose the stalk following a postlarval stage and take up a free existence as feather stars. Stalk loss and associated increased mobility may have been associated with the early Mesozoic diversification of durophagous predators, such as echinoids (Baumiller et al. 2010). The order has undergone extensive radiation since it initially appeared in the Jurassic (Meyer & Macurda 1977) and apparently since the early Paleogene (Meyer & Oji 1993) and is now found in virtually all seas at all depths (Messing 1997). Antedonidae is the most species-rich currently recognized family and encompasses more than one-quarter of all extant comatulids, about 150 species (Clark & Clark 1967, Hess & Messing 2011). Current morphologically-based taxonomy recognizes six subfamilies: Antedoninae, Heliometrinae, Thysanometrinae, Perometrinae, Isometrinae, and Bathymetrinae (Messing 2012). However, at least Heliometrinae appears to represent two separate clades based on both morphological (Eléaume 2006) and molecular data (Hemery 2011, Hemery et al. 2013, Rouse et al. 2013, in prep.). Messing & White (2001) elevated the former subfamily Zenometrinae to family level but restricted the group to only three genera. They treated the remaining former zenometrine genera as Antedonidae *incertae sedis*.

### B. *Morphology-based classification*

Crinoid classification has been based on skeletal morphology with occasional contributions from soft-part anatomy (e.g. AH Clark 1915, 1921, 1931, Messing 1981, 2003, Bohn and Heinzeller 1999, Hess and Messing 2011). Morphological characteristics used for higher taxonomic classification of Comatulida include stalk morphology, thecal structure, ray branching patterns and characteristics of articulations. All extant crinoids

belong to subclass Articulata, named for the ray articulations that include muscular as well as ligamentary bundles. Crinoid terminology follow Ubaughs (1978), Clark and Clark (1967), Messing and Dearborn (1990), and Hess and Messing (2011)

Basic articulate crinoid structure consists of a central visceral mass enclosed within or supported by a calyx composed of two or three circlets of skeletal ossicles (radials, basals, infrabasals) supported on a stalk composed of a series of columnal ossicles. Both mouth and anus lie on the upper aboral surface of the visceral mass. Five often branching rays, or arms, arise from the radial ossicles. Each consists of a linear series of articulated brachial ossicles, and the series of brachials between each branching point is referred to as a division series or brachitaxis (Fig. 1). The arms of all extant crinoids bear alternating unbranched side branches called pinnules that bear the podia and that, together with the arms, form the crinoid's suspension-feeding apparatus (e.g., Messing 1997, Roux et al. 2002).

Within Comatulida, most species are feather stars that lose the postlarval stalk but retain a single large aboral centrodorsal ossicle. Centrodorsals vary widely in shape and size and bear prehensile, hook-like cirri (Fig. 1) used for anchoring (Messing 1997, Hess & Messing 2011). Roux et al. (2002) discussed extant crinoid articulation structure in detail.

Hess and Messing (2011) placed Antedonidae in the superfamily Antedonoidea with the former antedonid subfamily Zenometridae and Pentametrocrinidae, the latter characterized by undivided rays. Most diagnostic characters are widely variable, but include basals transformed into a rosette with rod-shaped radiating portions ranging from absent to broad and tongue-like; centrodorsal cavity moderate to large; adoral paired muscle fossae forming tall, thin flanges almost parallel to the oral-aboral axis and meeting midradially at a  $\sim 90^\circ$  angle; radial cavity narrow or funnel shaped, without central plug; synarthry between brachials 1 and 2 usually embayed; syzygy generally between brachials 9 and 10, and distally at short intervals; and pinnules cylindrical to flattened and not carinate.

Antedonidae is currently distinguished chiefly on the basis of characters it does not share with the other families. The two genera Pentametrocrinidae have undivided rays, arising from five radials in *Pentametrocrinus* and ten in *Thaumatocrinus*. In



Antedoninae is diagnosed by a discoidal to subconical centrodorsal generally with a small, cirrus-free, smooth to tuberculate aboral apex and moderate central cavity; cirri usually 10-60, closely placed, generally with fewer than 20 cirrals, and without aboral spines or carinae; basal rosette lacking rod-shaped extensions; adoral muscle fossae moderate, slightly larger than interarticular ligament fossae, and broadly rounded, separated by broad, midradial ridge with median furrow, and shallow notch; synarthries between brachials 1 and 2 flat or slightly embayed. Recent genera are distinguished mainly on length and structure of proximal pinnules.

Bathymetrinae is characterized by a large centrodorsal cavity; small apex rounded or pointed, usually smooth; cirri typically 25-50 in irregular alternating rows; longest cirri laterally compressed; distal cirrals usually carinate or with aboral spine; longest cirrals up to six times longer than wide; basal rosette lacking rod-shaped extensions; radial articular facets high and steep, with low triangular ligament fossae and large, tall subtriangular muscular fossae separated by low narrow median ridge and small notch; radial cavity narrow; synarthry between primibrachials 1 and 2 commonly embayed; first pinnule stiff and slender with elongate pinnulars; second pinnule commonly the first genital pinnule.

Heliometrinae is diagnosed by a rounded centrodorsal with a low hemispheric to concave or deep pit-like aboral apex; cavity sometimes with shallow marginal pits or furrows; sockets numerous, regularly alternating; cirri up to 200, long, stout and laterally compressed with up to 90 cirrals; radial cavity moderate to rather large; radial articular facet high, commonly concave with muscle fossae narrow, tall and separated by a median ridge and notch; synarthrial articulations usually embayed; first pinnule long, flagellate, with numerous short pinnulars; distal pinnulars of proximal pinnules may bear rudimentary teeth forming a comb as in Comatulidae but weaker. Eléaume (2006) distinguished two groups of genera: *Anthometrina*, *Florometra*, *Heliometra* with two pairs of radial nerve canals and no basal rays, and *Solanometra*, *Promachocrinus* with only two radial nerve canals and basal rays present. Hemery et al. (2013) returned these groups as two separate clades, and Rouse et al. (2013, in prep.) returned *Promachocrinus* as separate from a *Florometra-Heliometra* clade. The subfamily is thus polyphyletic.

Isometrinae (Fet & Messing 2003) includes only genus *Isometra*, distinguished chiefly by viviparity and genital pinnules with expanded proximal pinnulars.

Perometrinae shares numerous features with other subfamilies but has distal cirrals bearing an aboral spine, triangular ligament fossae, and synarthry between brachials 1 and 2 usually embayed; first pinnule stout with fewer than 20 pinnulars; first interior pinnule frequently absent, and first exterior pinnule sometime absent; second pinnule differs from genital pinnules.

Thysanometrinae also shares numerous characters with other subfamilies, but bears 30-40 slender laterally compressed cirri lacking aboral projections and no rod-shaped basal extensions; centrodorsal adoral surface usually with interradian ridges; first pinnule long, flagellate, composed of 30-40 usually short pinnulars; second pinnule resembling those following. The radial articular facets differ substantially between the two included genera (*Thysanometra* and *Coccometra*).

Messing & White (2001) removed 15 genera from the former subfamily Zenometrinae and treated them as Antedonidae *incertae sedis*. They lack the diagnostic characteristics of the restricted Zenometridae, but most at least tend to have cirrus sockets arranged in distinct columns.

### C. Molecular-based phylogenies

Most classifications of articulate crinoids have been non-phylogenetic (see review in Hess & Messing 2011). Simms (1988) and Milsom et al. (1994) used phylogenetic approaches to reconstruct trees but included only limited numbers of fossil and extant taxa. Cohen et al. (2004) published the first combined morphological and molecular phylogenetic analysis of extant crinoids but included only a single concatenated feather star. Rouse et al. (2013) published the first extensive molecular-based analysis of extant crinoids, but among Antedonidae, included only a single *Antedon* terminal (*A. mediterranea*) and three heliometrines. In their maximum likelihood tree inferred from the concatenated five-gene complete dataset, the latter three conformed to Eléaume's (2006) assessment of subfamilial polyphyly, with heliometrines *Heliometra* and *Florometra* forming a monophyletic clade sister to *Aporometra* (Aporometridae) and *Promachocrinus* sister to the zenometrid *Psathyrometra*. *Antedon* returned as sister to *Tropiometra* (Tropiometridae). Hemery (2011) and Hemery et al. (2013) included 37

antedonids among 271 (Hemery 2011) and 105 (Hemery et al. 2013) crinoid terminals (81 Comatulida) in their reconstruction using two mitochondrial genes, COI and 16s rDNA, and two nuclear genes, 18s rDNA and 28s rDNA. Maximum likelihood and Bayesian Inference analyses were performed and tree topologies were compared by eye (Figs. 2A, 3). Their consensus tree returned Antedonidae as polyphyletic with multiple groups separated and rearranged among other taxa of Comatulida. For the purposes of analyses herein, antedonid clades are referred to by the names and letters in Hemery (2011) (Fig. 2B-F). Any inconsistencies between trees have been noted throughout.



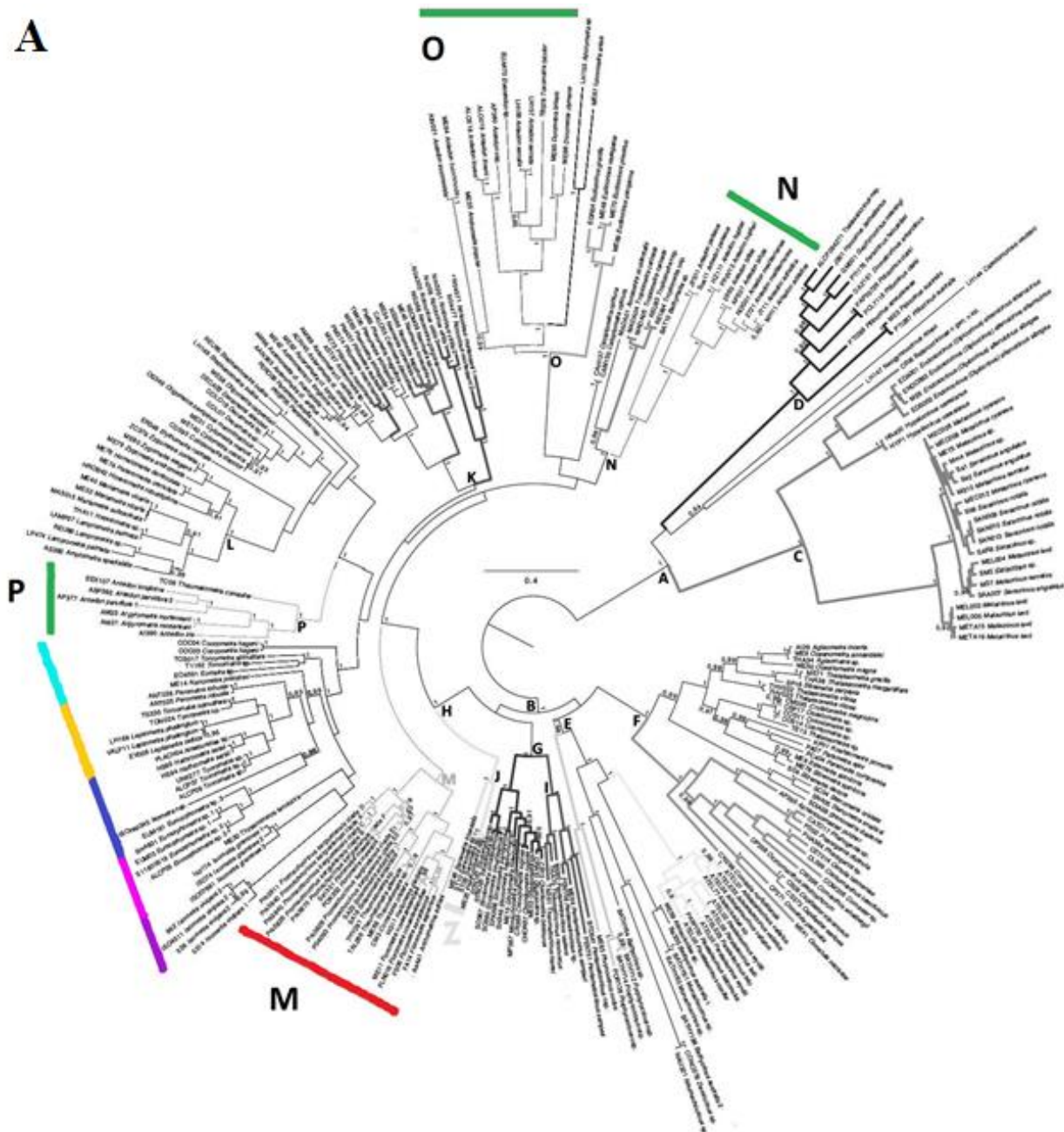


Fig. 2A: Crinoidea phylogeny from Bayesian Inference analysis using four combined genes (COI, 16S, 28S, and 18S). Clades M, N, O, P, and an 'unnamed' clade contain antedonid terminals. Colored bars indicate subfamily representatives: *Antedoninae* (green), *Bathymetrinae* (blue), *Heliometrinae* (red), *Isometrinae* (cyan), *Thysanometrinae* (yellow), *Perometrinae* (magenta), *Antedonidae i.s.* (orange), *Zenometridae* (yellow) (Hemery 2011).

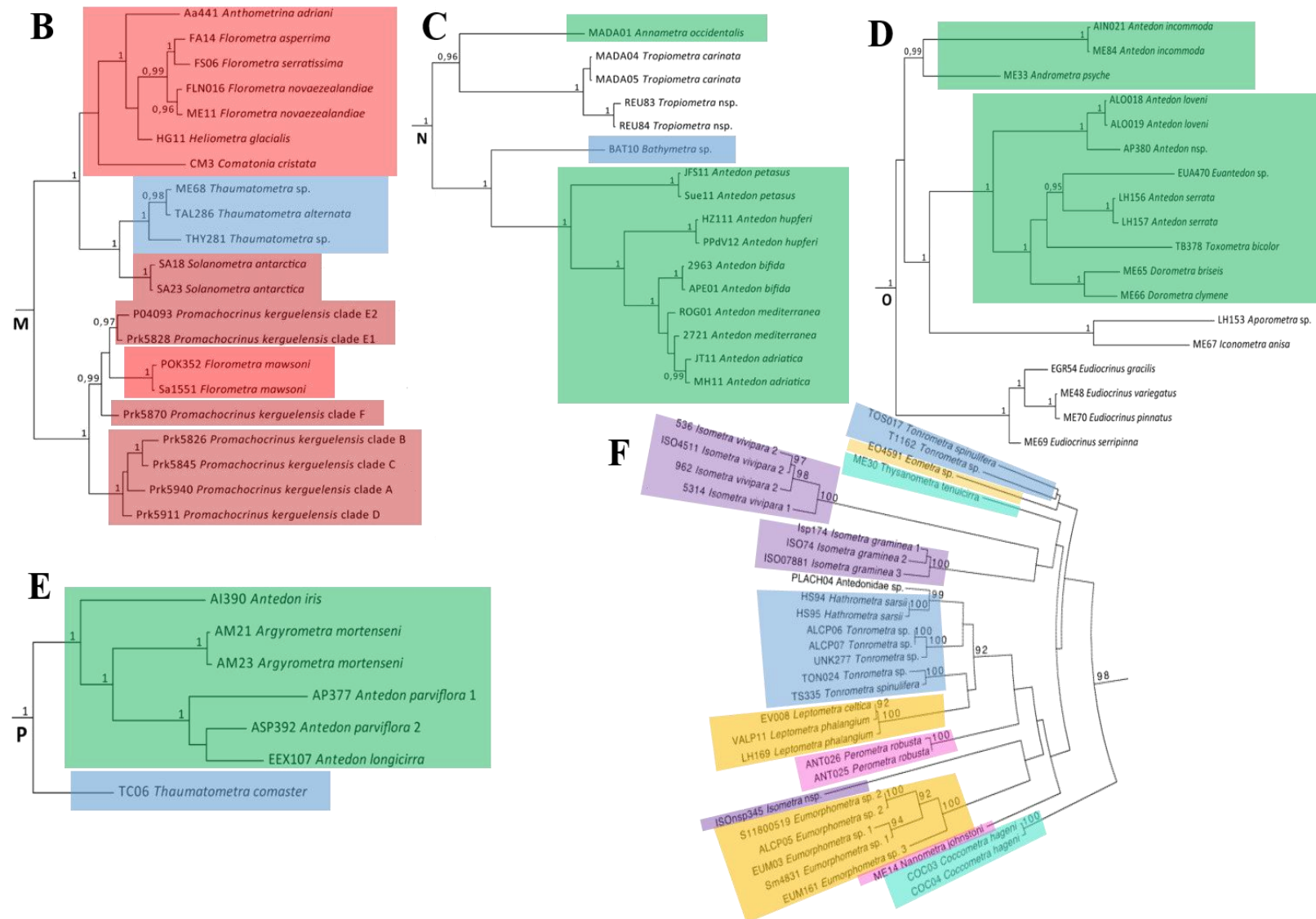


Fig. 2B-F: Close-up view of the five distinct antedonid clades in Fig. 2A. B: Hemery's clade M, C: clade N, D: clade O, E: clade P, F: 'unnamed' clade (Hemery 2011). (Antedoninae = green, Bathymetrinae = blue, Heliometrines = red, Isometrinae = purple, Thysanometrines = turquoise, Perometrines = pink, Antedonidae incertae sedis = orange, Zenometridae = yellow, not colored = Tropiometridae, Notocrinidae, Aporometridae)

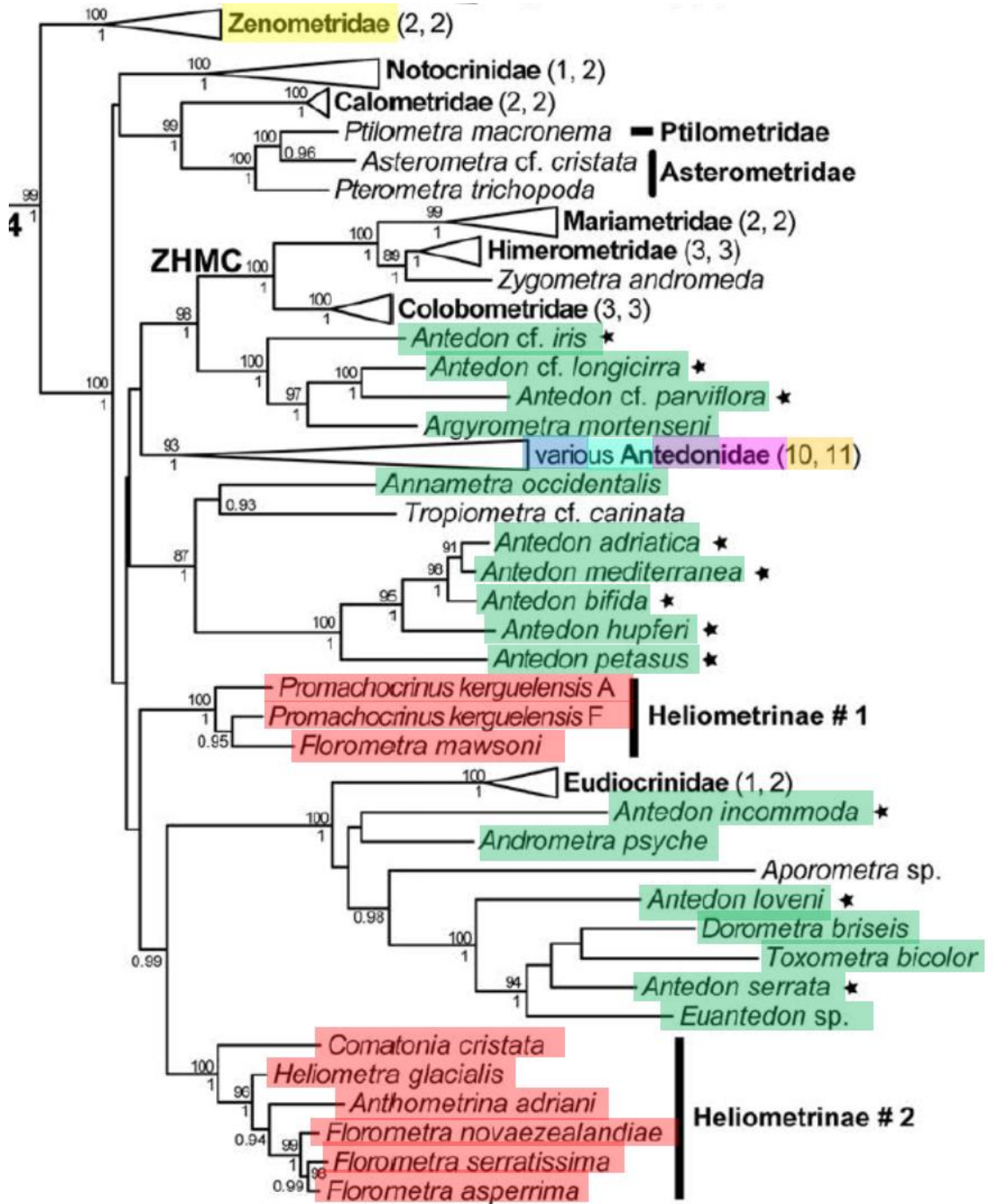


Fig. 3: Antedonid section of the cladogram from Hemery et al. 2013. Maximum likelihood bootstrap values (>80%) are given above branch lines, Bayesian posterior probability values (>0.9) below. Subfamily/family names are in **bold**; numbers in parentheses represent number of genera and species in the clade, respectively. Note: the equivalent of Hemery's 'unnamed' clade is the unspecified clade of "various Antedonidae."

Figure 4 shows the portion of the most recent available tree of Comatulida that includes morphology-based antedonid subfamilies (and Zenometridae) (Rouse et al. in prep.). The new tree presents former antedonid Zenometridae as paraphyletic and basal to a clade including all former Antedonidae and several other taxa (e.g., Mariametroidea, Aporometridae, Tropiometridae), with a basal *Psathyrometra* sp. + *Sarametra* sp. clade, and another clade composed of another *Psathyrometra* sp. and a *Monachocrinus* sp. (Bathycrinidae).

As in Eléaume (2006) and Hemery et al. (2013), the heliometrines in Rouse et al. (in prep.) are no longer considered a monophyletic group as they form two clades; *Promachocrinus* and *Florometra mawsoni* forming one clade, and *Comatonia*, *Florometra*, *Anthometrina*, and *Heliometra* spp. another. Hemery et al. (2013) and Rouse et al. (in prep.) include a paraphyletic subclade sister to the heliometrines, containing several antedonine genera, *Phrixometra* (Bathymetrinae), Eudiocrinidae, and Aporometridae. Eléaume (2006) removed *Promachocrinus* and *Solanometra* (the latter not included in Hemery et al. 2013 or Rouse et al. in prep.) to Antedonidae *incertae sedis* due to differences in basal and radial architecture. Sequence data nest *Florometra mawsoni* within the many sympatric clades of *Promachocrinus kerguelensis* (Eléaume 2006, Hemery et al. 2012).

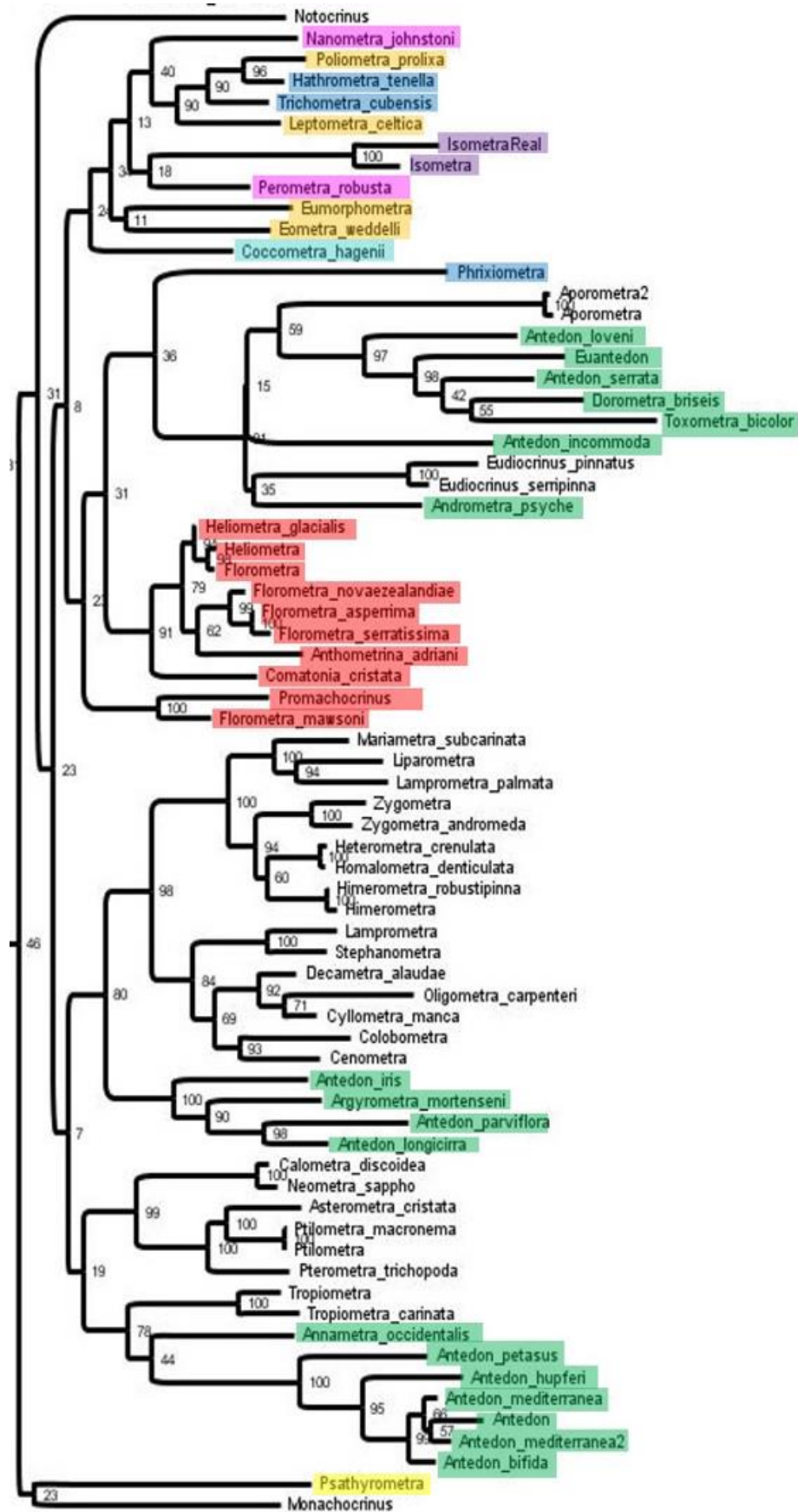


Fig 4. Portion of phylogenetic tree of Comatulida including terminals from antedonid subfamilies. Maximum likelihood bootstrap values given at branch nodes. Same color assignments as Figs. 2&3. Non-antedonid taxa are not highlighted (Rouse et al. in prep.).

Antedoninae returns as polyphyletic in all molecular phylogenies (Hemery 2011, Hemery et al. 2013, Rouse et al. in prep.) but with some paraphyletic and monophyletic subgroups. Representatives of several Indo-west Pacific antedonine genera (*Antedon*, *Euantedon*, *Toxometra*, *Dorometra*, and *Andrometra* terminals) form a paraphyletic grouping containing *Aporometra* (Aporometridae) and *Eudiocrinus* spp. (Eudiocrinidae) and sister to *Phrixometra* (Bathymetrinae). This larger clade arises from within Heliometrinae. An antedonine clade composed of *Argyrometra mortenseni* and three other Indo-west Pacific *Antedon* species is sister to a monophyletic Mariametroidea (minus Eudiocrinidae). The other antedonine clade is composed of North Atlantic *Antedon* species and South African *Annametra occidentalis* and is sister to Tropiometridae. This Atlantic antedonid-tropiometrid group is in turn sister to a larger clade containing other family members of Tropiometroidea (Asterometridae, Ptilometridae, and Calometridae).

A final clade composed of antedonid genera includes *Coccometra* (Thysanometrines), two perometrines (*Perometra* and *Nanometra*), two isometrines (*Isometra* spp.), two bathymetrines (*Hathrometra* and *Trichometra*; another bathymetrine (*Phrixometra*) returned distantly (see above)), and four Antedonidae *incertae sedis* terminals. Within this clade, four terminals, the bathymetrines *Hathrometra* and *Trichometra* and two former zenometrines (*Poliometra* and *Leptometra*) form a subclade restricted to the North Atlantic. The two thysanometrine genera, *Coccometra* and *Thysanometra*, were widely separated in Hemery's (2011) tree.

Although the trees in Rouse et al. (2013, in prep.), Hemery (2011) and Hemery et al. (2013) only contain a fraction of extant crinoid species, and exhibit lower than preferred confidence intervals at the basal nodes, they support the idea that previous morphologically-based taxonomy is based on homoplasy. Morphological comparisons within Antedonidae and among non-antedonid sister groups are required to identify possible characters that may support the molecular trees and produce a robust new classification (Hemery 2011, Hemery et al. 2013, Rouse et al. 2013, in prep., Roux et al. 2013).

## II. Objectives

The objective of this study was to search for morphological features that may support new relationships among groupings of former Antedonidae and their new non-antedonid sister groups based on Rouse et al.'s (in preparation), Hemery et al.'s (2013), and Hemery's (2011) molecular-based phylogenetic trees. Work initially focused on representatives distributed among the six former antedonid subfamilies plus examples of genera *incertae sedis* and the non-antedonid family Zenometridae, followed by representatives of the various clades distinguished in molecular trees and their non-antedonid sister groups (e.g., Notocrinoidea, Tropiometridae), to identify possible homologous features that may support molecular phylogenetic inferences, as well as to recognize homoplasies. The approach of studying certain skeletal components has proven successful in previous morphological examinations of feather star taxa, e.g., *Comatonia* moved from Comasteridae to Antedonidae (Messing 1981), Zenometridae removed from Antedonidae (Messing & White 2001), Heliometrinae divided (Eléaume 2006), and Atelecrinidae reassessed (Messing 2003, 2013). Character examples include details of centrodorsal shape and cavity (Purens 2016), features of cirrus sockets and cirri, basals, radials, brachials and pinnules, including articular structures. The particular ossicles examined in this study were the radials, as they are located below the visceral mass and are theoretically least likely affected by hydrodynamics and other environmental factors.

While the radials are not part of the vast suspension-feeding apparatus making up about 90 percent of the crinoid structure, they do play other vital roles in regards to the animal's water vascular system, as well as provide important attachment points and passages for muscles, ligaments, and nerve bundles (Clark & Clark 1967, Rasmussen 1978, Ubaghs 1978). The five radials (ten in *Promachocrinus* sp.) sit in a pentagon and are connected aborally to both the centrodorsal, by way of radial pits or furrows, and the internal basal rosette diagnostic of the family (Clark & Clark 1967, Hess & Messing 2011). The aboral nerve system passes from the centrodorsal through the basal structure, where lateral derivatives branch and form a circular commissure around the radial pentagon, and other derivatives partly fuse through the central canal on the articular face towards the brachials (Clark & Clark 1967, Ubaghs 1978). The articular face of each radial bears five fossae, four paired and one unpaired. The paired fossae include two

adoral muscle fossae and two interarticular ligament fossae separated by a thin ridge (Fig. 5). Aboral to the four paired fossae is the central canal, followed by a transversely-oriented fulcral ridge which accommodates the articular motion. Below the fulcral ridge is the unpaired aboral ligament fossa which houses the extensor ligament bundle and serves to antagonize the flexor muscles (Ubaghs 1978).

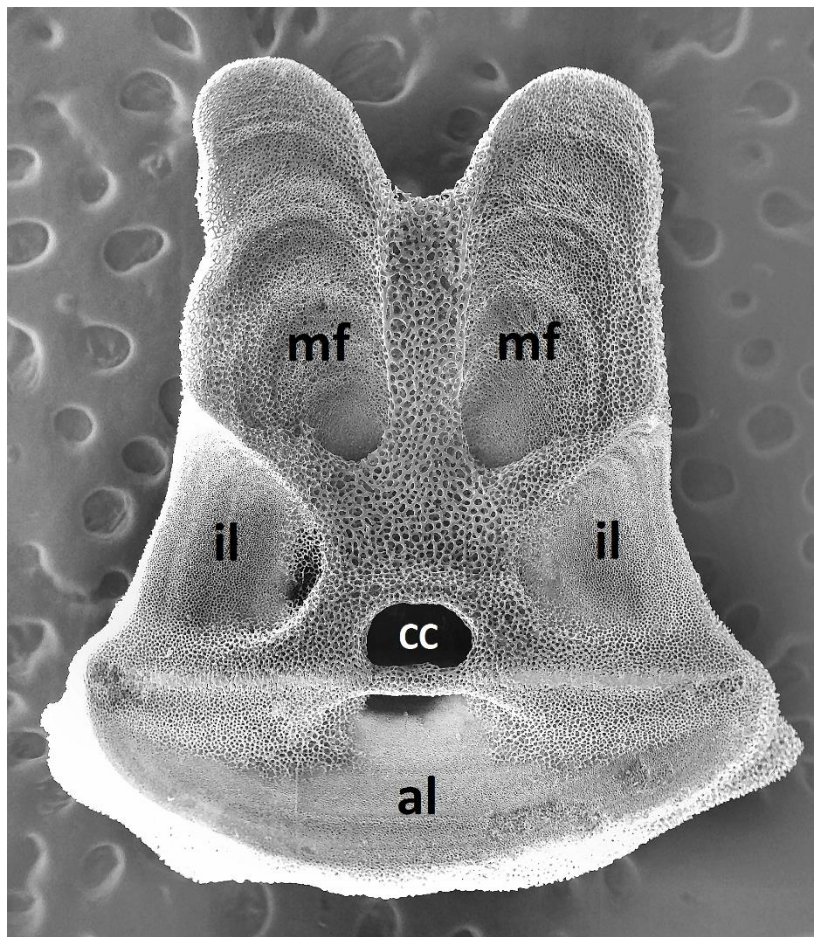


Fig. 5: SEM image of the articular facet view of a radial from *Florometra asperrima*; mf= adoral muscle fossae; il= interarticular ligament fossae; al= aboral ligament fossae; cc= central lumen.



Roux et al. (2013) discussed in detail the challenges involved in reconciling crinoid molecular and morphological phylogenies, emphasizing heterochronic trends and homoplastic evolutionary developmental patterns (e.g., paedomorphosis (Messing 1984); see also Rouse et al. 2013, Hemery et al. 2013) that confound attempts at classification based on morphology. While those trends were not able to be tested in this study, size was taken into account when looking at morphological variations. Because homoplasy is apparently so common, molecular-based trees formed the basis for review (Bull et al. 1993, Smith 1997, Roux et al. 2013). Morphological features that support molecular data do not imply a direct connection between processes at the genetic level and processes at the phenotypical level. Morphological support will, however, help to generate a more robust phylogeny upon which a stable classification can be built.

### III. Materials and Methods

#### A. *Specimens*

Due to the anatomical location of the radial ossicles, entire calices had to be dissolved for proper imaging. Therefore, specimens were selected from museum collections with larger sample sizes, and among them, those with the least intact number of arms and cirri were requested for loan. An attempt was made to obtain as large a sample as possible spanning the seven antedonid subfamilies (based on Hess & Messing 2011) as well as non-antedonid sisters, based on the taxa present in the three molecular phylogenies (Hemery 2011, Hemery et al. 2013, Rouse et al. in prep..) plus any other antedonids available. A total of 109 specimens from 40 species were obtained, primarily from NMNH and NSMT, with supplemental specimens from SIO, NSUOC, and MNHN (Table 1). Of the total number of species used, 16 were antedonines, four bathymetrines, five heliometrines, three perometrines, two thysanometrines, two isometrines, three from *Antedonidae incertae sedis*, one zenometrid, and three other non-antedonid sisters.

Table 1: Specimens and museum sources. Abbreviations: *NMNH*: National Museum of Natural History, Smithsonian Institution, Washington, DC; *NSMT*: National Museum of Nature and Science, Tokyo; *SIO*: Scripps Institution of Oceanography, UC San Diego; *NSUOC*: Nova Southeastern University, Oceanographic Center, Dania Beach, FL; *MNHN*: Muséum National d'Histoire Naturelle, Paris, France

Species	Sample Size	Museum/Collection
<b>Antedoninae</b>		
<i>Andrometra psyche</i>	3	NSMT
<i>Antedon bifida bifida</i>	4	NMNH
<i>Antedon hupferi</i>	4	NMNH
<i>Antedon c.f. incommoda</i>	2	NSUOC
<i>Antedon loveni</i>	5	NMNH
<i>Antedon c.f. loveni</i>	2	NSUOC
<i>Antedon mediterranea</i>	4	NMNH
<i>Antedon petasus</i>	3	NSUOC
<i>Antedon parviflora</i>	4	NSMT
<i>Antedon c.f. parviflora</i>	1	NSMT
<i>Antedon serrata</i>	2	NSMT
<i>Ctenantedon kinziei</i>	3	NMNH
<i>Dorometra briseis</i>	2	NSMT
<i>Dorometra c.f. briseis</i>	1	NSMT
<i>Dorometra parvicirra</i>	3	NSMT
<i>Iridometra adrestine</i>	2	NSMT
<b>Bathymetrinae</b>		
<i>Hathrometra tenella</i>	4	NMNH
<i>Thaumatometra tenuis</i>	1	NMNH
<i>Tonrometra spinulifera</i>	4	NMNH
<i>Trichometra cubensis</i>	1	NSUOC
<b>Heliometrinae</b>		
<i>Anthometrina adriani</i>	5	NMNH
<i>Comatonia cristata</i>	2	NSUOC
<i>Florometra asperrima</i>	5	NMNH
<i>Florometra serratissima</i>	1	SIO
<i>Promachocrinus kerguelensis</i>	1	SIO
<b>Perometrinae</b>		
<i>Erythrometra rubra</i>	2	NSMT
<i>Hypalometra defecta</i>	5	NMNH, NSUOC
<i>Perometra diomedea</i>	2	NSMT
<b>Thysanometrinae</b>		
<i>Coccometra hagenii</i>	4	NSUOC
<i>Thysanometra tenelloides</i>	5	NSMT
<b>Isometrinae</b>		
<i>Isometra graminea</i>	2	NMNH
<i>Isometra vivipara</i>	1	SIO

<i>Antedonidae incertae sedis</i>		
<i>Balanometra balanoides</i>	1	NSUOC
<i>Hybometra senta</i>	4	NMNH
<i>Poliometra proluxa</i>	2	NSUOC
Non-antedonids		
<i>Aporometra occidentalis</i>	3	NSUOC
<i>Notocrinus virilis</i>	3	NMNH
<i>Psathyrometra sp.</i>	4	MNHN
<i>Tropiometra carinata</i>	3	NMNH, NSUOC

---

After some identity hesitation following the dissolution of a few NSMT specimens, subsequent specimens were re-identified by both myself and Dr. Charles Messing upon reception from their respective museums. Using Clark's monograph (part 5, 1967), close examination of diagnostic characters under the dissecting microscope, with consideration from collection site and depth, resulted in most specimens keying out in agreement with the original identification label. There were some instances, however, where new identifications were agreed upon. An NMNH sample containing five specimens originally labeled as *Antedon bifida moroccana* was re-identified to be *Antedon hupferi* based upon the appearance of their proximal pinnules, division series and brachials (Clark & Clark 1967), as well as the collection site. The two subspecies of *Antedon bifida* (*A. b. bifida* and *A. b. moroccana*) and *Antedon hupferi* are morphologically very difficult to distinguish. Because of this, and their close geographic range, they may all be variations of the same species, *Antedon duebenii* (Clark & Clark 1967). The four specimens are treated as *Antedon hupferi* for this project, although more morphological and molecular work needs to be done (Hemery et al. 2009, 2009).

The original identifications of two NSMT samples from Japan, *Antedon parviflora* and *Dorometra briseis*, were accepted hesitantly, so a c.f. is included in their identifications. *Antedon c.f. parviflora* keyed out as an *Antedon*, since its third pinnule was of the same length and character as the succeeding pinnules, and was not distinctly smaller than the second pinnule (it was in fact larger). It keyed out to *A. parviflora* based on the length of its cirrus segments, but this was not definitive (Clark & Clark 1967). The specimen was too old to send out for genetic testing, so it was accepted as *Antedon c.f. parviflora* before dissolution. Similarly, identification of *Dorometra c.f. briseis* was not

definitive, as its third pinnule was indeed the longest and stoutest (in agreement with Clark & Clark 1967); however only among the proximal pinnules, not all pinnules.

Four NSUOC samples, two unknown *Antedon* spp. from Madang, Papua New Guinea and two *Antedon incommoda* from Midway Island, were re-identified, but hesitantly as well. Both unknown *Antedon* spp. were identified as *Antedon* c.f. *incommoda* as most of the diagnostic characteristics were not intact. The two individuals previously identified as *Antedon incommoda* were re-identified as *Antedon* c.f. *loveni*: one due to the number of cirrus segments, the other due to the centrodorsal being hemispherical, and both because their antepenultimate cirrus segments were longer than wide (Fig. 13, Clark & Clark 1967).

Four other NSMT specimens of *Antedon parviflora* were not re-identified but, due to substantial differences in their radial shape, were separated into two groups: *Antedon parviflora* B and E (with taller muscle fossae) from Shimane, Japan and *Antedon parviflora* C and D (with short muscle fossae) from the East China Sea. All four specimens were analyzed together and then by group for comprehensive analysis. Individuals identified with a c.f. were treated as a separate species from their non-c.f. counterparts for the purpose of unbiased statistical analysis.

Most of the specimens requested for loan were those least intact in the large sample jars, all diagnostic characters were absent in two instances (*Thaumatometra tenuis* and *Tonrometra spinulifera*), making accurate identification essentially impossible. In these instances, the original label identification was accepted and the dissolved radial ossicles were compared to literature descriptions and drawings.

Once each specimen was identified as precisely as possible, appendages not part of the calyx bundle were carefully removed with forceps; all cirri were separated from the centrodorsal at the first cirral whenever possible, and all arms were separated at one of two points: either between  $IBr_1$  and  $IBr_2$  or at the first syzygy at  $Br_{3+4}$ , whichever point minimized damage during dissection. The remaining centrodorsal with attached proximal brachials was placed in a 90% Chlorine Bleach/DI solution for at least 16 hours. Two additional washes with bleach were performed, each between 6 and 18 hours, to ensure all tissues had been thoroughly dissolved. Dissociated ossicles were then put through three separate washes in pure DI water, each soaking between 8 and 24 hours, to ensure

the bleach was removed from the ossicles. Radial ossicles that remained intact throughout the bleaching process were then carefully dried and mounted onto adhesive SEM stubs using a small paintbrush and a dissecting microscope, in preparation for SEM imaging.

### B. SEM imaging

Intact radial ossicles were imaged using an FEI Quanta 200 SEM with Inca X-sight (Oxford Instruments) at Nova Southeastern University's College of Dental Medicine. After a few preliminary sessions, three alignments were carried out to minimize variations in camera placement: 1) interior septum (which separates the two passages for the interradian nerve trunks) in line with the middle of the central lumen; 2) walls of the central lumen oriented so that no or little interior was visible, and 3) examination of the edges of all fossae so the ossicle appeared as "flat" as possible. Camera placement error was tested using *Coccometra hagenii* specimen F. Each of the specimen's five radial ossicles was imaged four times, with a reset of the image plane between each image capture. Each image was landmarked according to the protocol discussed below (see *Landmarking*) and a preliminary PCA, with accompanying ANOVA tests, was produced to test camera placement error (see Results). Satisfactory results allowed adoption of the alignment system for the rest of the ossicles and reduction of image number to one per ossicle. Once all ossicles were imaged, ossicles in a total of 233 images were deemed intact enough for landmarking (see Appendix B for all images).

### C. Landmarking

Before landmarking, each image was enhanced and, if necessary, rotated using Jasc Paint Shop Pro 9 software. The images were sharpened so stereom changes and slopes could easily be determined, and rotated so the scale bar was always horizontal; this was to reduce human error during measurements. Originally, 28 homologous landmarks were chosen, with the help of Dr. Lenaïg Hemery, to quantify the images for geometric morphometrics (Fig.6). All landmarks were based upon Bookstein's landmark types II and III (Table 2). None were of type I, as all ossicles lacked tissue (Bookstein 1991). No semi-landmarks were used. Individual *.tps* files were created from each image using tpsUtil 1.58, then measured and carefully digitized using tpsDig2 2.17 (Rohlf 2006,

Burrige 2012). The first images landmarked were two specimens of *Coccometra hagenii* and one specimen of *Dorometra briseis*. The image of one ossicle from each of these three specimens was landmarked ten times without reference, in three separate bouts, adding an additional error factor. PCAs and a nested ANOVA were then performed on the repetitions in order to test accuracy of landmark placement (Zelditch et al. 2012, Sherratt 2014, Liu et al. 2016). Repeatability percentages were found using the Mean Squares (MS) values from the nested ANOVA. The difference of bout value from total MS value was divided by number of reps, and the ratio of that value to total MS value revealed the repeatability percentage for that image (Sherratt 2015). Satisfactory results allowed confident landmark placement on the remaining images (see Results).

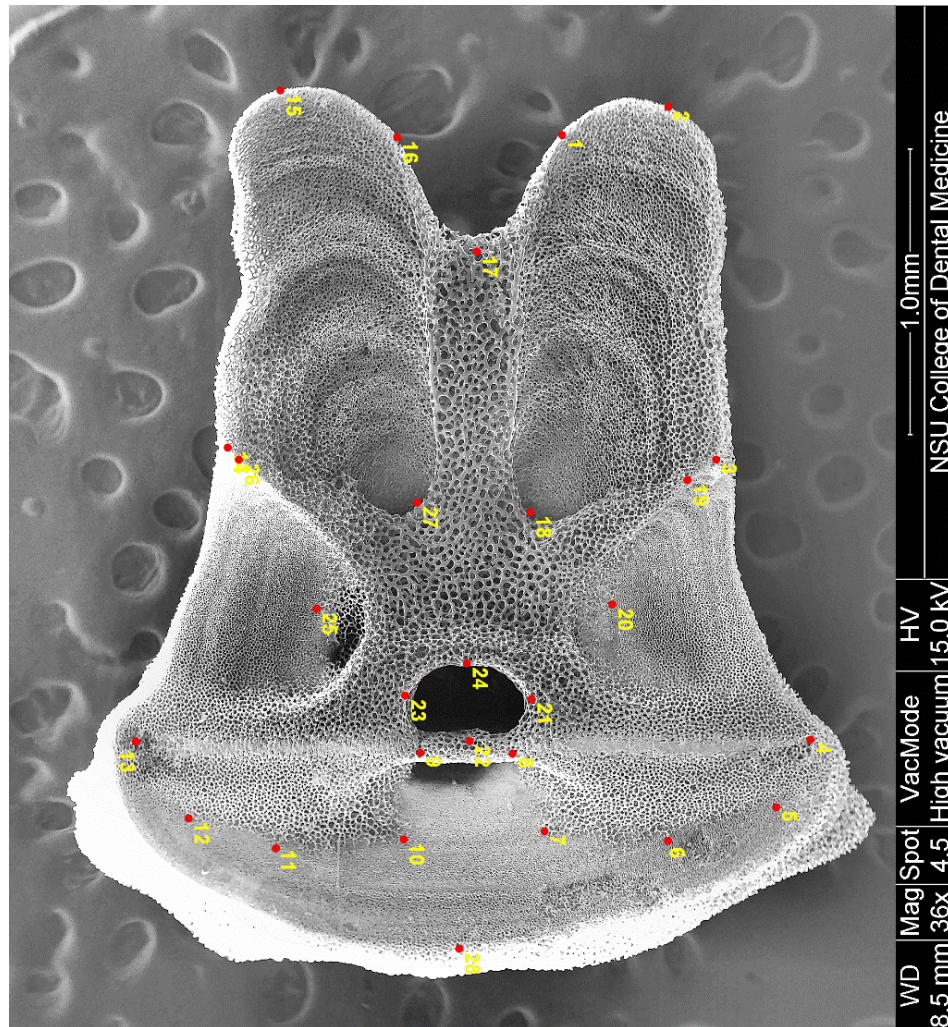


Fig. 6: Digitized SEM image of *Florometra asperrima* with 28 homologous landmarks based on Bookstein (1991).

Table 2: Description and landmark type assignment of the 28 homologous landmarks chosen based on Bookstein (1991).

n° point	Definition	Type
1	Start of curvature at end of right muscular area	III
2	Curvature maximum at right muscle area	II
3	Tip of ligamento-muscular ridge on right muscle area	II
4	End of transverse fulcral ridge, right side	II
5	Curvature max at stereom meeting on right aboral region	III
6	Lateral minimum point of aboral ridge stereom, right side	III
7	Median minimum point of aboral ridge stereom, right side	III
8	Inner minimum point of aboral ridge stereom, right side	III
9	Inner minimum point of aboral ridge stereom, left side	III
10	Median minimum point of aboral ridge stereom, left side	III
11	Lateral minimum point of aboral ridge stereom, left side	III
12	Curvature max at stereom meeting on left aboral region	III
13	End of transverse fulcral ridge, left side	II
14	Tip of ligamento-muscular ridge on left muscle area	II
15	Curvature maximum at left muscle area	II
16	Start of curvature at end of left muscle area	III
17	Curvature max at end of septum, within the ambulacral groove	II
18	Lowest, deepest point of right muscle fossa	III
19	Lowest meeting point on right ligamento-muscular ridge	II
20	Lowest point of right ligament area, middle of stereom curve	III
21	Curvature minimum on right side of central lumen	II
22	Curvature minimum on aboral side of central lumen	II
23	Curvature minimum on left side of central lumen	II
24	Curvature minimum on oral side of central lumen	II
25	Lowest point of left ligament area, middle of stereom curve	III
26	Lowest meeting point on left ligamento-muscular ridge	II
27	Lowest, deepest point of left muscle fossa	III
28	Projection of intermuscular septum axis on aboral ridge	II

After the 233 images were landmarked, each image was reviewed and landmarks moved if needed. Dr. Hemery carried out a third review of landmark placements. The repeated reviews were performed in an attempt to reduce human error as much as possible, as the digitizing process can be subjective. Any landmarks that could not be placed due to missing material were placed on the image margin for possible removal later. Once all landmark edits were completed for the images, the frequency of presence was calculated for each landmark using a simple excel table (rows depicted images, columns depicted landmarks, and 0/1 indicated presence or absence). Using the

frequency of presence data with a percent of lost data equation (Eqn 1, Cordeiro Estrela de Andrade Pinto 2005), two scenarios resulted in the least amount of lost data.

**Eqn 1**       $p = ((k*m*n) + (n*(K*m-k*m))*100) / (N*K*m)$

where K=total number of landmarks; m=dimension of the dataset (2D or 3D); N=total number of ossicles; k=number of removed landmarks, and n=number of removed ossicles.

Landmarks #5 and #12 were removed in both scenarios as they proved the most subjective and did not appear to provide crucial information. Scenario 1 also removed landmark #1 and a total of 14 images (Table 3), and yielded a loss of 5.37%. Scenario 2 retained landmark #1 but removed 18 total images (Table 4) and yielded a loss of 7.18%. As the results of both scenarios were both minimal and so similar, both were used to see if the results would differ *a posteriori*. Landmark removal and file appending was done with tpsUtil 1.58 (Rohlf 2006).

The process of landmarking an image creates coordinates (in this case, only x and y coordinates) for each landmark, which are used to quantify shape change. It is important to note that while coordinates can often be thought of as data, they are not discrete anatomical points and thus cannot be used individually as characters. In morphometric studies such as this one, an entire configuration of coordinates is the datum for a single individual that is used for morphometric analysis (Bookstein 1991, Bookstein 1997, Bookstein 2013, Rohlf 1999, Klingenberg 2008, Zelditch et al. 2012, Rohlf 2015).



Table 3: Scenario 1 landmark point table with 25 landmarks (used on 219 ossicles); type assignment based on Bookstein (1991).

<b>n° point</b>	<b>Definition</b>	<b>Type</b>
1	Curvature maximum at right muscle area	II
2	Tip of ligamento-muscular ridge on right muscle area	II
3	End of transverse fulcral ridge, right side	II
4	Lateral minimum point of aboral ridge stereom, right side	III
5	Median minimum point of aboral ridge stereom, right side	III
6	Inner minimum point of aboral ridge stereom, right side	III
7	Inner minimum point of aboral ridge stereom, left side	III
8	Median minimum point of aboral ridge stereom, left side	III
9	Lateral minimum point of aboral ridge stereom, left side	III
10	End of transverse fulcral ridge, left side	II
11	Tip of ligamento-muscular ridge on left muscle area	II
12	Curvature maximum at left muscle area	II
13	Start of curvature at end of left muscle area	III
14	Curvature max at end of septum, within the ambulacral groove	II
15	Lowest, deepest point of right muscle fossa	III
16	Lowest meeting point on right ligamento-muscular ridge	II
17	Lowest point of right ligament area, middle of stereom curve	III
18	Curvature minimum on right side of central lumen	II
19	Curvature minimum on aboral side of central lumen	II
20	Curvature minimum on left side of central lumen	II
21	Curvature minimum on oral side of central lumen	II
22	Lowest point of left ligament area, middle of stereom curve	III
23	Lowest meeting point on left ligamento-muscular ridge	II
24	Lowest, deepest point of left muscle fossa	III
25	Projection of intermuscular septum axis on aboral ridge	II

Table 4: Scenario 2 landmark point table with 26 landmarks (used on 215 ossicles): type assignment based on Bookstein (1991).

n° point	Definition	Type
1	Start of curvature at end of right muscular area	III
2	Curvature maximum at right muscle area	II
3	Tip of ligamento-muscular ridge on right muscle area	II
4	End of transverse fulcral ridge, right side	II
5	Lateral minimum point of aboral ridge stereom, right side	III
6	Median minimum point of aboral ridge stereom, right side	III
7	Inner minimum point of aboral ridge stereom, right side	III
8	Inner minimum point of aboral ridge stereom, left side	III
9	Median minimum point of aboral ridge stereom, left side	III
10	Lateral minimum point of aboral ridge stereom, left side	III
11	End of transverse fulcral ridge, left side	II
12	Tip of ligamento-muscular ridge on left muscle area	II
13	Curvature maximum at left muscle area	II
14	Start of curvature at end of left muscle area	III
15	Curvature max at end of septum, within the ambulacral groove	II
16	Lowest, deepest point of right muscle fossa	III
17	Lowest meeting point on right ligamento-muscular ridge	II
18	Lowest point of right ligament area, middle of stereom curve	III
19	Curvature minimum on right side of central lumen	II
20	Curvature minimum on aboral side of central lumen	II
21	Curvature minimum on left side of central lumen	II
22	Curvature minimum on oral side of central lumen	II
23	Lowest point of left ligament area, middle of stereom curve	III
24	Lowest meeting point on left ligamento-muscular ridge	II
25	Lowest, deepest point of left muscle fossa	III
26	Projection of intermuscular septum axis on aboral ridge	II

#### D. Additional factors

Allometry and its effect on radial shape was an additional factor explored during statistical analysis. Therefore, the sizes of the radials (Fig. 7), centrodorsal, and diameter at the first syzygy (Fig. 8) were measured (see Appendix Table A1). The radial height and width was measured before digitizing in tpsDig2 2.17 (Rohlf 2006). Centrodorsal height and diameter were measured under the dissecting scope following dissolution, and the diameter at the first syzygy, if available, was measured from images taken before dissolution, also using tpsDig2 2.17. Height to width (HW) ratios of the radials and the centrodorsal of each specimen were calculated, although only radial ratio was used as a

factor in statistical analyses. Specimens were assigned to either one of two factor levels based on their radial ratio: HW <1.0 (1) or  $\geq$ 1.0 (2). It was the original intention to use centrodorsal ratio as an additional factor, but as only two of the 40 species (non-antedonid sister *Psathyrometra* sp., and not sequenced *incertae sedis* species, *Balanometra balanoides*) had centrodorsal HW > 1.0, separate testing was not warranted. Arm length was not a contributor to size in this study, as none of the specimens had any completely intact.

In addition to measurements, biogeographic information such as depth, specific locality, general region, taxonomic assignment, and molecular clade assignment were compiled and also used as factors in statistical analyses (Table 5). Depth was separated into five range levels: 0-50m (1), 51-100m (2), 101-200m (3), 200-1000m (4), and 1001+m (5). Based on our and previous collection data (Clark & Clark 1967), species were assigned to the level in which they most frequently occurred, or the maximum if known to occur across several levels (e.g., *Poliometra prolixa* occurs from 20 to 1,960m and so was assigned to level 5). Specific locality separated species into 11 factor levels: Japan Sea, China Sea, Papua New Guinea, Australia, European North Atlantic, Antarctica, Northeast Pacific, West Africa, Northwest Atlantic, Caribbean Sea, and Mediterranean Sea. Japan and China seas were separated because of the preliminary observed shape differences between *Antedon parviflora* B&E (from the China Sea) and *Antedon parviflora* C&D (from the Japan Sea), and the anticipation that locality would be a significant factor. General region was separated into three factor levels: Atlantic, Pacific, and Antarctic. It is important to note that the factor “levels” are not used in a ranking manner, but simply for categorical purposes in the analyses. Although current speed is likely an influential factor in morphological adaptations of crinoids, it was not used here because nothing was known about the precise conditions under which the specimens lived (CG Messing, personal communication).

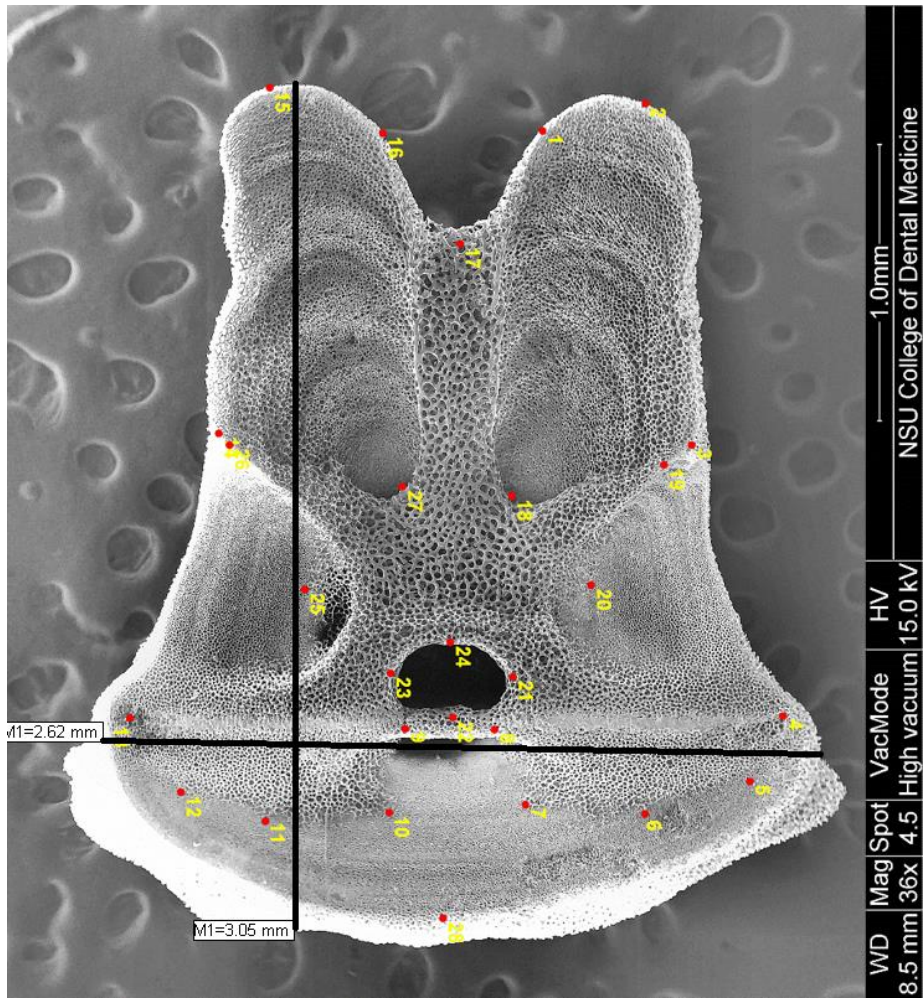


Fig. 7: Radial height and width measurements taken of *Florometra asperima*.

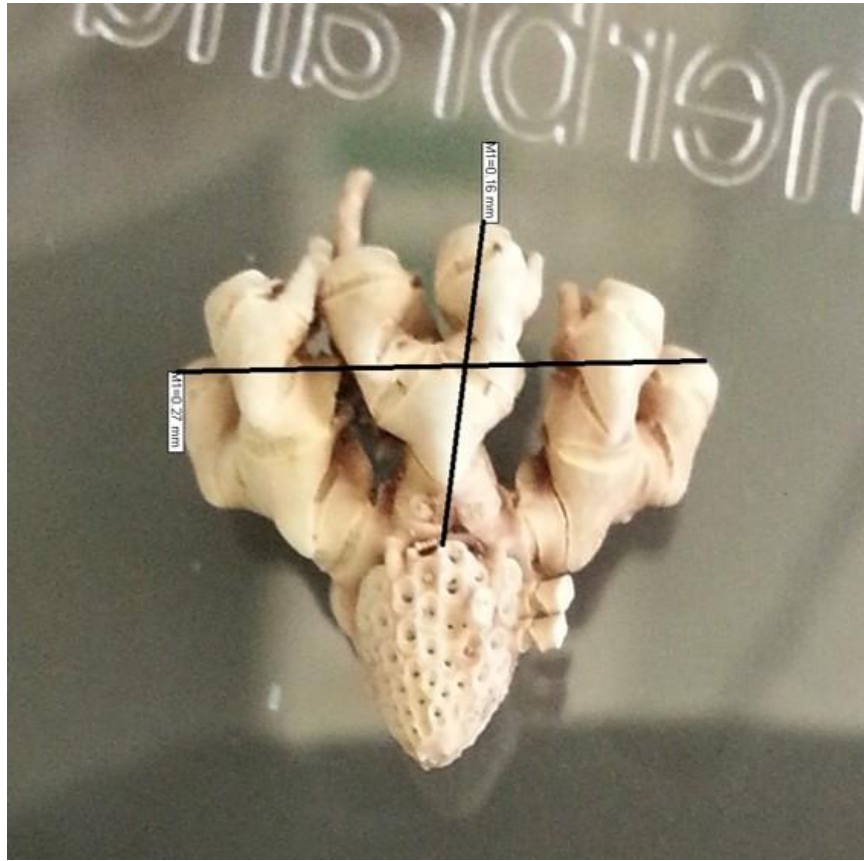


Fig. 8: Arm length (vertical line) and syzygy diameter (horizontal line) measurements taken of *Psathyrometra* sp.

Table 5: Comprehensive list of the 40 species in this study with their taxonomic classification, specific locality, general region, depth range, radial ratio, and molecular assignment; \*depth range data from Clark & Clark 1967, Meyer 1972, Eleaume et al. 2014, WoRMS

Subfamily/ Family	Species	Abbreviation (figs and tables)	Locality	Region (Ocean)	Collection depth (m)	Depth range* (m)	Radial ratio	Clade assignment
Antedoninae	<i>Andrometra psyche</i>	Andps	Tokyo, Japan	Pacific	145-161m	55-1000m	0.73	O
	<i>Antedon bifida bifida</i>	Antbb	United Kingdom	Atlantic	--	15-40m	0.69	N
	<i>Antedon hupferi</i>	Anthp	Cameroon	Atlantic	59m	0-120m	0.75	N
	<i>Antedon c.f. incommoda</i>	Acfm	Madang, PNG	Pacific	6.1-7.6 m	0-68m	0.79	O
	<i>Antedon loveni</i>	Antlv	NSW Australia	Pacific	--	0-18m	0.89	O
	<i>Antedon c.f. loveni</i>	Acfvl	Midway Island	Pacific	20-30 m	0-18m	0.71	O
	<i>Antedon mediterranea</i>	Antmd	Tunisia	Atlantic	--	0-420m	0.79	N
	<i>Antedon petasus</i>	Antpt	Sweden	Atlantic	20m	10-326m	0.86	N
	<i>Antedon parviflora</i> , B& E	AntpvBE	Eastern China Sea	Pacific	60m	0-275 (?400)m	0.87	P
	<i>Antedon parviflora</i> , C&D	AntpvCD	Shimane, Japan	Pacific	54-65m	0-275 (?400)m	0.8	P
	<i>Antedon c.f. parviflora</i>	Acfpv	Okinawa, Japan	Pacific	51-53 m	0-275 (?400)m	0.9	P
	<i>Antedon serrata</i>	Antse	Yamaguchi, Japan	Pacific	39-92m	0-180m	0.91	O
	<i>Ctenantedon kinziei</i>	Ctekz	Barbados	Atlantic	15-30m	0-36m	0.7	--
	<i>Dorometra briseis</i>	Dorbr	Kagoshima, Japan	Pacific	87-88m	108-728m	0.88	O
	<i>Dorometra c.f. briseis</i>	Dcfbr	Okinawa, Japan	Pacific	51-53 m	108-728m	0.97	O
	<i>Dorometra parvicirra</i>	Dorpv	Shimane, Japan	Pacific	60m	0-164m	1.08	--
	<i>Iridometra adrestine</i>	Iriad	Tosa Bay, Japan	Pacific	144-154m	80-731m	1.01	--
Bathymetrinae	<i>Hathrometra tenella</i>	Hattn	Massachusetts, US	Atlantic	335m	28-1783m	1.14	UN
	<i>Thaumatometra tenuis</i>	Thmtn	Hokkaido, Japan	Pacific	594m	(?35) 146-1500m	1.04	M, P
	<i>Tonrometra spinulifera</i>	Tonsp	Antarctica	Antarctic	606-638m	1266m	1.56	UN
	<i>Trichometra cubensis</i>	Tricb	NE Straits of FL	Atlantic	630m	293-2193m	1	UN

Table 5 cont'd: Comprehensive list of the 40 species in this study with their taxonomic classification, specific locality, general region, depth range, radial ratio, and molecular assignment;  
\*depth range data from Clark & Clark 1967, Meyer 1972, Eleaume et al. 2014, WoRMS

Subfamily/ Family	Species	Abbreviation (figs and tables)	Locality	Region (Ocean)	Collection depth (m)	Depth range* (m)	Radial ratio	Clade assignment
Heliometrinae	<i>Anthometrina adriani</i>	Anaad	Antarctica	Antarctic	--	55-1156m	1.13	M
	<i>Comatonia cristata</i>	Comcr	Great Bahama Bank	Atlantic	322-381m	14-366 (?411)m	1.13	M
	<i>Florometra asperrima</i>	Floas	Alaska, US	Pacific	291m	79-1574m	1.09	M
	<i>Florometra serratissima</i>	Flose	Off Santa Cruz, CA	Pacific	119-183	11-1252m	1.08	M
	<i>Promachocrinus kerguelensis</i>	Prmkg	Shag Rock, Antarctica	Antarctic	149-160m	20-2100m	1.74	M
Isometrinae	<i>Isometra graminea</i>	Isogr	Palmer Arch., Ross Sea*	Antarctic	--	59-714m	1.08	UN
	<i>Isometra vivpara</i>	Isovv	Elephant Island	Antarctic	222-247m	79-1228m	1.03	UN
Perometrinae	<i>Erythrometra rubra</i>	Eryru	Tokyo, Japan	Pacific	135-172m	(?95) 100-274m	0.92	--
	<i>Hypalometra defecta</i>	Hypdf	Venezuela	Atlantic	64m	60-386m	0.88	--
	<i>Perometra diomedea</i>	Perdi	Tosa Bay, Japan	Pacific	171m	71-254 (?278)m	0.95	UN
Thysanometrinae	<i>Coccometra hagenii</i>	Cocha	Gulf of Mexico	Atlantic	317m	14-1046m	1.05	UN
	<i>Thysanometra tenelloides</i>	Thyte	Suruga Bay	Pacific	240-410 m	128-360m	0.7	UN
Antedonidae i.s.	<i>Balanometra balanoides</i>	Balba	Midway to Hawaiian Isls	Pacific	108-298	142-150m	1.26	--
	<i>Hybometra senta</i>	Hybse	Angola, W Africa	Atlantic	1427m	42m	1.12	--
	<i>Poliometra proluxa</i>	Polpx	N of Iceland	Atlantic	--	20-1960m	1.38	UN
Zenometridae	<i>Psathyrometra</i> sp.	Pthsp	Indian Ocean & N Pacific*	Pacific	--	366-2903m	1.11	--
Aporometridae	<i>Aporometra occidentalis</i>	Apooc	Cape Northumberland, South Australia	Pacific	15m	0-18m	0.49	O
Notocrinidae	<i>Notocrinus virilis</i>	Notvi	Antarctica	Antarctic	174-192m	65-1120m	0.8	--
Tropiometridae	<i>Tropiometra carinata</i>	Troca	Colombia	Atlantic	3-12m	0-55 (?73)m	0.66	N

### *E. Statistical Analysis*

Analysis of the digitized images was performed in R using geomorph and shapes packages (Dryden & Dryden 2012, Adams & Otarola-Castillo 2013, Adams et al. 2014, R Core Team 2014). Morphometrics terminology follows Zelditch et al. (2012).

Configurations were aligned by generalized Procrustes superimposition (removing translation, rotation and scaling effects), and the superimposed configurations were projected as Euclidean distances onto an orthogonal plane using Principal Component analysis (PCA) (Kendall 1989, Rohlf & Slice 1990, Rohlf & Marcus 1993, Dryden & Mardia 1998, Klingenberg & McIntyre 1998, Rohlf 1999, Mitteroecker & Gunz 2009, Zelditch et al. 2012, Adams et al. 2013, Renaud et al. 2015). The purpose of PCA is to analyze all of the variance within a set of configurations and reduce it to a smaller set of factors or principal components (PCs), each of which encompasses decreasing amounts of variance (e.g., PC1 captures the largest variance, PC2 the second largest). PCA projected several levels of morphological variation. As mentioned above, first intra-ossicle and intra-image variation was projected via PCA to visualize inconsistencies in camera and landmark placements, respectively. Then a PCA was done for each individual with multiple digitized ossicles to identify any significant within-individual variation. Mean configurations of individuals were used to perform a PCA within each species to identify any significant within-species variations. Mean configurations from the latter were used for testing variations within genera, within subfamilies, and within clades.

As Principal Component Analysis only projects within-group variation, the variations between group means (subfamily or clade) were projected onto an orthogonal plane using Between Groups Principal Component Analysis (BGPCA). This method was chosen over using Canonical Variance Analysis (CVA) and Linear Discriminant Analysis (LDA) in order to maintain geometric integrity, which may be biased during the rescaling step required by CVA (Campbell & Atchley 1981, Mitteroecker and Bookstein 2011, Hernández-Ortiz et al. 2015, Renaud et al. 2015).

Both PCA and BGPCA are visualization tools only and, although they help describe shape variation through projection of PCs, they do not explain the variation or identify which factors cause the variation, nor do they provide any information about shape similarity. Procrustes ANOVA tests are used to explain shape variation in this



project, and Procrustes distances are calculated to explain similarity (Klingenberg & McIntyre 1998, Zelditch et al. 2012, Collyer et al. 2014). Procrustes ANOVA tests were performed within and between groups, testing the effects on shape variation by factors such as size (using centroid size), depth range, specific locality, general region and taxonomic and molecular assignments. Mean configurations were used when testing significance effects between species via Procrustes ANOVAs. Any ANOVA result that yielded significant results was followed by a pairwise test between individual configurations to identify which pairing(s) caused the significant variance. Because varying sample sizes caused an imbalance, permutations methods (999 iterations) were used in all ANOVA and pairwise testing to stabilize this error (Zelditch et al. 2012, Collyer et al. 2014).

While not used as a visualization tool in this project, Linear Discriminant Analysis (LDA) was used to classify individuals into species groups based on their Mahalanobis distances (Sheets et al. 2006, Mitteroecker & Gunz 2009, Mitteroecker & Bookstein 2011, Zelditch et al. 2012). Those classifications were then tested through leave-one-out cross validation (LOOCV), and, through comparisons to the known classifications of each individual, the overall correct classification rate, along with species-specific hit ratios (percent of correct classification) (Sheets et al. 2006, Cardini et al. 2009, Zelditch et al. 2012) were calculated for both scenarios. Finally, the patterns of similarity among species were visualized by way of “unweighted-pair grouping method using averages” (UPGMA) cluster analyses (Ramirez-Sanchez et al. 2016). UPGMA is a bottom-up method of cluster analysis, in which the two closest units are paired first, then their average distance is paired with the next closest unit, the average of the three paired with the next closest, and so on, until all taxa have been included (Zelditch et al. 2012, Hernández-Ortiz et al. 2015). This hierarchical clustering method was performed twice—once using the calculated Procrustes distances, the other using the Mahalanobis distances obtained from LDA—for each of the two scenarios, yielding a total of four phenograms.

Procrustes distance is the square root of the sum of squared differences in landmark positions between two shapes and is used during PCA, BGPCA, and Procrustes ANOVA testing (Dryden and Mardia 1998), while Mahalanobis distance is a measure of standard deviations from a reference shape or origin in a rescaled shape space and is used

during discriminant analyses (Zelditch et al. 2012). All non-zero PCs were used ( $2k-4$ , where  $k$  is the number of landmarks) when calculating both distances in order to include all possible shape characters and to obtain optimal results. The results based on Procrustes distances were of the most interest as they depict the degree of morphological similarities between species. Mahalanobis distances were included as an additional source of information regarding the strength of the phenogram clusters (Zelditch et al. 2012). The four phenogram results were visually compared to the molecular trees (Hemery 2011, Hemery et al. 2013, Rouse et al. in prep.). If congruent, these results, along with direct comparisons of Procrustes and Mahalanobis distance relatives, would support the notion of taxonomic revisions based on the phylogenies.

In an additional effort to find morphological connections, and possible character states within radial shape, 12 inter-landmark measurements were measured within each of the 233 ossicles (Zelditch et al. 1995, Rohlf 2000, Freudenstein 2005, Bookstein 2013, Ling et al. 2016). All measurements were taken from the original 28-landmark images to ensure landmark #1 could be measured and all landmark numbers would remain unchanged (Fig. 9, Table 6). All measurements were divided by a standard inter-landmark measurement (landmark 17 to landmark 28) in order to eliminate intra-individual variation (see Appendix Table A2), then independent-sample t-tests were performed for each measurement on all images; these t-tests used the average of data for each measurement and determined if there were significant variances or not between two species at a time (Ling et al. 2016). To reduce the number of t-tests performed, the impractical pairings were eliminated, grouping only by locality, subfamily, and clade, as well as closest distance-based relative if they were not included in any of the former groups. All non-significant pairings were noted and compared within taxonomic and molecular assignments, geographic factors, and the phenograms. In addition to the twelve inter-landmark measurements, nine of those measurements (both muscle fossae widths and aboral ligament fossa width excluded) were divided by radial height or width, depending on the measurement, resulting in nine fossa-to-ossicle measurement ratios. Those ratios were presented as a range for each species and compared directly with both the phenograms and phylogenies as well. Are phylogenetic forces a factor in constraining morphology, or is it a whole suite of interactions with their environment?

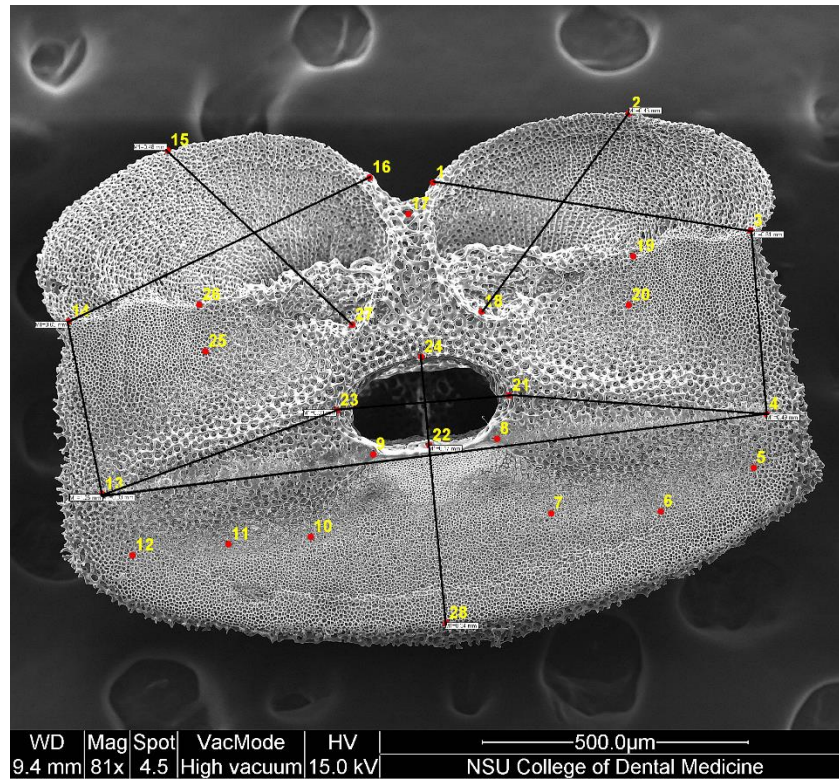


Fig. 9: Twelve inter-landmark measurements taken of *Antedon bifida bifida*.

Table 6: Table of the 12 inter-landmark measurements taken within each ossicle; all measurements were divided by the STANDARD to eliminate intra-individual variation

Landmark to Landmark (#=#)	Measurement
2=18	height of R adoral muscle fossae
1=3	width of R adoral muscle fossae
15=27	height of L adoral muscle fossae
14=16	width of L adoral muscle fossae
3=4	height of R interarticular ligament fossae
4=21	width of R interarticular ligament fossae
13=14	height of L interarticular ligament fossae
13=23	width of L interarticular ligament fossae
4=13	length of fulcral ridge/ width of aboral ligament fossae
22=28	height of aboral ligament fossae
21=23	width of central lumen
22=24	height of central lumen
17=28	STANDARD

#### IV. Test of the feasibility

##### A. Results

Preliminary results were obtained in order to accept both camera placement and landmark placement protocols through PCA and Procrustes ANOVA tests. Adequate results allowed for the completion of imaging and landmarking, and subsequent analyses. PCAs and Procrustes ANOVAs were performed on those individuals with more than one landmarked ossicle. Satisfactory results allowed for the usage of mean configurations as the datum for each individual in subsequent intra-specific testing. The results of the intra-specific testing, through between-group PCAs and Procrustes ANOVAs, then allowed usage of mean species configurations for all successive testing (i.e. intra-genus variability, intra-subfamily variability, etc).

##### i. *Camera placement variability*

The five radial ossicles of *Coccometra hagenii*, specimen F, were each imaged four times using the alignment protocol discussed above (see *SEM imaging*). The results of the PCA show tightly-formed clusters with no dramatically placed outliers within each ossicle (Fig 10). The overlap of the second and fifth ossicles simply infers a close similarity between their overall shapes; it does not infer any similarity between camera placements in comparison with the other ossicles. While the PCA does not show obvious outliers, the Procrustes ANOVA yielded significant variation ( $p = 0.001$ ) between camera placements. The results of the pairwise test identified the variability to be significant only within placements of the fourth ossicle. The other four ossicles showed no significant variance with camera placement.

## PCA of Camera Placement for *Coccometra hagenii* F

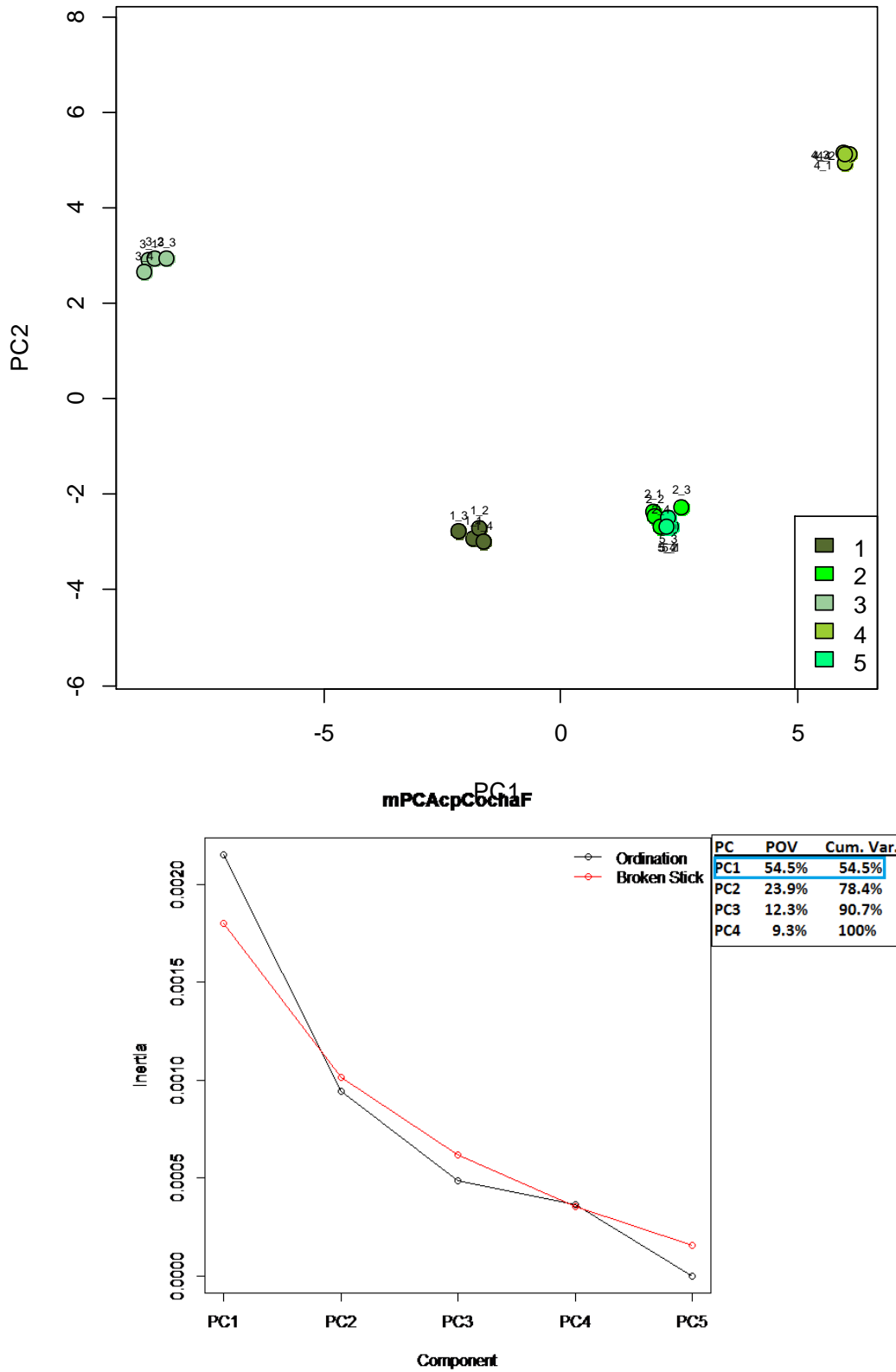


Fig. 10: Top: PCA of camera placement variation between the five radials of *Coccometra hagenii*, specimen F. Bottom: mean broken stick model, depicting PC1 as the interpretable variation

ii. *Landmark placement variability*

Three randomly-chosen images were selected to be landmarked ten times each, in three separate bouts (total of 30 repetitions for each image), in order to test for human error in landmark placements. The first two principal components of *Coccometra hagenii* specimen C encompass 68.5% of the total shape variance, both of which are interpretable and can be explained by non-random variation as they lie above the broken stick (Fig. 11, bottom). The PCA projection of *Coccometra hagenii* specimen C shows larger variations between the three bouts than within bouts although there are inconsistencies within each bout as well, especially within bout 2 (Fig. 11, top). The Procrustes ANOVA resulted in significant variance ( $p = 0.001$ ) between bouts only, specifically between bouts 2 and 3 according to the pairwise results. Results of the nested ANOVA revealed a repeatability of only 9.7% for *Coccometra hagenii*, specimen C.

Over half of the variation between all repetitions of *Coccometra hagenii* specimen D can be described by the first principal component (56.5%), with the first two PCs describing the interpretable variation (68.3%) (Fig. 12, bottom). The PCA projects the majority of the variation as between bout 1 and the other two bouts on the x-axis (PC1). There is significant overlap between bouts 2 and 3 on the x-axis and overlap of all three on the y-axis (PC2) (Fig. 12, top). Pairwise results after a significant Procrustes ANOVA ( $p = 0.001$ ) revealed that most of the between-bout variation is due to variances with bout 1, as depicted by the PCA, although there is variation between all three. As with *C. hagenii* specimen C, there was no significant variance within bouts, and the repeatability of landmark placement was only 9.8% after a nested ANOVA.

The interpretable variation for *Dorometra briseis* specimen A can be described by the first two PCs, encompassing 58.8% of the overall variance (Fig. 13, bottom). The clear source of variance from the PCA projection is bout 2, with significant overlap between bouts 1 and 3 along PC1 (Fig. 13, top). The Procrustes ANOVA was significant ( $p = 0.001$ ) for between-bout variation, with pairwise tests revealing the cause between bouts 1 and 2. Once again, no within-bout variation was significant and the results of the nested ANOVA revealed a repeatability of 6.9%.

# Landmark Placement PCA for CochaC

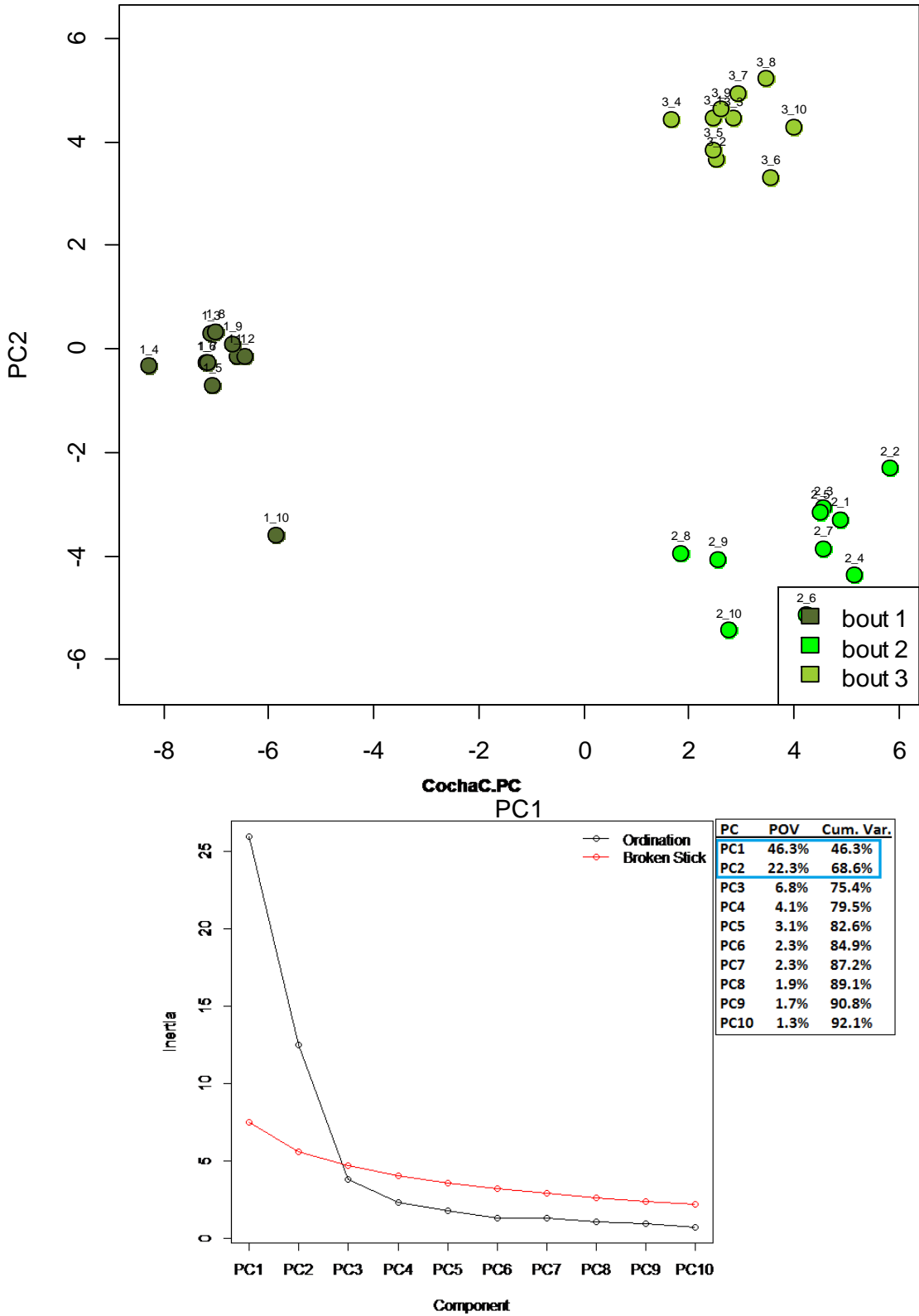


Fig. 11: Top: PCA of landmark placement variation between three bouts of 10 reps each with *Coccoetra hagenii*, specimen C. Bottom: broken stick model depicting the first two PCs (or x and y axes) as interpretable

# Landmark Placement PCA for CochaD

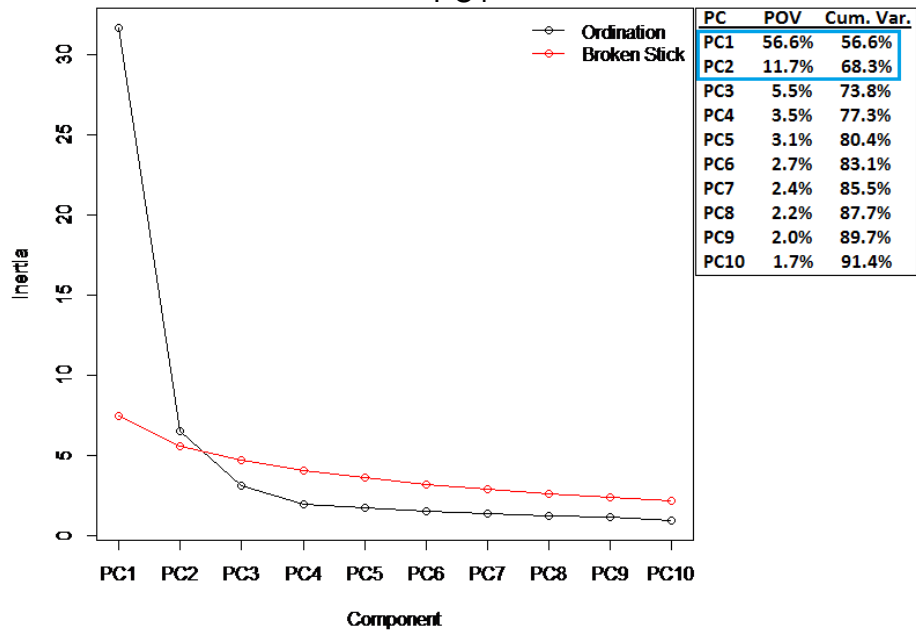
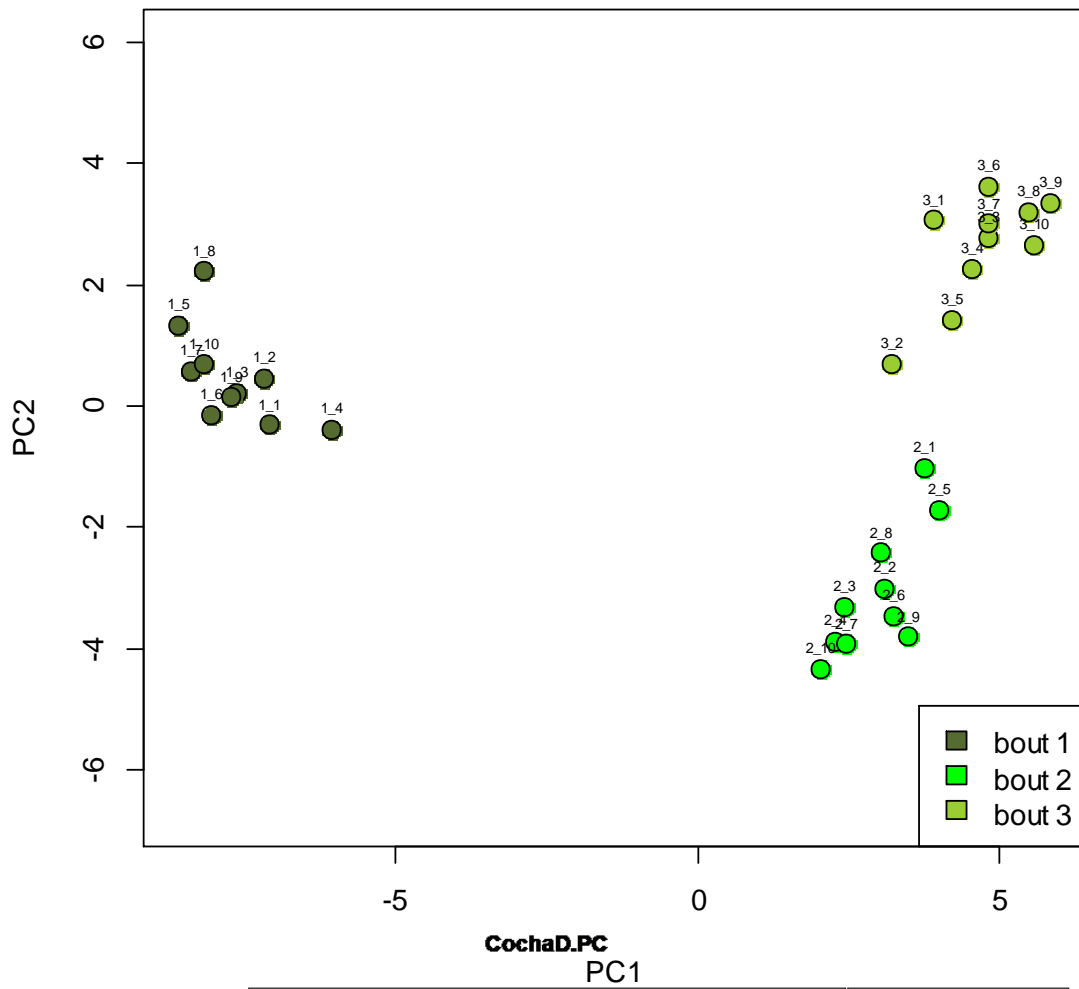


Fig. 12: Top: PCA of landmark placement variation between three bouts of 10 reps each with *Coccoetra hagenii*, specimen D. Bottom: broken stick model depicting the first two PCs (or x and y axes) as interpretable



# Landmark Placement PCA for Dorbra

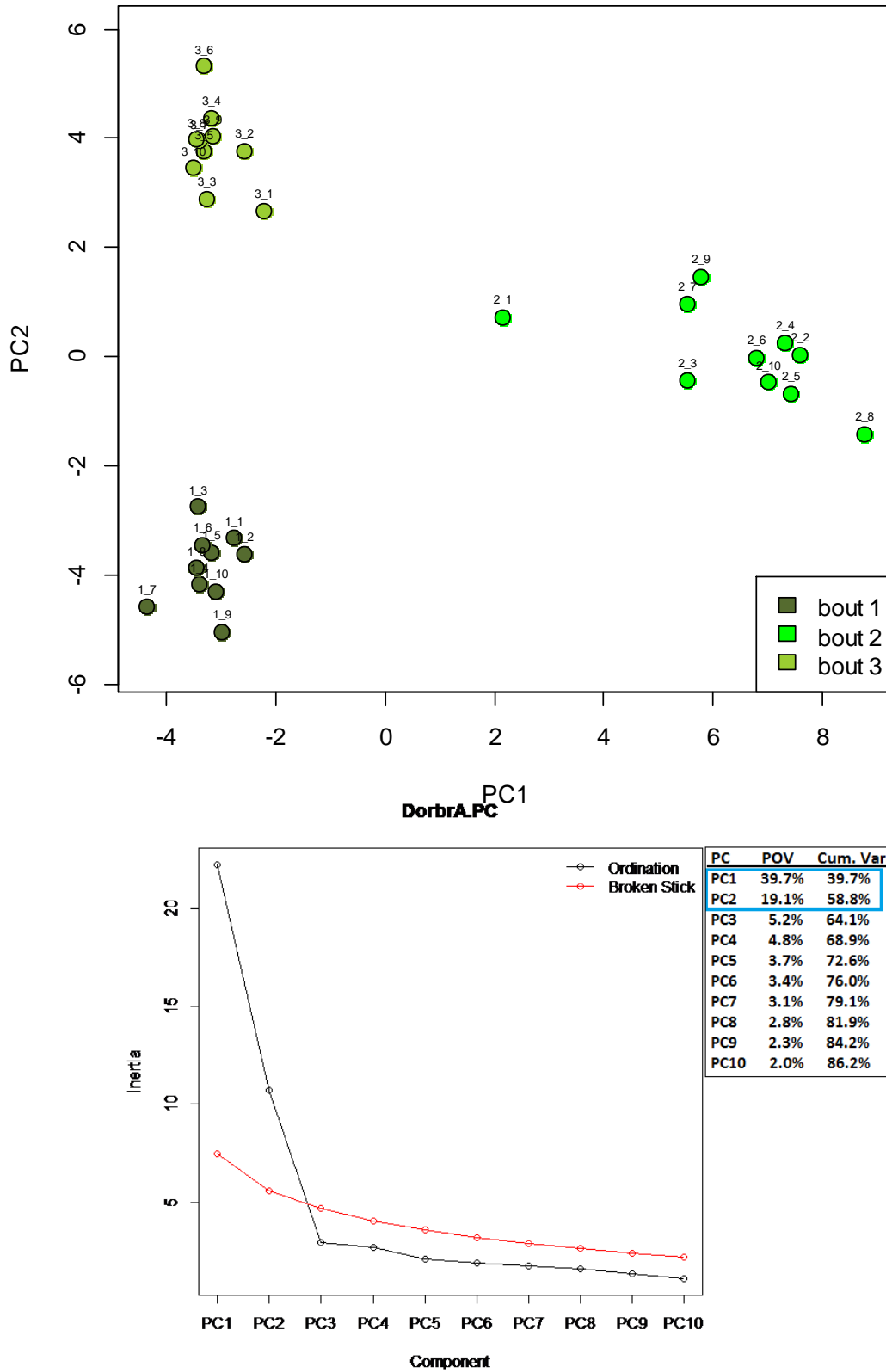


Fig. 13: Top: PCA of landmark placement variation between three bouts of 10 reps each with *Dorometra briseis*, specimen A. Bottom: broken stick model depicting the first two PCs (or x and y axes) as interpretable variation

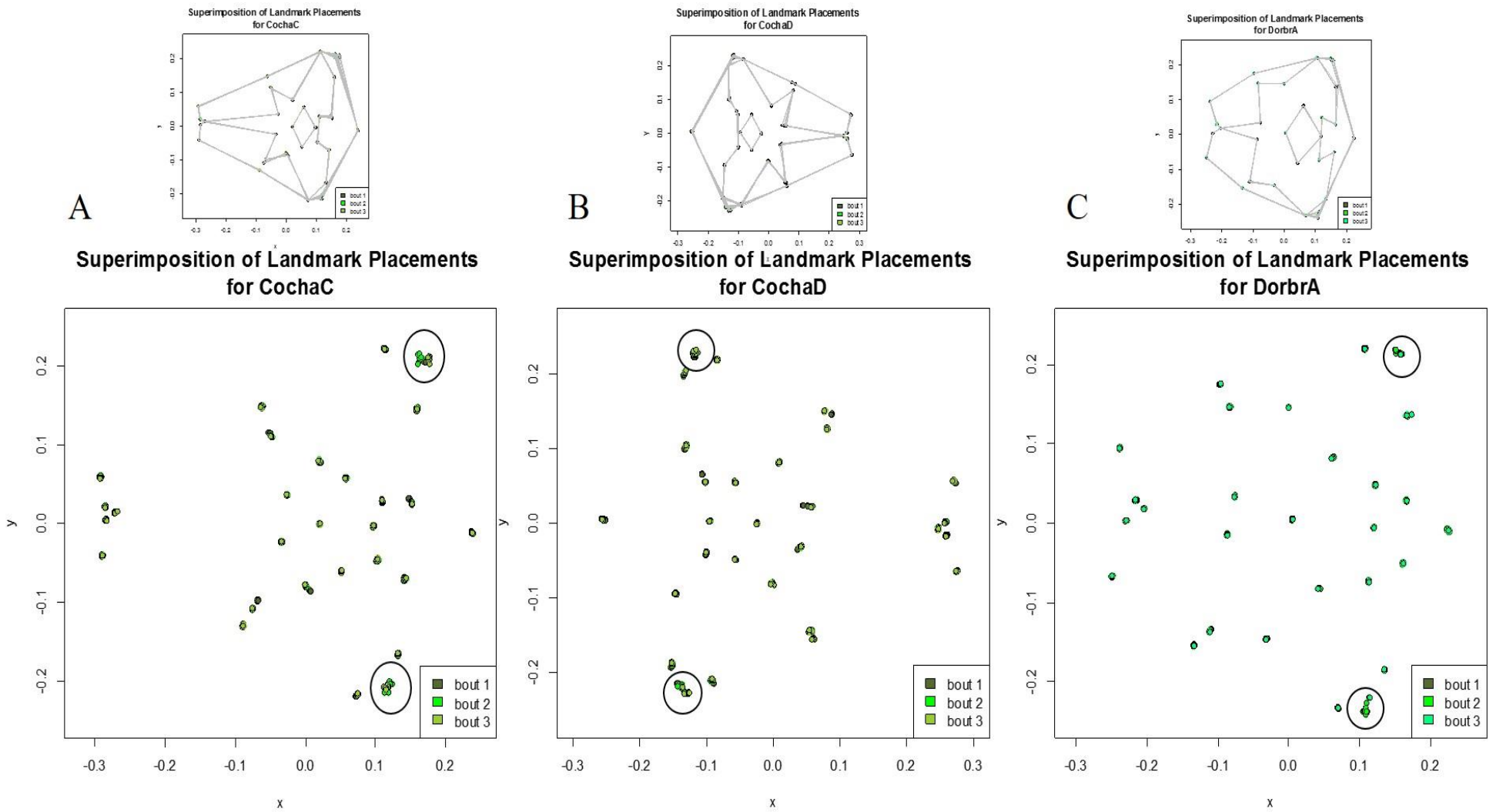


Fig. 14: superimposed landmarked configurations of all three bouts, with problematic landmarks (5 & 12) circled. A – *Coccometra hagenii*, specimen C, B – *Coccometra hagenii*, specimen D, C – *Dorometra briseis*, specimen A

## A. Discussion

Four of the five ossicles imaged for testing camera placement variability did not show any significant variances among their four replicates, therefore the camera alignment protocol (discussed above) was accepted and image number was reduced to one for subsequent ossicle imaging.

The result of the nested ANOVA for landmark placements was extremely low for all images, at less than 10% for all three species. However, both the number of repetitions (30 total) and the subjective nature of digitizing needs to be taken into account when interpreting repeatability. The majority of measurement error studies use around 2-3 repetitions for each individual or image (Liu et al. 2016, Sherratt 2014). In this study, in order to gain more digitizing practice as well as test repeatability, 10 digitizing repetitions were performed for each bout which greatly increased the probability for human error, as well as decreased the success of repeatability, so higher percentages were not really expected. Landmark digitizing in general is a very subjective practice. Each twitch of the hand creates a different coordinate from repetition to repetition, so additional precautions, such as second and third reviews of the digitized images, needed to be put in place (see *Landmarking*).

The specific landmarks causing the variations within and between bouts cannot be directly calculated, since the entire configuration is used as the datum for each ossicle, but they can be inferred through visualization of their superimposed configurations (Fig. 14A-C). Across the three digitized specimens, landmarks #5 and #12 seem to be causing the greatest amount of inconsistency (circled). These landmarks were removed (along with landmark 1 in Scenario 1) for subsequent testing (see *Landmarking*).

## V. Using geometric morphometrics to discriminate crinoids

### A. Results

#### i. *Intra-individual variability*

There was no significant variation within any of the 69 individuals with more than one ossicle imaged, for either of the two scenarios (25 landmarks and 219 ossicles in scenario 1 versus 26 landmarks and 215 ossicles in scenario 2). This allowed usage of

mean configurations as the individual datum in subsequent intra-specific testing. See the Appendix (Figs. A1-A20) for 20 examples of the non-significant results.

ii.. *Intra-specific variability*

Of the 40 species analyzed in this study, 21 species exhibited some significant variance among their individuals. Of the 21 species resulting in significant p-values with Procrustes ANOVA, only the following seven were discernable with the pairwise tests. *Antedon bifida bifida* was significantly variant ( $p = 0.001$ ) between individuals A & E in both scenarios, and C & E in scenario 1; individual C was not used in scenario 2 as the ossicles were missing landmark #1 (Fig. 15A&B). Although no effect of size on overall shape was recorded for this species, individual E did measure the largest radial height, as well as the largest diameter at the first syzygy (see Appendix Table A1), so size may be a factor in this variation.

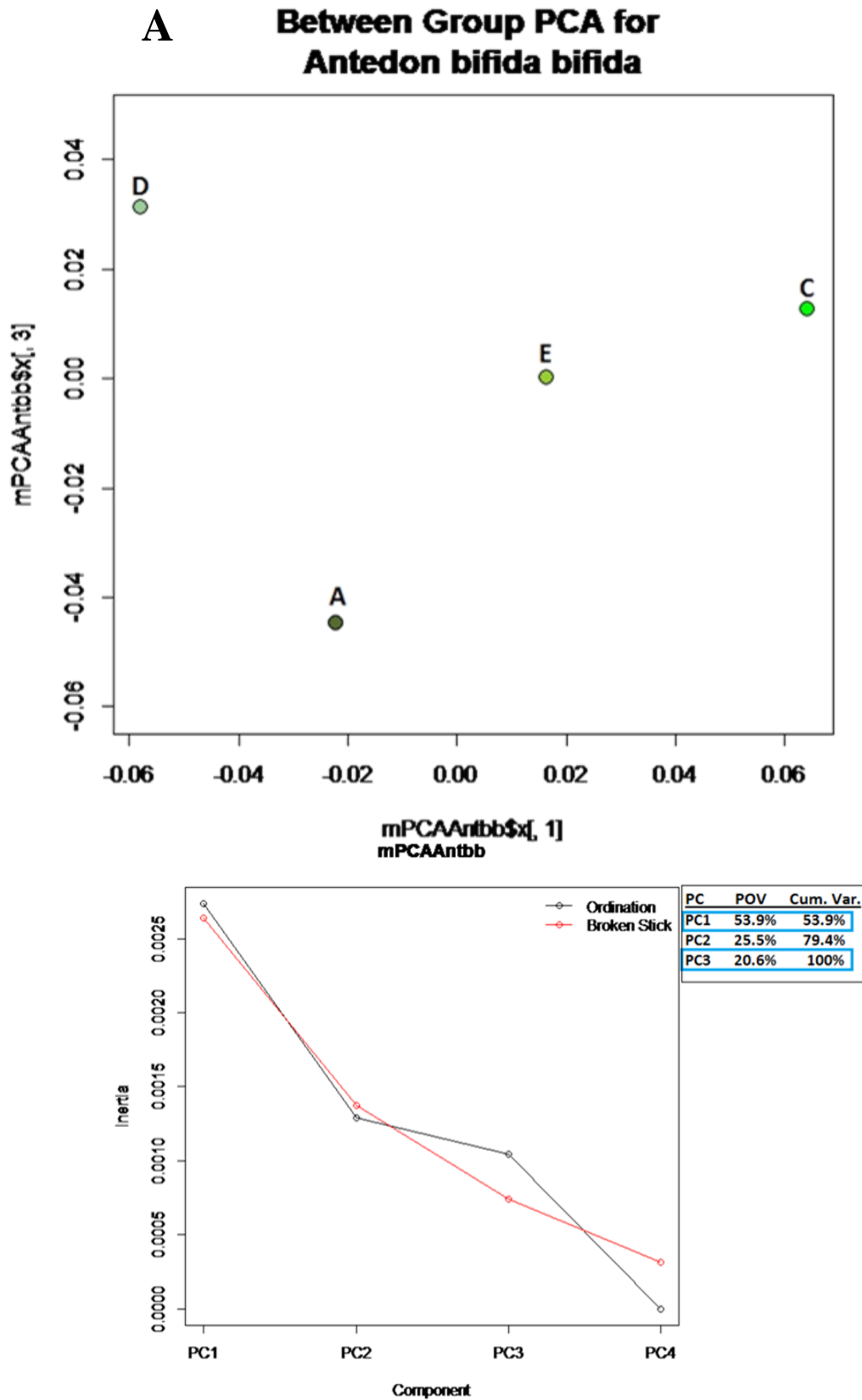


Fig. 15A: Scenario 1 results of intra-specific variation for *Antedon bifida bifida*. Scenario 1 yielded significant variances between individuals A & E and C & E.

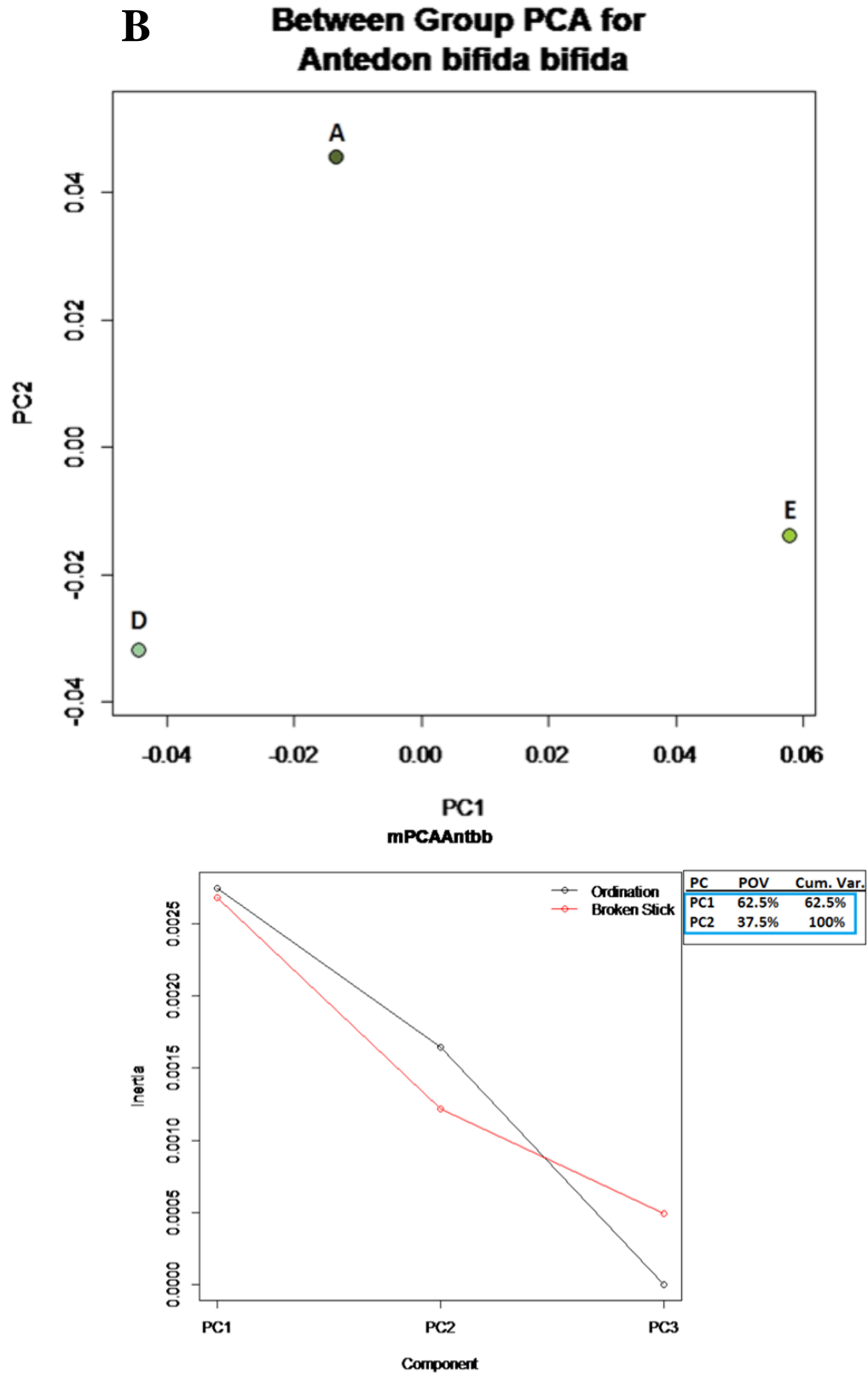


Fig. 15B: Scenario 2 results of intra-specific variation for *Antedon bifida bifida*. Scenario 2 yielded significant variance only between A & E.

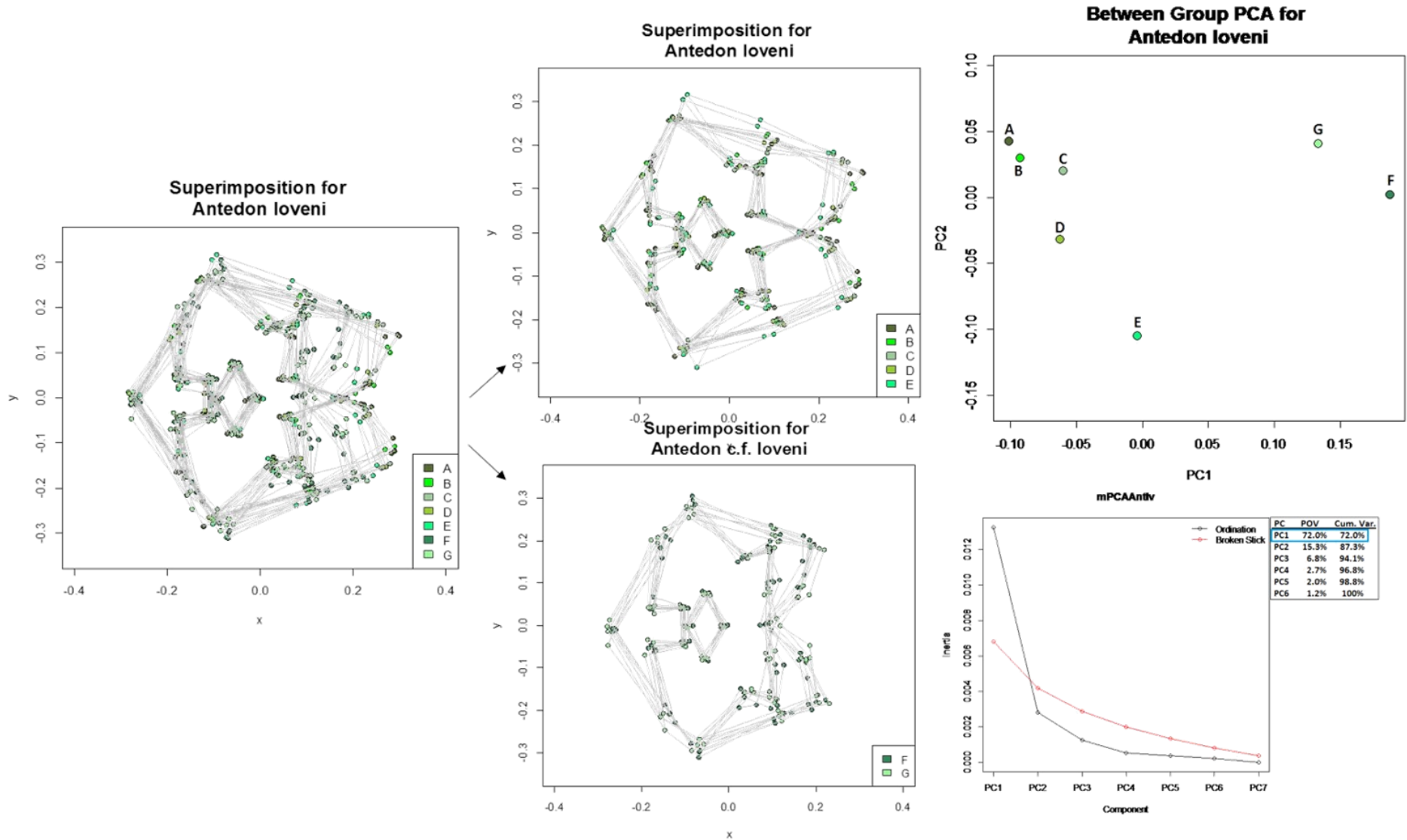


Fig. 16: Intra-species variation of all *Antedon loveni* specimens depicting notable differences in the superimposed configurations of the known *A. loveni* specimens A-E and *A. c.f. loveni* specimens F-G, as well as a clear separation in the BGPCA (note: this composite depicts scenario 2 results only, although there were no differences between the two; see Appendix Figure A21 for scenario 1 results).

Significant variance among *Antedon loveni* was tested first by combining the known *Antedon loveni* individuals with the *Antedon c.f. loveni* individuals. Three of the five *Antedon loveni* individuals (A, C and D) were significantly variant with *Antedon c.f. loveni* individual F ( $p = 0.001$ ) in both scenarios, supporting the separation of the species a priori (Fig. 16, Appendix Fig. A21). Among the individuals confidently deemed *Antedon loveni*, significant variation ( $p = 0.001$ ) was found between individuals A & C and B & C in both scenarios (25 landmarks and 219 ossicles in scenario 1 versus 26 landmarks and 215 ossicles in scenario 2). Individual C measured the largest diameter at the first syzygy and there was a significant effect of size on overall radial shape ( $p = 0.015$ ) within this species. Thus, size was the cause of variation here. As no significant variation appeared between the two individuals of *Antedon c.f. loveni*, they were both kept as a separate species for subsequent analyses.

The three groups of *Antedon parviflora* (*Antedon parviflora* B&E, *Antedon parviflora* C&D, and *Antedon c.f. parviflora*) were first combined to visualize any significant variations after Procrustes superimposition. Since four of the five individuals contained only one ossicle, proper Procrustes ANOVA could not be performed between the groups. However, evident differences in the superimposed configurations, as well as visible clustering in the BGPCA, provided enough evidence to keep the three groups separate for later analyses (Fig. 17, Appendix Fig. A22).

*Anthometrina adriani* revealed significant variance ( $p = 0.003$ ) between individuals A & C and C & E in both scenarios (Fig. 18, Appendix Fig. A23). No significant effect of size on shape appeared for this species ( $p = 0.331/0.369$ ), however individual C had a larger radial width than individual A, and a smaller radial height than individual E, which could be attributing to the overall variance.



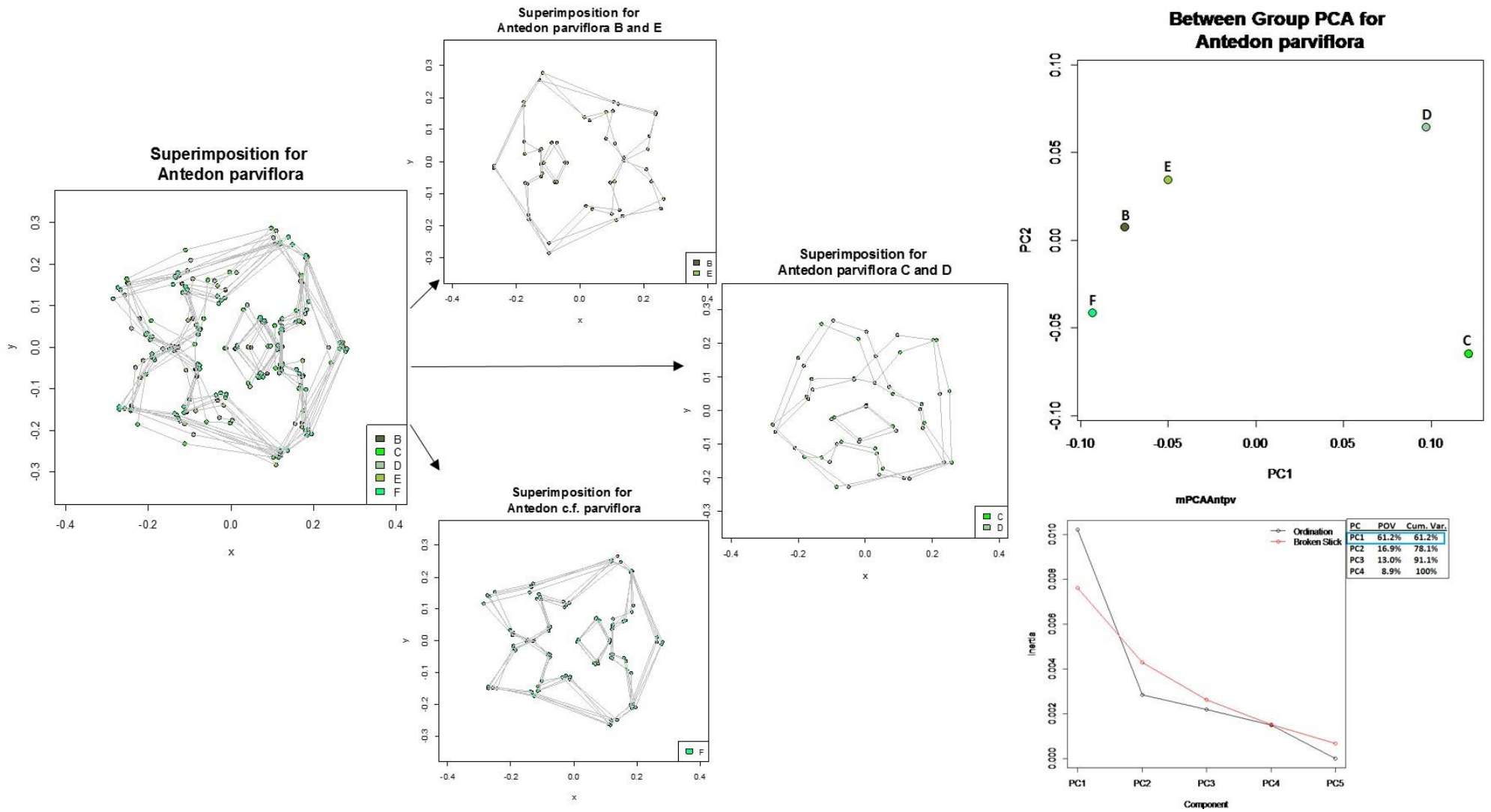


Fig. 17: Scenario 2 results of Intra-species variation of all *Antedon parviflora* specimens depicting notable differences in the superimposed configurations and PCA of three *A. parviflora* groups: specimens B&E, C&D, and F (see Appendix Fig. A22 for scenario 1 results).

### Between Group PCA for *Anthometrina adriani*

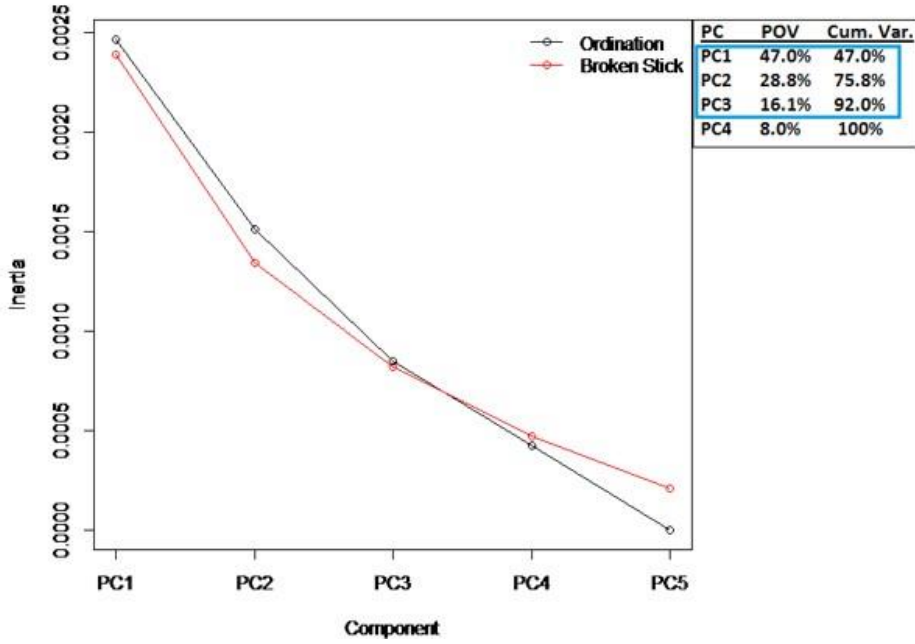
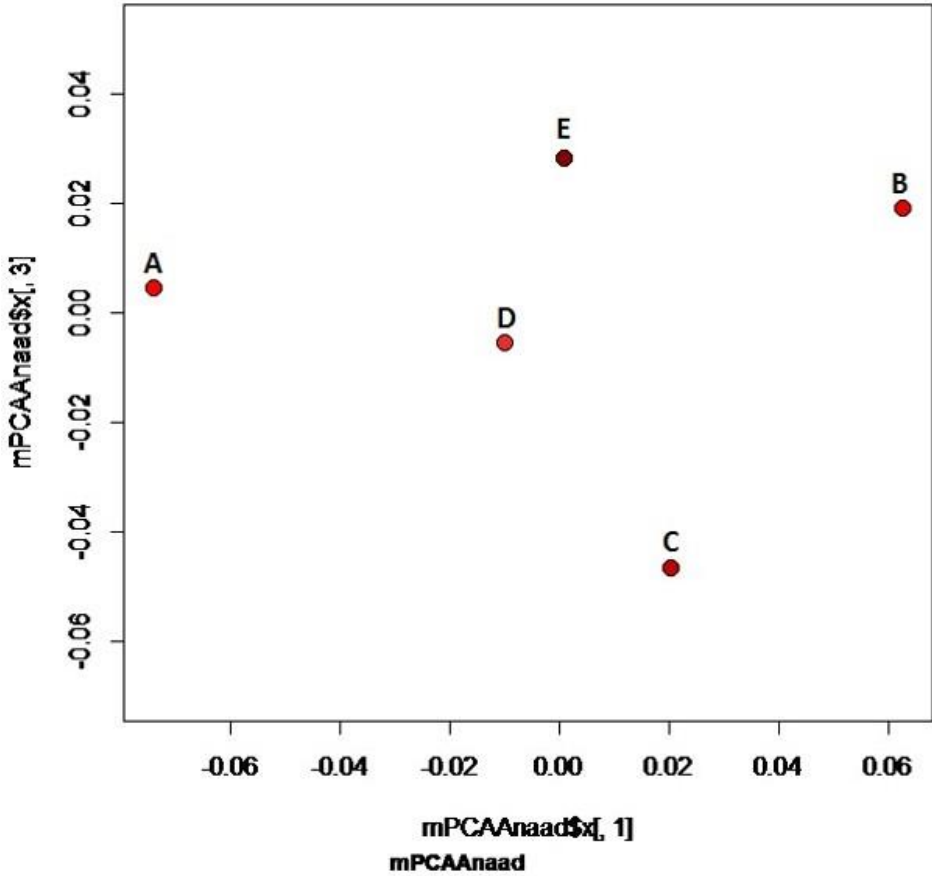


Fig. 18: Scenario 2 PCA and broken stick model depicting the intra-species variation of *Anthometrina adriani*. ANOVA results yielded significant variation between individuals A&E and C&E in both scenarios (see Appendix Fig. A23 for scenario 1 results).

### Between Group PCA for *Coccometra hagenii*

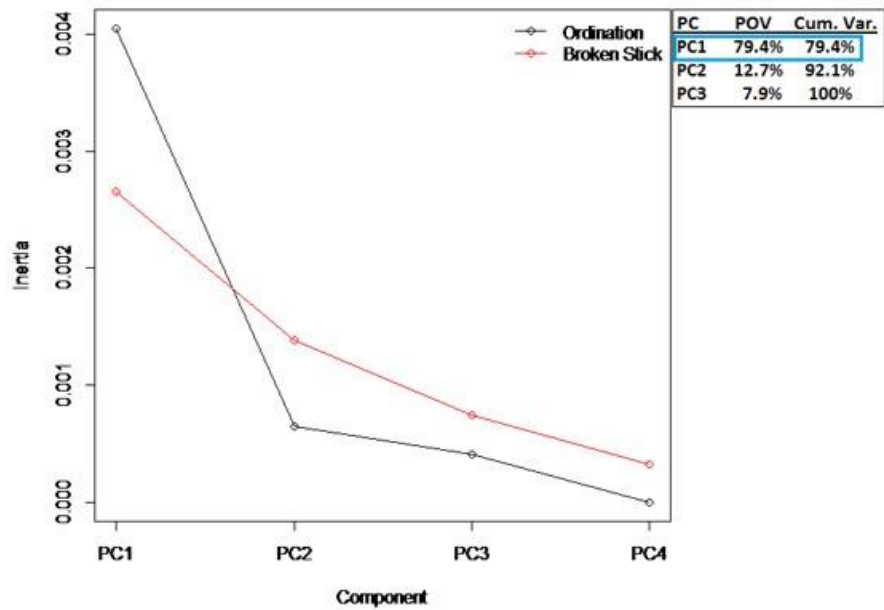
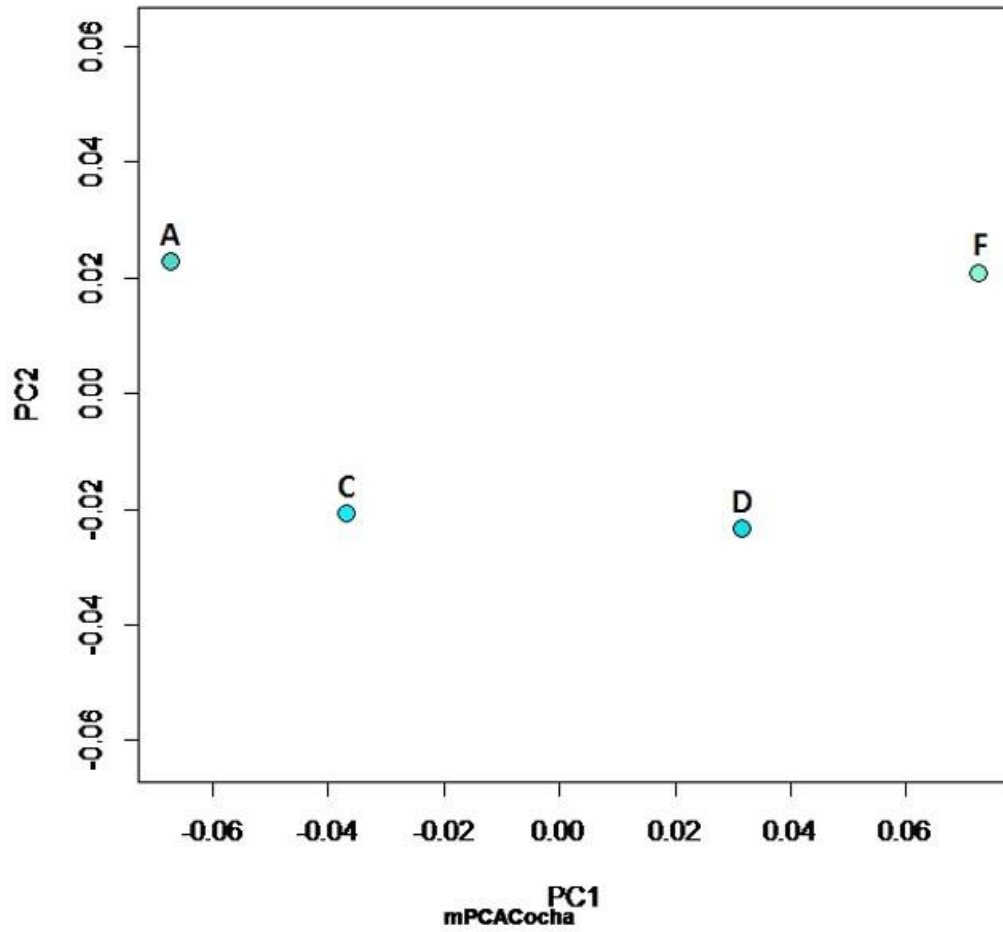


Fig. 19: Scenario 2 PCA and broken stick model depicting the intra-species variation of *Coccometra hagenii*. ANOVA results yielded significant variation between individuals C&D in both scenarios (see Appendix Fig. A24 for scenario 1 results).

Significant differences can be seen between *Coccometra hagenii* individuals C and D in both scenarios ( $p = 0.007/0.026$ ) (Fig. 19, Appendix Fig. A24). Of the four *C. hagenii* specimens, individual C measured the smallest ossicle height and width, while individual D measured the largest. Although there is no significant allometric effect in either scenario ( $p = 0.293/0.503$ ), size may be the cause of some variation between these two individuals.

*Dorometra briseis* and *Dorometra c.f. briseis* individuals were first combined to test for significant variations. Although the pairwise test was not significant, the Procrustes ANOVA resulted in significant variance between the two groups ( $p = 0.004$ ) in both scenarios. Furthermore, there was no significant variance within either group. These results, with support from the PCA (Fig. 20, Appendix Fig. A25), kept the two groups as separate species for further analyses.

Procrustes ANOVA and a pairwise test within *Florometra asperrima* resulted in significant variations ( $p = 0.001$ ) between individuals C&D in both scenarios, C&E in scenario 1, and B&C in scenario 2 (Fig. 21A&B). In all cases, the variation was between individual C, which measured the largest radial height, radial width, and diameter at the first syzygy. Individuals B & E had almost identical measurements of syzygy diameter, with individual B having a slightly smaller ossicle size (see Appendix Table A1).

Variations within *Hybometra senta* were found between individuals C&D in both scenarios ( $p = 0.0055/0.0065$ ) (Fig. 22, Appendix Fig. A26). Of the four individuals representing this species, these two were intermediate in size. Their ossicle widths were the same, but ossicle height and diameter at first syzygy were larger in individual C. There was no significant effect of size on overall shape ( $p = 0.217/0.232$ ).

Since there was no variation between ossicles in the same individual, variation between individuals was accepted and the mean configurations of species were used as representatives for subsequent analyses.

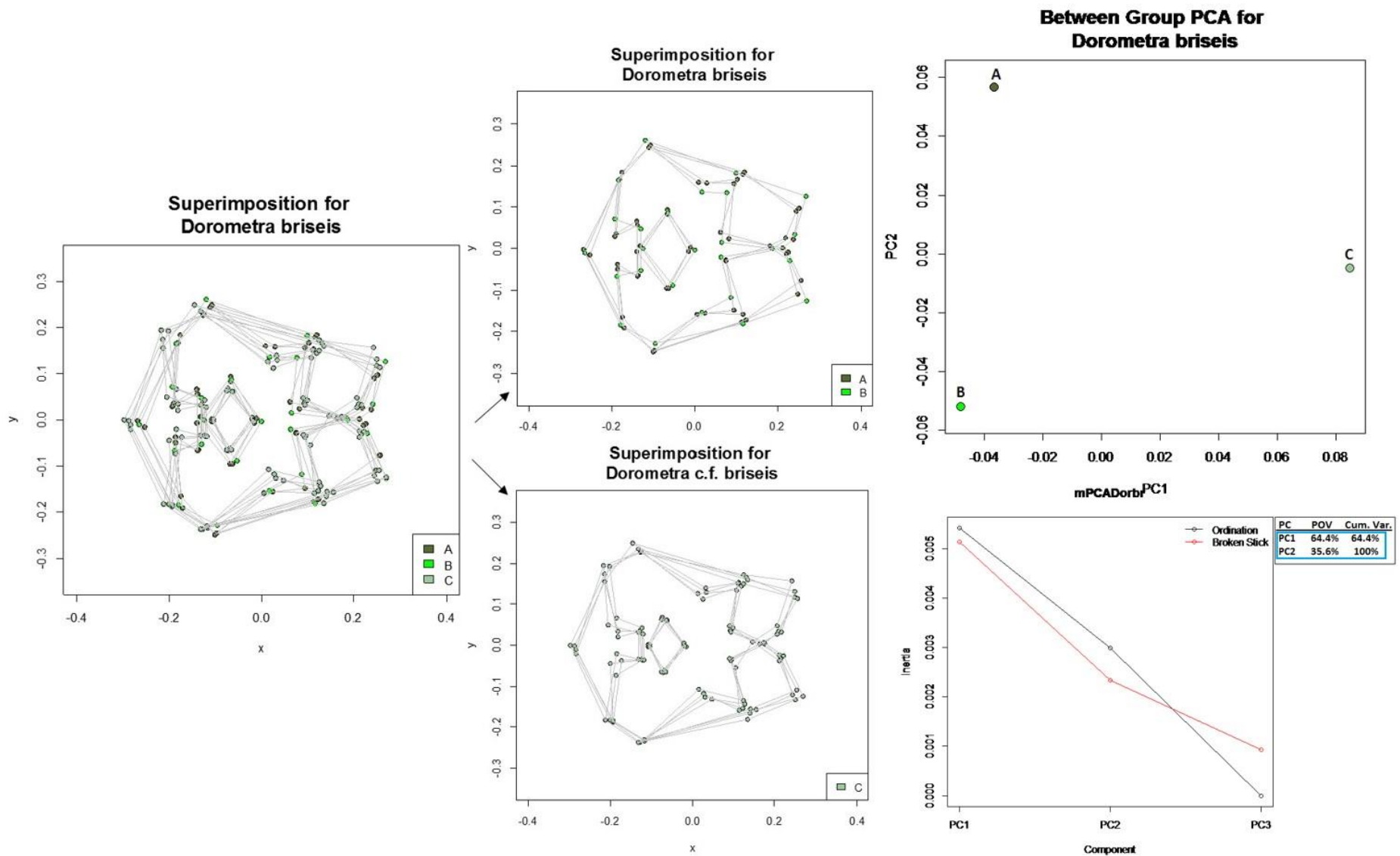


Fig. 20: Scenario 2 Intra-specific variation for all *Dorometra briseis* specimens, supporting the ANOVA results of significant variance between the two groups through clear differences in the superimpositions and PCA (see Appendix Fig. A25 for scenario 1 results).

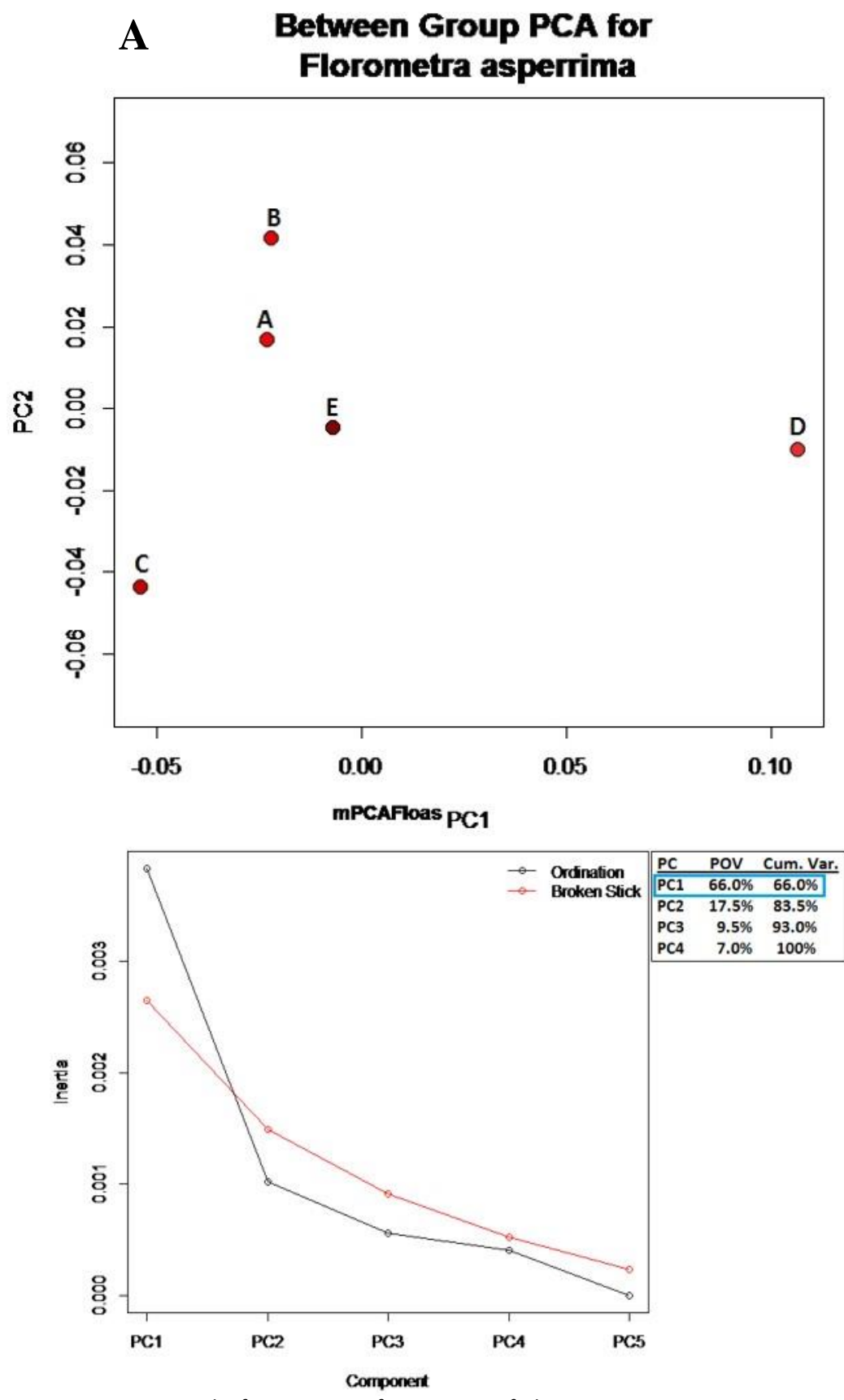


Fig. 21A: Scenario 1 results for intra-specific variation of *Florometra asperrima* supporting the significant variance between individuals C&D and C&E.

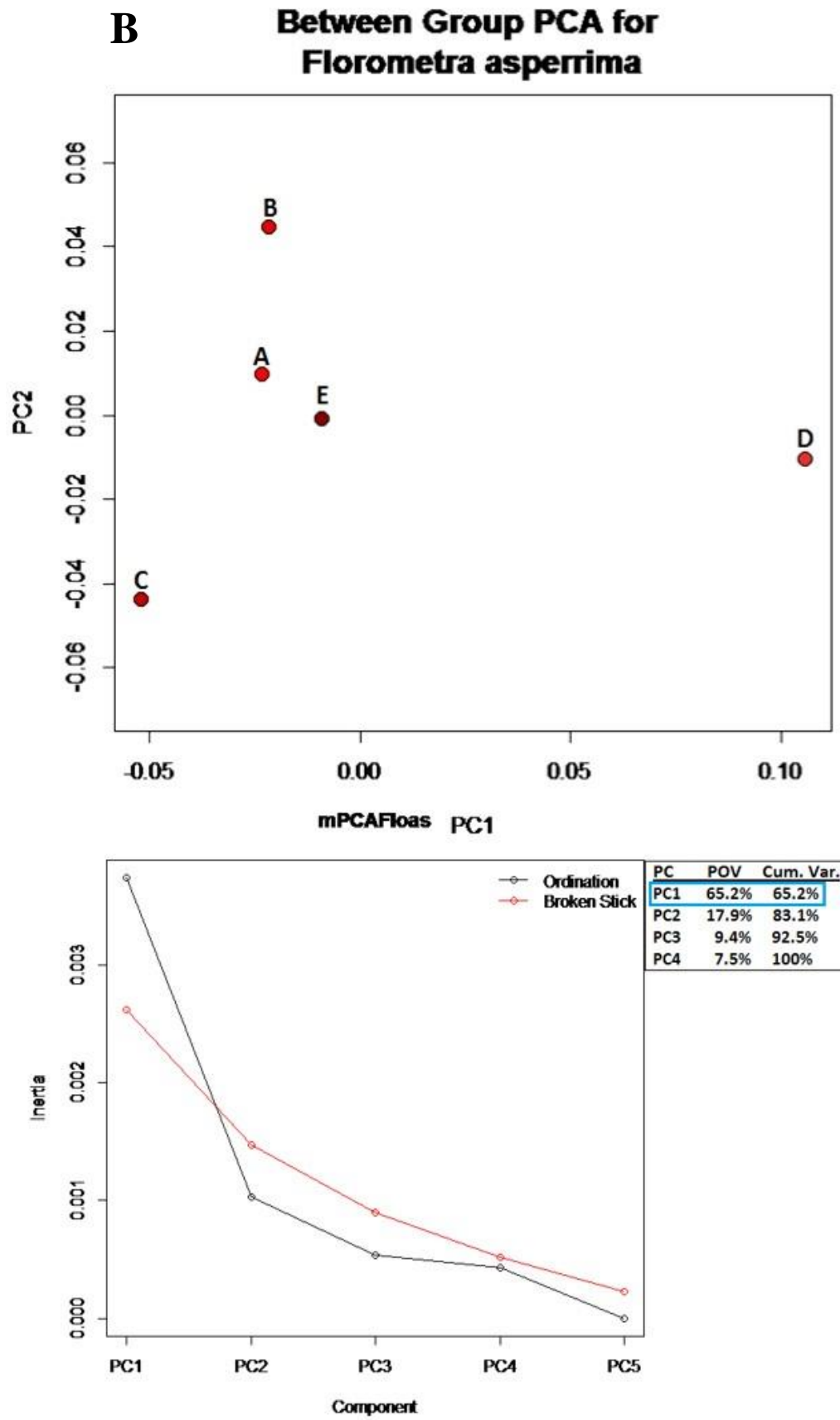


Fig. 21B: Scenario 2 results for intra-specific variation of *Florometra asperima* with significant variance between individuals C&D and B&C.

### Between Group PCA for *Hybometra senta*

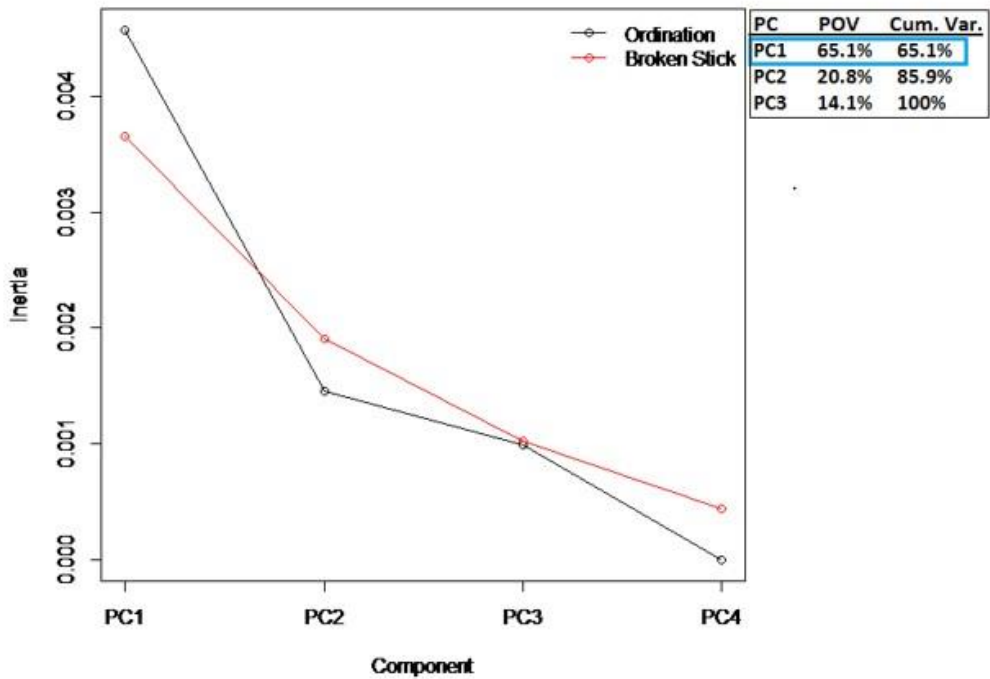
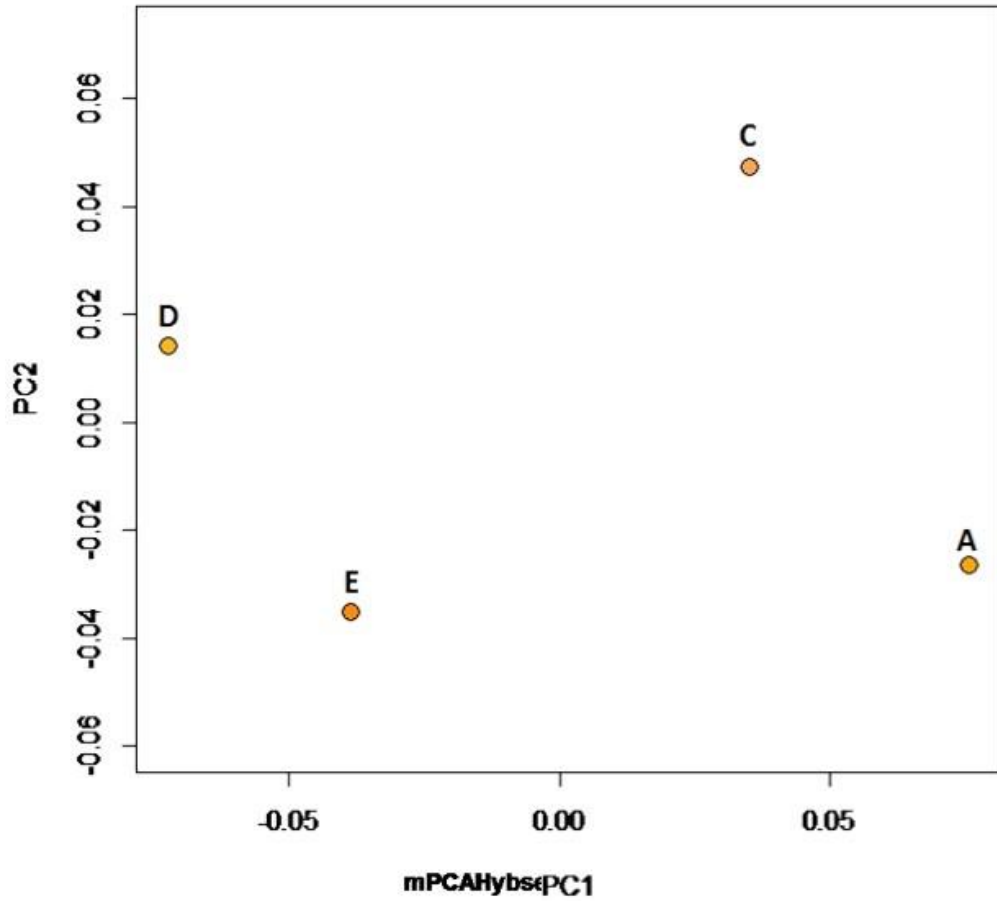


Fig. 22: Scenario 2 PCA and broken stick model of the intra-specific variation in *Hybometra senta*, supporting the ANOVA significant variance between individuals C&D (see Appendix Fig. A26 for scenario 1 results).



### iii. *Intra-generic variability*

Only four of the 26 genera in this project had more than one species present to test for intra-generic shape variations: *Antedon*, *Dorometra*, *Florometra* and *Isometra*.

#### a. *Antedon* spp.

Eleven species within the genus *Antedon* were available, spanning eight of the 11 localities and two of the five depth ranges (Table 5). Radial ratios were  $<1.0$  across all species, and so was not included in the Procrustes ANOVAs. The first principal component encompassed just under half of the total shape variation and explains all of the non-random variation in both scenarios (49.3% and 48.6%, respectively). While there was an allometric effect in scenario 1 ( $p = 0.031$ ), it was not present in scenario 2 ( $p = 0.085$ ), so size was ruled out as the factor causing variation. Significant factors were consistent between both scenarios (Fig. 23A, Appendix Fig. A27A). Of the four factors tested for effects on shape variation, general region ( $p = 0.011/0.014$ ) and phylogenetic assignment ( $p = 0.035/0.041$ ) proved significant, while depth range ( $p = 0.251/0.259$ ) and specific locality ( $p = 0.23/0.218$ ) provided no effect. The clear distinction between Atlantic and Pacific *Antedon* species can be seen in the PCA (Fig. 23B, Appendix Fig. A27B) and since there are only two factor levels in this case, a pairwise test was redundant. The pairwise test with molecular-based assignment resulted in a significant pairing between clade N and clade P species only. The variance is supported by the BGPCA, which returned a clear separation between the two clades, with overlap from clade O species (Fig. 23C, Appendix Fig. A27C). The phylogenetic effect supports the regional effect as clade N consists solely of Atlantic species, while clade P consists solely of species from the Pacific. However, clade O is also solely a Pacific clade, so several factors are at work here. The pairwise test between all *Antedon* species, with size taken into account, resulted in significantly variant pairings between clade N and P species, as well as between clades N and O. There were no significant pairings between clades O and P, supporting the regional effect. Also, interestingly, the only within-clade pairing was between clade O species, *Antedon loveni* and *Antedon c.f. loveni*. The true identity of *Antedon c.f. loveni* was investigated further in subsequent analyses.

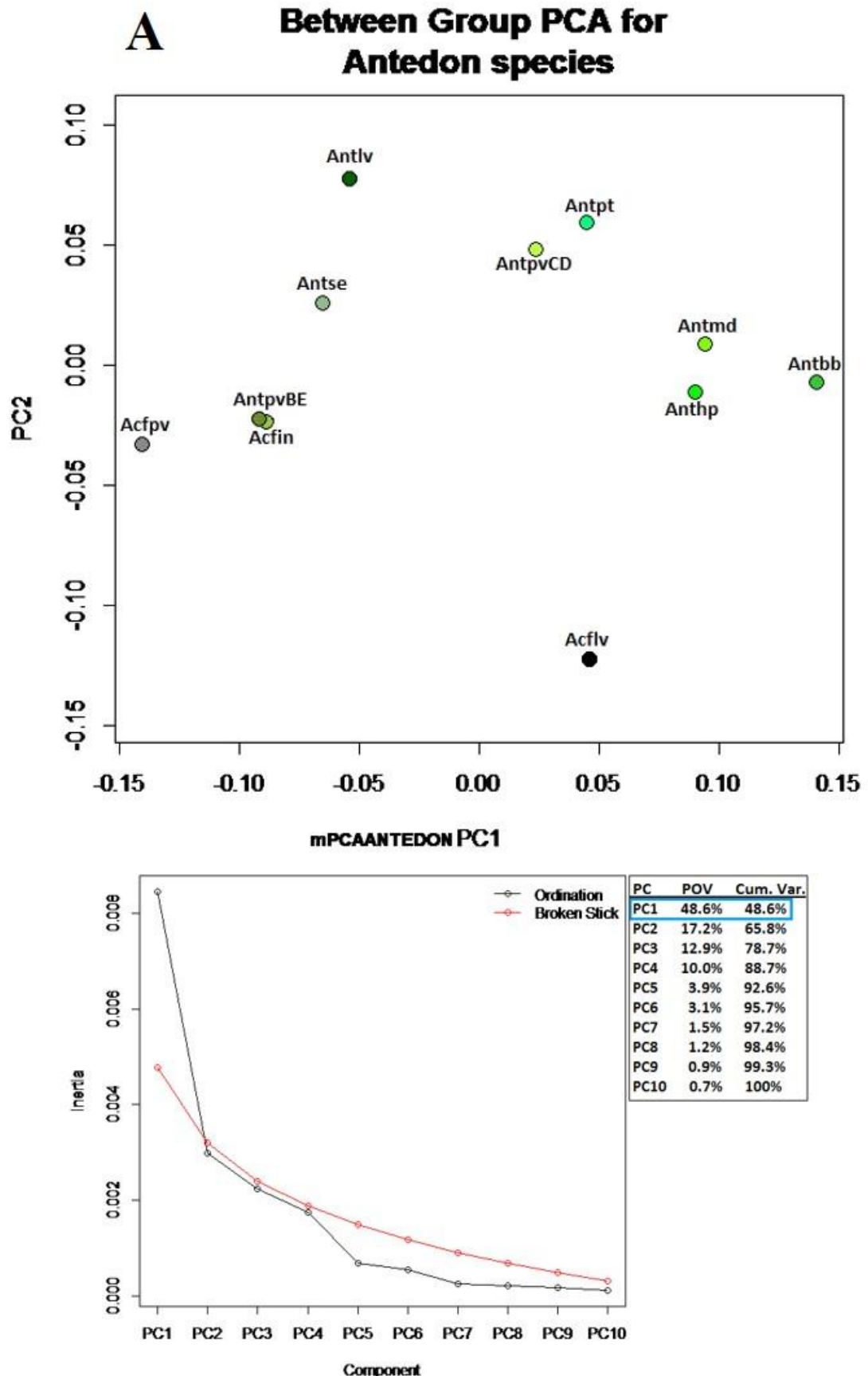


Fig. 23A: Scenario 2 intra-genus variation of *Antedon* spp. (see Appendix Fig. A2/A for scenario 1 results). A: between-group PCA (top) and broken stick model (bottom) (Acfin = *Antedon* c.f. *incommoda*, Acflv = *Antedon* c.f. *loveni*, Acfpv = *Antedon* c.f. *parviflora*, Antbb = *Antedon* *bifida bifida*, Anthp = *Antedon* *hufferi*, Antlv = *Antedon* *loveni*, Antmd = *Antedon* *mediterranea*, Antpt = *Antedon* *petasus*, AntpvBE = *Antedon* *parviflora* B&E, AntpvCD = *Antedon* *parviflora* C&D, Antse = *Antedon* *serrata*).

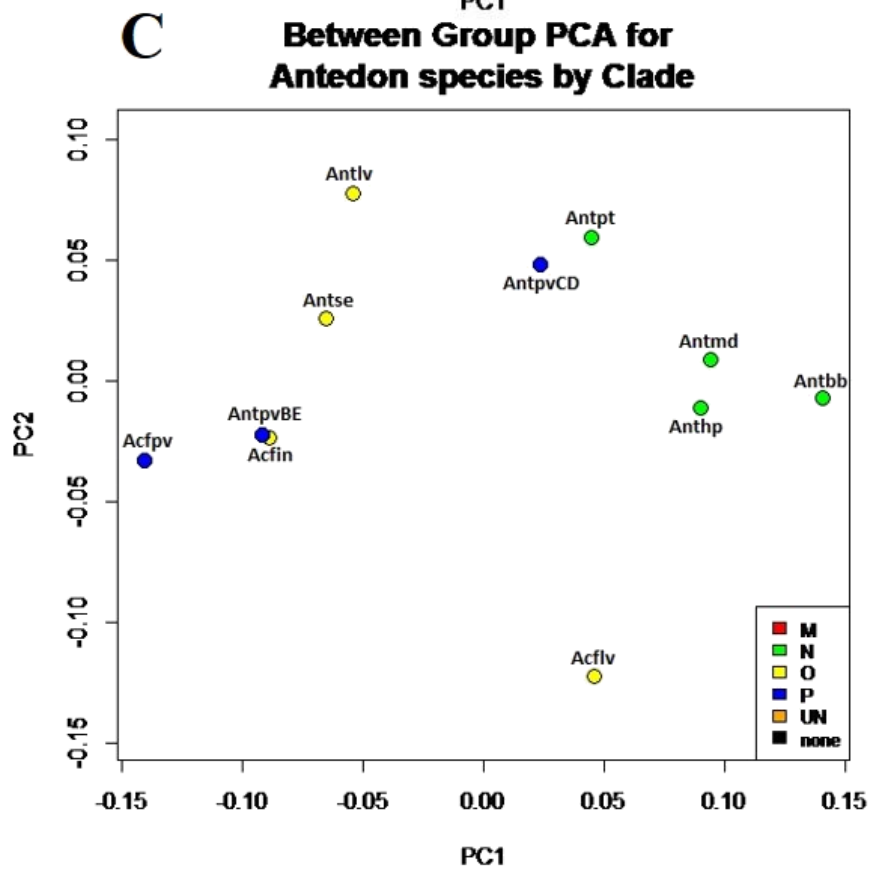
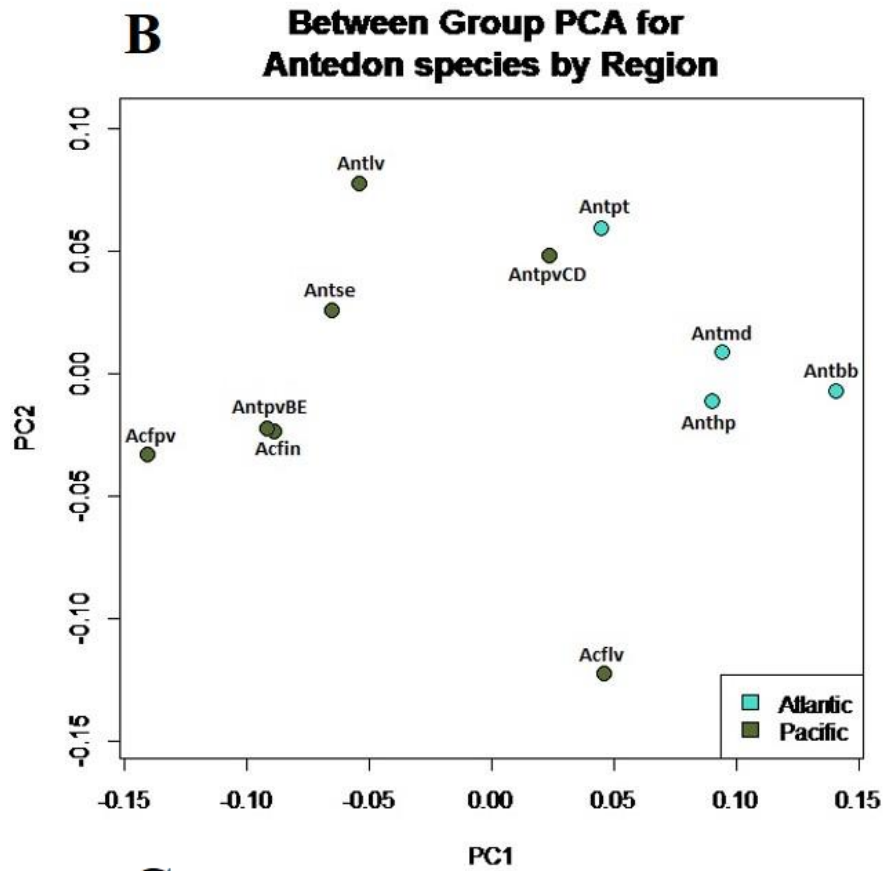


Fig. 23B-C: Scenario 2 intra-genus variation of *Antedon* spp. (see Appendix Fig. A27B-C for scenario 1 results). B: BGPCA colored by general region. C: BGPCA colored by clade assignment (see Fig. 23A for species abbreviation reference).

b. *Dorometra* spp.

Three species within genus *Dorometra* were available: *Dorometra briseis*, *Dorometra* c.f. *briseis*, and *Dorometra parvicirra*. All three species occur within the same depth range (51-100m), specific locality (Japan Sea), and general region (Pacific), so these factors were not included in ANOVA testing. Also, because *D. parvicirra* was not used in any tree, and thus placed in a different factor level by default, the results of any effect by clade assignment was not interpreted. Visual observations of the BGPCA suggested significant variations between the two *Dorometra briseis* groups and *Dorometra parvicirra* (Appendix Fig. A28A&B). Despite the visual separations and differing factor levels, neither scenario resulted in significant effects on shape by radial ratio ( $p = 0.1785/0.265$ ). Pairwise testing between the three species only resulted in a significant size difference between at least one specimen of *Dorometra* c.f. *briseis* and *Dorometra parvicirra*. Although this reflects an individual-specific size effect, it was not enough to cause an allometric effect on overall species shape in either scenario ( $p = 0.736/0.736$ ).

c. *Florometra* spp.

Both *Florometra* representatives in this study, *F. asperrima* and *F. serratissima*, share all tested factors except for collected depth. Procrustes ANOVAs were not performed on mean shape, as only two mean configurations could be compared, so individual configurations were tested for significant pairings between the two species (Appendix Fig. A29A&B). There was no significant effect on shape by depth ( $p = 0.758/0.732$ ), or any significant variation between the two species ( $p = 0.81/0.775$ ). Since they are almost completely identical morphologically and can be found at the same depths, they may represent a single species (Eléaume 2006). Their similarities were tested further in later analyses (see *Hierarchical Clustering* and *Inter-landmark measurements*).

d. *Isometra* spp.

Since one of the two *Isometra* species in this study, *Isometra vivipara*, was only represented by one specimen, neither Procrustes ANOVA nor pairwise testing was performed. Observations of the specimen PCA and broken stick model show that,

although some variation existed between the two species along PC1, this variance did not exceed the broken stick and was thus uninterpretable, random variation. The non-random variation lay along PC2, where considerable overlap existed between the species (Appendix Fig. A30A&B). As *I. vivipara* and *I. graminea* are distinguished almost entirely by size-related differences in the first two pinnules and share all biogeography factors, the possibility arose that they could be the same species. However, as they are still distinct in molecular analyses, it is more likely they are closely related sister species instead (Lenaïg Hemery, personal communication). Further analysis was performed later through independent-sample t-tests and hierarchical clustering.

#### iv. *Intra-subfamily variability*

Significant shape variations were tested for within each of the seven morphologically-based subfamilies, toward reconciling morphological features with the molecular phylogenies.

##### a. *Antedoninae*

The largest subfamily in this study, Antedoninae, was represented by 17 species across five genera (*Antedon*, *Andrometra*, *Ctenantedon*, *Dorometra*, and *Iridometra*). All biogeographic and measured factors were tested along with clade assignment, as the representative species spanned at least two factor levels for each. The first principal component described the interpretable variation within Antedoninae, encompassing over half of the total variance (55.2%) in both scenarios (Fig. 24A, Appendix Fig. A31A). Neither depth ( $p = 0.098/0.104$ ) nor specific locality ( $p = 0.27/0.252$ ) proved significant factors through the Procrustes ANOVAs with visual support by the BGPCA. There were significant effects on shape by general region ( $p = 0.008/0.008$ ), radial ratio ( $p = 0.009/0.0045$ ), and molecular clade assignment ( $p = 0.01/0.01$ ) (Fig. 24A-D, Appendix Fig. A31A-D). While there was some overlap between Atlantic and Pacific species in the BGPCA (Fig. 24B), a clear distinction remained between the two factor levels, supporting the ANOVA results. When both factor levels of radial ratio are present (as is the case here) a visual distinction will always exist between them in the BGPCA projections since it is directly associated with radial shape. Whether the factor is

significant in affecting the between-group variation is what is important, and this is not always the case (i.e. within the genus *Antedon*).

The representatives of Antedoninae in this study occur in three of the phylogenetic clades. Three other species were not included in the trees: *Ctenantedon kinziei*, *Dorometra parvicirra*, and *Iridometra adrestine*. The BGPCA (Fig. 24C) shows an almost complete separation of clades N (depicted in green) and P (blue) along the x-axis (the only interpretable PC) with overlap by clade O (yellow) species. Pairwise testing confirms this observation, with significant pairings between clades N and P and clades N and O. Significant pairings between the species not included in molecular phylogenies (black) and both clade N and clade O species exist as well. These results are misleading, however, and not used, as the three species not used in the phylogenies are a mixture of both Atlantic and Pacific species and would most likely separate into at least two of the three clades if included in the phylogenies.

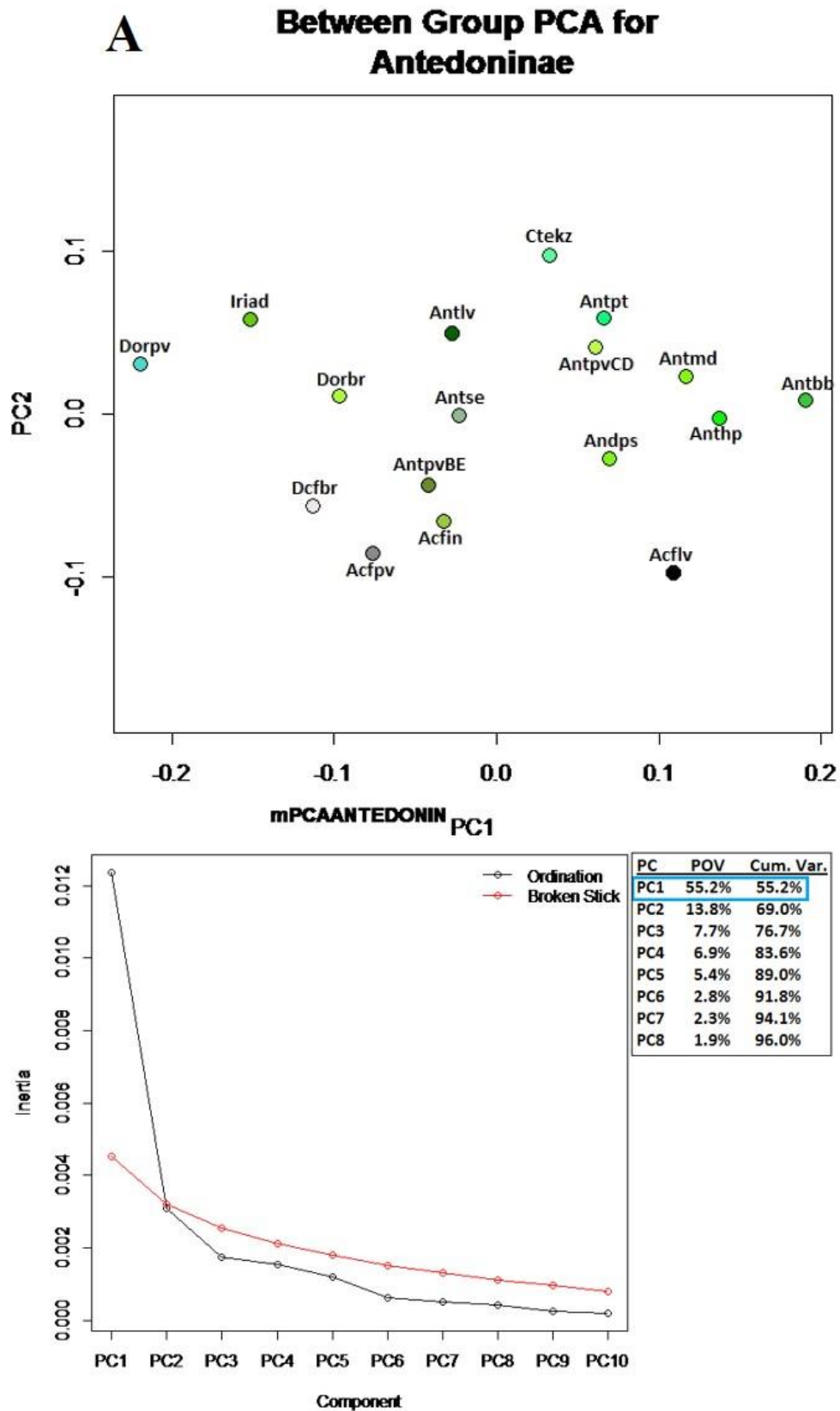
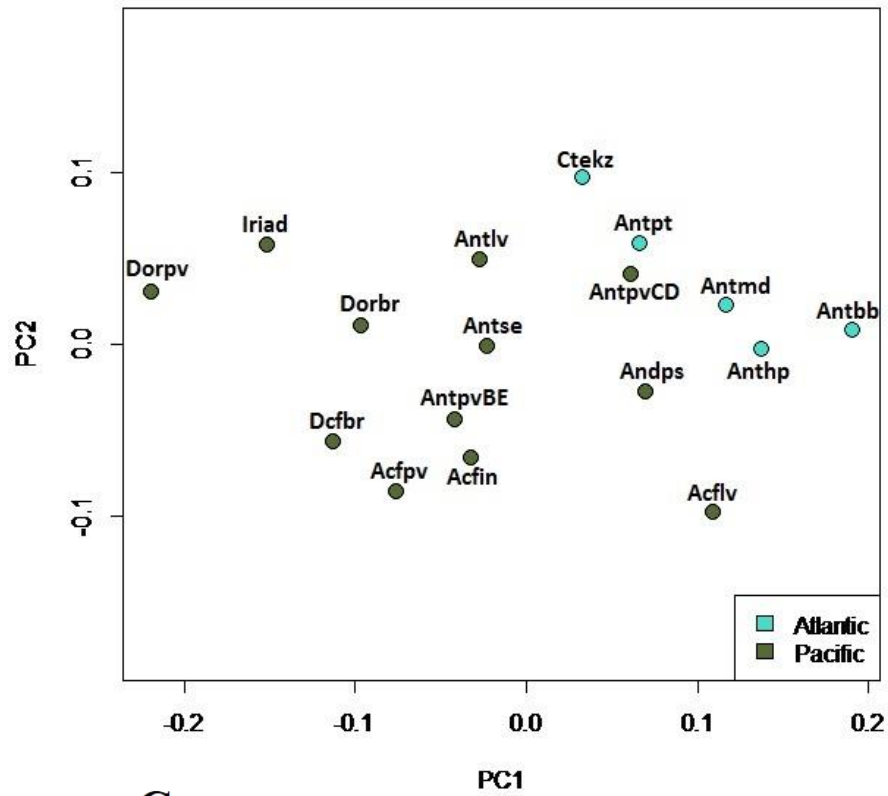


Fig. 24A: Scenario 2 intra-subfamily variation of Antedoninae. A: BGPCA (top) and broken stick model (bottom). (see Appendix Fig. A31 for scenario 1 results) (Acfin = *Antedon* c.f. *incommoda*, Acflv = *Antedon* c.f. *loveni*, Acfpv = *Antedon* c.f. *parviflora*, Andps = *Andrometra psyche*, Antbb = *Antedon bifida bifida*, Anthp = *Antedon hupferi*, Antlv = *Antedon loveni*, Antmd = *Antedon mediterranea*, Antpt = *Antedon petasus*, AntpvBE = *Antedon parviflora* B&E, AntpvCD = *Antedon parviflora* C&D, Antse = *Antedon serrata*, Ctekz = *Ctenantedon kinziei*, Dcfbr = *Dorometra* c.f. *briseis*, Dorbr = *Dorometra briseis*, Dorpv = *Dorometra parvicirra*, Iriad = *Iridometra adrestine*)

**B** **Between Group PCA for Antedoninae by Region**



**C** **Between Group PCA for Antedoninae species by Clade**

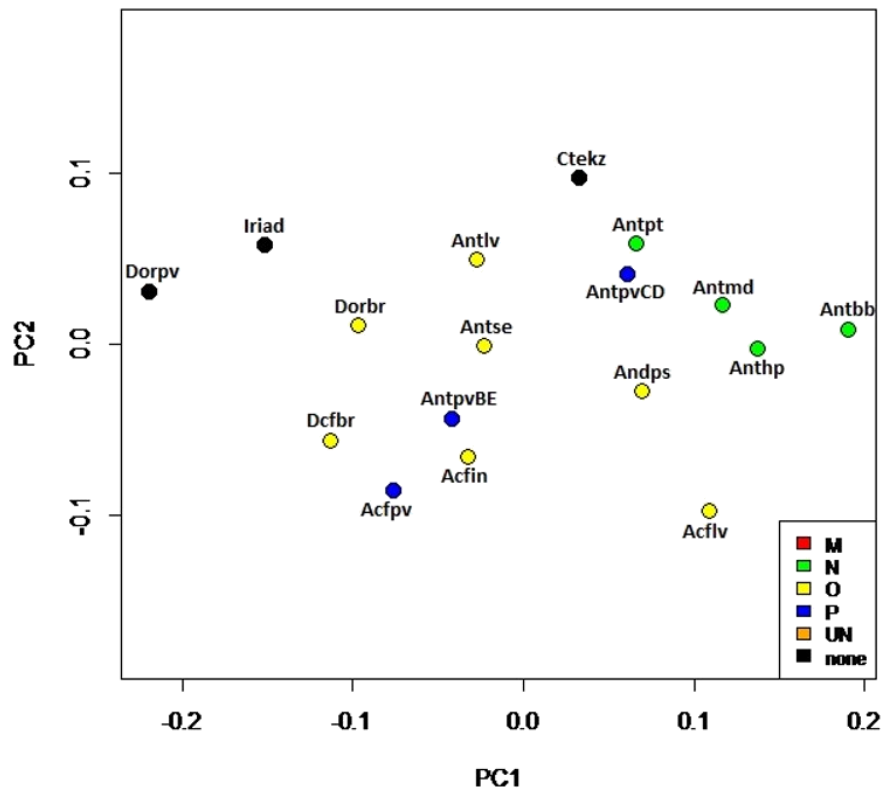


Fig. 24B-C: Scenario 2 intra-subfamily variation of Antedoninae.). B: BGPCA colored by general region. C: BGPCA colored by phylogenetic assignment. (see Appendix Fig. A31B-C for scenario 1 results; see Fig. 24A for species names).



**D** **Between Group PCA for Antedoninae species by Radial ratio**

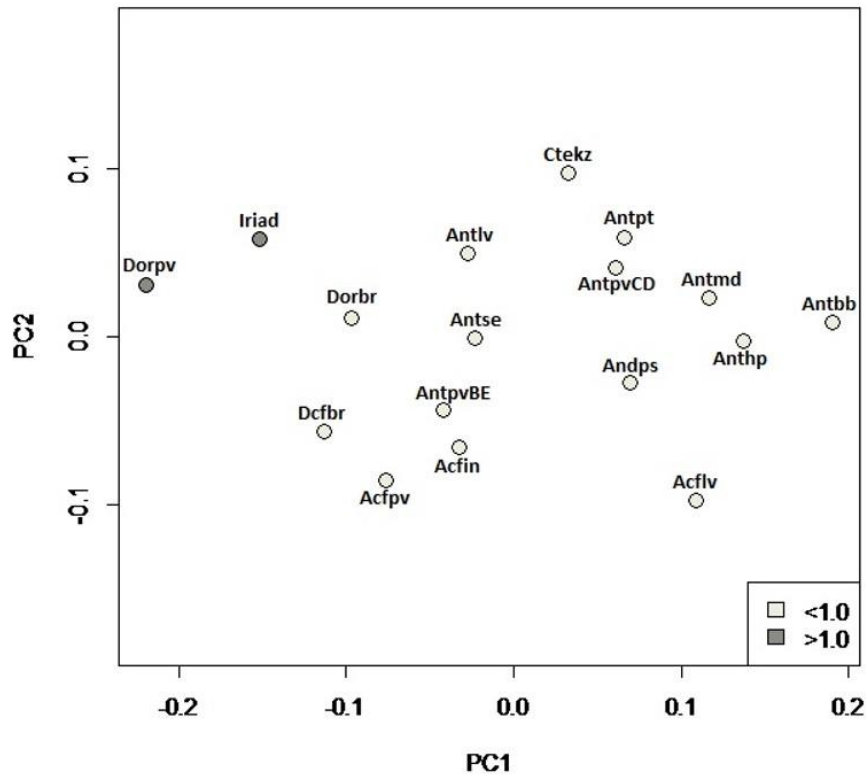


Fig. 24D: Scenario 2 intra-subfamily variation of Antedoninae. D: BGPCA colored by radial ratio (see Appendix Fig. A31D for scenario 1 results; see Fig. 24A for species abbreviations).

Pairwise results between all antedonines reveal 17 significant pairings in scenario 1 (25 landmarks) and 18 pairings in scenario 2 (26 landmarks), 12 of which occurred between an Atlantic and a Pacific species. Scenario 1 included a significant pairing between *Antedon parviflora* C&D and *Dorometra briseis*, two species that shared all other factors, assuming the identity of *A. parviflora* C&D is correct (see Discussion). Scenario 2 included a similar pairing between *Antedon parviflora* C&D and *Antedon serrata*. The additional pairing in scenario 2 was between two Atlantic species, *Antedon bifida bifida* and *Ctenantedon kinziei*. They shared all tested factors except for specific locality, and *C. kinziei* was not included in molecular analyses. The four remaining pairings in both scenarios involved variance between Pacific species and *Antedon* c.f. *loveni*. Two of the pairings were between the two antedonines with the larger radial ratios ( $\geq 1.0$ ): *Dorometra parvicirra* and *Iridometra adrestine*. The third pairing was between a fellow clade O species, *Dorometra* c.f. *briseis*, which differed in depth range and specific locality. Although neither of those factors proved significant enough to affect overall antedonine shape variation, they could be affecting the variation between these species specifically, or it could be the result of phylogenetic forces if one or both of them were misidentified morphologically. The final pairing of *Antedon* c.f. *loveni* was with *Antedon loveni*. Although these species differed in their specific locality (Australia versus North Pacific), it is more likely that *Antedon* c.f. *loveni* was misidentified and shape variations were caused by genetic differences. The true identity of *Antedon* c.f. *loveni* is investigated further in later analyses.

Although scenario 1 yielded significant results when testing the effect of size on shape ( $p = 0.014$ ), no such allometric effect appeared in scenario 2 ( $p = 0.056$ ). This inconsistency, with all other results constant between the scenarios, suggests the inclusion of landmark #1 as important in maintaining proper size depictions after Procrustes superimposition.

#### b. *Bathymetrinae*

The four species representing the bathymetrines in this study (*Hathrometra tenella*, *Thaumatometra tenuis*, *Trichometra cubensis*, and *Tonrometra spinulifera*) span four specific localities, all three general regions, and two molecular clade assignments (Table 5). They all shared the same factor levels of depth range (201-1000m) and radial ratio ( $\geq 1.0$ ), so these were not tested with Procrustes ANOVAs or pairwise tests. The majority of the shape variation within Bathymetrinae is interpretable in both scenarios (82.7%/83.1%) and can be described by the first principal component, or x-axis (Fig. 25, Appendix Fig. A32). Observations of the BGPCA suggest a significant difference between *Tonrometra spinulifera*, the only Antarctic representative, and the other three bathymetrines. However, Procrustes ANOVAs on mean shape revealed no significant shape variation between any species, and thus no significant effect by any factor (region:  $p = 0.443/0.274$ ; locality:  $p = 0.6335/0.2515$ ; clade:  $p = 0.6845/0.5985$ ). Pairwise tests supported the BGPCA projection with a regional pairing between Antarctic species, *Tonrometra spinulifera*, and the Atlantic species, *Hathrometra tenella* and *Trichometra cubensis*, and three locality pairings between *T. spinulifera* and the other bathymetrines. However, results based on individual configurations should not be used to properly represent variation within a subfamily since variability within species can give the illusion of variance when there is none. There was also no allometric effect on shape variation between any species. These results were consistent in both scenarios. Although there was non-random variation between bathymetrine species, it was not significant.

#### c. *Heliometrinae*

The five heliometrine species in this study (*Anthometrina adriani*, *Comatonia cristata*, *Florometra asperrima*, *F. serratissima*, and *Promachocrinus kerguelensis*) span two depth ranges, three specific localities and all three general regions (Table 5). They all measure radial ratios greater or equal to 1.0 and fall close to each other in molecular analyses (clade M for this study). PC1 describes the interpretable variation within Heliometrinae and encompasses over half of the total shape variation in both scenarios (64.7%/65.2%). Observations of the BGPCA suggest a significant variation between the Antarctic species with the widest depth range, *Promachocrinus kerguelensis*, and the

other four heliometrines (Fig. 26, Appendix Fig. A33). However, Procrustes ANOVAs on mean shape revealed no significant variation between any species, and thus no significant effect by any factor (depth:  $p = 0.549/0.5065$ ; locality:  $p = 0.616/0.6765$ ; region:  $p = 0.5935/0.6875$ ) in either scenario. Procrustes ANOVA tests between individuals yielded significant shape variance, with effects by depth ( $p = 0.003/0.003$ ), region ( $p = 0.001/0.002$ ), and locality ( $p = 0.001/0.002$ ). Pairwise tests resulted in the same single pairing for both region and locality: Antarctic species (*Anthometrina adriani* and *Promachocrinus kerguelensis*) and Pacific species (*Florometra serratissima* and *Florometra asperrima*). On the other hand, pairwise tests also paired the two depth range groups, as well as three species within the same depth range (*Comatonia cristata* against *Florometra asperrima* and *Anthometrina adriani*). None of these results are congruent with each other or the BGPCA and, as previously stated, pairwise tests can only be performed on individuals, so should not be used to suggest variation within the subfamily. Although there is interpretable variance between species, it is not significant within subfamily Heliometrinae.

## Between Group PCA for Bathymetrinae

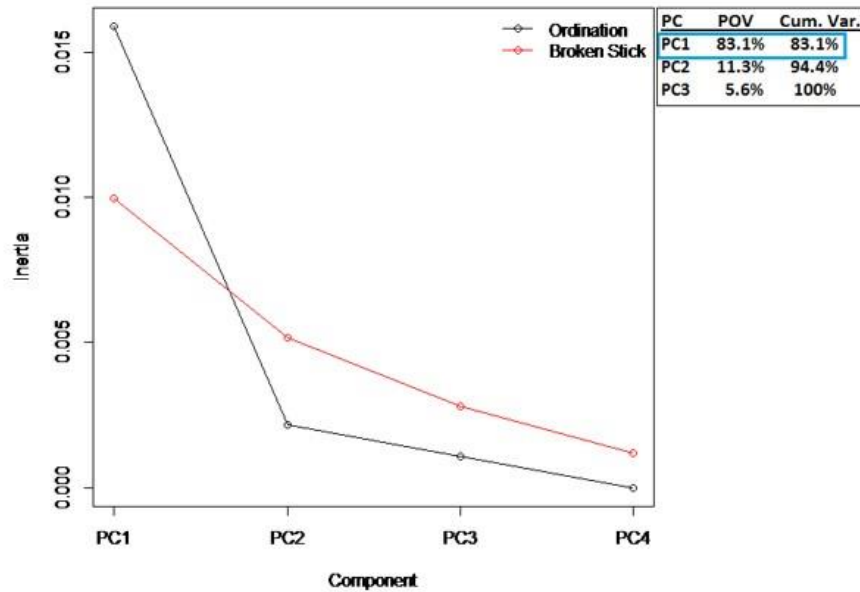
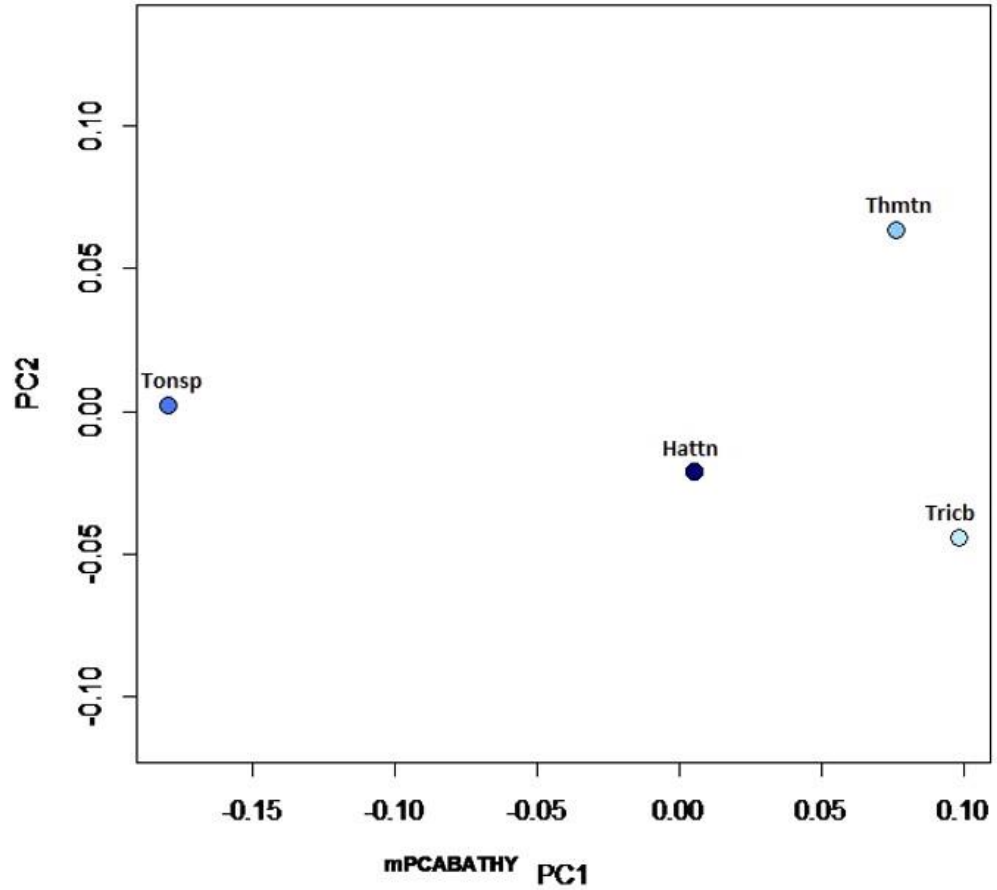


Fig. 25: Scenario 2 between group PCA (top) and broken stick model (bottom) depicting intra-subfamily variation of Bathymetrinae. Despite visual separations, there were no significant variations within this subfamily (see Appendix Fig. A32 for scenario 1 results) (Hattn = *Hathrometra tenella*, Thmtn = *Thaumatometra tenuis*, Tricb = *Trichometra cubensis*, Tonsp = *Tonrometra spinulfera*).

### Between Group PCA for Heliometrinae

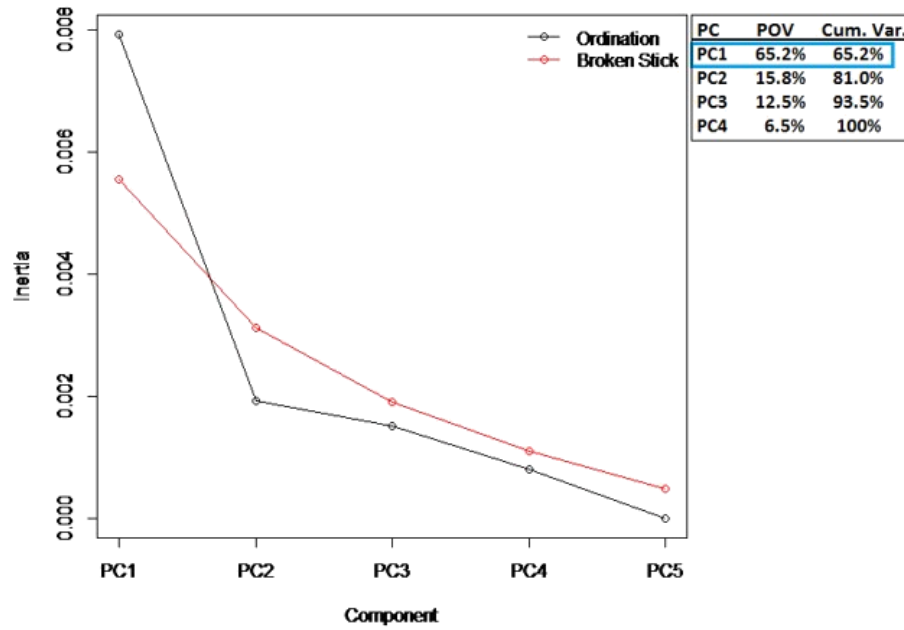
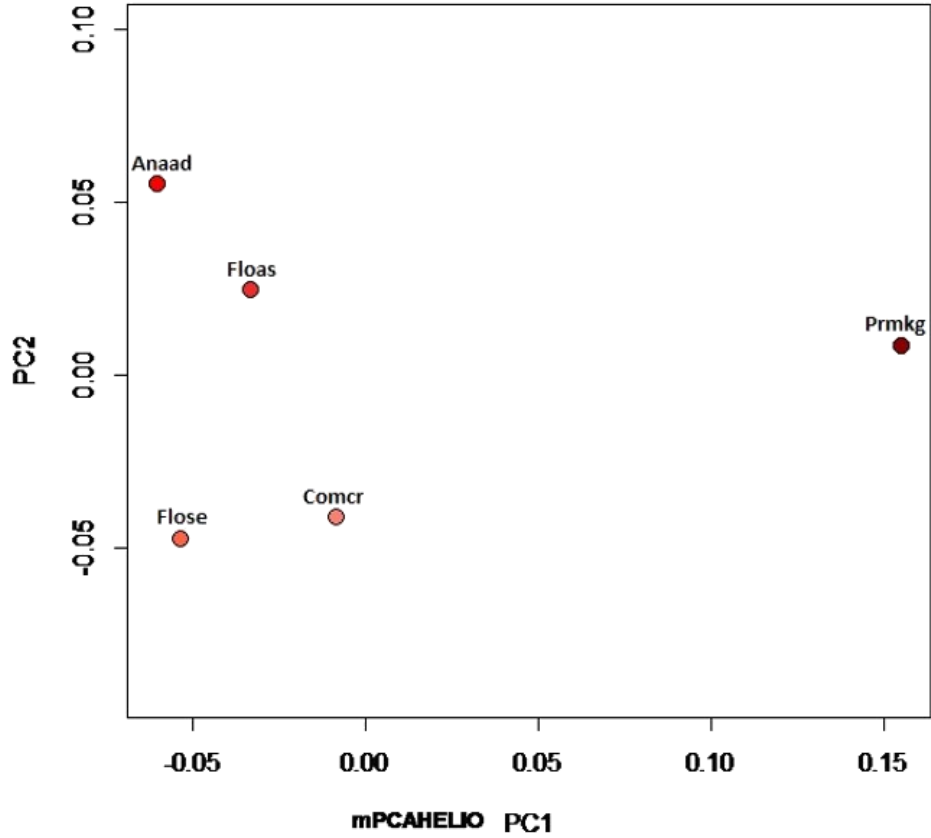


Fig. 26: Scenario 2 between group PCA (top) and broken stick model (bottom) depicting intra-subfamily variation of Heliometrinae. Despite visual separations, there were no significant variations within this subfamily (see Appendix Fig. A33 for scenario 1 results) (Anaad = *Anthometrina adriani*, Comcr = *Comatonia cristata*, Floas = *Florometra asperima*, Flose = *Florometra serratissima*, Prmkg = *Promachocrinus kerguelensis*).

d. *Isometrinae*

There was no significant variation between the two isometrines, *Isometra graminea* and *I. vivipara*. They share all tested factors and are distinguished almost entirely by size-related differences in the first two pinnules, but are still molecularly distinct, so it is most likely the two species are closely related sisters as part of a species flock (see *Isometra* results).

e. *Perometrinae*

The three perometrines represented here share a radial ratio factor level of less than 1.0 (Table 5). The two Pacific species, *Erythrometra rubra* and *Perometra diomedae*, shared all tested factors other than clade assignment (*E. rubra* was not used). As a shallower Atlantic species, the other perometrine, *Hypalometra defecta*, differs from the other two in all biogeographic factors. Despite these differences, no significant shape variation was present between perometrine species ( $p = 0.495/0.5005$ ), and thus there were no significant effects by any of the biogeographic factors (depth:  $p = 0.5195/0.5195$ ; locality:  $p = 0.437/0.437$ ; region:  $p = 0.5195/0.5195$ ). While all of the shape variation is interpretable by the first two principal components (Fig. 27, Appendix Fig. A34) and may be attributable to one or more biogeographical factors, the differences in shape between perometrine species were not significant. Phylogenetic effects could not be tested within this subfamily, as only a *Perometra* species was used in the phylogenetic trees (Hemery 2011, Rouse et al. in prep.). Additionally, the species used in the phylogenies (*P. robusta*) differed from the *Perometra* species used here (*P. diomedae*).

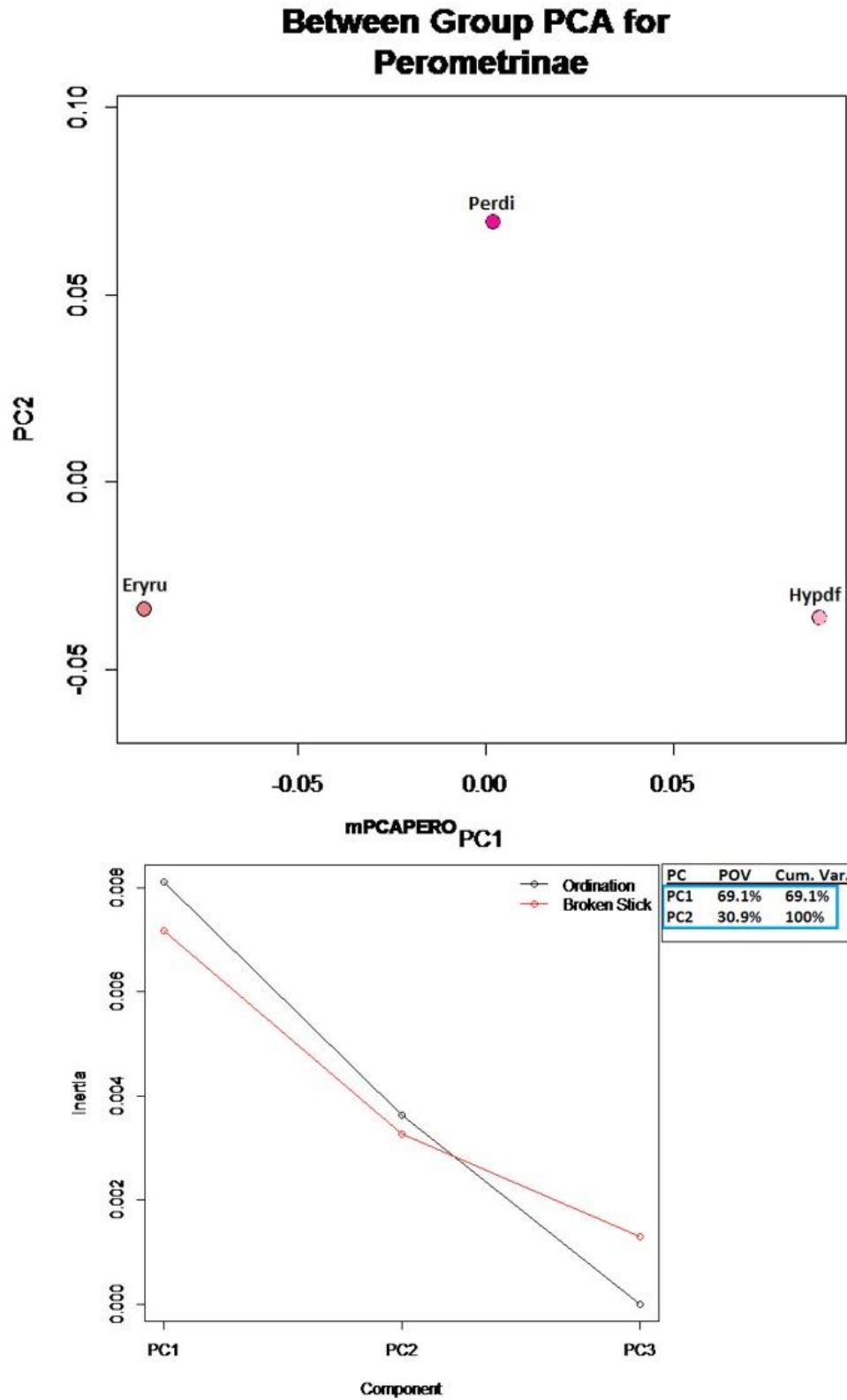


Fig. 27: Scenario 2 between group PCA (top) and broken stick model (bottom) depicting intra-subfamily variation of Perometrinae. Despite visual separations, there were no significant variations within this subfamily (see Appendix Fig. A34 for scenario 1 results) (Eryru = *Erythrometra rubra*, Hypdf = *Hypalometra defecta*, Perdi = *Perometra diomedae*).



f. *Thysanometrinae*

The two thysanometrines in this study represent both genera in this subfamily. The species share depth range (201-1000m) and phylogenetic assignment (clade ‘unnamed’), while differing in their specific locality, general region, and radial ratios: Caribbean *Coccometra hagenii* has a higher radial ratio ( $\geq 1.0$ ) and *Thysanometra tenelloides* from the Japan Sea has a smaller radial ratio ( $< 1.0$ ). Procrustes ANOVAs on mean shape could not be performed as there were only two mean configurations, so individual configurations were tested for significant pairings between the two species. Significant pairings between the two species occurred when testing all three factors ( $p = 0.001$ ) with the individual configurations. The PCA (Fig. 28, Appendix Fig. A35) shows a clear separation of the thysanometrines along PC1, which is the sole interpretable variance component in both scenarios (85.7%/85.9%). It is important to note, however, that PCA is based on the individuals and treats them as one group, so additional species within either or both genera would be needed to identify between-species variance through subsequent BGPCA and ANOVA testing.

g. *Antedonidae incertae sedis*

As with the perometrines, only one of the three species in *Antedonidae incertae sedis* examined here (*Poliometra prolixa*) was used in the phylogenetic trees (Hemery 2011, Hemery et al. 2013, Rouse et al. in prep.), so phylogenetic effects could not be tested among these taxa. Of the factors that could be tested, the species shared only a higher than wide radial ratio ( $H:W \geq 1.0$ ). *Hybometra senta* and *Poliometra prolixa* differ from *Balanometra balanoides* by depth range and general region, and all three differ in their specific localities (Table 5). The first principal component described the non-random shape variation in both scenarios (78.2%/78.55%), with a visual distinction between *Poliometra prolixa* and the other species in the BGPCA (Fig. 29, Appendix Fig. A36). Despite the graphical separation, the results of the Procrustes ANOVAs revealed no significant shape variation between any of the three species ( $p = 0.169/0.5005$ ), and thus no significant effects by depth ( $p = 0.429/0.429$ ), locality ( $p = 0.169/0.5005$ ), or region ( $p = 0.429/0.429$ ).

## PCA for Thysanometrinae

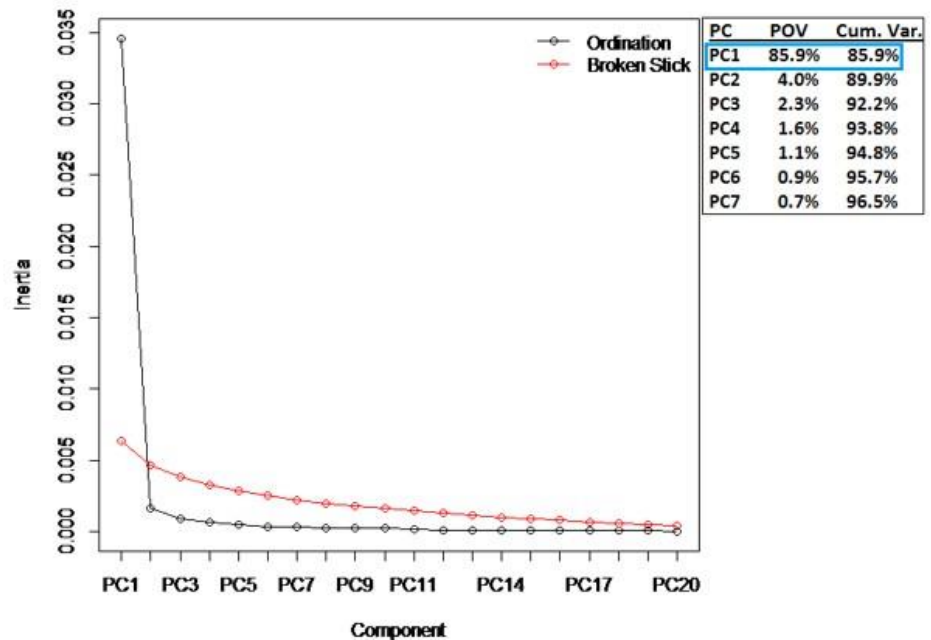
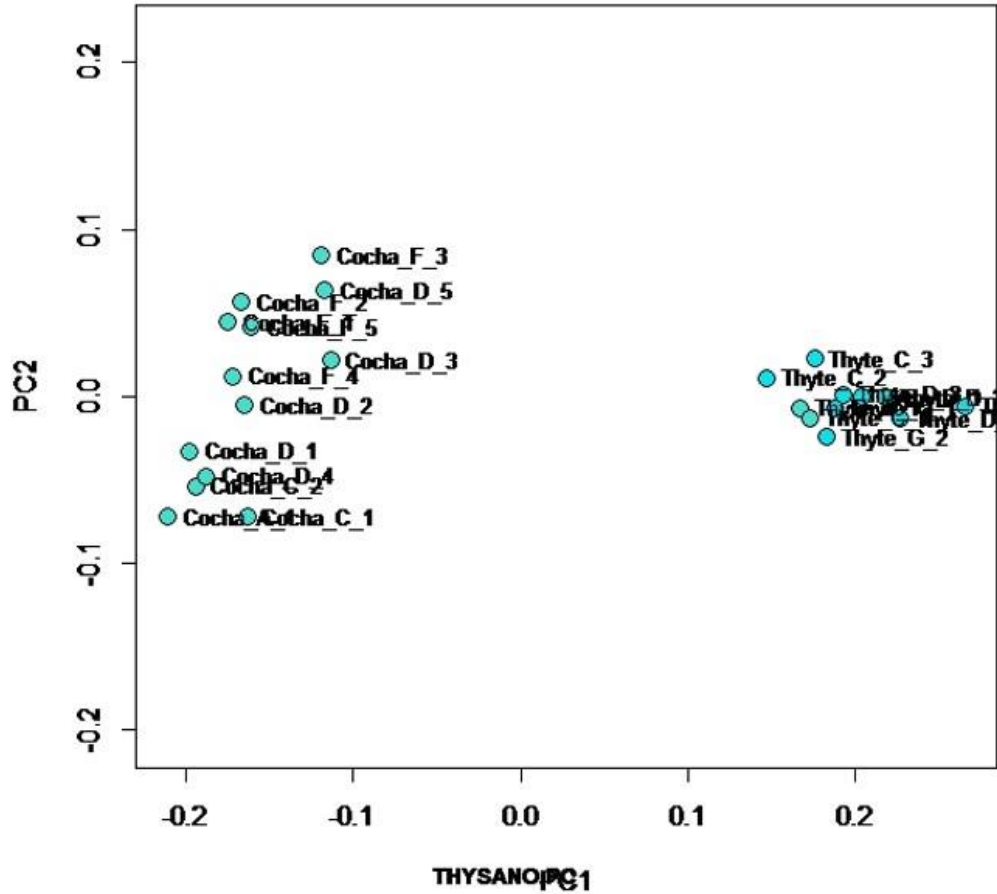


Fig. 28: Scenario 2 PCA (top) and broken stick model (bottom) depicting intra-subfamily variation of Thysanometrinae based on all individuals (see Appendix Fig. A35 for scenario 1 results) (Cocha = *Coccometra hagenii*, Thyte = *Thysanometra tenelloides*).

## Between Group PCA for Antedonidae incertae sedis

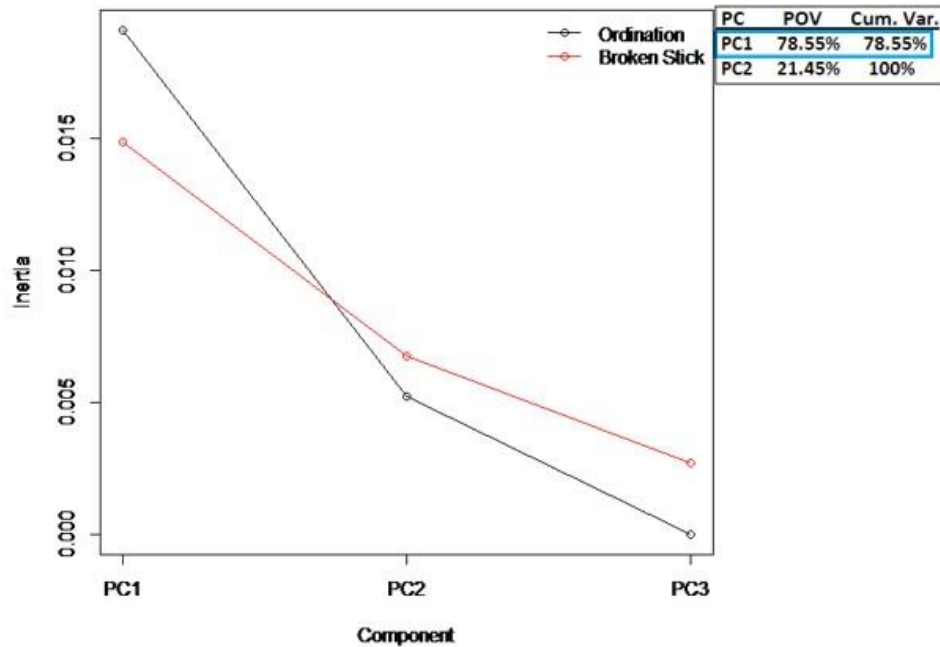
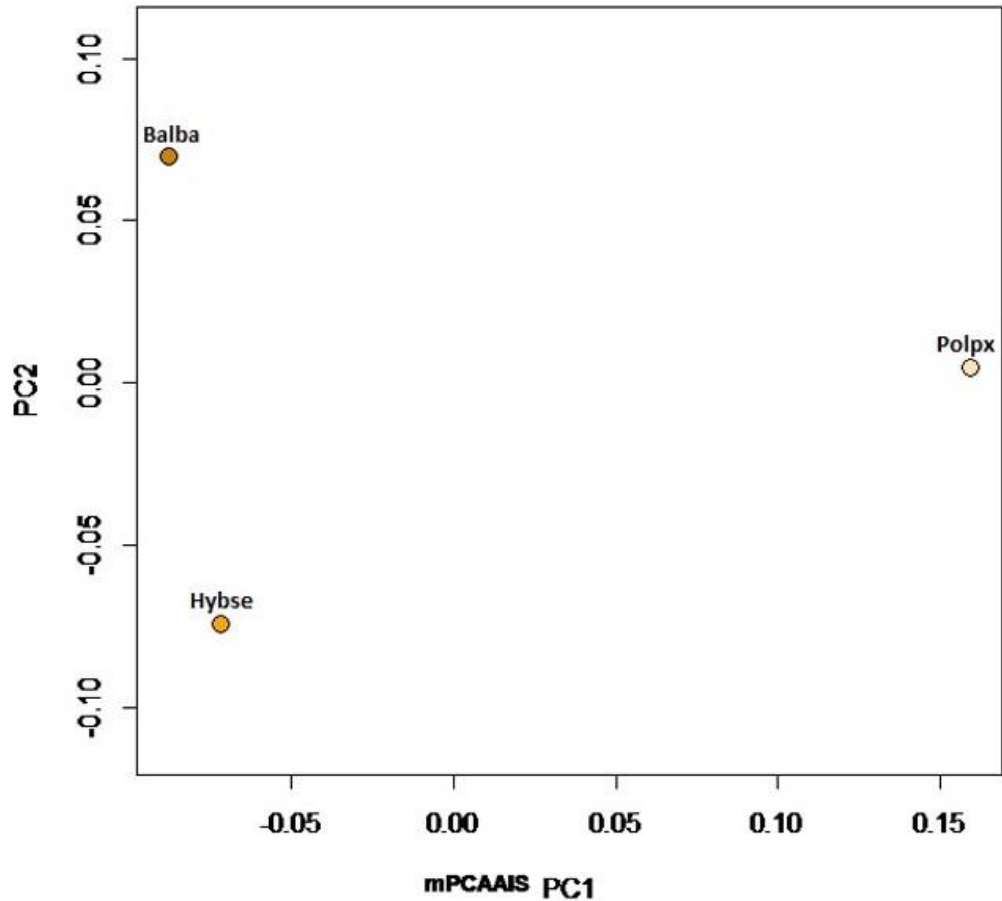


Fig. 29: Scenario 2 between group PCA (top) and broken stick model (bottom) depicting intra-subfamily variation of Antedonidae *incertae sedis*. Despite visual separations with *P. prolixa*, there were no significant variations within this subfamily (see Appendix Fig. A36 for scenario 1 results) (Balba = *Balanometra balanoides*, Hybse = *Hybometra senta*, Polpx = *Poliometra prolixa*).

v. *Intra-clade variability*

Significant shape variations were tested within each of the five clades that belonged to the former Antedonidae (Hemery 2011, Hemery et al. 2013, Rouse et al. in prep.). Limited variation within these clades based on the factors tested here would reinforce the molecular results and offer additional support for taxonomic revisions.

a. *Clade M (and other tree equivalents)*

Two heliometrine subclades, with an additional *Thaumatometra* species, make up Hemery's clade M (2011). This differs slightly from the other two trees (Hemery et al. 2013, Rouse et al. in prep.), which returned one heliometrine subclade (*Promachocrinus kerguelensis* and *Florometra mawsoni*) as sister to both the other subclade (*Heliometra glacialis*, *Anthometrina adriani*, *Florometra asperrima*, *F. serratissima*, and *Comatonia cristata*) and a clade equivalent to Hemery's (2011) clade O (Pacific antedonines, *Aporometra* sp., and *Eudiocrinus* spp.). For this study, both heliometrine subclades were included when testing variances within this clade, along with representatives of *Thaumatometra tenuis* (Hemery 2011). The phylogenetic return of *P. kerguelensis* as a sister and the close relationship of heliometrines to clade O was taken into account during result interpretations (see Discussion).

The tested factors within this group, and subsequent results, were similar to Heliometrinae (see results above); the inclusion of *Thaumatometra tenuis* added only one factor level in specific locality (Table 5). In accordance with the phylogenetics, a significant shape difference between members of heliometrine clade #2 (Hemery et al. 2013) and *P. kerguelensis* was expected. However, the results of the Procrustes ANOVA yielded no significant shape variation between any species, within or between the subclades, in both scenarios ( $p = 0.5005/0.5005$ ). There are observable differences between heliometrine clade #2 and *P. kerguelensis*, and (although less pronounced) between *T. tenuis*, on the BGPCA along PC1 (Fig. 30, Appendix Fig. A37), but these differences are not significant enough to warrant separation of the species into different taxonomic groups, supporting their placement on the trees.

### Between Group PCA for Clade M

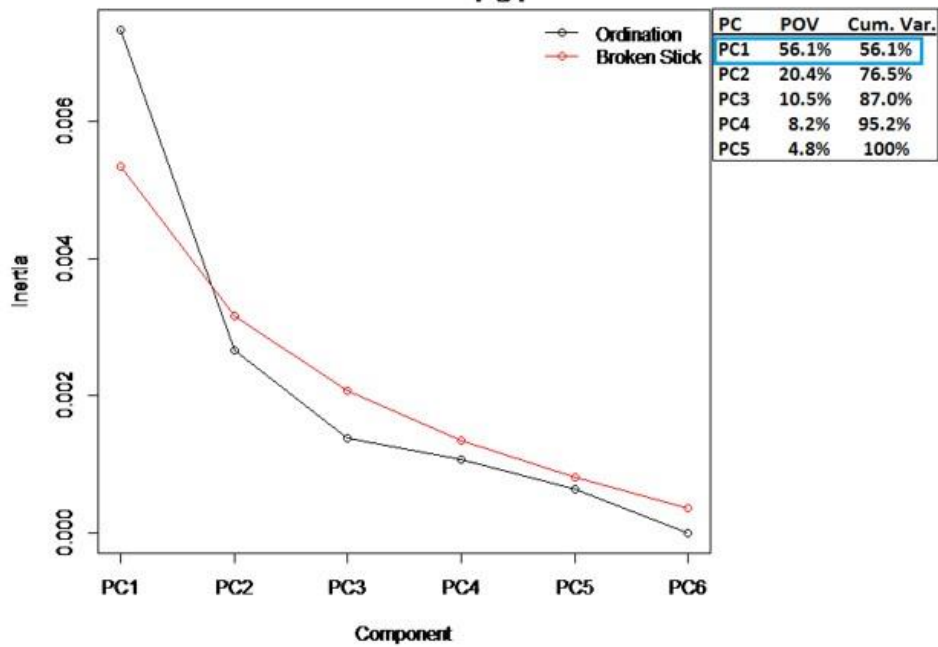
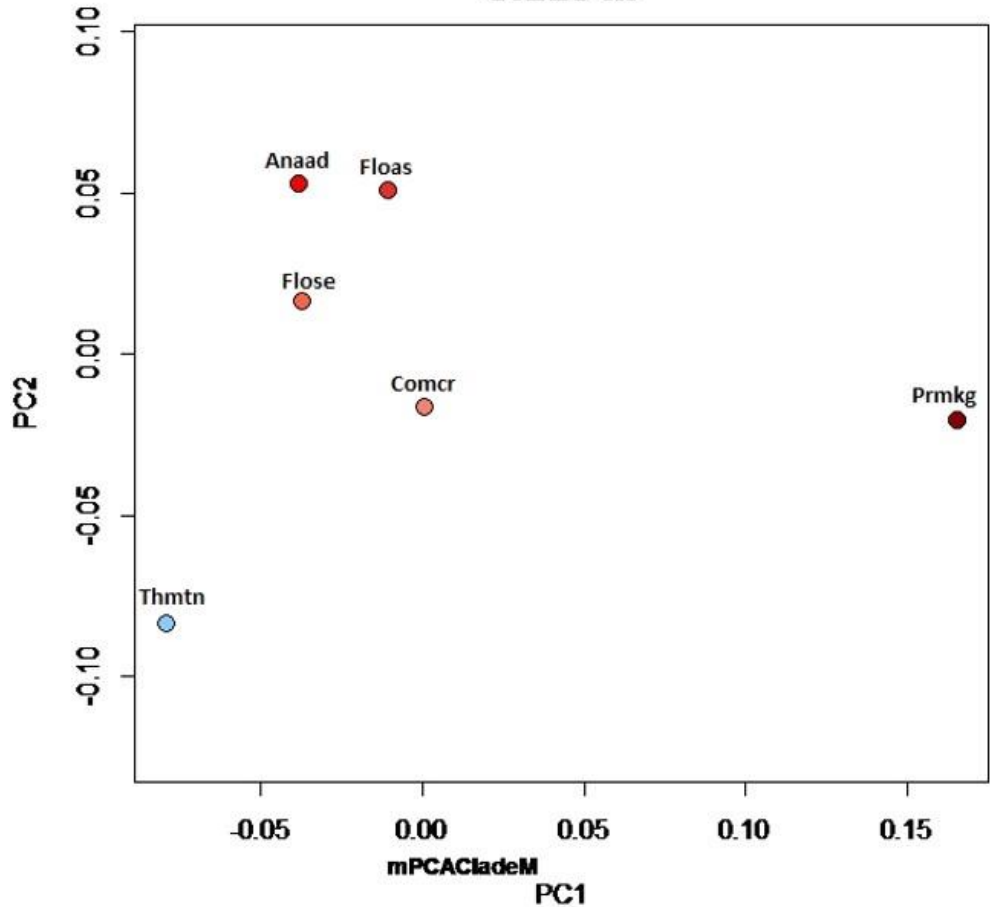


Fig. 30: Scenario 2 between group PCA (top) and broken stick model (bottom) depicting intra-clade variation of clade M and equivalents. Despite visual separation with *P. kerguelensis*, there were no significant variations within this clade (see Appendix Fig. A37 for scenario 1 results) (Anaad = *Anthometrina adriani*, Comcr = *Comatonia cristata*, Floas = *Florometra asperima*, Flose = *Florometra serratissima*, Prmkg = *Promachocrinus kerguelensis*, Thmtn = *Thaumatometra tenuis*).

b. *Clade N (and other tree equivalents)*

Hemery's clade N, and the other tree clade equivalents, are made up of two subclades, one containing solely Atlantic *Antedon* species, the other an Atlantic non-antedonid, *Tropiometra carinata* (*T. carinata* can also be found in the Indian Ocean, but the specimens in this study were Caribbean) (Hemery 2011, Hemery et al. 2013, Rouse et al. in prep.). Despite sharing a general region and measured factors, there is potential for shape variation through different localities and depth ranges (Table 5). BGPCA results show overlap between *A. bifida bifida* and *Tropiometra carinata* along the only non-random component (PC1), and very little variation between *A. petasus* and *A. mediterranea* (Fig. 31, Appendix Fig. A38). Separation of both groups from deeper species, *A. hupferi*, could suggest an effect on shape variation by depth. However, based on Procrustes ANOVA results, there was no significance in the overall shape variation between any clade N species ( $p = 0.5005/0.5005$ ). Whether region plays a role in shaping radial ossicles is unclear, as ANOVAs only test for differences, not similarities (see *Hierarchical Clustering*). Nevertheless, the phylogenetic results of all trees are supported here by radial morphology.

c. *Clade O (and other tree equivalents)*

Clade O, and its equivalents, is a solely Pacific clade composed of several antedonine species and three non-antedonid sisters, *Aporometra* sp. (*A. occidentalis* used here), *Eudiocrinus* spp. (not available) and *Iconometra anisa* (not available and only used in Hemery 2011). The eight representative species used in this project span three depth ranges, four specific localities, and two taxonomic classifications (Table 5). All species share a factor level for radial ratio ( $<1.0$ ), as well as region. Once again, the first principal component alone describes the interpretable variation in both scenarios ( $p = 67\%/66.3\%$ ), projecting a separation between the seven antedonines and sister, *Aporometra occidentalis* (Fig. 32, Appendix Fig. A39). While results of the Procrustes ANOVAs revealed no significant effects on shape variation by depth ( $p = 0.221/0.2265$ ) or locality ( $p = 0.323/0.313$ ), there was a significant effect by subfamily classification ( $p = 0.0255/0.0405$ ), supporting separation of *A. occidentalis* on the BGPCA. While there is

variation within this clade, it lies between the two subclades, supporting the phylogenetic placements.

d. *Clade P (and other tree equivalents)*

Clade P and equivalents consist of four Pacific antedonines (*Antedon iris*, *A. longicirra*, *A. parviflora*, and *Argyrometra mortenseni*), and is sister to a larger clade containing various non-antedonids (Hemery 2011, Hemery et al. 2013, Rouse et al. in prep.). Unfortunately, only one of the four clade P species (*A. parviflora*) was acquired for this study. However, due to uncertain identities, along with the addition of *Thaumatometra tenuis* (*T. comaster* used in Hemery 2011 only), four species could be tested for variance within this clade: *Antedon* c.f. *parviflora*, *A. parviflora* B&E, *A. parviflora* C&D, and *T. tenuis*. The three *A. parviflora* groups share all factor levels except for *A. parviflora* B&E, which differed in specific locality (Table 5). As a bathymetrine, *T. tenuis* differed from the others in taxonomic assignment, as well as depth range and radial ratio ( $\geq 1.0$ ). The majority of variance between species is interpretable (91.2%/91.1%) and described by the first two PCs (Fig. 33, Appendix Fig. A40). The BGPCA suggests variation between factor outlier, *T. tenuis*, and the *A. parviflora* groups along PC1. *A. parviflora* C&D also shows some separation along PC1, as well as PC2, suggesting a possibly misidentification (see *Misclassifications*). Despite the projected differences, Procrustes ANOVAs yielded no significant variation ( $p = 0.5005/0.378$ ) between any clade P representatives. This cannot confidently support the phylogenies, however, since only one representative was present and consistent across the three trees.

## Between Group PCA for Clade N

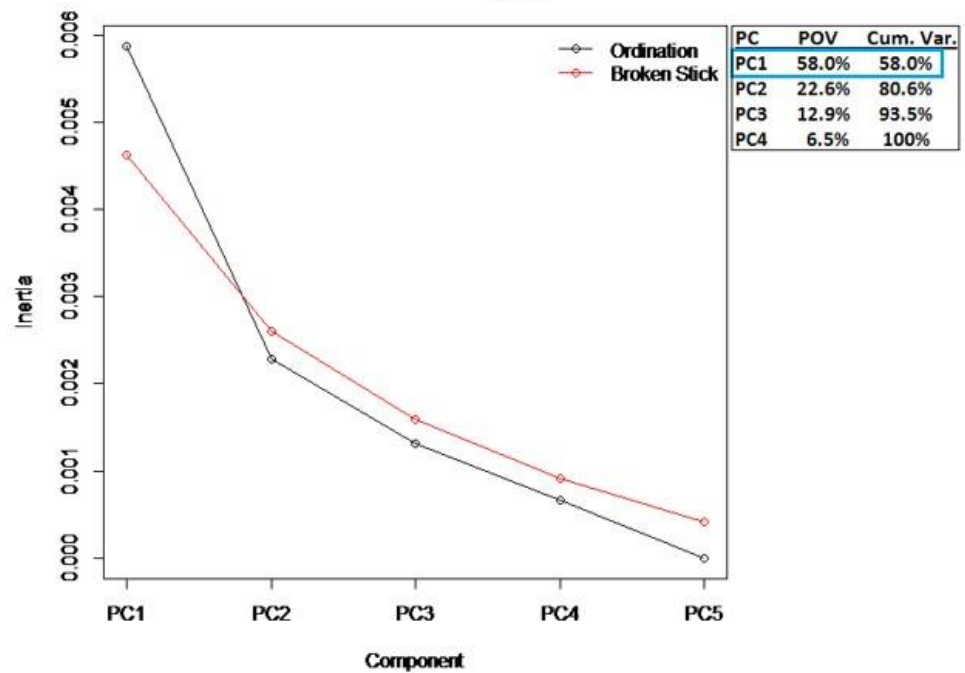
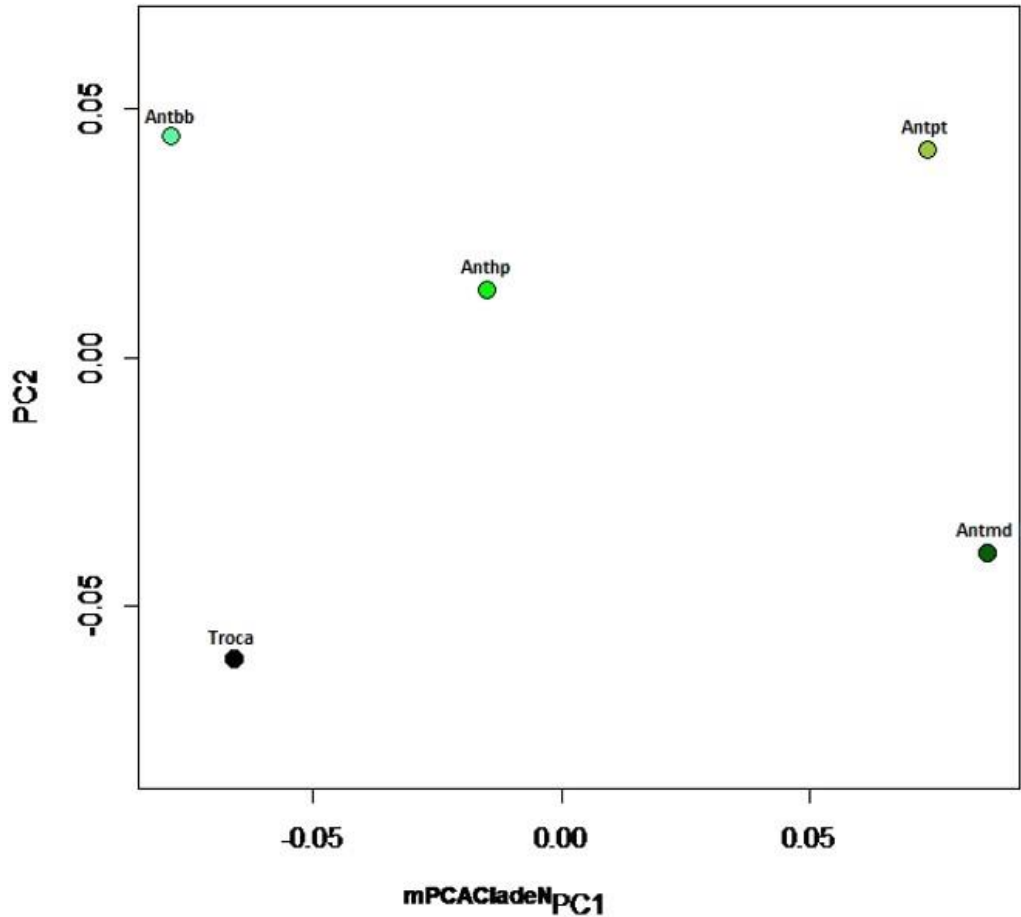


Fig. 31: Scenario 2 between group PCA (top) and broken stick model (bottom) depicting intra-clade variation of clade N and equivalents. Despite visual separations, there were no significant variations within this clade (see Appendix Fig. A38 for scenario 1 results) (Antbb = *Antedon bifida bifida*, Anthp = *Antedon hupferi*, Antmd = *Antedon mediterranea*, Antpt = *Antedon petasus*, Troca = *Tropiometra carinata*).



## Between Group PCA for Clade O

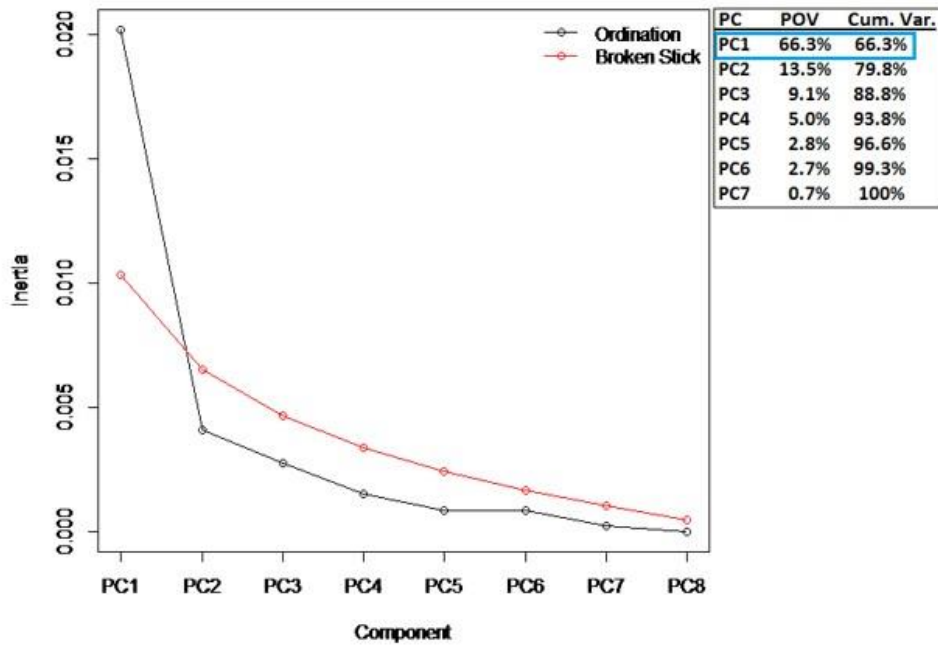
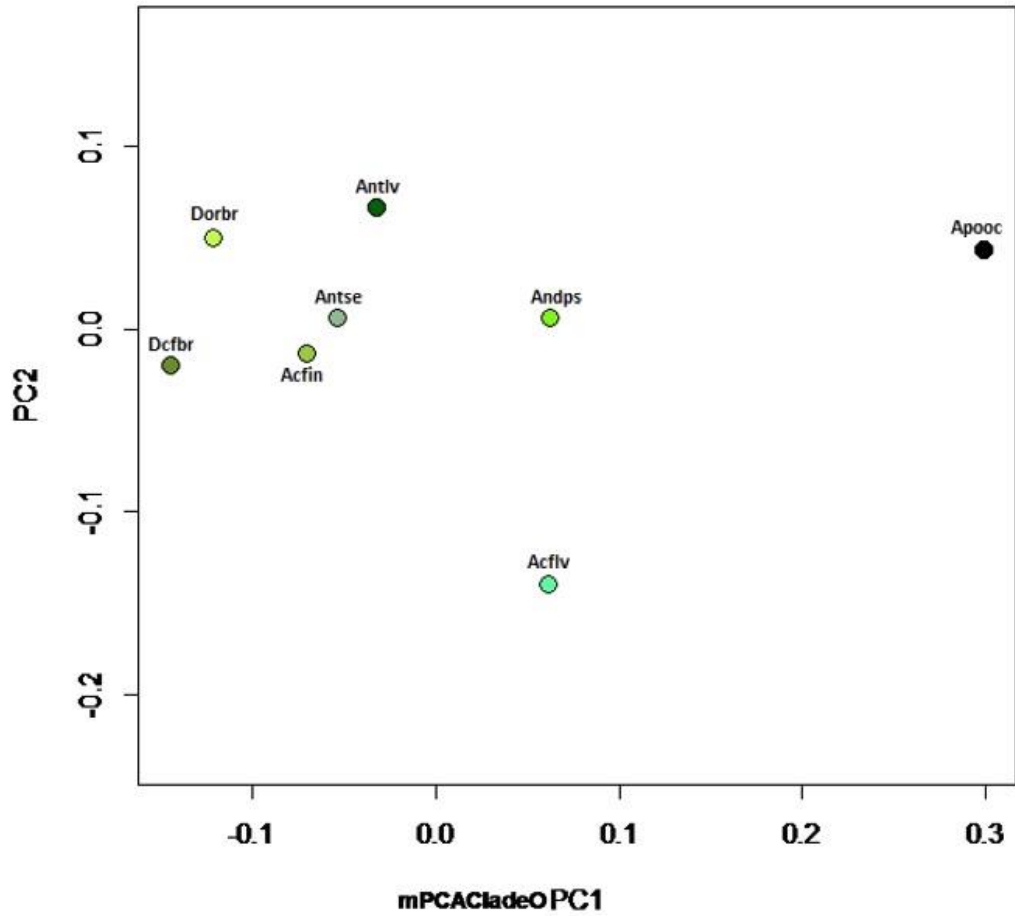


Fig. 32: Scenario 2 between group PCA (top) and broken stick model (bottom) depicting intra-clade variation of clade O and equivalents. There were significant affects by taxonomic classification within this clade, supporting the visual separation of *A. occidentalis* (see Appendix Fig. A39 for scenario 1 results) (Acfin = *Antedon* c.f. *incommoda*, Acflv = *Antedon* c.f. *loveni*, Andps = *Andrometra psyche*, Antlv = *Antedon loveni*, Antse = *Antedon serrata*, Dcfbr = *Dorometra* c.f. *briseis*, Dorbr = *Dorometra briseis*, Apooc = *Aporometra occidentalis*).

## Between Group PCA for Clade P

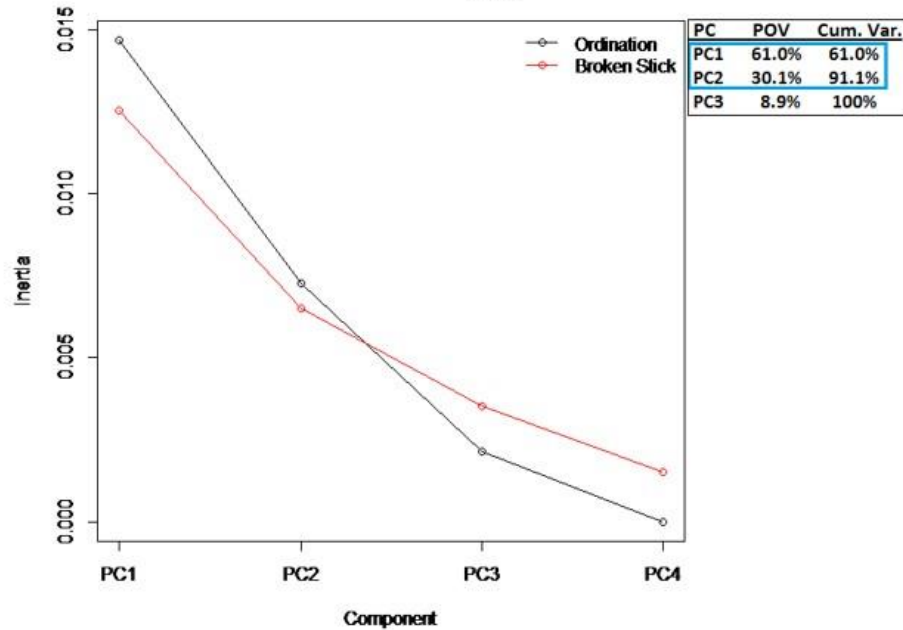
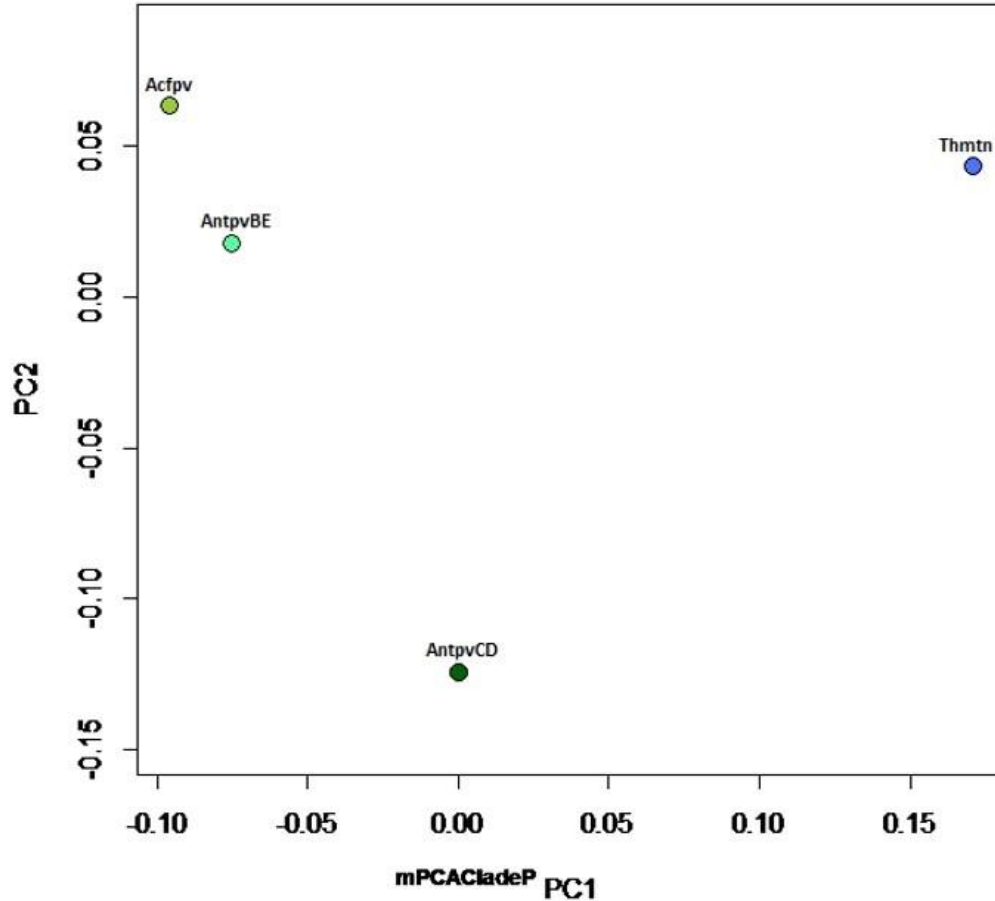


Fig. 33: Scenario 2 between group PCA (top) and broken stick model (bottom) depicting intra-clade variation of clade P and equivalents. Although the first two PCs are interpretable and there is visual separation of bathymetrine *T. tenuis*, there were no significant variations within this clade (see Appendix Fig. A40 for scenario 1 results) (Acfpv = *Antedon c.f. parviflora*, AntpvBE = *Antedon parviflora* B&E, AntpvCD = *Antedon parviflora* C&D, Thmtn = *Thaumatometra tenuis*).

e. Clade ‘unnamed’ (and other tree equivalents)

All three molecular phylogenies (Hemery 2011, Hemery et al. 2013, Rouse et al. in prep.) returned a similar ‘unnamed’ clade. The nine ‘unnamed’ species used in this study (bathymetrines *Hathrometra tenella*, *Trichometra cubensis* and *Tonrometra spinulifera*, isometrines *Isometra graminea* and *I. vivipara*, perometrine *Perometra diomedea*, thysanometrines *Coccometra hagenii* and *Thysanometra tenelloides*, and *incertae sedis* species *Poliometra prolixa*) consisted of antedonids from five different morphological subfamilies, five localities, all three general regions, the three deepest depth ranges, and both radial ratio levels (Table 5). Species inclusion is nearly consistent between all three, except for an additional bathymetrine (*Tonrometra spinulifera*) and thysanometrine (*Thysanometra tenuicirra*) in Hemery (2011). Hemery (2011) included *Hathrometra sarsii* and Rouse et al. (in prep.) included *H. tenella*, but there are likely the same taxon (Messing and Dearborn 1990).

The first principal component was the sole descriptor of non-random variation within clade ‘unnamed’, encompassing most of the overall variation as well in both scenarios (73.4%/74.6%). The BGPCA revealed no obvious clustering, although slight overlap appeared between the isometrines and Atlantic *Trichometra cubensis* (Fig. 34A, Appendix Fig. A41A). Results from the Procrustes ANOVAs revealed a significant effect on shape by radial ratio only ( $p = 0.0415/0.049$ ), indicating that *Thysanometra tenelloides* and *Perometra diomedea* differed significantly in shape from the other clade ‘unnamed’ species (Fig. 34B, Appendix Fig. A41B). The visual variance between the species with taller than wide radials ( $\geq 1.0$ ) was not large enough to register a significant difference in their radial shapes. As *Thysanometra* and *Perometra* are not sisters within clade ‘unnamed’, the results do not completely support the phylogenies. However, the *Thysanometra* and *Perometra* species used in this study differed from those used in either molecular tree, which may have affected the results (see Discussion).

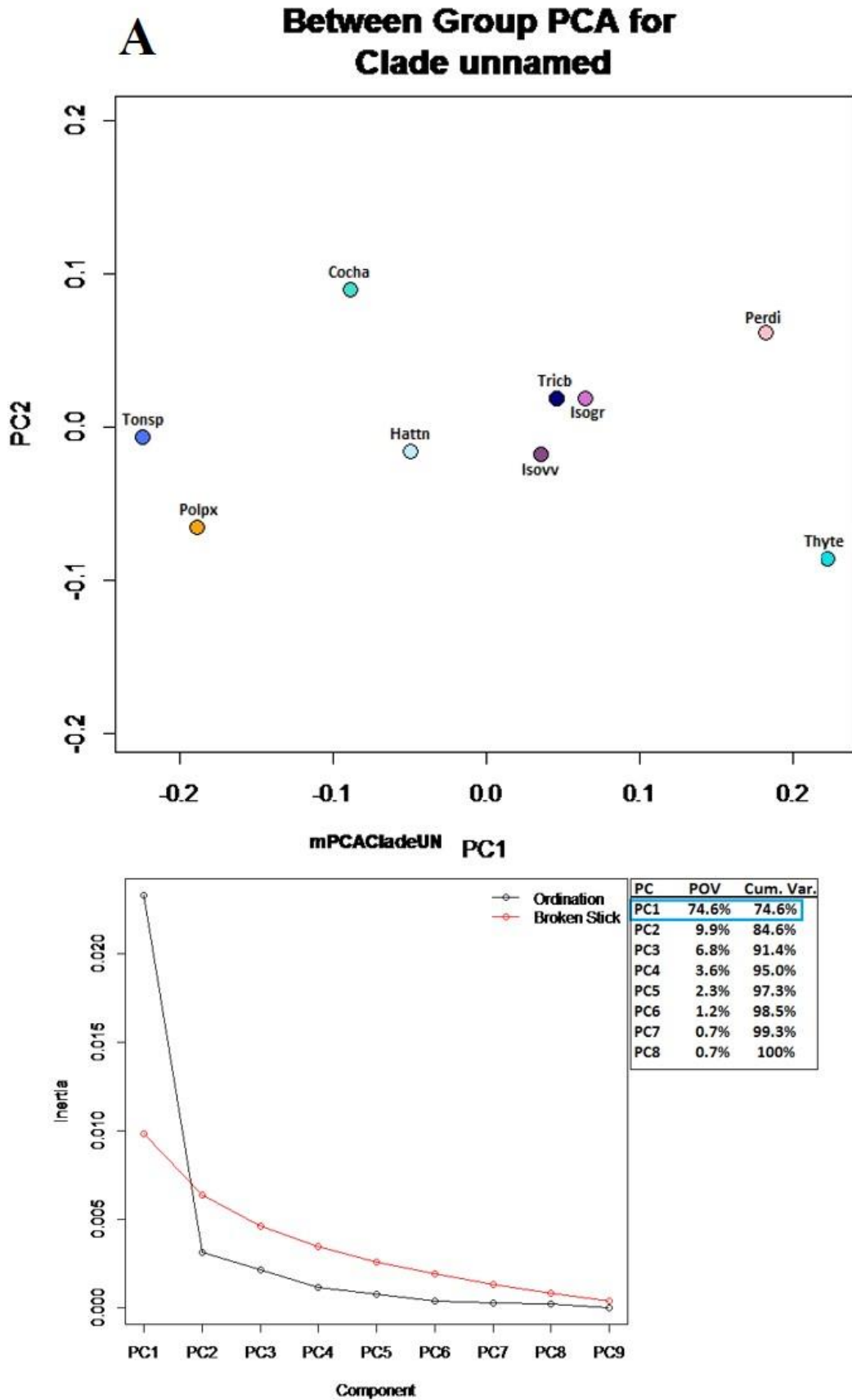


Fig. 34A: Scenario 2 between group PCA (top) and broken stick model (bottom) depicting intra-clade variation of clade 'unnamed' and equivalents (see Appendix Fig. A41A for scenario 1 results) (Cocha = *Coccometra hagenii*, Hattn = *Hathrometra tenella*, Isogr = *Isometra graminea*, Isov v = *Isometra vivipara*, Perdi = *Perometra diomedea*, Polpx = *Poliometra prolixa*, Thyte = *Thysanometra tenelloides*, Tonsp = *Tonrometra spinulifera*, Tricb = *Trichometra cubensis*).

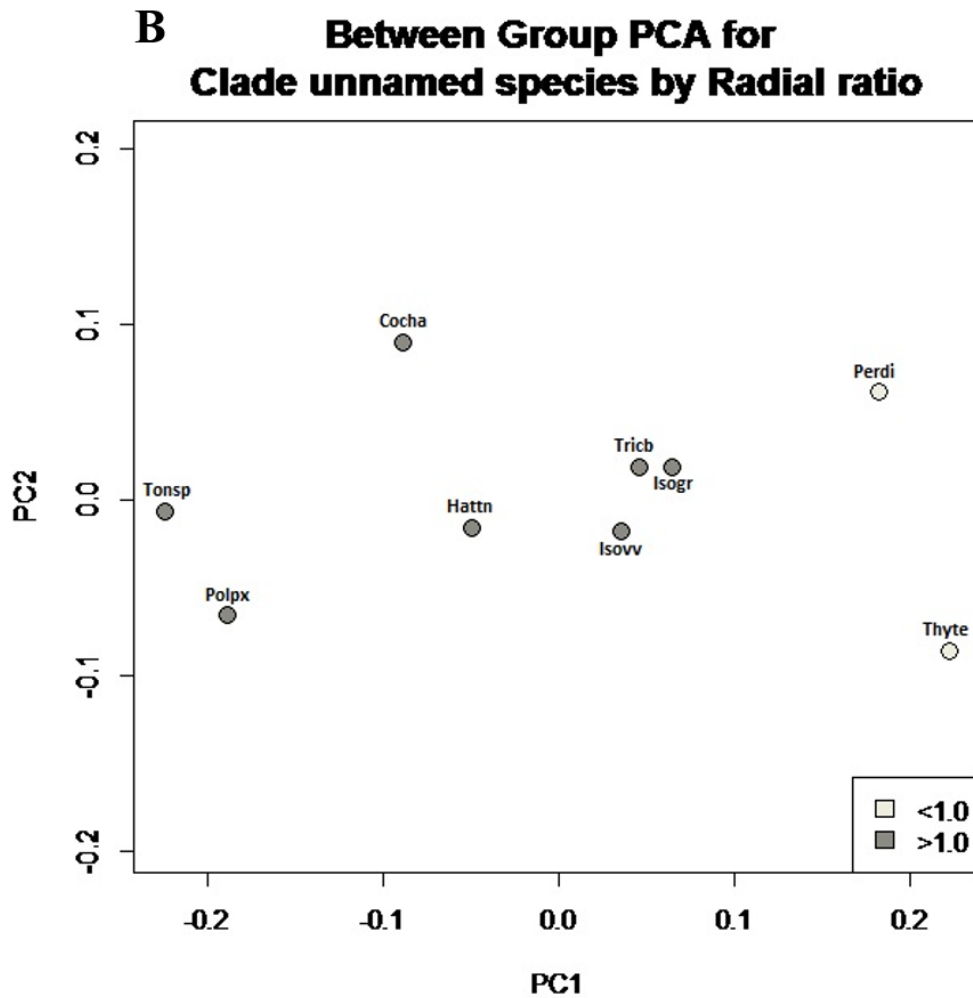


Fig. 34B: Scenario 2 results cont'd of intra-clade variation of clade 'unnamed' and equivalents. B: BGPCA colored by radial ratio showing separation of *P. diomedea* and *T. tenelloides*, supporting the Procrustes ANOVA results (see Appendix Fig. A41B for scenario 1 results; see Fig. 34A for abbreviation names).

vi. *Variation among all species*

After all of the within-subfamily and within-clade variation was examined, the entirety of species configurations was combined to test for significant shape variation among all of the species in this study. With all of the data included, six factors could be tested for significant effect on shape: depth range, specific locality, general region, radial ratio, taxonomic classification, and molecular clade assignment (Table 5). The first two principal components described the non-random variation between all species, encompassing over three-quarters of the total variance in both scenarios (76.0%/76.7%). Shape variation was significantly affected by four of the seven tested factors: depth ( $p =$

0.001/0.001), radial ratio ( $p = 0.001/0.001$ ), subfamily classification ( $p = 0.001/0.001$ ), and clade assignment ( $p = 0.001/0.001$ ). Pairwise tests for depth yielded significant pairings between species from the shallowest depth range (0-50m) and species from the three deepest ranges (101-200m, 201-1000m, and 1001+m) in both scenarios (25 landmarks in scenario 1 versus 26 landmarks in scenario 2). Additionally, scenario 1 paired the two shallowest depths as significant (0-50m and 51-100m), and scenario 2 paired the second range (51-100m) with the fourth range (201-1000m). It is important to keep in mind that pairwise tests are performed on individual configurations, not on mean species shape; thus, the pairings reflect significant differences between some individuals of the paired species, but not necessarily all. Nevertheless, the BGPCA supported the pairwise results for depth, as species lay in an overlapping series along PC1 from deepest (left) to shallowest (right) (Fig. 35B, Appendix Fig. A42B).

Pairwise tests for radial ratio yielded the only pairing possible, between the two levels  $<1.0$  and  $\geq 1.0$ , in both scenarios. There is an obvious connection with height to width ratio and overall shape variance, but testing is still necessary to prove significant or not between species (in this case, it is). A clear separation can be seen along PC1 in the BGPCA (Fig. 35C, Appendix Fig. A42C), with a slight overlap between *Dorometra briseis* ( $<1.0$ ) and *Isometra graminea* ( $\geq 1.0$ ) (see Discussion). As with depth, there is no variance of radial ratio along PC2.

Pairwise tests by subfamily assignment yielded the same nine significant pairings in both scenarios: bathymetrines, heliometrines, thysanometrines, and zenometrid *Psathyrometra* sp. each significantly varied from Antedoninae species and non-antedonoid sisters, with a ninth pairing between antedonines and species of Antedonidae *incertae sedis*. Again, pairwise testing is performed on individuals, so the pairings may not include all species in each subfamily/sister. This notion can be seen in the BGPCA with the pairing of Antedoninae and Thysanometrines species. The two thysanometrines, *Coccometra hagenii* and *Thysanometra tenelloides*, show a wide separation along PC1, and as *T. tenelloides* lies within the antedonines, the significant pairing is clearly only representative of the differences between antedonines and *C. hagenii* (Fig. 35D, Appendix Fig. A42D).

Complete separations between clade assignment can only be seen along PC1 between clades M and N, and clades M and O (Fig. 35E, Appendix Fig. A42E), which are supported by significant pairwise results. The latter is of greater interest, as clade O lies within clade M in the recent phylogenies (Hemery et al. 2013, Rouse et al. in prep.), and thus does not support the molecular work. In addition to these two pairings with clade M, both scenarios yielded significant pairings between clade ‘unnamed’ individuals and individuals of clades N and O after pairwise testing. Scenario 2 resulted in a fifth pairing between clade P and clade ‘unnamed’ individuals, as well (see Discussion).

# A Between Group PCA for ALL species

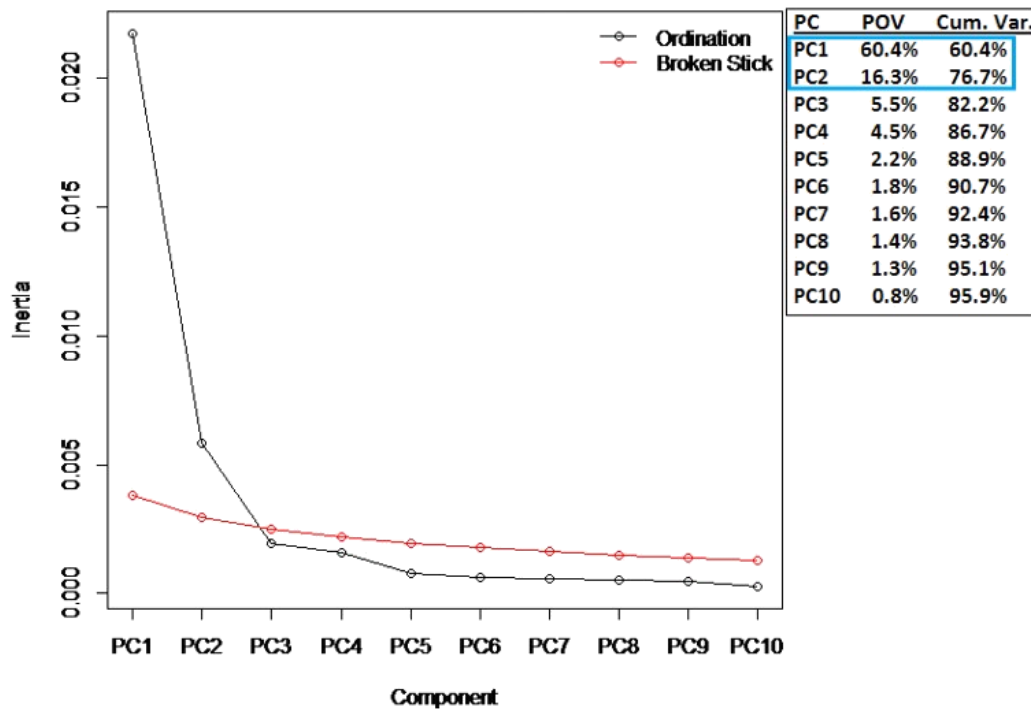
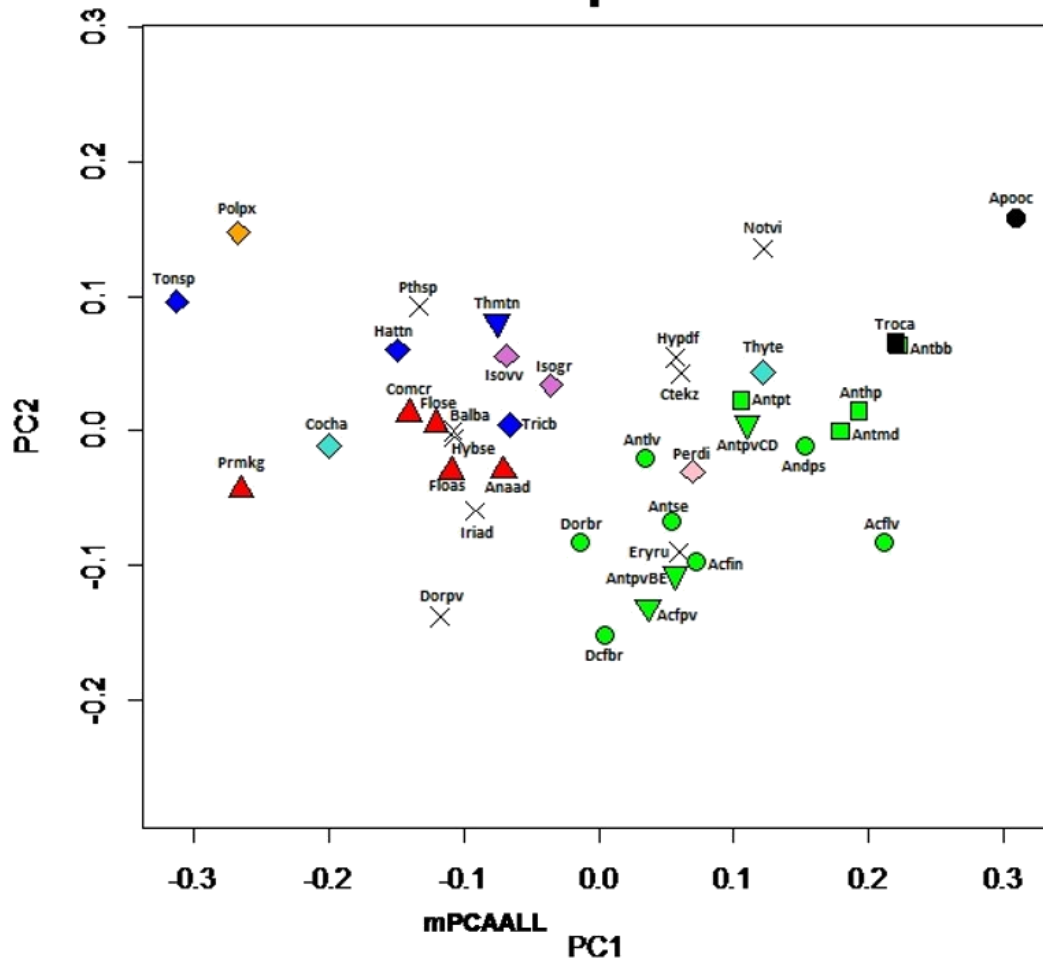


Fig. 35A: Scenario 2. A: BGPCA and broken stick model depicting significant variations between all species used in this study (see Appendix Fig. A42A for scenario 1 results; see Table 5 for species abbreviations) (colored by subfamily: *Antedoninae*, *Bathymetrinae*, *Heliometrinae*, *Isometrainae*, *Thysanometrinae*, *Perometrinae*, *A. incertae sedis*, non-antedonids; symbols by clade:  $\Delta$  = clade M,  $\square$  = clade N,  $\circ$  = clade O,  $\nabla$  = clade P,  $\diamond$  = clade 'unnamed', X = not used in molecular analyses)



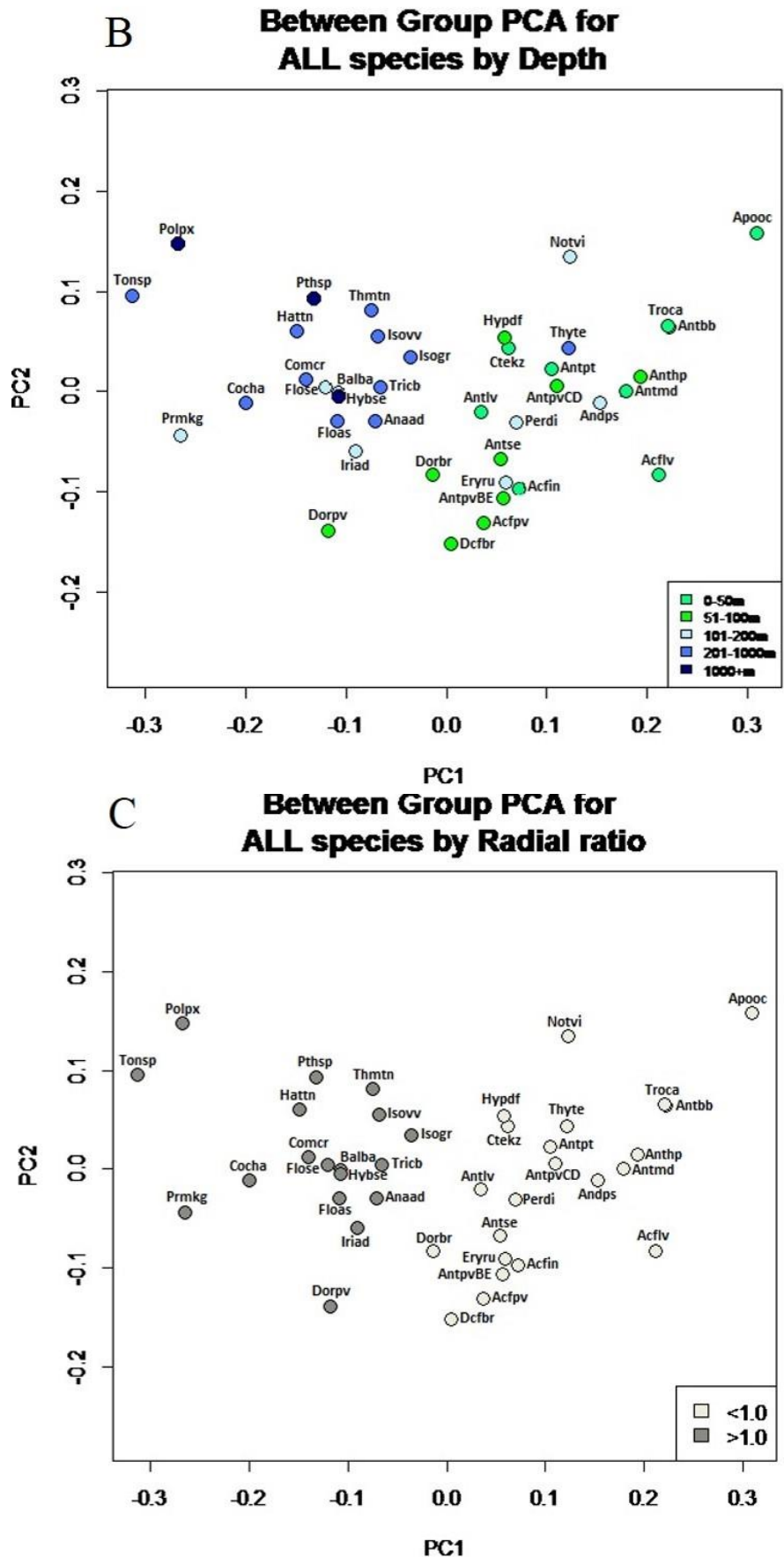


Fig. 35B-C: Scenario 2 results for variations between all species cont'd. B: BGPCA colored by depth. C: BGPCA colored by radial ratio assignment (see Appendix Fig. A42B-C for scenario 1 results; see Table 5 for species abbreviations).

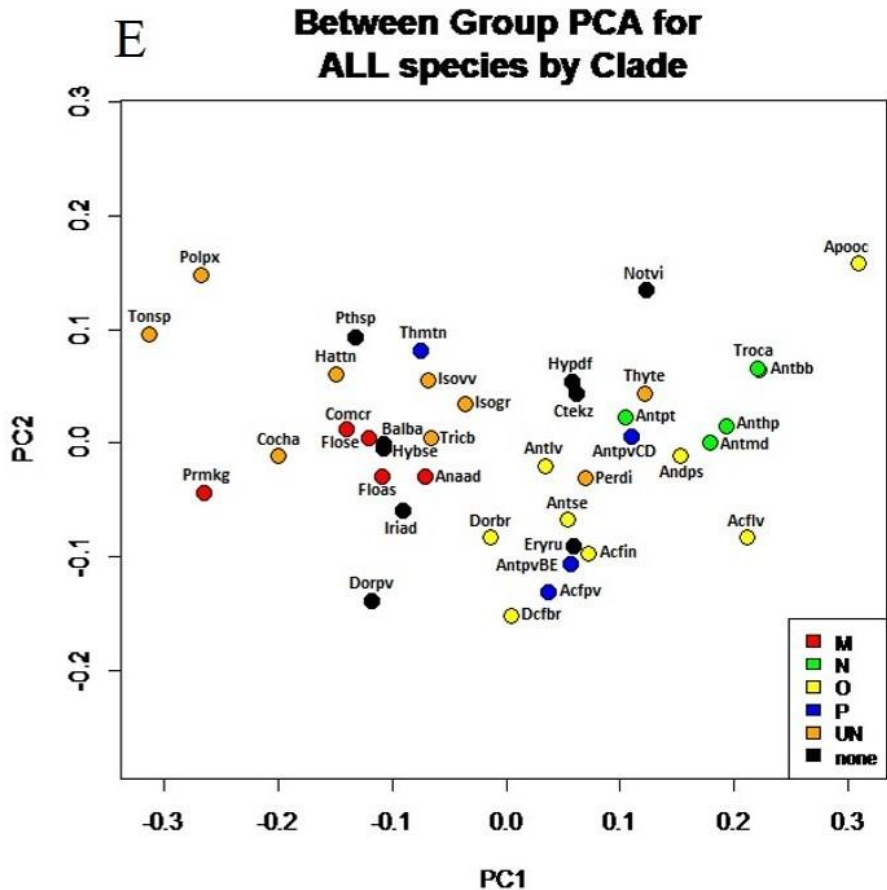
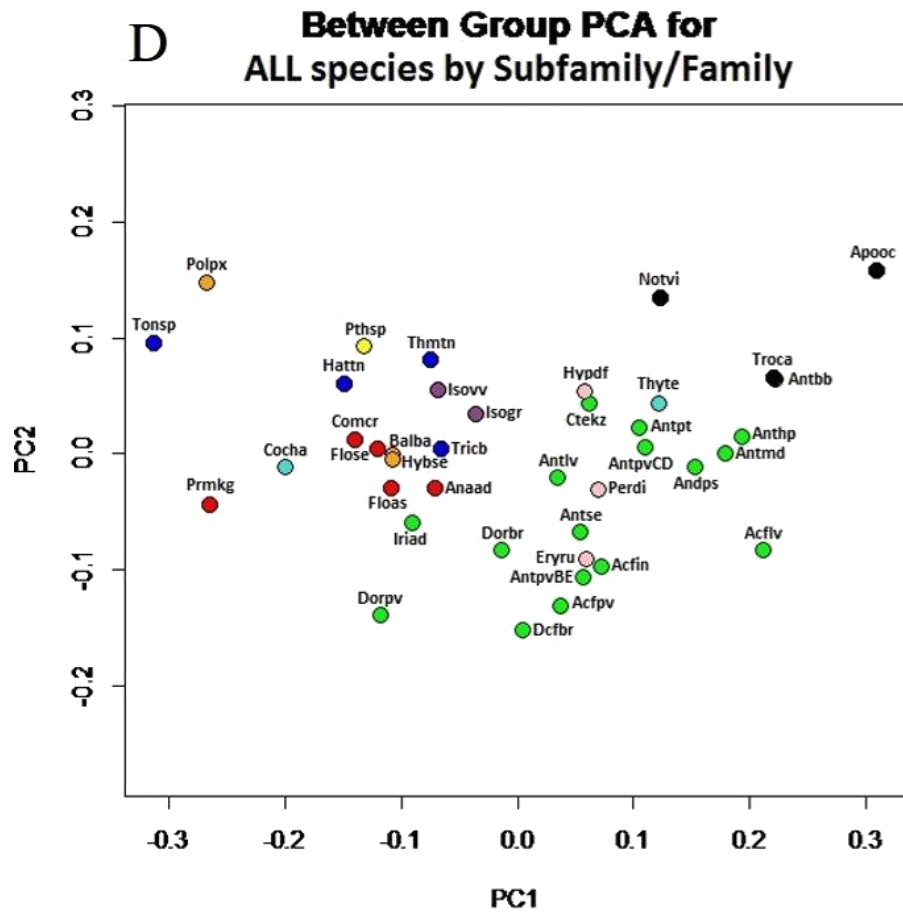


Fig. 35D-E: Scenario 2 results for variations between all species cont'd. D: BGPCA colored by subfamily/family. E: BGPCA colored by clade assignment (see Appendix Fig. A42D-E for scenario 1 results; see Table 5 for species abbreviations).

### vii. *Misclassifications through LOOCV*

The results of the leave-one-out cross validation (LOOCV) through Linear Discriminant Analysis (LDA) were almost identical in both scenarios, except for one fewer misclassification in scenario 2 (Appendix Tables A3 & A4). Two species could not be tested through cross-validation (*Balanometra balanoides* and *Isometra vivipara*), as only one individual was available for each. Four of the 40 study species had the lowest hit ratios of 0%, meaning that all of their individuals were misclassified as another species after cross-validation: both individuals of *Antedon* c.f. *incommoda* were misclassified as *Perometra diomedea*, both individuals of the group *Antedon parviflora* B&E were classified as *Antedon serrata*, the two *Erythrometra rubra* individuals were returned as *Andrometra psyche* and *Antedon loveni*, and the two *Iridometra adrestine* individuals were classified as *Antedon petasus* and *Dorometra parvicirra* (see Discussion).

Three species had the next lowest hit ratio (66.7%) in both scenarios with one individual misclassified: *Antedon serrata* returned as *Antedon loveni*, and both *Isometra graminea* and *Trichometra cubensis* returned as *Hybometra senta*. One individual of *Antedon petasus* was misclassified as *Antedon hupferi* (75% hit ratio), and vice versa (87.5% hit ratio) in both scenarios. One of the four *Comatonia cristata* specimens was returned as *Hathrometra tenella* (80% hit ratio). The group *Antedon parviflora* C&D had no misclassifications in scenario 2, but yielded only a 50% hit ratio in scenario 1, with the return of one individual as *Antedon loveni*. The remaining 27 species had no misclassifications in either scenario, yielding an overall correct classification rate of 92.24% for scenario 1 and 92.56% for scenario 2.

### B. Discussion

The lack of significant variance within any of the individuals examined in this study allowed usage of mean configurations as the individual datum in subsequent intra-specific testing. Of the 40 species examined for intra-specific variation, 21 showed some significant variance between their individuals. Of the seven species whose variances were discernable with pairwise testing, only one revealed any significant allometric effect (*Antedon loveni*). However, most of the significantly variant species varied between those

individuals with the largest differences in radial width or height, or syzygy diameter, so some sort of size effect is taking place. The shift in a significance pairing among *Florometra asperimma* individuals from C&E in scenario 1 to B&C in scenario 2 suggested the importance of landmark #1 in adding information to the configuration data, as there were no size differences between individuals B&E. Significant results within over half of the examined species seemed discouraging at first, but variation among individuals of other taxa (e.g. *Homo sapiens*) is common, and an individual may still be acceptable as a representative of a species as long as there is uniformity within the individual (i.e. identical hands) (Lenaïg Hemery, personal communication). Therefore, mean configurations were used as species datum for subsequent intra-generic, intra-subfamily, and intra-clade testing.

Of the four genera tested for intra-generic variability, only *Antedon* showed significant variances. Pairwise tests revealed significant shape differences between clade N Atlantic *Antedon* species and both clade O and P Pacific species. Region is the main factor affecting shape variance, at least among the factors in this study, although phylogenetics may also be playing a role.

Two of the seven morphologically-based subfamilies revealed significant variations during intra-subfamily testing. Antedoninae exhibited results similar to those within the genus *Antedon*, with regional and molecular effects on overall radial shape. Additionally, radial ratio has a significant affect, with several pairings between Atlantic antedonines and the two species with radial H:W ratio >1.0 (*Dorometra parvicirra* and *Iridometra adrestine*). This strengthens the regional effect on overall radial shape, at least within this subfamily. The two species representing the subfamily Thysanometrinae, *Coccometra hagenii* and *Thysanometra tenelloides*, varied significantly in radial ratio, general region, and specific locality. Although they fall within the same phylogenetic clade, they are not close sisters, and their otherwise clear differences support the disbanding of this morphological subfamily.

Clades O and ‘unnamed’ revealed significant variances during the intra-clade variability testing, although neither could strongly disprove morphological support. Clade O showed significant effect by taxonomic classification (the antedonine representatives

against non-antedonid *Aporometra occidentalis*) but still supports the inclusion of Pacific antedonids within the same clade as none were significantly variant with each other. Clade ‘unnamed’ results in significant variances affected by radial ratio. However, the two species that differed in radial ratio from the other clade ‘unnamed’ species examined in this study, *Perometra diomedea* and *Thysanometra tenelloides*, are not the same species as used in the molecular phylogenies, which may have affected the significance outcome within this clade.

The morphological variation between the species in this study has proven to be significantly associated with molecular clade assignment, as well as taxonomic assignment and depth range. All nine species assigned to the shallowest depth range (0-50m), and all but one of the nine species from 51-100 m (*Dorometra parvicirra* excepted) shared a radial ratio H:W <1.0. Half of the eight species recorded from 101-200m had ratios  $\geq 1.0$  and half <1.0. All but one of the eleven species from 201-1000 m (*Thysanometra tenelloides* excepted) and all three species from >1000 m had ratios  $\geq 1.0$ . This arrangement supports the morphometric results of this study, indicating that depth has a significant effect on radial shape. However, collected depth information was not available for all specimens in this study, so information had to be taken from other sources (e.g. *Anthometrina adriani* and *Isometra graminea* depths were taken from Eléaume et al. 2014). As many antedonids have wide depth ranges (Table 5), specimens from different depths could impede this pattern of radial shape with depth. It would be interesting to examine radial shape between specimens of the same species collected at their extreme depth range limits to determine if any significant intra-specific variations exist relative to depth.

Although shape varied significantly by region within the antedonines, no such effect appeared between all species. All geographic regions contain species with both H:W radial ratios <1.0 and >1.0, however species with H:W <1.0 were restricted to the shallower depths (0-200 m).

i. *Scenario 1 versus Scenario 2*

Two landmark/image combinations from the percent of lost data equation (Cordeiro Estrela de Andrade Pinto 2005) yielded the least percent of lost data for analysis (see *Landmarking*). Because the two scenarios were so similar, it was decided to analyze both and compare them. The two scenarios did not differ substantially in overall variance. However, inclusion of landmark #1, and possibly the smaller sample size of certain species, showed some minor effects on a few intra-group variances, as well as on the results of similarity testing.

*Florometra asperrima* was the only individual whose variance pairings differed between the scenarios. As sample size of this species did not change, it was the additional information from landmark #1 that caused a reduction in variance between individuals, C and E (which were variant in scenario 1), and created variance between individuals, C and B. An additional significant pairing between individuals within Antedoninae also arose in scenario 2, between *Ctenantedon kinziei* and *Antedon bifida bifida*. While the added coordinate information could have been the cause of this new pairing, it is also possible that the reduced sample size of *A. bifida bifida*, from 11 configurations to 9 between scenarios, could have also caused this result.

In testing variation among all species in this study, significant depth pairings changed between the two scenarios. There was a loss of variance between the first two ranges (0-50m and 51-100m) and an added variance between the second and fourth ranges (51-100m and 201-1000m) in scenario 2 compared to scenario 1. This change involved members belonging to the second depth range, and since none of these species had sample size changes between scenarios, this pairing alteration was the effect of additional information from landmark #1.

The overall correct classification rate from linear discriminant analysis (LDA) after leave-one-out cross validation (LOOCV) was very high for both scenarios (92.24%/92.56%), supporting the discriminatory strength of the LDA algorithm. The inclusion of landmark #1 in scenario 2 added the information necessary to correctly classify both individuals of *Antedon parviflora* C&D, and is the reason for the slightly higher correct classification rate.

Now that all of the variances between species' radial shape have been recognized, morphological similarities were examined through clustering models and independent sample t-tests.

## VI. Application for crinoid classification

### A. Results

#### i. UPGMA Hierarchical Clustering

The results of the clustering models based on Procrustes distances are almost identical between the two scenarios. This bottom-up clustering method begins with pairing the shortest Procrustes distances – those between *Hathrometra tenella* and *Comatonia cristata*, *Antedon serrata* and *A. parviflora* B&E, *A. bifida bifida* and *A. hupferi*, and *Iridometra adrestine* and *Trichometra cubensis*, then clustering by increasing distances using averages (Appendix Tables A5 & A6). Two main groups resulted from clustering by Procrustes distances, distinct in their radial ratio factor levels ( $<1.0$  and  $\geq 1.0$ ), with non-antedonid *Aporometra occidentalis* as the obvious outlier ( $<1.0$ ). Although *A. occidentalis* does have the smallest average radial ratio (0.49), the Procrustes distances are calculated from the sum of differences from all coordinate data (or PCs in this study), so it cannot be assumed (and is not the case) that the species with the shortest ratio will be least similar to the species with the largest ratio, and so on (see Discussion).

A few slight clustering differences appeared between the two scenarios, most likely due to the inclusion of landmark #1 in scenario 2. *Antedon parviflora* C&D, while measuring closest to *A. hupferi* in scenario 1, measured closest to *Ctenantedon kinziei* in scenario 2 (Table 7), causing it to join the *A. petasus* - *C. kinziei* pair sooner than in scenario 1 (Figs. 36 & 37). Four additional species (*Balanometra balanoides*, *Dorometra briseis*, *Thaumatometra tenuis*, and *Tropiometra carinata*) measured closest to different species in scenario 2 than in scenario 1 (Table 7). However, none of these changes had any effect on their position in the clustering models. The species' farthest relatives were consistent across the two scenarios, with the shorter radial ratio species farthest from *Tonrometra spinulifera* (with the second largest radial ratio) and all of the larger ratio

species farthest from *Aporometra occidentalis* (with the smallest radial ratio). One exception was *Notocrinus virilis* which was least similar to *Promachocrinus kerguelensis* (largest radial ratio) in scenario 1 and *T. spinulifera* in scenario 2.

Unlike the Procrustes based clustering models, results based on Mahalanobis distances showed several differences in species position between the two scenarios. (Figs. 38 & 39, Appendix Tables A7 & A8). Only two changes in closest morphological relative appeared between the scenarios (Table 7), although only one directly affected the primary cluster pairings. As a result, the majority of clustering differences between scenarios were likely affected by this new primary pairing, as well as by the addition of landmark #1 in scenario 2. This new primary pairing and additional landmark either increased or decreased Mahalanobis distances between certain species and also the subsequent clusters that resulted from the affected averages. An example of this cascade of effects was the pairings of *Antedon loveni* – *Isometra graminea* and *Perometra diomedea* – *Tropiometra carinata* in scenario 1 versus *A. loveni* – *P. diomedea*, *T. carinata* – *Aporometra occidentalis*, and *I. graminea* – (*Hybometra senta* – *Trichometra cubensis*) in scenario 2 (Fig. 39). It is important to note that the pairing of *A. occidentalis* and *T. carinata* in scenario 2 does not mean that they became more closely related with the addition of landmark #1. The distances between these two and between *A. occidentalis* and *Notocrinus virilis* are almost identical in both scenarios; but the primary pairing that occurred between *T. carinata* and *Perometra diomedea* in scenario 1 left *Notocrinus virilis* as the closest remaining relative to *A. occidentalis*. Both the measured distances and the effect of averages needed to be taken into account when reading these phenograms (see Discussion).

Morphological outliers are at least consistent between the two scenarios, with the majority of the shorter radial species furthest from *Poliometra prolixa* and most of the taller radial species furthest from either *Notocrinus virilis* or *Aporometra occidentalis*.

Both Procrustes and Mahalanobis distances included all variable data – coordinates or principal components – in their calculations, which yielded information about overall shape similarities between species. In order to determine similarities between specific areas within the radials, independent sample t-tests were performed on inter-landmark measurements of all images.



Table 7: Table of closest morphological relatives based on both Procrustes distances (P) and Mahalanobis distances (M) for both scenarios (SC1 & SC2)

Species	P - SC1	P - SC2	M - SC1	M - SC2
<i>Antedon c.f. incommoda</i> (Acfin)	Perdi	Perdi	Perdi	Perdi
<i>Antedon c.f. loveni</i> (Acflv)	Anthp	Anthp	AntpvBE	AntpvBE
<i>Antedon c.f. parviflora</i> (Acfpv)	Dcfbr	Dcfbr	Dcfbr	Dcfbr
<i>Anthometrina adriani</i> (Anaad)	Floas	Floas	Comcr	Comcr
<i>Andrometra psyche</i> (Andps)	Troca	Troca	Antlv	Antlv
<i>Antedon bifida bifida</i> (Antbb)	Anthp	Anthp	Anthp	Anthp
<i>Antedon hupferi</i> (Anthp)	Antbb	Antbb	Antpt	Antpt
<i>Antedon loveni</i> (Antlv)	Antse	Antse	Isogr	Perdi
<i>Antedon mediterranea</i> (Antmd)	Antpt	Antpt	Antpt	Antpt
<i>Antedon petasus</i> (Antpt)	Ctekz	Ctekz	Anthp	Anthp
<i>Antedon parviflora</i> B&E (AntpvBE)	Antse	Antse	Antse	Antse
<i>Antedon parviflora</i> C&D (AntpvCD)	Anthp	Ctekz	Antlv	Antlv
<i>Antedon serrata</i> (Antse)	AntpvBE	AntpvBE	AntpvBE	AntpvBE
<i>Aporometra occidentalis</i> (Apoooc)	Troca	Troca	Troca	Troca
<i>Balanometra balanoides</i> (Balba)	Isogr	Comcr	Hattn	Hattn
<i>Coccometra hagenii</i> (Cocha)	Hybse	Hybse	Comcr	Comcr
<i>Comatonia cristata</i> (Comcr)	Hattn	Hattn	Anaad	Anaad
<i>Ctenantedon kinziei</i> (Ctekz)	Antpt	Antpt	Antlv	Antlv
<i>Dorometra c.f. briseis</i> (Dcfbr)	Acfpv	Acfpv	Acfpv	Acfpv
<i>Dorometra briseis</i> (Dorbr)	Antse	Dcfbr	Iriad	Iriad
<i>Dorometra parvicirra</i> (Dorpv)	Iriad	Iriad	Iriad	Iriad
<i>Erythrometra rubra</i> (Eryru)	Antlv	Antlv	Antlv	Antlv
<i>Florometra asperrima</i> (Floas)	Flose	Flose	Flose	Flose
<i>Florometra serratissima</i> (Flose)	Floas	Floas	Floas	Floas
<i>Hathrometra tenella</i> (Hattn)	Comcr	Comcr	Comcr	Comcr
<i>Hybometra senta</i> (Hybse)	Tricb	Tricb	Tricb	Tricb
<i>Hypalometra defecta</i> (Hypdf)	Perdi	Perdi	Isogr	Isogr
<i>Iridometra adrestine</i> (Iriad)	Tricb	Tricb	Dorpv	Dorpv
<i>Isometra graminea</i> (Isogr)	Tricb	Tricb	Antlv	Antlv
<i>Isometra vivipara</i> (Isovv)	Isogr	Isogr	Hattn	Hattn
<i>Notocrinus virilis</i> (Notvi)	Hypdf	Hypdf	Hypdf	Hypdf
<i>Perometra diomedea</i> (Perdi)	Antlv	Antlv	Antlv	Antlv
<i>Poliometra prolixa</i> (Polpx)	Tonsp	Tonsp	Tonsp	Tonsp
<i>Promachocrinus kerguelensis</i> (Prmkg)	Comcr	Comcr	Comcr	Comcr
<i>Psathyrometra</i> sp. (Pthsp)	Hattn	Hattn	Thmtn	Thmtn
<i>Thaumatometra tenuis</i> (Thmtn)	Tricb	Isogr	Pthsp	Hattn
<i>Thysanometra tenelloides</i> (Thyte)	Antpt	Antpt	Antpt	Antpt
<i>Tonrometra spinulifera</i> (Tonsp)	Polpx	Polpx	Hattn	Hattn
<i>Trichometra cubensis</i> (Tricb)	Iriad	Iriad	Hybse	Hybse
<i>Tropiometra carinata</i> (Troca)	Antbb	Anthp	Anthp	Anthp

UPGMA Hierarchical clustering phenogram  
(Procrustes distance, scenario 1)

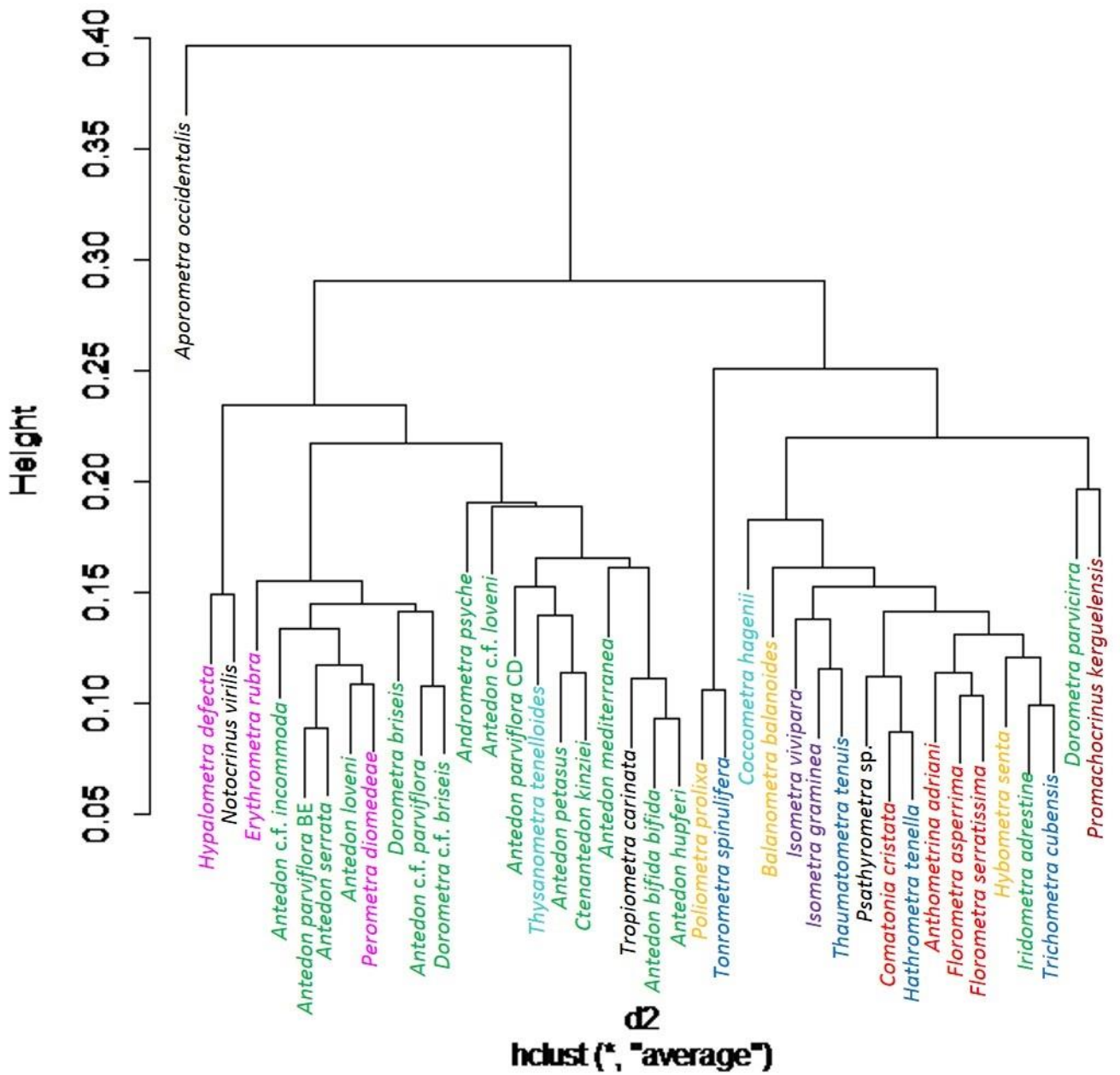


Fig. 36: UPGMA Hierarchical clustering model for scenario 1 data, based on Procrustes distances (see Appendix Table A5 for Procrustes distance values). The phenogram is colored by subfamily (reference Fig. 2A & 2B-F).

UPGMA Hierarchical clustering phenogram  
(Procrustes distance, scenario 2)

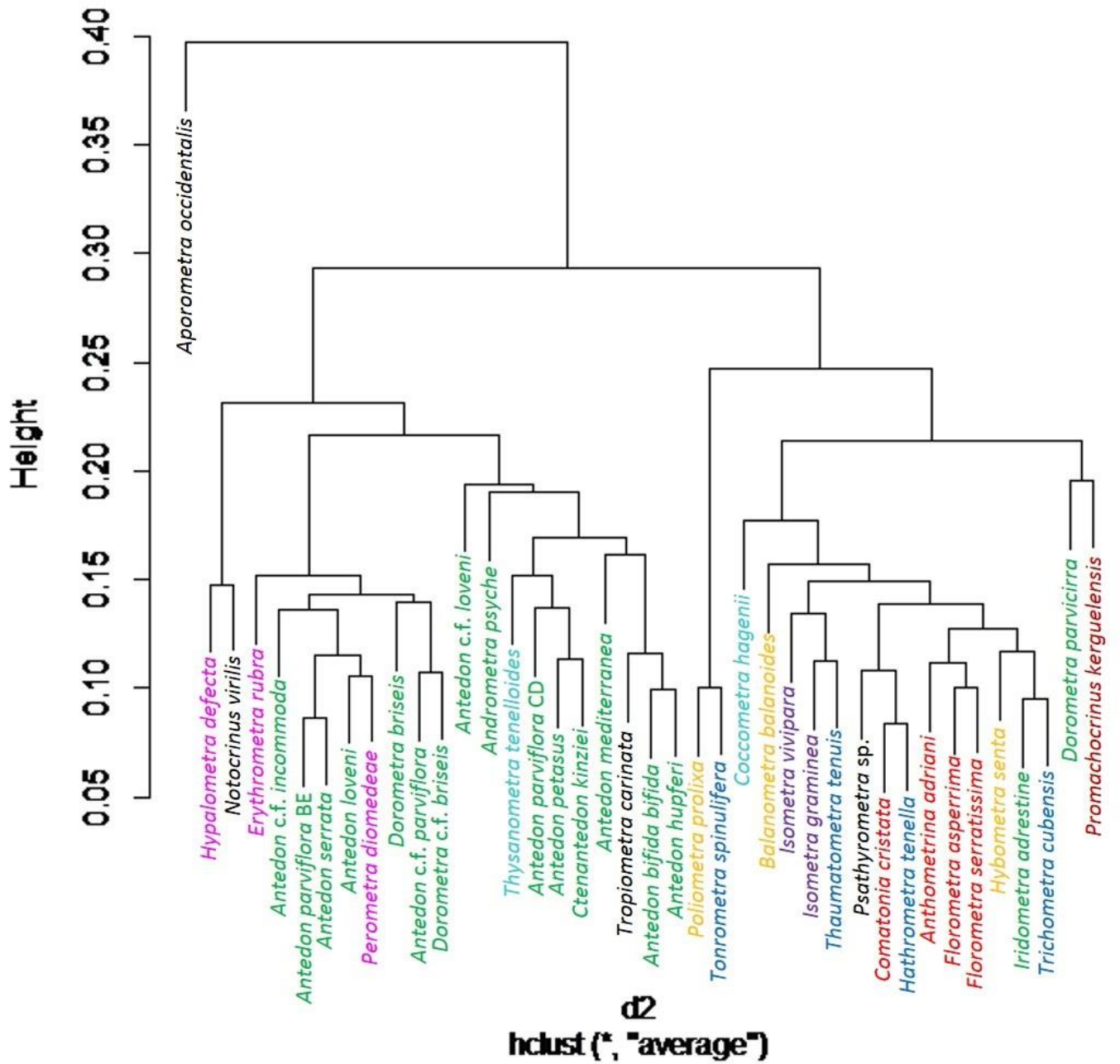


Fig. 37: UPGMA Hierarchical clustering model for scenario 2 data, based on Procrustes distances (see Appendix Table A6 for Procrustes distance values). The phenogram is colored by subfamily (reference Fig. 2A & 2B-F).

UPGMA Hierarchical clustering phenogram  
(Mahalanobis distance, scenario 1)

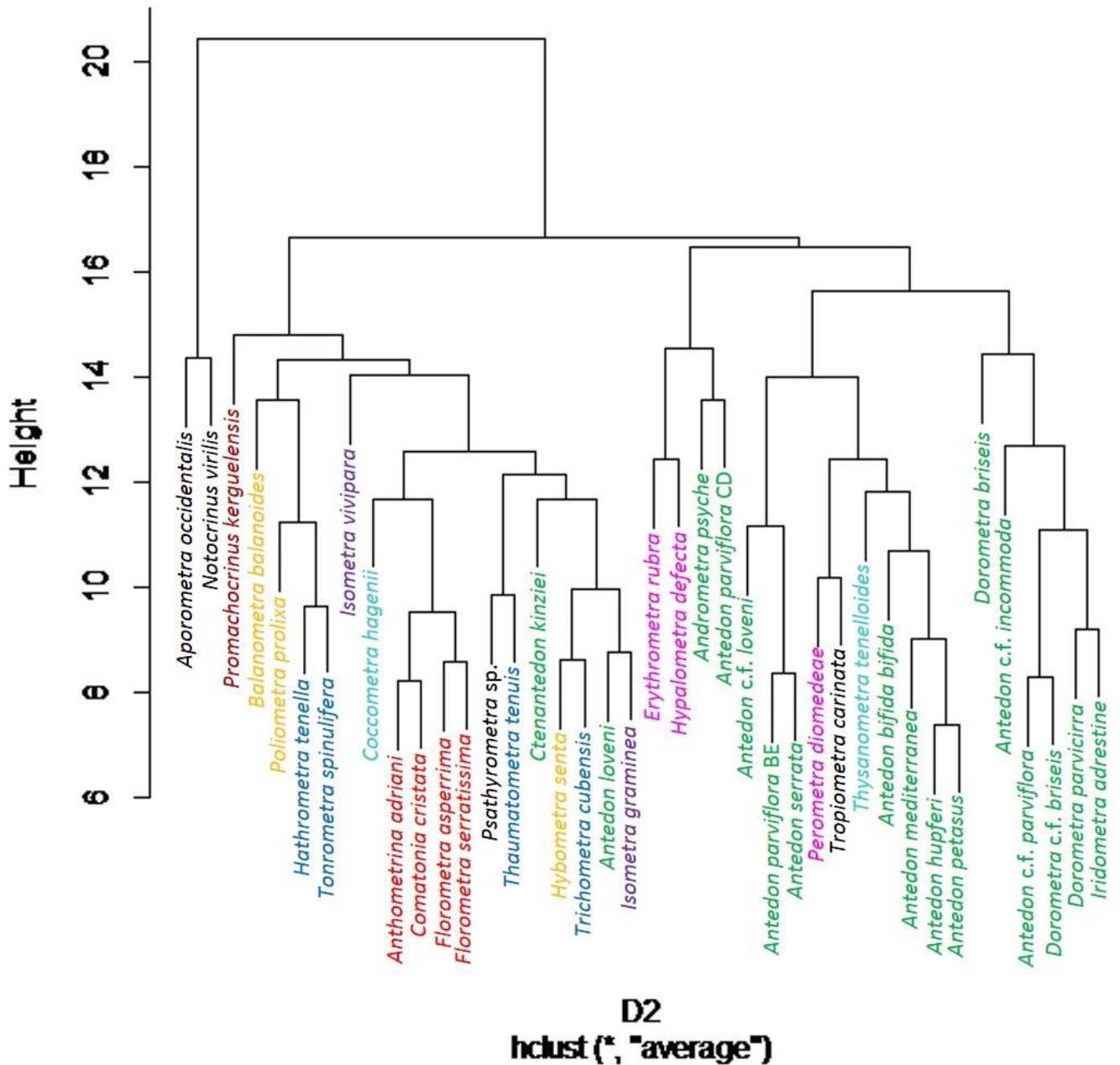


Fig. 38: UPGMA Hierarchical clustering model for scenario 1 data, based on Mahalanobis distances (see Appendix Table A7 for Procrustes distance values). The phenogram is colored by subfamily (reference Fig. 2A & 2B-F).

## UPGMA Hierarchical clustering phenogram (Mahalanobis distance, scenario 2)

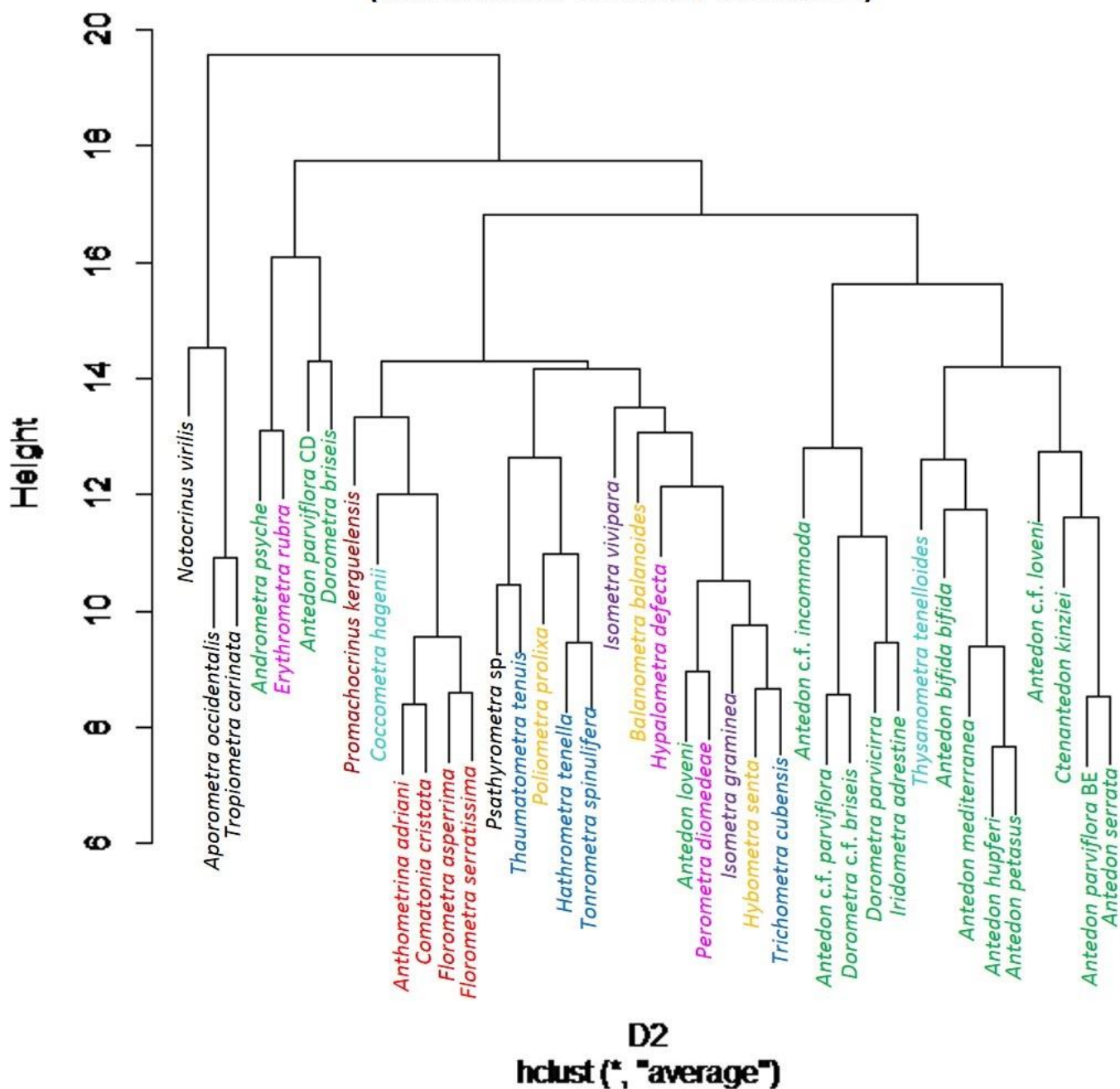


Fig. 39: UPGMA Hierarchical clustering model for scenario 2 data, based on Mahalanobis distances (see Appendix Table A8 for Procrustes distance values). The phenogram is colored by subfamily (reference Fig. 2A & 2B-F).

ii. *Inter-landmark measurements*

Twelve inter-landmark measurements were made on each radial image after digitizing (Fig. 9) with tpsDig2 1.58 (Rohlf 2006). Each measurement was divided by a standard measurement, between landmarks #17 and #28 (Table 6, Appendix Table A2), in order to remove any within-individual variation. Measurements included heights and widths of all attachment fossae, as well as measurements of the central canal, and were tested in a pairwise manner to identify significant differences between species. The non-significant results of the independent sample t-tests were of particular interest in this study, and are referred to as “sharing” measurements. They were used to find specific morphological connections between species and were compared with the phenograms. It is important to note that t-tests take into account measurements of all individuals in each species. The average of measurements is used to compare between species (a pair of species at a time and each inter-landmark measurement at a time); because not all species were represented by the same number of individuals, these results contain an element of bias.

a. *Clade O taxa*

*Antedon* c.f. *incommoda* shared between three (with *A. occidentalis*) and 11 (with *Antedon serrata*) measurements with the other clade O species (six antedonines, *Antedon* c.f. *loveni*, *A. loveni*, *A. serrata*, *Andrometra psyche*, *Dorometra briseis*, and *D.* c.f. *briseis*, and one non-antedonid, *Aporometra occidentalis*); all shared similarities in the height of their left interarticular ligament fossa and width of their central lumen. *Antedon* c.f. *incommoda* shared between six and 12 measurements with all other antedonines, the same ones shared by clade O species plus the widths of their right interarticular ligament fossa and aboral ligament fossa. *Antedon* c.f. *incommoda* shared all of its inter-landmark measurements with *Perometra diomedae*, supporting its misclassification under cross validation and the phenograms. However, it also shared all inter-landmark measurements with *Iridometra adrestine* but was not misclassified as this species.

*Antedon* c.f. *loveni* shared at least two of the twelve measurements with all antedonines except *Antedon loveni*. Although *A. cf. loveni* did not differ significantly from *A. loveni* in overall shape, the fact that it shares no inter-landmark measurements supports its original identification as tentative. *Antedon cf. loveni* shared the most (11)

measurements with *Antedon parviflora* C&D, nine with its closest Mahalanobis distance relative, *Antedon parviflora* B&E, and only three with its closest Procrustes distance relative, *Antedon hupferi*.

*Antedon loveni* shared at least some inter-landmark measurements with all antedonines (except *A. c.f. loveni*, as noted above), the most (11) with *Antedon parviflora* C&D. Fellow Australian and clade O species *Aporometra occidentalis* only shared one measurement with *A. loveni*: height of left adoral muscle fossa. Although *A. loveni* was not misclassified in cross validation, three separate species were misclassified as *A. loveni*, all of which shared several measurements with it: *Erythrometra rubra* and *Antedon serrata* (also its closest Procrustes distance-based relative) both shared 10 measurements and *Antedon parviflora* C&D shared 11. The closest Mahalanobis distance-based relatives (Table 7), *Isometra graminea* and *Perometra diomedea*, shared six and seven measurements with *A. loveni*, respectively.

*Andrometra psyche* shared between four and eleven measurements with all other antedonines and clade O species. It shared the most measurements (11) with fellow Japan species, *Antedon parviflora* C&D and *Iridometra adrestine*. Although *A. psyche* itself was not misclassified in the cross validation, one *Erythrometra rubra* specimen was misclassified as *A. psyche* in both scenarios; the two shared eight measurements. The closest Procrustes distance-based relative of *A. psyche*, *Tropiometra carinata*, shared seven measurements, six heights and one width. The closest Mahalanobis distance-based relative, *Antedon loveni*, shared nine measurements with *A. psyche*. All clade O species share similar height measurements of both fossae.

*Dorometra c.f. briseis* shared between one and eight measurements with all other antedonines except Atlantic *Ctenantedon kinziei*, and between two and seven measurements with all other clade O species except *Aporometra occidentalis*. It shared the most measurement similarities (10) with perometrine *Erythrometra rubra*, but only four with its closest distance-based relative, *Antedon c.f. parviflora*.

*Dorometra briseis* shared between one and 11 inter-landmark measurements with all other antedonines, between three and nine measurements with clade O species, but none with *A. occidentalis*. It shared seven and three measurements, respectively (both sharing muscle fossae heights), with its closest Procrustes-based relatives, *Antedon*

*serrata* and *Dorometra* c.f. *briseis*, and all measurements except for central lumen width with its closest Mahalanobis-based relative *Iridometra adrestine*. Additionally, it shared all measurements but width of the right muscle fossa with *Antedon parviflora* C&D.

*Antedon serrata* shared between two and 11 inter-landmark measurements with all antedonines, the majority (11) with other Pacific species *Antedon* c.f. *incommoda* and *Antedon* c.f. *parviflora*, along with perometrine *Erythrometra rubra*. It shared three to 11 measurements with all clade O species. Ten measurements were shared between *A. serrata* and its closest distance-based relative, *Antedon parviflora* B&E, differing in both muscle fossae heights. *A. serrata* also shared ten measurements with *Antedon loveni*, differing only in interarticular ligament fossae heights and causing a misclassification in the cross validation.

Non-antedonid sister *Aporometra occidentalis* shared few measurements with only four clade O species: *Antedon loveni* (shared one measurement), *Antedon* c.f. *incommoda* (shared three), *Antedon serrata* (shared three), and *Andrometra psyche* (five). Additionally, *A. occidentalis* shared four measurements with *Isometra graminea*, five measurements with *Notocrinus virilis*, and nine measurements with distance-based relative, *Tropiometra carinata*.

#### b. Clade N taxa

Among Atlantic *Antedon* species, *Antedon bifida bifida* shared between two and 10 measurements with the other antedonines, with the most (10) shared with Pacific *Andrometra psyche*. It shared three to six measurements with all other clade N species (four antedonines, *Antedon hupferi*, *A. mediterranea*, and *A. petasus*, and non-antedonid *Tropiometra carinata*), the most (6) with its closest distance-based relative (Table 7) *Antedon hupferi* and non-antedonid *Tropiometra carinata*. No measurements were constant throughout clade N.

Atlantic *Antedon hupferi* shared most measurements with Pacific species *Iridometra adrestine* and *Andrometra psyche* (eight and 10, respectively), despite being morphologically significantly different overall from *I. adrestine*. It shared three measurements with *Antedon mediterranea* and *Antedon petasus* (Mahalanobis distance-based relative and misclassification) and six measurements with *A. b. bifida* (Procrustes



distance-based relative) and non-antedonid *Tropiometra carinata*, all Atlantic specimens in clade N.

*Antedon mediterranea* was morphologically most similar to *Antedon petasus* based on both Procrustes and Mahalanobis distances. However, the two only shared six inter-landmark measurements. *A. mediterranea* shared three to six measurements with all other clade N species, as well as at least three with all antedonines. The most (10) was shared with clade O species *Andrometra psyche*.

*Antedon petasus* shared three measurements with fellow clade N species *A. b. bifida* and *A. hupferi* (its closest Mahalanobis distance-based relative and misclassification), and six measurements with other clade N species *A. mediterranea* and *Tropiometra carinata*. Despite having statistically different overall shapes, *A. petasus* shared the most measurements with *Iridometra adrestine* and was the results from a misclassification of *I. adrestine* in cross validation. The closest Procrustes distance-based relative, *Ctenantedon kinziei*, shared six measurements with *A. petasus*.

Non-antedonid sister, *Tropiometra carinata*, shared at least three inter-landmark measurements with its fellow clade N species, and at least one measurement with all other Caribbean species. The most measurements similarities occurred between *T. carinata* and four species (all of which share similar heights of the right interarticular ligament fossa and the central lumen): *Antedon bifida bifida* (the Procrustes distance-based relative for scenario 1), *Antedon hupferi* (the scenario 2 Procrustes and both Mahalanobis distance-based relatives), *Antedon petasus*, and *Trichometra cubensis*.

### c. Clade P taxa

*Antedon c.f. parviflora* shared between one and 11 measurements with all antedonines except for *Antedon mediterranea*, with which it is significantly variant. It shared measurements with all other clade P species (antedonines *Antedon parviflora* B&E and *A. parviflora* C&D, and bathymetrine *Thaumatometra tenuis*), although only two with non-antedonine *Thaumatometra tenuis*. *Antedon c.f. parviflora* shared the most measurements (11) with three species: *Antedon parviflora* C&D, *Antedon serrata*, and *Erythrometra rubra*. It only shared four measurements with distance-based relative *Dorometra c.f. briseis*. No measurements were shared between *A. c.f. parviflora* and the

other antedonines, but all clade P species shared the measurement of both right and left interarticular ligament fossae widths.

*Antedon parviflora* B&E shared inter-landmark measurements with all clade P species: eight measurements with *Antedon* c.f. *parviflora* and *Thaumatometra tenuis*, and all 12 measurements with *Antedon parviflora* C&D. Despite the two separated *A. parviflora* groups sharing their entirety of measurements, *A. parviflora* B&E is most likely not *Antedon parviflora*, but *Antedon serrata*. *A. serrata* was the closest morphological relative based on both Procrustes and Mahalanobis distances (Table 7), and shared 10 measurements with *A. parviflora* B&E (does not match either muscle fossae height). Procrustes distance-based relatives of *Antedon parviflora* C&D, *Antedon hupferi* and *Ctenantedon kinziei*, shared 11 and 10 measurements respectively, both differing in the right muscle fossa width. Mahalanobis distance-based relative *Antedon loveni* and *Dorometra briseis* both share 11 measurements with *A. parviflora* C&D, differing in the same measurement as the Procrustes distance relatives.

#### d. Clade M taxa

*Anthometrina adriani* shared between three (with *Promachocrinus kerguelensis*) and eight (*Florometra asperrima*) measurements with all heliometrines, although none were constant. It shared at least two measurements with all other clade M species (heliometrines *Comatonia cristata*, *Florometra asperrima*, *F. serratissima*, *Promachocrinus kerguelensis*, and bathymetrine *Thaumatometra tenuis*) and at least one with all Antarctic species, the most measurements shared with *Isometra vivipara* (nine shared measurements). Of the clade M species (and heliometrines), *A. adriani* shared the most measurements (eight) with Procrustes distance relative *Florometra asperrima* and the second most with Mahalanobis distance relative *Comatonia cristata* (six measurements).

*Comatonia cristata* shared at least four inter-landmark measurements with all heliometrine and clade M species, with the most (eight) between *Promachocrinus kerguelensis*. Two Atlantic bathymetrines shared the most measurements (nine) with *C. cristata* between all species: *Trichometra cubensis* and *Hathrometra tenella* (Procrustes distance-based closest relative and misclassification). The closest Mahalanobis distance-

based relative, fellow heliometrine (and clade M species) *Anthometrina adriani*, shared six measurements with *C. cristata*.

*Florometra asperrima* shared at least four similarities with all Heliometrinae and clade M species; the most shared by *Anthometrina adriani* (eight), followed by distance-based relative *Florometra serratissima* (seven). *Florometra serratissima* shared with all of the same species as *F. asperrima*, but with the most (eight) inter-landmark similarities between *Promachocrinus kerguelensis*.

*Promachocrinus kerguelensis* shared three to eight measurements with all heliometrine and clade M representatives. Eight measurements were shared with closest distance-based relative *Comatonia cristata*, the differences all related to width measurements. It shared the most (11) inter-landmark measurements with fellow Antarctic species, the isometrine *Isometra vivipara*, differing only in the height of the left muscle fossa.

e. Clade 'unnamed' taxa

*Hathrometra tenella* shared three to five measurements with its three other bathymetrine representatives, although only the left muscle fossa width was consistently similar. It also shared at least two measurements with all other clade 'unnamed' species in this study (two other bathymetrines, *Tonrometra spinulifera* and *Trichometra cubensis*, two thysanometrines, *Coccometra hagenii* and *Thysanometra tenelloides*, two isometrines, *Isometra graminea* and *I. vivipara*, perometrine *Perometra diomedea*, and one representative of Antedonidae *incertae sedis*, *Poliometra prolixa*), despite having significant overall shape variance with *Thysanometra tenelloides* and *Perometra diomedea*. The largest number of similarities with *H. tenella* exists between a fellow clade 'unnamed' species, *Isometra vivipara*, as well as its closest distance-based relative and cross validation companion, *Comatonia cristata*, with nine shared measurements.

Antarctic bathymetrine, *Tonrometra spinulifera*, shared at least two inter-landmark measurements with all of its regional and taxonomic sisters. Two to six measurements were also shared with all clade 'unnamed' species, with the exception of *Perometra diomedea* (shared no similarities with *T. spinulifera*). The closest Procrustes distance-based relative (Table 7) was fellow bathymetrine, *Hathrometra tenella*, with

which *T. spinulifera* shared only three muscle fossae measurements, while sharing five unsymmetrical measurements with non-bathymetrine and closest Mahalanobis distance-based relative, *Poliometra prolixa*. The most similarities were found with fellow Antarctic species, *Isometra vivipara*, with which *T. spinulifera* shared six unsymmetrical measurements.

Similar to fellow bathymetrine *Hathrometra tenella*, *Trichometra cubensis* shared at least one inter-landmark measurement with all of its taxonomic and cladistic counterparts. It also shared at least one measurement with all Caribbean species and non-antedonine Atlantic species. *Trichometra cubensis* shared seven measurements with its misclassification and closest Mahalanobis distance-based relative, *Hybometra senta*, and shared all but two measurements with closest Procrustes distance-based relative, *Iridometra adrestine* (does not share the heights of the right muscle fossa height or the left interarticular ligament fossa).

*Isometra graminea* differed significantly in overall shape from only one species, *Antedon c.f. parviflora*, and shared measurements with all other Antarctic species, clade ‘unnamed’ species, and its fellow isometrine, *I. vivipara*. All 12 measurements were shared with its subfamilial sister, supporting the idea of these two as variations of the same species (see Discussion). Six measurements were shared between *I. graminea* and closest Mahalanobis distance-based relative, *Antedon loveni*, and nine were shared with closest Procrustes distance-based relative, *Trichometra cubensis*. *Isometra graminea* shared no inter-landmark measurements with *Hybometra senta*, despite its misclassification after cross validation.

*Isometra vivipara* shared at least five inter-landmark measurements with all of its fellow clade ‘unnamed’ representatives and at least six with all other Antarctic species. Nine measurements were shared between *I. vivipara* and its closest Mahalanobis distance-based relative, *Hathrometra tenella*, and all 12 measurements were shared between *I. vivipara* and its closest Procrustes distance-based relative (and fellow isometrine), *I. graminea*.

*Coccometra hagenii* shared at least one inter-landmark measurement with all other representatives of clade ‘unnamed’ except for its previous taxonomic sister, *Thysanometra tenelloides*, with which it was significantly variant in overall morphology.

The most measurements shared with *C. hagenii* was with its closest Mahalanobis distance-based relative, *Comatonia cristata*, with six similarities, although no measurements were shared with its closest Procrustes distance-based relative, *Hybometra senta*.

*Thysanometra tenelloides* shared between two and six measurements with all clade ‘unnamed’ species (except for *C. hagenii*, as stated above). *Thysanometra tenelloides* also shared at least one measurement with all fellow Japan Sea species, especially *Iridometra adrestine*, with which it shared all but four height measurements. The closest distance-based relative, *Antedon petasus*, only shared two measurements with *T. tenelloides*, the heights of both interarticular ligament fossae.

*Poliometra prolixa* shared three to 10 measurements with all representatives from the Northeast Atlantic, all Antedonidae *incertae sedis* species, and all representatives from clade ‘unnamed’, with the exception of *Perometra diomedae*. With closest distance-based relative, *Tonrometra spinulifera*, *P. prolixa* shared five measurements, and with subfamily sister, *Balanometra balanoides*, *P. prolixa* shared all inter-landmark similarities but both aboral ligament fossae measurements.

*Perometra diomedae* shared three to seven of the 12 inter-landmark measurements with its fellow perometrines. It also shared at least two measurements with all other Japan species, the most with both *Antedon serrata* and *Iridometra adrestine* (shared 10 measurements). Muscle fossae height is consistent across the perometrine representatives, as well as with closest distance-based relative, *Antedon loveni*. *A. loveni* shared seven measurements with *P. diomedae*, including all inter-landmark heights.

#### f. *Cladistic outliers*

Cladistic outlier, *Psathyrometra* sp., shared between five and 11 measurements with all North Pacific species, except for *Antedon* c.f. *loveni*. Most inter-landmark similarities occurred with *Balanometra balanoides*, differing only in aboral ligament fossa height. Closest Procrustes distance-based relative, *Hathrometra tenella*, shared nine measurements with *Psathyrometra* sp., conflicting in aboral ligament fossa height as well as both central lumen measurements, while closest Mahalanobis distance-based relative,

*Thaumatometra tenuis*, shared only four measurements: both muscle fossae widths and both interarticular ligament fossae heights.

*Notocrinus virilis* shared at least one inter-landmark measurement with all other Antarctic species, the most (nine) with *Isometra vivipara*. Closest distance-based relative (Table 7), *Hypalometra defecta*, only shared four measurements with *N. virilis*: both muscle fossae heights and both interarticular ligament fossae heights.

*g. Taxa not included in molecular phylogenies*

The following species do not belong to any particular clade as they were not used in the molecular analyses. They are listed below according to morphological taxonomic classification.

*Dorometra parvicirra* shared at least one measurement with all other antedonines, despite some overall significant shape variation between it and *Antedon* c.f. *loveni* and *Antedon bifida bifida*. *D. parvicirra* also shared between two and 11 measurements with all Japan species, with the most similarities (11) shared with both *Erythrometra rubra* and *Iridometra adrestine* (closest distance-based relative).

*Iridometra adrestine* shared numerous inter-landmark similarities with almost half the species in this study, including its fellow Japan species as well as all other antedonines. It shared all twelve measurements with fellow Pacific species *E. rubra* and *A. c.f. incommoda*. It was misclassified after cross validation as *Antedon petasus* and *Dorometra parvicirra*, with which it shared nine and eleven measurements, respectively; it differed from *D. parvicirra* (its closest Mahalanobis distance-based relative) only in left interarticular ligament fossa height. It shared with its closest Procrustes distance-based relative, Atlantic *Trichometra cubensis*, all inter-landmark measurements except for the heights of the right muscle fossa and left interarticular ligament fossa.

Atlantic species *Ctenantedon kinziei*, shared measurements with all other antedonines except for Pacific *Dorometra* c.f. *briseis*. The most number of shared measurements occurred with Pacific antedonine *Iridometra adrestine*, with nine similarities. Closest Procrustes distance-based relative *Antedon petasus* shared six measurements with *C. kinziei*, and closest Mahalanobis relative *Antedon loveni* only shared three.

Among Perometrinae, *Erythrometra rubra* shared over half of its inter-landmark measurements, including muscle fossae heights, interarticular ligament fossae heights, and central lumen measurements, and all 12 of its measurements with fellow Japan species, the antedonine *Iridometra adrestine*. Although all distance-based relatives of *E. rubra* returned as *A. loveni*, and one specimen was misclassified as *A. loveni*, the two species shared no measurements. The other *E. rubra* specimen was misclassified as *Andrometra psyche* in cross validation, with which it shared seven similar measurements.

*Hypalometra defecta* shared at least three inter-landmark measurements with its fellow perometrines, *Perometra diomedae* and *Erythrometra rubra*, muscle fossae height being constant across the subfamily. *H. defecta* also shared at least four measurements with all other Caribbean species, the only constant being right interarticular ligament fossa height. *H. defecta* shared seven measurements with its closest Mahalanobis distance-based relative, *Isometra graminea*, but shared the most with subfamily sister *Erythrometra rubra*, only differing in the widths of both muscle fossae and the aboral ligament fossa.

*Thaumatometra tenuis* shared measurements with all other bathymetrines, including five with its closest scenario 2 Mahalanobis distance-based relative (Table 7), *Hathrometra tenella*, and six with its closest scenario 1 Procrustes distance-relative, *Trichometra cubensis*. Four measurements were shared with the closest Mahalanobis distance-based relative from scenario 1, *Psathryometra* sp., and three measurements were shared with the closest Procrustes distance-based relative from scenario 2, *Isometra graminea*, including both heights of the interarticular ligament fossae. *T. tenuis* shared most of its inter-landmark similarities with fellow Japan Sea species, *Erythrometra rubra*, differing only in muscle fossae and aboral ligament fossa widths.

*Balanometra balanoides* shared six to 12 measurements with seven other species: two fellow North Pacific species (*Florometra asperrima* and *Florometra serratissima*), the two other Antedonidae *incertae sedis* representatives (*Hybometra senta* and *Poliometra prolixa*), and the three species morphologically closest based on Procrustes and Mahalanobis distances. The species with the closest Mahalanobis distance, *Hathrometra tenella*, shared nine inter-landmark measurements, while the two species with the closest Procrustes distances, *Isometra graminea* (scenario 1) and *Comatonia*

*cristata* (scenario 2), joined *Florometra serratissima* in sharing all 12 inter-landmark measurements with *B. balanoides*.

*Hybometra senta* shared most of its inter-landmark measurements with fellow Antedonidae *incertae sedis* representative, *Balanometra balanoides*, excluding the three ligament fossae widths. It shared only the left muscle fossa height measurement with its other subfamily sister, *Poliometra prolixa*, and only the right muscle fossa height with fellow West African species, *Antedon hupferi*; it was significantly variant from both in overall radial shape. Both species misclassified as *H. senta* in cross validation, *Isometra graminea* and *Trichometra cubensis*, shared seven measurements with *H. senta*, five of which were consistent between the three species.

No inter-landmark measurements were shared between all of the species within the subfamilies Antedoninae, Bathymetrinae, Heliometrinae, or Thysanometrinae. One measurement, the height of the left adoral muscle fossa, was shared between all species of Antedonidae *incertae sedis*. Two measurements, the heights of the left and right adoral muscle fossae, were shared between the species of Perometrinae, and all twelve inter-landmark measurements were shared between the two representatives of Isometrinae (see Discussion). The only molecularly assigned clade to share landmark measurements between all of its species was clade P, in which only the widths of both left and right interarticular ligament fossae were shared.

### iii. *Character states in phenograms and phylogenies*

Nine fossa-to-ossicle measurement ratios were calculated for each specimen as size-independent data in an attempt to identify intra-radial character states that correspond to the molecular phylogenies (Appendix Table A9). The ratios were presented as a range for each species based on data from all of their individuals, and the ranges were compared with the phenograms and phylogenies. As with the inter-landmark measurement data, the unbalanced sample sizes between species most likely skewed the data to some degree, giving those with more individuals a larger range. This was taken into account during analysis.



a. *Character states in the phenograms*

Obtaining positive connections with specific intra-radial data and the hierarchical clustering models was unlikely, as the distance measurements used in hierarchical clustering are calculated from the entirety of the coordinate or PC data. Nevertheless, comparisons were made to rule out any missing connections. Only the clustering models based on the Procrustes distances were explored for intra-radial character states, because Mahalanobis distances are calculated in a rescaled space.

As stated above, the UPGMA Hierarchical clustering model based on Procrustes distances formed two main cluster groups in both scenarios, separated by radial ratio factor level, with *Aporometra occidentalis* as the outlier (see UPGMA Hierarchical clustering). The primary clusters, or closest distance-based relatives, were the only groupings to show any majority overlap in seven of the nine ratios (no majority overlap was apparent for muscle fossae height ratios). These results ruled out the idea of any one area skewing similarity data, and support the accuracy of using 2k-4 principal components as an equivalent to all coordinate data for Procrustes distance calculations.

In addition to comparing ratios within each radial (e.g., muscle fossae height to radial height), general radial H:W ratios were explored within the Procrustes distance-based phenograms. Character states were assigned to the two broad clusters, A and B, separated by factor level (with a 1 denoting a ratio  $<1.0$  and a 2 denoting a ratio  $\geq 1.0$ ); then radial ratios, averaged from all individuals for each species, were compared within the two broad clusters (Fig. 40). As with the within-radial ratio results, several, but not all, of the primary clusters (e.g., *Antedon parviflora* B&E – *Antedon serrata*, *Comatonia cristata* – *Hathrometra tenella*) had notably close radial ratios (Fig. 40, Appendix Fig. A43). There was no recognizable pattern of H:W ratios among the finer branches after these primary clusters (e.g., cluster D range (0.79-0.97) overlaps cluster E range (0.66-0.86), cluster H values (1.08 and 1.74) not close).

## UPGMA Hierarchical clustering phenogram (Procrustes distance, scenario 2)

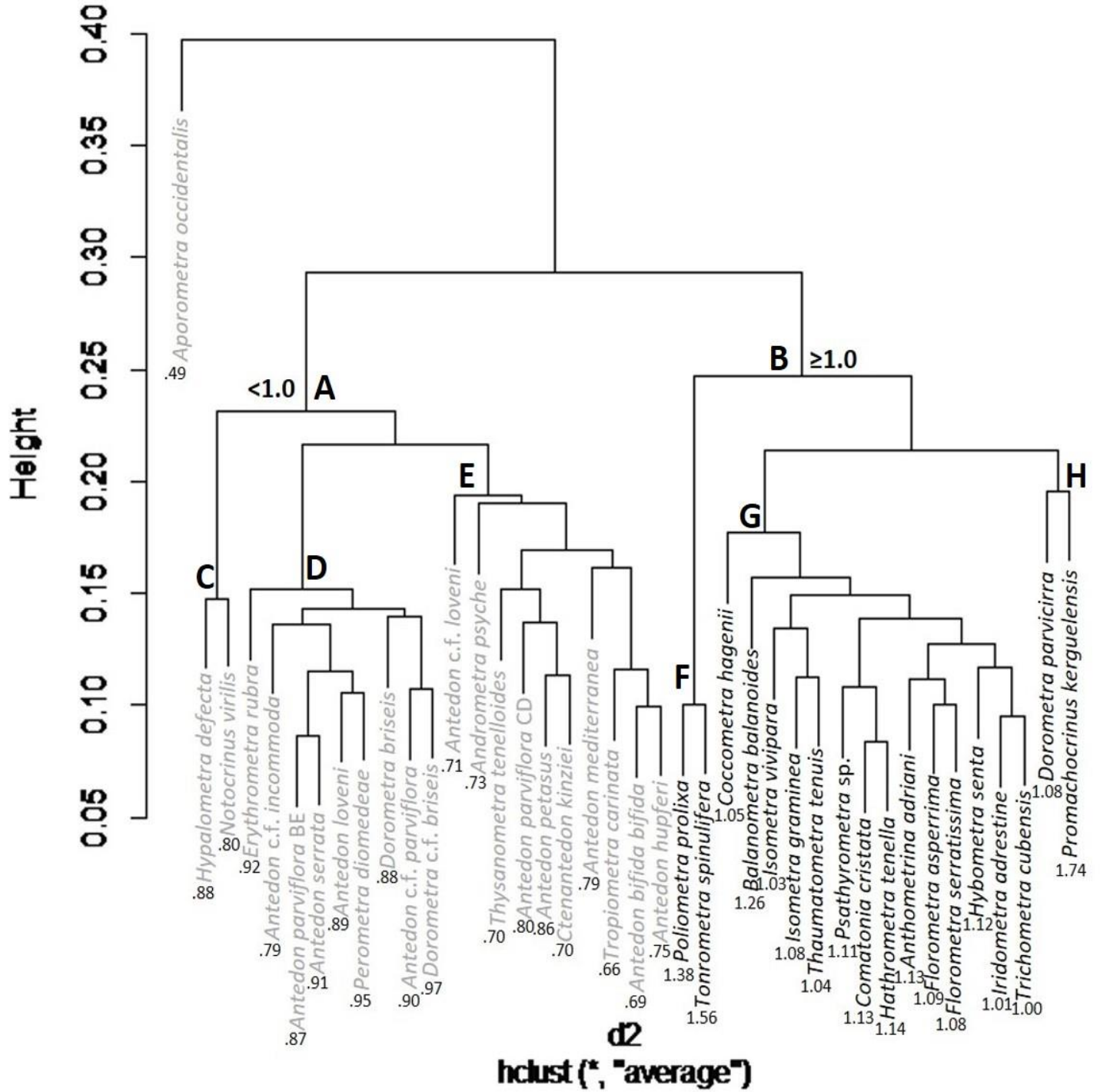


Fig. 40: Scenario 2 UPGMA Hierarchical clustering model based on Procrustes distances; colored by broad radial ratio ( $< 1.0$  = gray,  $\geq 1.0$  = black) with specific ratios at species terminals (see Appendix Fig. A43 for scenario 1 results).

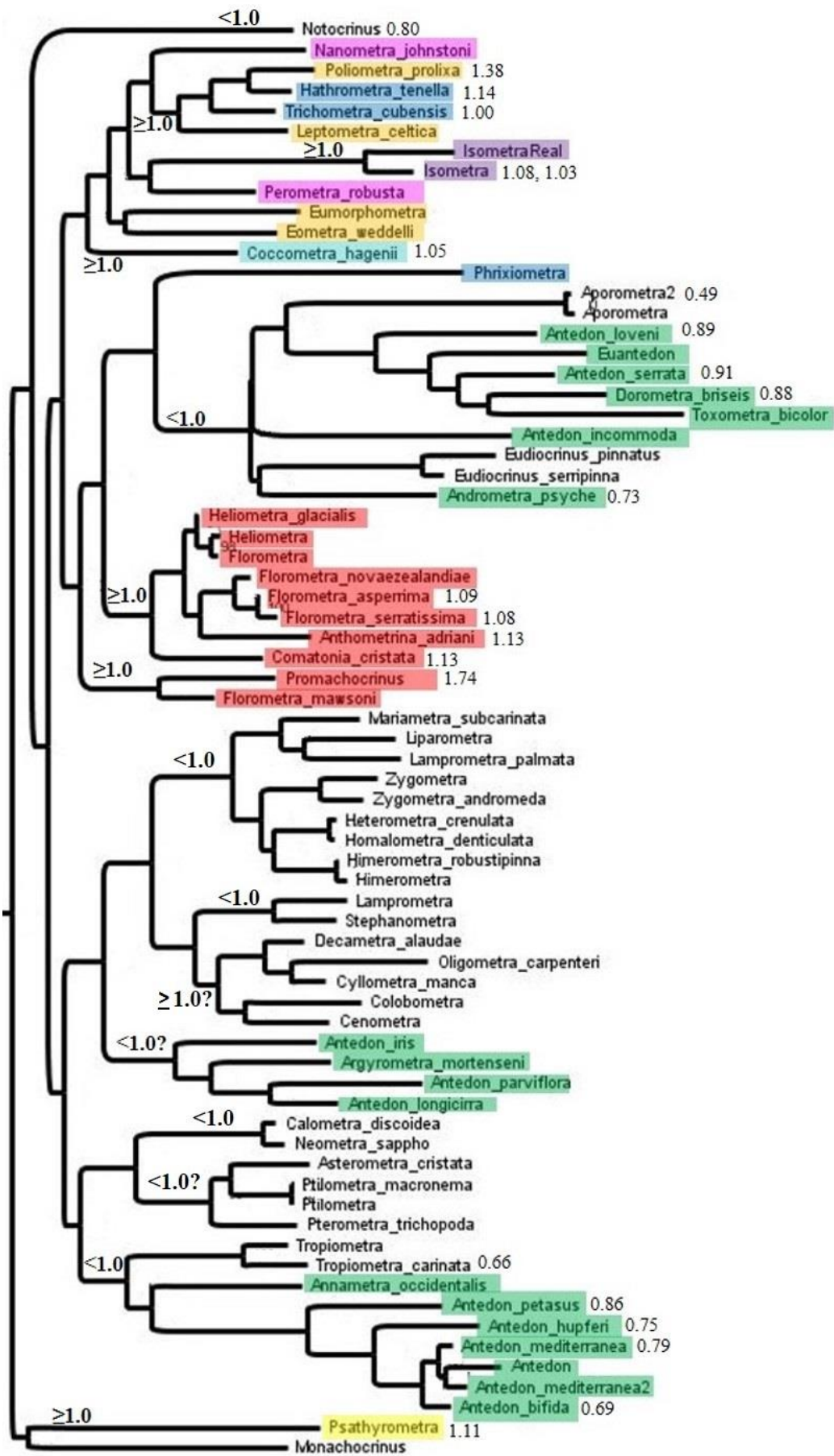


Fig. 41: Antedonid section of Rouse et al. in prep. with general radial ratio factor levels ( $<1.0$  or  $\geq 1.0$ ) at branch nodes; specific H:W radial ratios at terminals.

b. *Character states relative to the phylogenies*

The same within-radial ratios and H:W radial ratio data was used for investigation of character states within and between the phylogenetic clades. Again, any plausible character states would be suggested tentatively, due to the unbalanced sample sizes as well as the lack of availability of some terminals. The uncertain species were not used in comparing ratios for character state allocation.

There were no distinct states of any within-radial ratios within clade M. The interarticular ligament width ratios of *Anthometrina adriani* and *Promachocrinus kerguelensis* were both on the high end of the clade range (Appendix Table A9). However, as the ranges still overlapped with the other available clade members, it is not recognized as a separate character state and is most likely linked by their shared locality, if anything. All terminals within this clade have a radials higher (H) than wide (W) ( $H:W \geq 1.0$ ), making this a potential character state of clade M (Fig. 41), although thorough examination of all terminals is needed for concrete assignment and the character would have to undergo a state change to  $H:W < 1.0$  at the split between subclade #2 and clade O (Rouse et al. in prep.). Species H:W radial ratios configured well within the clade M subclades, with ratios for *Florometra asperrima* (1.09) and *F. serratissima* (1.08) almost identical, increasing slightly in close subclade #2 neighbors *Anthometrina adriani* (1.13) and *Comatonia cristata* (1.13), then increasing drastically in the subclade #1 representative, *Promachocrinus kerguelensis* (1.74). Recognition of more specific state changes, such as  $H:W 1.0-1.5$  for subclade #2 and  $H:W 1.5-2.0$  for subclade #1, is currently likely of little use due to the lack of data from the other subclade #1 terminal, *F. mawsoni*, as well as the positioning of subclade #1 in the phylogenies.

There were no discrete differences in intra-radial ratio ranges between the representatives of clade N and other tree equivalents. A small overlap exists between the greatest muscle fossae height ratio (in the largest *Antedon mediterranea*) and the smallest ratios of the other clade members, which eliminates any justification for separate character states. All representatives of this clade have radial H:W ratios  $> 1.0$ , so there is potential for a state assignment at the base branching node (Fig 41), but specimens of *Annametra occidentalis* (used in all trees) and *Antedon adriatica* (Hemery 2011, Hemery

et al. 2013) would be needed for confirmation. The species radial ratios within clade N have no discernable branching pattern, so no further states can be suggested.

Some intra-radial ratio ranges did not overlap between species of clade O, but the differences were not wide enough to warrant recognition of different character states. *Dorometra briseis* had a slightly larger ratio range for both central canal width and height, visible in SEM images, but the combination of it being only 2% greater than in other clade O members, and the small sample sizes, precluded recognition of multiple character states. *Aporometra occidentalis* has a smaller central canal width range with a larger gap, but without morphological data from its sister in Hemery's (2011) phylogeny, former colobometrid *Iconometra anisa*, character state suggestions cannot be made within this subclade. All eight examined members of clade O have H:W <1.0, although all terminals in phylogenies (12 in Rouse et al in prep.; 14 in Hemery 2011) are needed to define and assign character states. The subclade containing *Antedon loveni*, *A. serrata*, and *Dorometra briseis* shares very similar specific radial ratios (0.89, 0.91, and 0.88, respectively), distinct from that of subclade neighbor, *Aporometra occidentalis* (0.49). However, the branching neighbor, *Andrometra psyche*, has an intermediate average ratio, eliminating any justification for more finely differentiated character states.

No ratio ranges or averages were explored within clade P because, after re-identifications, this study included no taxa attributable to this clade.

As with the other clades, no intra-radial ratio differences were distinct enough to warrant specific character states within clade 'unnamed' and its other equivalents. *Coccometra hagenii* has a wider range of interarticular ligament width ratios than the other clade species, but this is most likely due to this species having the largest sample size (n = 14) relative to the others (n = 1 – 12). The slightly smaller aboral ligament height ratios and slightly larger central canal width ratios of *Tonrometra spinulifera* relative to the other clade members were not great enough (a gap of 1% or less) to warrant distinct character states. All clade 'unnamed' species examined for this study have radial H:W ratios  $\geq 1.0$  except for the representatives of *Perometra* (*P. diomedea*) and *Thysanometra* (*T. tenelloides*) with H:W <1.0. However, these two taxa were not the same ones as included in Hemery's (2011) phylogeny (*P. robusta* and *T. tenuicirra*), leaving the possibility of within-genus variation, so it remains uncertain if H:W  $\geq 1.0$  is

characteristic of all species and terminals included in the molecular clade ‘unnamed’. The specific radial ratios within clade ‘unnamed’ have no distinct pattern.

The most likely pattern in radial H:W ratio appears to be that  $H:W \geq 1.0$  was the ancestral state, given that it is characteristic of Zenometridae, the basalmost clade relative to all other clades containing former antedonids in both Hemery (2011) and Rouse et al. (in prep.): M, N, P, and ‘unnamed’. However, this statement is preliminary as the radial ratio of *Monachocrinus* sp. (Rouse et al. in prep – this specimen was misidentified as *M. caribbeus* and is actually *Rouxicrinus vestitus* (Mironov & Pawson 2014)) is not known. Among clades including former antedonids only clade O members (sister to clade M) consistently exhibit  $H:W < 1.0$ . Other non-antedonids arising among this group (e.g., Himerometroidea, several former Tropiometroidea families) have not been examined in enough detail. Limited depictions in AH Clark (1921) suggest that himerometroids (Colobometridae a possible exception) share a radial H:W ratio  $< 1.0$  while former tropiometroids vary by family (Tropiometridae, Ptilometridae and Calometridae with a H:W ratio  $< 1.0$ ; Thalassometridae and possibly Asterometridae with H:W ratio  $\geq 1.0$ ). This suggests that the radial character of  $H:W < 1.0$  arose several times throughout the tree (Fig. 41), although more radial examination need to be done across the comatulids.

## B. Discussion

There was no consistent sharing of intra-landmark measurements across subfamilies, clades, or other factor groups, nor did the radial ratios have any pattern past broad factor levels,  $< 1.0$  and  $\geq 1.0$ .

### i. Scenario 1 versus Scenario 2

Both distance-based UPGMA Hierarchical clustering models showed a few differences between the two scenarios. Five species changed closest Procrustes distance-based relatives from scenario 1 to scenario 2. However, only one of these changes caused cluster differences between the phenograms, and none involved species with sample size imbalance; therefore, the differences were caused by the additional landmark #1 data. The same is true for the differences in Mahalanobis distance-based relatives and their corresponding phenograms. Only two changes were made between the two scenarios and,

although yielding a cascade of cluster changes, did not involve any of the three species that had a reduced sample size in scenario #2.

Although larger sample sizes are preferred in shape analyses, it is clear from these results that having a comprehensive number of landmarks is just as, or more, important in order to acquire all necessary data and produce consistent results.

ii. *Identities of uncertain species*

Since the preservation time of the six uncertain species in this study exceeded the optimal time limit for obtaining proper genetic data (collected between 1984 and 2003) (and due to funding limitations), their true identities were inferred from the results of the cross validation, clustering models, and inter-landmark measurements, as well as from biogeographic information and overall morphological similarities.

a. *Antedon c.f. incommoda*

The identities of both individuals were uncertain, as most of their diagnostic features were not intact. The combination of alternating sockets, pinnules of <30 segments, and cirri lacking aboral spines placed them in Antedoninae, and apparently similar P<sub>2</sub> and P<sub>3</sub> suggested *Antedon*. Although there were no other *Antedon incommoda* species available to compare to, *A. incommoda* is only known from south and west Australia, while the specimens in this study were collected off Madang, Papua New Guinea, suggesting misidentification.

After cross validation, both individuals were misclassified as *Perometra diomedae*. Distance calculations yielded *P. diomedae* as the closest morphological relative, and the Procrustes-based clustering model joined the species with a larger cluster containing both *P. diomedae* and other Pacific antedonines. Additionally, the species shares all 12 inter-landmark measurements with *P. diomedae*, a closer Pacific locality, substantial overlap in the BGPCA along PC1, and no significant variance through Procrustes ANOVA testing.

Despite all of this evidence, direct visual comparisons with SEM images and the intact morphological characteristics indicated that this unknown species is not *Perometra diomedae*: the uncertain specimens lack the characteristic “skirt” at the base of all *P.*

*diomedeae* radials (Fig. 42A-B), lack a laterally close division series, and differ in centrodorsal shape (AH Clark, 1967). Even if some morphological features were modified by the environment, the prominent differences in radial features eliminate *P. diomedeae*. Visual comparisons of the SEM images, BGPCA, inter-landmark measurements, phenograms, and locality data, suggest it is most likely *Antedon serrata* (Fig. 42A&C), another Pacific antedonine, with which the unknowns share 11 measurements, the same locality, close Procrustes-based clustering, and no significant variance. This new identity does not change interpretations with the molecular results, as they fall in the same clade among the other Pacific antedonines.

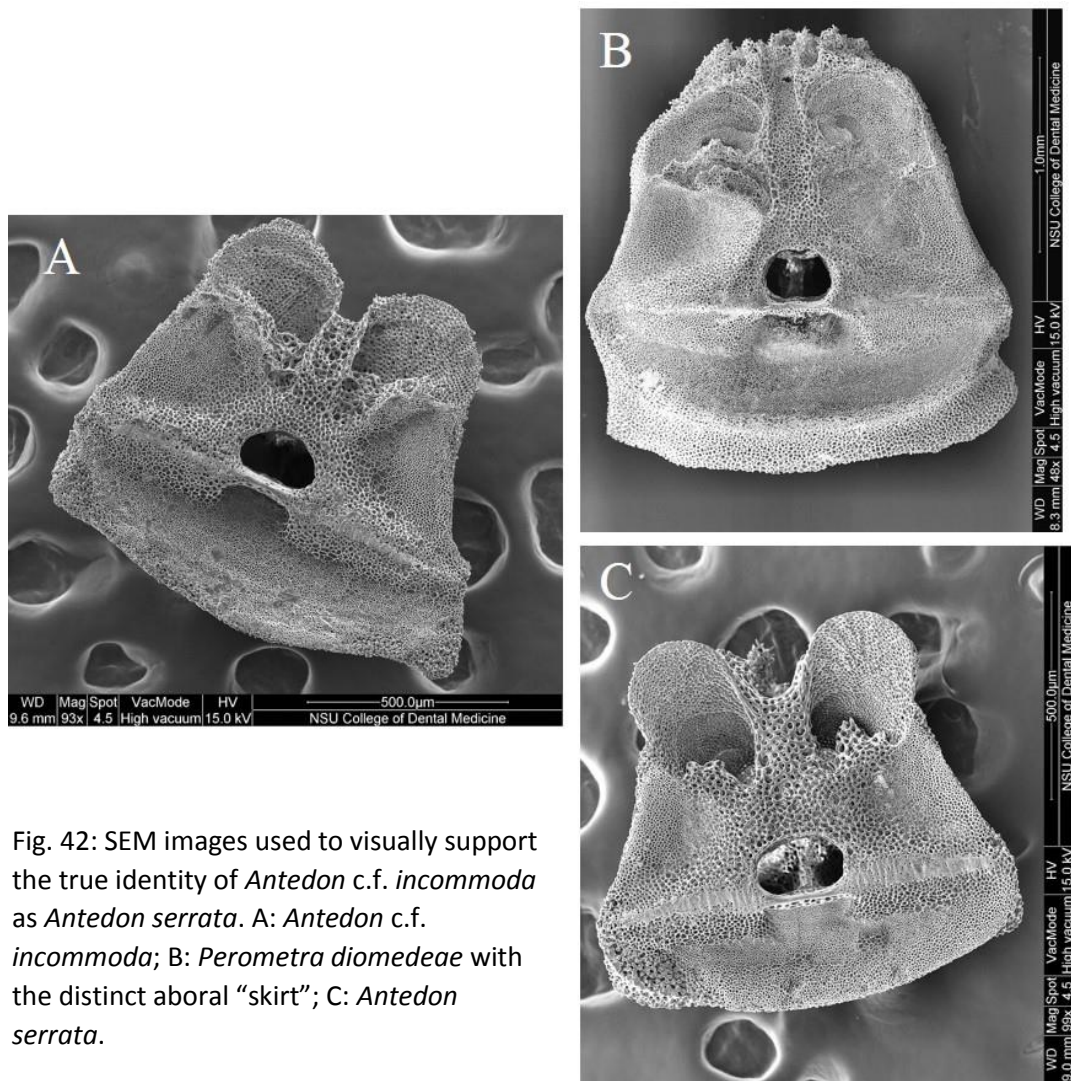


Fig. 42: SEM images used to visually support the true identity of *Antedon c.f. incommoda* as *Antedon serrata*. A: *Antedon c.f. incommoda*; B: *Perometra diomedeae* with the distinct aboral “skirt”; C: *Antedon serrata*.



b. *Antedon parviflora* groups

The *Antedon parviflora* specimens were among the first specimens dissociate and mounted for imaging, before the entire specimens were re-examined and identities verified. Because differences in several radial ossicle characters, e.g. muscle fossae height, inter-muscular ridge width, and central canal size, revealed that they were not all of the same species, they were split into two groups: B&E and C&D. Although other diagnostic characteristics were no longer available, the locality data also suggested misidentification: *Antedon parviflora* B&E was collected in the East China Sea and *Antedon parviflora* C&D in the Sea of Japan, both well north of the northernmost record of *A. parviflora* in the Philippines.

1. *Antedon parviflora* B&E

Both individuals in this group were misclassified as *Antedon serrata* after cross validations. Procrustes and Mahalanobis distance-based calculations yielded *Antedon serrata* as the closest morphological relative. *A. parviflora* B&E and *A. serrata* join as a primary cluster in all four UPGMA phenograms, they share 10 inter-landmark measurements, and have complete overlap along PC1 in the BGPCA. Visual comparisons of the radials show similarities as well (Fig. 43A-B), supporting the true identity of *Antedon parviflora* B&E as *Antedon serrata*. This could also have resulted from the lack of significant variation between clades P and O in ANOVA testing.

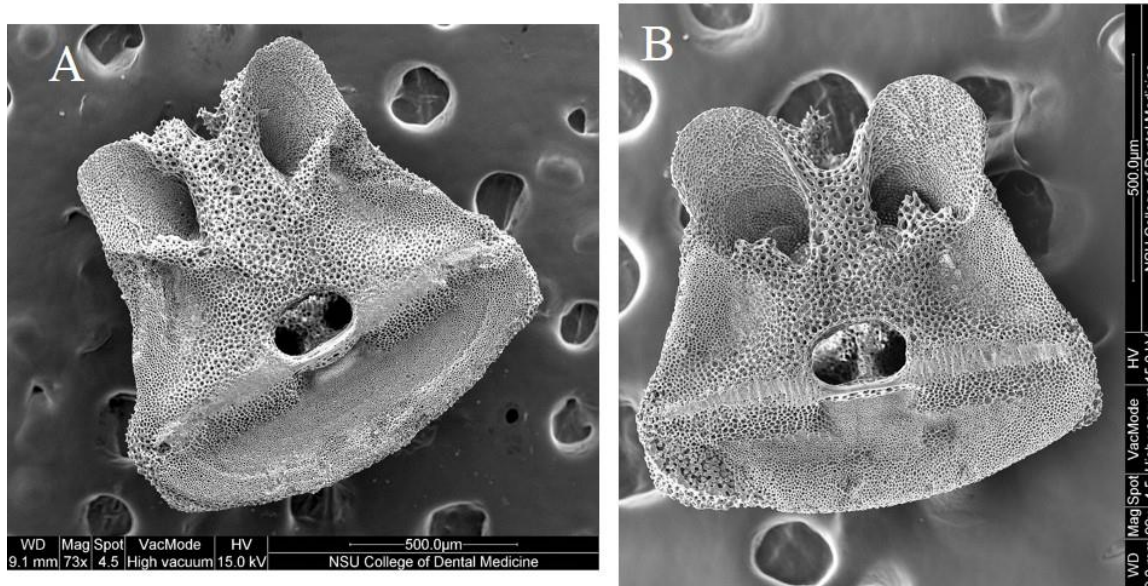


Fig. 43: SEM images used to visually support the true identity of *Antedon parviflora* B&E as *Antedon serrata*. A: *Antedon parviflora* B; B: *Antedon serrata*

## 2. *Antedon parviflora* C&D

Only one of the individuals of this species was misclassified, and only in scenario 1, as *Antedon loveni*. Mahalanobis distance calculations yielded *Antedon loveni* as this species' closest relative as well, with 11 inter-landmark measurement similarities as support. However, because *A. loveni* is restricted to southern Australia, and the Procrustes distance-based results yielded the closest morphological relatives as Atlantic antedonines, *Antedon hupferi* and *Ctenantedon kinziei*, the SEM images were examined in greater detail.

Messing (1984) suggested that ossicle stereom may be relatively coarser in juvenile specimens and becomes finer during development. The *A. parviflora* C&D specimens exhibit such relatively coarser stereom, as well as smaller size and underdeveloped interarticular fossae and ridges, suggesting they are juveniles, which produced the inconsistent morphological pairings through distance calculations and measurement similarities. The next most similar species, based on the hierarchical clustering models, are *Andrometra psyche* and *Dorometra briseis*. *Dorometra briseis* has a very large central canal relative to its size, a feature not shared by any other species but

*Antedon parviflora* C&D in this study (Fig 44A-B). This similarity, along with locality, overall morphology, and inter-landmark measurement similarities (the two share all but their right muscle fossa width), support the true identity of *A. parviflora* C&D as *Dorometra briseis*. It also helps explain the significant individual pairing with *D. briseis* in scenario 1 (and with *A. serrata* in scenario 2) as due to its underdeveloped juvenile form, not phylogenetic factors. This identity change also further reduces the number of terminals in clade P, and most likely contributed to the lack of significance between clades P and O in the Procrustes ANOVA and BGPCA results.

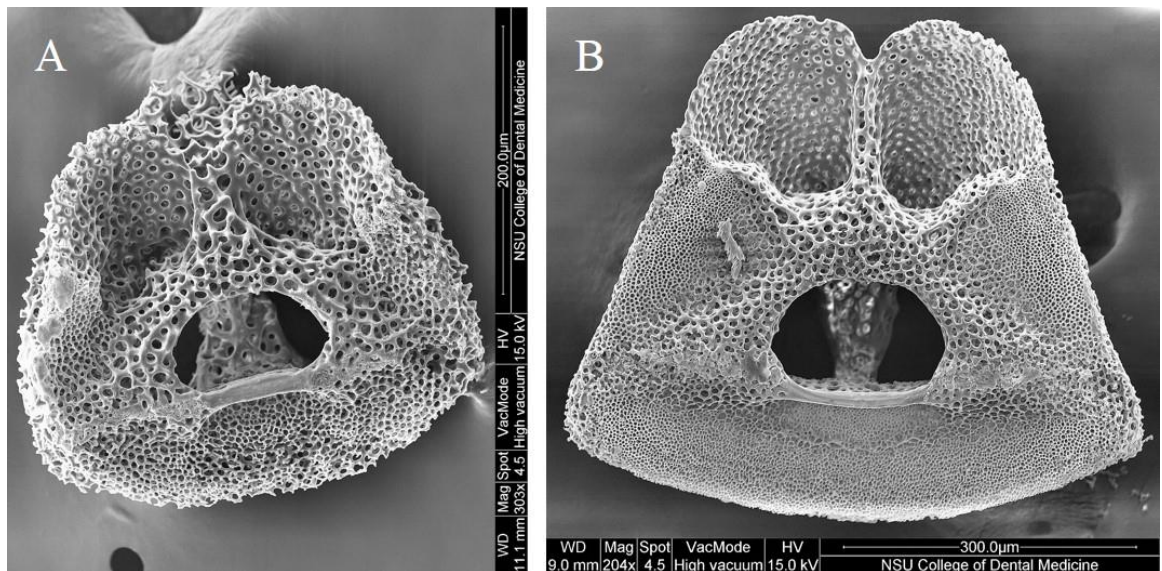


Fig. 44: SEM images used to visually support the true identity of *Antedon parviflora* C&D as a juvenile *Dorometra briseis*. A: *Antedon parviflora* D; B: *Dorometra briseis*

### 3. *Antedon* c.f. *parviflora*

This specimen was obtained later toward improving comparison with the other two *A. parviflora* groups. However, its diagnostic features were not fully congruent with any species (closest to *A. parviflora* based on cirral length, but also similar to *A. longicirra*). As the other two *A. parviflora* groups were also uncertain, the new specimen could not be compared with any definitively identified specimens; it also was not misclassified. The closest morphological relative to this species, based on distance measurements and all four phenograms, is *Dorometra* c.f. *briseis*. The two share the same locality (Sea of Japan, outside the ranges of *A. parviflora* and *A. longicirra*) and extremely similar radial featurettes (Fig. 45A-B). However, as the identity of *Dorometra* c.f. *briseis* is uncertain as well (below), the identity of *A. c.f. parviflora* remains unclear.

#### c. *Dorometra* c.f. *briseis*

As noted above, *Dorometra* c.f. *briseis* is morphologically most similar to *Antedon* c.f. *parviflora* based on distance calculations, clustering models, and image observations. Although this specimen could not be compared with a definitive *A. parviflora*, the two were compared with a definitive *Dorometra briseis*, with which neither share a distinctly wide central canal. Aside from *D. briseis*, the two lie very close to both *Antedon serrata* and *Erythrometra rubra* in the BGPCA along PC1, and overlap *Dorometra parvicirra* along PC2. They share the most inter-landmark measurement similarity with *E. rubra*, and cluster with all three in the phenograms. Direct comparisons of SEM images did not contribute to definitive identification; in fact, their radial morphologies are not closely similar to any of the other species examined. Since there was no definitive *A. parviflora* for comparison, this alternative remains uncertain. Although their known distributions about – *D. briseis* is southern Japan and *A. parviflora* from the Bonin (Ogasawara) Islands – the former might alternatively be a Pacific *Dorometra* species not used in this study. If so, no true representative of clade P remain in this study.

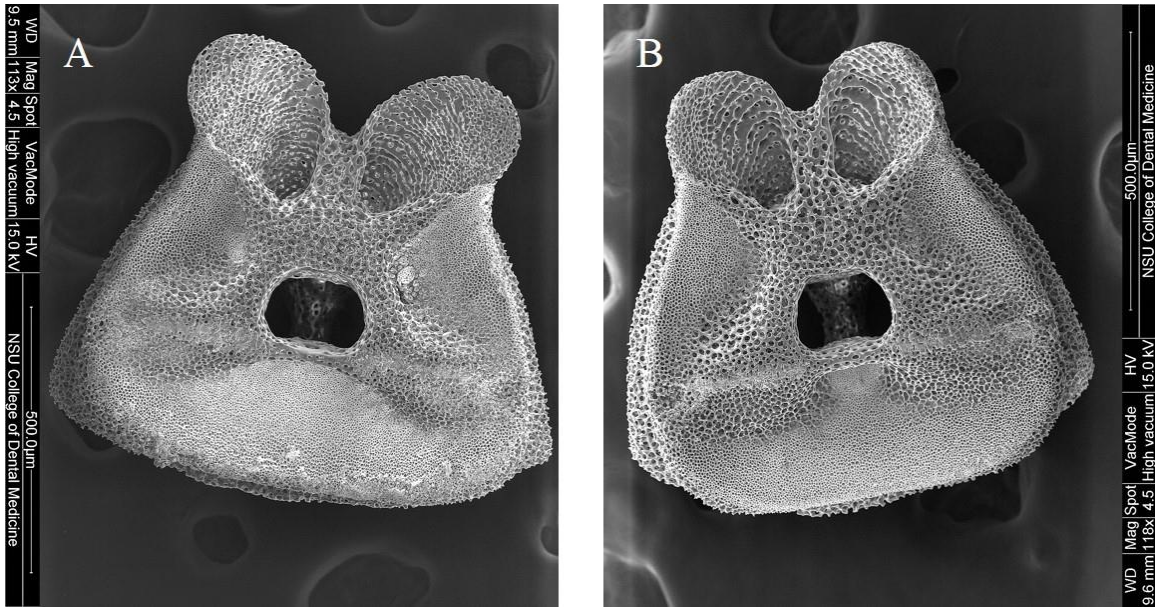


Fig. 45: SEM images used to visually support their similar identities, although what that identity is, is unclear. A: *Antedon* c.f. *parviflora*; B: *Dorometra* c.f. *briseis*.

d. *Antedon* c.f. *loveni*

Specimens of *Antedon* c.f. *loveni* were compared with definitive *A. loveni* specimens, with which they share no measurement or locality similarities, were not close relatives based on distance calculations, and did not cluster closely in the phenograms. Instead, *A. c.f. loveni* clustered in a group containing clade N species, with *Thysanometra tenelloides* and *Antedon parviflora* C&D (now thought to be *D. briseis*). It shared the most measurements with this newly identified *D. briseis*, overlapped it along PC2 in the BGPCA, and was its closest morphological relative based on Mahalanobis distances. *Antedon* c.f. *loveni* overlapped *Antedon hupferi* along PC1 and is its closest relative based on Procrustes distances. However, *A. hupferi* is an Atlantic species and is thus ruled out.

The widely separated muscle fossae of *Antedon* c.f. *loveni* radials is distinct from any other species in this study, so its true identity remains uncertain.

e. *Summary of reassigned taxa*

The examination of the radials above and the re-assignments, strongly suggest that this project included no actual representatives of clade P. As a result, the significant differences between these re-assigned or unidentified species and the members of clade N

(see Intra-subfamily variability) could no longer be presented as variance between clades N and P. Two of the three groups were re-identified as Clade O species, *Antedon serrata* and a *Dorometra briseis* juvenile. Although this juvenile and another clade O species (*Dorometra briseis*) differed significantly in pairwise tests, the juvenile did not differ significantly from any clade N species. The only pairwise result between clades N and P was between clade N species *Antedon mediterranea* and the specimen previously identified as *Antedon c.f. parviflora*, which was re-identified as an uncertain *Dorometra* species that was definitively not *D. briseis*. These results explain why there was significant variance between Atlantic and Pacific species, but not between clades N and O. Thus, it can now be said that there is no significant variance in mean radial shape between any clades containing antedonine species.

### iii. Comparing morphological relatives to the phylogenies

The closest morphological relatives of each species based on distance calculations (mainly Procrustes distances, with support if needed from Mahalanobis distances) were compared with their placements in the molecular phylogenies in order to support the connection between radial morphology and phylogenetics.

#### a. Clade M (and equivalents)

The morphological similarities between the available species of clade M (Heliometrinae and *Thaumatometra*) coincided with their phylogenetic placement fairly well. *Thaumatometra tenuis* was not taken into account in comparisons as the phylogenies used different species from different localities. This left four heliometrines in two subclades to be compared. Eleaume's (2006) morphological comparison reflected the later molecular phylogenies: subclade #1 with *Promachocrinus kerguelensis*, *Solanometra antarctica*, and *Florometra mawsoni* characterized by a single pair of nerve canals in the interior face of the radials, and a fine radial intermuscular septum, versus subclade #2 with *Anthometrina adriani*, *F. asperrima*, *F. serratissima*, *F. magellanica*, and *Heliometra glacialis* characterized by two pairs of nerve canals and a thick

intermuscular septum. The phylogenies also included *Comatonia cristata* and *F. novaezealandiae* in subclade #2.

In the current study, both distance-based relatives of *Anthometrina adriani* - *Florometra asperrima* and *Comatonia cristata* - are also close subclade #2 phylogenetic relatives (Fig. 46). *Florometra asperrima* and *F. serratissima* are each other's closest phylogenetic and morphological relative. The only known difference between the two appears to be the location of the third syzygy, and as this characteristic is linked to arm autotomy and may be variable depending on environmental conditions, it is plausible the two are morphotypes (or perhaps ecophenotypes) of the same species (Eléaume 2006). The closest morphological relative to *Comatonia cristata* based on Procrustes distances, *Hathrometra tenella*, does not lie within clade M, or even its neighbor, clade O, meaning the two are not phylogenetically similar. It is possible, however, that if either *Florometra novaezealandiae* (subclade #2) or *F. mawsoni* (subclade #1) were available for this study, they would be more morphologically similar to *C. cristata* than *H. tenella*. The closest Mahalanobis distance-based relative to *C. cristata*, *Anthometrina adriani*, is molecularly related to it as well. The closest distance-based relative of *Promachocrinus kerguelensis* is *Comatonia cristata* (Table 7), although they differ in number of radial nerve canals and lie in neighboring subclades.

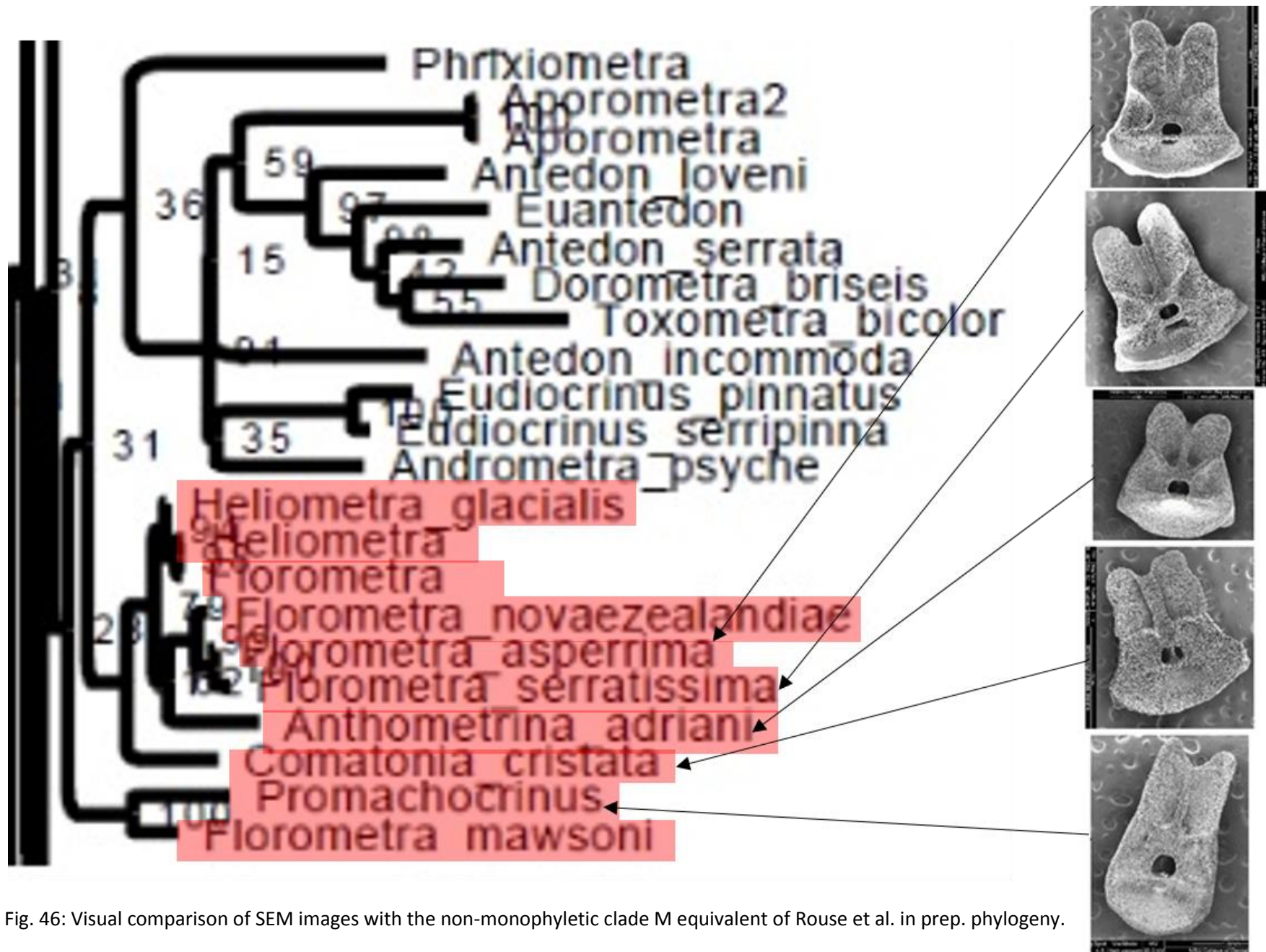


Fig. 46: Visual comparison of SEM images with the non-monophyletic clade M equivalent of Rouse et al. in prep. phylogeny.



b. *Clade N (and equivalents)*

Clade N consists of six Atlantic *Antedon* spp. and South African *Annametra occidentalis* as a clade sister to the non-antedonid *Tropiometra carinata*, also from the Atlantic (although its range extends to the western Indian Ocean). *Antedon bifida bifida* and *Antedon hupferi* are the closest morphological relatives to *T. carinata*. The closest Procrustes distance-based relative to *Antedon petasus*, *Ctenantedon kinziei*, was not used in any of the phylogenies, so its morphological and phylogenetic placements cannot be compared. However, molecular sister taxa *A. petasus* and *A. hupferi* are also closest based on Mahalanobis distances. Both closest distance-based relatives of *Antedon hupferi* - *A. bifida bifida* and *A. petasus* - are closely related molecularly as well, although not direct sisters. The same goes for *A. bifida bifida*, which is closest morphologically to fellow clade N species, *Antedon hupferi*, although is closest molecularly to *A. mediterranea*. Finally, *Antedon mediterranea* is morphologically most similar to *Antedon petasus*. Although not closest molecularly, they still lie within the same subclade of a genetically tight clade N (Fig. 47).

c. *Clade O (and equivalents)*

This clade includes eight former antedonids: Australian *Antedon loveni*, *A. incommoda*, and *Toxometra bicolor*; east Asian *A. serrata*, *D. briseis*, and *Andrometra psyche*; an unidentified *Euantedon* sp. (western to central Pacific) (all antedonines), and the South Atlantic bathymetrine *Phrixometra*, as well as two non-antedonids: South Australian *Aporometra occidentalis* (Aporometridae) and western Pacific *Eudiocrinus* sp. (formerly in Colobometridae). Among the taxa examined in this study, *Antedon* c.f. *incommoda* was re-identified as *Antedon serrata* based on measurement data and visual comparisons, although its identity remains questionable. Its closest morphological relative is *Perometra diomedae*, although genetic similarities cannot be compared as *P. diomedae* was not used in the molecular analyses. The closest morphological relative to *Andrometra psyche*, based on Procrustes distances, is *Tropiometra carinata*, an Atlantic clade N species; no phylogenetic connection here. The closest Mahalanobis distance-based relative to *A. psyche* is *Antedon loveni* (Table 7), which, although not in the same

subclade, still lies in the same genetic clade O. The closest Procrustes distance-based relative of *A. loveni* is also its closest molecular relative, *Antedon serrata*. The relatives of *A. loveni* based on Mahalanobis distances have no close phylogenetic association. *Antedon serrata* returned closest to *Antedon parviflora* B&E based on both distances. Since *A. parviflora* B&E was re-identified as *Antedon serrata*, comparisons are redundant. The second closest morphological relative to *Antedon serrata* was *Antedon loveni*, a close phylogenetic neighbor. The closest Procrustes distance-based relative of *Dorometra briseis* from scenario 1 was subclade companion, *Antedon serrata*. In scenario 2, the closest Procrustes relative of *D. briseis* was *Dorometra c.f. briseis* of uncertain identity; its closest Mahalanobis distance-based relative, *Iridometra adrestine*, was not used in the phylogenies. The aporometrid *Aporometra occidentalis* is morphologically similar to the tropiometrid *Tropiometra carinata*, but they return on widely separated branches in the phylogenies, and are geographically widely separated as well (Fig. 48).

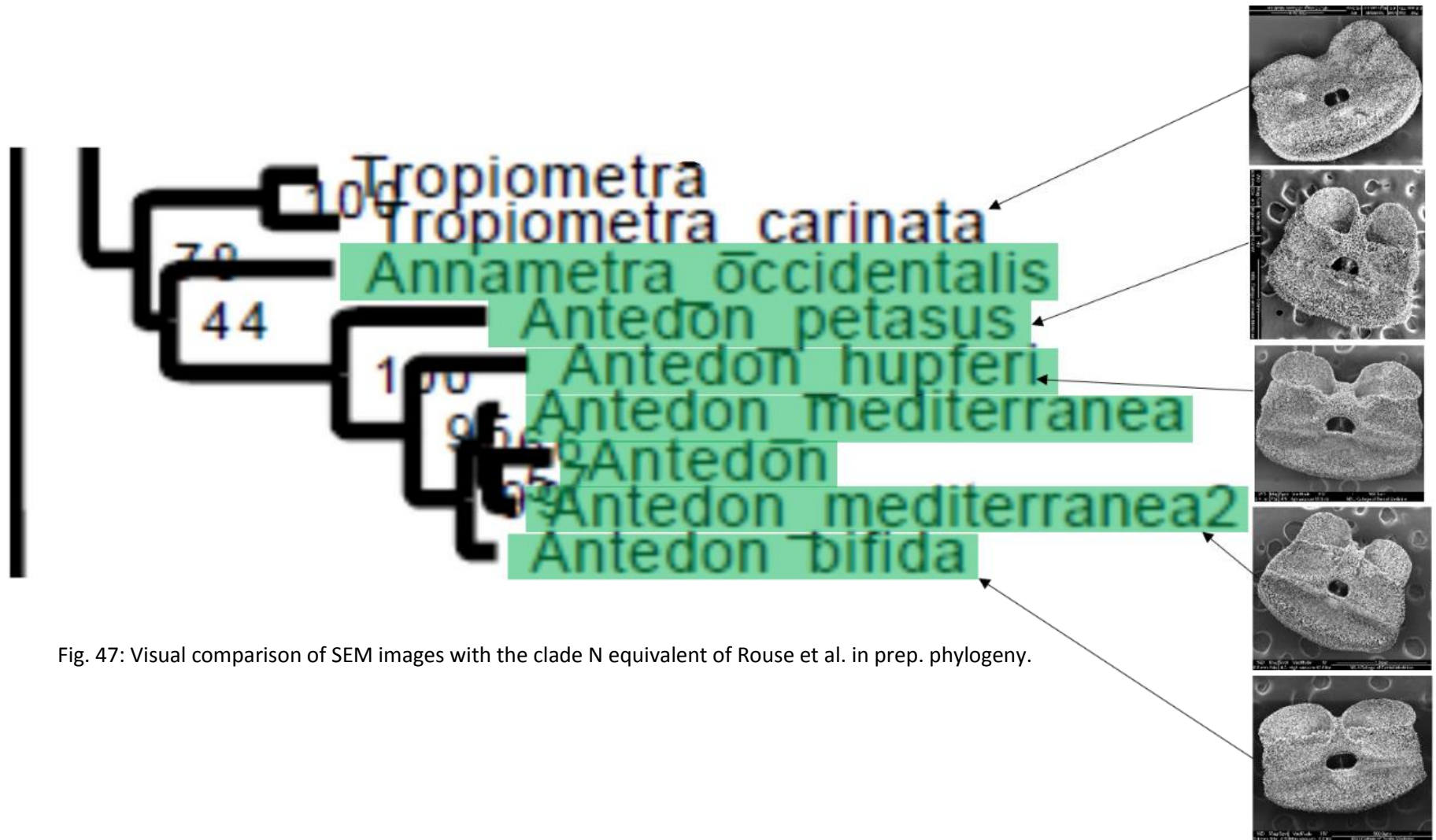


Fig. 47: Visual comparison of SEM images with the clade N equivalent of Rouse et al. in prep. phylogeny.

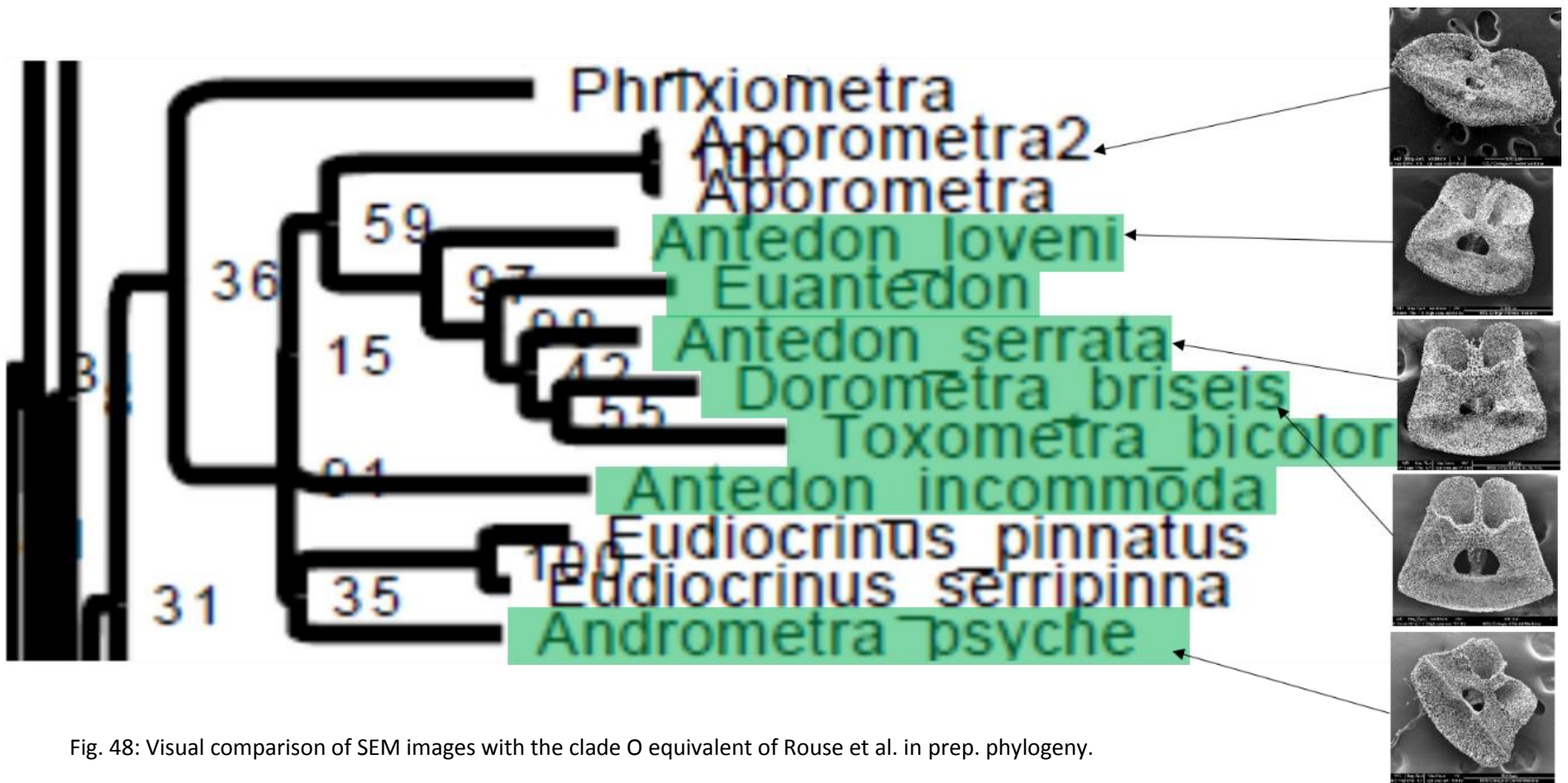


Fig. 48: Visual comparison of SEM images with the clade O equivalent of Rouse et al. in prep. phylogeny.

d. *Clade P (and equivalents)*

Since all of the species previously thought to be *Antedon parviflora* were either re-identified or are still uncertain, there were no definitive clade P species to compare morphologically with the molecular results.

e. Clade 'unnamed' (and equivalents)

Hemery (2011) and Rouse et al. (in prep..) returned a clade including representatives of eight genera in common (*Nanometra*, *Hathrometra*, *Leptometra*, *Perometra*, *Isometra*, *Eumorphometra*, *Eometra*, and *Coccometra*) (plus *Tonrometra* and *Thysanometra* in Hemery (2011) and *Poliometra* and *Trichometra* in Rouse et al. (in prep..)), although their interior relationship differed (Fig. 49). Although *Tonrometra spinulifera* was only sequenced in Hemery (2011), it returned in the current study as closest morphologically to *Poliometra prolixa*. *Tonrometra spinulifera* returned closest to *Hathrometra sarsii* in Hemery et al. (2013), and *P. prolixa* returned close to *Hathrometra tenella* in Rouse et al. (in prep..). The likely identity of the two *Hathrometra* species (Messing & Dearborn 1990) suggests that *T. spinulifera* and *P. prolixa* are molecularly close as well.

The thysanometrine *Thysanometra tenelloides* from Japan was morphologically closest in the current study to Atlantic *Antedon petasus* – a clade N species in Rouse et al. (in prep..). Hemery (2011) returned *Thysanometra tenuicirra* at a distance as sister to an Isometrainae clade. These two *Thysanometra* species, the only taxa in the genus, are closely similar based on traditional morphology (Clark and Clark 1967), so the placement of *T. tenelloides* closest to *A. petasus* here remains unexplained. Similarly, *Perometra diomedea* was closest morphologically in the current study to clade O species, *Antedon loveni*, whereas *Perometra robusta* returned in Hemery (2011) as sister to a clade of several genera (*Hathrometra*, *Leptometra*, *Tonrometra*). These two *Perometra* species are distinguished only by variations of P<sub>1</sub> ornamentation (Clark and Clark 1967), so, the similarity of *P. diomedea* and *A. loveni* remains unexplained as well.

*Isometra graminea* was the closest Procrustes distance-based relative of its phylogenetic sister, *Isometra vivipara*. *Hathrometra tenella* was closest to *I. vivipara* based on Mahalanobis distances and returned in this clade 'unnamed', but in a separate subclade. Although no close phylogenetic relationship exists between *Isometra graminea* and its closest Mahalanobis distance-based relative, *Antedon loveni*, its closest Procrustes-based relative, *Trichometra cubensis*, also returned in this clade 'unnamed' but again in a separate subclade (Fig. 49). However, no morphological, geographic, or molecular support was found for *Comatonia cristata*, the closest distance-based relative

of *Hathrometra tenella* or *Iridometra adrestine*, the closest Procrustes relative of *Trichometra cubensis* (Table 7). The closest Mahalanobis relative of *T. cubensis* was *Hybometra senta*, a species not included in any phylogeny. Traditional morphology placed *H. senta* close to *Eumorphometra* and *Leptometra* (Clark and Clark 1967), both *Antedonidae incertae sedis* and both members of clade ‘unnamed’. Strengthening the possibility of placing *H. senta* in clade ‘unnamed’ was that its closest Procrustes-based relative was *Coccometra hagenii*, also in clade ‘unnamed’. However, given the distant phylogenetic relationships noted above between several taxa despite close Mahalanobis or Procrustes similarities, i.e. *P. diomedea* and *A. loveni*, and *T. tenelloides* and *A. petasus*, it may be premature to suggest that *H. senta* belongs in clade ‘unnamed’.

In general, there is a notable connection between overall radial shape and the phylogenies. Whether phylogenetic forces are an influential factor in constraining morphology or whether both phylogenetics and morphology are influenced similarly by environmental factors is unclear, and thus have been explored further through comparisons of biogeography, intra-radial measurements, and additional morphological features.

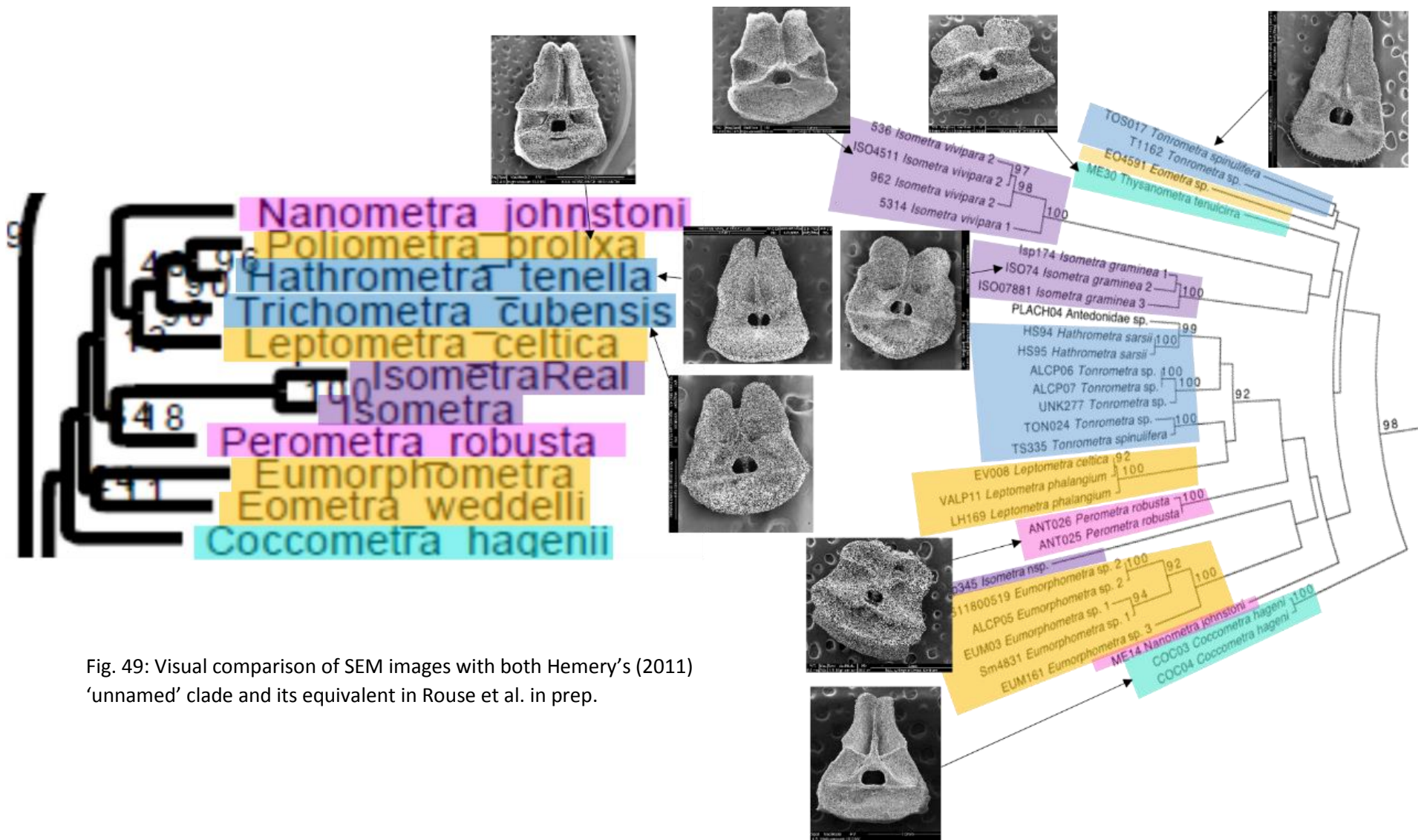


Fig. 49: Visual comparison of SEM images with both Hemery's (2011) 'unnamed' clade and its equivalent in Rouse et al. in prep.



#### iv. *Visual comparisons of SEM images to phylogenies*

Visually obvious morphological similarities in many ways reflected the molecular results better than the morphometrics did, due to the limitation of 25 (scenario #1) or 26 (scenario #2) landmarks as an overall shape representation in the statistical analyses. The clade M representatives in this study all share a H:W ratio  $\geq 1.0$ , but more specifically have tall muscle fossae, a thick intermuscular ridge, and interarticular ligament fossae that visually seem as wide as high (Fig. 46). Clade N representatives all share wide muscle fossae well separated by a thick intermuscular ridge, as well as wider than high interarticular ligament fossae (Fig. 47). Although all clade O representatives have  $H:W < 1.0$  radial ratios, only the antedonids share muscle fossae that are visually either higher or as high as wide and situated closer together than the antedonids in clade N (Fig. 48). They also seem to have a larger central canal than those in clade N. Clade ‘unnamed’ representatives (*Perometra diomedea* and *Thysanometra tenelloides* excepted) share tall muscle fossae (although varying degrees), wider or as wide as high interarticular ligament fossae, and thin interarticular ridges within their tall radials (Fig. 49).

#### v. *Taxonomic revisions*

Antedoninae was the only subfamily that definitively yielded significant variation among its tested species. Additional morphometric data from antedonines not used in the phylogenies confirmed that significant differences exist between antedonines from different regions: Atlantic versus Indo-west Pacific. The morphologically similar radials within clades are both visually apparent and reinforced by Procrustes distance calculations (Tables 7, A5, A6), supporting the need for in-depth examinations between regional antedonines, specifically within the genus *Antedon*. One potential outcome, as suggested by Hemery et al. (2009), is the restoration of genus *Compsometra* (type species *Antedon loveni* Bell, 1882), which formerly included Indo-west Pacific species in clades O and P: *loveni*, *incommoda*, *serrata*, *iris*, *longicirra* and *parviflora*. The genus was placed in synonymy under *Antedon* by Gislén (1955). *Antedon* would remain the genus for Atlantic and Mediterranean species, following the type species *Antedon bifida* (Pennant, 1777).

An expectation at the outset of this study was that, if significant morphometric distinctions conformed with molecular data to support taxonomic revisions, the polyphyly of Antedonidae would likely require shuffling of generic assignments, elevation of former subfamilies to familial status, or establishment of new families, with taxa morphologically closest to the type species, *Antedon bifida*, retained in that genus and in Antedonidae. Although this study offers no formal taxonomic revision, such an outcome is still likely, as the closest molecular relatives of clade N are non-antedonids. Some possible taxonomic revisions are suggested below, based on support of the phylogenies by the morphometric results presented here, as well as by diagnostic features of the proximal-most ossicles, thought least likely constrained by the environment.

In addition to their radial morphology coinciding with the molecular results, there are a few other morphological features shared between the antedonines and *Tropiometra* spp. of clade N (Hemery 2011, Hemery et al. 2013, Rouse et al. in prep.), such as their cirrus socket arrangement, lack of cirral ornamentations, proximal syzygy pattern, and third pinnule as similar to those succeeding (Clark & Clark 1967, Hess & Messing 2011). Also, all examined representatives occur in the Atlantic, although *T. carinata* extends to the Indian Ocean, and other *Tropiometra* species occur as far as Japan and Australia. A clade containing representatives of other families from superfamily Tropiometroidea (Asterometridae, Calometridae, Ptilometridae) is sister to clade N in Rouse et al. (in prep.), although with very low support numbers (19% ML), and returns at a distance (as clade K) as sister to Notocrinidae in Hemery (2011) and Hemery et al. (2013). All phylogenies have returned Tropiometroidea as polyphyletic. Hemery's (2011) clade N and Rouse et al.'s equivalent (in prep.) also include *Bathymetra* (not included in Hemery et al. 2013); However, no morphological or geographic support currently exists for its inclusion.

The antedonine members of clade P, although not included in this study, only share a hemispherical centrodorsal, cirrus socket arrangement, and a third pinnule characteristically similar to those succeeding, along with those characters shared by all antedonines: basal rosette, proximal syzygy pattern, and lack of cirral ornamentation (Clark and Clark 1967, Hess & Messing 2011). The addition of *Thaumatometra comaster* in Hemery's tree (2011) reduces the morphological similarities to centrodorsal shape,

socket arrangement, syzygy pattern, and a basal rosette (Clark and Clark 1967). Clade P is phylogenetically related to representatives from the superfamily Himerometroidea in all three phylogenies, with which it only consistently shares cirrus socket arrangement and a basal rosette – characters found in other feather star clades as well. The diagnostic features that distinguish himerometroid families are not shared by clade P members, or any antedonids, so the taxonomic placement of these species remains unclear.

No morphological support exists for the molecular pairing of *Aporometra occidentalis* to the Pacific antedonines of clade O. The two taxonomic groups proved significantly variant in ANOVA and pairwise testing, and share no diagnostic characteristics. Grouping of Aporometridae and Notocrinidae together in Notocrinoidea has some morphological basis (e.g., radial pits in centrodorsal) (Clark and Clark 1967, Hess & Messing 2011), but they otherwise differ in morphology and distribution, whereas *Aporometra* species and clade O antedonines have overlapping ranges.

Except for *Thaumatometra* spp. (Hemery 2011), clade M and its recent tree equivalents contain members within the same antedonid subfamily, Heliometrinae, which lends support to the morphometrics and former morphological taxonomy (Clark & Clark 1967, Hess & Messing 2011, Hemery et al. 2013, Rouse et al. in prep.). Eléaume (2006) recognized two morphological groups of heliometrine genera based on, e.g., two versus four nerve canals in the interior face of the radials. All three molecular phylogenies also recognize two heliometrine clades, but the subfamily consistently returns as paraphyletic, with a *Promachocrinus kerguelensis* and *Florometra mawsoni* clade basal to the remaining heliometrines and clade O (antedonines, *Aporometra* and Eudiocrinidae).

Additionally, over two-thirds of all the species imaged in this study had four radial nerve canal openings (two pairs) instead of two on the interior face of each radial, but neither number was consistent among species of the same clade or subfamily (e.g., of the three perometrines examined, *Erythrometra rubra* had two nerve canals while *Hypalometra defecta* and *Perometra diomedea* had four; of the four bathymetrines, only *Tonrometra spinulifera* had two nerve canals). Thysanometrinae was the only morphological subfamily, represented by *Coccometra hagenii* and *Thysanometra tenelloides*, which had a consistent number of nerve canals, but the morphology of the two representatives was otherwise completely different.

Heliometrines is not monophyletic, as the clade containing the two M subclades also includes clade O (Hemery et al. 2013, Rouse et al. in prep.). Revisions based on the molecular phylogenies suggest a new clade to include both clade M and clade O. If treated as a superfamily, the appropriate name would be Eudiocrinoidea. Eudiocrinidae AH Clark, 1907, is senior to the other available family-group names: Heliometrines AH Clark, 1909, and Apometrines HL Clark, 1938. This revision suggestion is rather far-fetched as of now, however, due to such low support at the basal nodes (Hemery et al. 2013, Rouse et al. in prep). Although Hemery (2011) returned *Thaumatometra* spp. in clade M, none are *T. tenuis*, which is morphologically distinct from the other *Thaumatometra* species based on its size and proximal pinnule length (Clark and Clark 1967). *Thaumatometra tenuis* is not morphologically similar to the heliometrines in clade M, but since it is also distinct from the other *Thaumatometra* species, it cannot yet be considered during taxonomic revisions.

As clade ‘unnamed’ and its equivalents contain members from five of the seven antedonid subfamilies, major taxonomic revisions would have to be performed in order to match the phylogenies. Still, some can be suggested. Regardless of species sequenced, the bathymetrines and *incertae sedis* members tend to fall together. Members of both share a conical centrodorsal (although not all bathymetrines) with a large cavity, elongate segments of the proximal pinnules, and laterally close primibrachials (although ornamentation may vary). These same general characteristics are shared by the perometrines, the representatives of which are neighbors to the other two subfamilies in the phylogenies. It could be suggested that the bathymetrines and *incertae sedis* species either be combined into Bathymetrines, or kept as separate subfamilies (due to the differences in cirrus socket arrangement) under a new family, Bathymetridae. Although perometrines share the socket arrangement of Bathymetrines, they are not apparently similar to either this subfamily or *incertae sedis* based on morphometric results, and thus should remain their own group, either as a subfamily under the new bathymetrine family or alone. Isometrines species form their own subclade but are molecularly close to the previous subfamilies, and are morphometrically similar to the bathymetrines. Their non-radial diagnostic features, however, are most similar to those of the heliometrines, so taxonomic placement of this group remains unclear.

Significant pairings between thysanometrine individuals, distinct separation within the BGPCA, differing locality ranges, and differences in radial ratio (at least between the species examined in this study) yield enough evidence to warrant a closer look at their other morphological features. The Mahalanobis-based results support diagnostic similarities between *Coccometra* species and the heliometrines, including centrodorsal and primibrachial shapes, a moderate cavity, and characteristically stout and flagellate proximal pinnules (Clark & Clark 1967, Hess & Messing 2011), although the latter feature is shared by *Thysanometra* as well. However, the Procrustes-based morphometrics suggest *Coccometra hagenii* is most closely related to *incertae sedis* and bathymetrine species, a result consistent with the phylogenies (Hemery 2011, Hemery et al. 2013, Rouse et al. in prep.), which returned this genus as basal to a clade including *Eometra*, *Eumorphometra*, *Hathrometra*, *Leptometra*, *Perometra* and *Nanometra*. This clade also included *Thysanometra*, but at a considerable distance from *Coccometra*. All results so far support dismembering Thysanometrinae, although more thysanometrine species, as well as more features within those species, need to be sequenced and examined.

The suggestions proposed above are extremely hesitant and based on general and limited data. Much more examination needs to be done for actual consideration of any formal taxonomic revisions. Even though more evidence is better when suggesting taxonomic revisions, the fact that radial morphology seems to be the only consistent similarity within clades reinforces the notion that the majority of the crinoid body is highly moldable by the environment, and supports this study's choice of using the radial ossicles for finding morphological connections with the phylogenetics.

## VII. General Discussion

### A. *Study Limitations / pros and cons*

The morphological exploration of only one ossicle was not considered one of the limitations of this study as it was chosen specifically as the single skeletal element thought least likely to be affected by the environment. Imaging proved to be an important limitation. The original plan was to obtain three-dimensional images of the radial ossicles for morphometric analysis, but that resource proved unavailable due to many delays.

Additional features that might have contributed to molecular support (e.g., fossae depth, ossicle depth and overall shape, thickness of muscle fossae) were thus not included. As a result, two-dimensional SEM imaging was used. The articular facet was chosen, as it has the most topographical variance. Additionally, Miriam Zelditch (personal communication) raised a concern about use of type 3 landmarks instead of semilandmarks. Documented problems associated with the subjectivity of semilandmarks (Gunz & Mitteroecker 2013, Klingenberg 2008, Zelditch et al. 2012) influenced the decision to use type 3 landmarks in this study. However, towards the end, after all landmarking was complete and statistical analyses had begun, it was clarified that between the two options, type 3 landmark and semilandmarks, semilandmarks are much less arbitrary than type 3 landmarks if digitized correctly and are associated with a distinct anatomical position – a feature not accompanied with type 3 landmarks (Mitteroecker & Gunz 2009, Zelditch et al. 2012, Adams et al. 2013, Zelditch et al. 2015, Miriam Zelditch, personal communication). Because of the timing of this clarification, it was decided that analyses would continue with the already digitized type 3 landmarks, with a change to semilandmarks for publication.

Another major limitation of this study, noted throughout, was the incomplete representation of terminals, as well as low and unbalanced sample sizes within and between terminals. These sampling limitations could have affected the connection between radial morphology and phylogenetics; inclusion of all terminals in the morphometric analyses could have returned different results.

A few differences in locality data extracted from Genbank (Benson et al. 2009, Sayers et al. 2009) existed between the species sequenced by Hemery (2011, 2013) and Rouse (in prep.) and those used for morphometric analysis here. Of the five species with collection site differences, four remained in the same general region (*Trichometra cubensis*, *Hathrometra tenella*, *Dorometra briseis*, and *Andrometra psyche*), so are of less concern than *Tropiometra carinata*, which was collected off the southern tip of Madagascar for sequencing and off Colombia for morphometric analysis. Torrence et al. (2012) found two substantially divergent genetic lineages across the species' range, suggesting the possible existence of a species complex. Although both occurred in sympatry in both Indian and Atlantic oceans, the material discussed here for sequencing

versus morphometrics could have derived from different genetic lineages. Additionally, for the several instances in which one or more biogeographic factors were not available for a species, data from Clark & Clark (1967) were used for factor assignment. Although locality was not a significant factor affecting shape between species, locality differences were not tested within a species and could have affected our results.

Aside from limitations due to missing data, unknown data also limited possible conclusions in this study. Because not enough is known about development and age in comatulids, ontogenetic effects on radial shape formation could not be tested. The presumed recognition of *Antedon parviflora* C&D as juvenile *Dorometra briseis* specimens allowed a preliminary look at the differences between juvenile and adult radials. Those initially identified as *A. parviflora* C&D shared all but one inter-landmark measurement (right muscle fossa width) with *D. briseis*. Overall radial morphology did not differ significantly between these two, although there was a notable size difference (radial height was 0.30 mm for *A. parviflora* C&D and 0.51 mm for *D. briseis*), suggesting that radials do not exhibit the substantial morphological changes with development that can be seen with other ossicles (i.e. axils, Messing 2013). The larger relative stereom size of the juveniles seen in the specimens originally identified as *Antedon parviflora* C&D suggests that relative mesh sizes may also vary ontogenetically (Messing 1984).

The idea arose, during measurements of inter-landmarks, that dimensional differences in fossae might be linked to interspecific locomotory differences. However, as far as is known, all antedonids, as well as representatives of several other clades (e.g., Thalassometridae, Mariametridae), can swim in the same manner, by alternately thrusting and lifting their arms (Ubaghs 1978). However, the ability to swim is not consistently distributed among clades in current phylogenies, e.g., thalassometrids swim, but members of their sister Comatulidae cannot; among Himerometroidea, mariametrids swim, but himerometrids do not. Effects of current velocity on radial shape could not be tested, because ambient environmental conditions and variations associated with individual specimens were completely unknown.

## B. *Future morphological focus*

Aside from the overall support that radial morphology has lent in this study to molecular work, the features of this one ossicle are not enough to support the drastic taxonomic changes that the molecular phylogenies suggest for Antedonidae; additional morphological features need to be examined, not only across all taxa, but across locality and depth ranges within taxa.

Although the radials, as proximal-most ossicles not involved in the suspension feeding apparatus, were anticipated to be the skeletal components least likely affected by hydrodynamics and other environmental factors, the patterns seen between the morphometrics and both depth and region in this study indicate that even the radials are somewhat affected by their environment. Regardless, additional morphological support is needed, and continuing to focus on the proximal ossicles at least reduces the probability of environmentally associated phenotypic plasticity within species.

Away from the radial pentagon, promising ossicles for analysis include the two primibrachials making up the division series, with secondary support from the proximal pinnules not involved in suspension feeding. Although the latter are often modified for different purposes, e.g., putative tactile and defensive functions, they may be less likely to be affected by environmental factors than their distal counterparts. However, the number of these modified pinnules varies within and between taxa, in some cases at least with growth (e.g. Rankin & Messing 2008), and it is not clear how they respond to environmental conditions.

Aboral to the radials lie the basals, which differ structurally in different extant comatulid groups, e.g., Antedonidae versus Zenometridae (Messing & White 2001). The basals were considered at the outset similar to the radials in ostensibly being “concealed” from environmental variation. However, it became clear during dissociation that these structures may not be a dependable diagnostic feature. Apart from their extremely delicate nature, there were inconsistencies across antedonid taxa, e.g., single compound basals were found in all specimens of the bathymetrine, *Tonrometra spinulifera*, and the thysanometrine, *Thysanometra tenelloides*, although they are described with a rosette form characteristic of their family (Hess & Messing 2011). Both species were thought to



be fully grown (from the limited size records in Clark and Clark 1967), so this was not a developmental occurrence. Rosette forms across taxa need to be reexamined.

Cirrus length, ornamentation, and arrangement around the centrodorsal have tentative potential as supportive features for the phylogenies. However, they are likely subject to variation based on their chosen substrate. Therefore, it is suggested that the adoral features (primibrachials and proximal pinnules) and possibly characters of the centrodorsal itself (Purens 2016) should be the primary focus in continuing the search for morphological support for molecular results.

### C. Conclusions

Despite their location within the visceral mass, radial ossicles are not immune from the effects of environmental factors. However, the factors that appeared to have an effect on radial morphology in this study are depth and region, which may reflect a combination of evolution and biogeography. The Atlantic antedonines differed significantly in overall radial appearance and a reduced H:W ratio from the Pacific antedonines, so a more comprehensive examination, and possible taxonomic revisions, should follow. All examined species with a radial H:W ratio  $<1.0$  were restricted to the shallower depths (0-200 m), although several individuals of each species should be collected at their depth extremes for comparisons. Aside from biogeographic factors, there were notable morphological similarities of the radials of species within molecular clades (Hemery 2011, Hemery et al. 2013, Rouse et al. in prep.) In many cases, the visually apparent morphological similarities better reflected the molecular results than did the results of the morphometrics. Morphometrics results could be improved upon through use of semilandmarks instead of type 3 landmarks, or possibly through more carefully chosen landmark choices and placements in future studies. Nonetheless, the limited variations of radial morphology within molecular clades support further morphological studies of this nature that will strengthen our understanding of extant crinoid phylogeny (Bull et al. 1993, Littlewood et al. 1997, Hemery 2011, Rouse et al. 2013, Roux et al. 2013). Three-dimensional imaging needs to be done on the radials, and other proximal ossicles across as many antedonid terminals as possible. Only then can morphology be

fully used as a guide for revising this crinoid family's chaotic taxonomy in congruence with molecular phylogenetics.

## VIII. Appendices

### A. Appendix A

Table A1: Radial, centrodorsal, and syzygy measurement table for all imaged ossicles

Subfamily/ Family	Species_specimen_ossicle #	Radial Height ±0.02 (mm)	Radial Width ±0.02 (mm)	Radial Height to CD Height ±0.02 Width Ratio	CD Diameter ±0.02 (mm)	CD Height to Weight Ratio	Diameter at 1 <sup>st</sup> syzygy ±0.01 (mm)	
Antedoninae	Andrometra psyche_A_1	0.74 mm	0.95 mm	0.7789	0.75 mm	1.5 mm	0.5	No data
	A. psyche_A_2	0.69 mm	0.95 mm	0.7263	0.75 mm	1.5 mm	0.5	No data
	A. psyche_B_1	0.58 mm	0.82 mm	0.7073	0.75 mm	1.4 mm	0.5357	No data
	A. psyche_C_1	0.69 mm	0.97 mm	0.7113	0.75 mm	1.5 mm	0.5	No data
	Antedon bifida bifida_A_1	1.02 mm	1.48 mm	0.6892	0.75 mm	2.75 mm	0.2727	7.14 mm
	A. bifida bifida_A_2	0.98 mm	1.45 mm	0.6759	0.75 mm	2.75 mm	0.2727	7.14 mm
	A. bifida bifida_A_3	0.98 mm	1.42 mm	0.6901	0.75 mm	2.75 mm	0.2727	7.14 mm
	A. bifida bifida_C_1	1.06 mm	1.67 mm	0.6347	0.75 mm	2.75 mm	0.2727	8.16 mm
	A. bifida bifida_C_2	1.12 mm	1.65 mm	0.6788	0.75 mm	2.75 mm	0.2727	8.16 mm
	A. bifida bifida_D_1	0.94 mm	1.45 mm	0.6483	0.75 mm	2.25 mm	0.3333	9.18 mm
	A. bifida bifida_D_2	0.95 mm	1.43 mm	0.6643	0.75 mm	2.25 mm	0.3333	9.18 mm
	A. bifida bifida_D_3	0.98 mm	1.48 mm	0.6622	0.75 mm	2.25 mm	0.3333	9.18 mm
	A. bifida bifida_E_1	1.19 mm	1.57 mm	0.758	0.75 mm	2.5 mm	0.3	9.6 mm
	A. bifida bifida_E_2	1.20 mm	1.59 mm	0.7547	0.75 mm	2.5 mm	0.3	9.6 mm
	A. bifida bifida_E_3	1.12 mm	1.61 mm	0.6956	0.75 mm	2.5 mm	0.3	9.6 mm
	Antedon hupferi_A_1	1.52 mm	1.93 mm	0.7876	1.0 mm	3.25 mm	0.3077	9.69 mm
	A. hupferi_B_1	1.04 mm	1.41 mm	0.7376	0.75 mm	2.25 mm	0.3333	6.63 mm
	A. hupferi_B_2	1.04 mm	1.41 mm	0.7376	0.75 mm	2.25 mm	0.3333	6.63 mm
	A. hupferi_B_3	1.04 mm	1.42 mm	0.7324	0.75 mm	2.25 mm	0.3333	6.63 mm
	A. hupferi_C_1	1.29 mm	1.60 mm	0.8062	0.9 mm	2.5 mm	0.36	8.16 mm
	A. hupferi_D_1	1.31 mm	1.74 mm	0.7529	0.9 mm	2.75 mm	0.3273	8.16 mm
	A. hupferi_D_2	1.28 mm	1.75 mm	0.7314	0.9 mm	2.75 mm	0.3273	8.16 mm
	A. hupferi_D_3	1.30 mm	1.73 mm	0.7514	0.9 mm	2.75 mm	0.3273	8.16 mm
Antedon c.f. incommoda_A_1	0.97 mm	No data	No data	No data	No data	No data	No data	6.0 mm
A. c.f. incommoda_B_1	0.75 mm	0.95 mm	0.7895	0.5 mm	1.75 mm	0.2857	5.4 mm	

Table A1 cont'd: Radial, centrodorsal, and syzygy measurement table for all imaged ossicles

Subfamily/ Family	Species_specimen_ossicle #	Radial Height ±0.02 (mm)	Radial Width ±0.02 (mm)	Radial Height to Width Ratio	CD Height ±0.02 (mm)	CD Diameter ±0.02 (mm)	CD Height to Weight Ratio	Diameter at 1 <sup>st</sup> syzygy ±0.01 (mm)
	<i>Antedon loveni_A_1</i>	0.83 mm	0.89 mm	0.9326	0.5 mm	1.5 mm	0.3333	5.1 mm
	<i>A. loveni_A_2</i>	0.82 mm	0.89 mm	0.9213	0.5 mm	1.5 mm	0.3333	5.1 mm
	<i>A. loveni_A_3</i>	0.82 mm	0.88 mm	0.9318	0.5 mm	1.5 mm	0.3333	5.1 mm
	<i>A. loveni_B_1</i>	0.82 mm	0.90 mm	0.9111	0.6 mm	1.5 mm	0.4	5.1 mm
	<i>A. loveni_B_2</i>	0.86 mm	0.92 mm	0.9348	0.6 mm	1.5 mm	0.4	5.1 mm
	<i>A. loveni_C_1</i>	0.75 mm	0.82 mm	0.9146	0.5 mm	1.5 mm	0.3333	6.12 mm
	<i>A. loveni_C_2</i>	0.76 mm	0.81 mm	0.9383	0.5 mm	1.5 mm	0.3333	6.12 mm
	<i>A. loveni_D_1</i>	0.68 mm	0.75 mm	0.9067	0.5 mm	1.25 mm	0.4	4.59 mm
	<i>A. loveni_D_2</i>	0.67 mm	0.75 mm	0.8933	0.5 mm	1.25 mm	0.4	4.59 mm
	<i>A. loveni_E_1</i>	0.76 mm	0.96 mm	0.7917	0.5 mm	1.5 mm	0.3333	4.8 mm
	<i>A. loveni_E_2</i>	0.76 mm	1.01 mm	0.7525	0.5 mm	1.5 mm	0.3333	4.8 mm
	<i>Antedon c.f. loveni_F_1</i>	0.68 mm	1.00 mm	0.68	0.6 mm	1.75 mm	0.3429	6.05 mm
	<i>A. c.f. loveni_F_2</i>	0.68 mm	0.92 mm	0.7391	0.6 mm	1.75 mm	0.3429	6.05 mm
	<i>A. c.f. loveni_F_3</i>	0.65 mm	0.95 mm	0.6842	0.6 mm	1.75 mm	0.3429	6.05 mm
	<i>A. c.f. loveni_F_4</i>	0.67 mm	0.98 mm	0.6837	0.6 mm	1.75 mm	0.3429	6.05 mm
	<i>A. c.f. loveni_G_1</i>	0.67 mm	0.96 mm	0.6979	0.75 mm	1.8 mm	0.4167	4.59 mm
	<i>A. c.f. loveni_G_2</i>	0.72 mm	0.96 mm	0.75	0.75 mm	1.8 mm	0.4167	4.59 mm
	<i>A. c.f. loveni_G_3</i>	0.72 mm	0.97 mm	0.7423	0.75 mm	1.8 mm	0.4167	4.59 mm
	<i>A. c.f. loveni_G_4</i>	0.71 mm	0.99 mm	0.7172	0.75 mm	1.8 mm	0.4167	4.59 mm
	<i>Antedon mediterranea_A_1</i>	1.40 mm	1.67 mm	0.8383	0.75 mm	2.75 mm	0.2727	7.65 mm
	<i>A. mediterranea_A_2</i>	1.39 mm	1.67 mm	0.8323	0.75 mm	2.75 mm	0.2727	7.65 mm
	<i>A. mediterranea_C_1</i>	1.44 mm	1.88 mm	0.766	0.75 mm	2.75 mm	0.2727	9.18 mm
	<i>A. mediterranea_D_1</i>	1.58 mm	1.95 mm	0.8103	0.75 mm	2.75 mm	0.2727	8.67 mm
	<i>A. mediterranea_D_2</i>	1.58 mm	2.02 mm	0.7822	0.75 mm	2.75 mm	0.2727	8.67 mm
	<i>A. mediterranea_D_3</i>	1.64 mm	1.98 mm	0.8283	0.75 mm	2.75 mm	0.2727	8.67 mm
	<i>A. mediterranea_E_1</i>	1.78 mm	2.39 mm	0.7448	1.0 mm	3.5 mm	0.2857	10.71 mm
	<i>A. mediterranea_E_2</i>	1.68 mm	2.29 mm	0.7336	1.0 mm	3.5 mm	0.2857	10.71 mm

Table A1 cont'd: Radial, centrodorsal, and syzygy measurement table for all imaged ossicles

Subfamily/ Family	Species_specimen_ossicle #	Radial Height ±0.02 (mm)	Radial Width ±0.02 (mm)	Radial Height to Width Ratio	CD Height ±0.02 (mm)	CD Diameter ±0.02 (mm)	CD Height to Weight Ratio	Diameter at 1 <sup>st</sup> syzygy ±0.01 (mm)
	<i>Antedon petasus_A_1</i>	1.58 mm	1.85 mm	0.854	1.5 mm	3.5 mm	0.4286	No data
	<i>A. petasus_A_2</i>	1.53 mm	1.81 mm	0.8453	1.5 mm	3.5 mm	0.4286	No data
	<i>A. petasus_C_1</i>	1.44 mm	1.65 mm	0.8727	1.0 mm	2.75 mm	0.3636	No data
	<i>A. petasus_D_1</i>	1.75 mm	2.02 mm	0.8663	1.5 mm	3.5 mm	0.4286	No data
	<i>Antedon parviflora_B_1</i>	1.21 mm	1.33 mm	0.9098	0.8 mm	2.0 mm	0.4	No data
	<i>A. parviflora_E_1</i>	1.03 mm	1.23 mm	0.8374	0.75 mm	2.0 mm	0.375	No data
	<i>A. parviflora_C_1</i>	0.30 mm	0.40 mm	0.75	No data	No data	No data	No data
	<i>A. parviflora_D_1</i>	0.30 mm	0.35 mm	0.8571	No data	No data	No data	No data
	<i>Antedon c.f. parviflora_F_1</i>	0.85 mm	0.96 mm	0.8852	1.0 mm	1.75 mm	0.5714	4.8 mm
	<i>A. c.f. parviflora_F_2</i>	0.87 mm	0.97 mm	0.8969	1.0 mm	1.75 mm	0.5714	4.8 mm
	<i>A. c.f. parviflora_F_3</i>	0.88 mm	0.96 mm	0.9167	1.0 mm	1.75 mm	0.5714	4.8 mm
	<i>A. c.f. parviflora_F_4</i>	0.89 mm	0.97 mm	0.9175	1.0 mm	1.75 mm	0.5714	4.8 mm
	<i>Antedon serrata_A_1</i>	0.68 mm	0.72 mm	0.9444	0.6 mm	1.25 mm	0.48	No data
	<i>A. serrata_A_2</i>	0.64 mm	0.73 mm	0.8767	0.6 mm	1.25 mm	0.48	No data
	<i>A. serrata_B_1</i>	0.94 mm	1.03 mm	0.9126	0.75 mm	1.75 mm	0.4286	No data
	<i>Ctenantedon kinziei_A_1</i>	1.06 mm	1.54 mm	0.6883	1.0 mm	3.0 mm	0.3333	6.12 mm
	<i>C. kinziei_A_2</i>	1.14 mm	1.54 mm	0.7403	1.0 mm	3.0 mm	0.3333	6.12 mm
	<i>C. kinziei_C_1</i>	1.04 mm	1.58 mm	0.6582	0.9 mm	3.0 mm	0.3	5.1 mm
	<i>C. kinziei_C_2</i>	1.04 mm	1.57 mm	0.6624	0.9 mm	3.0 mm	0.3	5.1 mm
	<i>C. kinziei_D_1</i>	0.75 mm	1.03 mm	0.7281	0.5 mm	2.0 mm	0.25	4.59 mm
	<i>C. kinziei_D_2</i>	0.73 mm	1.02 mm	0.7157	0.5 mm	2.0 mm	0.25	4.59 mm
	<i>C. kinziei_D_3</i>	0.74 mm	1.00 mm	0.74	0.5 mm	2.0 mm	0.25	4.59 mm
	<i>Dorometra briseis_A_1</i>	0.51 mm	0.60 mm	0.85	0.3 mm	0.75 mm	0.4	No data
	<i>D. briseis_A_2</i>	0.51 mm	0.58 mm	0.8793	0.3 mm	0.75 mm	0.4	No data
	<i>D. briseis_B_1</i>	0.45 mm	0.50 mm	0.9	0.3 mm	0.7 mm	0.4286	No data

Table A1 cont'd: Radial, centrodorsal, and syzygy measurement table for all imaged ossicles

Subfamily/ Family	Species_specimen_ossicle #	Radial Height ±0.02 (mm)	Radial Width ±0.02 (mm)	Radial Height to Width Ratio	CD Height ±0.02 (mm)	CD Diameter ±0.02 (mm)	CD Height to Weight Ratio	Diameter at 1 <sup>st</sup> syzygy ±0.01 (mm)
	<i>Dorometra</i> c.f. <i>briseis</i> _C_1	0.83 mm	0.86 mm	0.9651	1.0 mm	1.6 mm	0.625	3.6 mm
	<i>D.</i> c.f. <i>briseis</i> _C_2	0.83 mm	0.87 mm	0.954	1.0 mm	1.6 mm	0.625	3.6 mm
	<i>D.</i> c.f. <i>briseis</i> _C_3	0.82 mm	0.85 mm	0.9647	1.0 mm	1.6 mm	0.625	3.6 mm
	<i>D.</i> c.f. <i>briseis</i> _C_4	0.86 mm	0.87 mm	0.9885	1.0 mm	1.6 mm	0.625	3.6 mm
	<i>Dorometra</i> <i>parvicirra</i> _A_1	1.31 mm	1.20 mm	1.0917	1.0 mm	2.0 mm	0.5	No data
	<i>D.</i> <i>parvicirra</i> _B_1	1.31 mm	1.25 mm	1.048	1.0 mm	2.0 mm	0.5	No data
	<i>D.</i> <i>parvicirra</i> _B_2	1.42 mm	1.27 mm	1.1181	1.0 mm	2.0 mm	0.5	No data
	<i>D.</i> <i>parvicirra</i> _B_3	1.35 mm	1.27 mm	1.063	1.0 mm	2.0 mm	0.5	No data
	<i>D.</i> <i>parvicirra</i> _C_1	1.31 mm	1.22 mm	1.0738	1.0 mm	2.0 mm	0.5	8.16 mm
	<i>Iridometra</i> <i>adrestine</i> _B_1	1.37 mm	1.54 mm	0.8896	No data	No data	No data	No data
	<i>I.</i> <i>adrestine</i> _C_1	1.35 mm	1.20 mm	1.125	1.0 mm	2.6 mm	0.3846	7.14 mm
Bathymetrinae	<i>Hathrometra</i> <i>tenella</i> _A_1	1.61 mm	1.32 mm	1.2197	1.75 mm	2.5 mm	0.7	6.0 mm
	<i>H.</i> <i>tenella</i> _A_2	1.55 mm	1.31 mm	1.1832	1.75 mm	2.5 mm	0.7	6.0 mm
	<i>H.</i> <i>tenella</i> _A_3	1.49 mm	1.28 mm	1.1641	1.75 mm	2.5 mm	0.7	6.0 mm
	<i>H.</i> <i>tenella</i> _B_1	1.89 mm	1.66 mm	1.1385	2.5 mm	3.0 mm	0.8333	9.0 mm
	<i>H.</i> <i>tenella</i> _D_1	1.91 mm	1.74 mm	1.0977	2.5 mm	2.75 mm	0.9091	7.8 mm
	<i>H.</i> <i>tenella</i> _E_1	1.57 mm	1.46 mm	1.0753	2.0 mm	2.5 mm	0.8	7.2 mm
	<i>H.</i> <i>tenella</i> _E_2	1.56 mm	1.44 mm	1.0833	2.0 mm	2.5 mm	0.8	7.2 mm
	<i>Thaumatometra</i> <i>tenuis</i> _B_1	1.87 mm	1.78 mm	1.0506	1.25 mm	3.0 mm	0.4167	11.55 mm
	<i>T.</i> <i>tenuis</i> _B_2	1.83 mm	1.76 mm	1.0398	1.25 mm	3.0 mm	0.4167	11.55 mm
	<i>T.</i> <i>tenuis</i> _B_3	1.80 mm	1.76 mm	1.0227	1.25 mm	3.0 mm	0.4167	11.55 mm

Table A1 cont'd: Radial, centrodorsal, and syzygy measurement table for all imaged ossicles

Subfamily/ Family	Species_specimen_ossicle #	Radial Height ±0.02 (mm)	Radial Width ±0.02 (mm)	Radial Height to Width Ratio	CD Height ±0.02 (mm)	CD Diameter ±0.02 (mm)	CD Height to Weight Ratio	Diameter at 1 <sup>st</sup> syzygy ±0.01 (mm)
	<i>Tonrometra spinulifera_A_1</i>	2.11 mm	1.30 mm	1.6231	1.9 mm	2.25 mm	0.8444	6.12 mm
	<i>T. spinulifera_A_2</i>	2.17 mm	1.30 mm	1.6692	1.9 mm	2.25 mm	0.8444	6.12 mm
	<i>T. spinulifera_B_1</i>	1.88 mm	1.28 mm	1.4687	1.9 mm	2.0 mm	0.95	6.63 mm
	<i>T. spinulifera_C_1</i>	2.36 mm	1.54 mm	1.5325	2.0 mm	2.5 mm	0.8	10.2 mm
	<i>T. spinulifera_E_1</i>	2.20 mm	1.43 mm	1.5385	1.9 mm	2.5 mm	0.76	7.2 mm
	<i>T. spinulifera_E_2</i>	2.23 mm	1.44 mm	1.5486	1.9 mm	2.5 mm	0.76	7.2 mm
	<i>T. spinulifera_E_3</i>	2.23 mm	1.43 mm	1.5594	1.9 mm	2.5 mm	0.76	7.2 mm
	<i>Trichometra cubensis_E_1</i>	1.07 mm	1.09 mm	0.9816	1.0 mm	1.5 mm	0.6667	No data
	<i>T. cubensis_E_2</i>	1.05 mm	1.06 mm	0.9906	1.0 mm	1.5 mm	0.6667	No data
	<i>T. cubensis_E_3</i>	1.09 mm	1.09 mm	1	1.0 mm	1.5 mm	0.6667	No data
<b>Heliometrinae</b>	<i>Anthometrina adriani_A_1</i>	2.36 mm	2.05 mm	1.1512	2.75 mm	3.5 mm	0.7857	15.95 mm
	<i>A. adriani_A_2</i>	2.39 mm	2.04 mm	1.1716	2.75 mm	3.5 mm	0.7857	15.95 mm
	<i>A. adriani_A_3</i>	2.33 mm	2.04 mm	1.1422	2.75 mm	3.5 mm	0.7857	15.95 mm
	<i>A. adriani_B_1</i>	2.69 mm	2.42 mm	1.1116	3.25 mm	4.5 mm	0.7222	11.55 mm
	<i>A. adriani_B_2</i>	2.61 mm	2.42 mm	1.0785	3.25 mm	4.5 mm	0.7222	11.55 mm
	<i>A. adriani_C_1</i>	2.31 mm	2.12 mm	1.0896	3.0 mm	3.75 mm	0.8	13.2 mm
	<i>A. adriani_C_2</i>	2.31 mm	2.15 mm	1.0744	3.0 mm	3.75 mm	0.8	13.2 mm
	<i>A. adriani_D_1</i>	3.12 mm	2.68 mm	1.1642	3.5 mm	4.5 mm	0.7778	17.6 mm
	<i>A. adriani_E_1</i>	2.61 mm	2.23 mm	1.1704	3.0 mm	4.0 mm	0.75	12.6 mm
	<i>A. adriani_E_2</i>	2.61 mm	2.29 mm	1.1397	3.0 mm	4.0 mm	0.75	12.6 mm
	<i>A. adriani_E_3</i>	2.60 mm	2.25 mm	1.1555	3.0 mm	4.0 mm	0.75	12.6 mm
	<i>Comatonia cristata_B_1</i>	2.63 mm	2.39 mm	1.1004	2.5 mm	4.0 mm	0.625	No data
	<i>C. cristata_B_2</i>	2.69 mm	2.31 mm	1.1645	2.5 mm	4.0 mm	0.625	No data
	<i>C. cristata_B_3</i>	2.54 mm	2.35 mm	1.0808	2.5 mm	4.0 mm	0.625	No data
	<i>C. cristata_C_1</i>	1.15 mm	0.99 mm	1.1616	1.25 mm	1.75 mm	0.7143	No data
	<i>C. cristata_C_2</i>	1.15 mm	1.00 mm	1.15	1.25 mm	1.75 mm	0.7143	No data



Table A1 cont'd: Radial, centrodorsal, and syzygy measurement table for all imaged ossicles

Subfamily/ Family	Species_specimen_ossicle #	Radial Height ±0.02 (mm)	Radial Width ±0.02 (mm)	Radial Height to Width Ratio	CD Height ±0.02 (mm)	CD Diameter ±0.02 (mm)	CD Height to Weight Ratio	Diameter at 1 <sup>st</sup> syzygy ±0.01 (mm)
	<i>Florometra asperrima_A_1</i>	3.12 mm	3.07 mm	1.0163	2.0 mm	5.25 mm	0.3809	15.95 mm
	<i>F. asperrima_A_2</i>	3.06 mm	2.87 mm	1.0662	2.0 mm	5.25 mm	0.3809	15.95 mm
	<i>F. asperrima_A_3</i>	3.09 mm	2.85 mm	1.0842	2.0 mm	5.25 mm	0.3809	15.95 mm
	<i>F. asperrima_B_1</i>	3.10 mm	2.84 mm	1.0915	2.25 mm	5.5 mm	0.4091	13.75 mm
	<i>F. asperrima_B_2</i>	3.00 mm	2.77 mm	1.083	2.25 mm	5.5 mm	0.4091	13.75 mm
	<i>F. asperrima_C_1</i>	3.84 mm	3.28 mm	1.1707	2.5 mm	6.0 mm	0.4167	17.05 mm
	<i>F. asperrima_C_2</i>	3.69 mm	3.25 mm	1.1354	2.5 mm	6.0 mm	0.4167	17.05 mm
	<i>F. asperrima_D_1</i>	2.02 mm	1.85 mm	1.0919	1.25 mm	3.5 mm	0.3571	10.45 mm
	<i>F. asperrima_D_2</i>	1.95 mm	1.89 mm	1.0317	1.25 mm	3.5 mm	0.3571	10.45 mm
	<i>F. asperrima_E_1</i>	3.26 mm	3.01 mm	1.083	2.5 mm	5.75 mm	0.4348	13.8 mm
	<i>F. asperrima_E_2</i>	3.24 mm	2.84 mm	1.1408	2.5 mm	5.75 mm	0.4348	13.8 mm
	<i>F. asperrima_E_3</i>	3.36 mm	2.99 mm	1.1237	2.5 mm	5.75 mm	0.4348	13.8 mm
	<i>Florometra serratissima_B_1</i>	3.14 mm	2.95 mm	1.0644	2.5 mm	5.25 mm	0.4762	10.5 mm
	<i>F. serratissima_B_2</i>	3.25 mm	2.94 mm	1.1054	2.5 mm	5.25 mm	0.4762	10.5 mm
	<i>Promachocrinus kerguelensis_A_1</i>	2.52 mm	1.46 mm	1.726	2.0 mm	3.5 mm	0.5714	18.15 mm
	<i>P. kerguelensis_A_2</i>	2.56 mm	1.45 mm	1.7655	2.0 mm	3.5 mm	0.5714	18.15 mm
Isometrinae	<i>Isometra graminea_A_1</i>	1.48 mm	1.38 mm	1.0725	1.5 mm	1.75 mm	0.8571	7.2 mm
	<i>I. graminea_A_2</i>	1.54 mm	1.43 mm	1.0769	1.5 mm	1.75 mm	0.8571	7.2 mm
	<i>I. graminea_C_1</i>	1.50 mm	1.39 mm	1.0791	1.25 mm	1.75 mm	0.7143	7.8 mm
	<i>Isometra vivipara_A_1</i>	2.97 mm	2.88 mm	1.031	2.25 mm	3.75 mm	0.6	No data
Perometrinae	<i>Erythrometra rubra_A_1</i>	0.81 mm	0.88 mm	0.9204	1.0 mm	1.5 mm	0.6667	No data
	<i>E. rubra_B_1</i>	0.52 mm	0.56 mm	0.9286	0.75 mm	1.0 mm	0.75	2.55 mm

Table A1 cont'd: Radial, centrodorsal, and syzygy measurement table for all imaged ossicles

Subfamily/ Family	Species_specimen_ossicle #	Radial Height ±0.02 (mm)	Radial Width ±0.02 (mm)	Radial Height to Width Ratio	CD Height ±0.02 (mm)	CD Diameter ±0.02 (mm)	CD Height to Weight Ratio	Diameter at 1 <sup>st</sup> syzygy ±0.01 (mm)
	<i>Hyalometra defecta</i> _A_1	0.55 mm	0.62 mm	0.8871	0.75 mm	1.0 mm	0.75	No data
	<i>H. defecta</i> _B_1	0.67 mm	0.82 mm	0.8171	0.75 mm	1.5 mm	0.5	No data
	<i>H. defecta</i> _B_2	0.66 mm	0.83 mm	0.7952	0.75 mm	1.5 mm	0.5	No data
	<i>H. defecta</i> _D_1	0.87 mm	0.91 mm	0.956	1.0 mm	1.5 mm	0.6667	4.59 mm
	<i>H. defecta</i> _F_1	0.84 mm	0.88 mm	0.9545	1.0 mm	1.25 mm	0.8	4.59 mm
	<i>H. defecta</i> _G_1	0.74 mm	0.82 mm	0.9024	0.75 mm	1.25 mm	0.6	2.5 mm
	<i>H. defecta</i> _G_2	0.71 mm	0.81 mm	0.8765	0.75 mm	1.25 mm	0.6	2.5 mm
	<i>Perometra diomedeeae</i> _A_1	2.27 mm	2.22 mm	1.0225	1.8 mm	3.8 mm	0.4737	No data
	<i>P. diomedeeae</i> _A_2	2.12 mm	2.20 mm	0.9636	1.8 mm	3.8 mm	0.4737	No data
	<i>P. diomedeeae</i> _B_1	1.83 mm	2.10 mm	0.8714	2.0 mm	3.5 mm	0.5714	No data
	<i>P. diomedeeae</i> _B_2	1.93 mm	2.05 mm	0.9415	2.0 mm	3.5 mm	0.5714	No data
<i>Thysanometrinae</i>	<i>Coccometra hagenii</i> _A_1	1.73 mm	1.57 mm	1.1019	1.5 mm	2.75 mm	0.5454	No data
	<i>C. hagenii</i> _C_1	1.67 mm	1.49 mm	1.1208	1.4 mm	2.75 mm	0.5091	8.67 mm
	<i>C. hagenii</i> _C_2	1.66 mm	1.49 mm	1.1141	1.4 mm	2.75 mm	0.5091	8.67 mm
	<i>C. hagenii</i> _C_3	1.68 mm	1.48 mm	1.1351	1.4 mm	2.75 mm	0.5091	8.67 mm
	<i>C. hagenii</i> _D_1	1.88 mm	1.81 mm	1.0387	1.5 mm	3.45 mm	0.4348	No data
	<i>C. hagenii</i> _D_2	1.78 mm	1.85 mm	0.9622	1.5 mm	3.45 mm	0.4348	No data
	<i>C. hagenii</i> _D_3	1.76 mm	1.83 mm	0.9617	1.5 mm	3.45 mm	0.4348	No data
	<i>C. hagenii</i> _D_4	1.87 mm	1.79 mm	1.0447	1.5 mm	3.45 mm	0.4348	No data
	<i>C. hagenii</i> _D_5	1.73 mm	1.76 mm	0.9829	1.5 mm	3.45 mm	0.4348	No data
	<i>C. hagenii</i> _F_1	1.73 mm	1.62 mm	1.068	1.75 mm	3.25 mm	0.5385	No data
	<i>C. hagenii</i> _F_2	1.77 mm	1.71 mm	1.0351	1.75 mm	3.25 mm	0.5385	No data
	<i>C. hagenii</i> _F_3	1.69 mm	1.70 mm	0.9941	1.75 mm	3.25 mm	0.5385	No data
	<i>C. hagenii</i> _F_4	1.76 mm	1.69 mm	1.0414	1.75 mm	3.25 mm	0.5385	No data
	<i>C. hagenii</i> _F_5	1.82 mm	1.69 mm	1.0769	1.75 mm	3.25 mm	0.5385	No data

Table A1 cont'd: Radial, centrodorsal, and syzygy measurement table for all imaged ossicles

Subfamily/ Family	Species_specimen_ossicle #	Radial Height ±0.02 (mm)	Radial Width ±0.02 (mm)	Radial Height to Width Ratio	CD Height ±0.02 (mm)	CD Diameter ±0.02 (mm)	CD Height to Weight Ratio	Diameter at 1 <sup>st</sup> syzygy ±0.01 (mm)
	<i>Thysanometra tenelloides_B_1</i>	1.99 mm	2.70 mm	0.737	1.5 mm	5.0 mm	0.3	15.81 mm
	<i>T. tenelloides_C_1</i>	1.81 mm	2.77 mm	0.6534	1.75 mm	5.5 mm	0.3182	10.71 mm
	<i>T. tenelloides_C_2</i>	1.85 mm	2.76 mm	0.6703	1.75 mm	5.5 mm	0.3182	10.71 mm
	<i>T. tenelloides_C_3</i>	1.87 mm	2.80 mm	0.6678	1.75 mm	5.5 mm	0.3182	10.71 mm
	<i>T. tenelloides_D_1</i>	1.91 mm	2.81 mm	0.6797	1.5 mm	5.0 mm	0.3	12.24 mm
	<i>T. tenelloides_D_2</i>	1.86 mm	2.78 mm	0.6691	1.5 mm	5.0 mm	0.3	12.24 mm
	<i>T. tenelloides_D_3</i>	1.88 mm	2.85 mm	0.6596	1.5 mm	5.0 mm	0.3	12.24 mm
	<i>T. tenelloides_D_4</i>	1.85 mm	2.74 mm	0.6752	1.5 mm	5.0 mm	0.3	12.24 mm
	<i>T. tenelloides_E_1</i>	1.96 mm	2.91 mm	0.6735	1.5 mm	5.0 mm	0.3	11.73 mm
	<i>T. tenelloides_G_1</i>	1.93 mm	2.34 mm	0.8248	1.5 mm	4.25 mm	0.3529	11.22 mm
	<i>T. tenelloides_G_2</i>	2.00 mm	2.35 mm	0.8511	1.5 mm	4.25 mm	0.3529	11.22 mm
<i>Antedonidae i.s.</i>	<i>Balanometra balanoides_A_1</i>	1.73 mm	1.37 mm	1.2628	3.5 mm	2.5 mm	1.4	No data
	<i>Hybometra senta_A_1</i>	1.70 mm	1.56 mm	1.0897	2.5 mm	2.75 mm	0.9091	8.16 mm
	<i>H. senta_A_2</i>	1.74 mm	1.61 mm	1.0807	2.5 mm	2.75 mm	0.9091	8.16 mm
	<i>H. senta_C_1</i>	1.60 mm	1.38 mm	1.1594	2.25 mm	2.5 mm	0.9	8.16 mm
	<i>H. senta_C_2</i>	1.69 mm	1.38 mm	1.2246	2.25 mm	2.5 mm	0.9	8.16 mm
	<i>H. senta_D_1</i>	1.55 mm	1.36 mm	1.1397	2.0 mm	2.5 mm	0.8	7.14 mm
	<i>H. senta_D_2</i>	1.55 mm	1.40 mm	1.1071	2.0 mm	2.5 mm	0.8	7.14 mm
	<i>H. senta_E_1</i>	1.54 mm	1.43 mm	1.0769	2.0 mm	2.5 mm	0.8	6.6 mm
	<i>Poliometra proluxa_A_1</i>	3.80 mm	2.76 mm	1.3768	4.25 mm	5.5 mm	0.7727	No data
	<i>P. proluxa_A_2</i>	3.86 mm	2.89 mm	1.3356	4.25 mm	5.5 mm	0.7727	No data
	<i>P. proluxa_B_1</i>	4.05 mm	2.83 mm	1.4311	4.5 mm	3.75 mm	1.2	No data

Table A1 cont'd: Radial, centrodorsal, and syzygy measurement table for all imaged ossicles

Subfamily/ Family	Species_specimen_ossicle #	Radial Height ±0.02 (mm)	Radial Width ±0.02 (mm)	Radial Height to CD Height ±0.02 Width Ratio	CD Diameter ±0.02 (mm)	CD Height to Weight Ratio	Diameter at 1 <sup>st</sup> syzygy ±0.01 (mm)	
Zenometridae	Psathyrometra sp_B_1	2.59 mm	2.32 mm	1.1164	3.75 mm	3.7 mm	1.0135	No data
	Psathyrometra sp_C_1	3.06 mm	2.58 mm	1.186	4.5 mm	4.25 mm	1.0588	12.825 mm
	Psathyrometra sp_C_2	3.22 mm	2.58 mm	1.2481	4.5 mm	4.25 mm	1.0588	12.825 mm
	Psathyrometra sp_D_1	3.10 mm	3.04 mm	1.0197	7.0 mm	5.5 mm	1.2727	12.35 mm
	Psathyrometra sp_D_2	3.31 mm	3.05 mm	1.0852	7.0 mm	5.5 mm	1.2727	12.35 mm
	Psathyrometra sp_E_1	3.04 mm	2.84 mm	1.0704	4.8 mm	4.75 mm	1.0105	10.45 mm
	Psathyrometra sp_E_2	3.01 mm	2.80 mm	1.075	4.8 mm	4.75 mm	1.0105	10.45 mm
Aporometridae	Aporometra occidentalis_A_1	0.54 mm	1.17 mm	0.4615	1.25 mm	2.0 mm	0.625	No data
	A. occidentalis_B_1	0.73 mm	1.43 mm	0.5105	2.25 mm	3.0 mm	0.75	No data
	A. occidentalis_B_2	0.74 mm	1.43 mm	0.5175	2.25 mm	3.0 mm	0.75	No data
	A. occidentalis_B_3	0.71 mm	1.44 mm	0.493	2.25 mm	3.0 mm	0.75	No data
	A. occidentalis_C_1	0.76 mm	1.49 mm	0.5101	2.5 mm	2.75 mm	0.9091	No data
	A. occidentalis_C_2	0.71 mm	1.48 mm	0.4797	2.5 mm	2.75 mm	0.9091	No data
Notocrinidae	Notocrinus virilis_A_1	3.37 mm	4.44 mm	0.759	6.0 mm	7.25 mm	0.8276	17.85 mm
	N. virilis_A_2	3.27 mm	4.22 mm	0.7749	6.0 mm	7.25 mm	0.8276	17.85 mm
	N. virilis_A_3	3.20 mm	4.03 mm	0.794	6.0 mm	7.25 mm	0.8276	17.85 mm
	N. virilis_B_1	3.42 mm	4.42 mm	0.7737	6.5 mm	7.25 mm	0.8965	17.4 mm
	N. virilis_C_1	2.46 mm	2.83 mm	0.8693	3.75 mm	4.5 mm	0.8333	14.85 mm
	N. virilis_C_2	2.34 mm	2.86 mm	0.8182	3.75 mm	4.5 mm	0.8333	14.85 mm
	N. virilis_C_3	2.33 mm	2.90 mm	0.8034	3.75 mm	4.5 mm	0.8333	14.85 mm
Tropiometridae	Tropiometra carinata_A_1	1.48 mm	2.28 mm	0.6491	1.5 mm	3.75 mm	0.4	No data
	T. carinata_A_2	1.46 mm	2.24 mm	0.6518	1.5 mm	3.75 mm	0.4	No data
	T. carinata_D_1	0.96 mm	1.44 mm	0.6667	1.0 mm	2.0 mm	0.5	7.65 mm
	T. carinata_D_2	0.95 mm	1.41 mm	0.6738	1.0 mm	2.0 mm	0.5	7.65 mm
	T. carinata_D_3	0.94 mm	1.48 mm	0.6351	1.0 mm	2.0 mm	0.5	7.65 mm
	T. carinata_E_1	1.13 mm	1.64 mm	0.689	1.0 mm	2.75 mm	0.3636	8.16 mm

Table A2: Inter-landmark measurements of all imaged ossicles after standardization (see Table 6 for measurement names)

Subfamily/ Family	Species_specimen_ossicle #	2=18	1=3	15=27	14=16	3=4	4=21	13=14	13=23	4=13	22=28	21=23	22=24
Antedoninae	<i>Andrometra psyche_A_1</i>	0.46	0.46	0.39	0.46	0.54	0.65	0.57	0.68	1.63	0.44	0.35	0.24
	<i>A. psyche_A_2</i>	0.37	0.49	0.39	0.46	0.46	0.56	0.47	0.61	1.49	0.41	0.34	0.2
	<i>A. psyche_B_1</i>	0.58	0.6	0.6	0.65	0.53	0.74	0.53	0.7	1.79	0.51	0.37	0.23
	<i>A. psyche_C_1</i>	0.49	0.51	0.47	0.51	0.57	0.63	0.63	0.67	1.67	0.53	0.41	0.25
	<i>Antedon bifida bifida_A_1</i>	0.6	0.79	0.6	0.85	0.425	0.61	0.4	0.64	1.625	0.45	0.41	0.19
	<i>A. bifida bifida_A_3</i>	0.59	0.83	0.57	0.8	0.43	0.64	0.44	0.61	1.64	0.44	0.41	0.2
	<i>A. bifida bifida_C_1</i>	0.51	NA	0.55	0.67	0.46	0.7	0.49	0.73	1.79	0.44	0.38	0.2
	<i>A. bifida bifida_C_2</i>	0.51	NA	0.45	0.68	0.46	0.66	0.44	0.68	1.71	0.43	0.38	0.19
	<i>A. bifida bifida_D_1</i>	0.57	0.92	0.59	0.82	0.54	0.71	0.59	0.76	1.9	0.48	0.46	0.24
	<i>A. bifida bifida_D_2</i>	0.62	0.84	0.57	0.78	0.54	0.73	0.51	0.71	1.81	0.44	0.41	0.23
	<i>A. bifida bifida_D_3</i>	0.55	0.77	0.57	0.71	0.55	0.7	0.53	0.67	1.74	0.44	0.41	0.22
	<i>A. bifida bifida_E_1</i>	0.58	0.66	0.6	0.64	0.5	0.59	0.51	0.62	1.51	0.4	0.35	0.18
	<i>A. bifida bifida_E_2</i>	0.59	0.63	0.51	0.68	0.52	0.63	0.45	0.58	1.49	0.4	0.33	0.19
<i>A. bifida bifida_E_3</i>	0.6	0.82	0.52	0.64	0.375	0.67	0.4	0.65	1.66	0.43	0.35	0.2	
<i>Antedon hupferi_A_1</i>	0.52	0.63	0.56	0.65	0.57	0.62	0.53	0.61	1.51	0.48	0.31	0.23	
<i>A. hupferi_B_1</i>	0.55	0.63	0.57	0.63	0.52	0.64	0.51	0.69	1.67	0.47	0.37	0.21	
<i>A. hupferi_B_2</i>	0.55	0.61	0.53	0.6	0.53	0.65	0.54	0.65	1.63	0.46	0.36	0.2	
<i>A. hupferi_B_3</i>	0.54	0.7	0.6	0.66	0.53	0.66	0.57	0.66	1.62	0.49	0.35	0.21	
<i>A. hupferi_C_1</i>	0.48	0.6	0.53	0.61	0.54	0.62	0.5	0.61	1.54	0.45	0.35	0.18	
<i>A. hupferi_D_1</i>	0.59	0.6	0.625	0.6	0.53	0.65	0.54	0.66	1.65	0.46	0.375	0.18	
<i>A. hupferi_D_2</i>	0.59	0.68	0.61	0.66	0.54	0.73	0.55	0.72	1.78	0.48	0.37	0.18	
<i>A. hupferi_D_3</i>	0.6	0.66	0.6	0.61	0.56	0.72	0.54	0.68	1.7	0.46	0.34	0.18	
<i>Antedon c.f. incommoda_A_1</i>	0.54	0.46	0.55	0.47	0.59	0.59	0.55	0.47	1.34	0.45	0.3	0.19	
<i>A. c.f. incommoda_B_1</i>	0.53	0.47	0.53	0.46	0.65	0.51	0.63	0.56	1.46	0.44	0.39	0.19	
<i>Antedon loveni_A_1</i>	0.56	0.46	0.61	0.49	0.51	0.47	0.49	0.44	1.21	0.36	0.33	0.2	
<i>A. loveni_A_2</i>	0.58	0.5	0.56	0.5	0.52	0.44	0.48	0.45	1.17	0.36	0.31	0.19	
<i>A. loveni_A_3</i>	0.49	0.46	0.55	0.48	0.52	0.45	0.51	0.45	1.15	0.37	0.31	0.15	
<i>A. loveni_B_1</i>	0.49	0.48	0.46	0.54	0.48	0.46	0.48	0.45	1.18	0.4	0.31	0.18	
<i>A. loveni_B_2</i>	0.51	0.51	0.51	0.6	0.51	0.46	0.51	0.48	1.21	0.4	0.31	0.18	
<i>A. loveni_C_1</i>	0.51	0.44	0.54	0.44	0.47	0.43	0.46	0.44	1.15	0.36	0.33	0.2	
<i>A. loveni_C_2</i>	0.54	0.44	0.52	0.44	0.46	0.4	0.49	0.42	1.12	0.37	0.34	0.2	
<i>A. loveni_D_1</i>	0.52	0.46	0.5	0.48	0.48	0.44	0.44	0.44	1.18	0.41	0.35	0.2	
<i>A. loveni_D_2</i>	0.52	0.46	0.52	0.48	0.48	0.41	0.5	0.43	1.15	0.39	0.35	0.22	
<i>A. loveni_E_1</i>	0.48	0.55	0.5	0.55	0.45	0.52	0.43	0.6	1.4	0.4	0.33	0.22	
<i>A. loveni_E_2</i>	0.52	0.53	0.51	0.64	0.46	0.59	0.42	0.63	1.52	0.41	0.32	0.25	
<i>Antedon c.f. loveni_F_1</i>	0.33	0.42	0.375	0.33	0.65	0.7	0.67	0.67	1.8	0.5	0.46	0.25	
<i>A. c.f. loveni_F_2</i>	0.375	0.35	0.29	0.375	0.69	0.56	0.65	0.56	1.58	0.48	0.46	0.27	
<i>A. c.f. loveni_F_3</i>	0.35	0.45	0.37	0.37	0.53	0.63	0.57	0.63	1.69	0.47	0.45	0.25	
<i>A. c.f. loveni_F_4</i>	0.45	0.35	0.41	0.33	0.53	0.61	0.53	0.61	1.67	0.51	0.45	0.22	
<i>A. c.f. loveni_G_1</i>	0.42	0.42	0.42	0.42	0.5	0.56	0.5	0.52	1.48	0.5	0.42	0.23	
<i>A. c.f. loveni_G_2</i>	0.4	0.36	0.4	0.36	0.49	0.49	0.54	0.45	1.33	0.47	0.38	0.42	
<i>A. c.f. loveni_G_3</i>	0.46	0.37	0.41	0.43	0.55	0.54	0.55	0.55	1.5	0.46	0.41	0.22	
<i>A. c.f. loveni_G_4</i>	0.35	0.46	0.4	0.39	0.54	0.54	0.51	0.53	1.44	0.46	0.39	0.21	
<i>Antedon mediterranea_A_1</i>	0.42	0.51	0.5	0.58	0.49	0.58	0.48	0.59	1.4	0.48	0.27	0.19	
<i>A. mediterranea_A_2</i>	0.4	0.59	0.46	0.58	0.46	0.625	0.46	0.64	1.51	0.44	0.28	0.2	
<i>A. mediterranea_C_1</i>	0.41	0.59	0.46	0.51	0.47	0.65	0.49	0.66	1.58	0.45	0.29	0.2	
<i>A. mediterranea_D_1</i>	0.45	0.6	0.44	0.59	0.4	0.62	0.39	0.68	1.52	0.48	0.25	0.2	
<i>A. mediterranea_D_2</i>	0.45	0.61	0.43	0.58	0.4	0.67	0.45	0.65	1.57	0.48	0.26	0.2	
<i>A. mediterranea_D_3</i>	0.42	0.58	0.46	0.55	0.34	0.48	0.42	0.63	1.31	0.49	0.25	0.2	
<i>A. mediterranea_E_1</i>	0.3	0.57	0.28	0.54	0.47	0.69	0.45	0.67	1.58	0.44	0.26	0.22	
<i>A. mediterranea_E_2</i>	0.35	0.61	0.33	0.58	0.43	0.74	0.47	0.71	1.67	0.46	0.26	0.23	

Table A2 cont'd: Inter-landmark measurements of all imaged ossicles after standardization (see Table 6 for measurement names)

Subfamily/ Family	Species_specimen_ossicle #	2=18	1=3	15=27	14=16	3=4	4=21	13=14	13=23	4=13	22=28	21=23	22=24
	<i>Antedon petasus_A_1</i>	0.47	0.5	0.41	0.65	0.45	0.53	0.43	0.56	1.325	0.43	0.26	0.17
	<i>A. petasus_A_2</i>	0.49	0.71	0.49	0.59	0.37	0.56	0.44	0.57	1.4	0.47	0.3	0.19
	<i>A. petasus_C_1</i>	0.48	0.51	0.46	0.53	0.45	0.49	0.43	0.46	1.19	0.39	0.26	0.17
	<i>A. petasus_D_1</i>	0.49	0.59	0.47	0.62	0.45	0.51	0.43	0.57	1.34	0.4	0.28	0.18
	<i>Antedon parviflora_B_1</i>	0.44	0.34	0.43	0.34	0.6	0.47	0.63	0.49	1.25	0.36	0.3	0.19
	<i>A. parviflora_E_1</i>	0.41	0.45	0.4	0.45	0.56	0.55	0.59	0.55	1.38	0.38	0.29	0.18
	<i>A. parviflora_C_1</i>	0.65	0.55	0.6	0.6	0.65	0.65	0.65	0.55	1.65	0.5	0.55	0.3
	<i>A. parviflora_D_1</i>	0.5	0.54	0.46	0.54	0.5	0.42	0.54	0.42	1.25	0.33	0.5	0.25
	<i>Antedon c.f. parviflora_F_1</i>	0.52	0.41	0.5	0.36	0.625	0.47	0.625	0.45	1.22	0.36	0.34	0.25
	<i>A. c.f. parviflora_F_2</i>	0.52	0.39	0.54	0.38	0.72	0.52	0.7	0.47	1.26	0.41	0.34	0.26
	<i>A. c.f. parviflora_F_3</i>	0.53	0.35	0.45	0.41	0.62	0.44	0.61	0.45	1.2	0.39	0.32	0.24
	<i>A. c.f. parviflora_F_4</i>	0.57	0.38	0.56	0.36	0.77	0.49	0.69	0.51	1.29	0.38	0.34	0.25
	<i>Antedon serrata_A_1</i>	0.52	0.42	0.52	0.46	0.6	0.44	0.58	0.46	1.25	0.38	0.36	0.17
	<i>A. serrata_A_2</i>	0.51	0.49	0.51	0.51	0.63	0.49	0.63	0.51	1.35	0.35	0.37	0.22
	<i>A. serrata_B_1</i>	0.54	0.4	0.54	0.4	0.54	0.47	0.54	0.46	1.22	0.35	0.31	0.2
	<i>Ctenantedon kinziei_A_1</i>	0.68	0.63	0.65	0.61	0.48	0.68	0.55	0.59	1.59	0.34	0.34	0.22
	<i>C. kinziei_A_2</i>	0.59	0.59	0.59	0.63	0.48	0.57	0.51	0.63	1.48	0.31	0.3	0.2
	<i>C. kinziei_C_1</i>	0.54	0.65	0.53	0.58	0.47	0.49	0.42	0.51	1.31	0.36	0.35	0.23
	<i>C. kinziei_C_2</i>	0.56	0.575	0.59	0.64	0.425	0.41	0.54	0.59	1.25	0.36	0.3	0.225
	<i>C. kinziei_D_1</i>	0.72	0.7	0.75	0.66	0.45	0.53	0.47	0.57	1.45	0.36	0.4	0.23
	<i>C. kinziei_D_2</i>	0.68	0.74	0.7	0.75	0.43	0.55	0.45	0.57	1.45	0.32	0.38	0.24
	<i>C. kinziei_D_3</i>	0.72	0.66	0.72	0.66	0.47	0.53	0.43	0.47	1.34	0.36	0.38	0.24
	<i>Dorometra briseis_A_1</i>	0.41	0.43	0.41	0.43	0.48	0.35	0.5	0.35	1.06	0.24	0.39	0.26
	<i>D. briseis_A_2</i>	0.42	0.42	0.42	0.42	0.51	0.33	0.51	0.35	1.09	0.3	0.42	0.28
	<i>D. briseis_B_1</i>	0.51	0.43	0.51	0.46	0.49	0.32	0.51	0.4	1.08	0.3	0.38	0.27
	<i>Dorometra c.f. briseis_C_1</i>	0.37	0.33	0.39	0.33	0.6	0.4	0.63	0.43	1.06	0.39	0.28	0.19
	<i>D. c.f. briseis_C_2</i>	0.4	0.38	0.44	0.35	0.6	0.4	0.6	0.41	1.08	0.43	0.3	0.21
	<i>D. c.f. briseis_C_3</i>	0.39	0.31	0.4	0.33	0.61	0.4	0.6	0.4	1.01	0.4	0.27	0.19
	<i>D. c.f. briseis_C_4</i>	0.44	0.32	0.38	0.32	0.62	0.38	0.57	0.38	1.01	0.4	0.28	0.19
	<i>Dorometra parvicirra_A_1</i>	0.52	0.37	0.54	0.38	0.55	0.4	0.53	0.38	1.03	0.36	0.27	0.22
	<i>D. parvicirra_B_1</i>	0.49	0.3	0.47	0.32	0.53	0.37	0.54	0.37	0.97	0.34	0.25	0.18
	<i>D. parvicirra_B_2</i>	0.52	0.35	0.57	0.33	0.56	0.37	0.55	0.38	0.96	0.33	0.25	0.18
	<i>D. parvicirra_B_3</i>	0.51	0.33	0.53	0.31	0.54	0.39	0.57	0.37	0.97	0.36	0.24	0.17
	<i>D. parvicirra_C_1</i>	0.48	0.43	0.48	0.4	0.52	0.4	0.53	0.38	1.01	0.3	0.26	0.19
	<i>Iridometra adrestine_B_1</i>	0.52	0.49	0.54	0.49	0.41	0.45	0.51	0.52	1.2	0.41	0.25	0.16
	<i>I. adrestine_C_1</i>	0.51	0.41	0.53	0.38	0.47	0.34	0.5	0.35	0.93	0.31	0.25	0.19
Bathymetrinae	<i>Hathrometra tenella_A_1</i>	0.65	0.61	0.65	0.61	0.38	0.34	0.34	0.34	0.91	0.31	0.26	0.17
	<i>H. tenella_A_2</i>	0.65	0.55	0.67	0.59	0.4	0.35	0.4	0.35	0.93	0.35	0.27	0.18
	<i>H. tenella_A_3</i>	0.63	0.65	0.64	0.59	0.37	0.34	0.35	0.32	0.92	0.36	0.29	0.18
	<i>H. tenella_B_1</i>	0.55	0.65	0.57	0.63	0.28	0.32	0.26	0.33	0.9	0.33	0.27	0.17
	<i>H. tenella_D_1</i>	0.61	0.62	0.6	0.61	0.29	0.33	0.325	0.35	0.925	0.31	0.26	0.18
	<i>H. tenella_E_1</i>	0.6	0.7	0.61	0.65	0.28	0.39	0.32	0.39	1.05	0.32	0.29	0.2
	<i>H. tenella_E_2</i>	0.6	NA	0.61	0.67	0.26	0.37	0.27	0.375	1.03	0.31	0.3	0.19
	<i>Thaumatometra tenuis_B_1</i>	0.71	0.66	0.75	0.66	0.34	0.45	0.42	0.45	1.14	0.34	0.29	0.18
	<i>T. tenuis_B_2</i>	0.73	0.73	0.68	0.72	0.35	0.46	0.34	0.45	1.17	0.34	0.3	0.2
	<i>T. tenuis_B_3</i>	0.7	0.71	0.73	0.68	0.37	0.47	0.35	0.45	1.16	0.33	0.29	0.19
	<i>Tonrometra spinulifera_A_1</i>	0.63	0.63	0.64	0.71	0.21	0.22	0.21	0.21	0.61	0.24	0.2	0.14
	<i>T. spinulifera_A_2</i>	0.66	0.69	0.67	0.69	0.22	0.24	0.21	0.23	0.63	0.23	0.19	0.14
	<i>T. spinulifera_B_1</i>	0.64	0.65	0.66	0.65	0.28	0.26	0.26	0.24	0.7	0.23	0.22	0.17
	<i>T. spinulifera_C_1</i>	0.65	0.69	0.65	0.65	0.25	0.25	0.27	0.25	0.68	0.26	0.2	0.14
	<i>T. spinulifera_E_1</i>	0.62	0.68	0.58	0.63	0.26	0.27	0.25	0.25	0.71	0.25	0.22	0.17
	<i>T. spinulifera_E_2</i>	0.63	0.67	0.58	0.63	0.27	0.26	0.25	0.24	0.71	0.24	0.23	0.17
	<i>T. spinulifera_E_3</i>	0.61	0.61	0.64	0.73	0.25	0.25	0.22	0.24	0.66	0.23	0.22	0.17

Table A2 cont'd: Inter-landmark measurements of all imaged ossicles after standardization (see Table 6 for measurement names)

Subfamily/ Family	Species_specimen_ossicle #	2=18	1=3	15=27	14=16	3=4	4=21	13=14	13=23	4=13	22=28	21=23	22=24
	<i>Trichometra cubensis_E_1</i>	0.59	0.5	0.56	0.57	0.44	0.43	0.41	0.44	1.1	0.34	0.26	0.19
	<i>T. cubensis_E_2</i>	0.61	0.62	0.63	0.52	0.39	0.46	0.44	0.43	1.14	0.38	0.28	0.2
	<i>T. cubensis_E_3</i>	0.63	0.54	0.58	0.52	0.42	0.43	0.44	0.39	1.07	0.38	0.27	0.2
<i>Heliometrinae</i>	<i>Anthometrina adriani_A_1</i>	0.58	0.41	0.6	0.41	0.49	0.39	0.52	0.4	0.99	0.39	0.22	0.14
	<i>A. adriani_A_2</i>	0.54	0.45	0.55	0.41	0.44	0.38	0.46	0.38	0.91	0.37	0.18	0.12
	<i>A. adriani_A_3</i>	0.51	0.44	0.53	0.41	0.47	0.38	0.46	0.39	0.94	0.36	0.21	0.14
	<i>A. adriani_B_1</i>	0.55	0.48	0.55	0.43	0.43	0.38	0.44	0.38	0.95	0.33	0.21	0.14
	<i>A. adriani_B_2</i>	0.54	0.49	0.52	0.49	0.39	0.39	0.42	0.41	1	0.35	0.22	0.15
	<i>A. adriani_C_1</i>	0.6	0.38	0.62	0.44	0.45	0.4	0.49	0.39	0.97	0.35	0.22	0.15
	<i>A. adriani_C_2</i>	0.63	0.48	0.58	0.41	0.38	0.4	0.42	0.4	1	0.37	0.21	0.15
	<i>A. adriani_D_1</i>	0.64	0.44	0.62	0.49	0.42	0.39	0.45	0.4	0.99	0.33	0.21	0.14
	<i>A. adriani_E_1</i>	0.55	0.45	0.53	0.44	0.41	0.37	0.42	0.37	0.91	0.32	0.2	0.13
	<i>A. adriani_E_2</i>	0.53	0.42	0.52	0.45	0.43	0.36	0.42	0.37	0.92	0.32	0.21	0.13
	<i>A. adriani_E_3</i>	0.53	0.45	0.53	0.42	0.4	0.36	0.44	0.38	0.9	0.34	0.19	0.13
	<i>Comatonia cristata_B_1</i>	0.49	0.53	0.5	0.51	0.3	0.38	0.3	0.36	0.89	0.33	0.16	0.13
	<i>C. cristata_B_2</i>	0.49	0.52	0.51	0.51	0.28	0.31	0.28	0.3	0.78	0.31	0.17	0.12
	<i>C. cristata_B_3</i>	0.51	0.53	0.53	0.52	0.25	0.32	0.31	0.39	0.88	0.32	0.18	0.12
	<i>C. cristata_C_1</i>	0.63	0.58	0.58	0.56	0.46	0.33	0.45	0.32	0.95	0.33	0.33	0.19
	<i>C. cristata_C_2</i>	0.59	0.48	0.6	0.55	0.44	0.33	0.42	0.33	0.94	0.32	0.31	0.2
	<i>Florometra asperrima_A_1</i>	0.65	0.48	0.61	0.5	0.48	0.43	0.4	0.39	1.06	0.31	0.24	0.12
	<i>F. asperrima_A_2</i>	0.6	0.51	0.62	0.51	0.44	0.39	0.46	0.41	1.02	0.3	0.23	0.11
	<i>F. asperrima_A_3</i>	0.59	0.48	0.62	0.47	0.41	0.42	0.46	0.41	1.05	0.32	0.22	0.12
	<i>F. asperrima_B_1</i>	0.62	0.52	0.63	0.51	0.42	0.4	0.44	0.4	0.96	0.3	0.18	0.11
	<i>F. asperrima_B_2</i>	0.73	0.46	0.71	0.47	0.47	0.45	0.48	0.44	1.09	0.32	0.22	0.11
	<i>F. asperrima_C_1</i>	0.62	0.52	0.58	0.52	0.36	0.38	0.4	0.36	0.92	0.32	0.19	0.11
	<i>F. asperrima_C_2</i>	0.64	0.57	0.64	0.52	0.37	0.39	0.42	0.37	0.94	0.31	0.2	0.12
	<i>F. asperrima_D_1</i>	0.44	0.44	0.45	0.42	0.52	0.33	0.51	0.35	0.9	0.33	0.24	0.13
	<i>F. asperrima_D_2</i>	0.45	0.4	0.46	0.42	0.53	0.38	0.55	0.36	0.99	0.33	0.26	0.13
	<i>F. asperrima_E_1</i>	0.51	0.5	0.6	0.5	0.43	0.4	0.43	0.37	0.98	0.29	0.22	0.11
	<i>F. asperrima_E_2</i>	0.6	0.53	0.59	0.53	0.44	0.43	0.44	0.43	1.08	0.3	0.23	0.13
	<i>F. asperrima_E_3</i>	0.56	0.53	0.55	0.55	0.41	0.38	0.41	0.36	0.93	0.28	0.2	0.1
	<i>Florometra serratissima_B_1</i>	0.75	0.53	0.74	0.52	0.43	0.43	0.45	0.43	1.06	0.31	0.22	0.14
	<i>F. serratissima_B_2</i>	0.71	0.58	0.78	0.54	0.42	0.43	0.45	0.44	1.08	0.31	0.22	0.15
	<i>Promachocrinus kerguelensis_A_1</i>	0.53	0.48	0.53	0.48	0.37	0.26	0.38	0.24	0.61	0.32	0.16	0.15
	<i>P. kerguelensis_A_2</i>	0.59	0.47	0.57	0.5	0.37	0.24	0.4	0.25	0.59	0.32	0.16	0.16
<i>Isometrinae</i>	<i>Isometra graminea_A_1</i>	0.55	0.5	0.53	0.55	0.45	0.41	0.39	0.44	1.06	0.39	0.26	0.17
	<i>I. graminea_A_2</i>	0.63	0.58	0.57	0.56	0.42	0.43	0.4	0.47	1.09	0.43	0.28	0.17
	<i>I. graminea_C_1</i>	0.51	0.48	0.53	0.58	0.37	0.41	0.42	0.42	1.07	0.41	0.27	0.16
	<i>Isometra vivipara_A_1</i>	0.56	0.5	0.55	0.57	0.34	0.37	0.33	0.37	0.95	0.37	0.23	0.15
<i>Perometrinae</i>	<i>Erythrometra rubra_A_1</i>	0.4	0.39	0.39	0.44	0.5	0.48	0.44	0.44	1.19	0.52	0.3	0.19
	<i>E. rubra_B_1</i>	0.47	0.39	0.5	0.39	0.63	0.45	0.6	0.39	1.13	0.5	0.37	0.26
	<i>Hypalometra defecta_A_1</i>	0.47	0.64	0.44	0.71	0.35	0.38	0.31	0.42	1.09	0.4	0.38	0.27
	<i>H. defecta_B_1</i>	0.52	0.55	0.46	0.59	0.45	0.45	0.41	0.39	1.14	0.5	0.36	0.23
	<i>H. defecta_B_2</i>	0.51	0.58	0.45	0.6	0.51	0.45	0.45	0.44	1.13	0.53	0.36	0.22
	<i>H. defecta_D_1</i>	0.51	0.72	0.54	0.71	0.25	0.46	0.26	0.47	1.17	0.39	0.29	0.22
	<i>H. defecta_F_1</i>	0.61	0.67	0.59	0.62	0.43	0.51	0.44	0.44	1.25	0.43	0.34	0.25
	<i>H. defecta_G_1</i>	0.52	0.67	0.55	0.63	0.33	0.42	0.37	0.45	1.13	0.4	0.32	0.23
	<i>H. defecta_G_2</i>	0.5	0.65	0.53	0.64	0.38	0.41	0.38	0.45	1.15	0.4	0.34	0.22
	<i>Perometra diomedea_A_1</i>	0.49	0.48	0.5	0.46	0.54	0.52	0.51	0.52	1.31	0.38	0.28	0.18
	<i>P. diomedea_A_2</i>	0.53	0.54	0.48	0.53	0.5	0.53	0.47	0.51	1.31	0.4	0.29	0.19
	<i>P. diomedea_B_1</i>	0.54	0.58	0.5	0.61	0.54	0.61	0.5	0.54	1.44	0.45	0.32	0.23
	<i>P. diomedea_B_2</i>	0.48	0.51	0.49	0.55	0.48	0.58	0.49	0.54	1.37	0.48	0.27	0.19

Table A2 cont'd: Inter-landmark measurements of all imaged ossicles after standardization (see Table 6 for measurement names)

Subfamily/ Family	Species_specimen_ossicle #	2=18	1=3	15=27	14=16	3=4	4=21	13=14	13=23	4=13	22=28	21=23	22=24
Thysanometrinae	<i>Coccometra hagenii_A_1</i>	0.5	0.475	0.49	0.46	0.33	0.28	0.37	0.31	0.79	0.29	0.21	0.13
	<i>C. hagenii_C_1</i>	0.53	0.5	0.51	0.47	0.37	0.35	0.37	0.31	0.87	0.27	0.23	0.15
	<i>C. hagenii_C_2</i>	0.54	NA	0.53	0.47	0.38	0.32	0.37	0.31	0.86	0.28	0.24	0.13
	<i>C. hagenii_C_3</i>	0.51	0.46	0.53	0.49	0.36	0.26	0.36	0.29	0.77	0.28	0.24	0.13
	<i>C. hagenii_D_1</i>	0.51	0.48	0.49	0.53	0.33	0.3	0.35	0.3	0.79	0.27	0.21	0.15
	<i>C. hagenii_D_2</i>	0.47	0.47	0.47	0.48	0.35	0.31	0.32	0.32	0.85	0.3	0.22	0.15
	<i>C. hagenii_D_3</i>	0.49	0.49	0.47	0.45	0.33	0.34	0.36	0.33	0.86	0.31	0.21	0.14
	<i>C. hagenii_D_4</i>	0.52	0.47	0.51	0.43	0.33	0.28	0.34	0.31	0.8	0.3	0.21	0.14
	<i>C. hagenii_D_5</i>	0.41	0.39	0.49	0.49	0.38	0.3	0.37	0.32	0.83	0.33	0.23	0.15
	<i>C. hagenii_F_1</i>	0.46	0.39	0.48	0.42	0.37	0.27	0.37	0.32	0.75	0.34	0.19	0.14
	<i>C. hagenii_F_2</i>	0.47	0.45	0.46	0.39	0.37	0.275	0.39	0.29	0.75	0.32	0.2	0.14
	<i>C. hagenii_F_3</i>	0.41	0.39	0.44	0.45	0.41	0.33	0.36	0.27	0.79	0.33	0.21	0.16
	<i>C. hagenii_F_4</i>	0.46	0.39	0.47	0.42	0.37	0.27	0.34	0.29	0.75	0.32	0.21	0.15
	<i>C. hagenii_F_5</i>	0.45	0.39	0.48	0.42	0.39	0.29	0.38	0.32	0.8	0.34	0.19	0.14
	Thysanometra tenelloides_B_1	<i>T. tenelloides_B_1</i>	0.65	0.72	0.56	0.73	0.41	0.59	0.39	0.59	1.5	0.31	0.33
<i>T. tenelloides_C_1</i>		0.72	0.81	0.65	0.74	0.42	0.61	0.44	0.63	1.55	0.34	0.31	0.19
<i>T. tenelloides_C_2</i>		0.58	0.7	0.62	0.7	0.45	0.59	0.46	0.62	1.51	0.35	0.31	0.2
<i>T. tenelloides_C_3</i>		0.66	0.65	0.6	0.67	0.46	0.6	0.51	0.66	1.57	0.36	0.32	0.21
<i>T. tenelloides_D_1</i>		0.56	0.72	0.54	0.72	0.41	0.61	0.43	0.64	1.57	0.37	0.34	0.2
<i>T. tenelloides_D_2</i>		0.61	0.76	0.57	0.73	0.4	0.68	0.41	0.66	1.66	0.35	0.33	0.21
<i>T. tenelloides_D_3</i>		0.61	0.8	0.6	0.68	0.4	0.67	0.51	0.68	1.68	0.37	0.34	0.21
<i>T. tenelloides_D_4</i>		0.56	0.71	0.54	0.77	0.41	0.64	0.38	0.65	1.58	0.35	0.3	0.21
<i>T. tenelloides_E_1</i>		0.6	0.82	0.64	0.8	0.43	0.69	0.44	0.65	1.67	0.34	0.35	0.21
<i>T. tenelloides_G_1</i>		0.66	0.72	0.66	0.69	0.56	0.65	0.53	0.59	1.57	0.39	0.35	0.19
<i>T. tenelloides_G_2</i>	0.64	0.76	0.59	0.84	0.47	0.61	0.5	0.61	1.53	0.38	0.34	0.16	
Antedonidae l.s.	<i>Balanometra balanoides_A_1</i>	0.42	0.49	0.42	0.46	0.35	0.29	0.34	0.31	0.82	0.37	0.24	0.17
	<i>Hybometra sents_A_1</i>	0.53	0.57	0.53	0.52	0.47	0.41	0.47	0.42	1.05	0.39	0.26	0.18
	<i>H. sents_A_2</i>	0.48	0.54	0.49	0.55	0.41	0.39	0.41	0.41	0.99	0.36	0.23	0.19
	<i>H. sents_C_1</i>	0.48	0.48	0.51	0.48	0.41	0.38	0.46	0.39	0.95	0.41	0.22	0.16
	<i>H. sents_C_2</i>	0.54	0.41	0.55	0.43	0.5	0.34	0.47	0.36	0.89	0.39	0.22	0.15
	<i>H. sents_D_1</i>	0.58	0.5	0.58	0.51	0.43	0.37	0.44	0.39	0.96	0.36	0.24	0.18
	<i>H. sents_D_2</i>	0.63	0.5	0.58	0.5	0.46	0.37	0.45	0.39	0.97	0.36	0.24	0.18
	<i>H. sents_E_1</i>	0.5	0.5	0.52	0.51	0.38	0.39	0.44	0.4	0.98	0.36	0.24	0.17
	<i>Poliometra proluxa_A_1</i>	0.58	0.6	0.58	0.63	0.21	0.29	0.23	0.28	0.69	0.3	0.15	0.12
<i>P. proluxa_A_2</i>	0.6	0.67	0.61	0.69	0.21	0.27	0.19	0.29	0.68	0.27	0.15	0.13	
<i>P. proluxa_B_1</i>	0.59	0.68	0.56	0.71	0.17	0.29	0.18	0.3	0.72	0.27	0.15	0.14	
Zenometridae	<i>Psathyrometra sp_B_1</i>	0.69	0.64	0.65	0.6	0.33	0.39	0.3	0.35	1.01	0.31	0.28	0.15
	<i>Psathyrometra sp_C_1</i>	0.61	0.65	0.65	0.59	0.33	0.35	0.33	0.36	0.9	0.27	0.21	0.13
	<i>Psathyrometra sp_C_2</i>	0.57	0.56	0.64	0.64	0.32	0.27	0.34	0.35	0.83	0.26	0.21	0.13
	<i>Psathyrometra sp_D_1</i>	0.57	0.75	0.57	0.78	0.29	0.46	0.31	0.43	1.12	0.28	0.26	0.15
	<i>Psathyrometra sp_D_2</i>	0.58	0.72	0.54	0.71	0.31	0.38	0.28	0.38	0.99	0.27	0.25	0.15
	<i>Psathyrometra sp_E_1</i>	0.74	0.79	0.73	0.82	0.35	0.47	0.36	0.47	1.17	0.33	0.26	0.16
	<i>Psathyrometra sp_E_2</i>	0.7	0.8	0.71	0.8	0.35	0.43	0.33	0.43	1.09	0.33	0.25	0.16
Aporometridae	<i>Aporometra occidentalis_A_1</i>	0.66	1.13	0.42	1.16	0.42	0.92	0.47	0.84	2.18	0.58	0.45	0.26
	<i>A. occidentalis_B_1</i>	0.55	1	0.57	0.875	0.375	0.79	0.43	0.71	1.875	0.5	0.39	0.21
	<i>A. occidentalis_B_2</i>	0.58	0.93	0.64	0.93	0.49	0.76	0.45	0.74	1.89	0.53	0.4	0.22
	<i>A. occidentalis_B_3</i>	0.57	1.02	0.64	0.98	0.39	0.79	0.39	0.77	1.875	0.52	0.375	0.21
	<i>A. occidentalis_C_1</i>	0.68	0.96	0.67	1.04	0.39	0.78	0.43	0.87	1.93	0.48	0.33	0.24
	<i>A. occidentalis_C_2</i>	0.57	1.09	0.625	1.11	0.36	0.73	0.41	0.71	1.75	0.48	0.34	0.21



Table A2 cont'd: Inter-landmark measurements of all imaged ossicles after standardization (see Table 6 for measurement names)

Subfamily/ Family	Species_specimen_ossicle #	2=18	1=3	15=27	14=16	3=4	4=21	13=14	13=23	4=13	22=28	21=23	22=24
Notocrinidae	Notocrinus virilis_A_1	0.46	0.81	0.45	0.81	0.23	0.58	0.29	0.52	1.31	0.52	0.23	0.16
	N. virilis_A_2	0.55	0.82	0.52	0.87	0.31	0.65	0.32	0.58	1.46	0.54	0.27	0.18
	N. virilis_A_3	0.51	0.81	0.53	0.79	0.27	0.61	0.3	0.58	1.41	0.51	0.26	0.17
	N. virilis_B_1	0.55	0.81	0.52	0.9	0.32	0.59	0.25	0.62	1.39	0.49	0.22	0.2
	N. virilis_C_1	0.59	0.65	0.57	0.64	0.46	0.52	0.45	0.48	1.19	0.5	0.24	0.16
	N. virilis_C_2	0.63	0.75	0.6	0.69	0.46	0.58	0.47	0.58	1.39	0.5	0.28	0.16
	N. virilis_C_3	0.58	0.75	0.57	0.78	0.42	0.57	0.41	0.57	1.34	0.47	0.25	0.16
Tropiometridae	Tropiometra carinata_A_1	0.65	0.71	0.65	0.69	0.38	0.82	0.4	0.78	1.84	0.47	0.26	0.17
	T. carinata_A_2	0.63	0.7	0.59	0.72	0.43	0.8	0.45	0.82	1.88	0.46	0.26	0.18
	T. carinata_D_1	0.46	0.71	0.51	0.69	0.47	0.69	0.53	0.76	1.75	0.53	0.33	0.21
	T. carinata_D_2	0.58	0.64	0.44	0.76	0.58	0.71	0.5	0.75	1.74	0.51	0.32	0.22
	T. carinata_D_3	0.55	0.74	0.44	0.73	0.47	0.77	0.41	0.78	1.82	0.49	0.31	0.22
	T. carinata_E_1	0.57	0.61	0.48	0.71	0.57	0.75	0.53	0.75	1.82	0.51	0.34	0.19

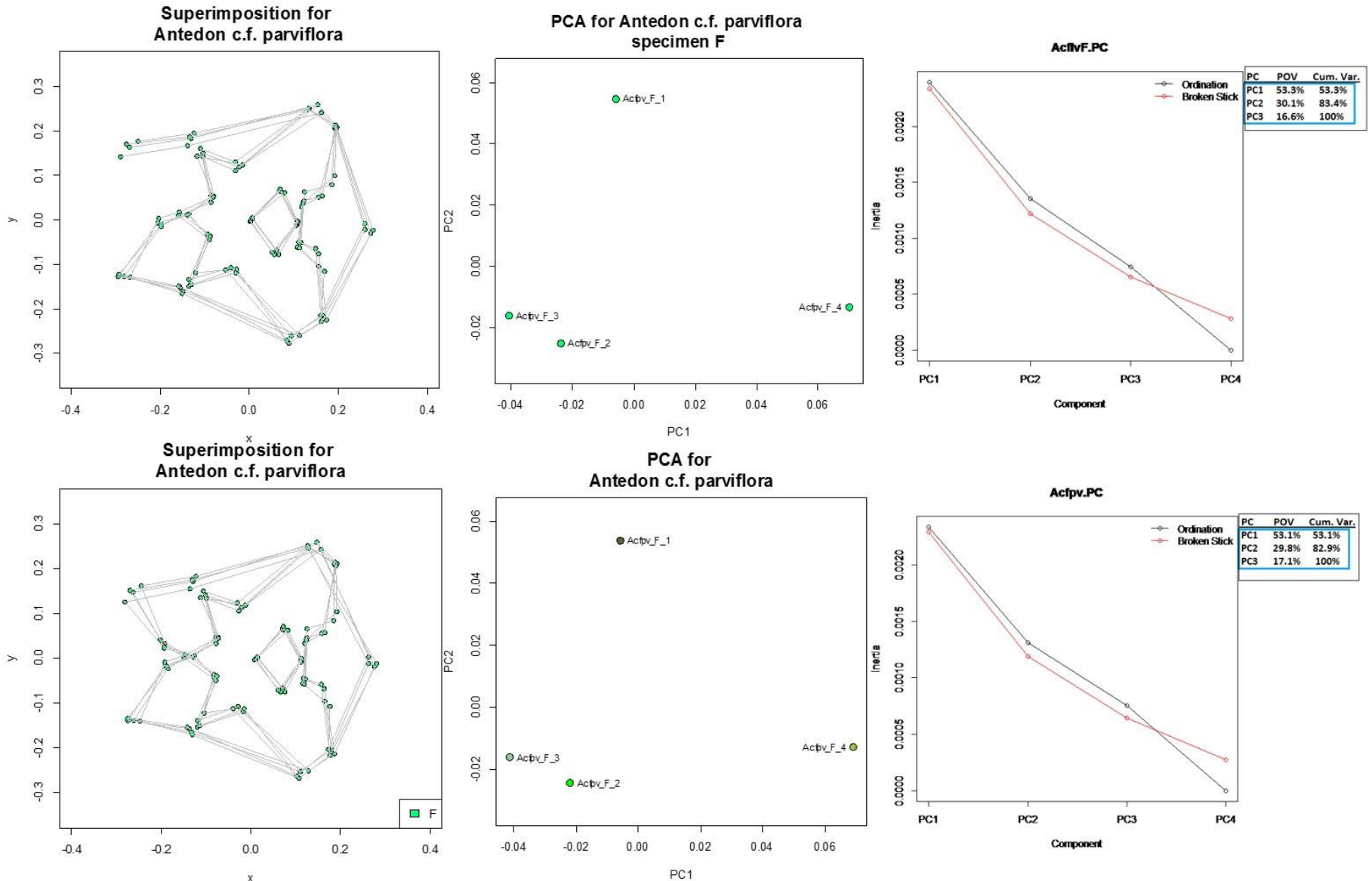


Fig. A1: Superimposed configuration, PCA, and broken stick model for ossicles within *Antedon c.f. parviflora*, specimen F (top: scenario 1; bottom: scenario 2). There is no significant variance within this individual.

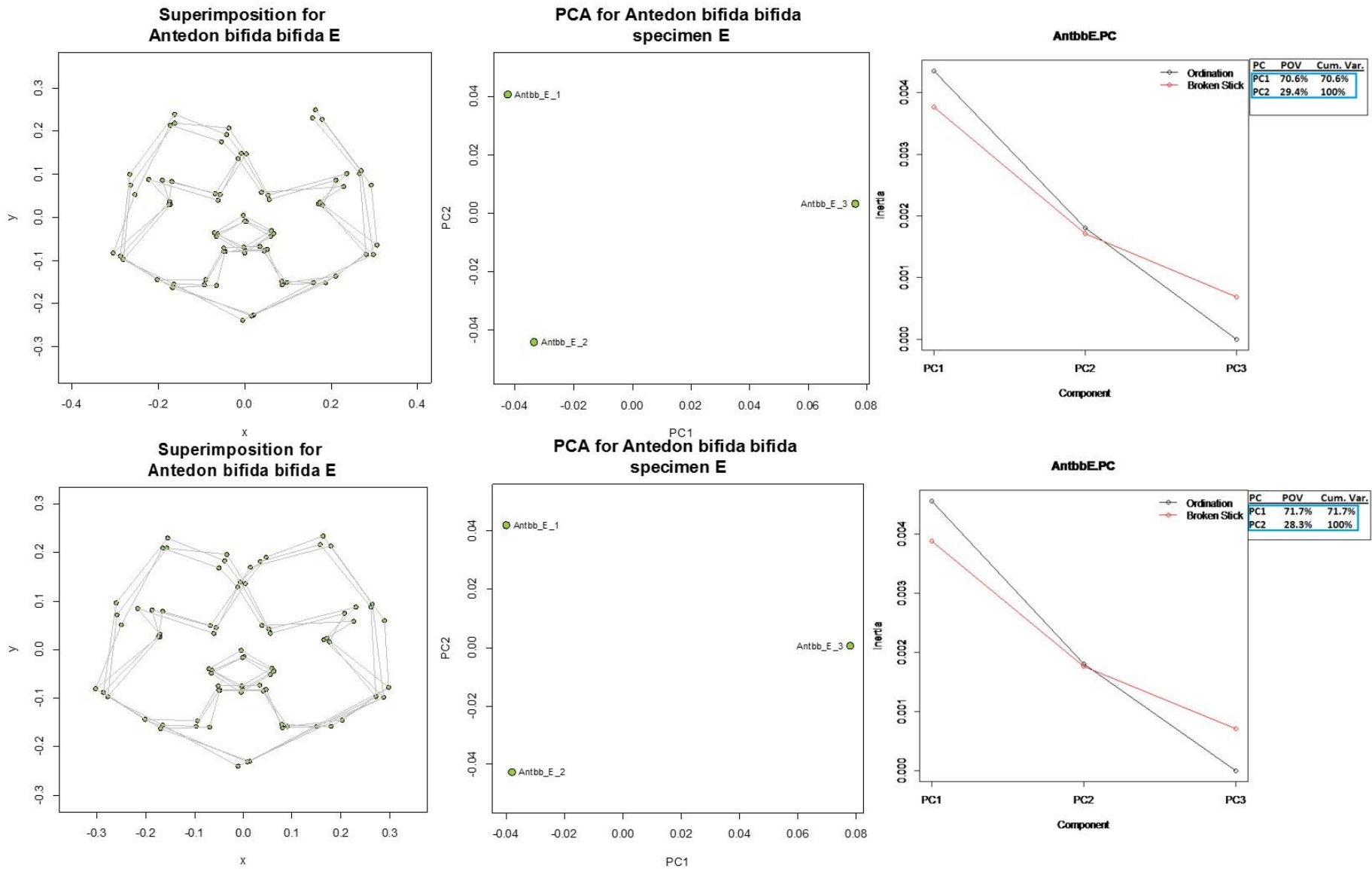


Fig. A2: Superimposed configuration, PCA, and broken stick model for ossicles within *Antedon bifida bifida*, specimen E (top: scenario 1; bottom: scenario 2). There is no significant variance within this individual.

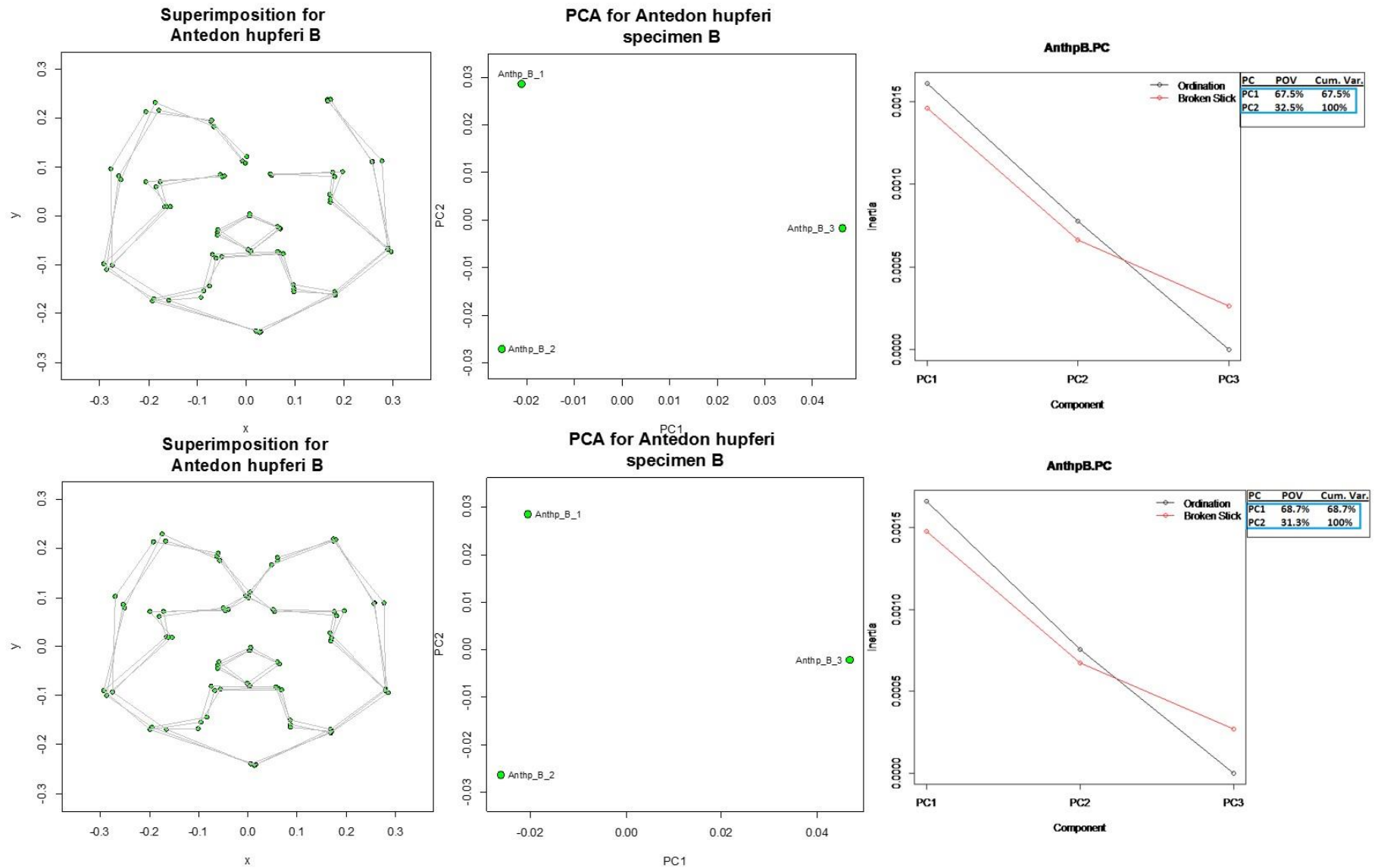


Fig. A3: Superimposed configuration, PCA, and broken stick model for ossicles within *Antedon hupferi*, specimen B (top: scenario 1; bottom: scenario 2). There is no significant variance within this individual.

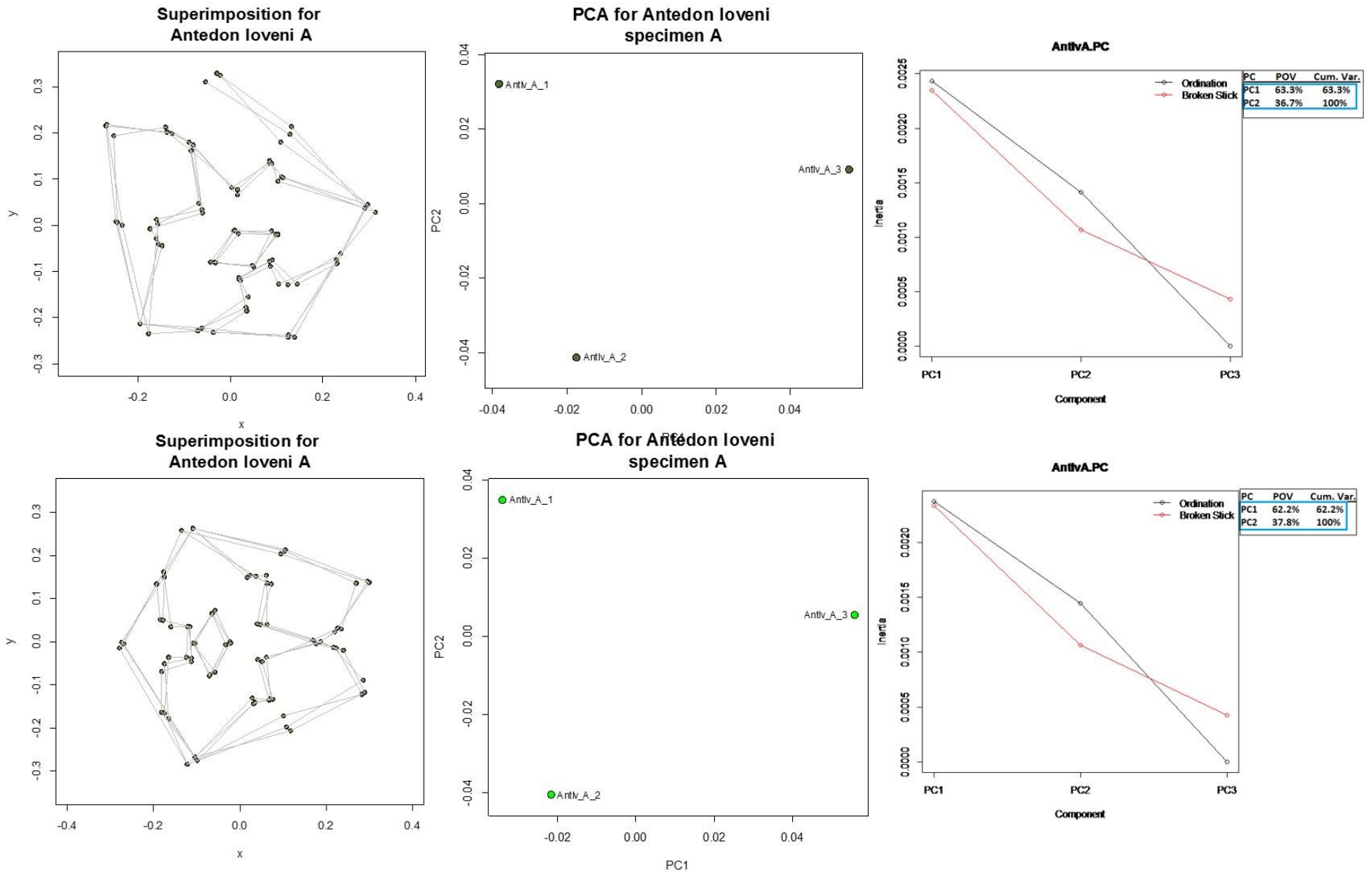


Fig. A4: Superimposed configuration, PCA, and broken stick model for ossicles within *Antedon loveni*, specimen A (top: scenario 1; bottom: scenario 2). There is no significant variance within this individual.

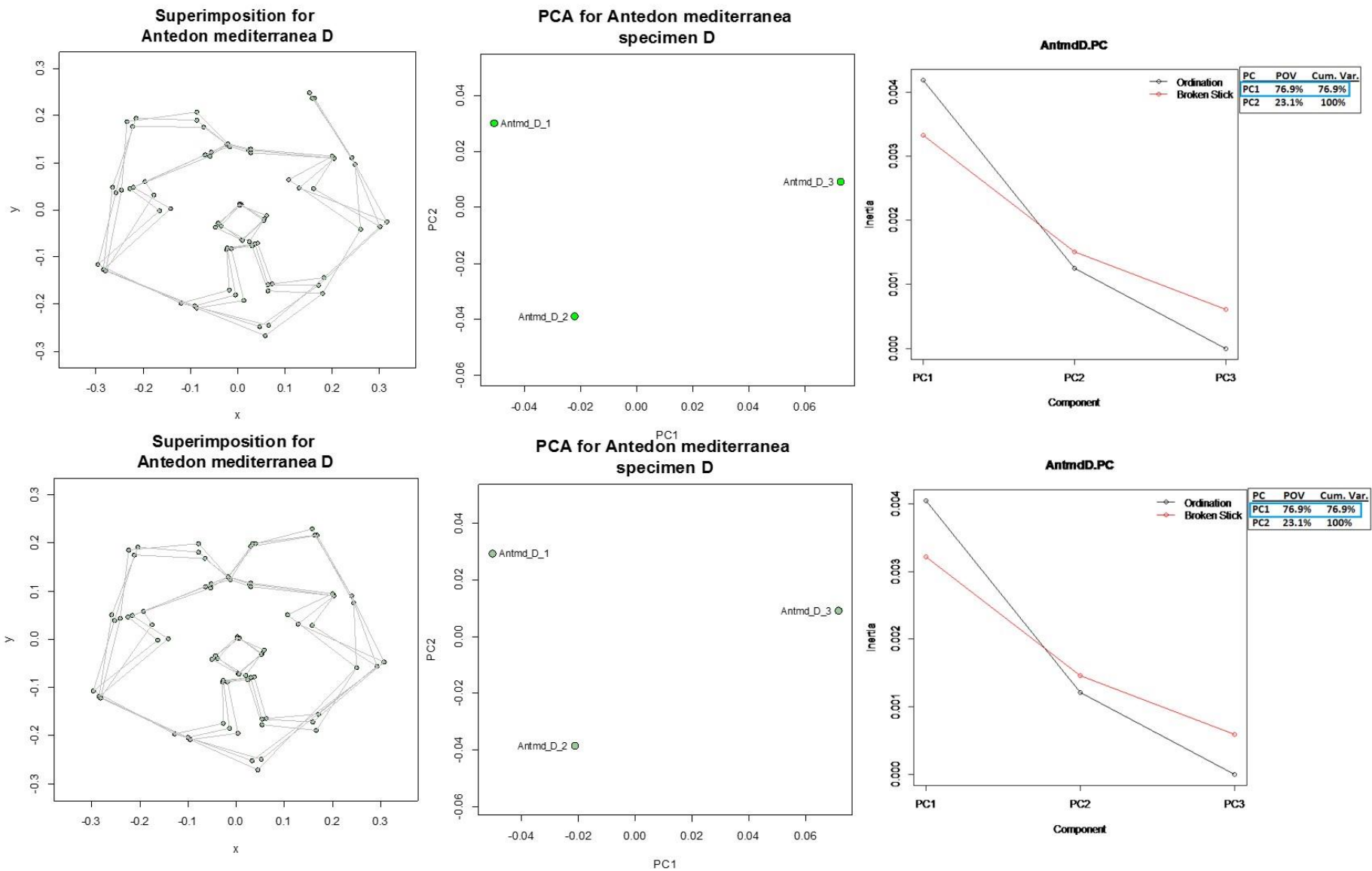


Fig. A5: Superimposed configuration, PCA, and broken stick model for ossicles within *Antedon mediterranea*, specimen D (top: scenario 1; bottom: scenario 2). There is no significant variance within this individual.

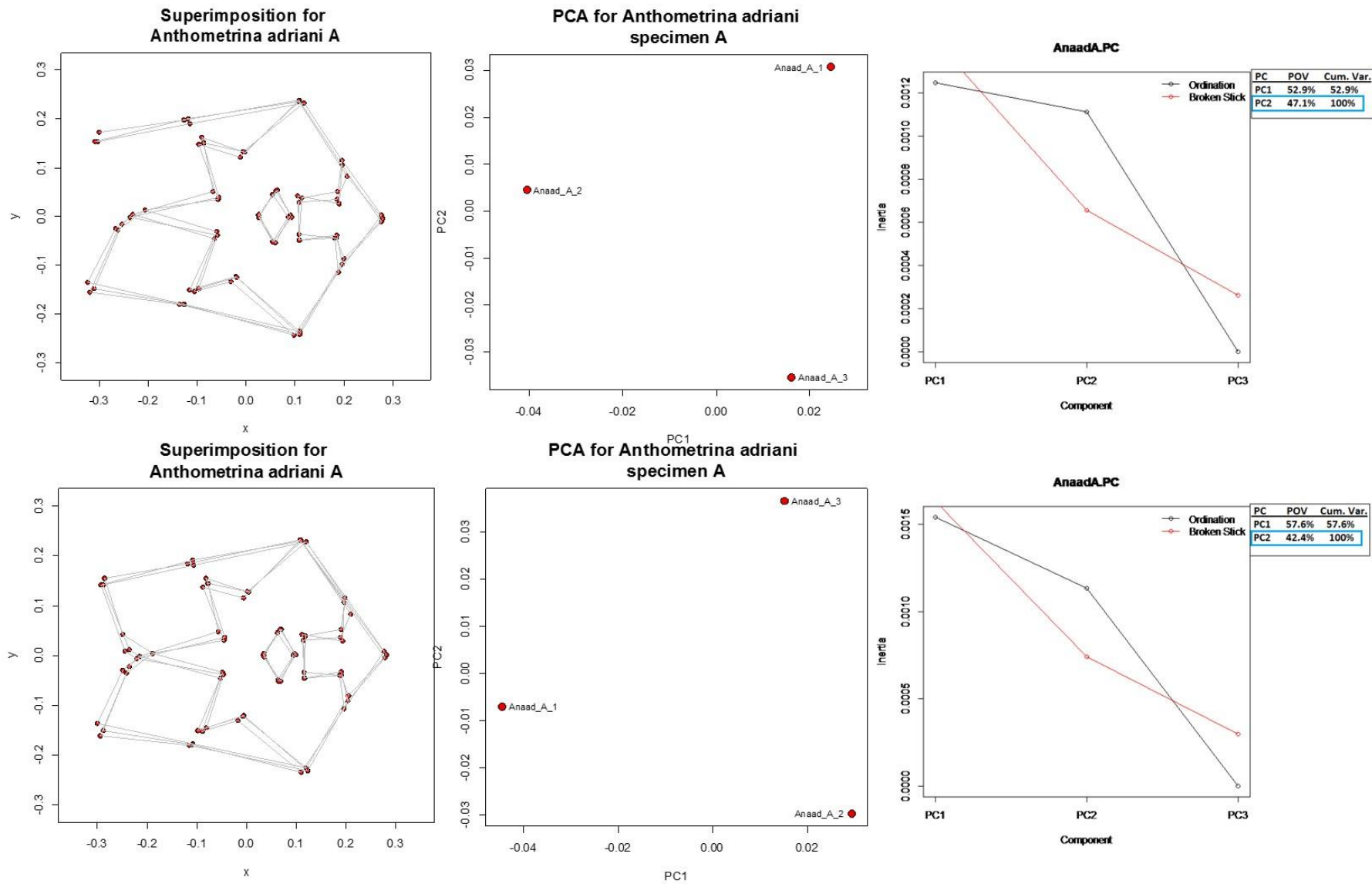


Fig. A6: Superimposed configuration, PCA, and broken stick model for ossicles within *Anthometrina adriani*, specimen A (top: scenario 1; bottom: scenario 2). There is no significant variance within this individual.

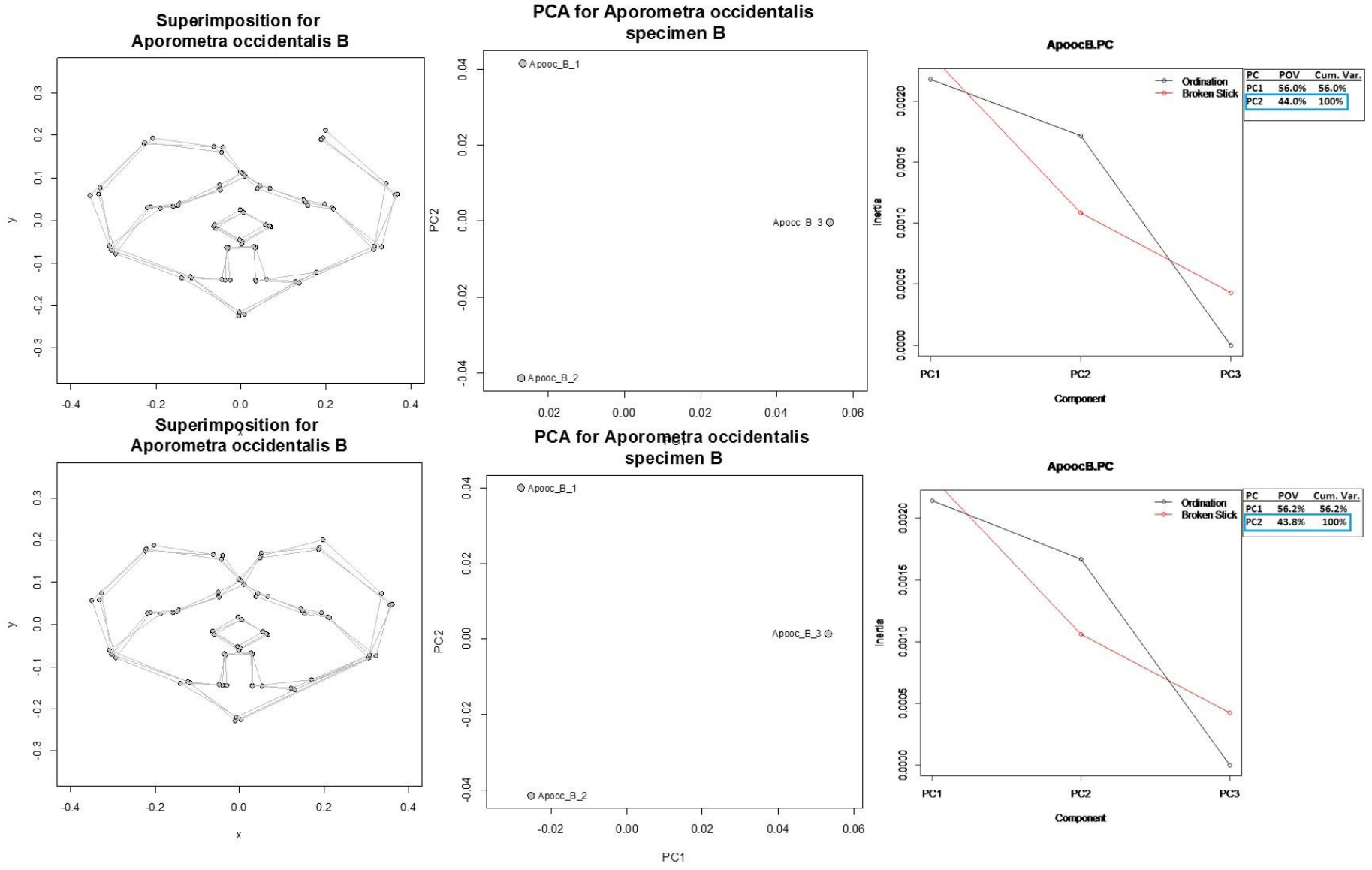


Fig. A7: Superimposed configuration, PCA, and broken stick model for ossicles within *Apometra occidentalis*, specimen B (top: scenario 1; bottom: scenario 2). There is no significant variance within this individual.



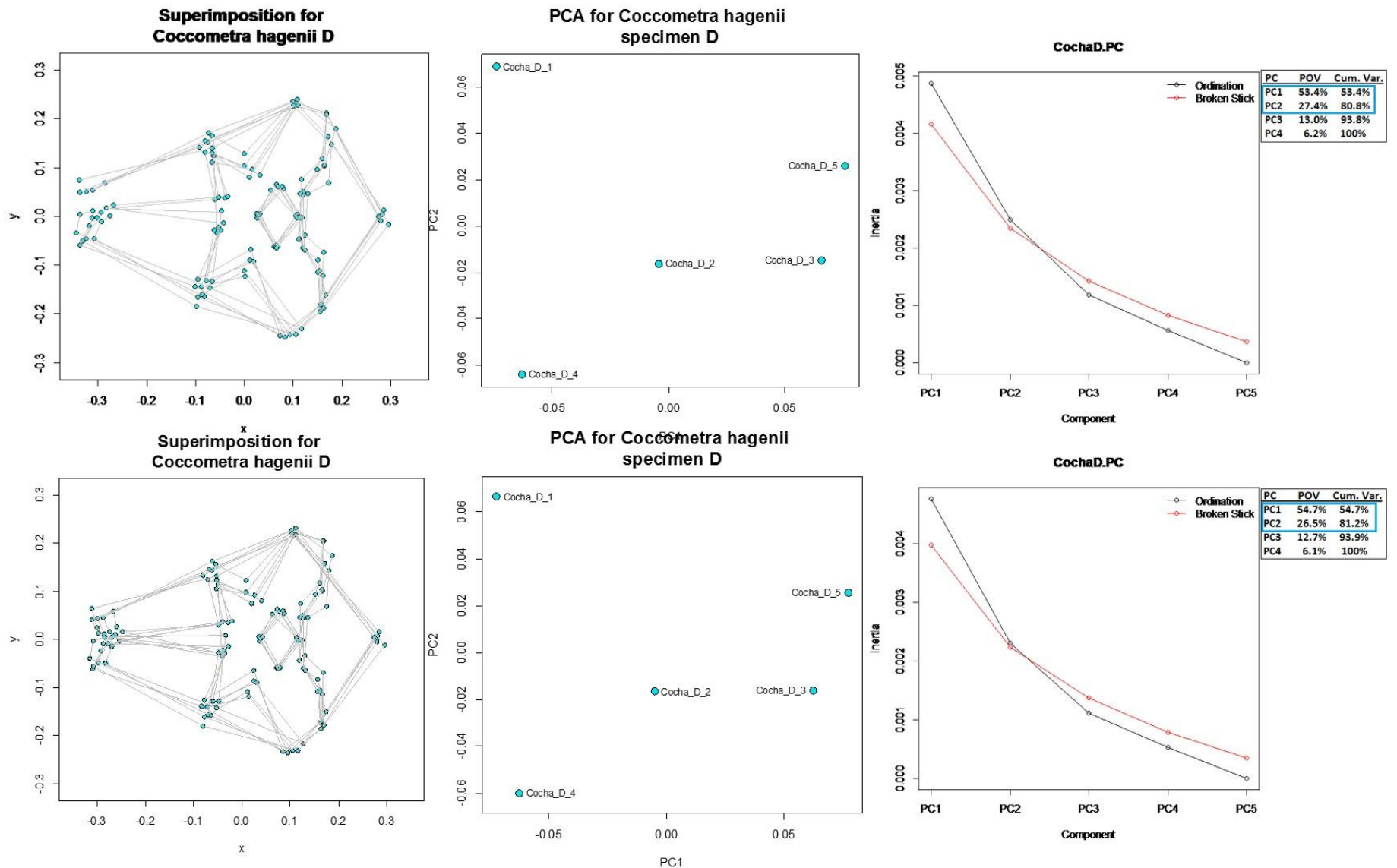


Fig. A8: Superimposed configuration, PCA, and broken stick model for ossicles within *Coccoetra hagenii*, specimen D (top: scenario 1; bottom: scenario 2). There is no significant variance within this individual.

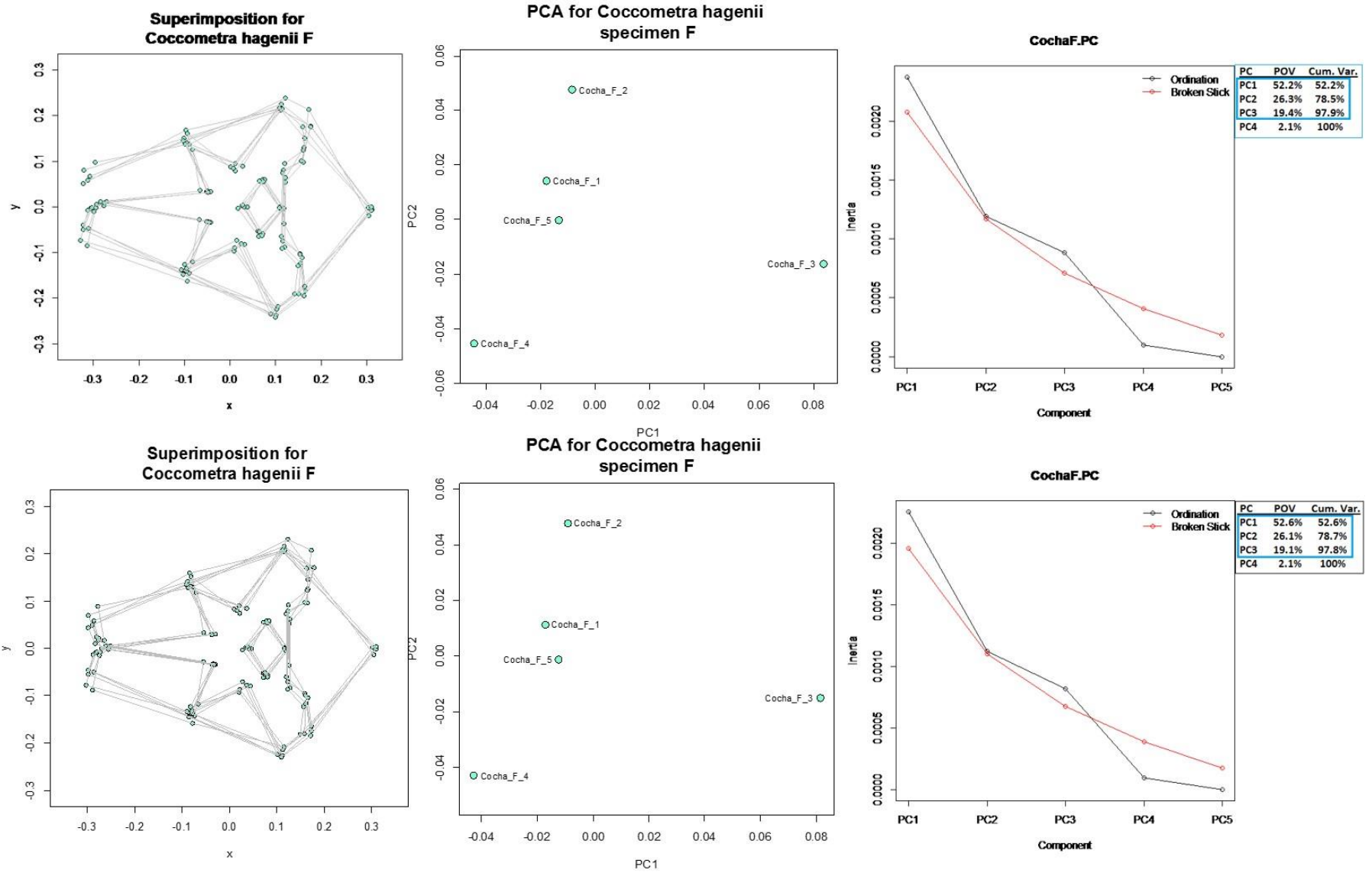


Fig. A9: Superimposed configuration, PCA, and broken stick model for ossicles within *Coccoetra hagenii*, specimen F (top: scenario 1; bottom: scenario 2). There is no significant variance within this individual.

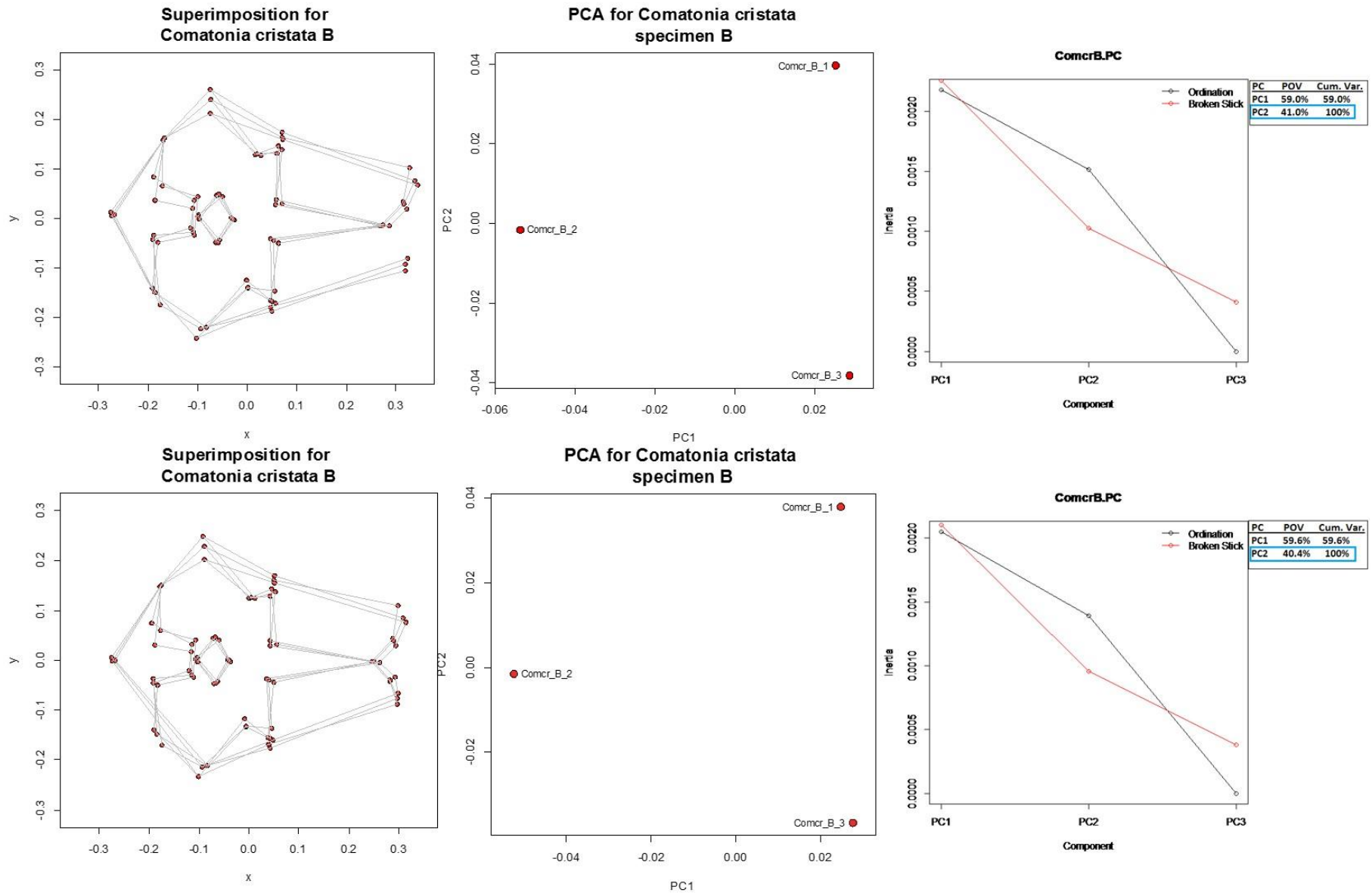


Fig. A10: Superimposed configuration, PCA, and broken stick model for ossicles within *Comatonia cristata*, specimen B (top: scenario 1; bottom: scenario 2). There is no significant variance within this individual.

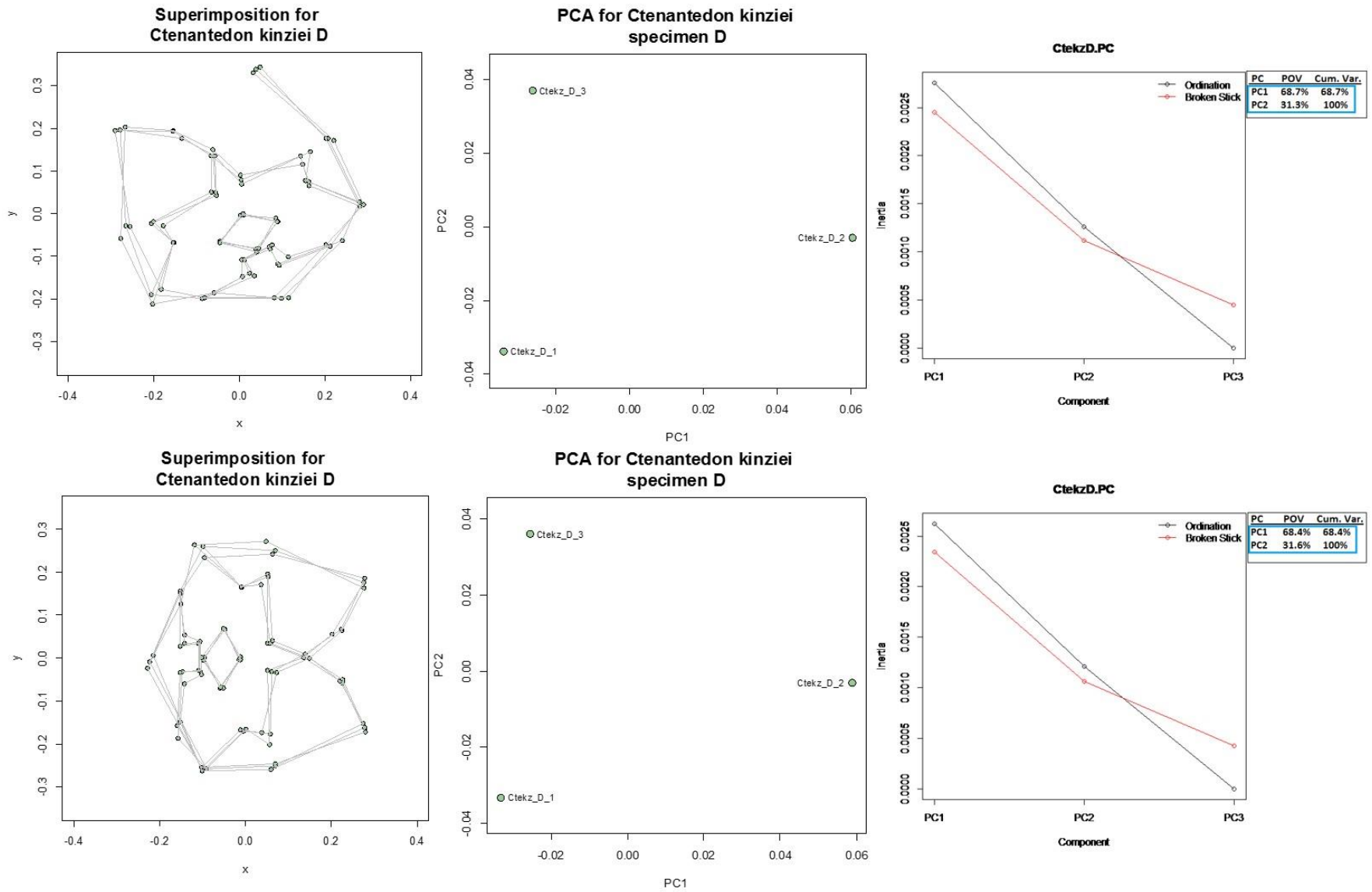


Fig. A11: Superimposed configuration, PCA, and broken stick model for ossicles within *Ctenantedon kinziei*, specimen D (top: scenario 1; bottom: scenario 2). There is no significant variance within this individual.

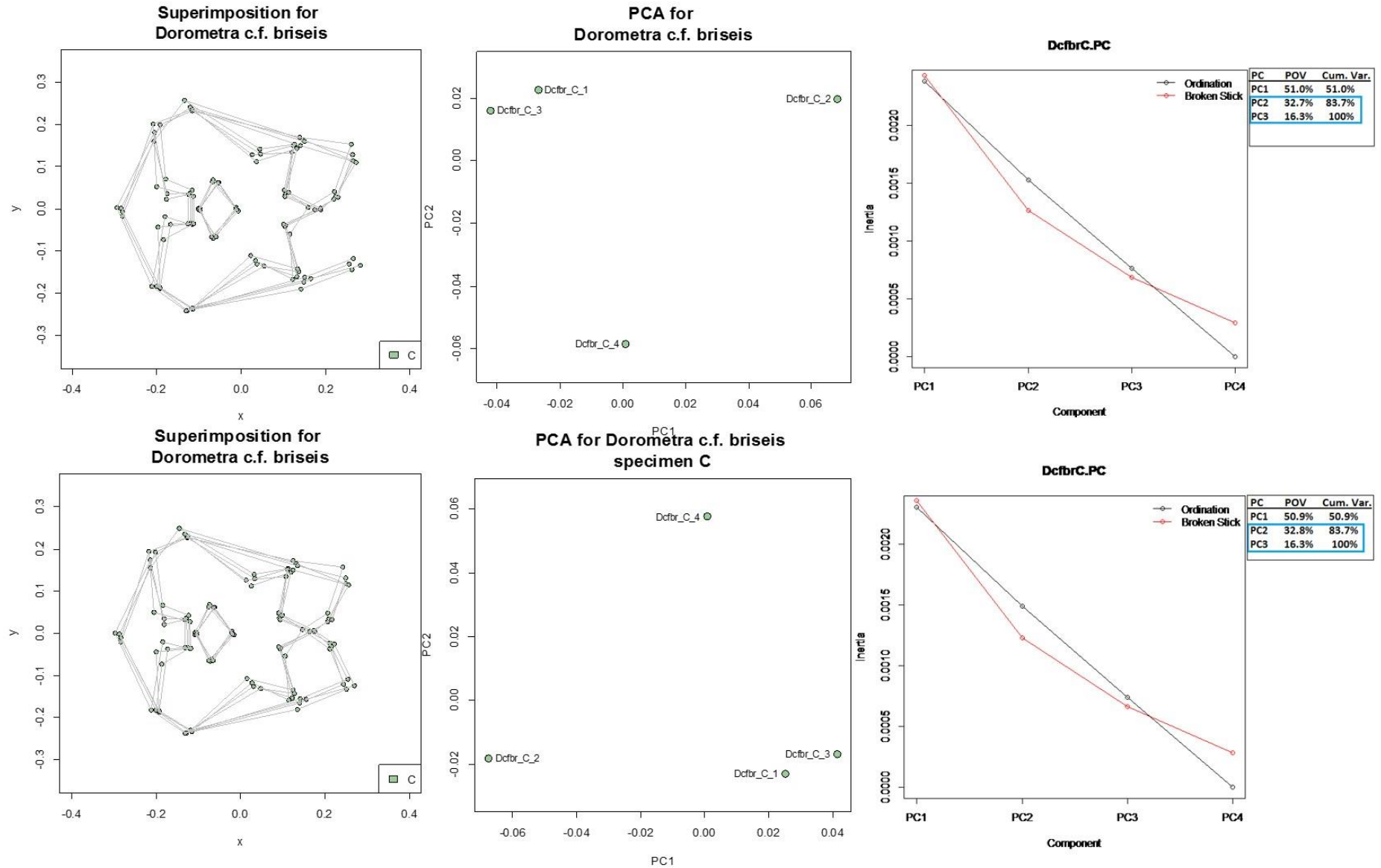


Fig. A12: Superimposed configuration, PCA, and broken stick model for ossicles within *Dorometra c.f. briseis*, specimen C (top: scenario 1; bottom: scenario 2). There is no significant variance within this individual.

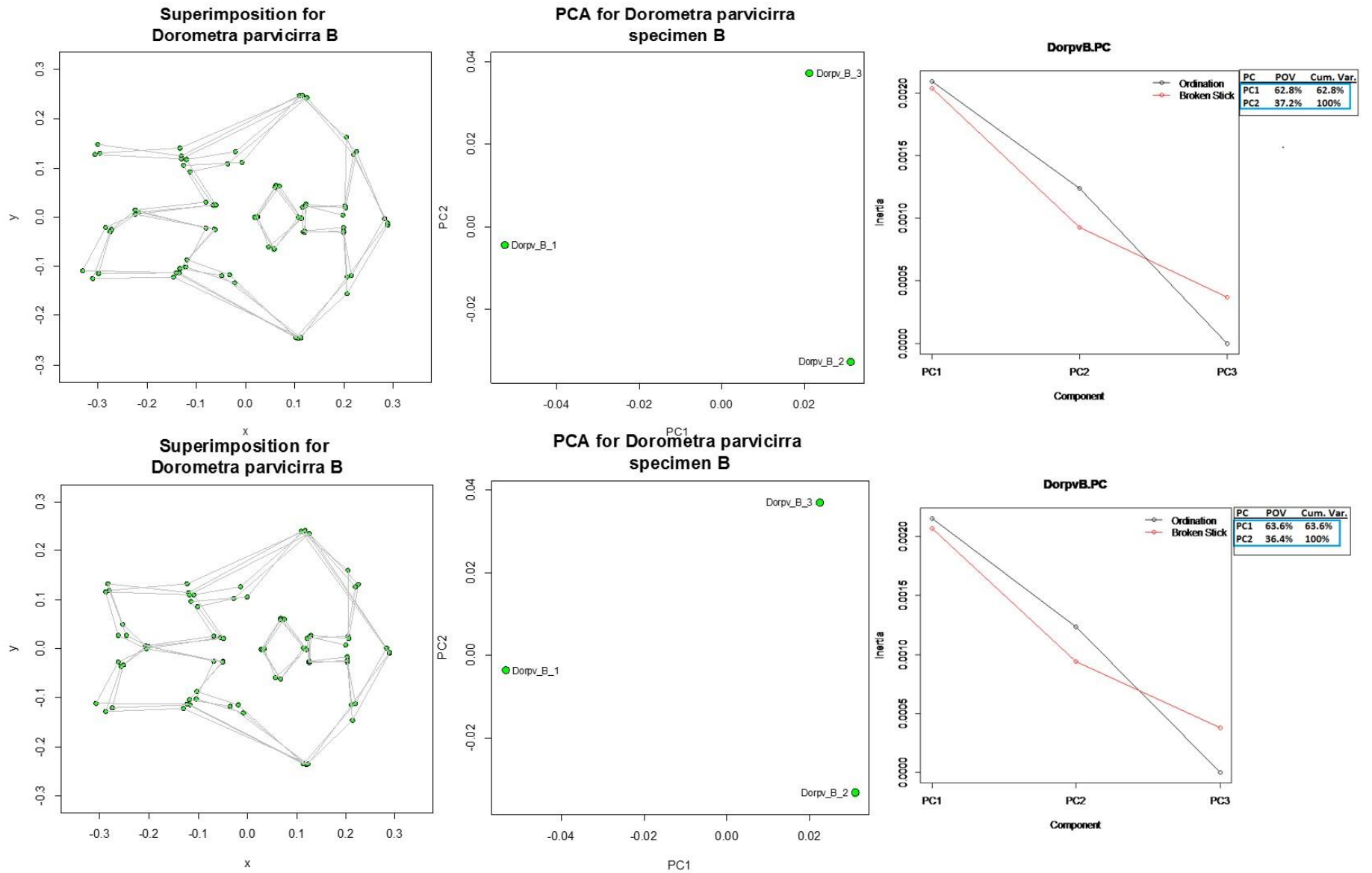


Fig. A13: Superimposed configuration, PCA, and broken stick model for ossicles within *Dorometra parvicirra*, specimen B (top: scenario 1; bottom: scenario 2). There is no significant variance within this individual.

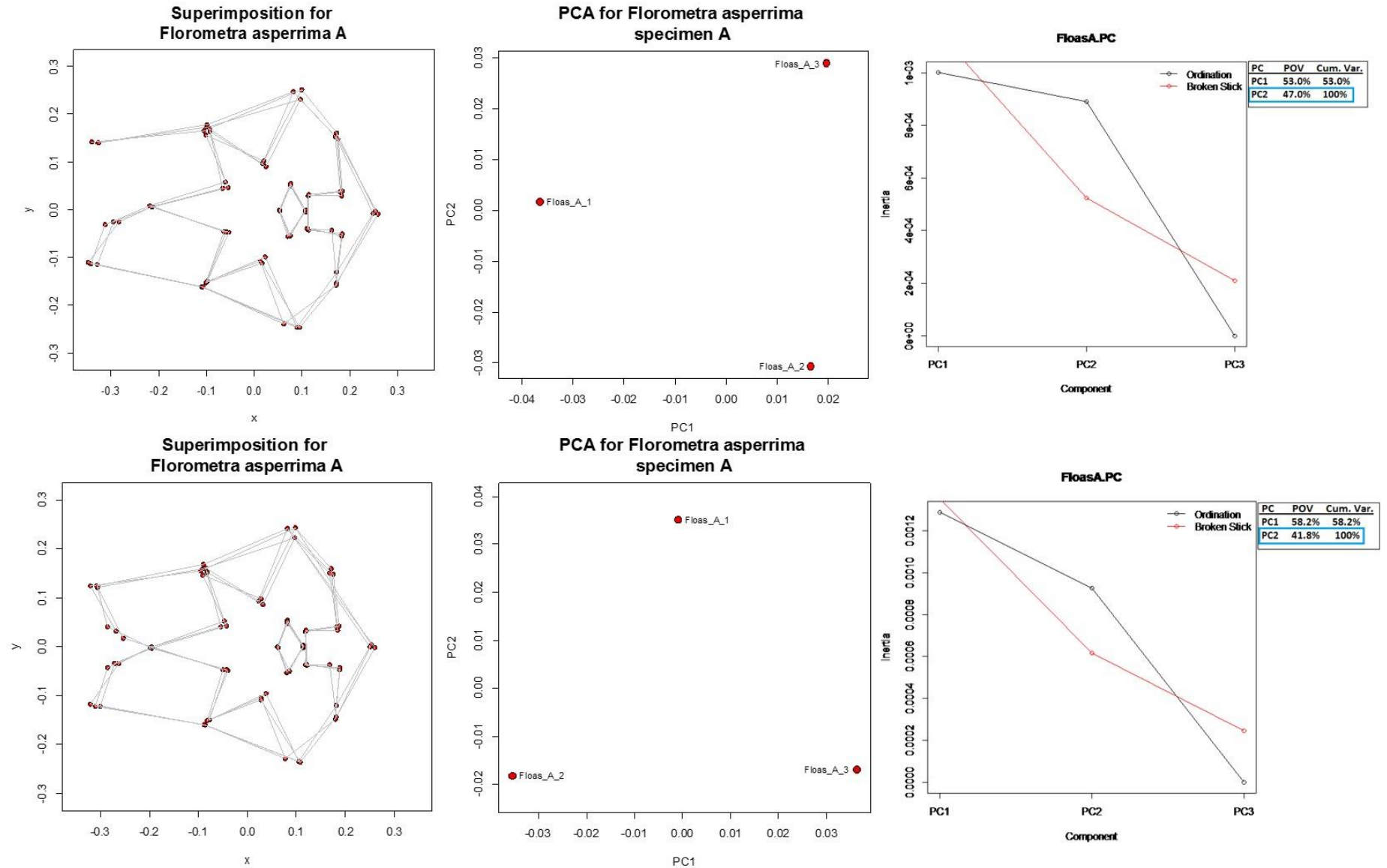


Fig. A14: Superimposed configuration, PCA, and broken stick model for ossicles within *Florometra asperima*, specimen A (top: scenario 1; bottom: scenario 2). There is no significant variance within this individual.

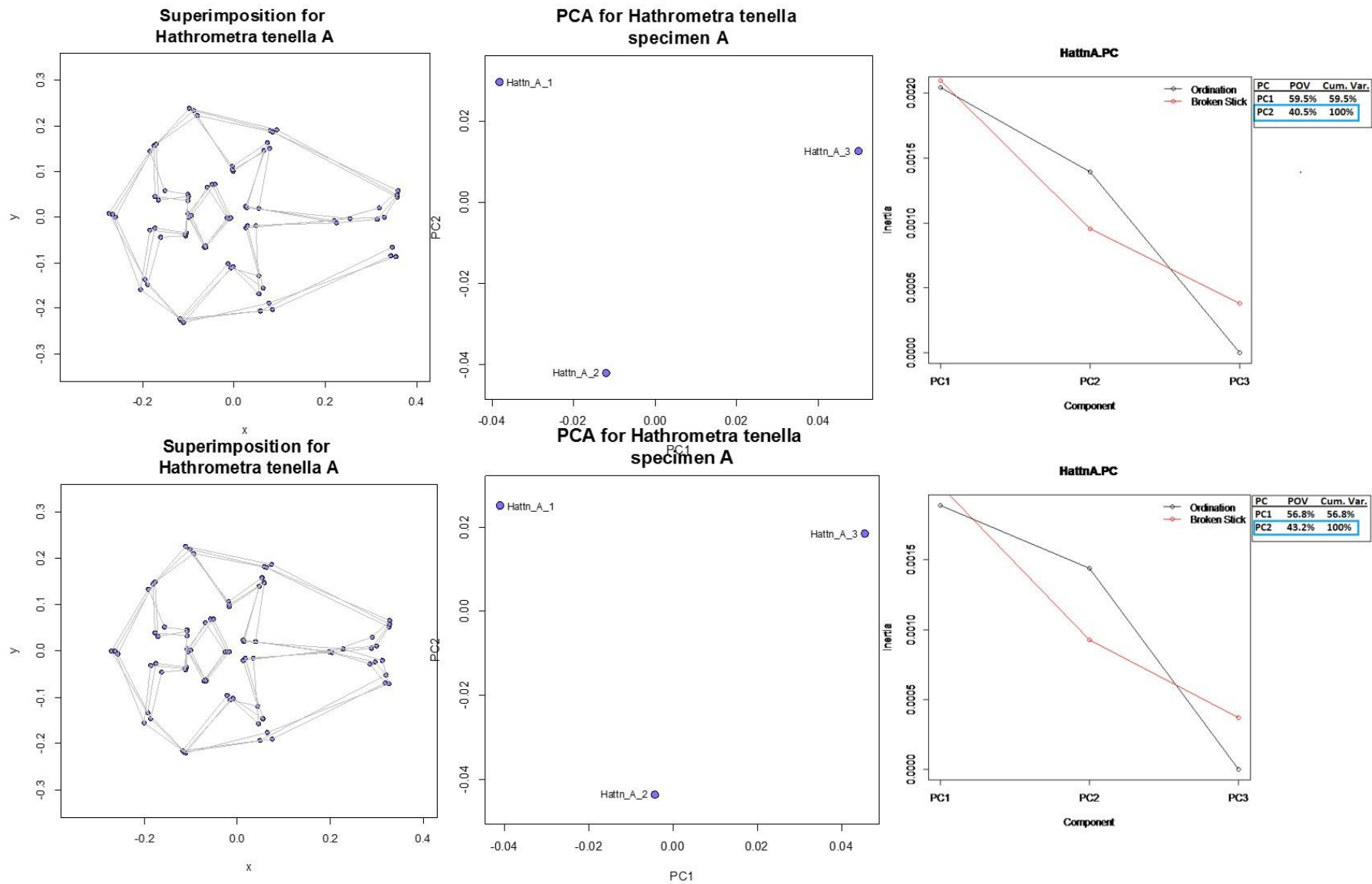


Fig. A15: Superimposed configuration, PCA, and broken stick model for ossicles within *Hathrometra tenella*, specimen A (top: scenario 1; bottom: scenario 2). There is no significant variance within this individual.



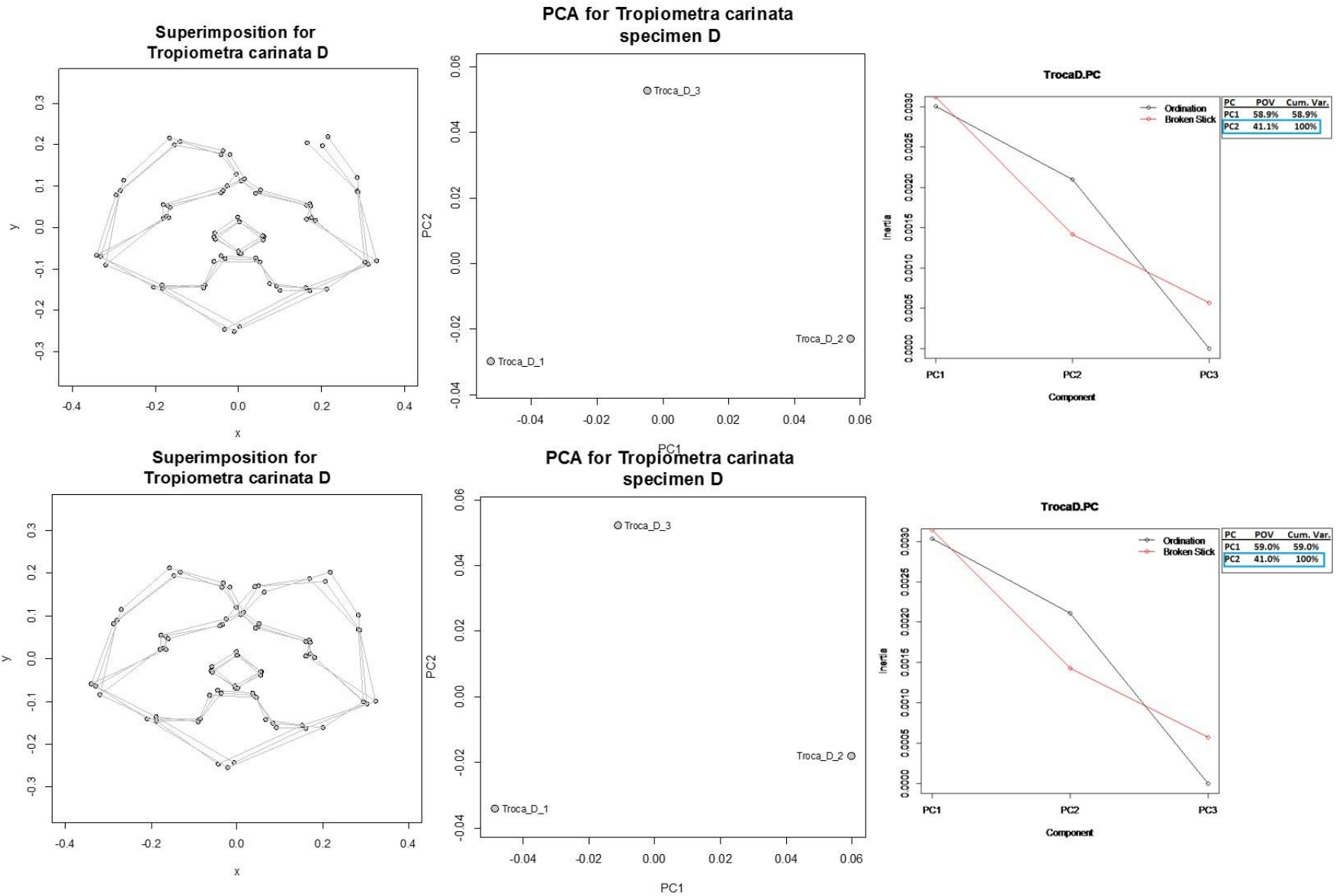


Fig. A16: Superimposed configuration, PCA, and broken stick model for ossicles within *Tropiometra carinata*, specimen D (top: scenario 1; bottom: scenario 2). There is no significant variance within this individual.

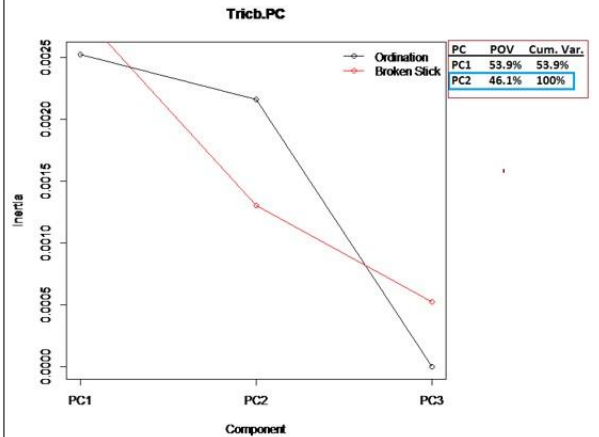
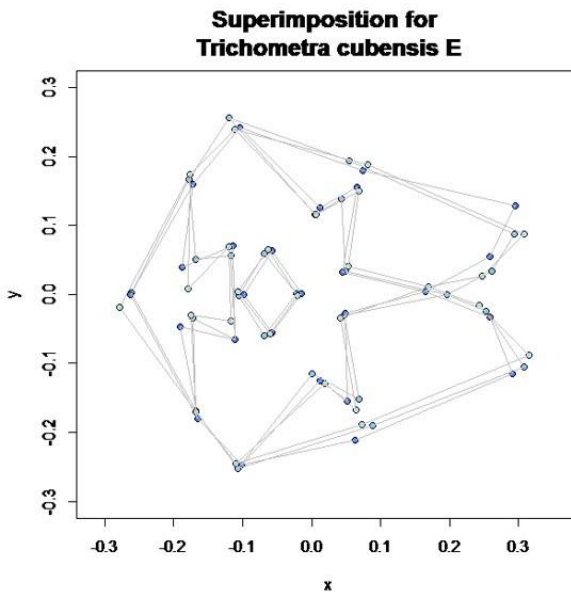
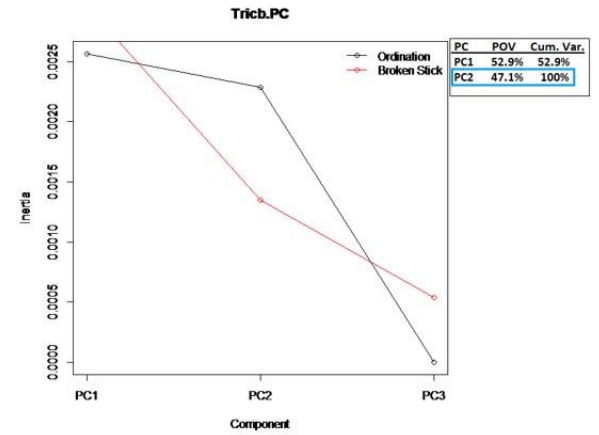
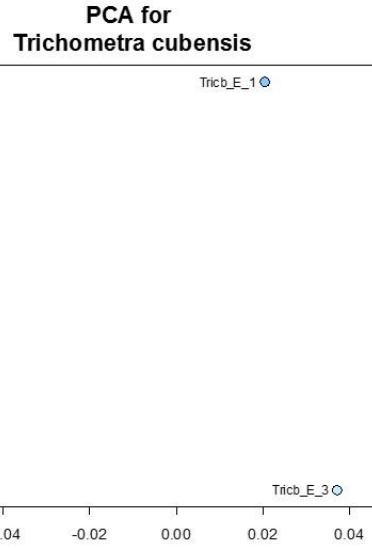
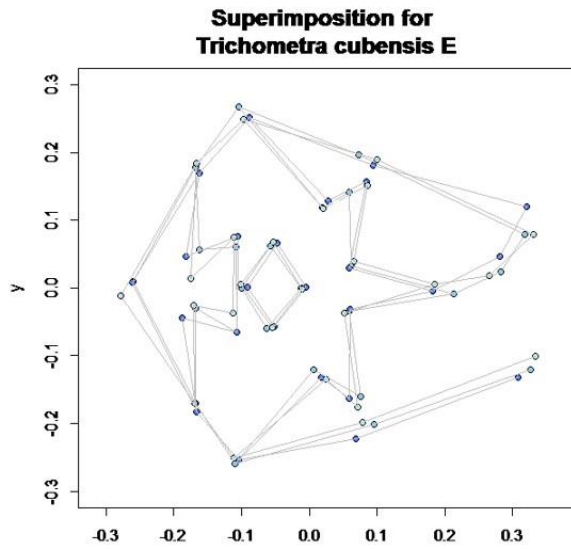


Fig. A17: Superimposed configuration, PCA, and broken stick model for ossicles within *Trichometra cubensis*, specimen E (top: scenario 1; bottom: scenario 2). There is no significant variance within this individual.

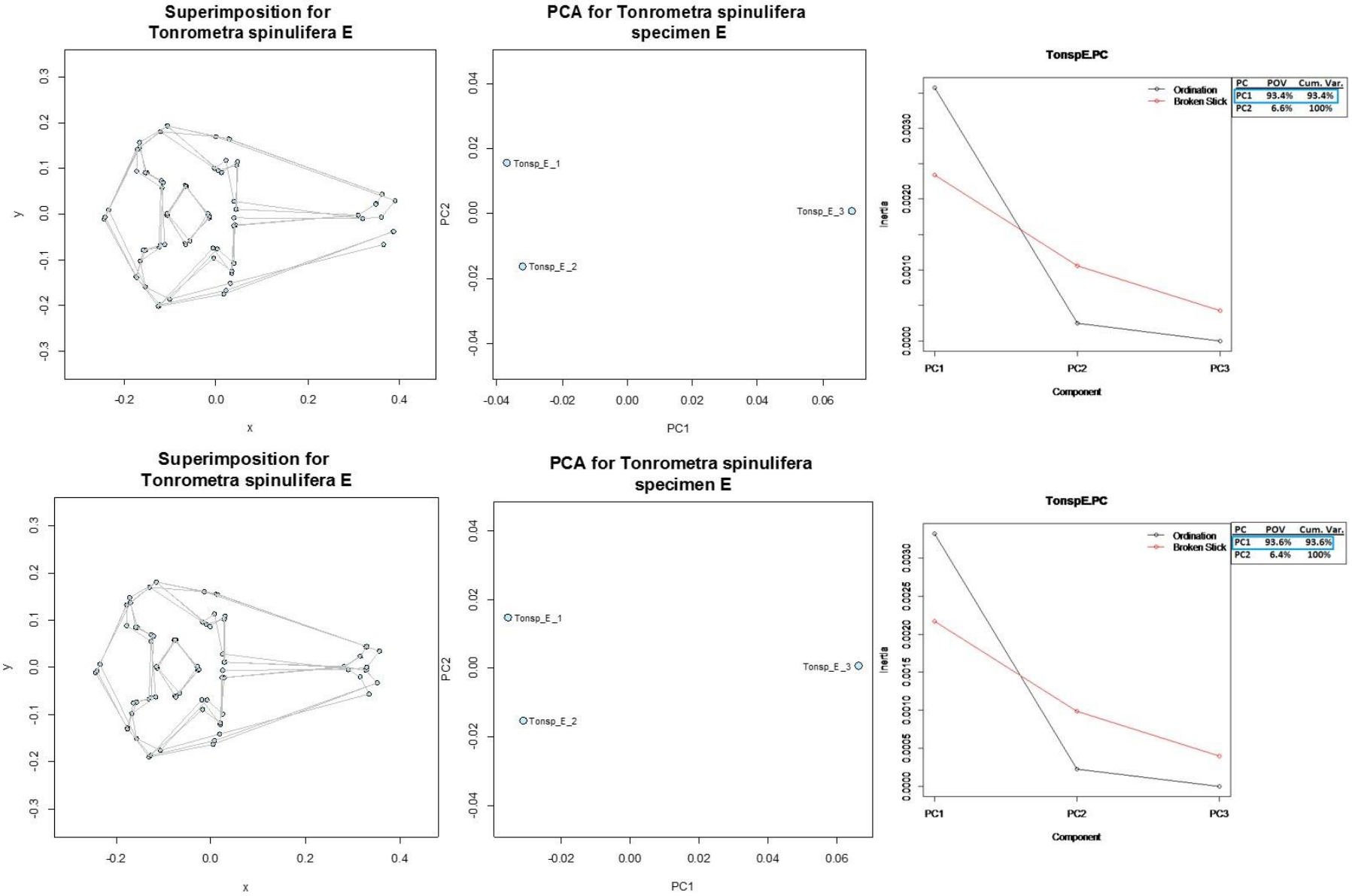


Fig. A18: Superimposed configuration, PCA, and broken stick model for ossicles within *Tonrometra spinulifera*, specimen E (top: scenario 1; bottom: scenario 2). There is no significant variance within this individual.

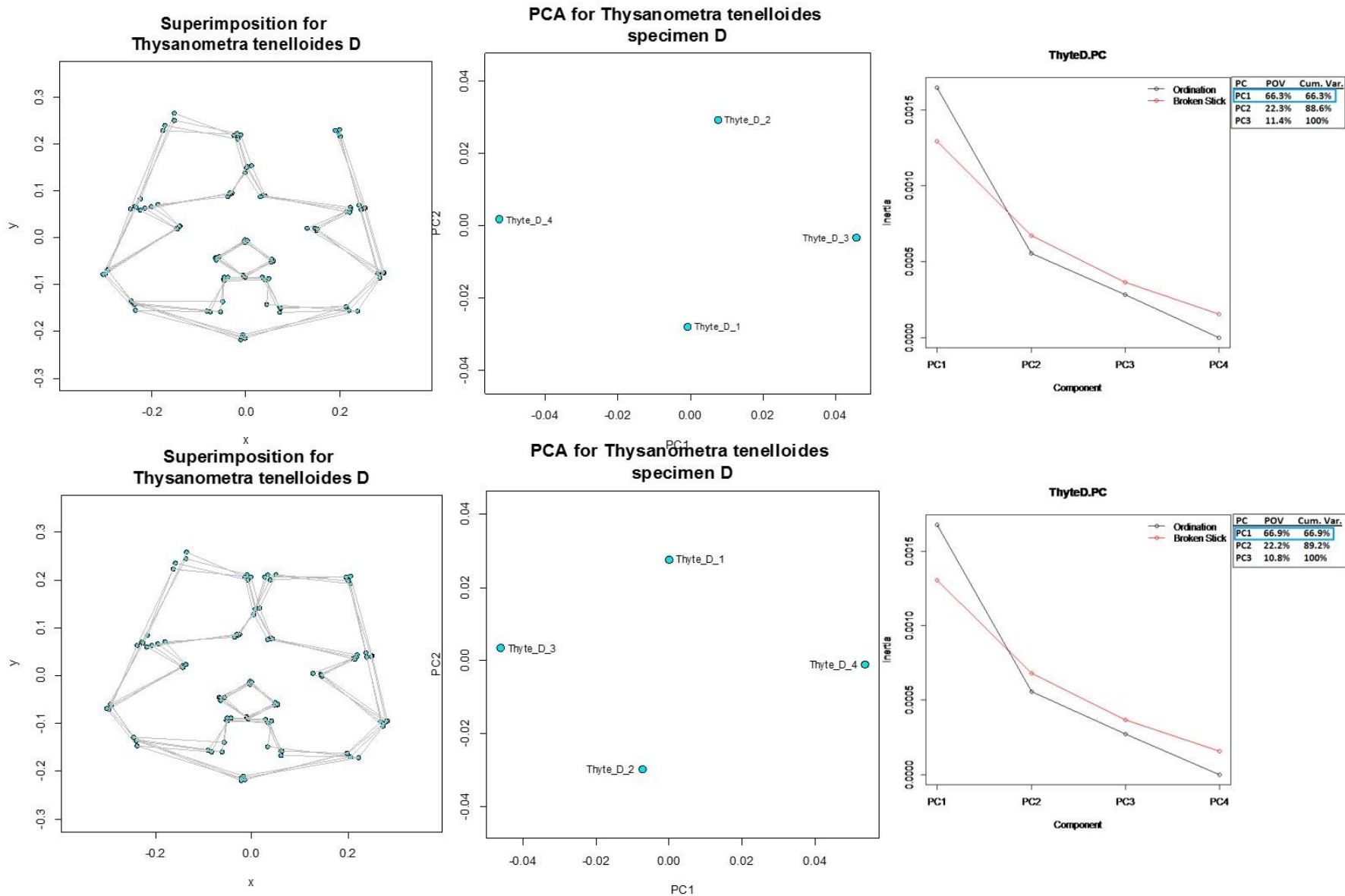


Fig. A19: Superimposed configuration, PCA, and broken stick model for ossicles within *Thyasnometra tenelloides*, specimen D (top: scenario 1; bottom: scenario 2). There is no significant variance within this individual.

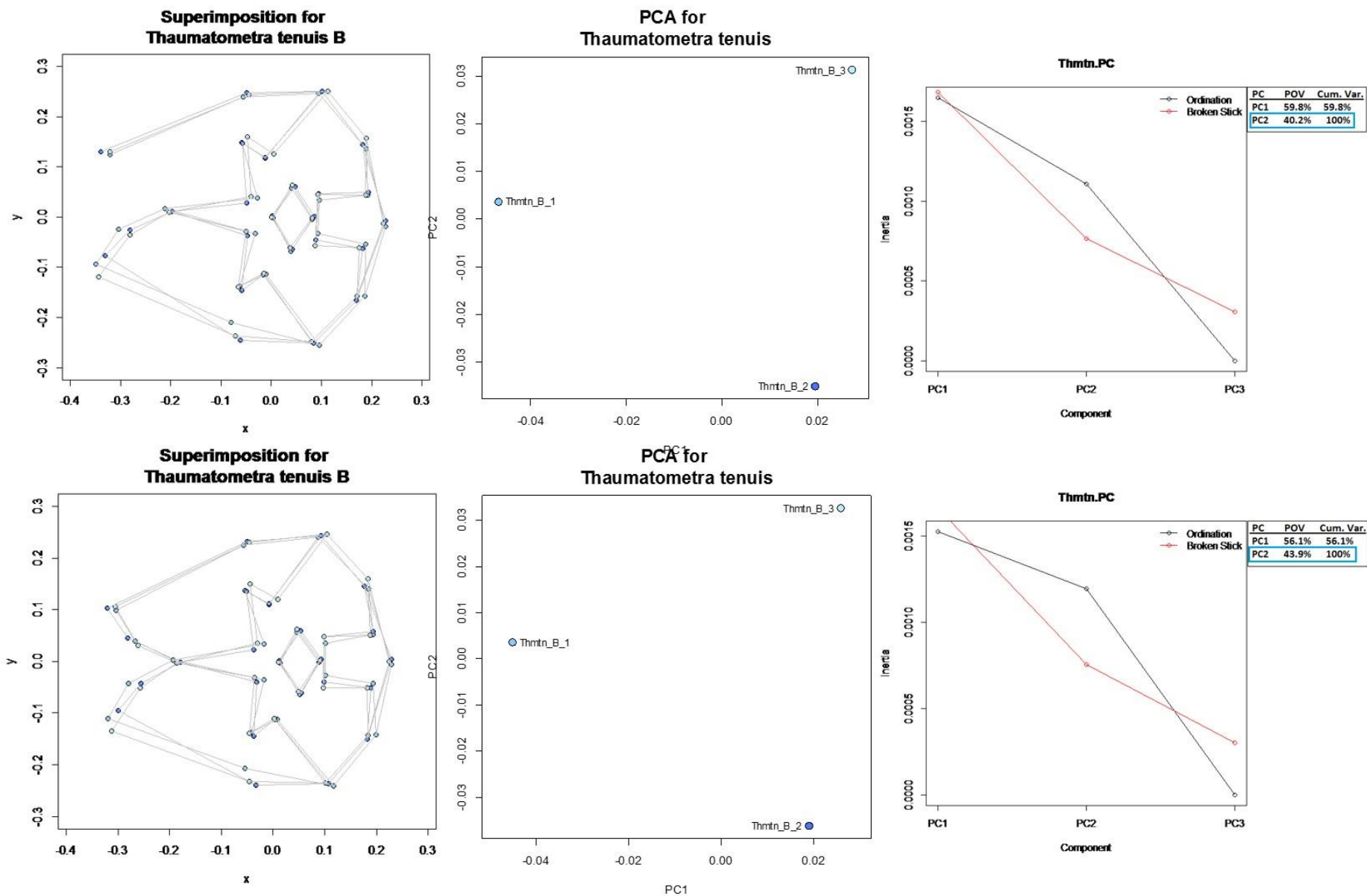


Fig. A20: Superimposed configuration, PCA, and broken stick model for ossicles within *Thaumatometra tenuis*, specimen B (top: scenario 1; bottom: scenario 2). There is no significant variance within this individual.

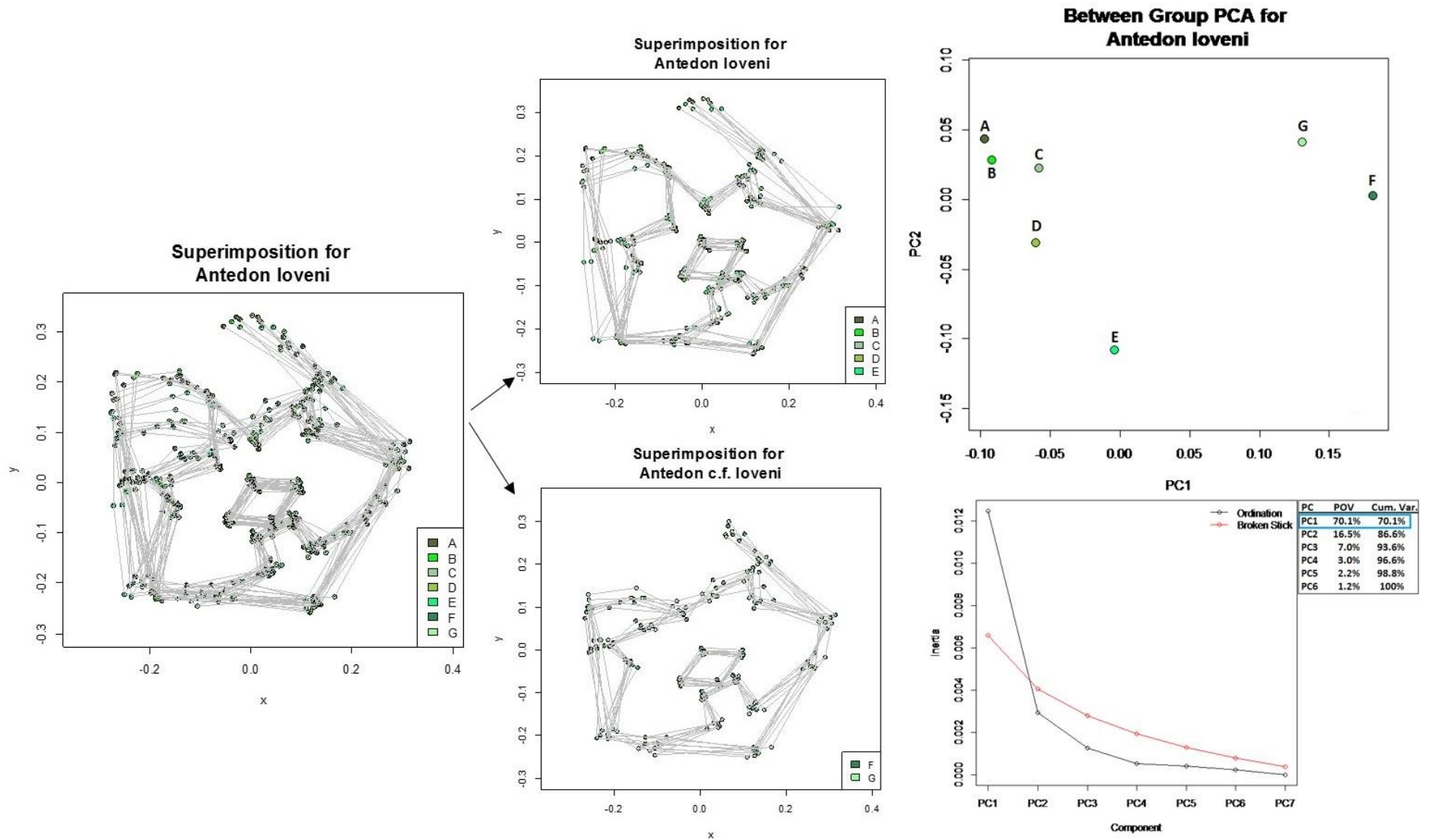


Fig. A21: Scenario 1 results of Intra-species variation for all *Antedon loveni* specimens depicting notable differences in the superimposed configurations of the known *A. loveni* specimens A-E and *A. c.f. loveni* specimens F-G, as well as a clear separation in the PCA (see Figure 16 for scenario 2 results).

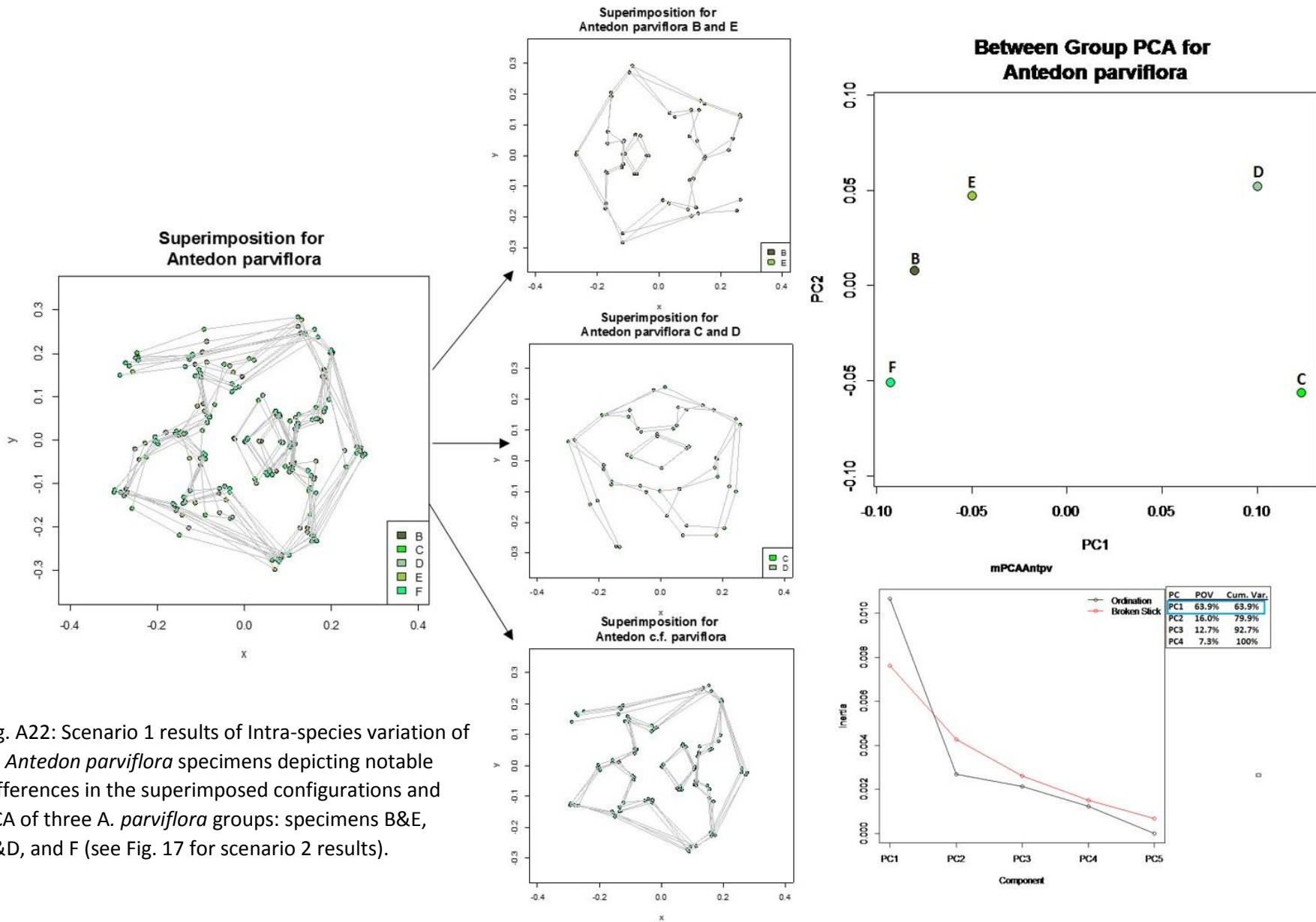


Fig. A22: Scenario 1 results of Intra-species variation of all *Antedon parviflora* specimens depicting notable differences in the superimposed configurations and PCA of three *A. parviflora* groups: specimens B&E, C&D, and F (see Fig. 17 for scenario 2 results).

### Between Group PCA for *Anthometrina adriani*

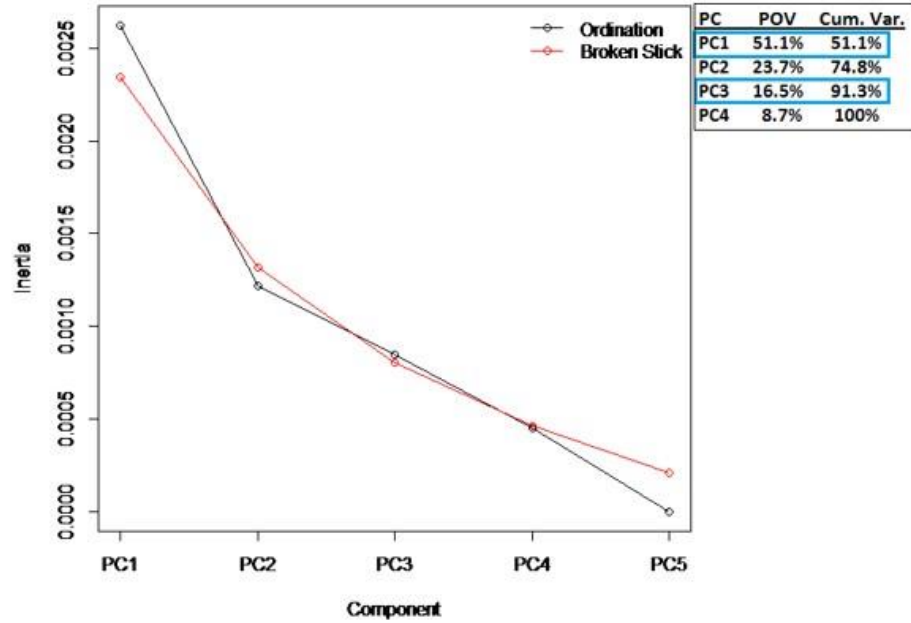
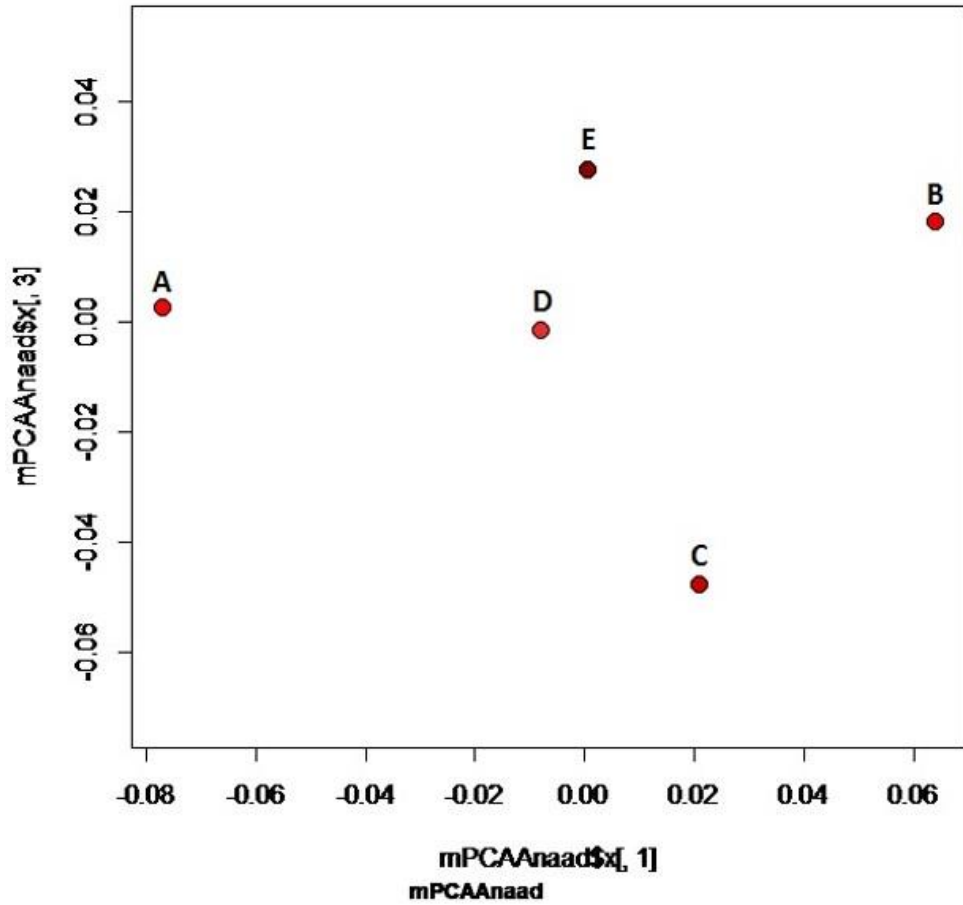


Fig. A23: Scenario 1 PCA and broken stick model depicting the intra-species variation of *Anthometrina adriani*. ANOVA results yielded significant variation between individuals A&E and C&E in both scenarios (see Fig. 18 for scenario 2 results).



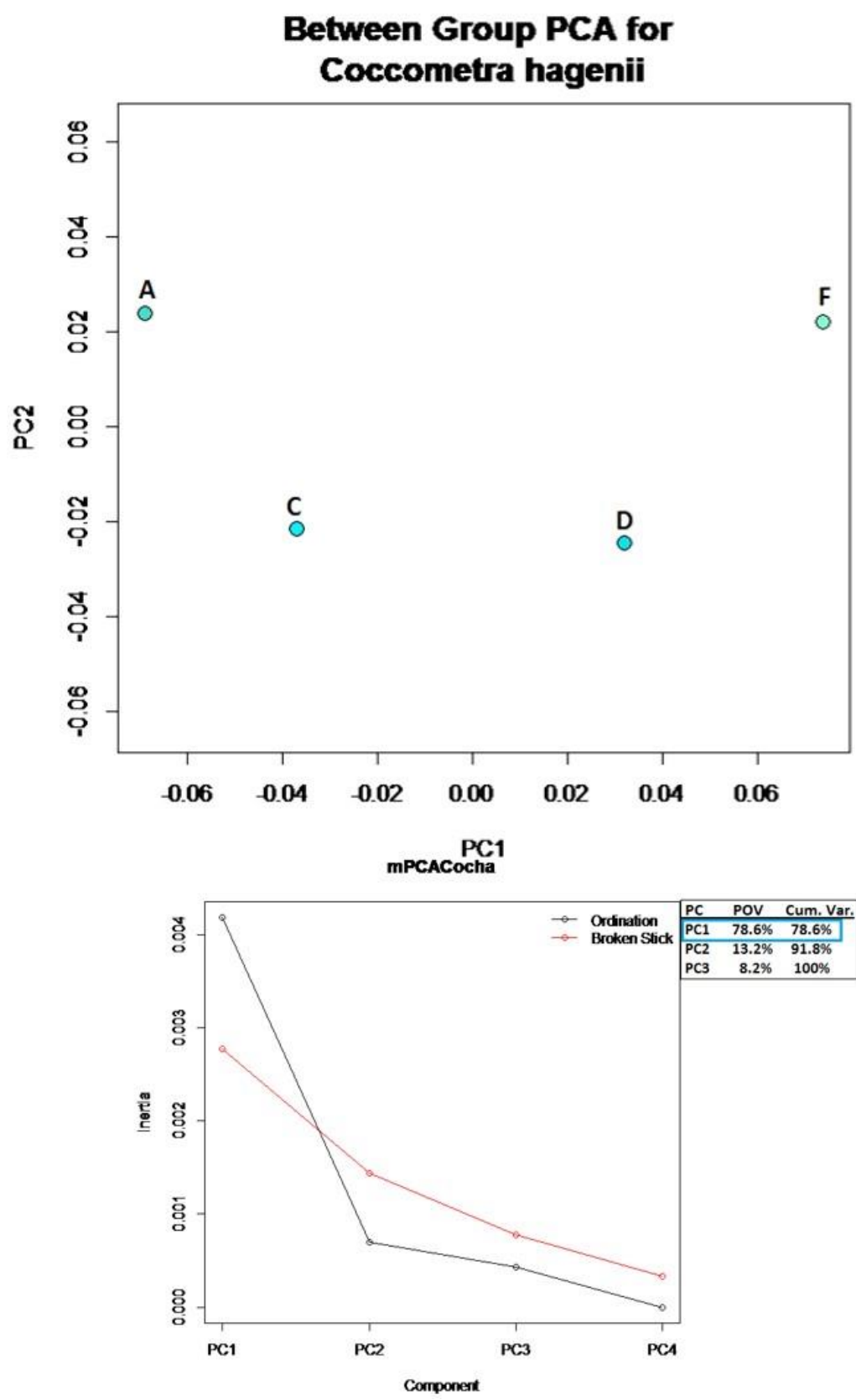


Fig. A24: Scenario 1 PCA and broken stick model depicting the intra-species variation of *Coccometra hagenii*. ANOVA results yielded significant variation between individuals C&D in both scenarios (see Fig. 19 for scenario 2 results).

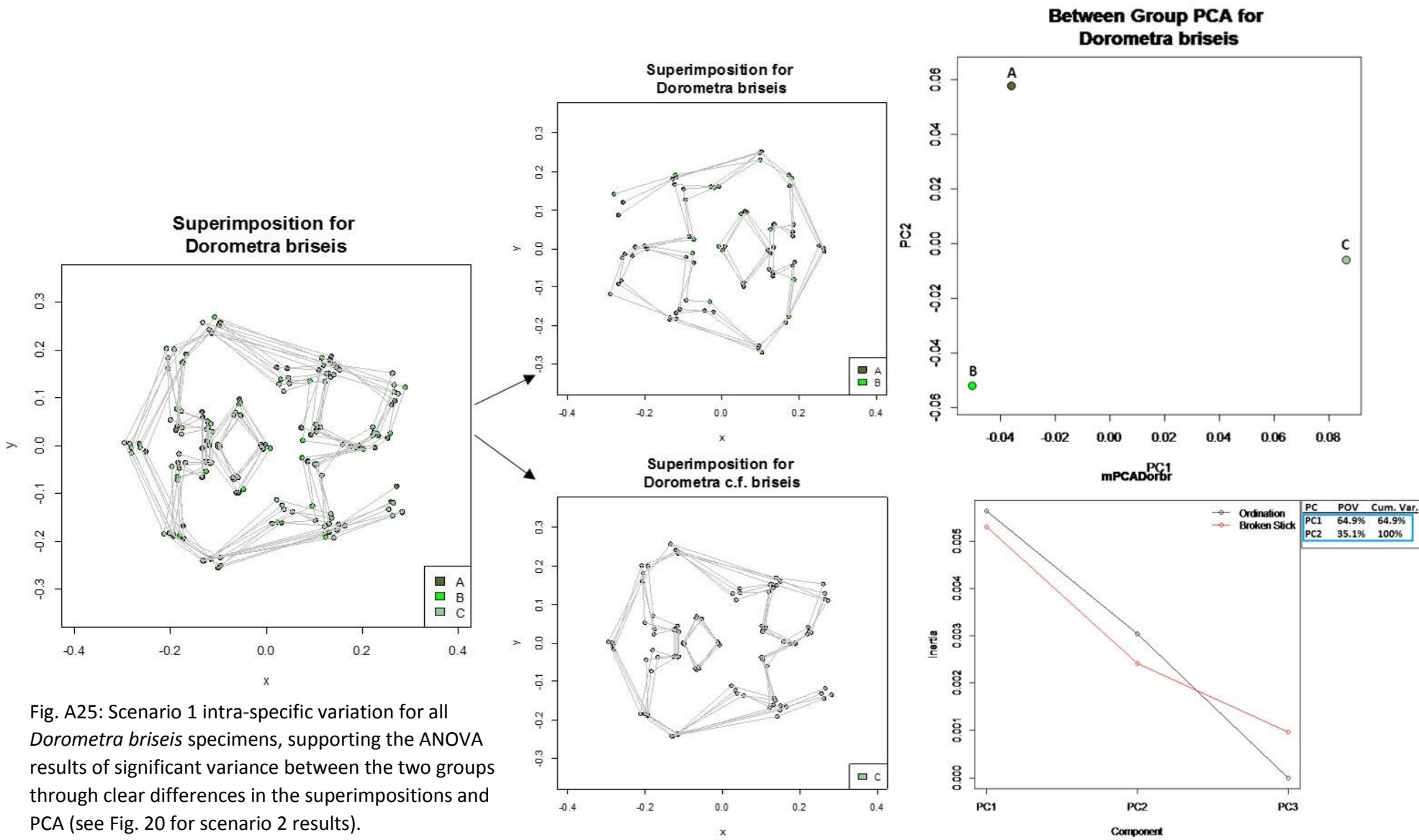


Fig. A25: Scenario 1 intra-specific variation for all *Dorometra briseis* specimens, supporting the ANOVA results of significant variance between the two groups through clear differences in the superimpositions and PCA (see Fig. 20 for scenario 2 results).

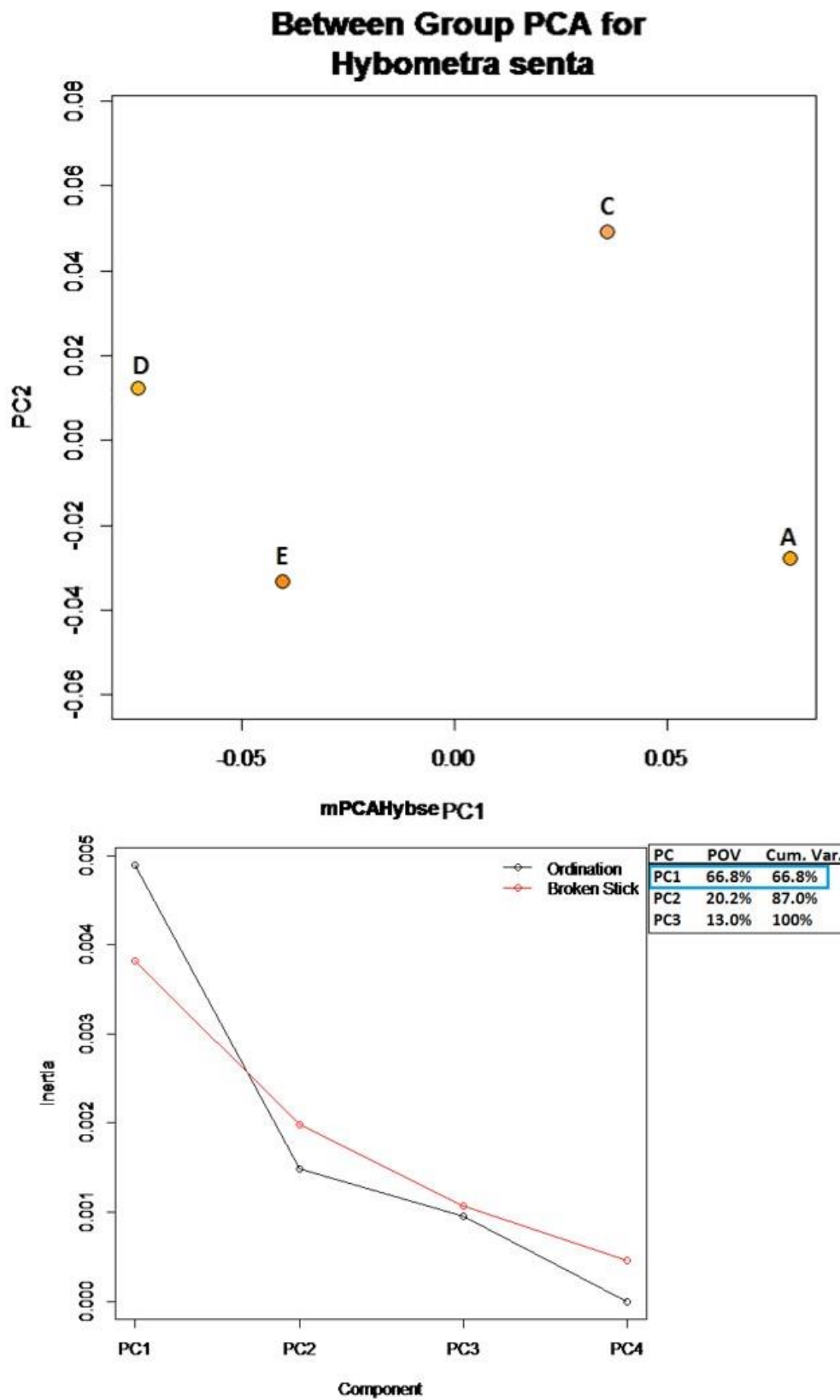


Fig. A26: Scenario 1 PCA and broken stick model of the intra-specific variation in *Hybometra senta*, supporting the ANOVA significant variance between individuals C&D (see Fig. 22 for scenario 2 results).

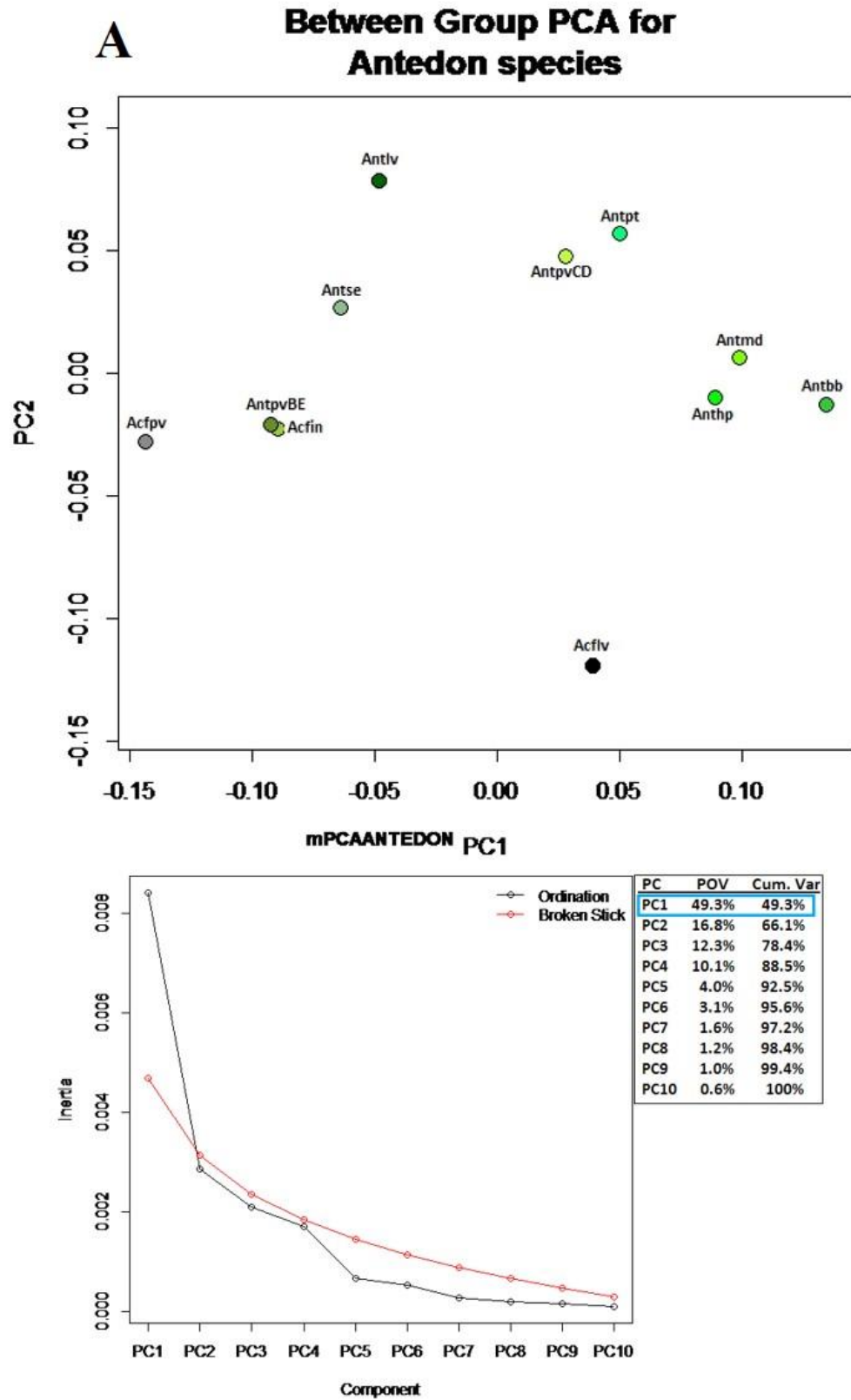
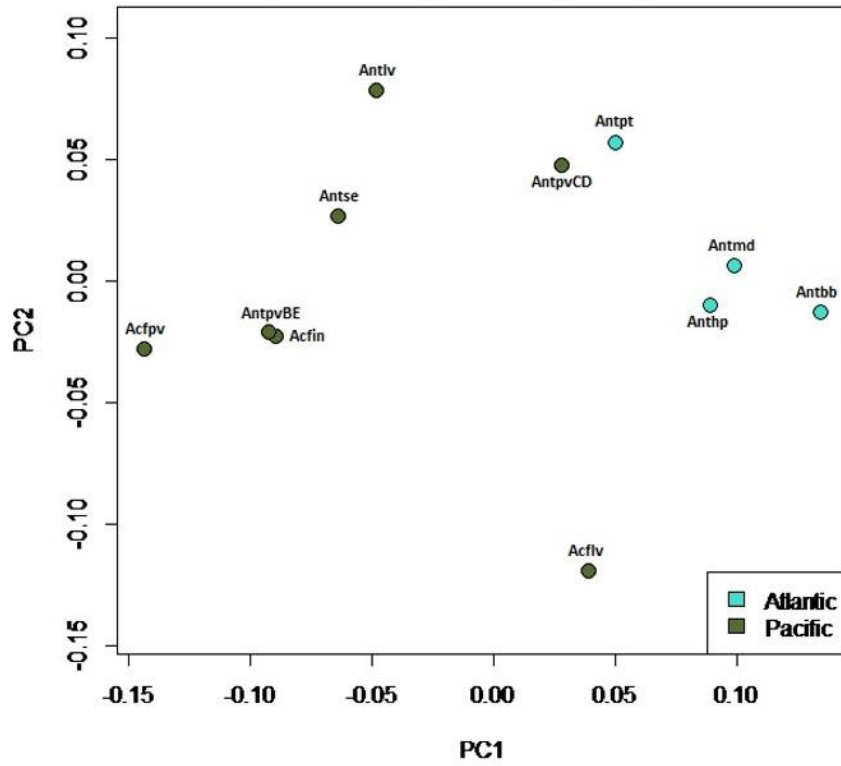


Fig. A27A: Scenario 1 intra-genus variation of *Antedon* spp. (see Fig. 23A for scenario 2 results). A: between-group PCA (top) and broken stick model (bottom). (Acfin = *Antedon* c.f. *incommoda*, Acflv = *Antedon* c.f. *loveni*, Acfpv = *Antedon* c.f. *parviflora*, Antbb = *Antedon* *bifida* *bifida*, Anthp = *Antedon* *hupferi*, Antlv = *Antedon* *loveni*, Antmd = *Antedon* *mediterranea*, Antpt = *Antedon* *petasus*, AntpvBE = *Antedon* *parviflora* B&E, AntpvCD = *Antedon* *parviflora* C&D, Antse = *Antedon* *serrata*).

**B** Between Group PCA for *Antedon* species by Region



**C** Between Group PCA for *Antedon* species by Clade

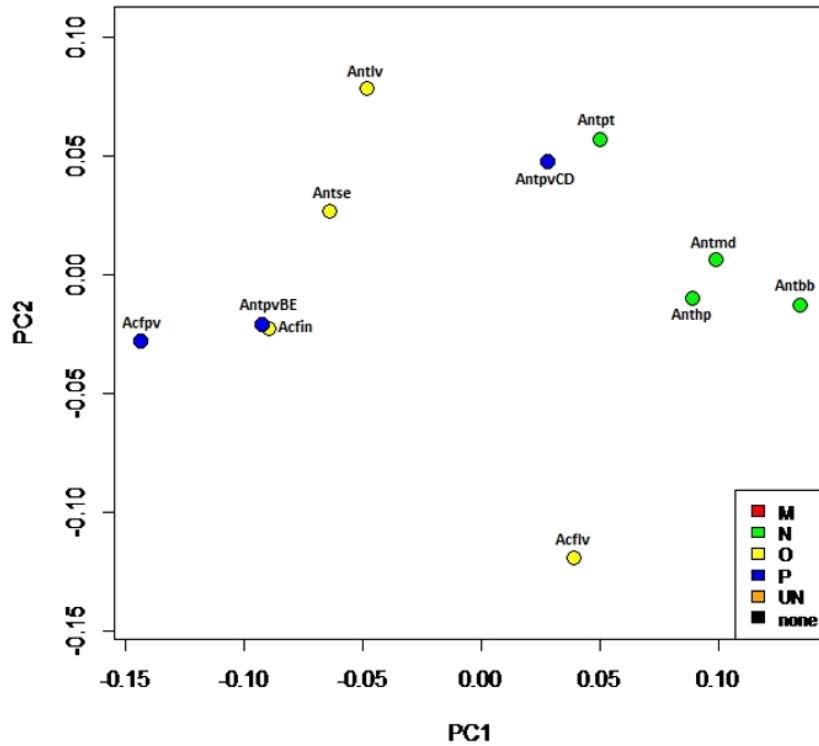


Fig. A27B-C: Scenario 1 intra-genus variation of *Antedon* spp. (see Fig. 23B-C for scenario 2 results). B: BGPCA colored by general region. C: BGPCA colored by clade assignment (see Fig. A27A for species abbreviation reference).

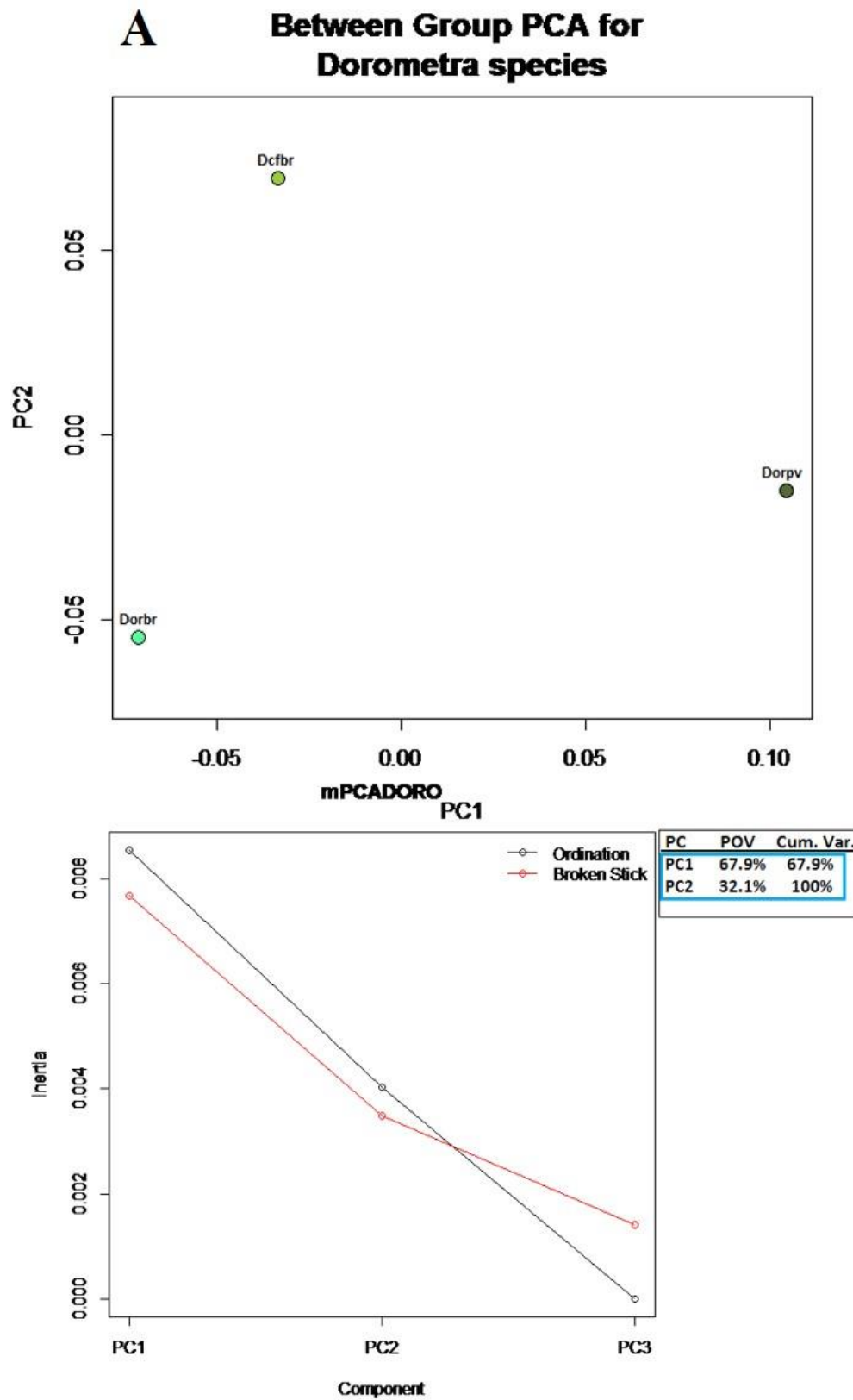


Fig. A28A: Scenario 1 results of intra-genus variation BGPCA and broken stick model for *Dorometra* spp. Despite their separations along both axes, there is no significant variance within this genus. (Dorbr = *Dorometra briseis*, Dcfbr = *Dorometra c.f. briseis*, Dorpv = *Dorometra parvicirra*).

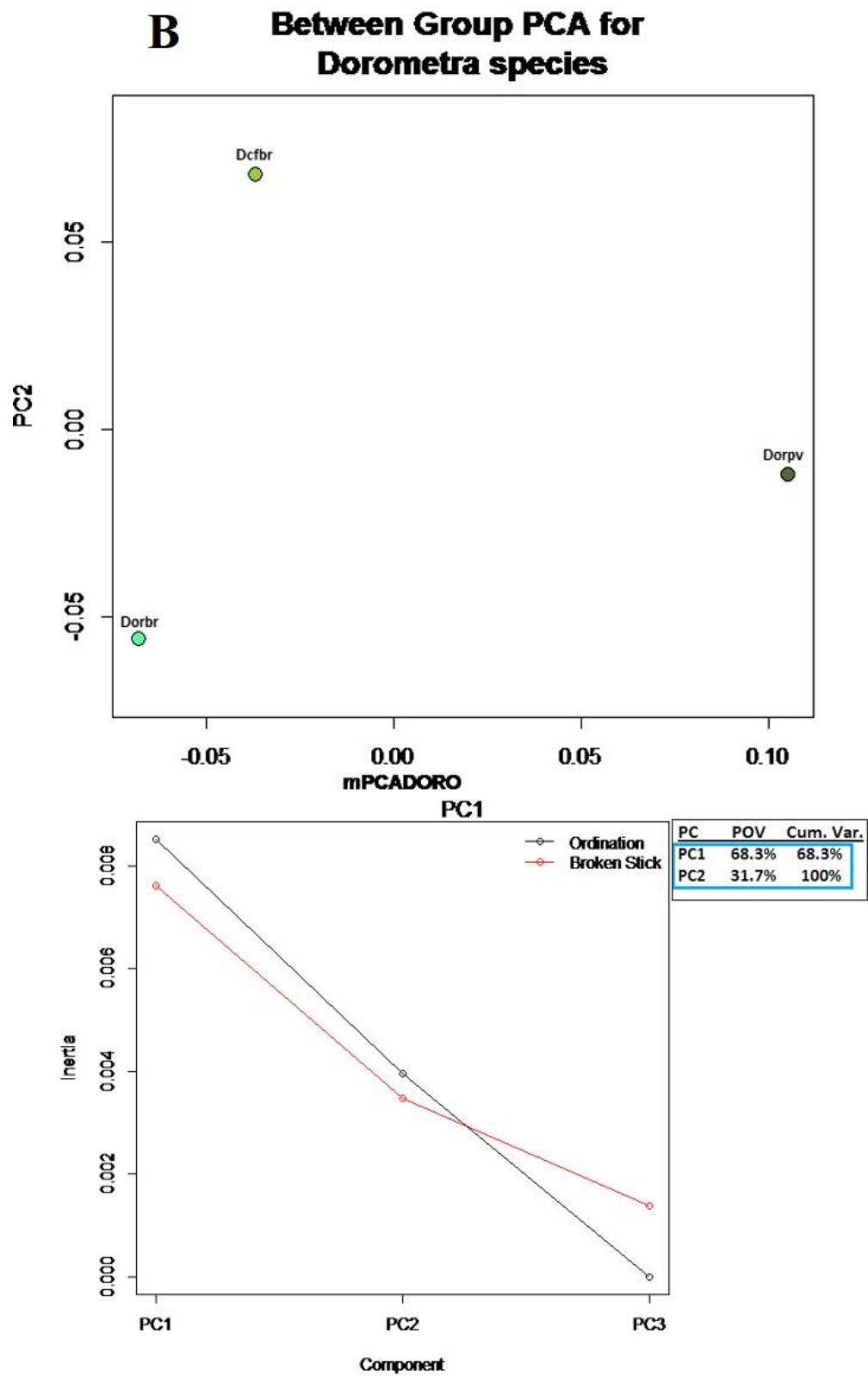


Fig. A28B: Scenario 2 results of intra-genus variation BGPCA and broken stick model for *Dorometra* spp. Despite their separations along both axes, there is no significant variance within this genus. (Dorbr = *Dorometra briseis*, Dcfbr = *Dorometra* c.f. *briseis*, Dorpv = *Dorometra parvicirra*).

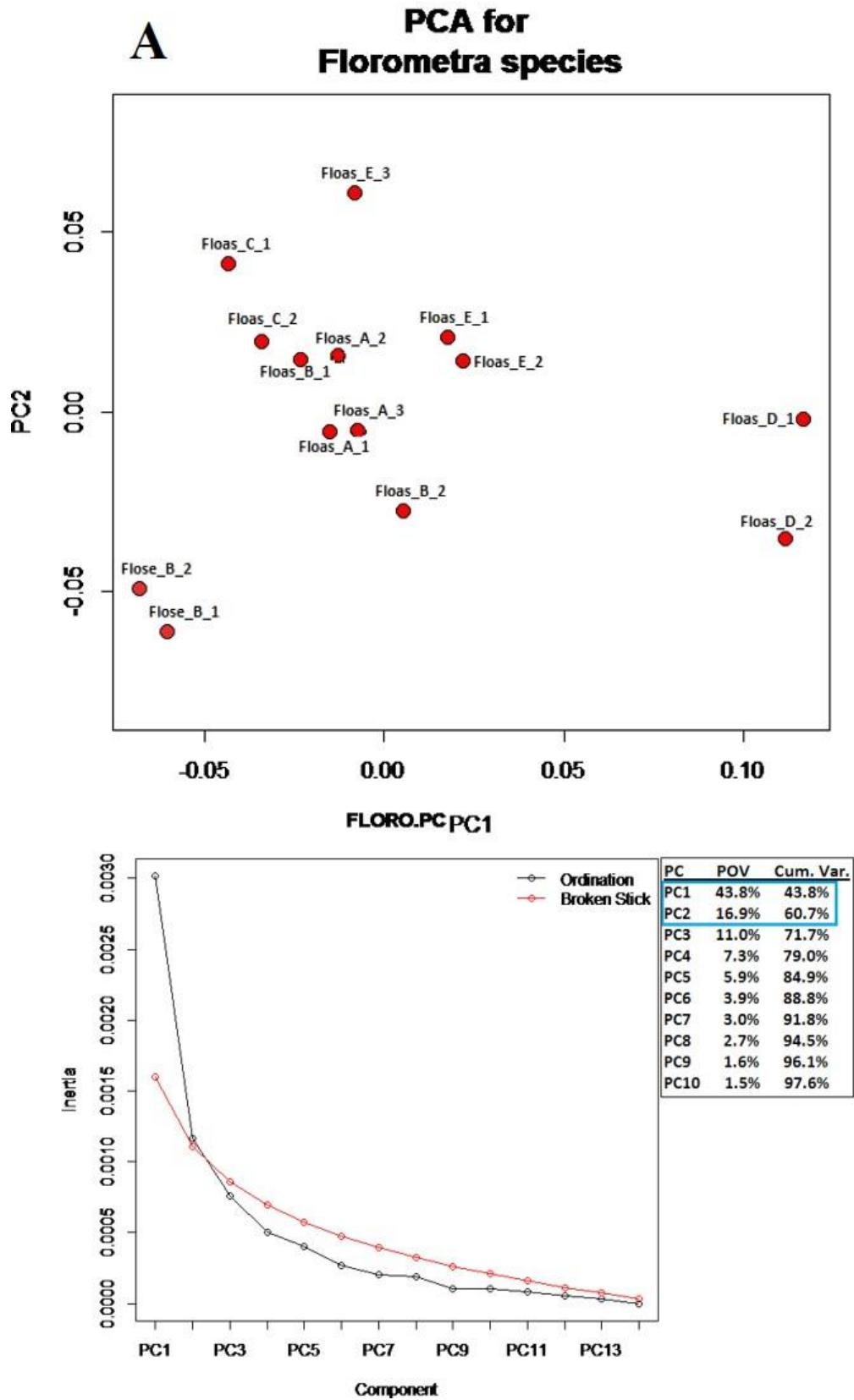


Fig. A29A: Scenario 1 results of intra-genus variation PCA and broken stick model for individuals of *Florometra* spp. There is no significant variance between *F. asperima* and *F. serratissima* in this study. (Floas = *Florometra asperima*, Flose = *Florometra serratissima*).



## B PCA for Florometra species

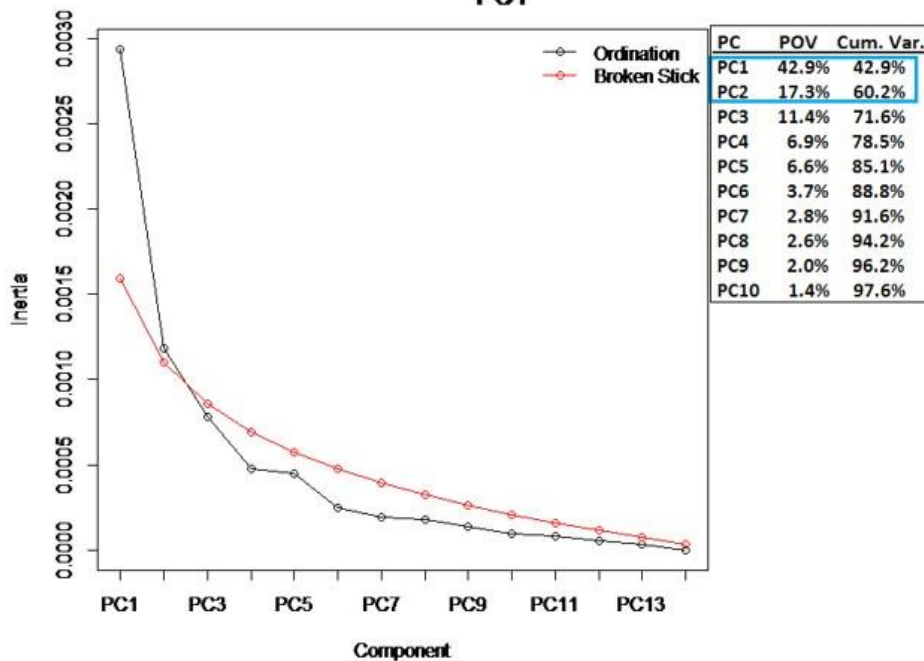
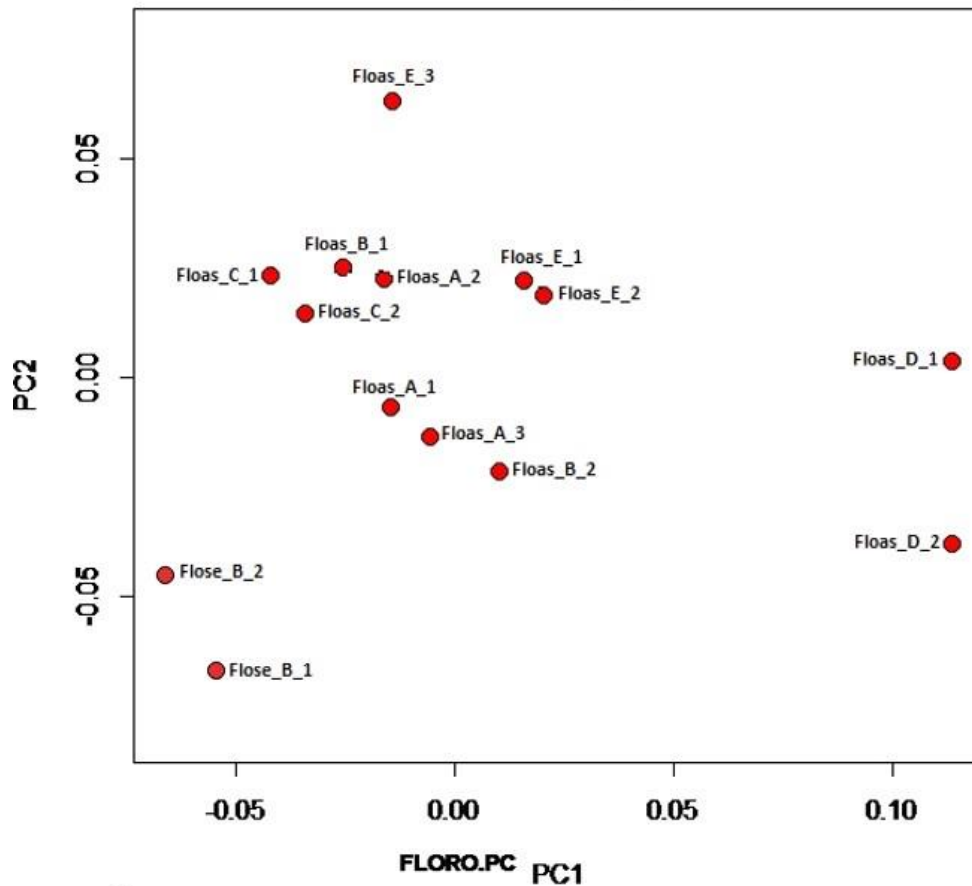


Fig. A29B: Scenario 2 results of intra-genus variation PCA and broken stick model for individuals of *Florometra* spp. There is no significant variance between *F. asperrema* and *F. serratissima* in this study. (Floas = *Florometra asperrema*, Flose = *Florometra serratissima*).

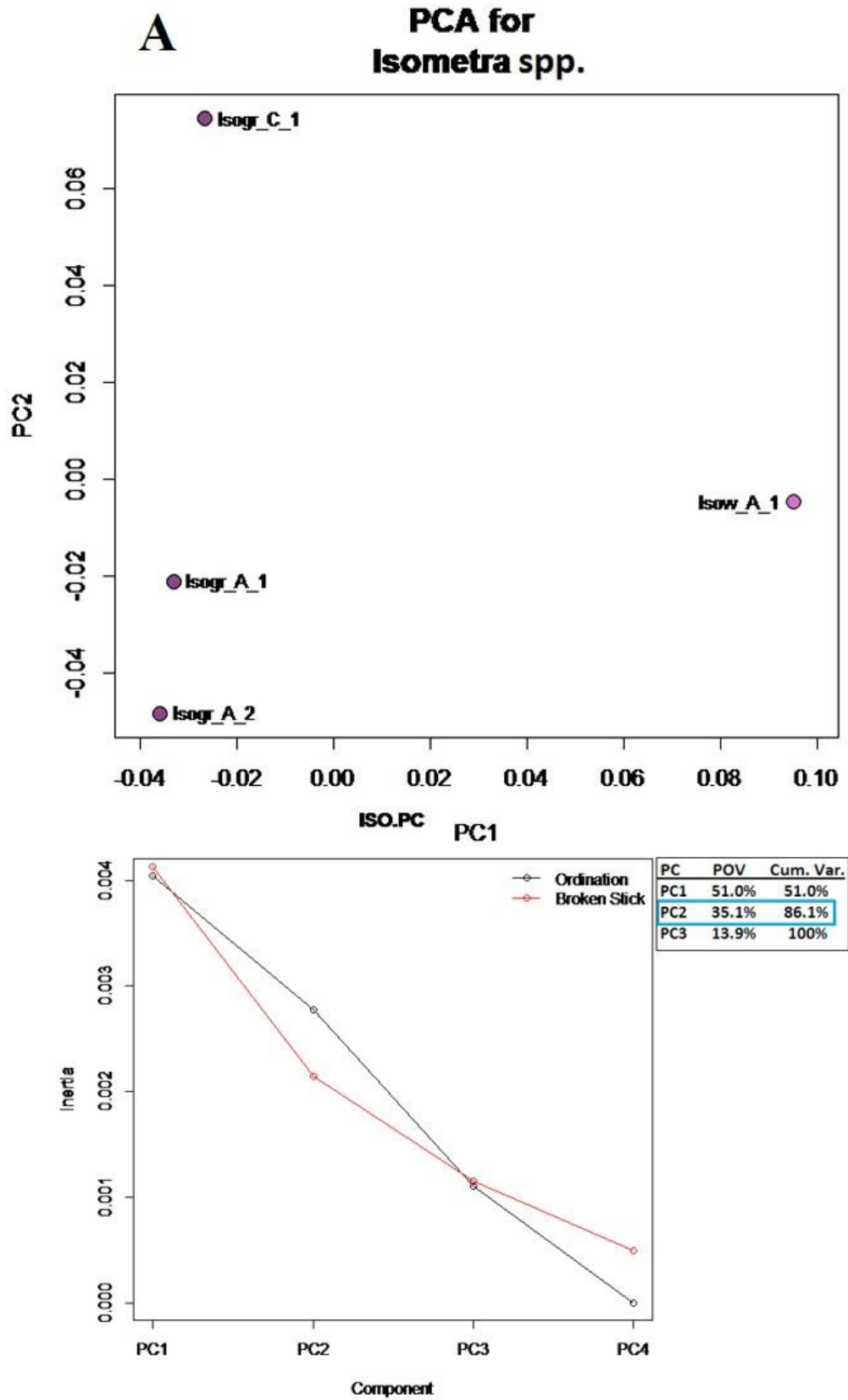


Fig. A30A: Scenario 1 results of intra-genus variation PCA and broken stick model for individuals of *Isometra* spp. There is no significant variance between *I. graminea* and *I. vivipara* in this study. (Isogr = *Isometra graminea*, Isovv = *Isometra vivipara*).

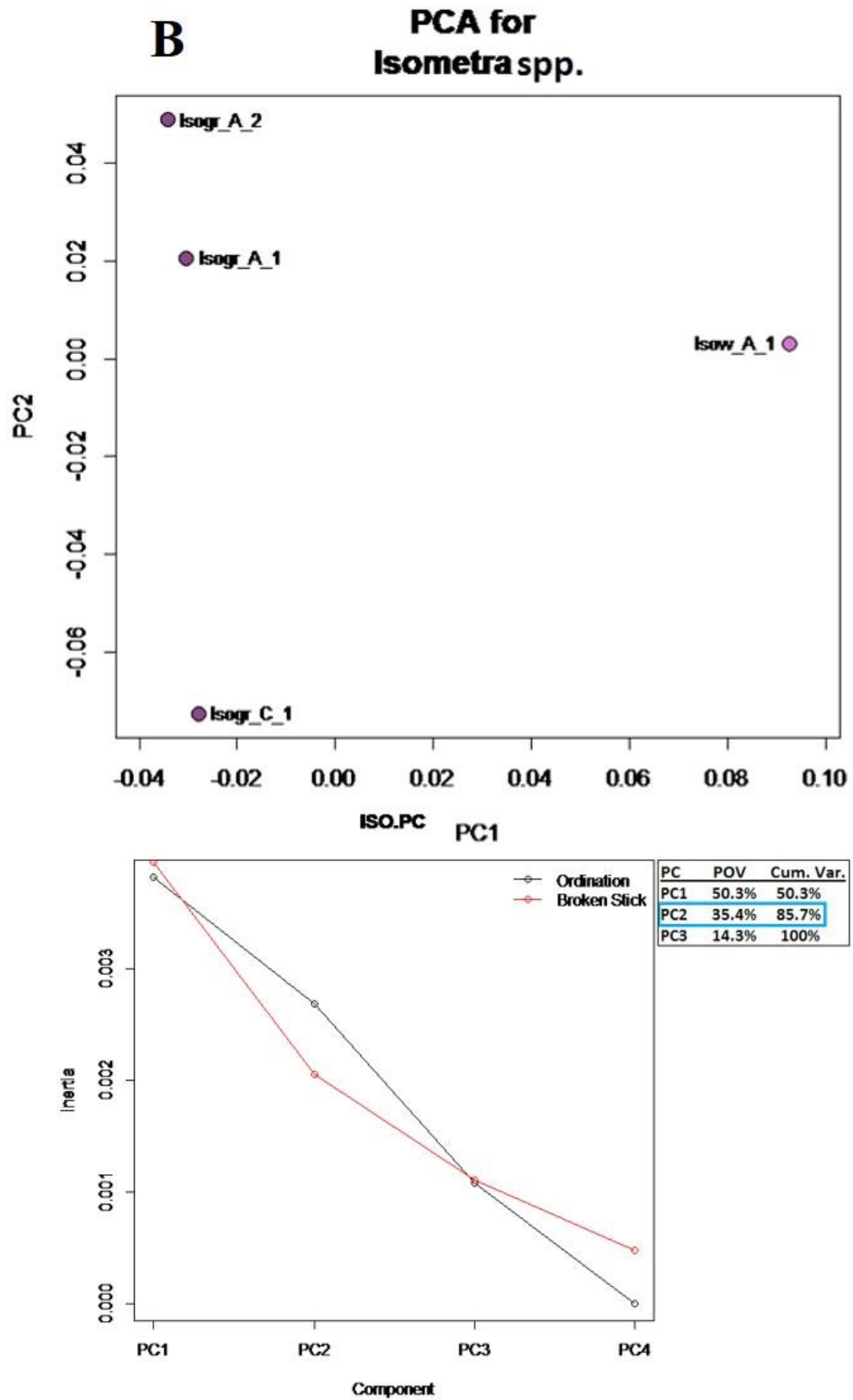


Fig. A30B: Scenario 2 results of intra-genus variation PCA and broken stick model for individuals of *Isometra* spp. There is no significant variance between *I. graminea* and *I. vivipara* in this study. (Isogr = *Isometra graminea*, Isowv = *Isometra vivipara*).

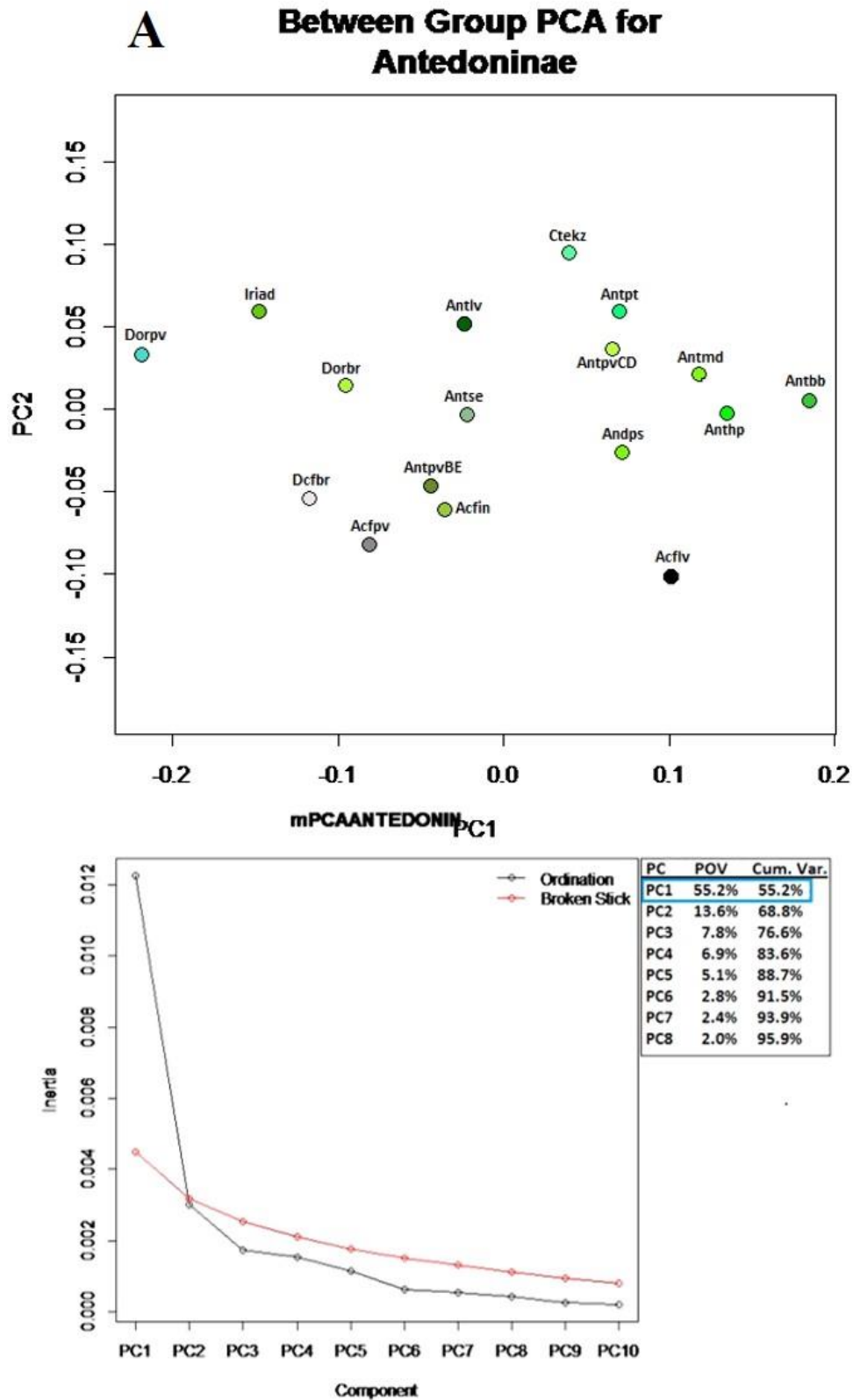


Fig. A31A: Scenario 1 intra-subfamily variation of Antedoninae. BGPCA (top) and broken stick model (bottom) (see Fig. 24A for scenario 2 results) (Acfin = *Antedon* c.f. *incommoda*, Acflv = *Antedon* c.f. *loveni*, Acfpv = *Antedon* c.f. *parviflora*, Andps = *Andrometra psyche*, Antbb = *Antedon bifida bifida*, Anthp = *Antedon hupferi*, Antlv = *Antedon loveni*, Antmd = *Antedon mediterranea*, Antpt = *Antedon petasus*, AntpvBE = *Antedon parviflora* B&E, AntpvCD = *Antedon parviflora* C&D, Antse = *Antedon serrata*, Ctekz = *Ctenantedon kinziei*, Dcfbr = *Dorometra* c.f. *briseis*, Dorbr = *Dorometra briseis*, Dorpv = *Dorometra parvicirra*, Iriad = *Iridometra adrestine*).

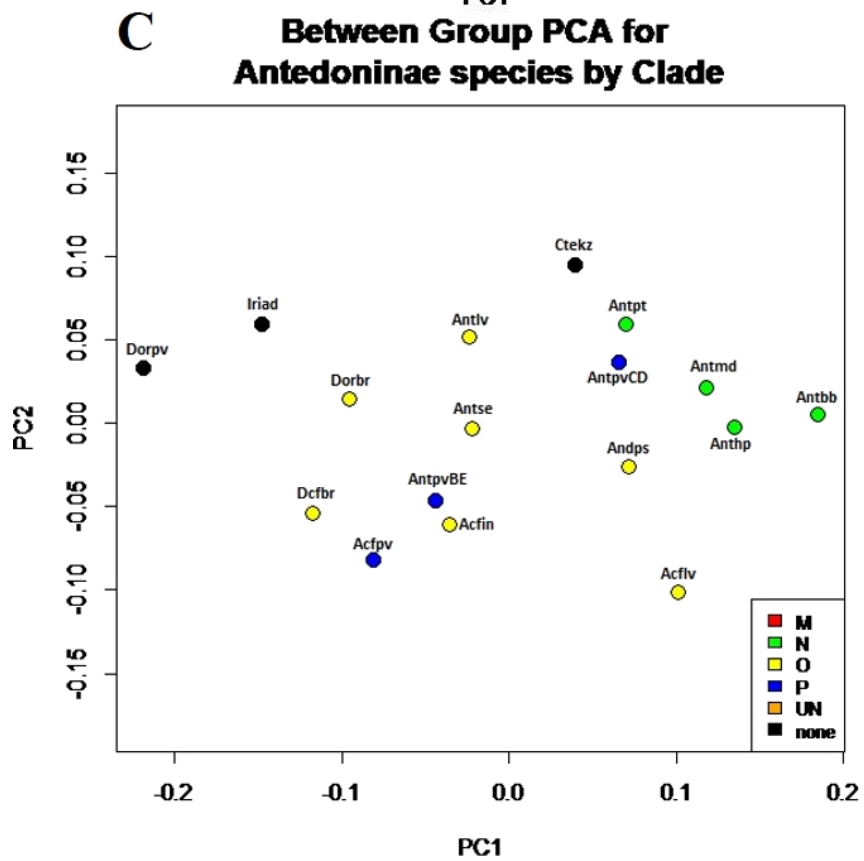
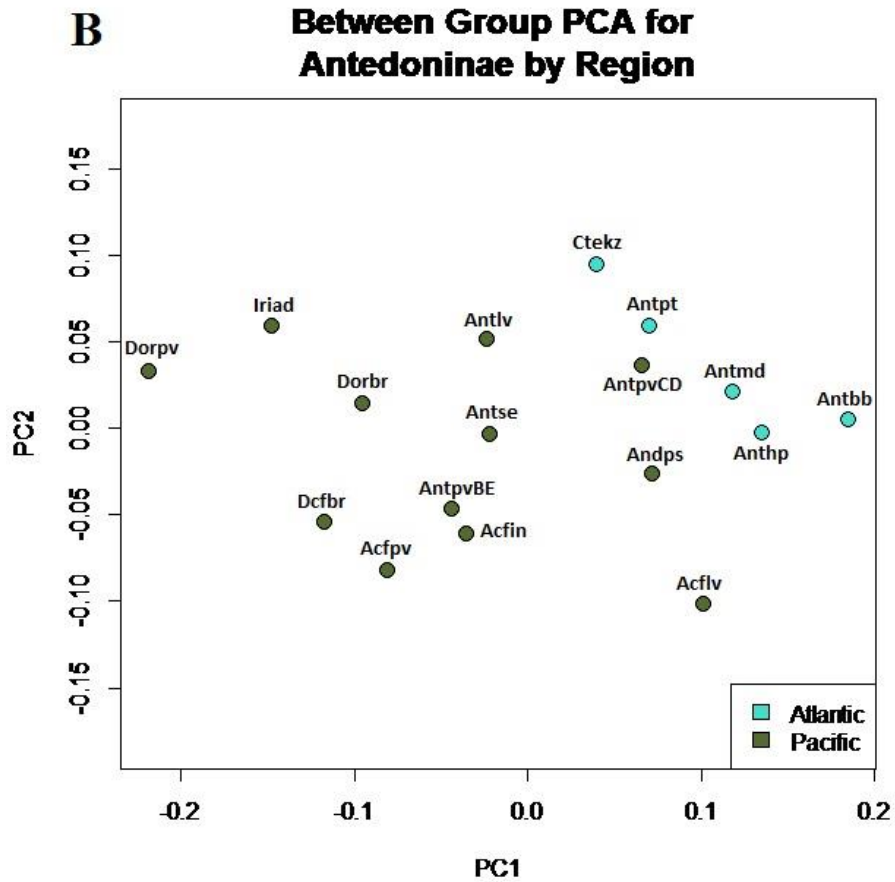


Fig. A31B-C: Scenario 1 intra-subfamily variation of Antedoninae. B: BGPCA colored by general region. C: BGPCA colored by phylogenetic assignment. (see Fig. 24B-D for scenario 2 results; see Fig A31A for species abbreviations).

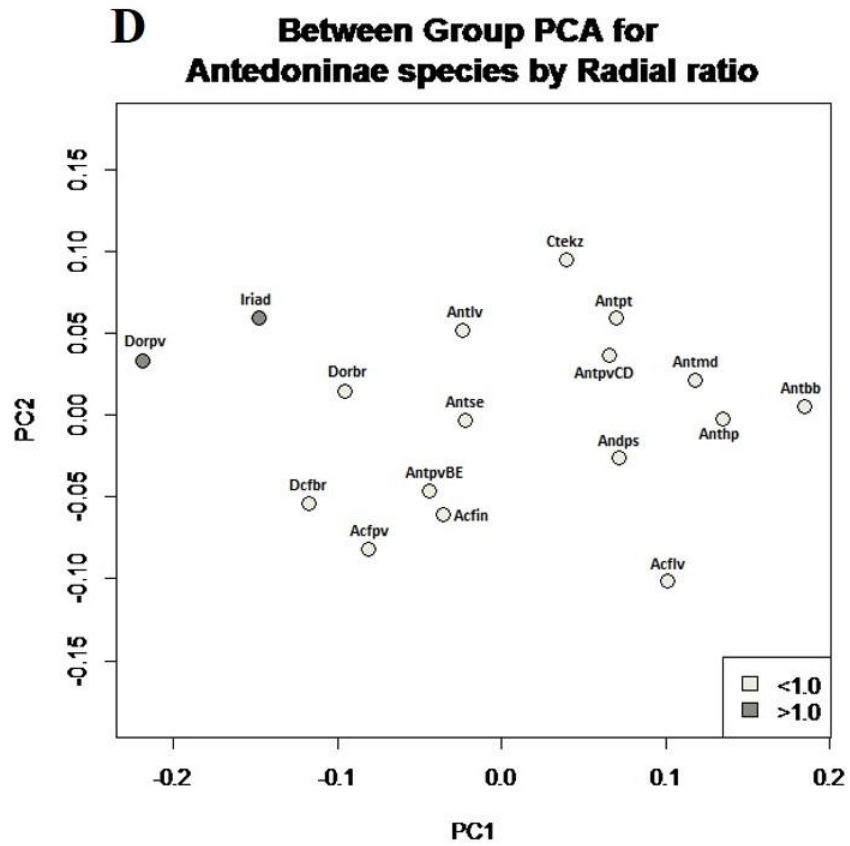


Fig. A31D: Scenario 1 intra-subfamily variation of Antedoninae. D: BGPCA colored by radial ratio (see Fig. 24B-D for scenario 2 results; see Fig. A31A for species abbreviations).

## Between Group PCA for Bathymetrinae

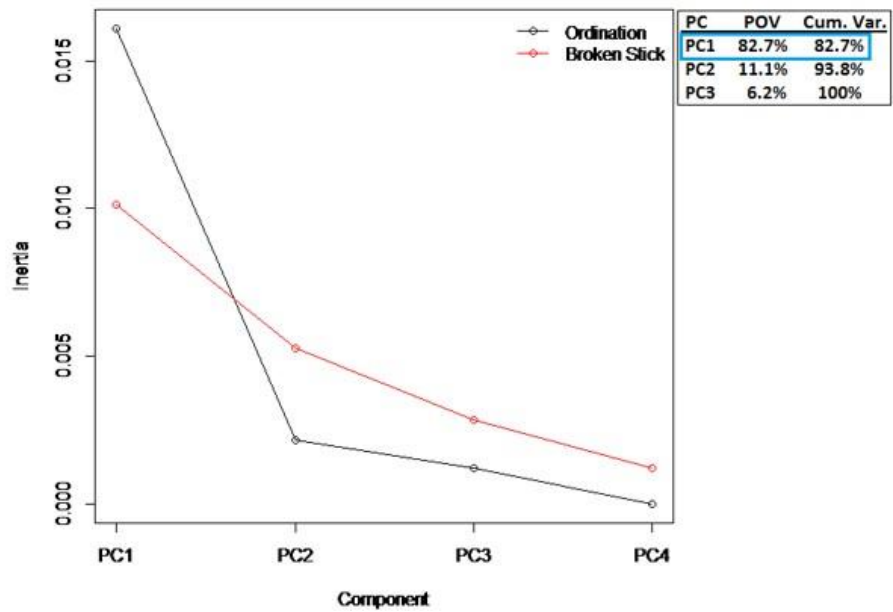
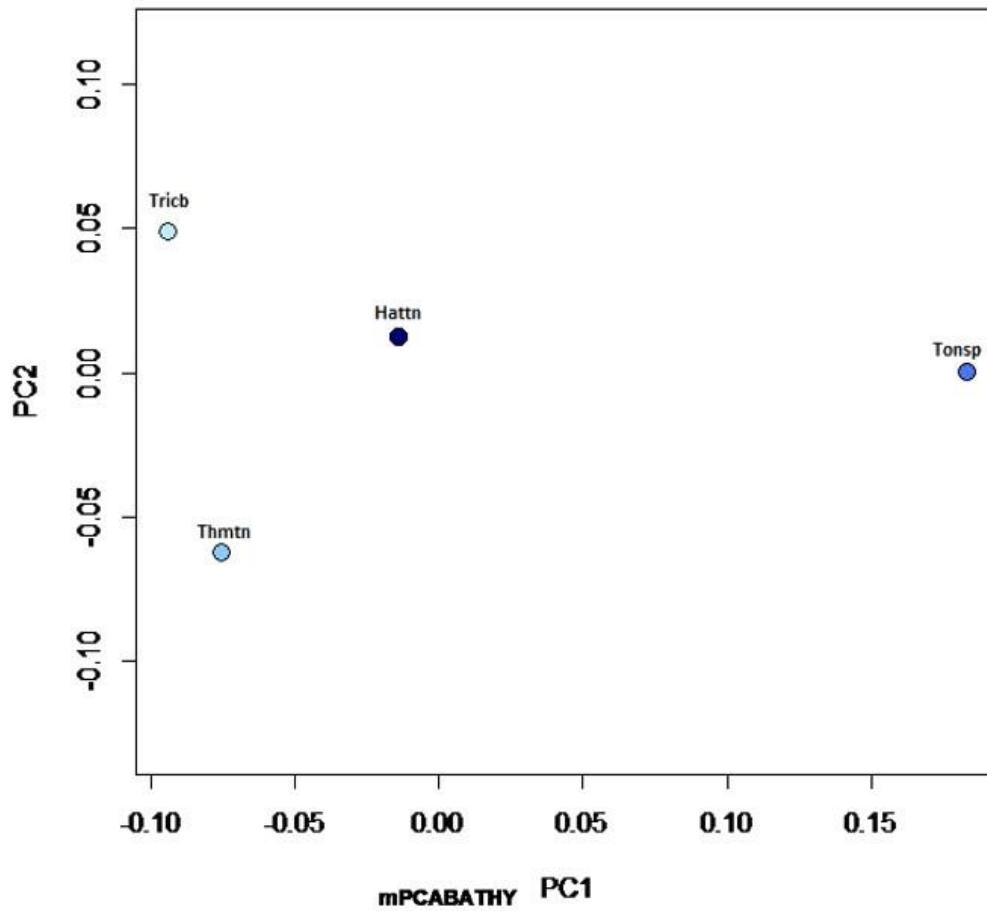


Fig. A32: Scenario 1 between group PCA (left) and broken stick model (right) depicting intra-subfamily variation of Bathymetrinae. Despite visual separations, there were no significant variations within this subfamily (see Fig. 25 for scenario 2 results) (Hattn = *Hathrometra tenella*, Thmtn = *Thaumatometra tenuis*, Tricb = *Trichometra cubensis*, Tonsp = *Tonrometra spinulifera*).

### Between Group PCA for Heliometrinae

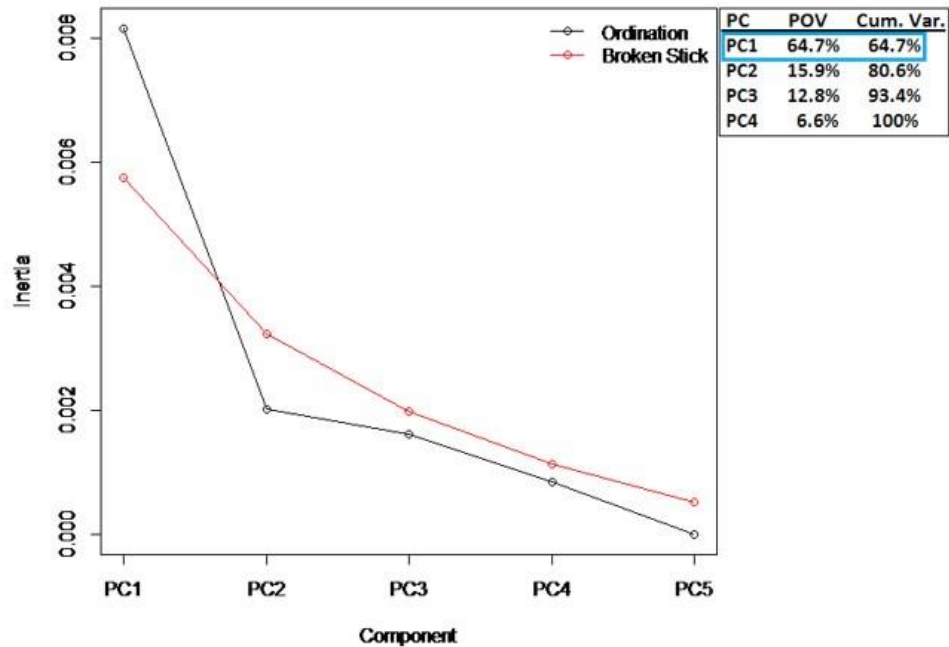
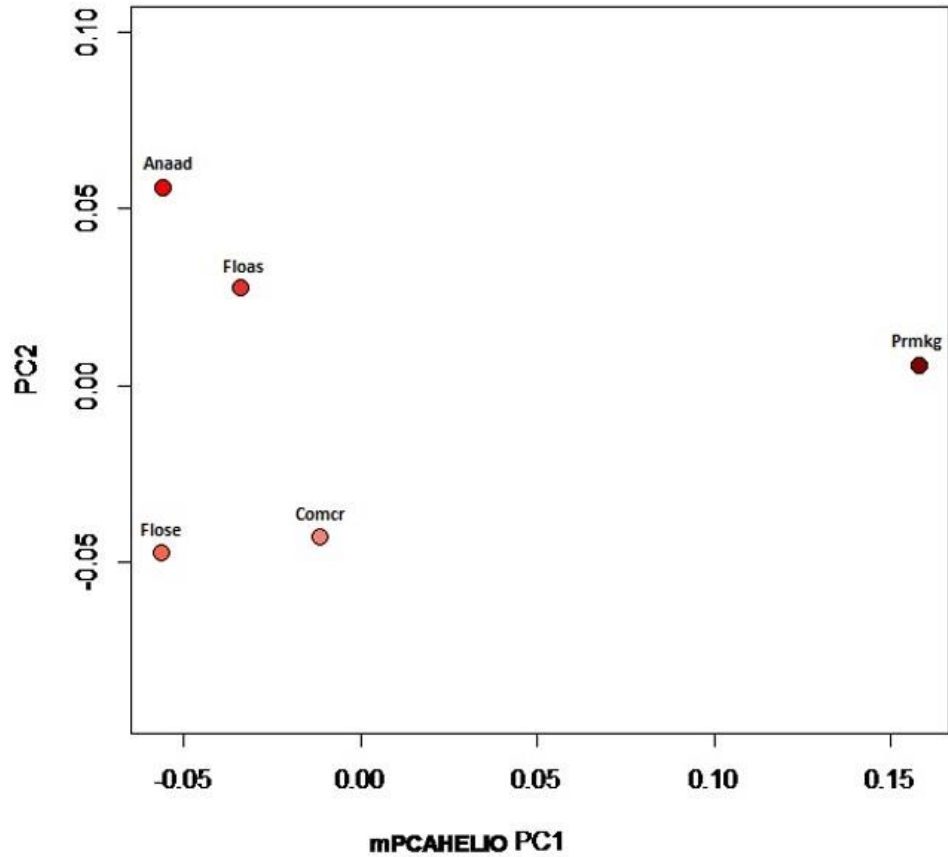


Fig. A33: Scenario 1 between group PCA (left) and broken stick model (right) depicting intra-subfamily variation of Heliometrinae. Despite visual separations, there were no significant variations within this subfamily (see Fig. 26 for scenario 2 results) (Anaad = *Anthometrina adriani*, Comcr = *Comatonia cristata*, Floas = *Florometra asperrima*, Flose = *Florometra serratissima*, Prmkg = *Promachocrinus kerguelensis*).



### Between Group PCA for Perometrinae

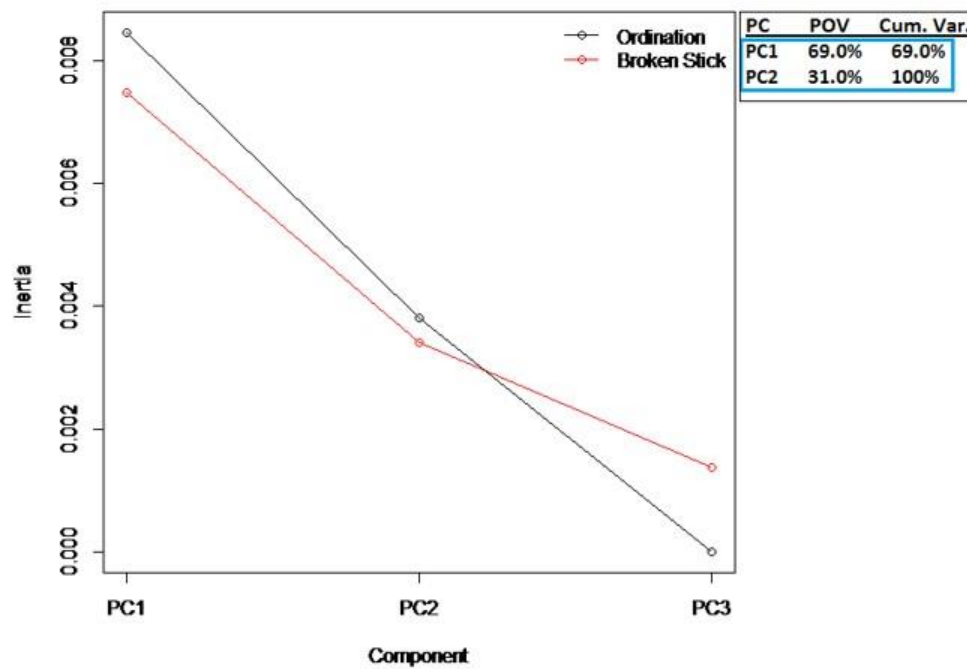
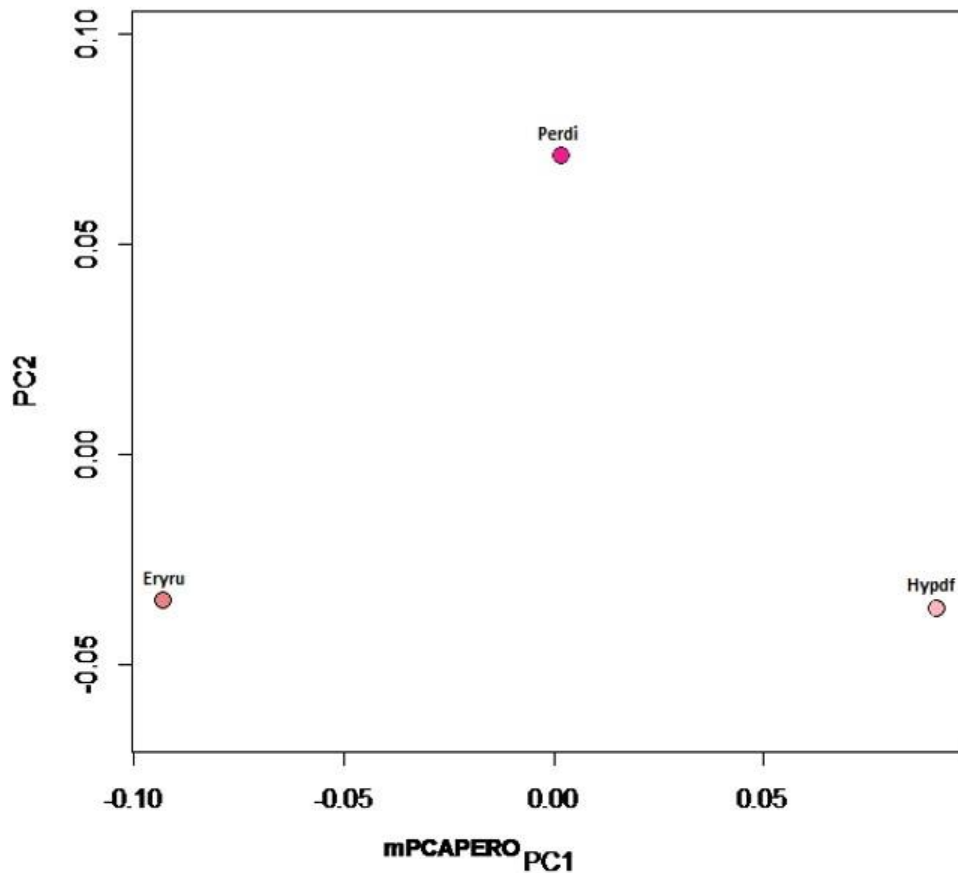


Fig. A34: Scenario 1 between group PCA (top) and broken stick model (bottom) depicting intra-subfamily variation of Perometrinae. Despite visual separations, there were no significant variations within this subfamily (see Fig. 27 for scenario 2 results) (Eryru = *Erythrometra rubra*, Hypdf = *Hypalometra defecta*, Perdi = *Perometra diomedae*).

## PCA for Thysanometrinae

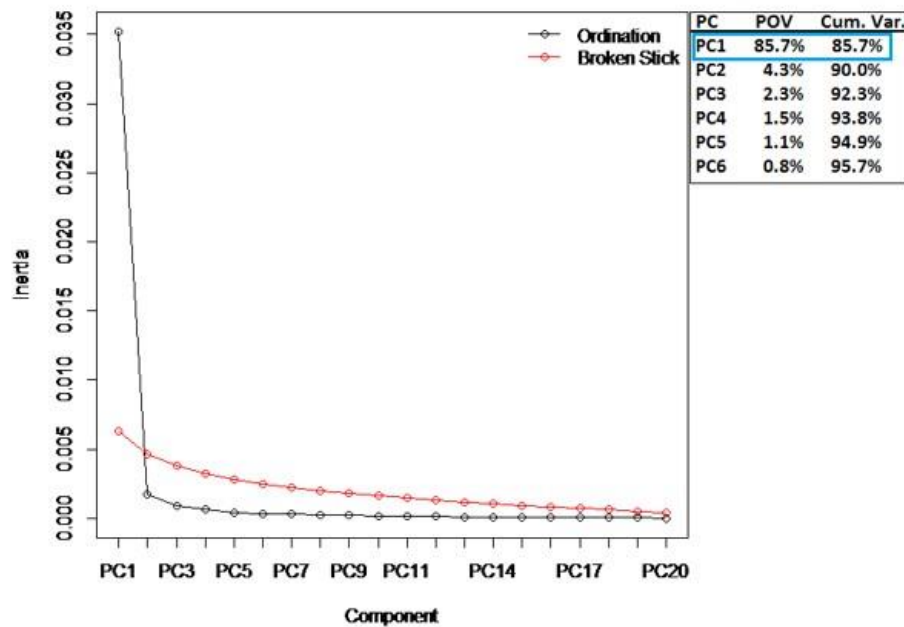
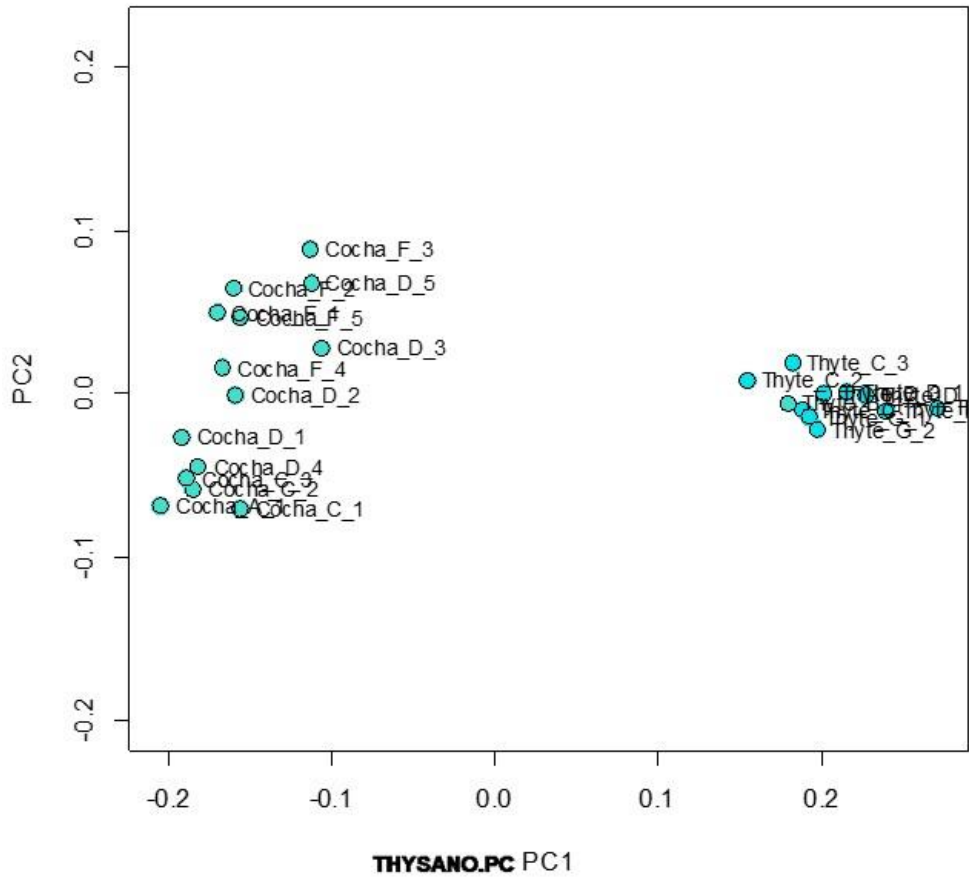


Fig. A35: Scenario 1 PCA (top) and broken stick model (bottom) depicting intra-subfamily variation of Thysanometrinae based on all individuals (see Fig. 28 for scenario 2 results) (Cocha = *Coccometra hagenii*, Thyte = *Thysanometra tenelloides*).

## Between Group PCA for *Antedonidae incertae sedis*

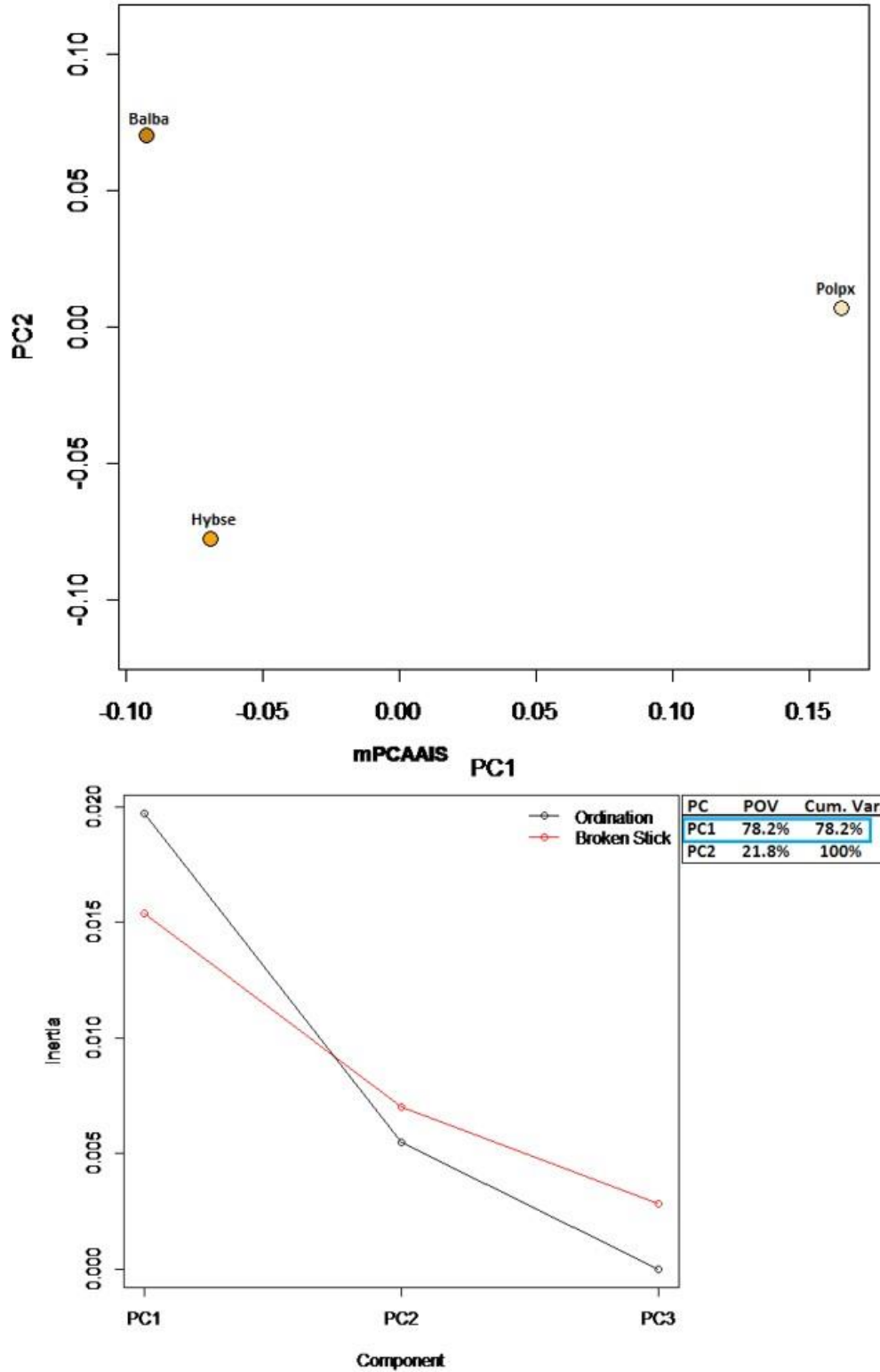


Fig. A36: Scenario 1 between group PCA (top) and broken stick model (bottom) depicting intra-subfamily variation of *Antedonidae incertae sedis*. Despite visual separations with *P. prolixa*, there were no significant variations within this subfamily (see Fig. 29 for scenario 2 results) (Balba = *Balanometra balanoides*, Hybse = *Hybometra senta*, Polpx = *Poliometra prolixa*).

## Between Group PCA for Clade M

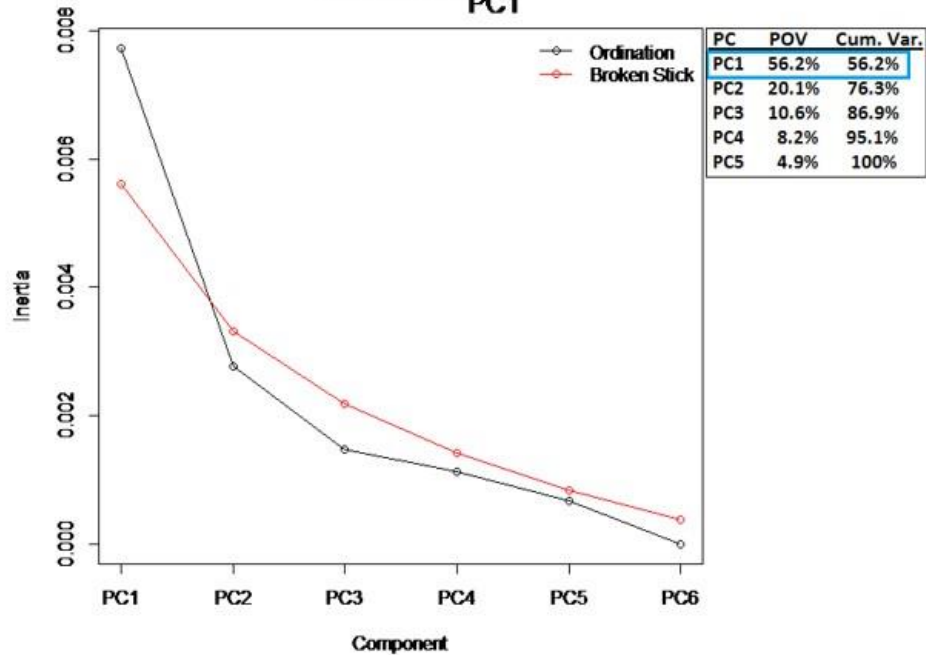
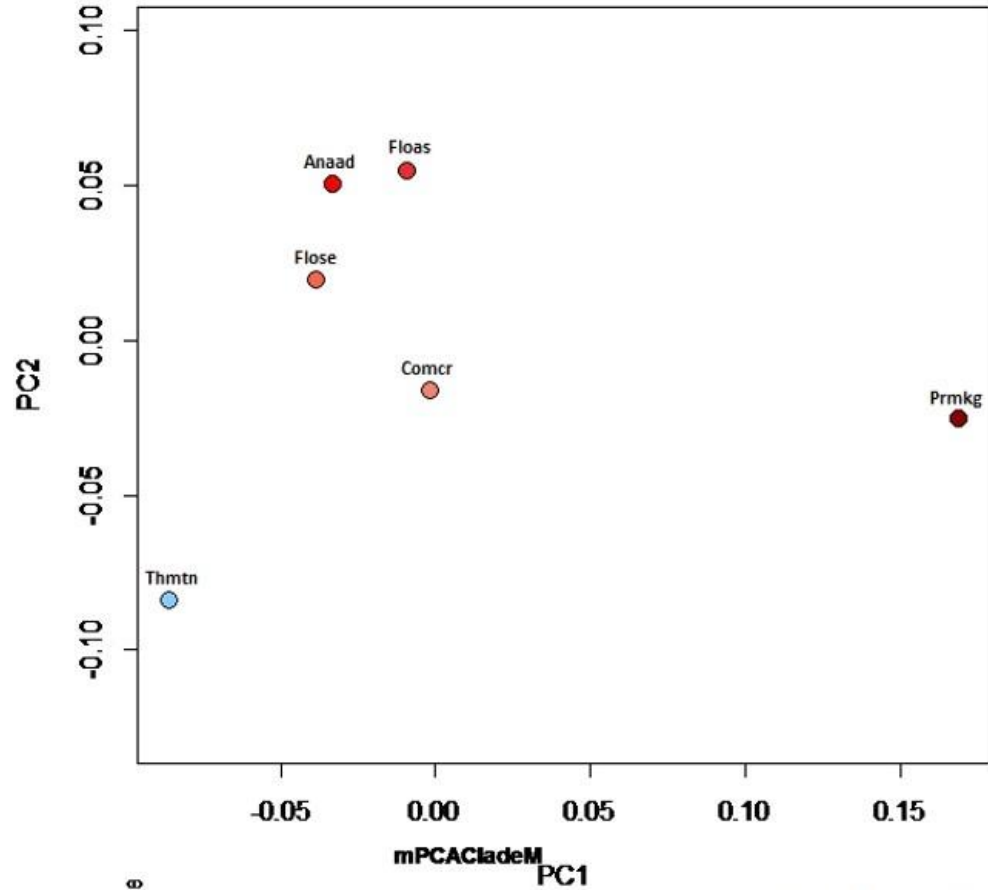


Fig. A37: Scenario 1 between group PCA (top) and broken stick model (bottom) depicting intra-clade variation of clade M and equivalents. Despite visual separation with *P. kerguelensis*, there were no significant variations within this clade (see Fig. 30 for scenario 2 results) (Anaad = *Anthometrina adriani*, Floas = *Florometra asperrima*, Flose = *Florometra serratissima*, Comcr = *Comatonia cristata*, Prmkg = *Promachocrinus kerguelensis*, Thmtn = *Thaumatometra tenuis*).

## Between Group PCA for Clade N

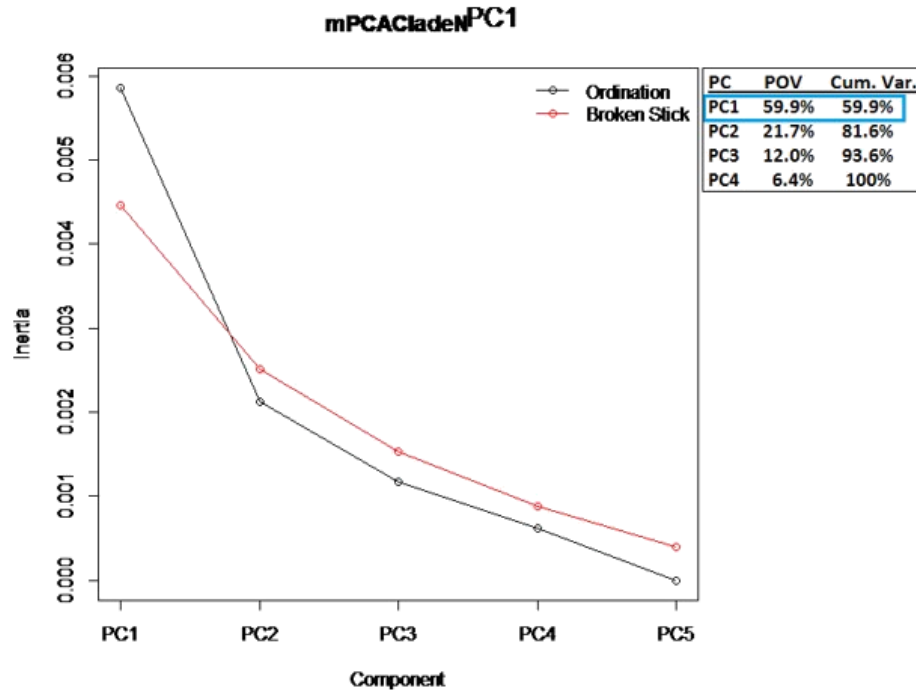
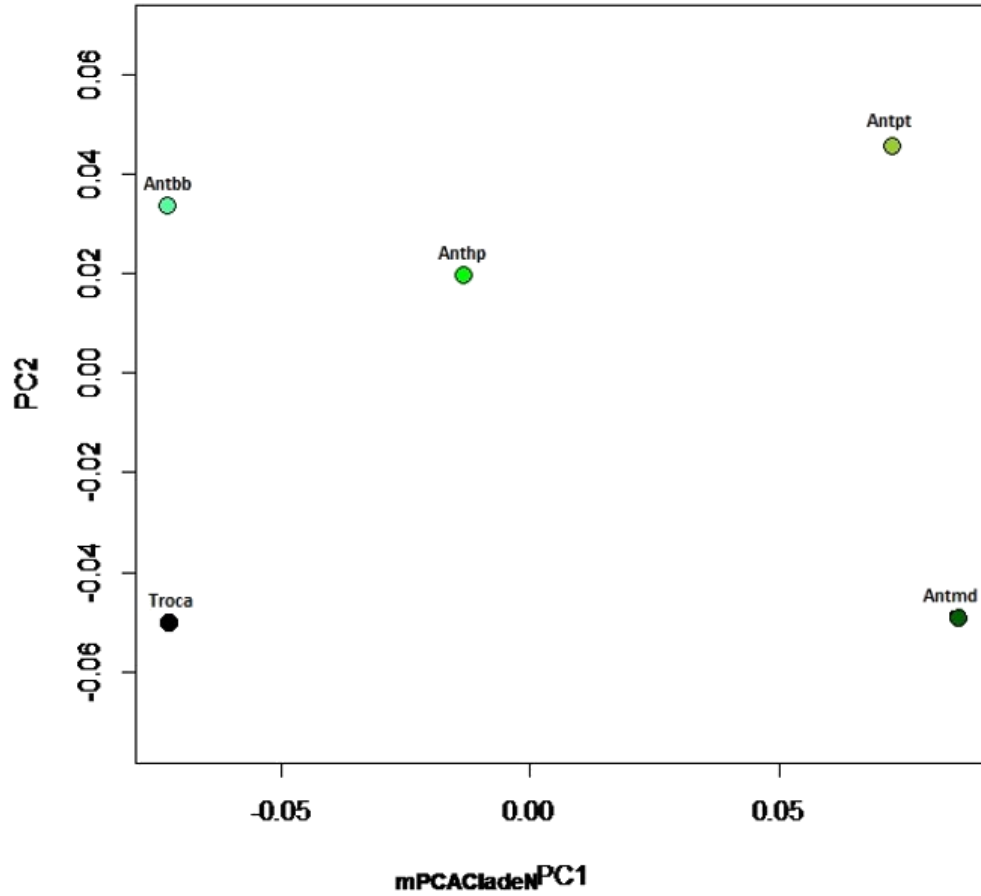


Fig. A38: Scenario 1 between group PCA (top) and broken stick model (bottom) depicting intra-clade variation of clade N and equivalents. Despite visual separations, there were no significant variations within this clade (see Fig. 31 for scenario 2 results) (Antbb = *Antedon bifida bifida*, Anthp = *Antedon hupferi*, Antmd = *Antedon mediterranea*, Antpt = *Antedon petasus*, Troca = *Tropiometra carinata*).

## Between Group PCA for Clade O

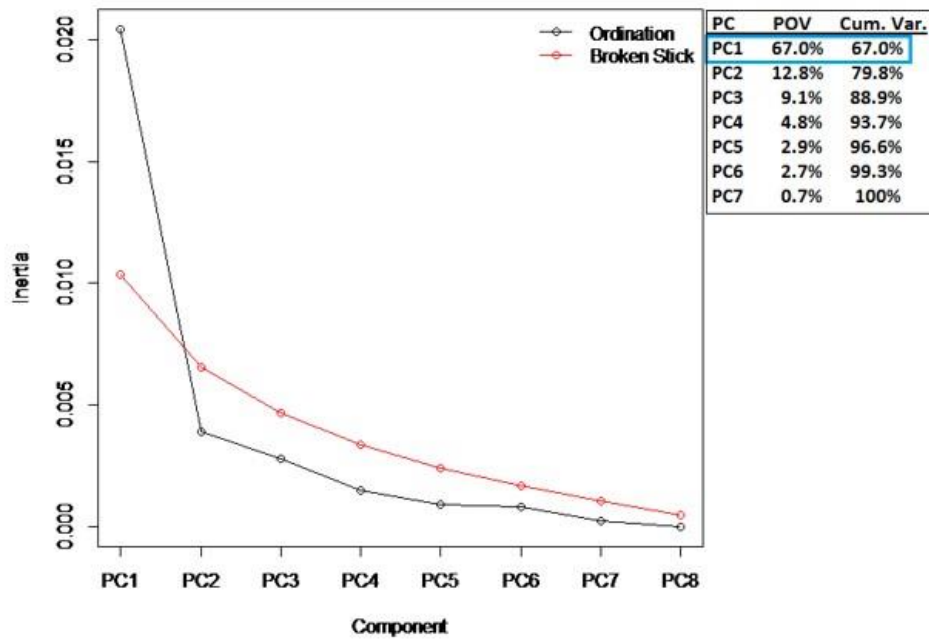
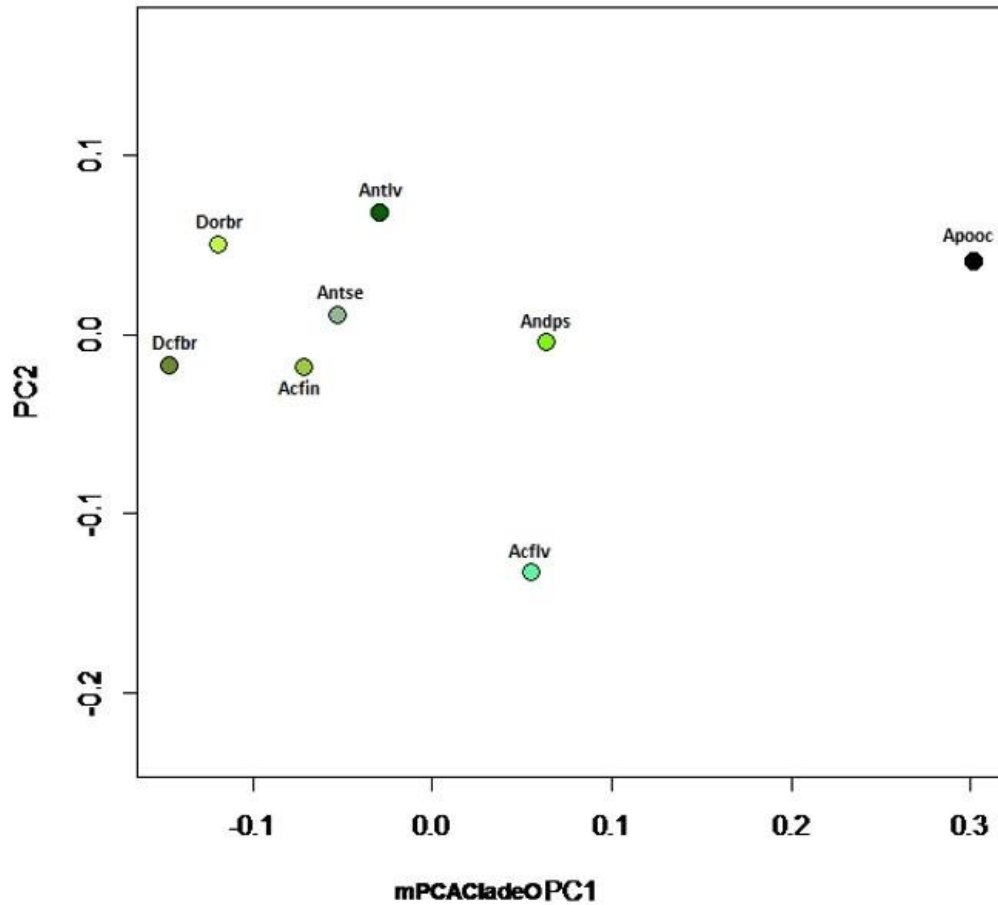


Fig. A39: Scenario 1 between group PCA (top) and broken stick model (bottom) depicting intra-clade variation of clade O and equivalents. There were significant affects by taxonomic classification within this clade, supporting the visual separation of *A. occidentalis* (see Fig. 32 for scenario 2 results) (*Acfin* = *Antedon c.f. incommoda*, *Acflv* = *Antedon c.f. loveni*, *Andps* = *Andrometra psyche*, *Antlv* = *Antedon loveni*, *Antse* = *Antedon serrata*, *Dcfbr* = *Dorometra c.f. briseis*, *Dorbr* = *Dorometra briseis*, *Apooc* = *Aporometra occidentalis*).

## Between Group PCA for Clade P

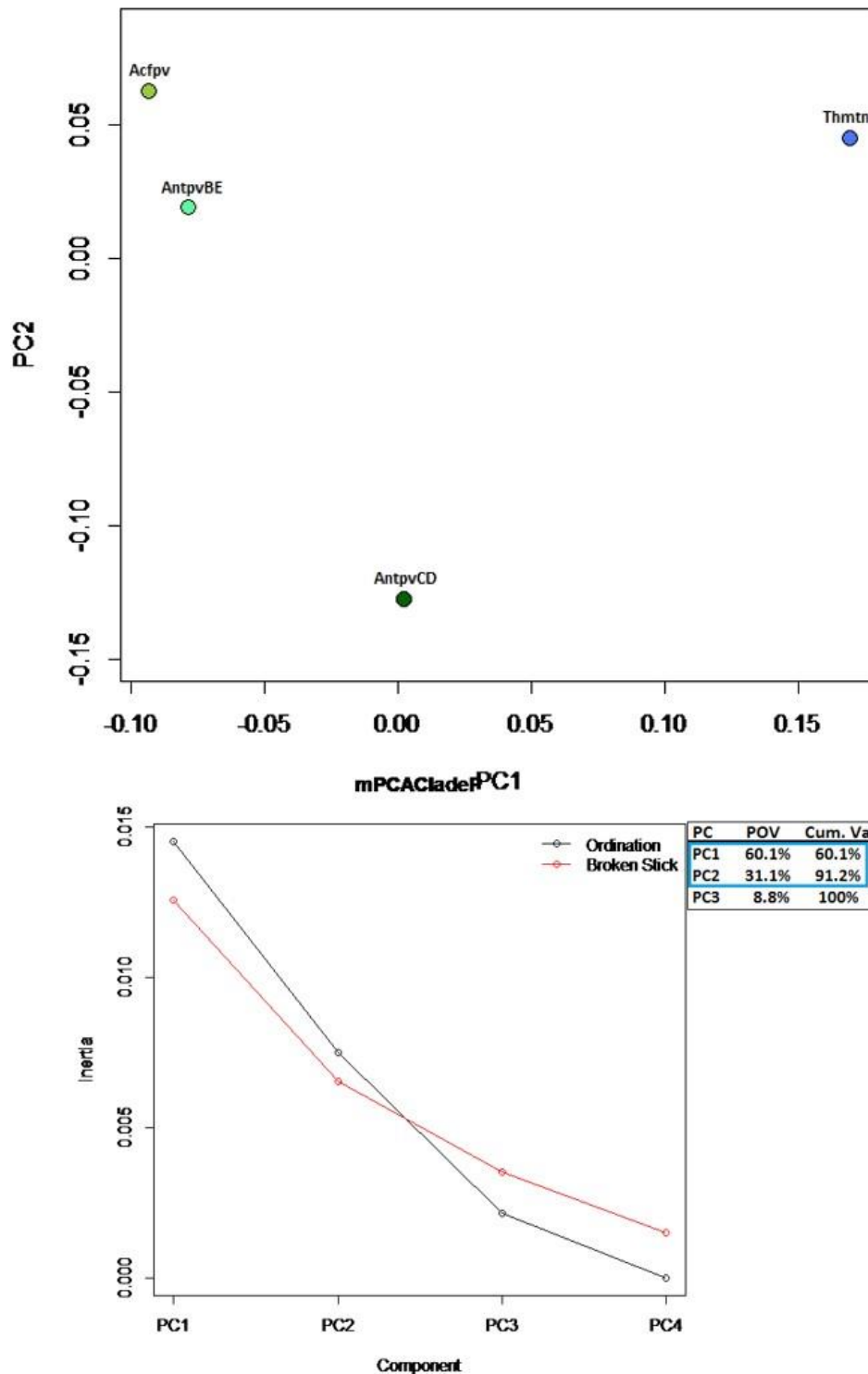


Fig. A40: Scenario 1 between group PCA (top) and broken stick model (bottom) depicting intra-clade variation of clade P and equivalents. Although the first two PCs are interpretable and there is visual separation of bathymetrine *T. tenuis*, there were no significant variations within this clade (see Fig. 33 for scenario 2 results) (Acfpv = *Antedon c.f. parviflora*, AntpvBE = *Antedon parviflora* B&E, AntpvCD = *Antedon parviflora* C&D, Thmtn = *Thaumatometra tenuis*).

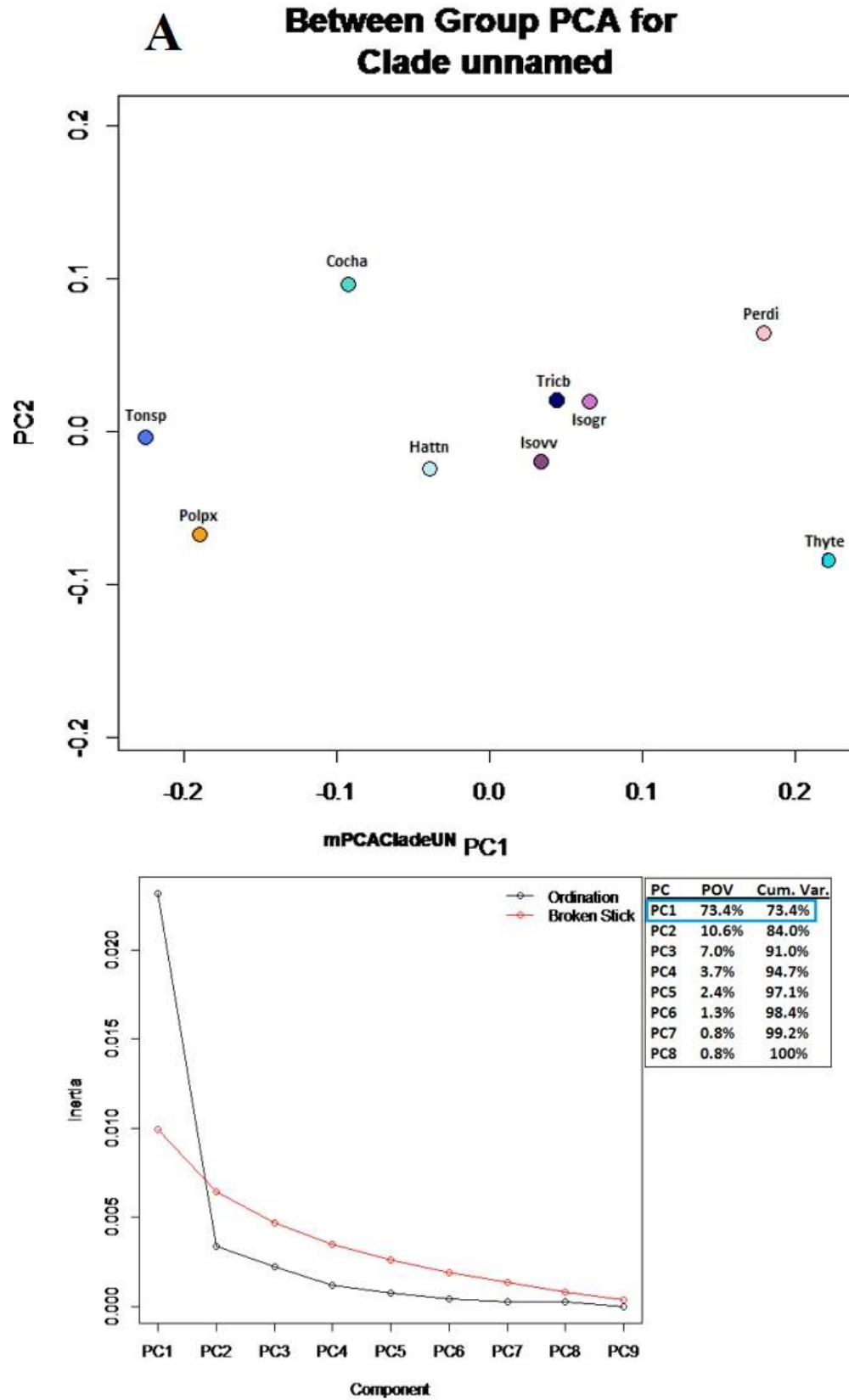


Fig. A41A: Scenario 1 between group PCA (top) and broken stick model (bottom) depicting intra-clade variation of clade ‘unnamed’ and equivalents (see Fig. 34A for scenario 2 results) (Cocha = *Coccometra hagenii*, Hattn = *Hathrometra tenella*, Isogr = *Isometra graminea*, Isov = *Isometra vivipara*, Perdi = *Perometra diomedea*, Polpx = *Poliometra prolixa*, Thyte = *Thysanometra tenelloides*, Tonsp = *Tonrometra spinulifera*, Tricb = *Trichometra cubensis*).



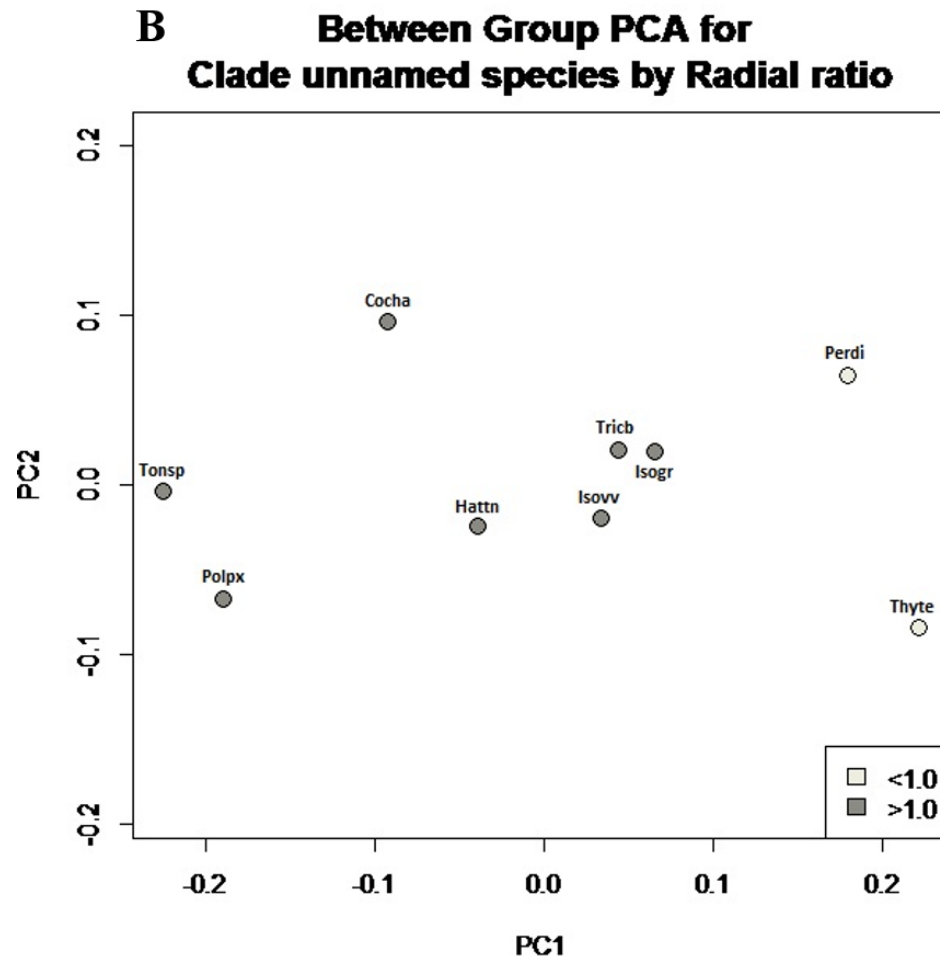


Fig. A41B: Scenario 1 results cont'd for intra-clade variation of clade 'unnamed' and equivalents. B: BGPCA colored by radial ratio showing separation of *P. diomedea* and *T. tenelloides*, supporting the Procrustes ANOVA results (see Fig. 34B for scenario 2 results).

# A Between Group PCA for ALL species

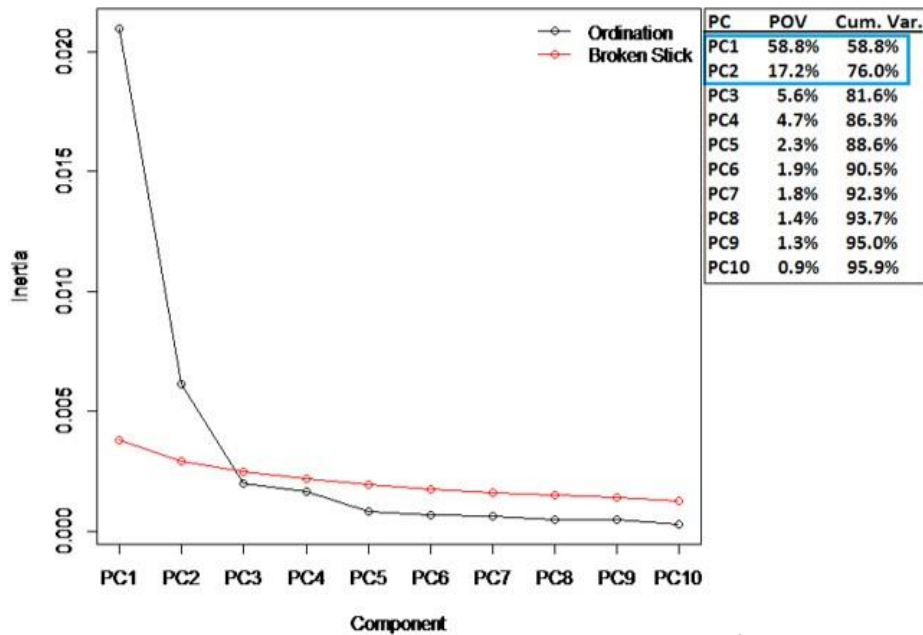
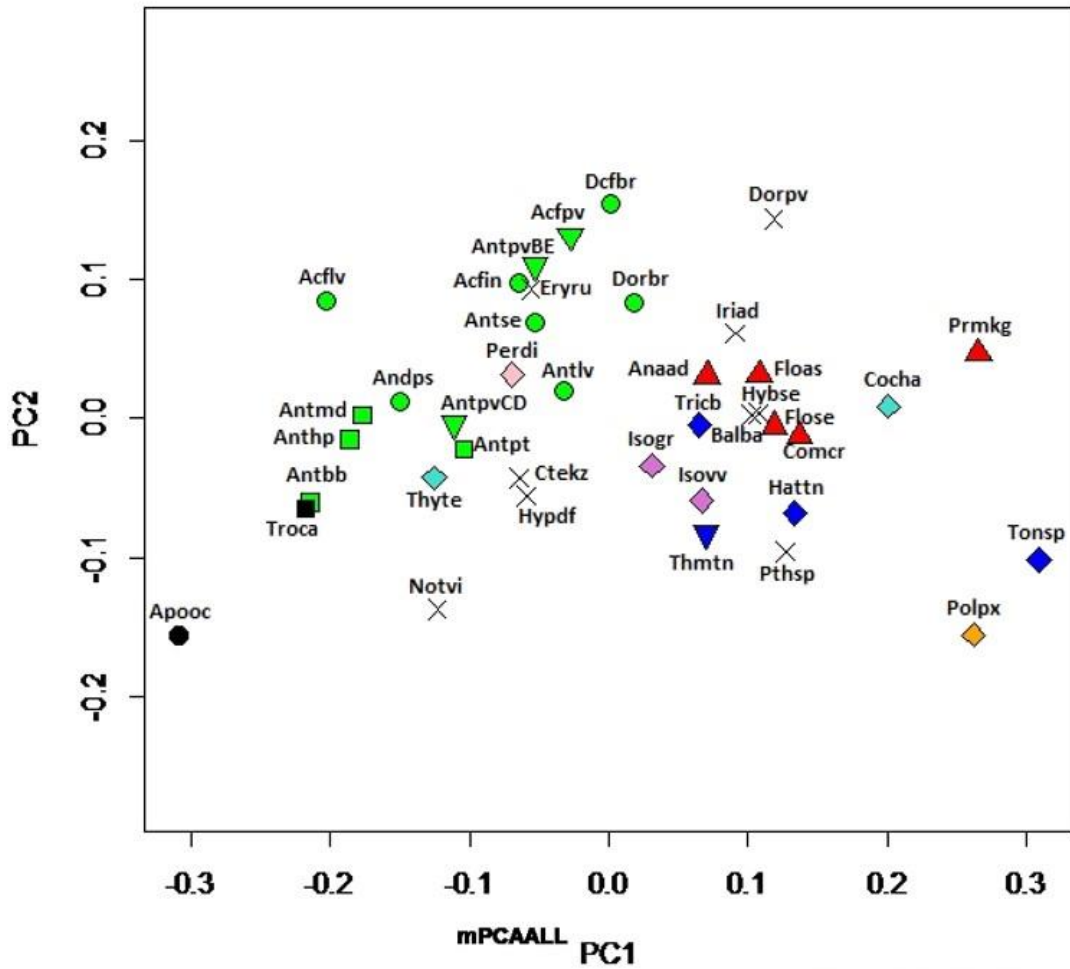
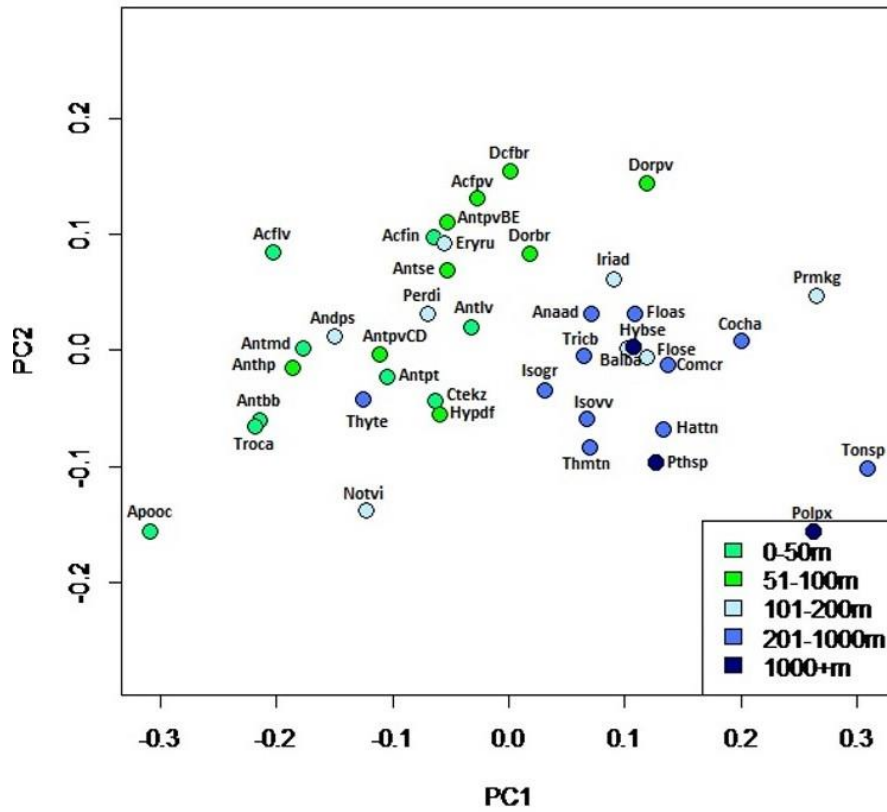


Fig. A42A: Scenario 1. A: BGPCA and broken stick model depicting significant variations between all species used in this study (see Appendix Fig. 35A for scenario 2 results; see Table 5 for species abbreviations) (colored by subfamily: *Antedoninae*, *Bathymetrinae*, *Heliometrinae*, *Isometrinae*, *Thysanometrinae*, *Perometrinae*, *A. incertae sedis*, non-antedonids; symbols by clade: Δ = clade M, □ = clade N, ○ = clade O, ▽ = clade P, ◇ = clade 'unnamed', X = not used in molecular analyses)

**B** **Between Group PCA for ALL species**



**C** **Between Group PCA for ALL species by Radial ratio**

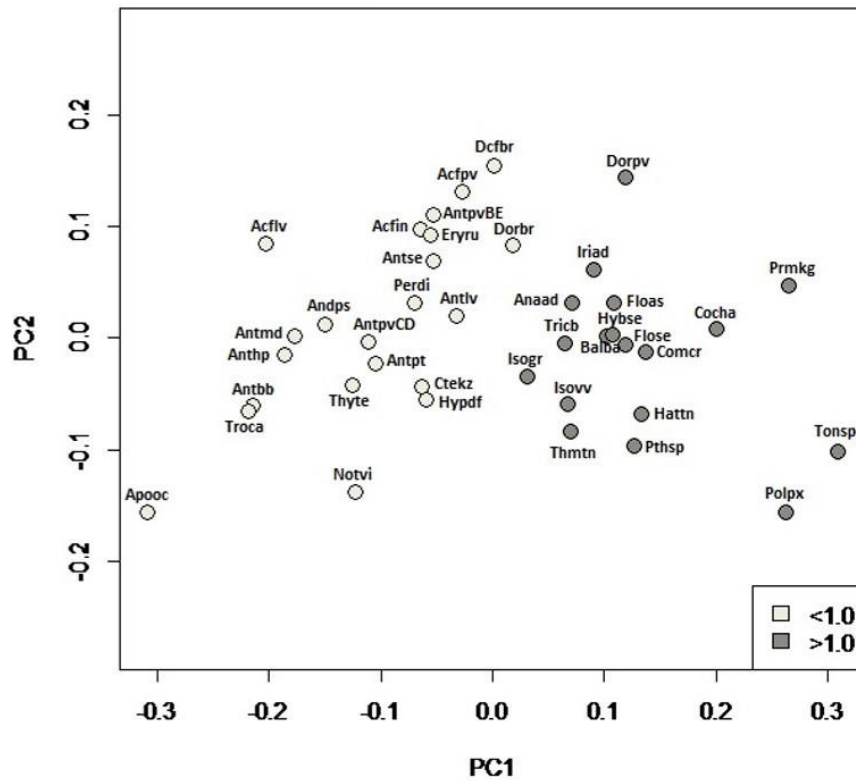


Fig. A42B-C: Scenario 1 results model of variations between all species cont'd. B: BGPCA colored by depth. C: BGPCA colored by radial ratio (see Fig. 35B-C for scenario 2 results; see Table 5 for species abbreviations).  
209

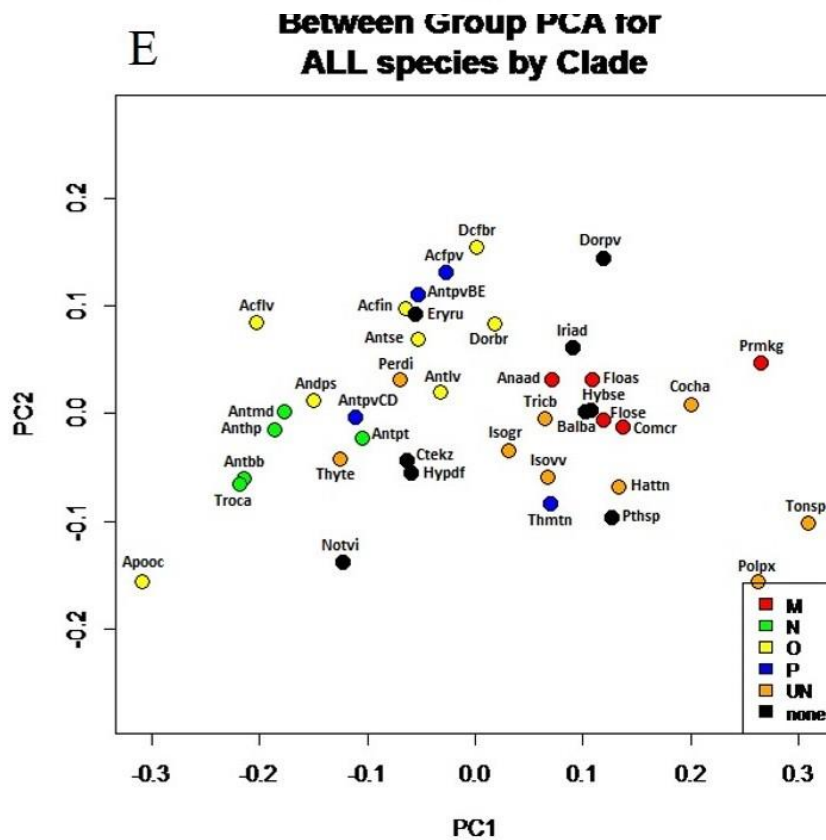
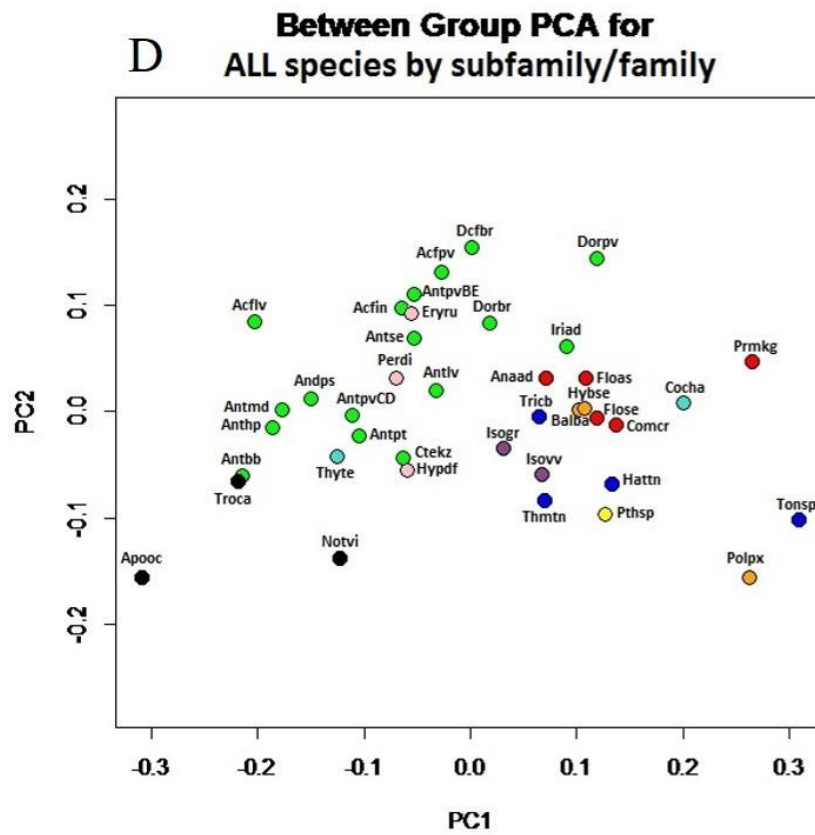


Fig. A42D-E: Scenario 1 results model of variations between all species cont'd. D: BGPCA colored by subfamily/family. E: BGPCA colored by clade assignment (see Fig. 35D-E for scenario 2 results; see Table 5 for species abbreviations).





Table 43. Table of Procrustes distances between all species in scenario 1 (closest Procrustes distances between species pairs in bold; see Table 7)

	Acfn	Acflv	Acfpv	Anaad	Andps	Antbb	Anthp	Antlv	Antmd	Antpt	AntpvBE	AntpvCD	Antsa	Apooc	Balba	Cocha	Comcr	Ctek	Dcfbr	Dorbr	Dorpv	Eryru	Floas	Flose	Hattn	Hybsb	Hypdf	Iriad	Isogr	Isov	Notvi	Pardi	Poljx	Pmkg	Pthsp	Thmtn	Thyta	Tonsp	Trich		
Acfn	0.200786																																								
Acflv	0.13943	0.126488																																							
Acfpv	0.212641	0.314569	0.20121																																						
Anaad	0.204736	0.19814	0.227037	0.273485																																					
Andps	0.241735	0.191948	0.294177	0.519415	0.204903																																				
Antbb	0.206489	<b>0.148789</b>	0.242015	0.276365	0.173369	<b>0.092557</b>																																			
Anthp	0.15027	0.221653	0.173115	0.126374	0.177829	0.227344	0.181041																																		
Antlv	0.241197	0.175115	0.27536	0.18347	0.193648	0.179959	0.132097	0.194918																																	
Antmd	0.196108	0.192458	0.228951	0.211736	0.200393	0.161202	0.113511	0.132235	<b>0.115276</b>																																
AntpvBE	0.143604	0.175051	0.139628	0.190437	0.211508	0.261638	0.202328	0.133652	0.215845	0.178751																															
AntpvCD	0.215438	0.189047	0.21541	0.230772	0.171668	0.181646	<b>0.139869</b>	0.142197	0.190049	0.139789	0.185688																														
Antsa	0.131671	0.189075	0.132583	0.152025	0.203563	0.222934	0.168629	<b>0.089003</b>	0.203369	0.140299	<b>0.08851</b>	0.146289																													
Apooc	0.390219	0.305557	0.441817	0.43458	0.291864	0.206283	0.226665	0.336116	0.243605	0.271766	0.39089	0.291594	0.366177																												
Balba	0.237089	0.355359	0.246344	0.13811	0.284711	0.365979	0.321478	0.177715	0.317697	0.236776	0.241251	0.268608	0.22547	0.458134																											
Cocha	0.305838	0.43396	0.28051	0.198067	0.37903	0.436107	0.406619	0.268311	0.422092	0.342987	0.297645	0.348378	0.28827	0.569635	0.179448																										
Comcr	0.298624	0.368994	0.260096	0.119013	0.328623	0.384192	0.329702	0.183211	0.333847	0.232788	0.242397	0.275151	0.219115	0.477691	0.139653	0.141265																									
Ctek	0.214873	0.225118	0.239611	0.194217	0.217521	0.190655	0.158481	0.120009	0.185286	<b>0.118155</b>	0.170663	0.199669	0.145415	0.292095	0.247956	0.31855	0.22295																								
Dcfbr	0.154545	0.246802	0.107741	0.180655	0.261911	0.327111	0.268869	0.167246	0.263863	0.224586	0.118474	0.23933	0.140295	0.454181	0.215041	0.277538	0.234053	0.238488																							
Dorbr	0.153441	0.159392	0.151149	0.157956	0.243243	0.296648	0.248972	0.131361	0.267585	0.201287	0.143814	0.18893	<b>0.129217</b>	0.425422	0.180207	0.232387	0.190791	0.197017	0.129932																						
Dorpv	0.241265	0.359482	0.216911	0.156114	0.326125	0.421189	0.365287	0.208186	0.351295	0.305829	0.2174	0.312142	0.223666	0.527329	0.181364	0.229246	0.1873	0.288926	0.161489	0.179398																					
Eryru	0.157312	0.223481	0.174213	0.197315	0.188157	0.276982	0.221422	<b>0.130091</b>	0.226122	0.19845	0.105879	0.19197	0.146237	0.378452	0.213575	0.317936	0.253378	0.223927	0.154398	0.166738	0.212584																				
Floas	0.246345	0.354405	0.216559	<b>0.105773</b>	0.317889	0.360448	0.314317	0.177628	0.31748	0.245424	0.198191	0.264419	0.187952	0.473858	0.174083	0.181848	0.194462	0.208025	0.199367	0.185984	0.166132	0.232218																			
Flose	0.246168	0.361706	0.243685	0.121755	0.326612	0.352404	0.318784	0.189059	0.338137	0.254156	0.239664	0.272557	0.210890	0.474952	0.192901	0.175956	0.104261	0.211246	0.242482	0.203475	0.200216	0.267192	<b>0.103626</b>																		
Hattn	0.275389	0.38606	0.287941	0.172401	0.338968	0.359734	0.333754	0.208925	0.34257	0.258564	0.178873	0.286499	0.251624	0.467361	0.167906	0.168753	<b>0.086791</b>	0.22121	0.275207	0.213726	0.243953	0.284406	0.161784	0.121794																	
Hybsb	0.233764	0.348985	0.206338	0.144889	0.299364	0.348369	0.307744	0.184636	0.333669	0.248104	0.221143	0.254908	0.197332	0.476052	0.149444	<b>0.133072</b>	0.122984	0.228731	0.209851	0.166809	0.205593	0.233496	0.159633	0.144939	0.141792																
Hypdf	0.223371	0.256432	0.223554	0.217036	0.173205	0.226178	0.199934	0.153631	0.237336	0.183287	0.22582	0.176303	0.19163	0.317751	0.205851	0.304005	0.231597	0.190246	0.248348	0.213471	0.301143	0.184002	0.262284	0.269057	0.253195	0.217535															
Iriad	0.196427	0.31269	0.181542	0.119996	0.272866	0.347963	0.302191	0.154286	0.302628	0.237936	0.178962	0.250647	0.177859	0.471594	0.146996	0.168417	0.118885	0.214037	0.16107	0.134124	<b>0.128559</b>	0.199239	0.12047	0.131439	0.156348	0.152218	0.237192														
Isogr	0.209642	0.294997	0.21688	0.139082	0.219083	0.286204	0.246448	0.110016	0.28641	0.191411	0.200918	0.193518	0.173583	0.576459	<b>0.139776</b>	0.225519	0.149691	0.156886	0.214691	0.165889	0.215718	0.18077	0.16985	0.16946	0.155851	0.148401	0.147736	0.161449													
Isov	0.237311	0.339412	0.260528	0.188358	0.286432	0.310283	0.298581	0.186721	0.314028	0.232208	0.238823	0.264089	0.235548	0.410962	0.185652	0.216539	0.160699	0.206851	0.256997	0.202297	0.256651	0.24619	0.199873	0.176367	0.134266	0.179329	0.21166	0.163739	<b>0.126992</b>												
Notvi	0.302039	0.306022	0.316929	0.311415	0.211204	0.241309	0.228396	0.244606	0.268868	0.239288	0.308963	0.248097	0.280971	0.26646	0.302531	0.390441	0.347144	0.240147	0.348165	0.324642	0.401669	0.281315	0.340126	0.344586	0.331429	0.30558	<b>0.140184</b>	0.33674	0.231562	0.278977											
Pardi	0.113076	0.189048	0.14253	0.188436	0.152099	0.204758	0.163449	<b>0.108578</b>	0.200828	0.149569	0.13297	0.16269	0.111441	0.339203	0.218443	0.285133	0.236153	0.165748	0.171165	0.151591	0.250453	0.141819	0.221095	0.234789	0.24947	0.198817	<b>0.139812</b>	0.187194	0.160903	0.207637	0.218547										
Poljx	0.431166	0.52974	0.421433	0.287387	0.468207	0.495363	0.476227	0.354747	0.480106	0.39746	0.418899	0.41268	0.395999	0.585498	0.239896	0.202257	0.204152	0.361895	0.412159	0.357275	0.353107	0.428095	0.26119	0.240178	0.177219	0.243023	0.365853	0.286634	0.283796	0.253118	0.42235	0.390855									
Pmkg	0.386597	0.494638	0.358884	0.221279	0.45707	0.521777	0.479379	0.316397	0.480795	0.395102	0.354833	0.408238	0.344817	0.614147	0.214861	0.214928	<b>0.184928</b>	0.365437	0.506956	0.399521	0.1985																				





Table A7: Table of Mahalanobis distances between all species in Scenario 1 (closest Mahalanobis distances between species pairs in bold; see Table 7)

	Acfn	Acfv	Acfv	Anead	Andos	Antbb	Anthp	Antlv	Antmd	Antpt	AntpvBE	AntpvCD	Antse	Apoc	Balbs	Cocha	Comcr	Cteks	Ocfbr	Dorbr	Dorpv	Eryru	Floes	Flose	Hattn	Hvbs	Hvpdf	Iriad	Isogr	Isovv	Notvi	Perdi	Polpx	Pmkg	Pthsp	Thmnt	Thyte	Tonsp	Tricb			
Acfn	16.09946																																									
Acfv	12.17078	16.55156																																								
Anaad	13.27700	17.54143	13.91283																																							
Andps	15.51012	15.19038	15.7469	15.86169																																						
Antbb	12.84517	14.71303	17.90049	13.58347	15.30433																																					
Anthp	13.3697	14.25232	16.97218	13.57287	15.22254	<b>7.992043</b>																																				
Antlv	12.17618	13.07149	12.81084	9.120119	<b>10.99041</b>	11.96064	12.04765																																			
Antmd	15.02038	15.90570	16.73813	14.76423	15.21146	13.23295	9.537657	13.62597																																		
Antpt	13.1864	16.40132	16.36357	11.75739	16.26649	10.97977	<b>7.383382</b>	11.67793	<b>8.489109</b>																																	
AntpvBE	13.98272	<b>10.67278</b>	13.04617	13.82293	16.61097	14.45216	13.21545	12.46539	14.80199	14.82956																																
AntpvCD	17.96325	16.49283	17.51464	16.55279	13.55966	16.39039	15.8474	11.77219	17.79948	15.77511	17.74206																															
Antse	11.98262	11.88261	12.95249	11.1254	14.92448	10.37744	9.874594	<b>8.844025</b>	13.13729	11.26972	<b>8.389606</b>	14.10132																														
Apoc	20.60807	20.15687	24.11621	19.44266	18.24529	13.49044	13.52481	16.44626	17.21013	15.84248	20.11348	10.93145	18.17537																													
Balbs	17.44487	20.84228	19.00132	13.7919	16.73793	19.35456	18.95279	12.56474	18.59126	16.08957	20.9772	18.02639	18.02149	21.62595																												
Cocha	16.70006	21.40879	17.53787	10.3006	19.33133	18.89741	19.72624	12.78114	20.87854	17.02793	19.03919	18.04822	16.36623	24.09091	12.40409																											
Comcr	15.23051	17.90144	16.78214	<b>8.218979</b>	17.93419	15.49294	15.03157	9.345177	16.13978	12.21628	16.14225	15.39045	12.61777	20.51798	12.36272	<b>9.067045</b>																										
Cteks	15.74564	16.82942	14.34045	12.66485	16.81868	13.89613	11.81902	<b>9.520092</b>	14.43946	11.97718	12.39603	13.96419	10.44938	16.23363	17.90456	16.73642	12.23641																									
Ocfbr	11.50476	16.32974	<b>8.30484</b>	12.77599	16.87493	17.87579	15.60498	13.01608	14.32131	14.1998	12.29255	18.44724	13.10139	23.33364	17.79929	17.07671	15.09221	14.30398																								
Dorbr	15.99154	18.57631	15.09515	16.28033	17.20119	19.00846	18.17522	13.04875	18.94629	16.98869	16.92937	13.82467	13.23491	23.83229	17.59345	16.6703	15.10651	15.32546	15.42668																							
Dorpv	14.85417	17.74755	12.26395	11.899	16.06183	19.50635	17.37632	12.33104	15.79629	16.12286	13.97675	17.02029	13.30013	24.66262	16.98119	16.03915	13.13432	14.97496	9.895227	13.03907																						
Eryru	16.48639	16.28928	17.78785	15.88361	12.49742	17.35182	16.10805	11.91876	15.33387	15.3761	18.535	14.74985	15.61134	20.36239	15.7881	18.09727	14.85066	17.687	17.086	17.23147	15.80762																					
Floes	16.20075	16.98237	15.9072	9.132554	19.69182	15.85578	14.66848	12.56226	16.81578	15.24353	12.90506	18.13582	12.11993	20.81797	18.12997	15.72987	10.79978	11.88405	14.19627	18.97858	15.92504	20.44797																				
Flose	15.42029	19.63975	16.08581	8.920292	19.63927	15.2776	14.29263	12.63653	16.88228	13.11797	15.33217	17.67246	12.9501	21.30623	18.04381	13.04796	9.402339	11.95545	15.04739	17.74814	13.37073	19.12725	<b>8.568013</b>																			
Hattn	16.00934	21.20745	18.39657	13.55756	19.79752	17.29164	17.04275	12.73626	17.60144	13.22191	20.54768	16.63644	16.30076	21.97715	11.45153	11.86663	<b>9.074346</b>	14.27593	17.36777	16.53889	16.91261	16.71828	15.14324	13.14125																		
Hvbs	16.14064	19.88631	16.46605	10.79331	17.5073	17.30424	15.8384	11.53186	17.78899	13.36164	18.20691	16.55371	15.11277	20.1893	12.47201	10.45162	9.638849	13.63895	15.26077	16.88648	15.80926	15.17046	13.05676	12.37906	11.47919																	
Hvpdf	16.30997	18.56248	17.98848	15.84902	14.87614	15.76769	16.04065	12.401	17.61323	15.5208	19.84458	16.03108	16.55305	17.20702	13.30547	17.25911	14.93251	16.9174	17.82821	18.08774	18.99343	12.440	19.50486	19.06107	15.10278	13.04002																
Iriad	12.1957	16.92464	11.4957	10.75078	15.4862	16.2547	14.84344	10.3488	14.18468	12.98979	15.79785	15.17368	11.16096	23.08856	15.32723	18.48719	10.88881	13.1681	10.58545	<b>12.99915</b>	<b>9.210291</b>	15.48769	12.58132	12.01597	12.57526	15.41589	17.25621															
Isogr	15.18448	16.8636	16.43438	11.86063	13.88101	15.40258	14.60783	<b>8.796936</b>	16.70283	13.25799	16.90203	14.90631	14.46915	16.86977	11.74362	13.87387	11.18107	12.08781	15.23905	17.60209	16.00564	13.3673	13.62517	14.53298	12.34294	9.305875	<b>10.83322</b>	13.44536														
Isovv	16.85438	20.64932	19.54177	15.42455	19.95734	17.13777	17.08642	14.1789	19.00964	14.14857	20.40526	19.2802	17.53689	20.0951	14.47407	14.47456	13.2536	15.86693	18.39281	19.49386	20.04125	16.50034	17.12757	15.83102	<b>11.57895</b>	13.00179	15.12565	15.74607	15.6987													
Notvi	22.10471	14.65028	25.01895	20.52024	20.86863	19.07345	18.7677	19.5928	21.89549	19.07624	24.4622	23.6973	22.5923	14.37435	20.16373	22.17965	24.30305	21.02993	24.18249	26.93323	26.48332	21.1198	22.06241	22.38398	21.71474	16.87504	<b>13.92892</b>	24.75133	15.60915	18.2318												
Perdi	<b>10.45706</b>	14.98767	13.4098	11.52309	13.90288	12.14915	12.05401	<b>8.934998</b>	14.03849	11.3346	13.72821	16.06068	11.75333	16.44236	14.22806	14.34664	12.6606	12.91039	13.21098	16.2319	15.39432	13.52863	14.25773	14.90039	14.48318	11.23705	11.42801	15.13328	11.03232	13.70179	16.70127											
Polpx	24.00384	28.0588	25.40599	17.86373	28.28846	24.30132	24.28137	19.62031	25.17042	20.31394	27.02161	25.91893	25.90629	26.06484	15.37145	14.0895	14.47708	21.22921	24.22176	24.5004	24.04214	22.80722	19.17087	18.28506	12.71675	12.92112	18.93751	21.05605	16.56274	15.20985	21.24055	19.48822										
Pmkg	19.9709	22.93237	17.84304	12.80413	22.07854	22.96409	21.20197	15.81005	19.68825	17.95272	19.95933	20.43879</																														



Table A9: Table of inter-landmark measurement ratios (see Table A2 for standardized measurements)

mf = muscle fossae; al = aboral ligament fossae; il = interarticular ligament fossae; CC = central canal

H % = height to radial height %, W% = width to radial width %; R = right; L = left

Specimen	R mf H %	L mf H %	al H %	R il H %	L il H %	R il W %	L il W %	CC W %	CC H %
<i>Andrometra psyche_A_1</i>	34	28	32	39	42	74	78	20	17
<i>A. psyche_A_2</i>	32	33	35	39	40	69	76	21	17
<i>A. psyche_B_1</i>	43	45	38	40	40	78	73	19	17
<i>A. psyche_C_1</i>	36	35	39	42	46	66	70	22	19
<i>Antedon bifida bifida_A_1</i>	47	47	35	33	31	66	69	22	15
<i>A. bifida bifida_A_2</i>	48	49	35	36	34	67	65	23	17
<i>A. bifida bifida_A_3</i>	45	44	34	33	34	68	65	22	15
<i>A. bifida bifida_C_1</i>	41	44	36	38	40	72	75	20	16
<i>A. bifida bifida_C_2</i>	40	36	34	37	35	71	74	21	15
<i>A. bifida bifida_D_1</i>	38	39	32	36	39	62	66	20	16
<i>A. bifida bifida_D_2</i>	44	41	32	39	37	70	67	20	17
<i>A. bifida bifida_D_3</i>	41	43	33	41	40	69	66	20	16
<i>A. bifida bifida_E_1</i>	44	46	31	39	39	69	73	20	14
<i>A. bifida bifida_E_2</i>	47	41	32	41	36	75	69	19	15
<i>A. bifida bifida_E_3</i>	47	41	34	29	31	73	71	19	16
<i>Antedon hupferi_A_1</i>	36	39	33	39	37	67	66	17	16
<i>A. hupferi_B_1</i>	38	41	34	37.5	36	68	74	20	15
<i>A. hupferi_B_2</i>	41	39	35	39	40	72	72	20	15
<i>A. hupferi_B_3</i>	39	44	36	38	41	70	70	19	15
<i>A. hupferi_C_1</i>	36	39	34	40	38	75	74	21	14
<i>A. hupferi_D_1</i>	43	46	34	39	40	71	72	21	13
<i>A. hupferi_D_2</i>	42	44	34	39	40	77	75	19	13
<i>A. hupferi_D_3</i>	43	43	33	40	38	77	73	18	13
<i>Antedon c.f. incommoda_A_1</i>	41	42	34	45	42	--	--	--	14
<i>A. c.f. incommoda_B_1</i>	40	40	33	49	48	61	67	23	15
<i>Antedon loveni_A_1</i>	41	45	26	37	36	65	61	22	14
<i>A. loveni_A_2</i>	45	44	28	40	38	63	65	22	15
<i>A. loveni_A_3</i>	39	44	29	41	40	66	66	23	12
<i>A. loveni_B_1</i>	39	36	32	38	38	67	64	22	15
<i>A. loveni_B_2</i>	38	38	30	38	38	65	67	22	14
<i>A. loveni_C_1</i>	41	44	29	39	37	63	66	24	16
<i>A. loveni_C_2</i>	42	41	29	35	38	57	62	25	16
<i>A. loveni_D_1</i>	41	40	32	38	35	64	64	25	16
<i>A. loveni_D_2</i>	42	42	31	39	40	59	61	25	18
<i>A. loveni_E_1</i>	38	39	32	35	34	65	75	21	17
<i>A. loveni_E_2</i>	41	39	32	35	33	69	73	19	20
<i>Antedon c.f. loveni_F_1</i>	23	26	35	46	47	66	64	22	18
<i>A. c.f. loveni_F_2</i>	26	21	34	48	46	59	59	24	19
<i>A. c.f. loveni_F_3</i>	26	28	35	40	43	65	65	23	18
<i>A. c.f. loveni_F_4</i>	33	30	37	39	39	61	61	22	16
<i>A. c.f. loveni_G_1</i>	33	33	39	39	39	60	56	23	18
<i>A. c.f. loveni_G_2</i>	30	30	36	37.5	42	56	52	22	17
<i>A. c.f. loveni_G_3</i>	35	30	35	42	42	60	62	23	17
<i>A. c.f. loveni_G_4</i>	28	32	37	44	41	63	61	22	17
<i>Antedon mediterranea_A_1</i>	30	36	34	35	34	69	71	16	14
<i>A. mediterranea_A_2</i>	30	34	33	34	34	78	80	17	15
<i>A. mediterranea_C_1</i>	30	34	33	35	37	74	75	16	15
<i>A. mediterranea_D_1</i>	33	33	35	30	29	75	82	15	14
<i>A. mediterranea_D_2</i>	32	31	34	28	32	75	72	15	14
<i>A. mediterranea_D_3</i>	31	34	37	25	31	60	78	15	15
<i>A. mediterranea_E_1</i>	23	21	33	35	34	78	75	15	17
<i>A. mediterranea_E_2</i>	26	24	34	33	36	82	79	14	17

Table A9 cont'd: Table of inter-landmark measurement ratios (see Table A2 for standardized measurements)

mf = muscle fossae; al = aboral ligament fossae; il = interarticular ligament fossae; CC = central canal

H % = height to radial height %, W% = width to radial width %; R = right; L = left

Specimen	Rmf H %	Lmf H %	al H %	Ril H %	Lil H %	Ril W %	Lil W %	CC W %	CCH %
<i>Antedon petasus</i> _A_1	37	32	33	35	33	70	75	17	13
<i>A. petasus</i> _A_2	37	37	35	28	33	72	73	19	14
<i>A. petasus</i> _C_1	37.5	36	30	35	33	67	63	18	13
<i>A. petasus</i> _D_1	37	35	30	34	33	67	74	18	14
<i>Antedon parviflora</i> _B_1	35	34	29	48	50	68	71	22	15
<i>A. parviflora</i> _E_1	31	30	29	43	45	70	70	19	14
<i>A. parviflora</i> _C_1	43	40	33	43	43	65	55	27	20
<i>A. parviflora</i> _D_1	40	37	27	40	43	57	57	34	20
<i>Antedon</i> c.f. <i>parviflora</i> _F_1	39	38	27	47	47	62.5	60	23	19
<i>A. c.f. parviflora</i> _F_2	37	38	29	51	49	66	60	22	18
<i>A. c.f. parviflora</i> _F_3	40	34	29	46	45	60	62.5	22	18
<i>A. c.f. parviflora</i> _F_4	39	38	26	53	47	62	64	22	17
<i>Antedon serrata</i> _A_1	40	40	29	46	44	64	67	26	13
<i>A. serrata</i> _A_2	39	39	27	48	48	66	68	25	17
<i>A. serrata</i> _B_1	42	42	28	42	42	68	66	22	16
<i>Ctenantedon kinziei</i> _A_1	45	43	23	32	37	62	54	16	15
<i>C. kinziei</i> _A_2	42	42	22	34	36	60	66	16	14
<i>C. kinziei</i> _C_1	40	39	27	36	32	48	51	17	17
<i>C. kinziei</i> _C_2	43	45	28	33	41	42	60	15	17
<i>C. kinziei</i> _D_1	51	53	25	32	33	54	58	20	16
<i>C. kinziei</i> _D_2	49	51	23	31	33	57	59	20	18
<i>C. kinziei</i> _D_3	51	51	26	34	31	56	50	20	18
<i>Dorometra briseis</i> _A_1	37	37	22	43	45	53	53	30	23
<i>D. briseis</i> _A_2	35	35	25	43	43	48	52	31	23
<i>D. briseis</i> _B_1	42	42	24	40	42	48	60	28	22
<i>Dorometra</i> c.f. <i>briseis</i> _C_1	30	31	31	48	51	63	67	22	16
<i>D. c.f. briseis</i> _C_2	30	34	32	46	46	57	60	22	16
<i>D. c.f. briseis</i> _C_3	32	33	33	50	49	63	63	21	16
<i>D. c.f. briseis</i> _C_4	35	30	31	49	45	60	60	22	15
<i>Dorometra parvicirra</i> _A_1	40	41	27	42	40	67	63	22	17
<i>D. parvicirra</i> _B_1	42	40	29	45	46	66	66	22	15
<i>D. parvicirra</i> _B_2	41	44	26	44	43	65	66	22	14
<i>D. parvicirra</i> _B_3	42	44	30	44	47	68	65	21	14
<i>D. parvicirra</i> _C_1	38	39	24	42	43	69	66	22	15
<i>Iridometra adrestine</i> _B_1	42	43	33	33	41	65	74	18	13
<i>I. adrestine</i> _C_1	43	44	26	39	42	65	67	23	15
<i>Hathrometra tenella</i> _A_1	53	53	25	30	27	67	67	26	14
<i>H. tenella</i> _A_2	51	52	27	32	31	64	64	25	14
<i>H. tenella</i> _A_3	50	50	28	29	27	62	59	27	14
<i>H. tenella</i> _B_1	47	48	27	23	22	61	63	26	14
<i>H. tenella</i> _D_1	51	50	26	25	27	61	64	24	15
<i>H. tenella</i> _E_1	48	49	26	22	25	67	67	25	16
<i>H. tenella</i> _E_2	49	50	26	21	22	65	67	26	15
<i>Thaumatometra tenuis</i> _B_1	51	54	25	25	30	68	68	22	13
<i>T. tenuis</i> _B_2	52	49	24	25	25	68	67	22	14
<i>T. tenuis</i> _B_3	52	54	24	27	26	72	68	22	14
<i>Tonrometra spinulifera</i> _A_1	56	56	21	19	19	63	61	28	12
<i>T. spinulifera</i> _A_2	57	58	20	19	18	69	68	28	12
<i>T. spinulifera</i> _B_1	55	57	20	24	22	66	61	27	14
<i>T. spinulifera</i> _C_1	56	56	23	22	23	67	67	27	12
<i>T. spinulifera</i> _E_1	53	49	21	22	21	70	64	29	14
<i>T. spinulifera</i> _E_2	53	49	21	22	21	68	64	30	14
<i>T. spinulifera</i> _E_3	52	55	20	21	19	66	63	29	14

Table A9 cont'd: Table of inter-landmark measurement ratios (see Table A2 for standardized measurements)

mf = muscle fossae; al = aboral ligament fossae; il = interarticular ligament fossae; CC = central canal

H % = height to radial height %, W% = width to radial width %; R = right; L = left

Specimen	R mf H %	L mf H %	al H %	R il H %	L il H %	R il W %	L il W %	CC W %	CC H %
<i>Trichometra cubensis</i> _E_1	48	45	27	35	33	68	70	20	15
<i>T. cubensis</i> _E_2	46	48	29	30	33	68	64	21	15
<i>T. cubensis</i> _E_3	47	43	28	31	33	64	59	20	15
<i>Anthometrina adriani</i> _A_1	46	47	31	39	41	72	74	20	11
<i>A. adriani</i> _A_2	46	47	32	38	40	76	75	19	10
<i>A. adriani</i> _A_3	43	45	30	40	39	72	74	20	12
<i>A. adriani</i> _B_1	46	47	28	36	37	72	71	20	12
<i>A. adriani</i> _B_2	45	44	29	33	35	71	73	20	12
<i>A. adriani</i> _C_1	50	51	29	38	41	72	71	20	12
<i>A. adriani</i> _C_2	52	48	30	32	35	72	72	19	12
<i>A. adriani</i> _D_1	52	50	26	34	36	74	75	19	11
<i>A. adriani</i> _E_1	49	47	28	36	37	76	77	21	12
<i>A. adriani</i> _E_2	47	47	29	38	38	73	75	21	12
<i>A. adriani</i> _E_3	47	47	30	36	39	74	77	20	12
<i>Comatonia cristata</i> _B_1	42	43	28	26	26	73	69	15	12
<i>C. cristata</i> _B_2	44	46	28	26	25	66	62	18	11
<i>C. cristata</i> _B_3	46	47	29	22	28	62	76	17	11
<i>C. cristata</i> _C_1	46	43	24	34	33	57	54	28	14
<i>C. cristata</i> _C_2	46	47	25	35	33	60	60	28	16
<i>Florometra asperrima</i> _A_1	48	45	23	35	29	64	59	18	9
<i>F. asperrima</i> _A_2	46	48	23	34	35	63	66	19	9
<i>F. asperrima</i> _A_3	44	47	24	30	35	68	66	18	9
<i>F. asperrima</i> _B_1	49	50	23	33	35	69	68	16	9
<i>F. asperrima</i> _B_2	53	51	23	34	35	70	69	17	8
<i>F. asperrima</i> _C_1	49	45	25	28	31	70	66	17	8
<i>F. asperrima</i> _C_2	49	49	24	28	32	68	64	17	9
<i>F. asperrima</i> _D_1	35	35	26	41	40	57	59	20	10
<i>F. asperrima</i> _D_2	35	36	26	42	44	62	59	21	10
<i>F. asperrima</i> _E_1	39	46	23	33	34	67	62	18	9
<i>F. asperrima</i> _E_2	43	43	22	32	32	70	70	19	9
<i>F. asperrima</i> _E_3	44	43	22	32	32	68	63	18	8
<i>Florometra serratissima</i> _B_1	54	54	23	31	33	66	66	17	10
<i>F. serratissima</i> _B_2	51	56	22	30	32	69	70	17	10
<i>Promachocrinus kerguelensis</i> _A_1	45	46	27	32	32	75	70	24	13
<i>P. kerguelensis</i> _A_2	49	48	27	31	34	70	73	24	13
<i>Isometra graminea</i> _A_1	44	42	31	36	31	70	74	22	13
<i>I. graminea</i> _A_2	45	41	31	30	29	67	73	22	12
<i>I. graminea</i> _C_1	40	42	32	29	33	69	72	23	13
<i>Isometra vivipara</i> _A_1	46	46	31	28	28	64	64	20	13
<i>Erythrometra rubra</i> _A_1	32	31	41	39	35	70	64	22	15
<i>E. rubra</i> _B_1	35	36	36	46	44	61	54	25	19
<i>Hypalometra defecta</i> _A_1	38	36	33	29	25	55	61	27	22
<i>H. defecta</i> _B_1	43	39	42	37	34	61	54	24	19
<i>H. defecta</i> _B_2	42	38	44	42	38	60	58	24	18
<i>H. defecta</i> _D_1	42	45	32	21	22	72	75	23	18
<i>H. defecta</i> _F_1	44	43	31	31	32	70	61	24	18
<i>H. defecta</i> _G_1	42	45	32	27	30	61	66	23	19
<i>H. defecta</i> _G_2	41	44	32	31	31	59	64	25	18
<i>Perometra diomedea</i> _A_1	34	34	26	37	35	73	74	20	13
<i>P. diomedea</i> _A_2	37	33	27	34	32	70	67	19	13
<i>P. diomedea</i> _B_1	36	33	30	37	33	71	63	19	15
<i>P. diomedea</i> _B_2	35	35	35	35	35	79	74	18	14

Table A9 cont'd: Table of inter-landmark measurement ratios (see Table A2 for standardized measurements)

mf = muscle fossae; al = aboral ligament fossae; il = interarticular ligament fossae; CC = central canal

H % = height to radial height %, W% = width to radial width %; R = right; L = left

Specimen	R mf H %	L mf H %	al H %	R il H %	L il H %	R il W %	L il W %	CC W %	CC H %
<i>Coccometra hagenii</i> _A_1	47	45	27	31	34	57	64	22	12
<i>C. hagenii</i> _C_1	47	45	24	33	33	70	63	23	14
<i>C. hagenii</i> _C_2	48	47	25	34	33	64	62	23	11
<i>C. hagenii</i> _C_3	45	48	25	32	32	53	59	24	12
<i>C. hagenii</i> _D_1	47	45	24	31	32	57	57	20	14
<i>C. hagenii</i> _D_2	43	43	27	32	29	55	57	19	13
<i>C. hagenii</i> _D_3	43.75	42	28	30	32	58	56	18	12.5
<i>C. hagenii</i> _D_4	47	46	26	30	31	54	59	19	13
<i>C. hagenii</i> _D_5	36	42	29	33	32	51	54	19	13
<i>C. hagenii</i> _F_1	44	46	32	35	36	55	65	19	14
<i>C. hagenii</i> _F_2	42	41	29	33	35	51	55	19	12
<i>C. hagenii</i> _F_3	37	40	30	37	32	59	48	19	15
<i>C. hagenii</i> _F_4	42	43	29	33	31	51	54	20	14
<i>C. hagenii</i> _F_5	41	43	31	35	34	57	63	18	13
<i>Thysanometra tenelloides</i> _B_1	48	42	23	30	29	64	64	18	14
<i>T. tenelloides</i> _C_1	52	47	24	30	31	58	59	14	14
<i>T. tenelloides</i> _C_2	42	44	25	32	33	56	59	15	14
<i>T. tenelloides</i> _C_3	45	42	25	32	35	56	61	15	14
<i>T. tenelloides</i> _D_1	42	40	27	30	32	62	65	17	15
<i>T. tenelloides</i> _D_2	45	42	26	30	31	68	65	16	16
<i>T. tenelloides</i> _D_3	44	44	27	29	37	64	65	16	15
<i>T. tenelloides</i> _D_4	43	42	27	32	29	66	68	16	16
<i>T. tenelloides</i> _E_1	43	46	24	31	32	67	63	17	15
<i>T. tenelloides</i> _G_1	46	46	27	39	37	74	67	20	13
<i>T. tenelloides</i> _G_2	45	41	26.5	33	35	73	73	20	11.5
<i>Balanometra balanoides</i> _A_1	36	36	32	30	29	64	67	26	14
<i>Hybometra senta</i> _A_1	40	40	29	36	36	68	69	21	13
<i>H. senta</i> _A_2	38	40	29	33	33	67	71	20	15
<i>H. senta</i> _C_1	38.75	41	33	33	37	71	72	21	13
<i>H. senta</i> _C_2	44	44	32	41	38	68	72	22	12
<i>H. senta</i> _D_1	46	46	28	34	35	68	71	21	14
<i>H. senta</i> _D_2	48	44	28	35	35	63	66	21	13
<i>H. senta</i> _E_1	41	42	30	31	36	68	70	21	14
<i>Poliometra prolixa</i> _A_1	53	53	28	19	21	74	70	18	11
<i>P. prolixa</i> _A_2	55	55	24	18	17	65	69	18	11
<i>P. prolixa</i> _B_1	50	48	23	14	16	72	73	18	12
<i>Psathyrometra</i> sp_B_1	52	49	24	25	23	65	59	24	12
<i>Psathyrometra</i> sp_C_1	51	54	23	28	28	68	70	20	11
<i>Psathyrometra</i> sp_C_2	49	54	22	27	29	58	74	23	11
<i>Psathyrometra</i> sp_D_1	46	45	23	23	25	75	70	21	12
<i>Psathyrometra</i> sp_D_2	48	45	22	26	23	67	68	22	12
<i>Psathyrometra</i> sp_E_1	53	53	24	25	26	72	72	20	12
<i>Psathyrometra</i> sp_E_2	52	52	25	26	24	69	69	20	12
<i>Aporometra occidentalis</i> _A_1	46	30	41	30	33	60	55	14	18
<i>A. occidentalis</i> _B_1	42	44	38	29	33	61	56	15	16
<i>A. occidentalis</i> _B_2	43	47	39	36	34	59	57	15	16
<i>A. occidentalis</i> _B_3	45	51	41	31	31	61	60	15	17
<i>A. occidentalis</i> _C_1	49	47	34	28	30	56	63	12	17
<i>A. occidentalis</i> _C_2	45	49	38	28	32	55	54	13	17

Table A9 cont'd: Table of inter-landmark measurement ratios (see Table A2 for standardized measurements)

mf = muscle fossae; al = aboral ligament fossae; il = interarticular ligament fossae; CC = central canal

H % = height to radial height %, W% = width to radial width %; R = right; L = left

Specimen	R mf H %	L mf H %	al H %	R il H %	L il H %	R il W %	L il W %	CC W %	CC H %
<i>Notocrinus virilis_A_1</i>	35	34	39	17	22	67	60	13	12
<i>N. virilis_A_2</i>	38	36	37	21	23	70	62	14	12
<i>N. virilis_A_3</i>	37	38	37	20	22	69	66	15	12.5
<i>N. virilis_B_1</i>	38	36	34	22	17	63	66	12	14
<i>N. virilis_C_1</i>	43	41	37	33	32	66	61	15	11
<i>N. virilis_C_2</i>	44	42	35	32	33	66	66	16	11
<i>N. virilis_C_3</i>	43	42	34	31	30	67	68	14	12
<i>Tropiometra carinata_A_1</i>	0.51	0.51	37	30	32	83	80	13	13
<i>T. carinata_A_2</i>	0.49	0.46	36	34	35	80	83	13	14
<i>T. carinata_D_1</i>	0.34	0.38	40	35	40	69	76	17	16
<i>T. carinata_D_2</i>	0.44	0.34	39	44	38	72	77	16	17
<i>T. carinata_D_3</i>	0.42	0.34	38	36	32	76	77	15	17
<i>T. carinata_E_1</i>	0.41	0.35	37	42	39	76	76	17	14

## UPGMA Hierarchical clustering phenogram (Procrustes distances, scenario 1)

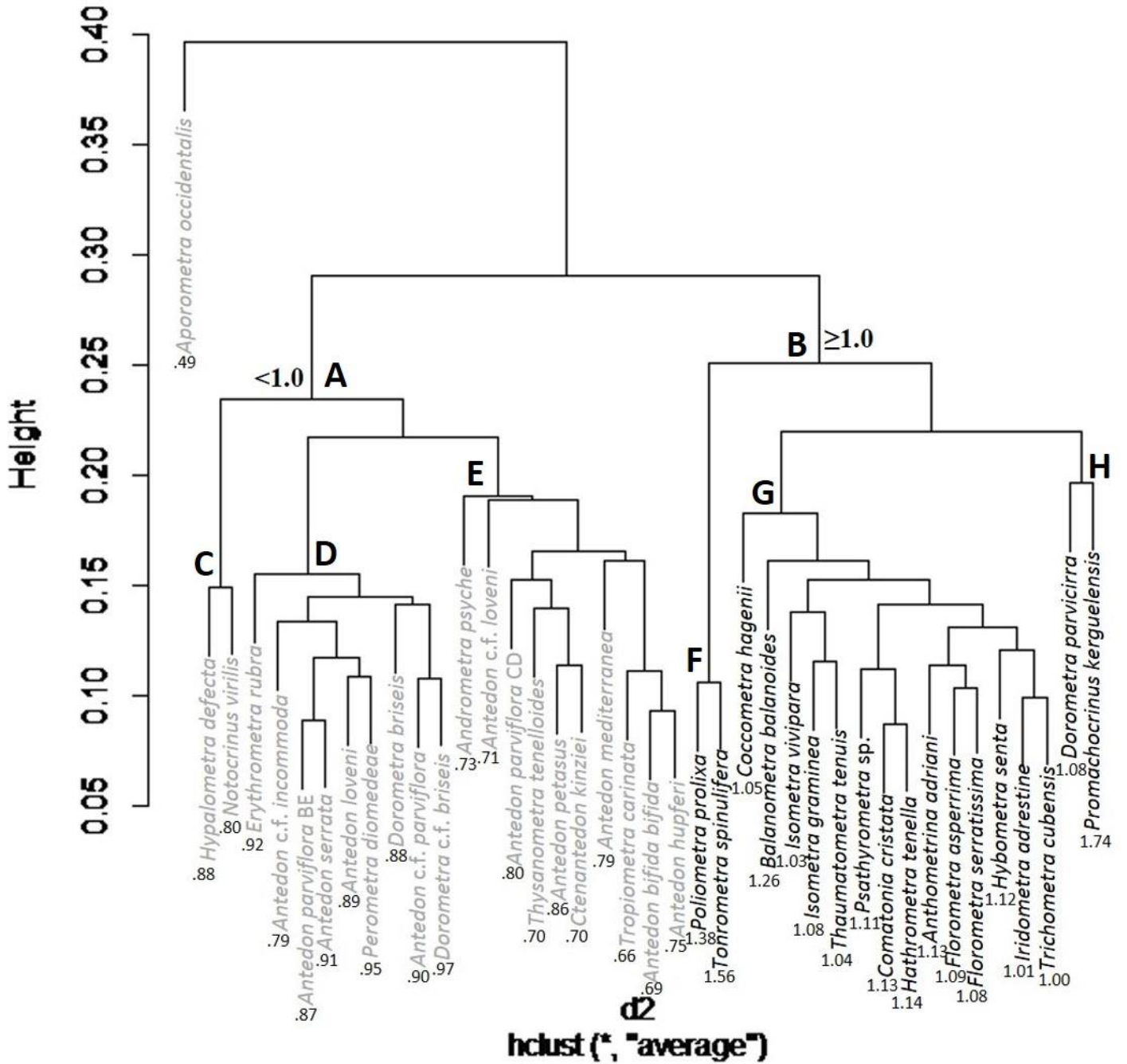


Fig. A43: Scenario 1 UPGMA Hierarchical clustering model based on Procrustes distances; colored by broad radial ratio (<math>< 1.0</math> = gray, <math>\geq 1.0</math> = black) with specific ratios at species terminals (see Fig. 40 for scenario 2 results).



B. Appendix B

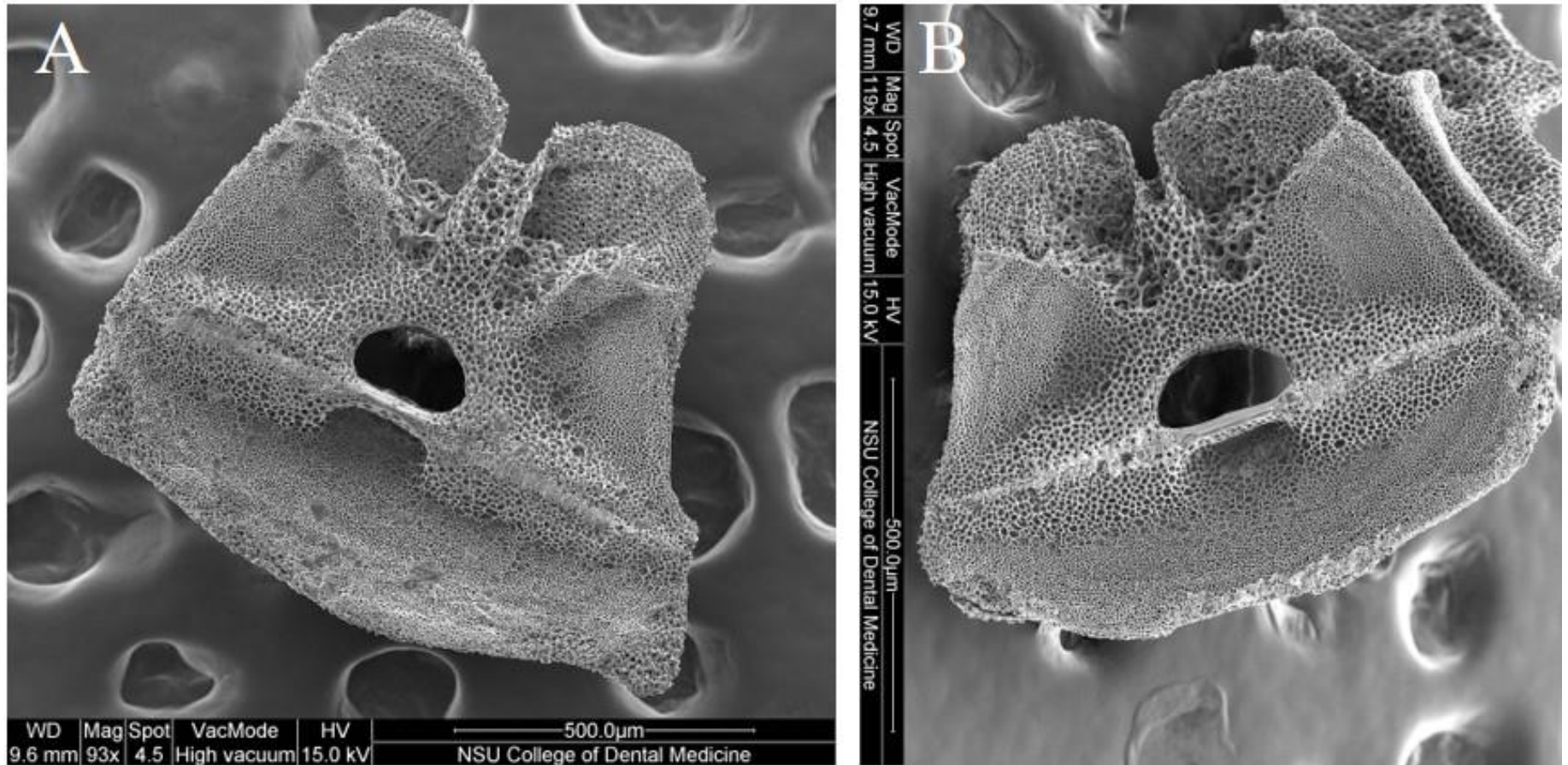


Fig. B1: SEM images of *Antedon* c.f. *incommoda*. A: specimen A; B: specimen B.

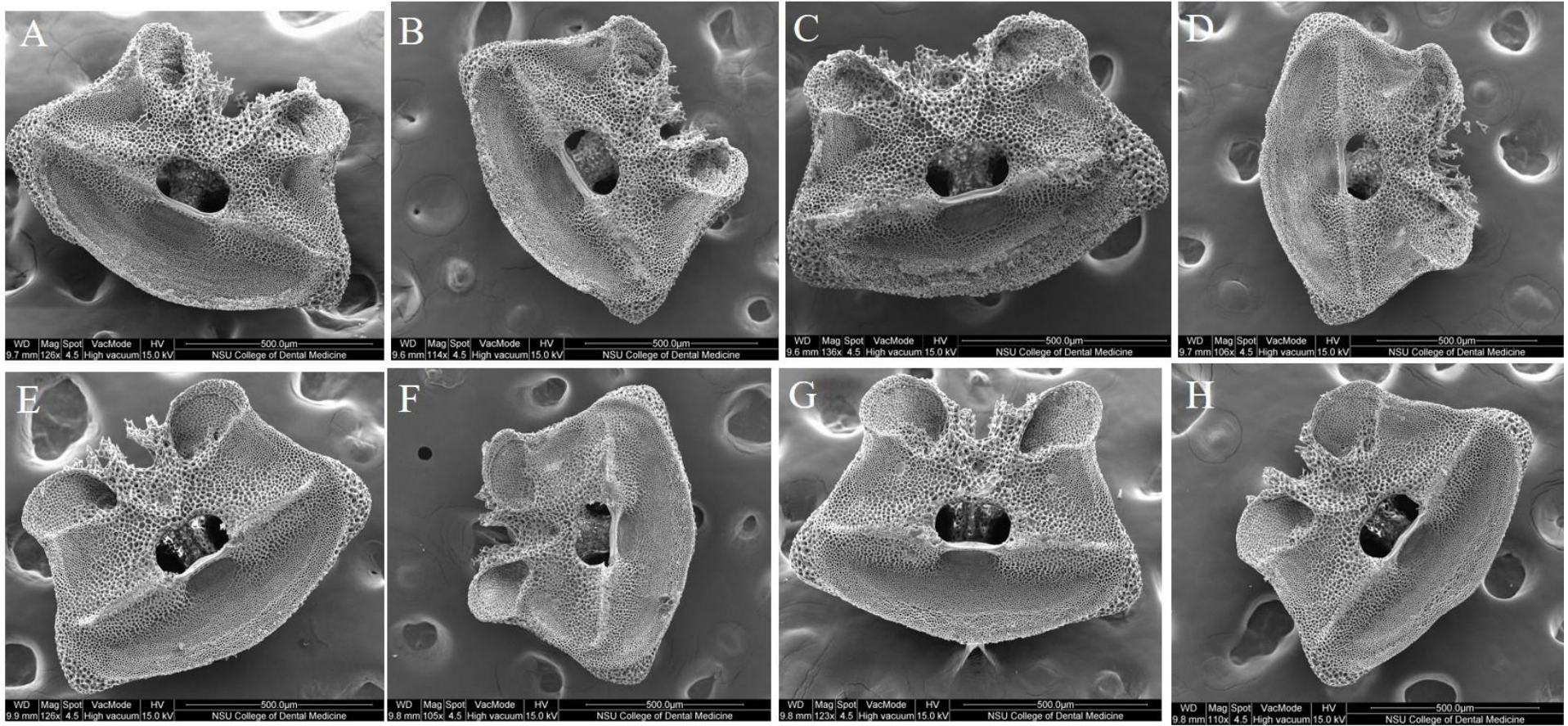


Fig. B2: SEM images of *Antedon c.f. loveni*. A-D: specimen F; E-H: specimen G

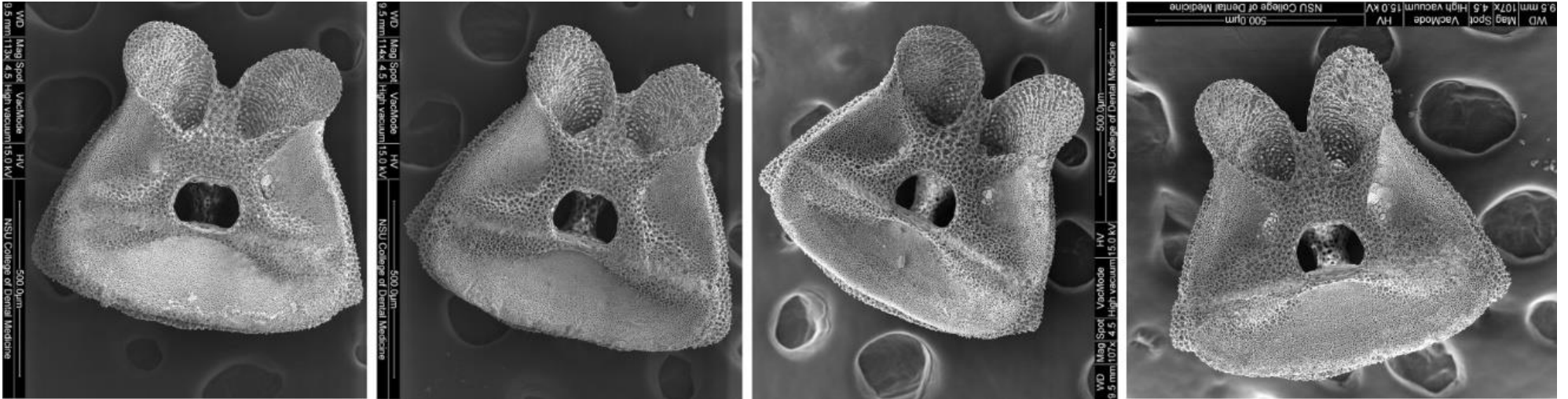


Fig. B3: SEM images of *Antedon c.f. parviflora*, specimen F.

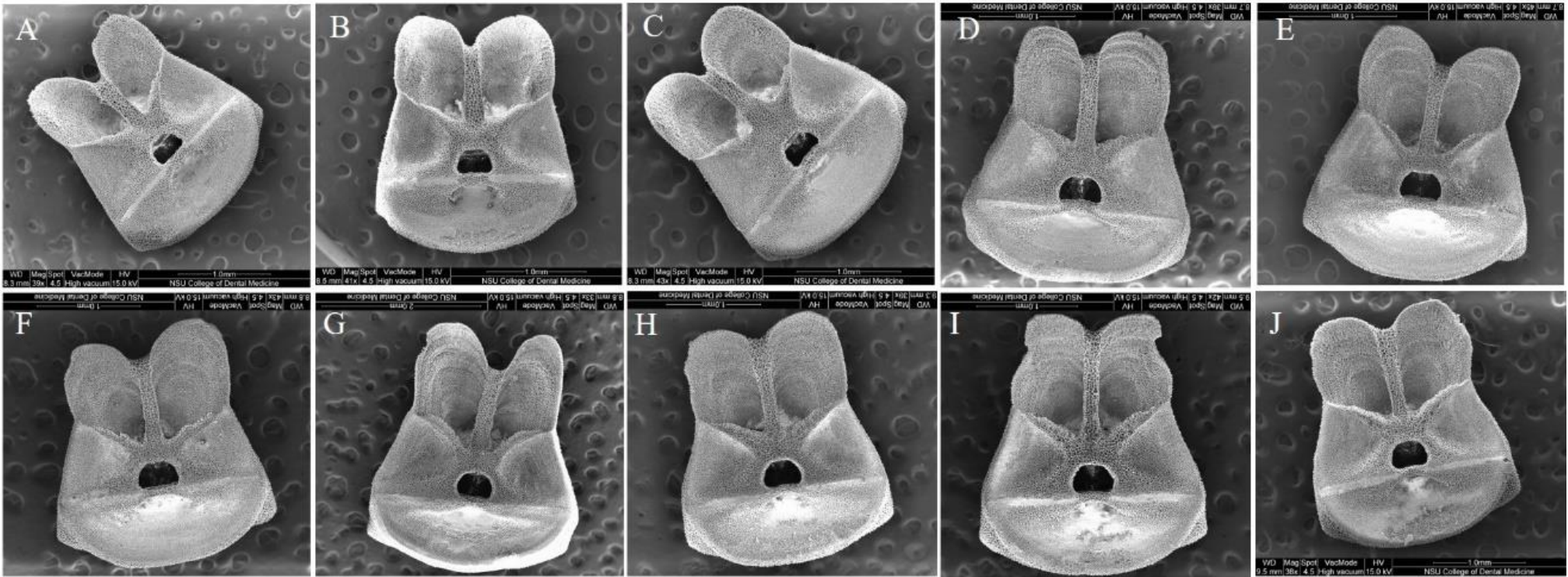


Fig. B4: SEM images of *Anthometrina adriani*. A-C: specimen A; D: specimen B; E-F: specimen C; G: specimen D; H-J: specimen E

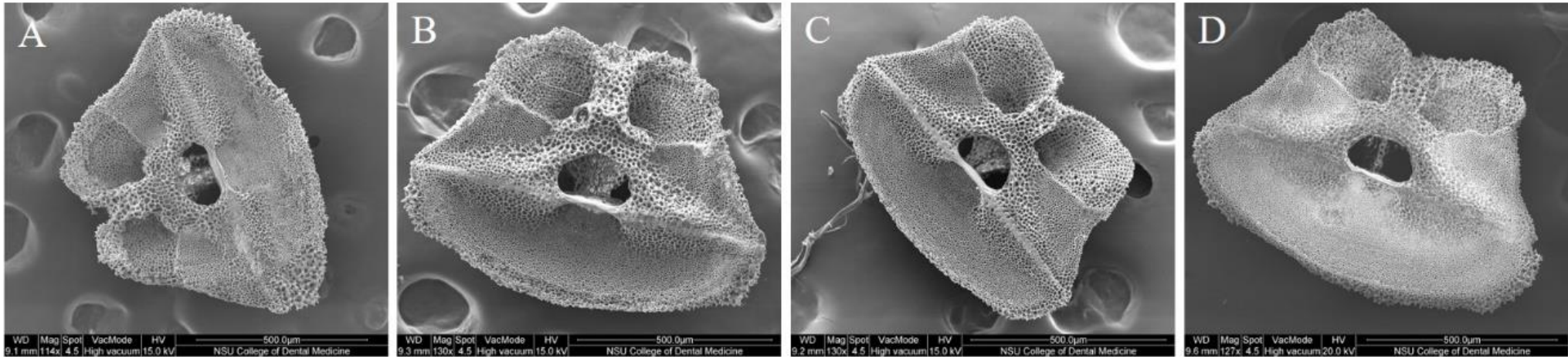


Fig. B5: SEM images of *Andrometra psyche*. A-B: specimen A; C: specimen B; D: specimen C

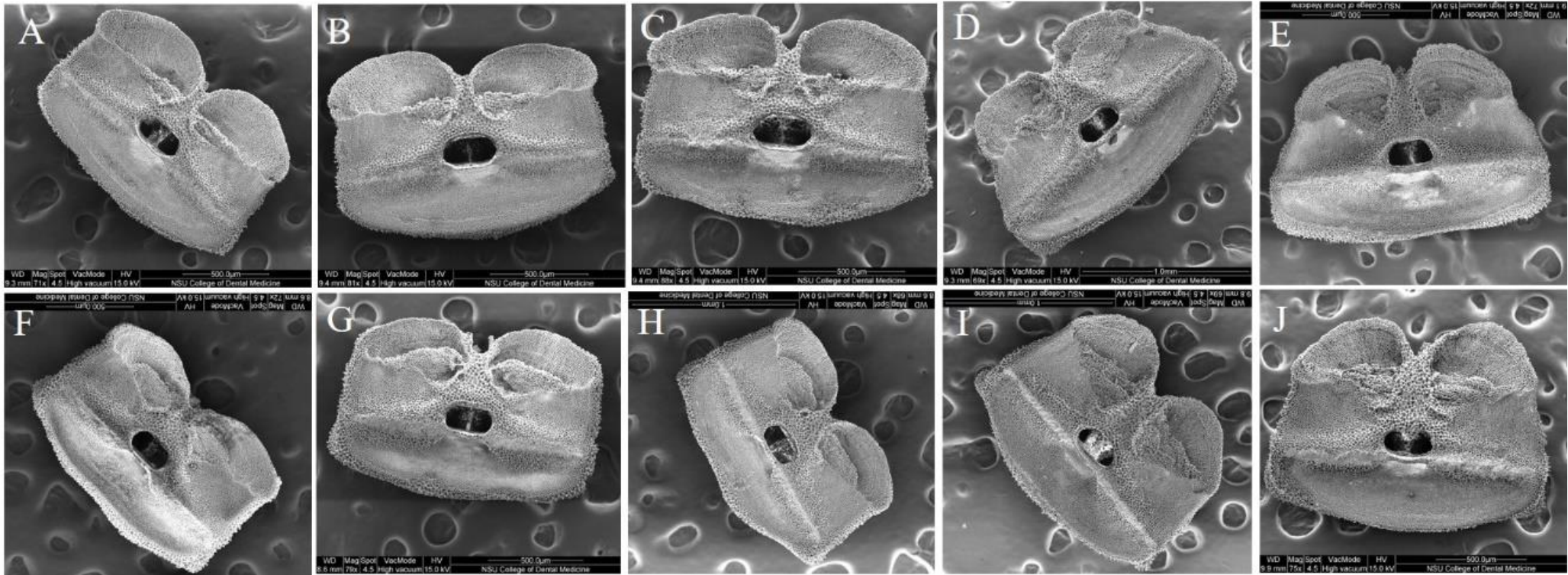


Fig. B6: SEM images of *Antedon bifida bifida*. A-C: specimen A; D-E: specimen C; F-H: specimen D; I-J: specimen E.

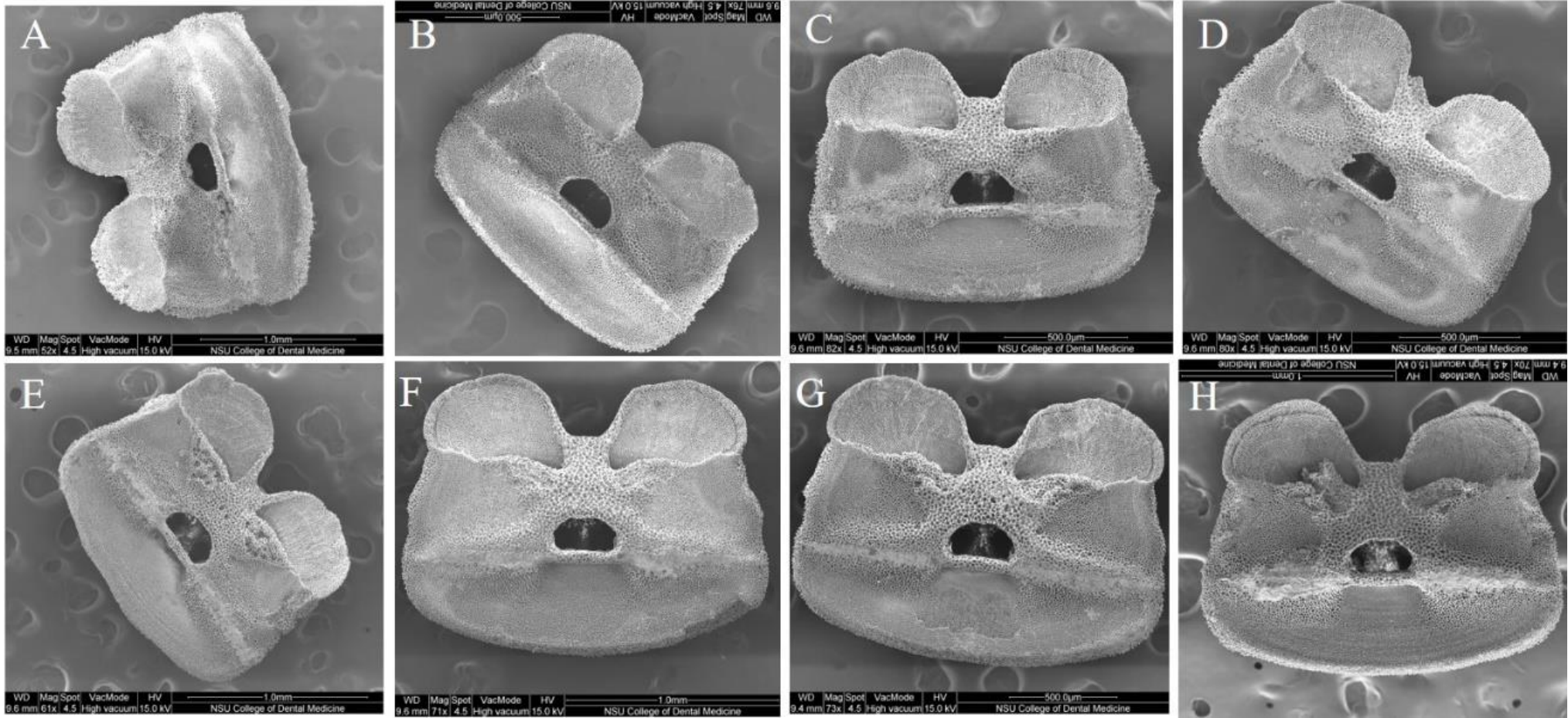


Fig. B7: SEM images of *Antedon hupferi*. A: specimen A; B-D: specimen B; E: specimen C; F-H: specimen D.

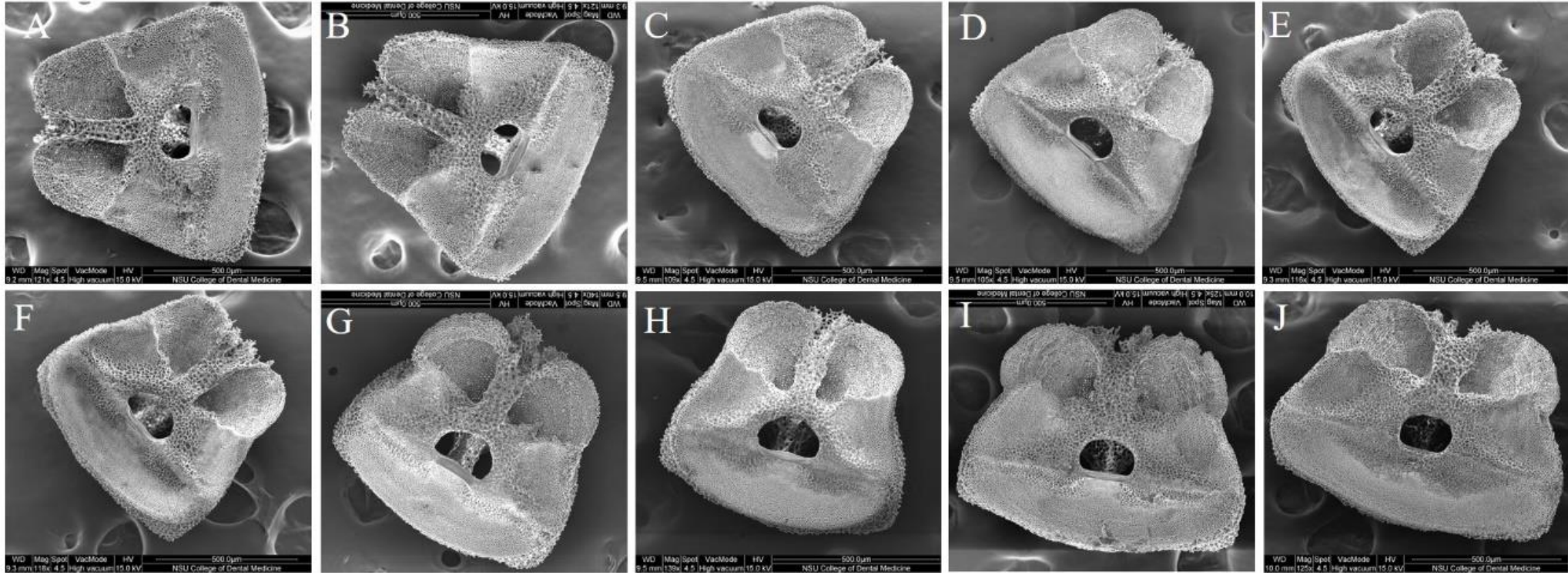


Fig. B8: SEM images of *Antedon loveni*. A-B: specimen A; C-D: specimen B; E-F: specimen C; G-H: specimen D; I-J: specimen E



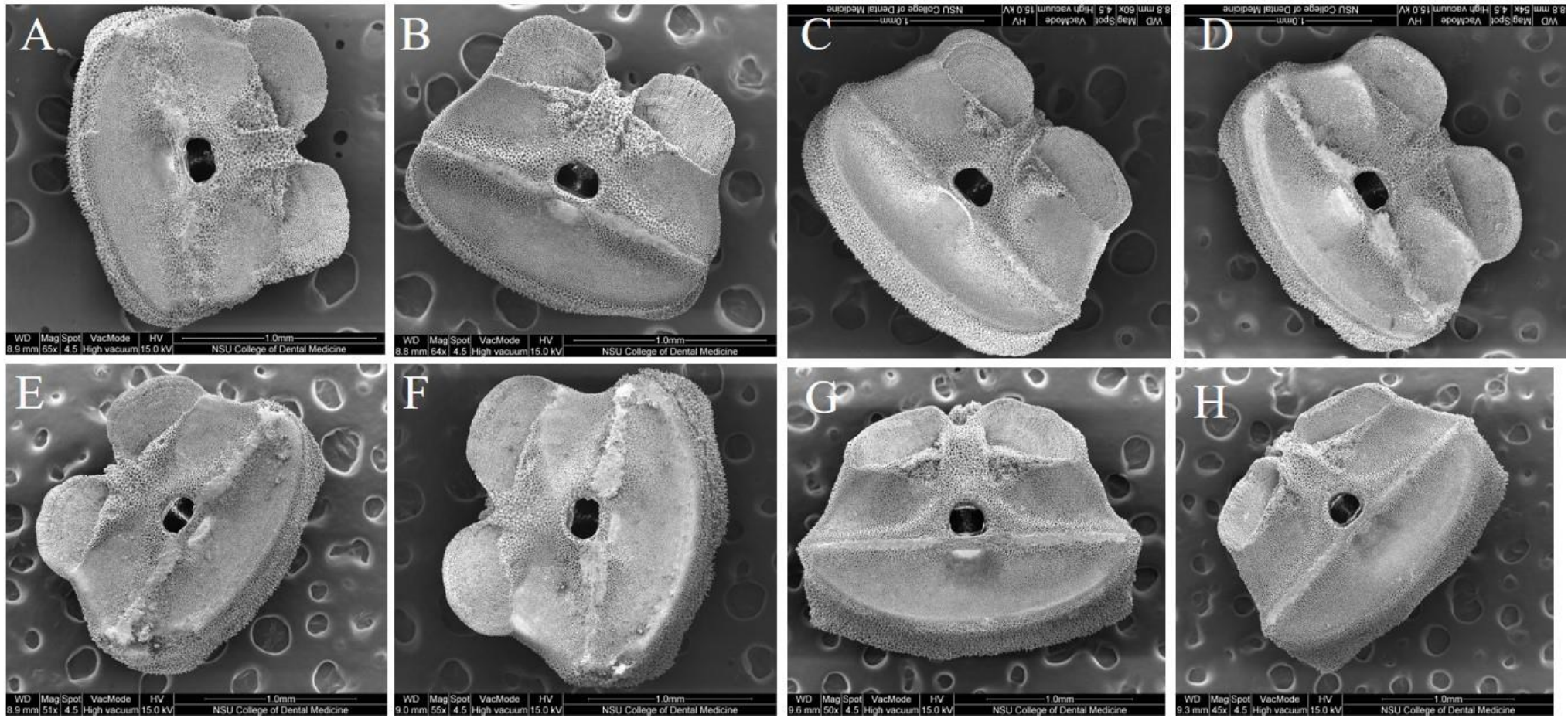


Fig. B9: SEM images of *Antedon mediterranea*. A-B: specimen A; C: specimen C; D-F: specimen D; G-H: specimen E

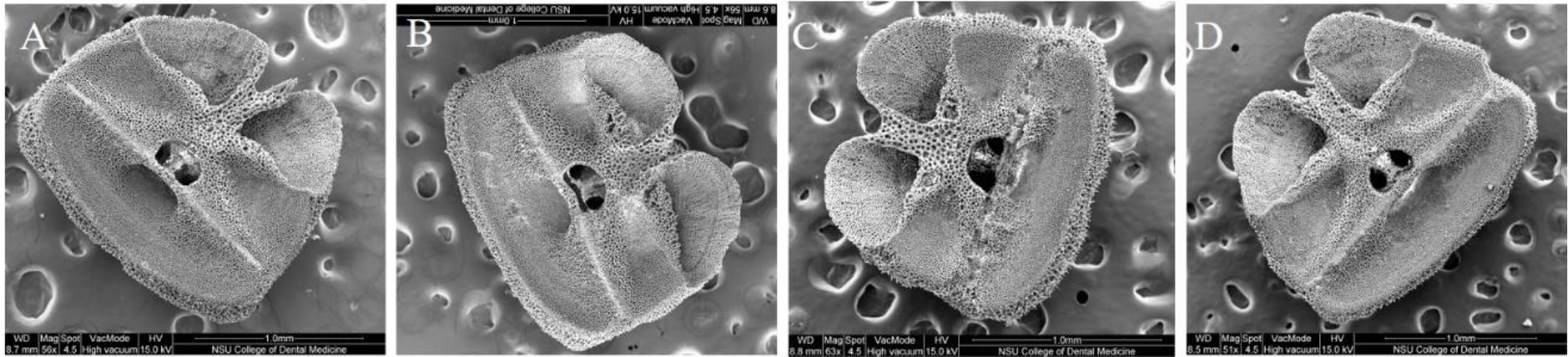


Fig. B10: SEM images of *Antedon petasus*. A-B: specimen A; C: specimen C; D: specimen D.

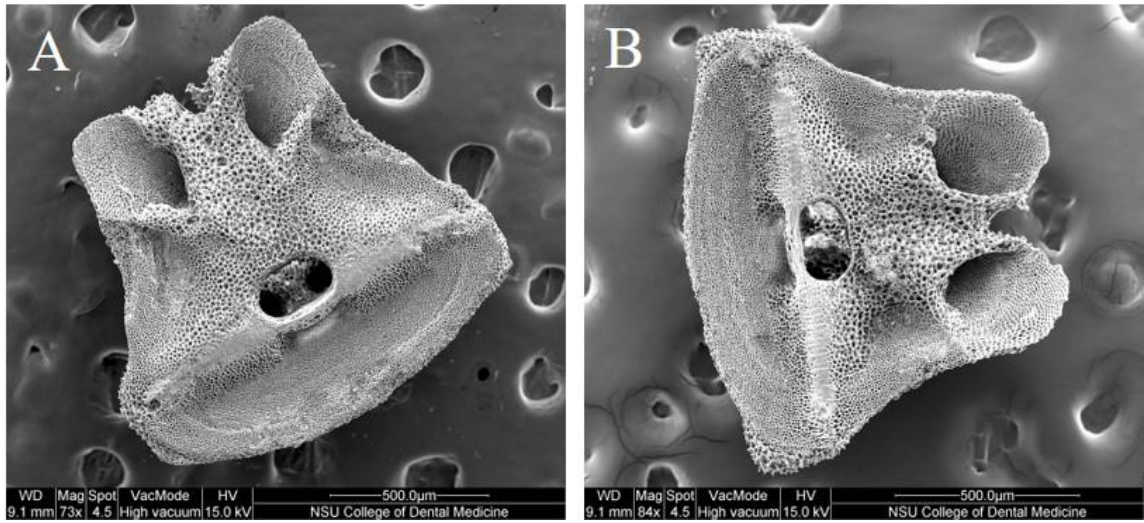


Fig. B11: SEM images of *Antedon parviflora* B & E. A: specimen B; B: specimen E.

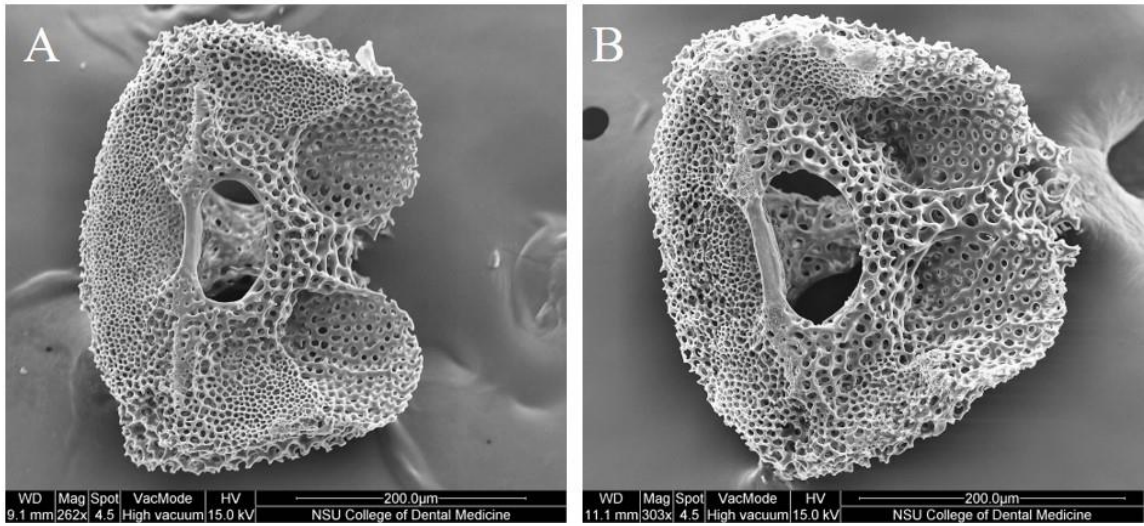


Fig. B12: SEM images of *Antedon parviflora* C & D. A: specimen C; B: specimen D.

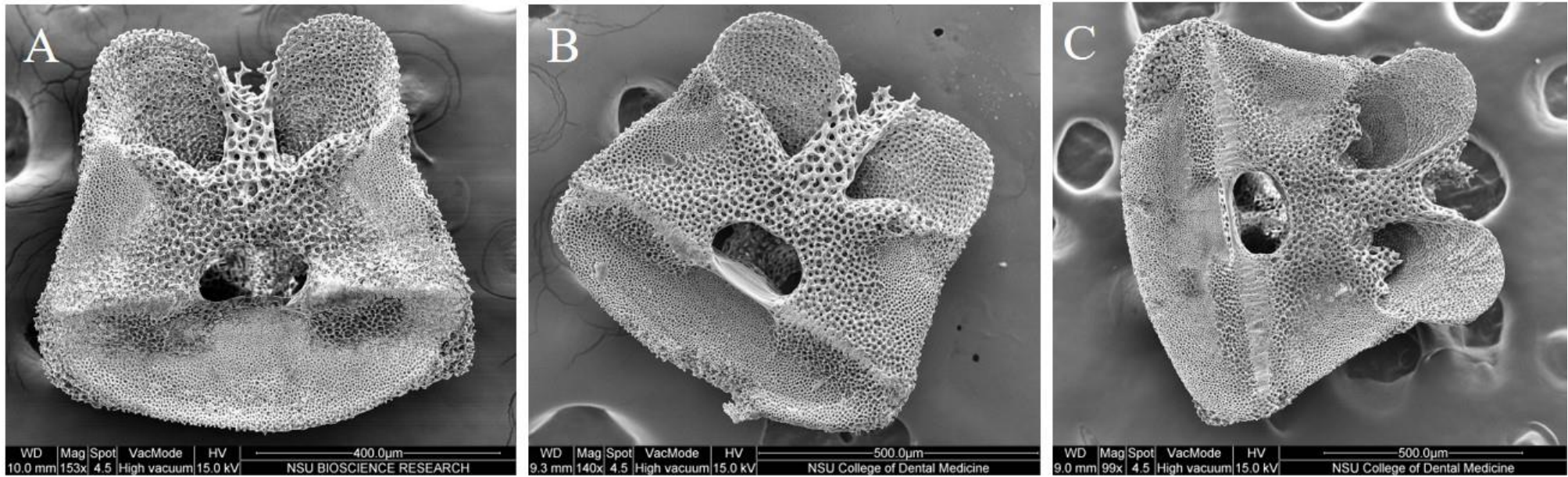


Fig. B13: SEM images of *Antedon serrata*. A-B: specimen A; C: specimen B.

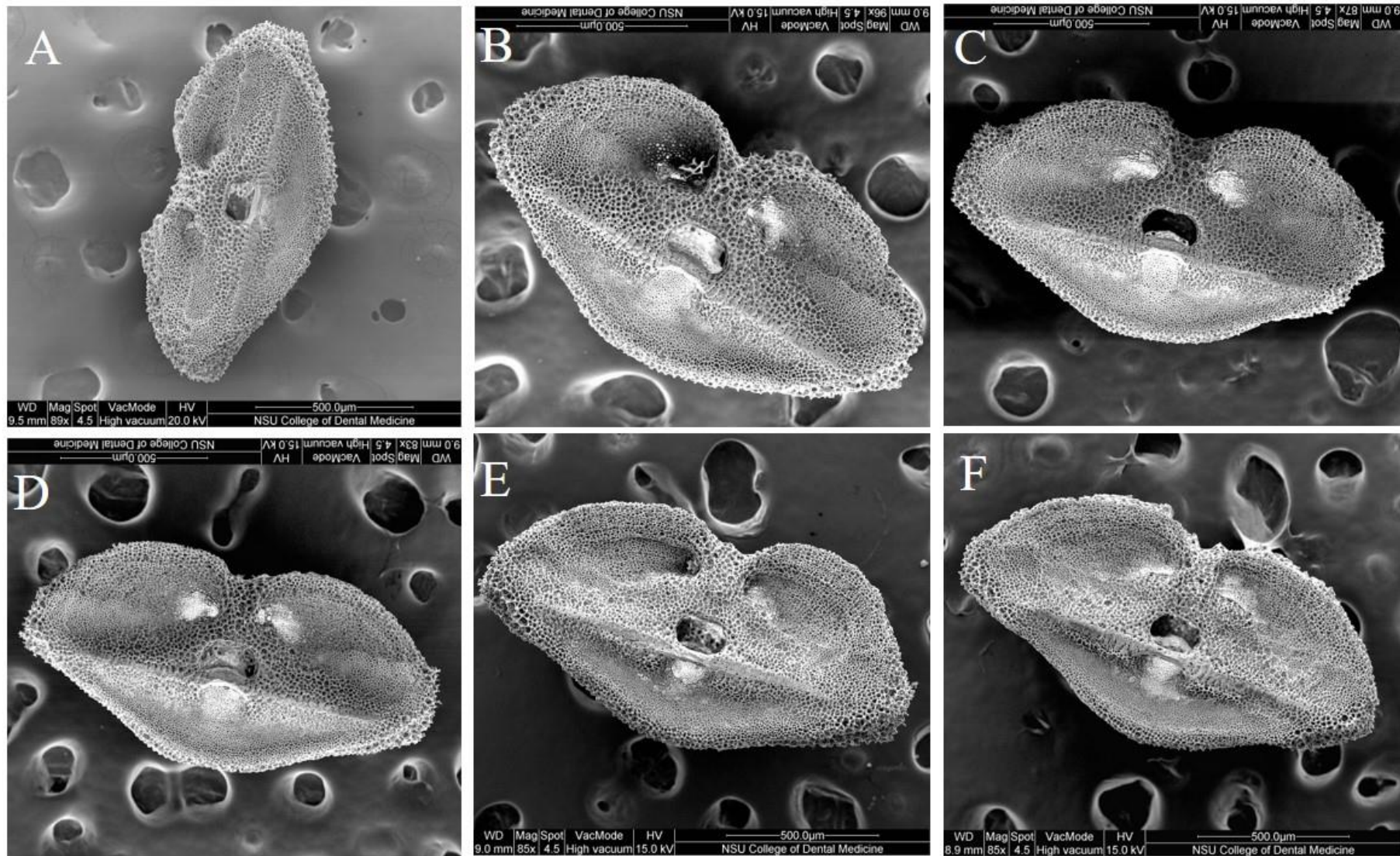


Fig. B14: SEM images of *Aporometra occidentalis*. A: specimen A; B-D: specimen B; E-F: specimen C.

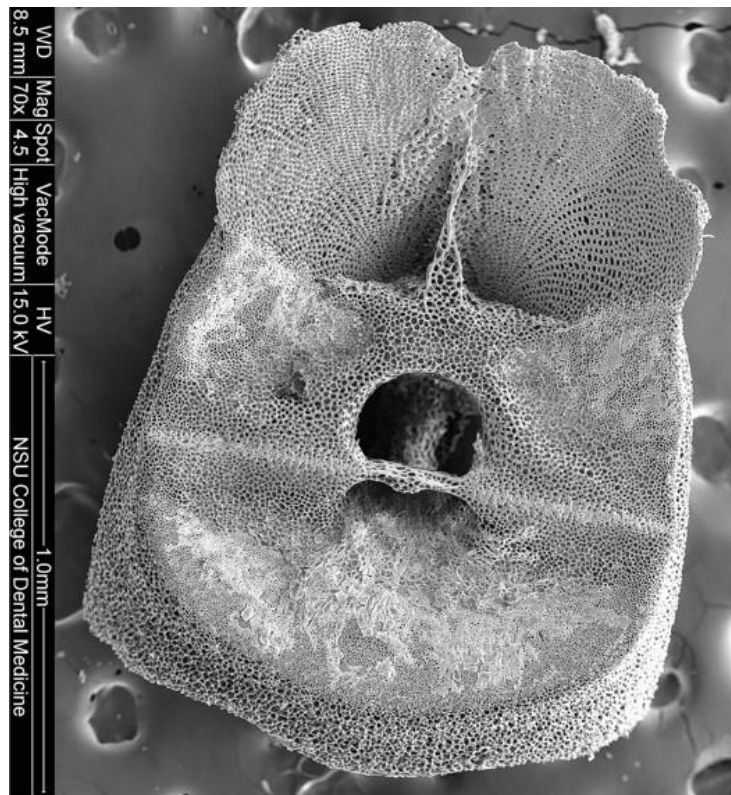


Fig. B15: SEM image of *Balanometra balanoides* (only one ossicle was successfully imaged in this study).

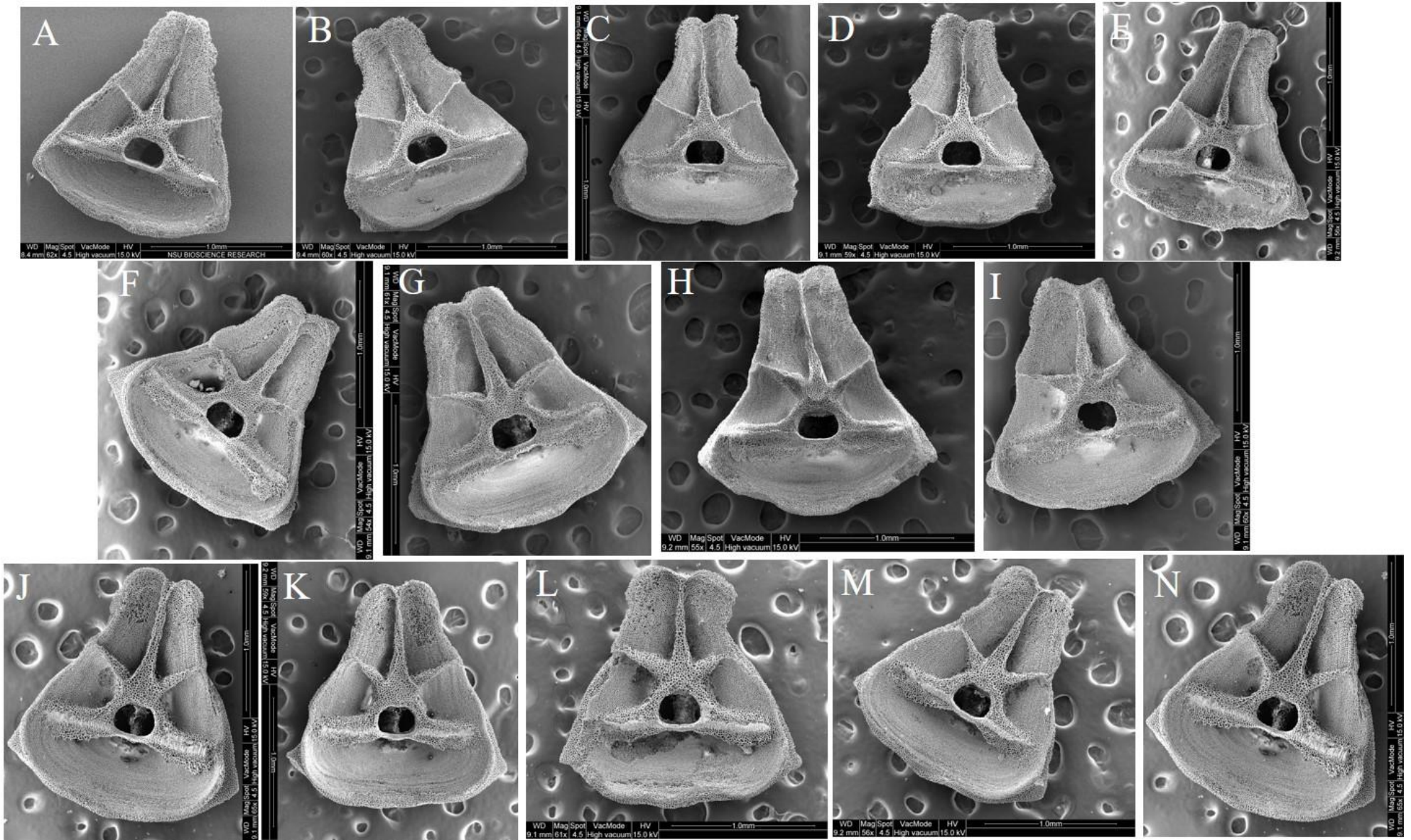


Fig. B16: SEM images of *Coccometra hagenii*. A: specimen A; B-D: specimen C; E-I: specimen D; J-N: specimen F.

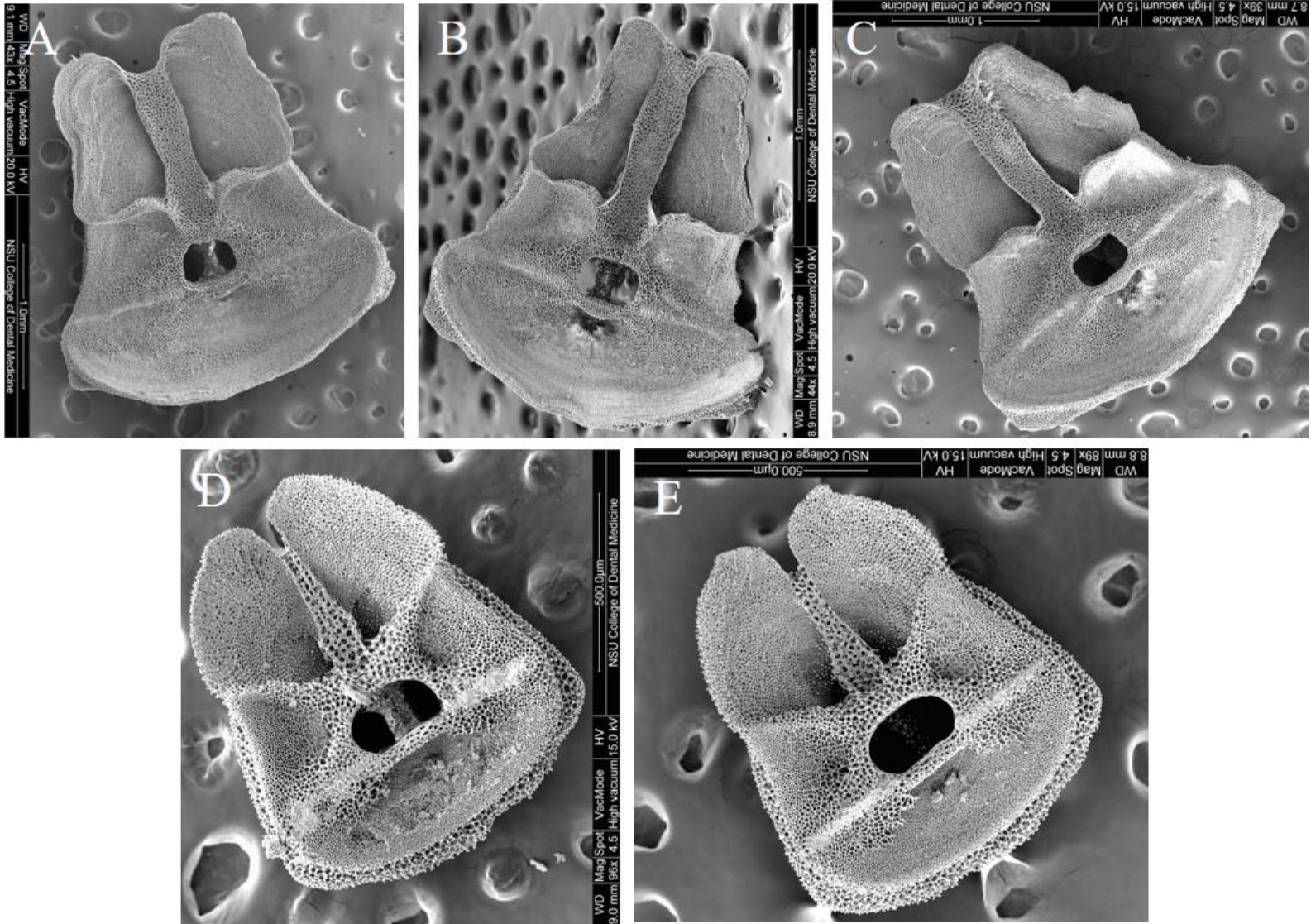


Fig. B17: SEM images of *Comatonia cristata*. A-C: specimen B; D-E: specimen C.



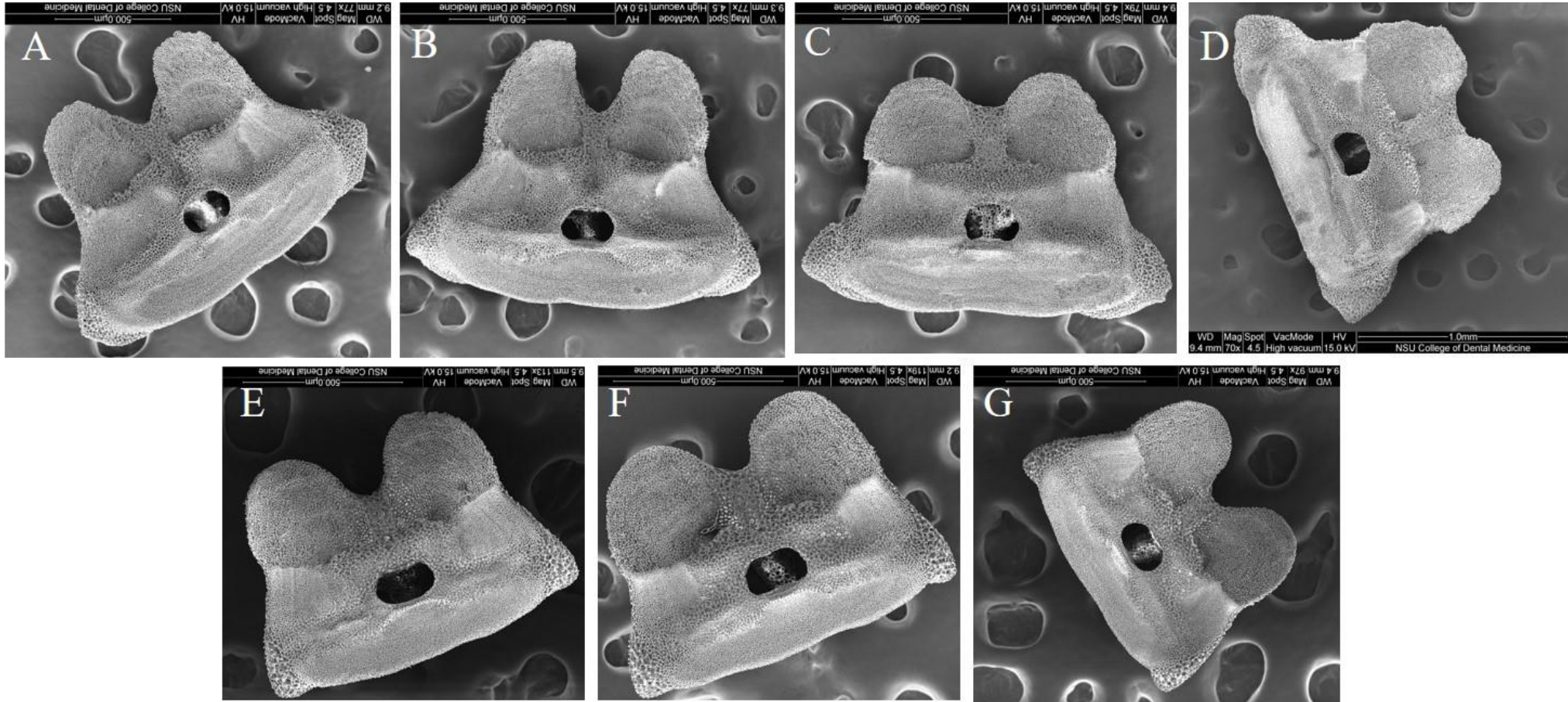


Fig. B18: SEM images of *Ctenantedon kinziei*. A-B: specimen A; C-D: specimen C; E-G: specimen D.

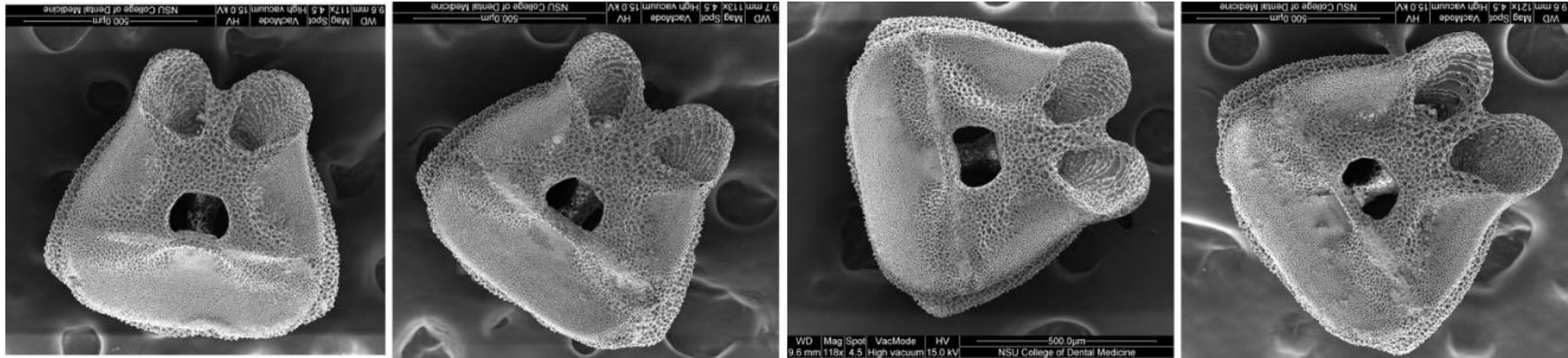


Fig. B19: SEM images of *Dorometra c.f. briseis*, specimen C.

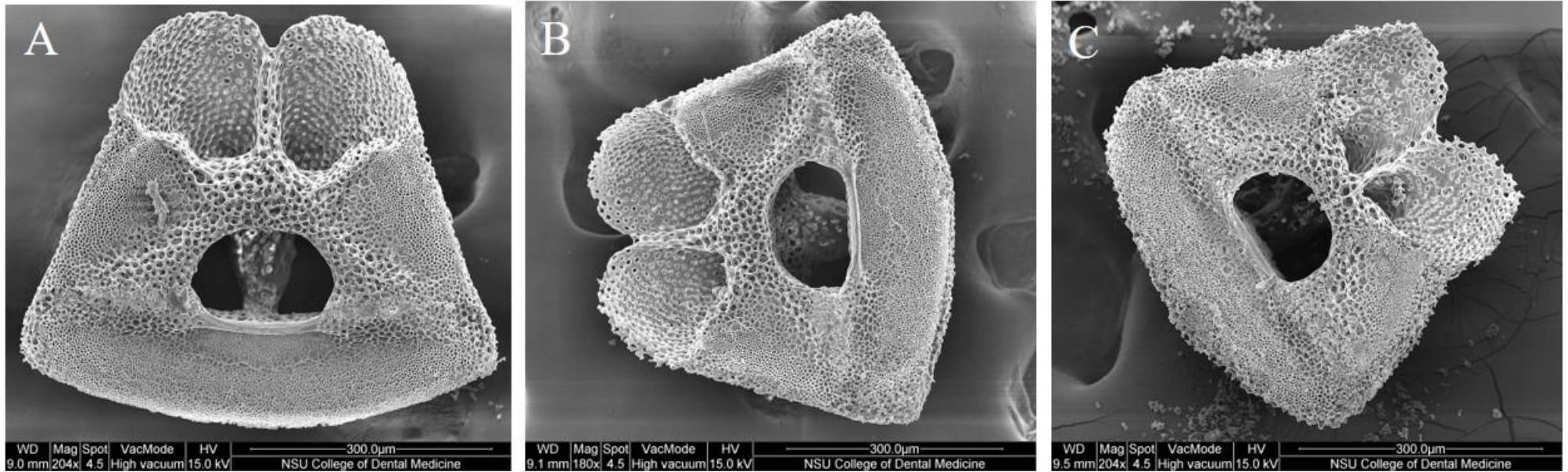


Fig. B20: SEM images of *Dorometra briseis*. A-B: specimen A; C: specimen B.

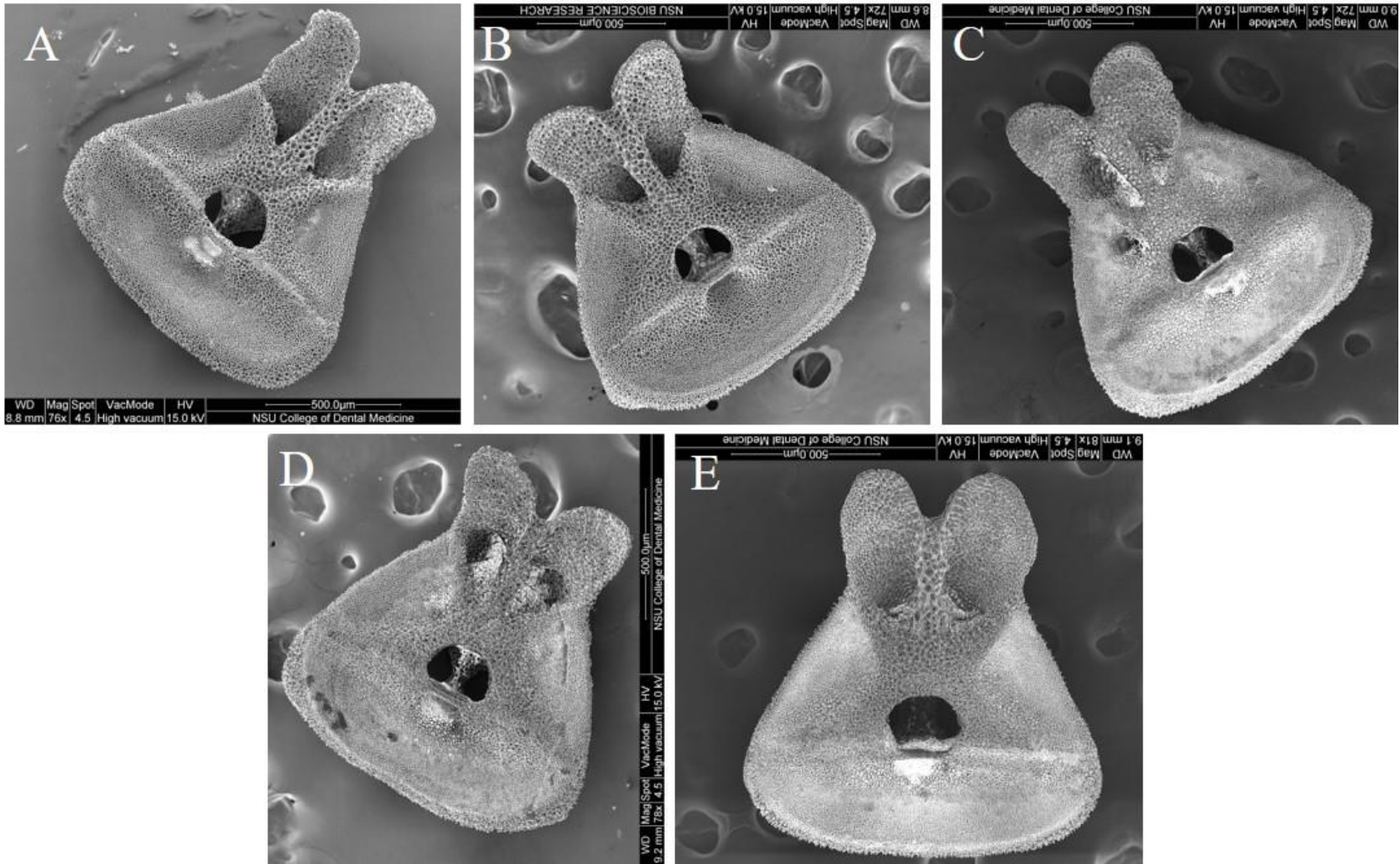


Fig. B21: SEM images of *Dorometra parvicirra*. A: specimen A; B-D: specimen B; E: specimen C.

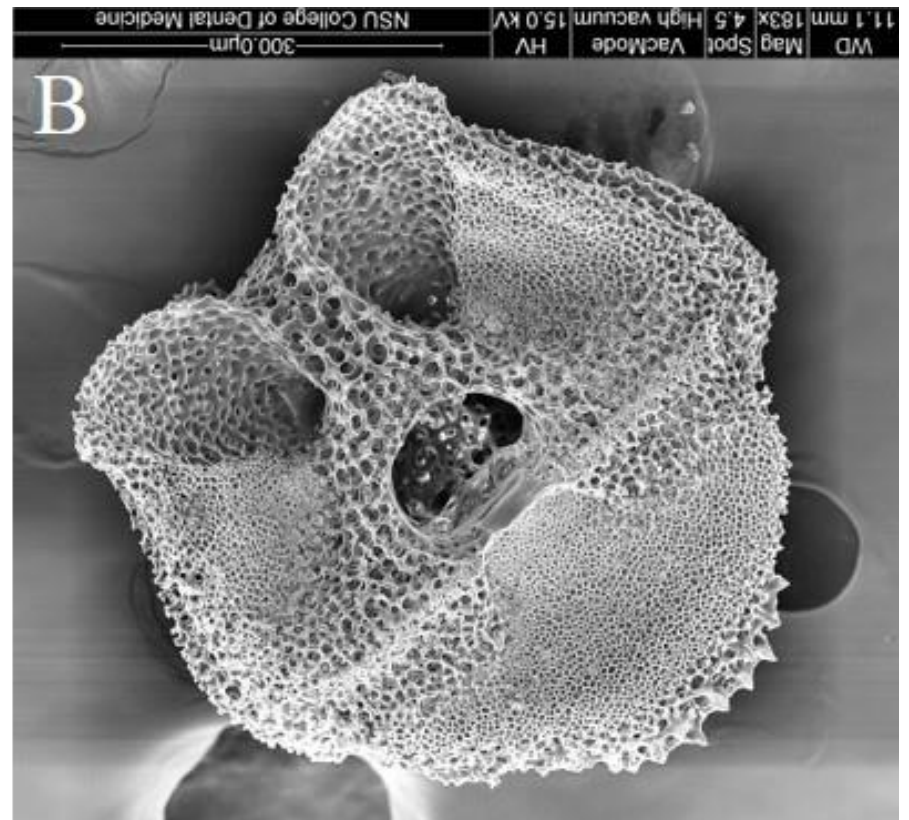
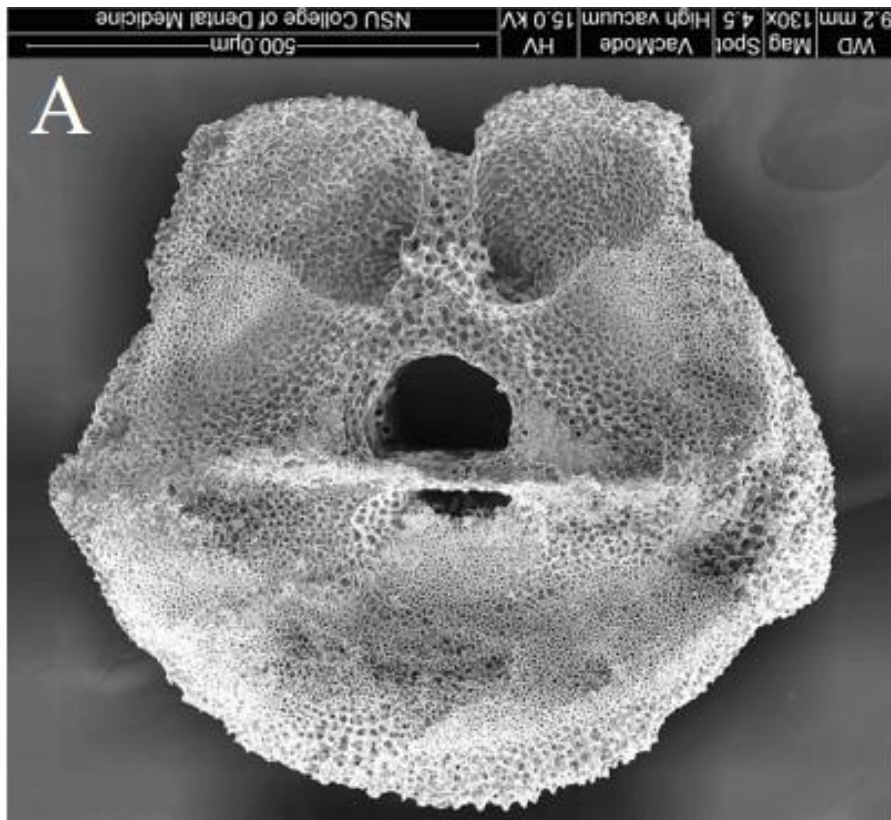


Fig. B22: SEM images of *Erythrometra rubra*. A: specimen A; B: specimen B.

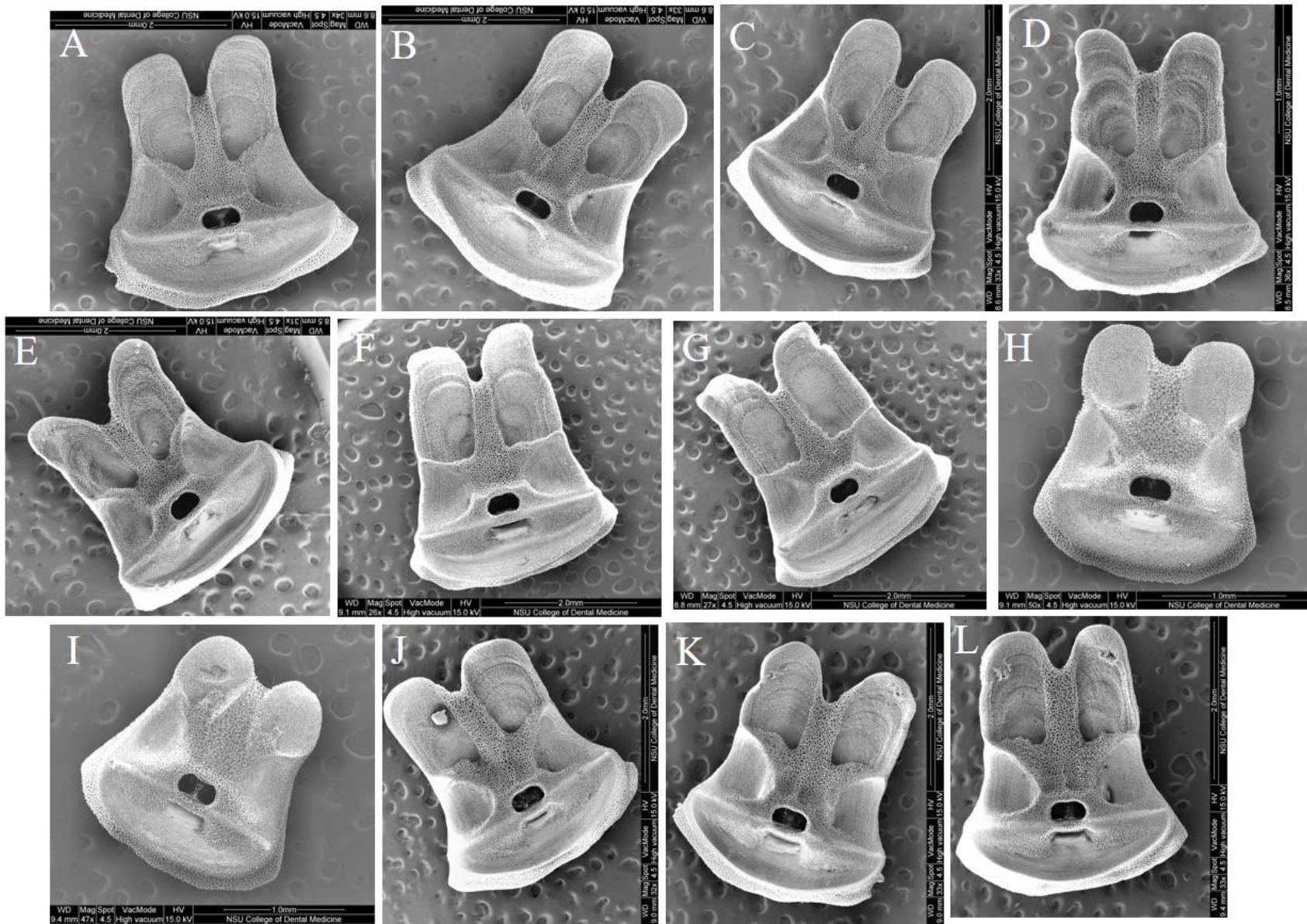


Fig. B23: SEM images of *Florometra asperirma*. A-C: specimen A; D-E: specimen B; F-G: specimen C; H-I: specimen D; J-L: specimen E.

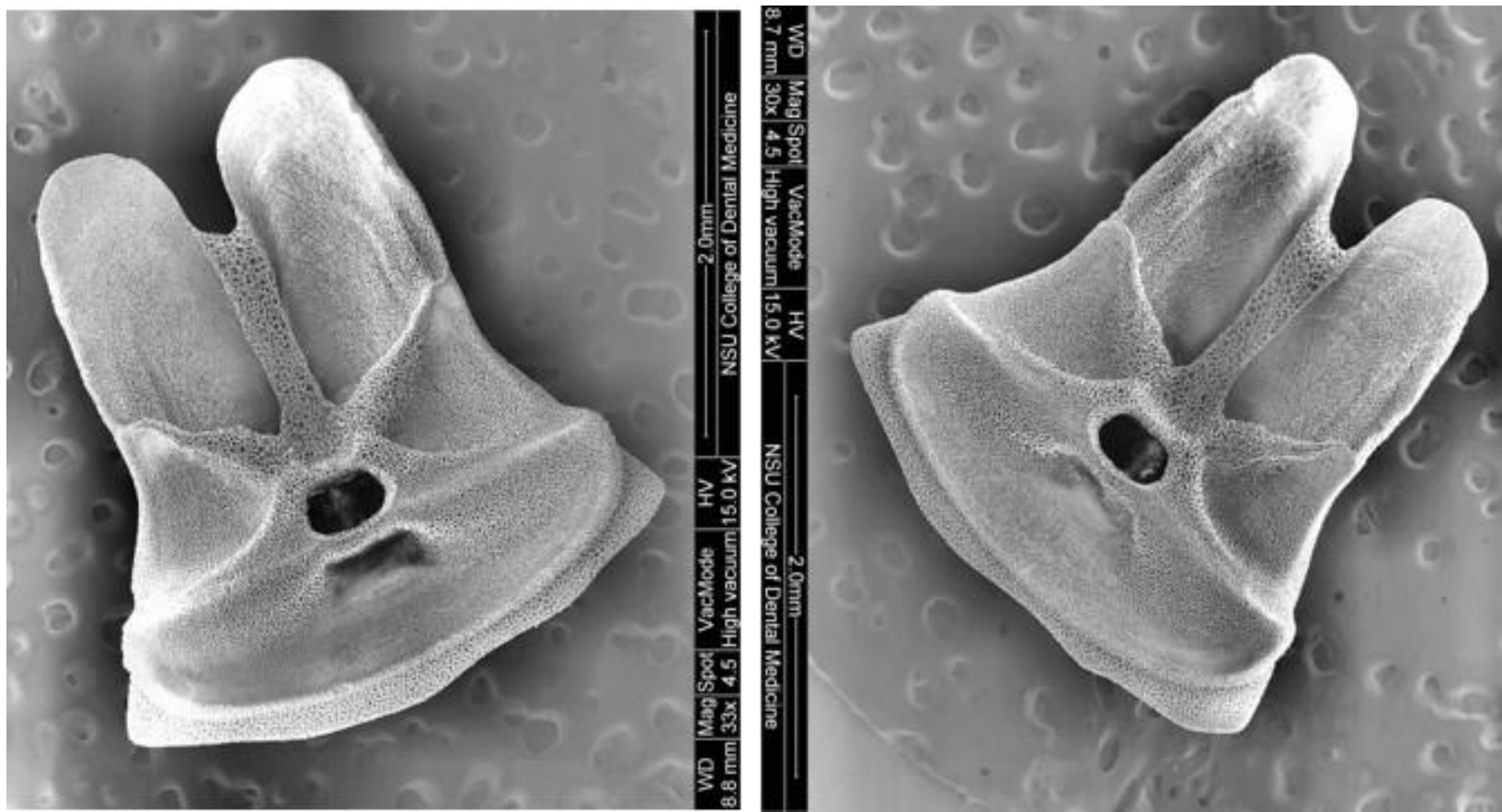


Fig. B24: SEM images of *Florometra serratissima*, specimen B.

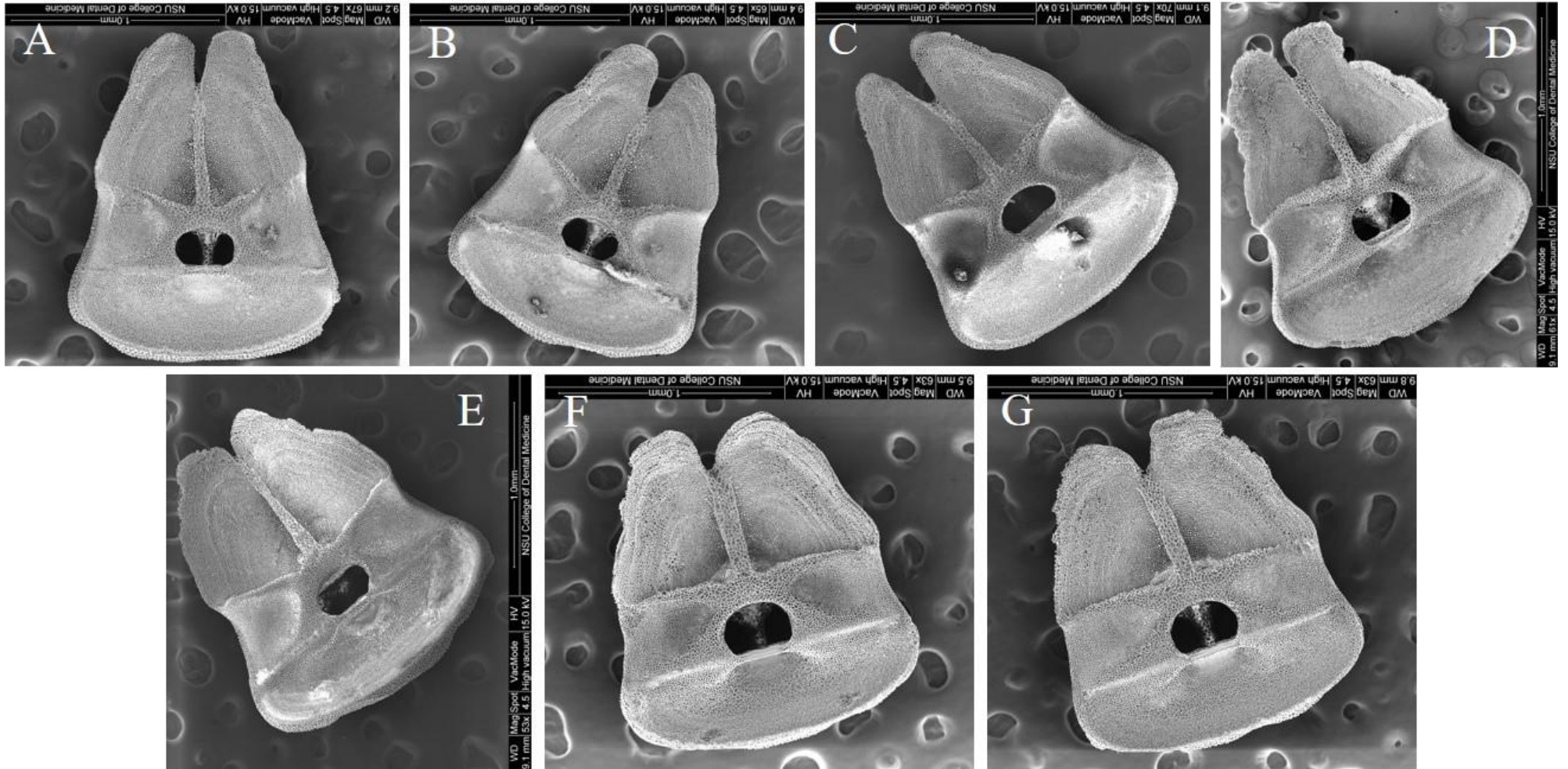


Fig. B25: SEM images of *Hathrometra tenella*. A-C: specimen A; D: specimen B; E: specimen D; F-G: specimen E.



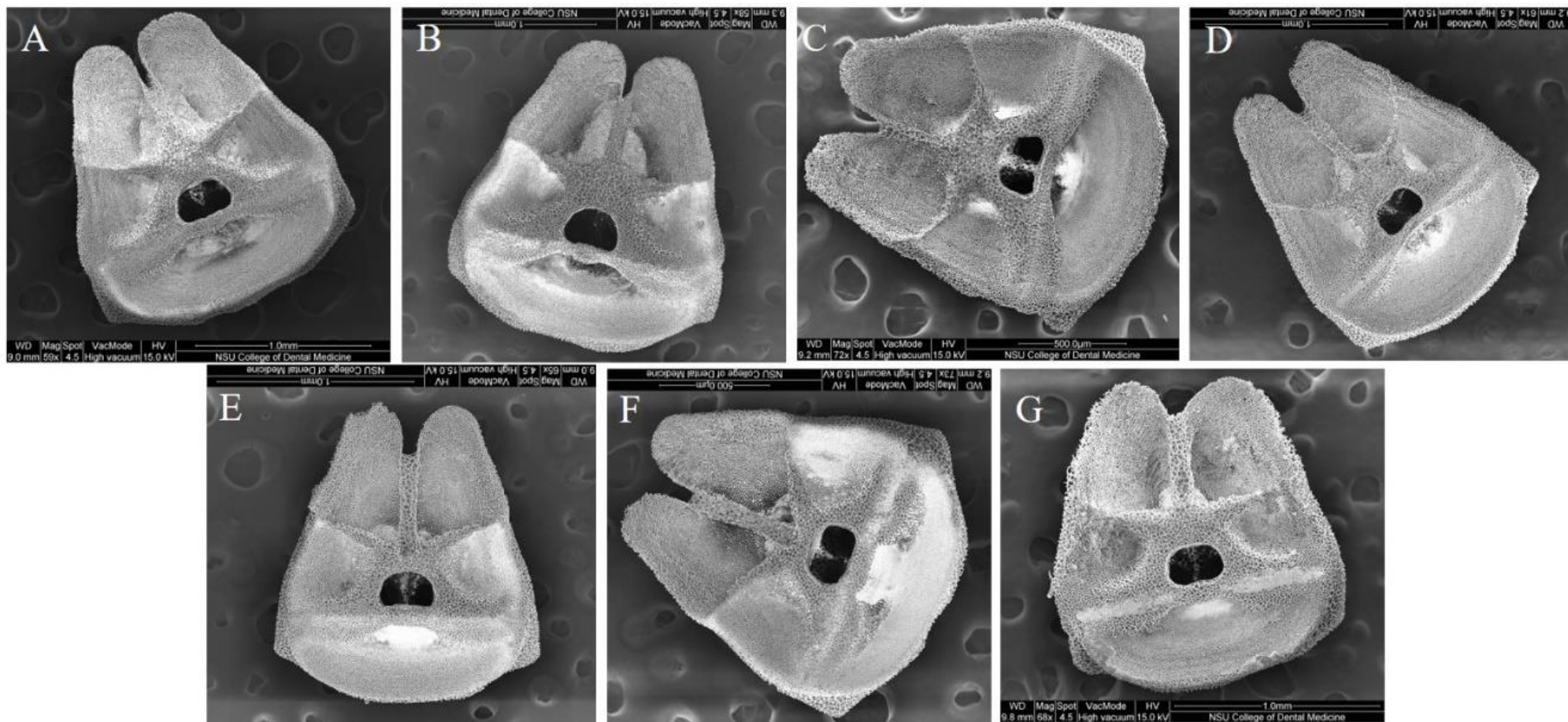


Fig. B26: SEM images of *Hybometra senta*. A-B: specimen A; C-D: specimen C; E-F: specimen D; G: specimen E.

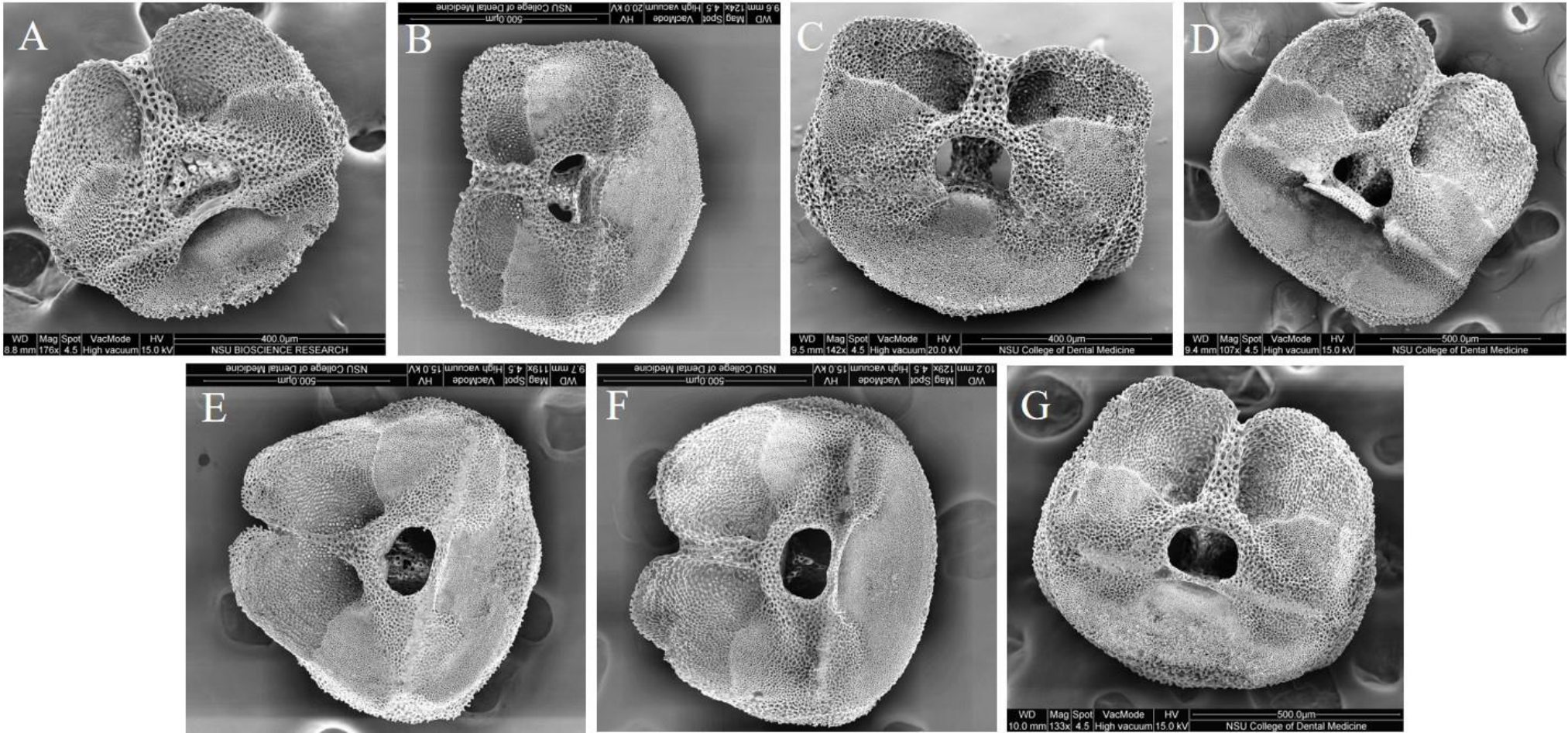


Fig. B27: SEM images of *Hypalometra defecta*. A: specimen A; B-C: specimen B; D: specimen D; E: specimen F; F-G: specimen G.

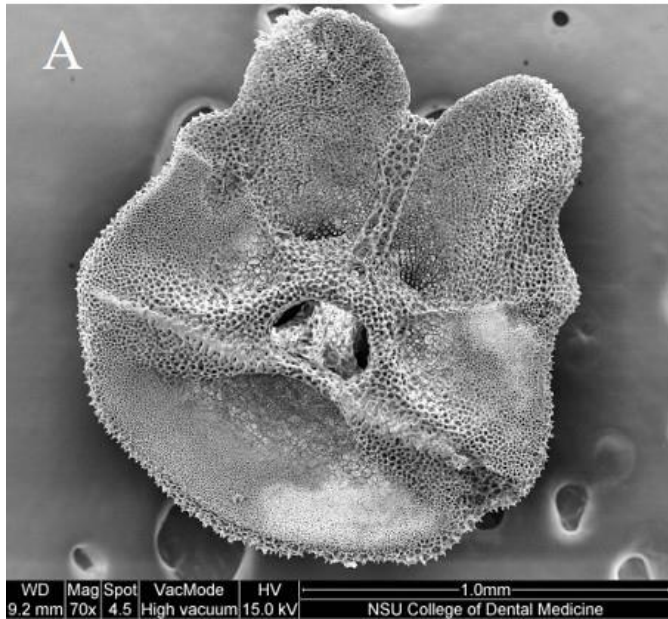


Fig. B28: SEM images of *Isometra graminea*. A-B: specimen A; C: specimen C.

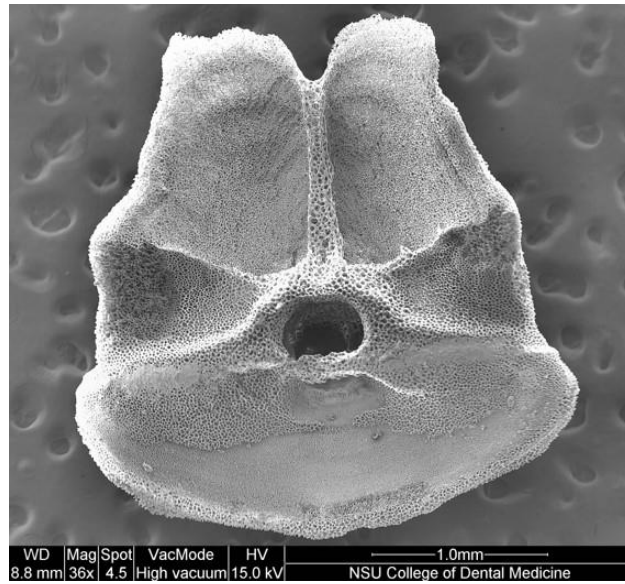


Fig. B29; SEM image of *Isometra vivipara* (only one ossicle was successfully images in this study).

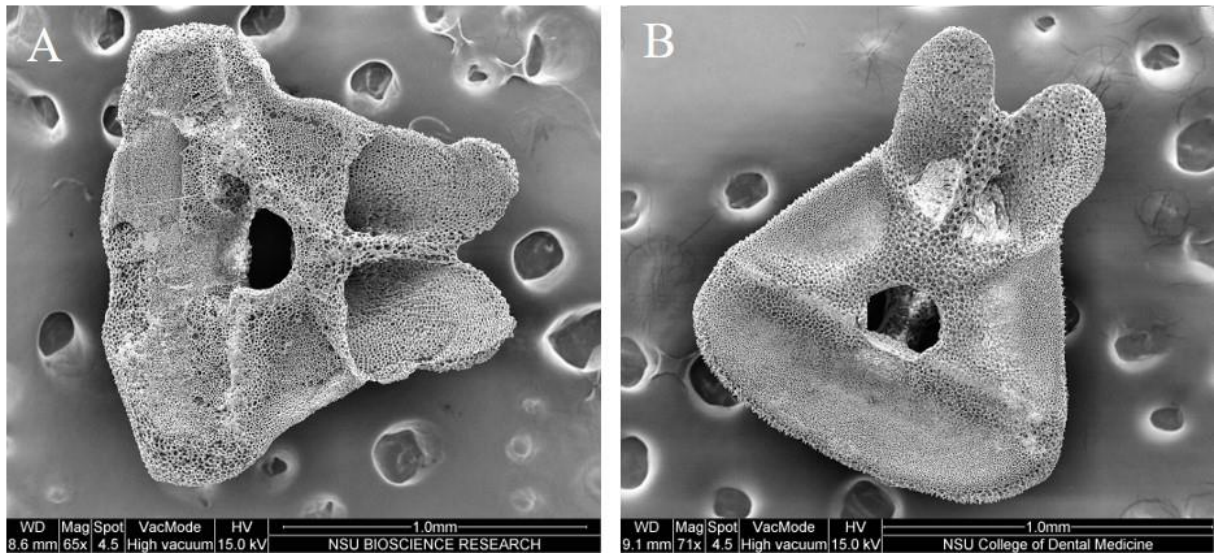


Fig. B30: SEM images of *Iridometra adrestine*. A: specimen B; B: specimen C.

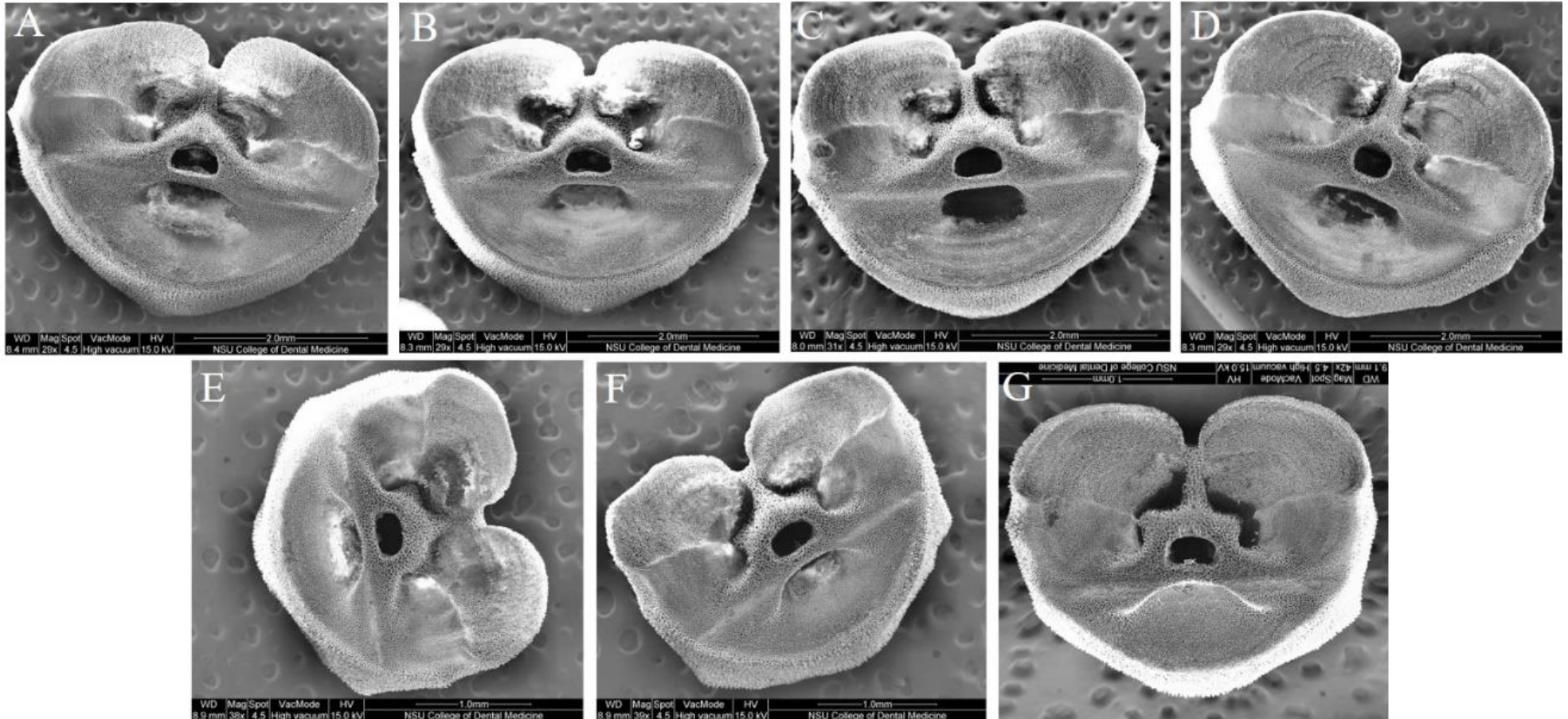


Fig. B31: SEM images of *Notocrinus virilis*. A-C: specimen A; D: specimen B; E-G: specimen C.

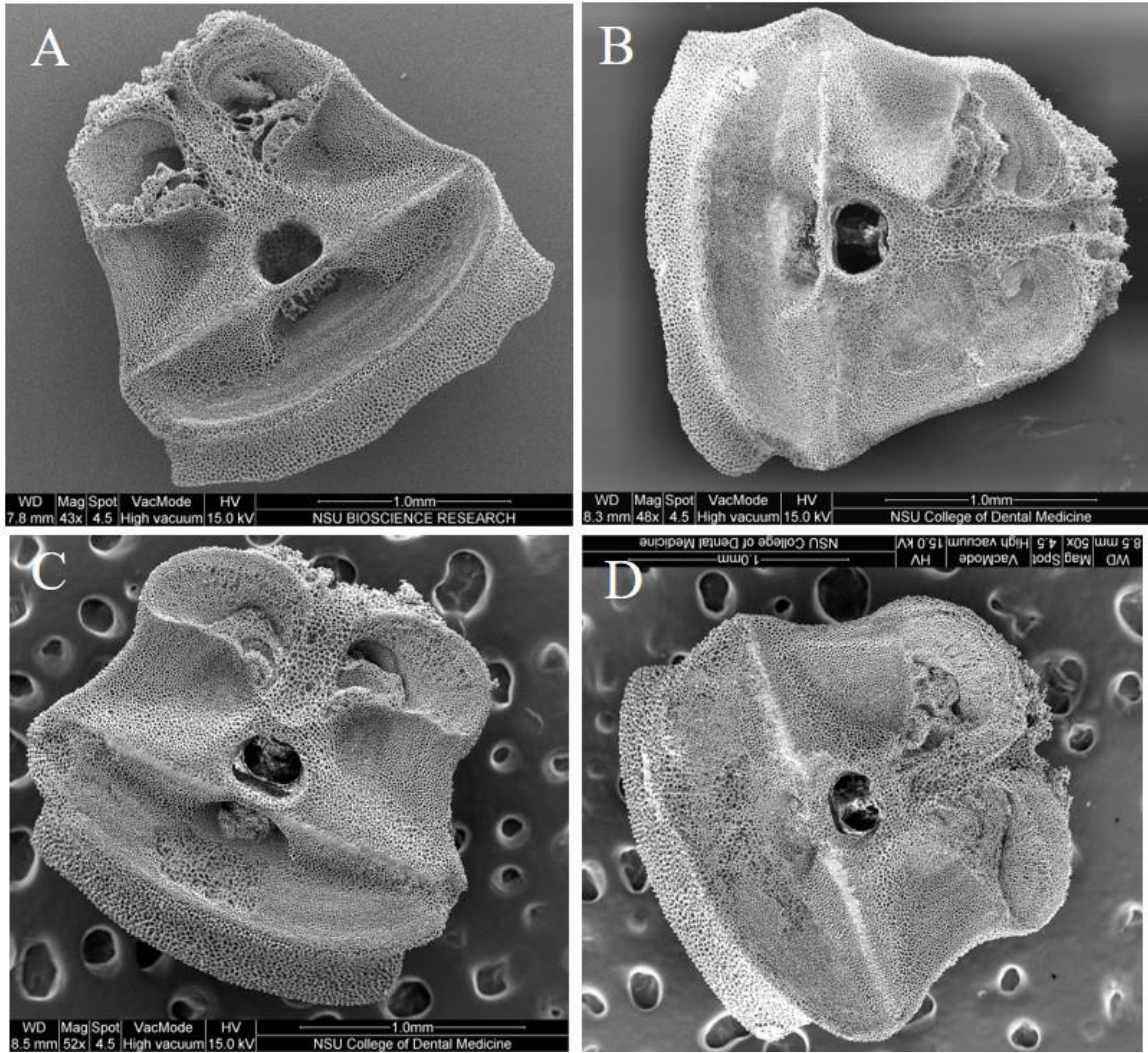


Fig. B32: SEM images of *Perometra diomedea*. A-B: specimen A; C-D: specimen B.

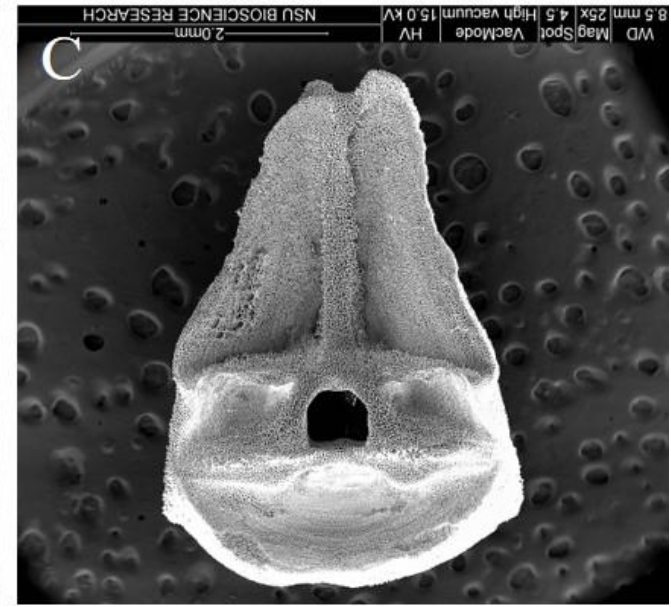


Fig. B33: SEM images of *Poliometra prolixa*. A-B: specimen A; C: specimen B.

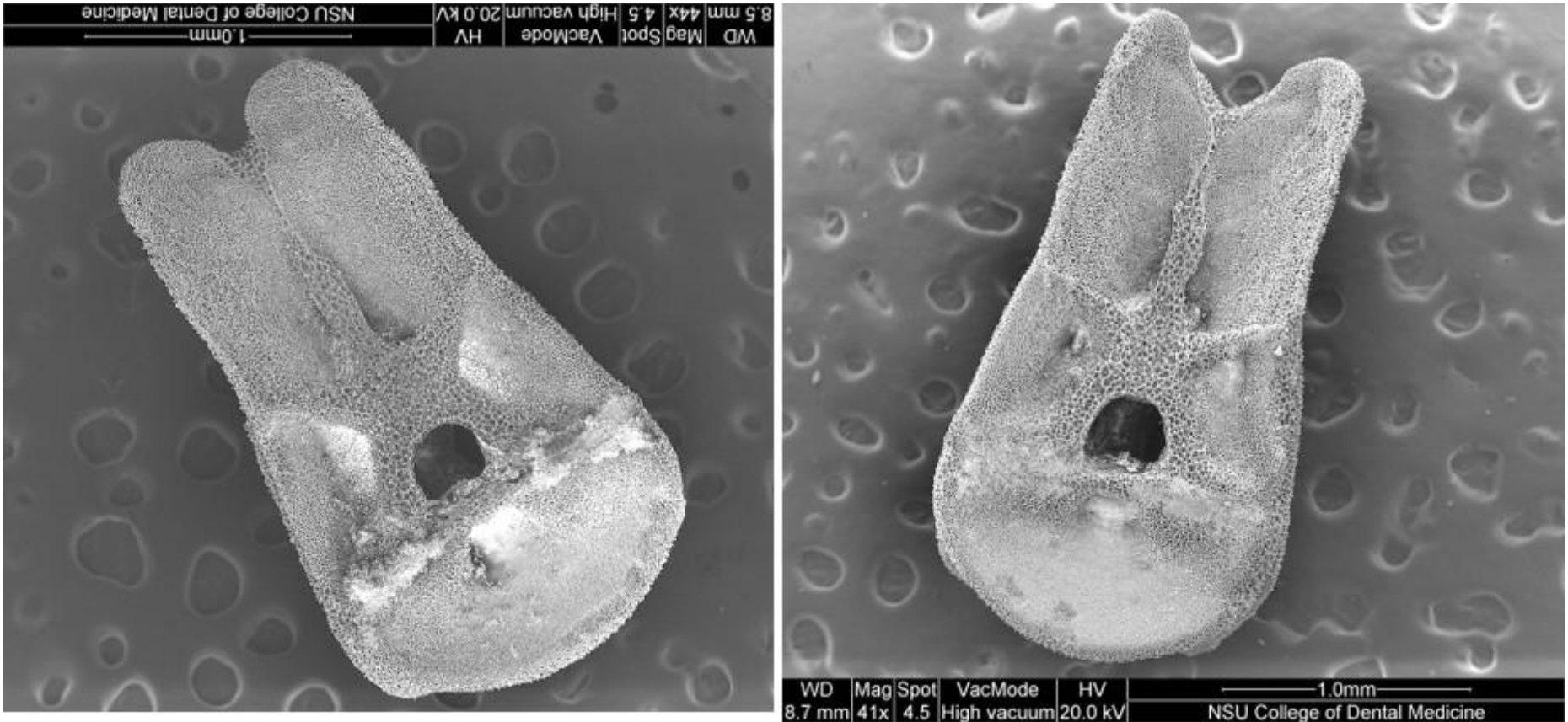


Fig. B34: SEM images of *Promachocrinus kerguelensis*, specimen A.



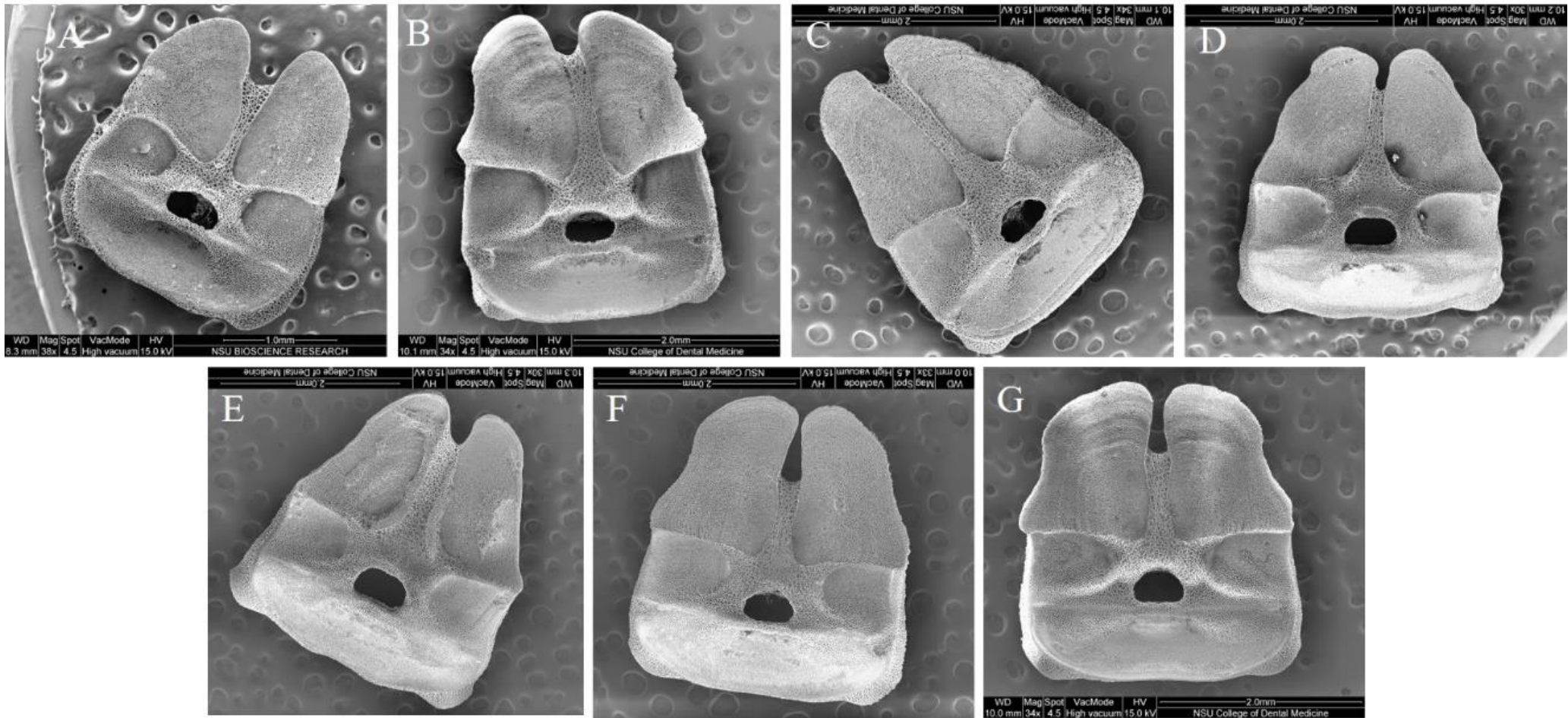


Fig. B35: SEM images of *Psathyrometra* sp. A: specimen B; B-C: specimen C; D-E: specimen D; F-G: specimen E.

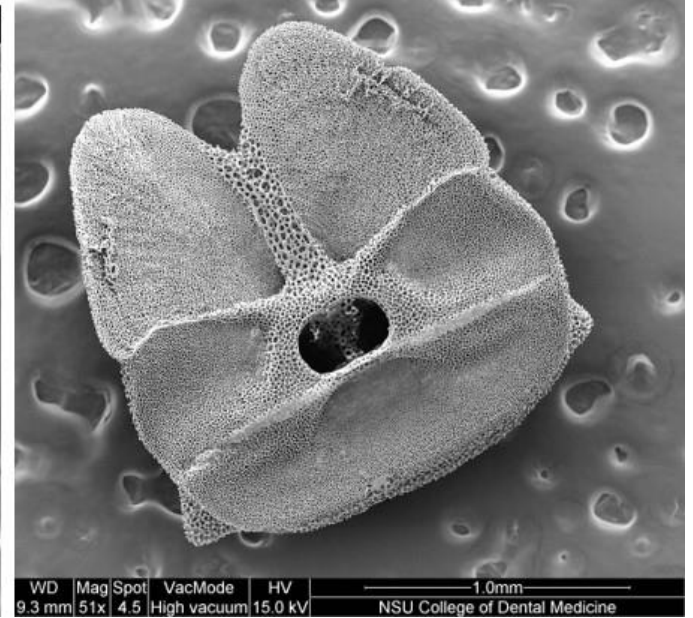
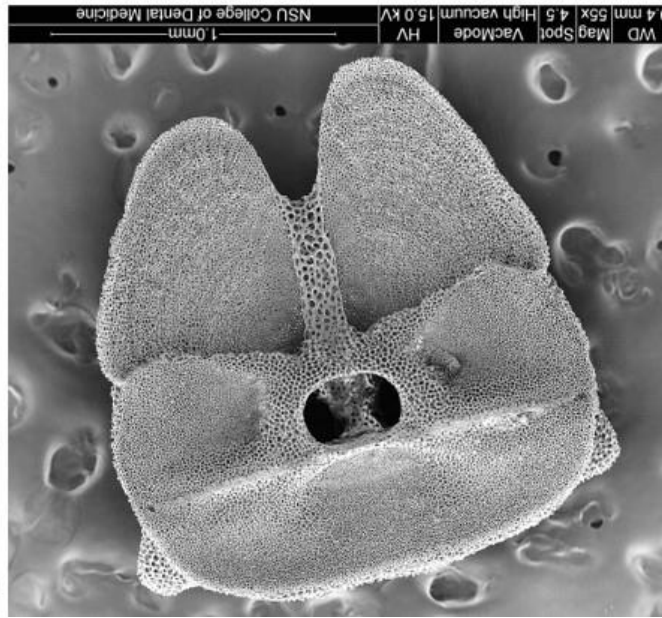
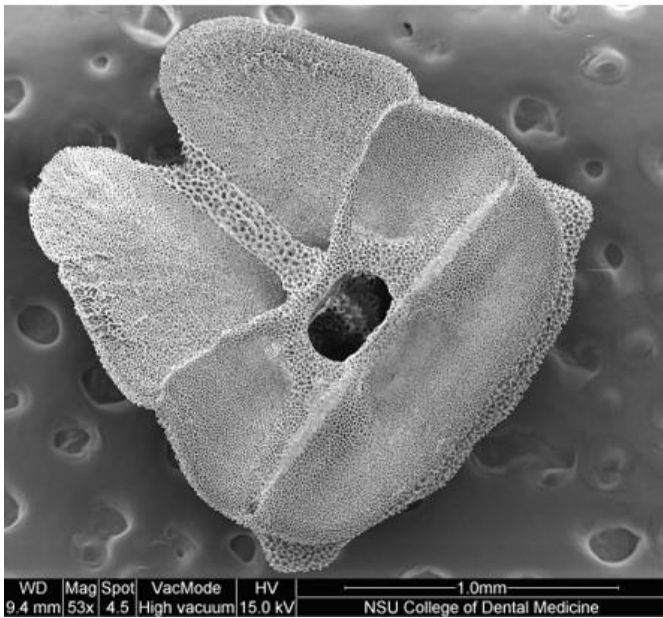


Fig. B36: SEM images of *Thaumatometra tenuis*, specimen B.

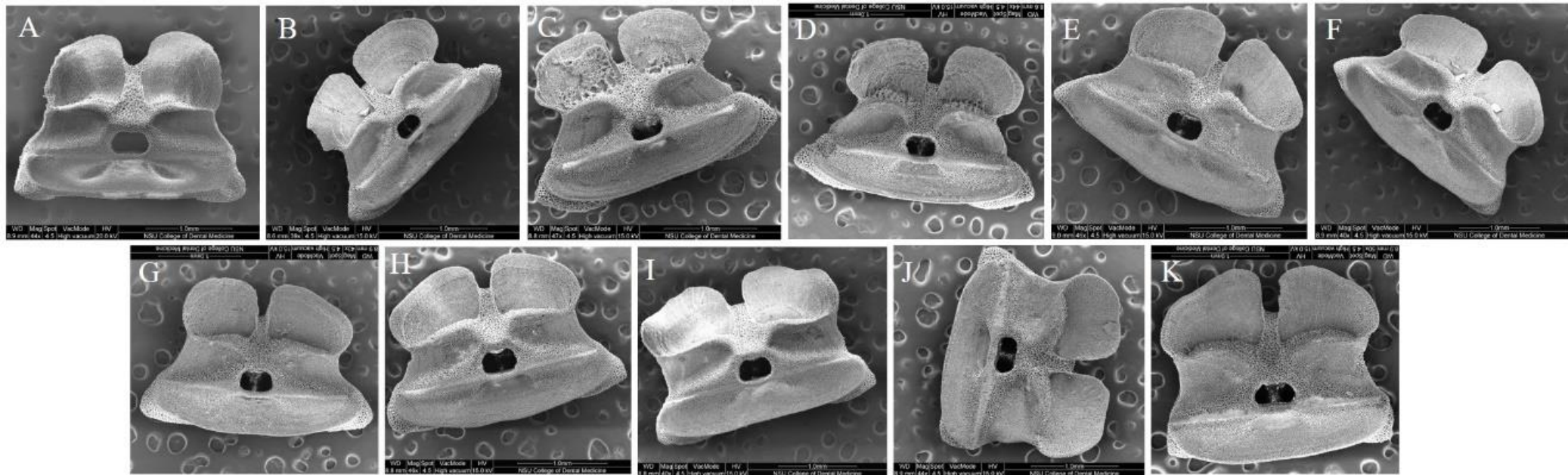


Fig. B37: SEM images of *Thysanometra tenelloides*. A: specimen B; B-D: specimen C; E-H: specimen D; I: specimen E; J-K: specimen G.

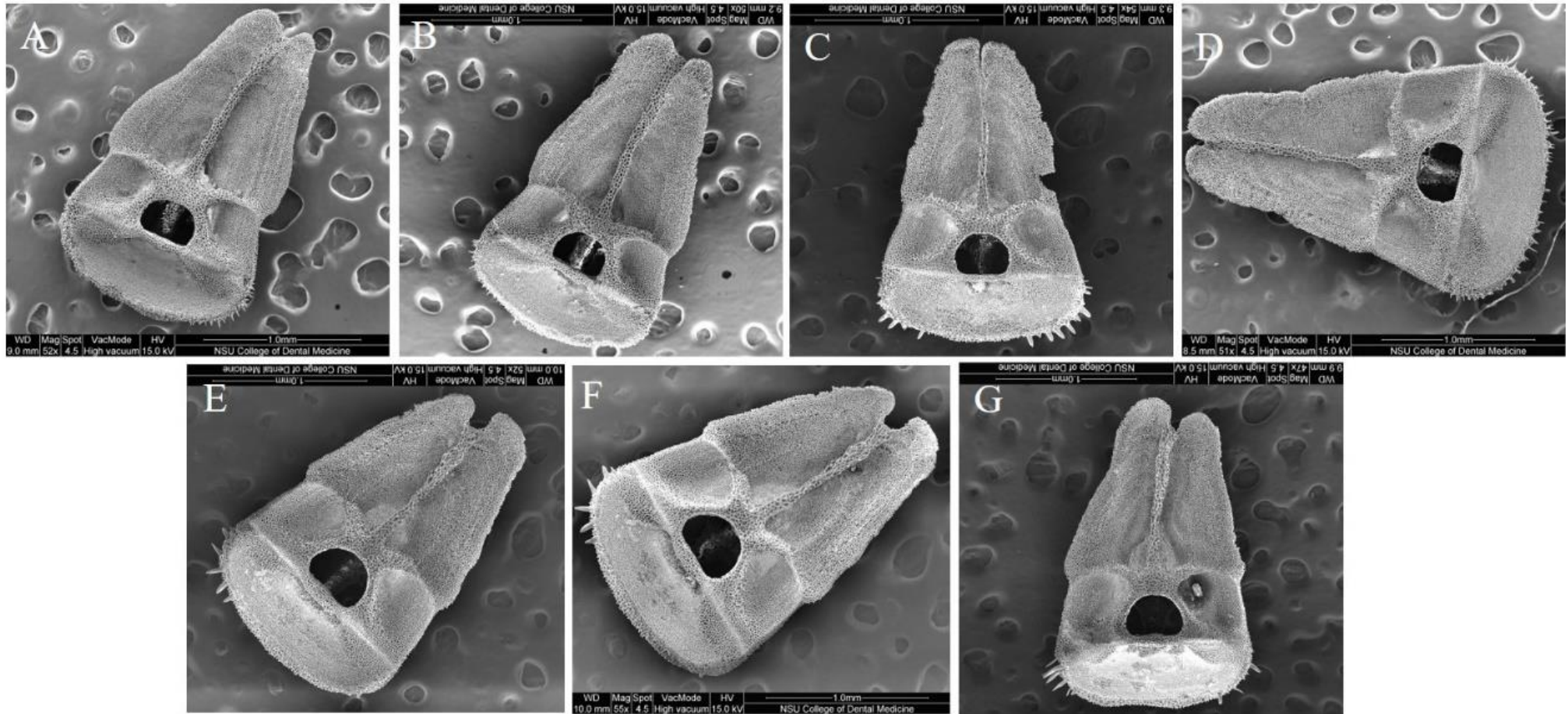


Fig. B38: SEM images of *Tonrometra spinulifera*. A-B: specimen A; C: specimen B; D: specimen C; E-G: specimen E.

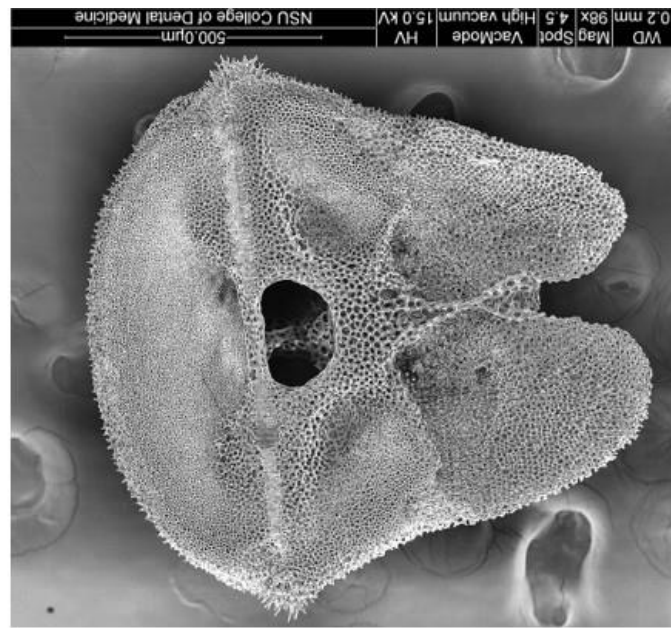
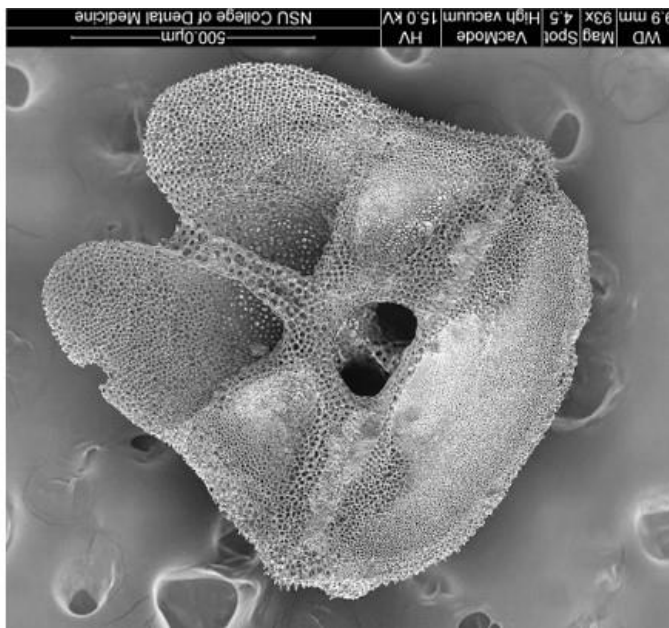
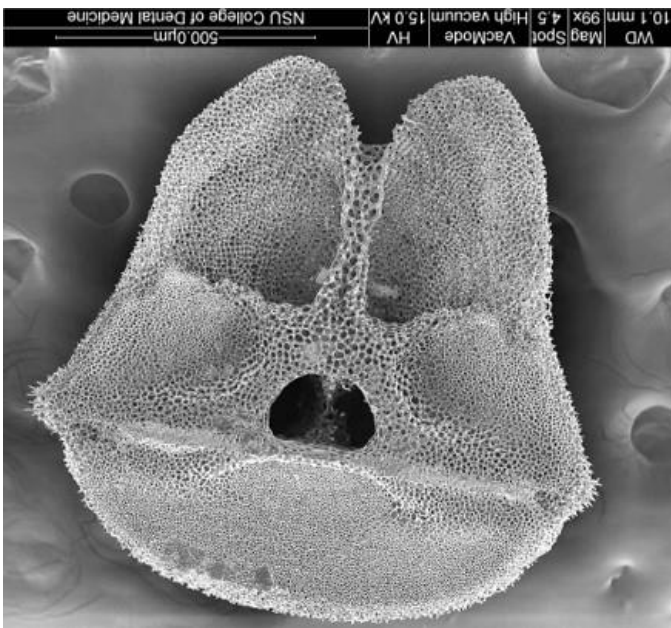


Fig. B39: SEM images of *Trichometra cubensis*, specimen E.

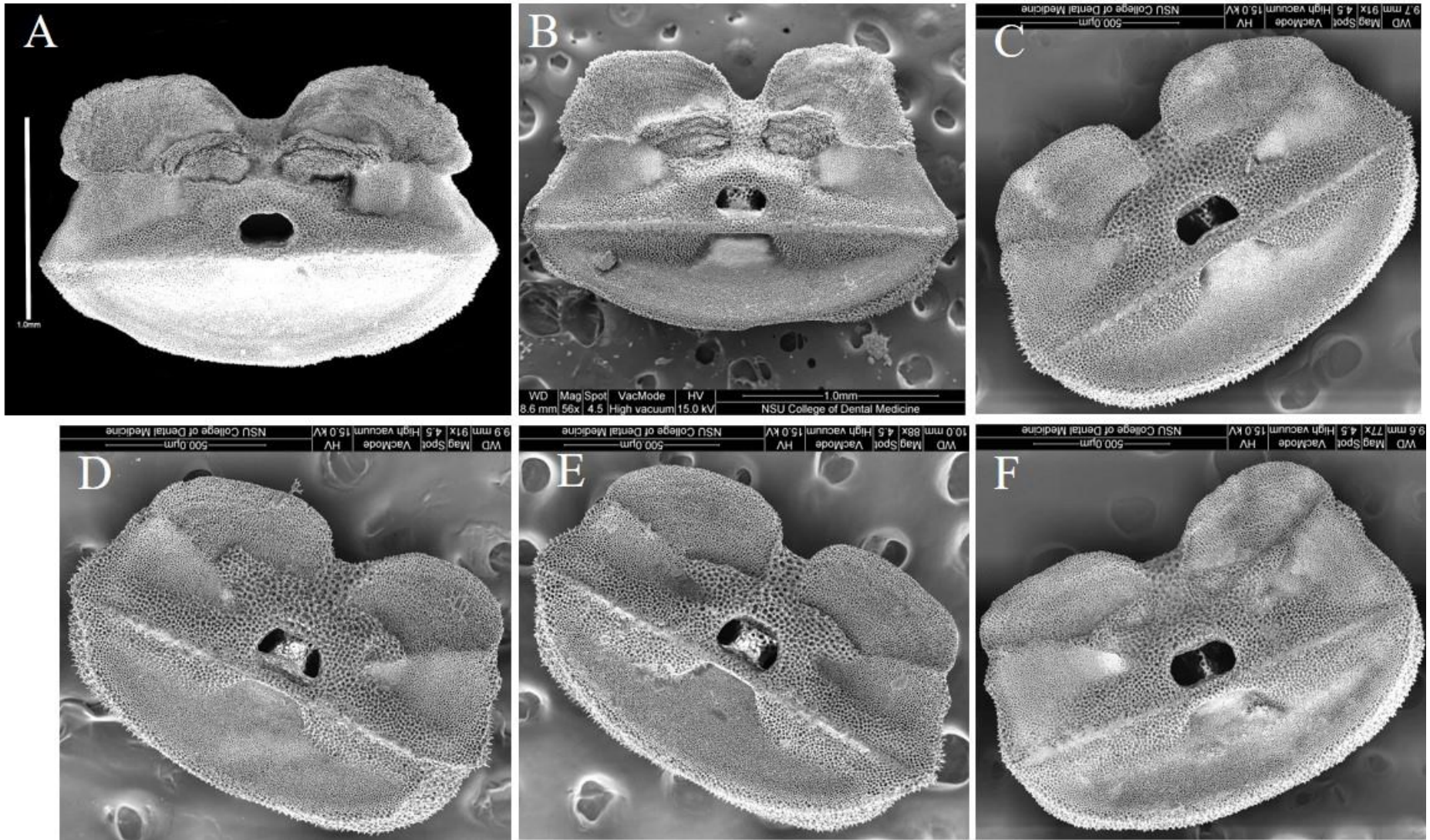


Fig. B40: SEM images of *Tropiometra carinata*. A-B: specimen A; C-E: specimen D; F: specimen E.

## IX. References

- Adams, D. C. and Otárola-Castillo, E. 2013. geomorph: an R package for the collection and analysis of geometric morphometric shape data. *Methods in Ecology and Evolution* 4(4): 393-399.
- Adams, D. C., Rohlf, F. J., and Slice, D. E. 2013. A field comes of age: geometric morphometrics in the 21st century. *Hystrix*, 24(1): 7.
- Adams, D. C., Otárola-Castillo, E., and Sherratt, E. 2014. geomorph: Software for geometric morphometric analyses. R packages version 2.1. 2. <http://CRAN.R-project.org/package=geomorph>.
- Baumiller, T. K., Salamon, M. A., Gorzelak, P., Mooi, R., Messing, C. G., and Gahn, F. J. 2010. Post-Paleozoic crinoid radiation in response to benthic predation preceded the Mesozoic marine revolution. *Proceedings of the National Academy of Sciences* 107(13): 5893-5896.
- Benson DA, Karsch-Mizrachi I, Lipman DJ, Ostell J, and Sayers EW. 2009. GenBank. *Nucleic Acids Res.* 2009 Jan; 37(Database issue): D26-31. Epub 2008 Oct 21.
- Bohn, J. M. and Heinzeller, T. 1999. Morphology of the bourgueticrinid and isocrinid aboral nervous system and its possible phylogenetic implications (Echinodermata, Crinoidea). *Acta Zoologica* 80: 241-249.
- Bookstein, F. L. (2013, October). Can biometrical shape be a homologous character?. In *Elsevier Inc.*.
- Bookstein, F. L. 1997. *Morphometric tools for landmark data: geometry and biology.* Cambridge University Press.
- Bull, J. J., Huelsenbeck, J. P., Cunningham, C. W., Swofford, D. L., and Waddell, P. J. 1993. Partitioning and combining data in phylogenetic analysis. *Systematic Biology*, 42(3): 384-397.
- Burrige, A.K. (2012-2014). A short introduction using TpsUtil, TpsDig2, and TpsRelw developed by F. James Rohlf.
- Campbell, N. A., and Atchley, W. R. 1981. The geometry of canonical variate analysis. *Systematic Biology*, 30(3): 268-280.
- Cardini, A., Nagorsen, D., O'Higgins, P., Polly, P. D., Thorington Jr, R. W., and Tongiorgi, P. 2009. Detecting biological distinctiveness using geometric

morphometrics: an example case from the Vancouver Island marmot. *Ethology Ecology & Evolution* 21(3-4): 209-223.

- Clark, A. H. 1915. A monograph of the existing crinoids, 1(1). *Bulletin of the United States National Museum* (82): vi + 406, 17 pls.
- Clark, A. H. 1921. A monograph of the existing crinoids, 1(2). *Bulletin of the United States National Museum* (82): xxvi + 795, 57 pls.
- Clark, A. H. 1931. A monograph of the existing crinoids, 1(3) Superfamily Comasterida. *Bulletin of the United States National Museum* (82): viii + 816 pp., 82 pls.
- Clark, A. H. and Clark, A.M. 1967. A monograph of existing crinoids. *Bulletin of the United States National Museum* 82 1(5): 1-860.
- Cohen B.L., Améziane N., Eléaume M. and Richer de Forges B. 2004. Crinoid phylogeny: a preliminary analysis (Echinodermata: Crinoidea). *Marine Biology*, 144: 605-617.
- Collyer, M. L., Sekora, D. J., and Adams, D. C. 2014. A method for analysis of phenotypic change for phenotypes described by high-dimensional data. *Heredity*.
- Cordeiro Estrela de Andrade Pinot P. 2005. Systématique et évolution morphologique du genre *Calomys* Waterhouse 1837 (Rodentia, Cricetidae, Sigmodontidae, Phyllotini). Application de méthodes de morphométrie géométrique, de reconnaissances de patrons et de reconstructions phylogénétiques en systématique évolutive. Thèse de l'Université Paris VI – Pierre et Marie Curie, Paris, 1-199.
- Dryden, I., and Dryden, M. I. 2012. *Shapes package. Vienna, Austria: R Foundation for Statistical Computing.*
- Dryden, I. L., and Mardia, K. V. 1998. *Statistical shape analysis* (Vol. 4). Chichester: J. Wiley.
- Eléaume, M. 2006. Approche morphométrique de la variabilité phénotypique: conséquences systématiques et évolutives. Applications aux crinoïdes actuels (Crinoidea: Echinodermata). Muséum national d'Histoire naturelle, Paris. PhD Dissertation: 402
- Eléaume, M., Hemery, L.G., Roux, M., and Améziane, N. 2014. Chapter 5.25. Southern Ocean Crinoids. In: De Broyer, C., Koubbi, P., Griffiths, H.J., Raymond, B., Udekem d'Acoz, C., et al. (eds.). *Biogeographic Atlas of the Southern Ocean*. Scientific Committee on Antarctic Research, Cambridge, pp. 208-212.



- Fet, V., and Messing, C. G. 2003. Case 3270: Isometrinae Clark, 1917 (Ecinodermata, Crinoidea): Proposed Emendation of Spelling to Isometraineae to Remove Homonymy with Isometrinae Kraepelin, 1891 (Arachnida, Scorpiones). *Bulletin of Zoological Nomenclature* 60(4): 293.
- Freudenstein, J.V. 2005. Characters, States, and Homology. *Systematic Biology* 54(6): 965-973.
- Gislen, T. 1955. West African crinoids. *Atlantide Rep* 3: 83-92.
- Gunz, P., and Mitteroecker, P. 2013. Semilandmarks: a method for quantifying curves and surfaces. *Hystrix, the Italian Journal of Mammalogy* 24(1): 103-109.
- Hemery L.G., Eléaume M., Chevaldonné P., Dettai A., and Améziane N. (2009, January). The genus *Antedon* (Crinoidea, Echinodermata): an example of evolution through vicariance. Poster presented at the 13<sup>th</sup> International Echinoderm Conference, Hobart, Tasmania.
- Hemery L.G., Eléaume M., Chevaldonné P., Dettai A., and Améziane N. (2009, January). The genus *Antedon* (Crinoidea, Echinodermata): discontinuous distribution or problem of definition? Poster presented at the 13<sup>th</sup> International Echinoderm Conference, Hobart, Tasmania.
- Hemery L.G. 2011. Diversité moléculaire, phylogéographie et phylogénie des Crinoïdes (Echinoderms) dans un environnement extrême: l'océan Austral. Partie IV: Phylogénie des crinoïdes. PhD dissertation, Muséum national d'Histoire naturelle, Paris. 381 pp.
- Hemery, L. G., Eléaume, M., Roussel, V., Améziane, N., Gallut, C., Steinke, D., ... and Wilson, N. G. 2012. Comprehensive sampling reveals circumpolarity and sympatry in seven mitochondrial lineages of the Southern Ocean crinoid species *Promachocrinus kerguelensis* (Echinodermata). *Molecular Ecology* 21(10): 2502-2518.
- Hemery L.G., Roux M., Améziane N., and Eléaume M. 2013. High-resolution crinoid phyletic inter-relationships derived from molecular data. *Cahiers de Biologie Marine*. 54: 511-523.
- Hernández-Ortiz, V., Canal, N. A., Salas, J. O. T., Ruíz-Hurtado, F. M., and Dzul-Cauich, J. F. 2015. Taxonomy and phenotypic relationships of the *Anastrepha fraterculus* complex in the Mesoamerican and Pacific Neotropical dominions (Diptera, Tephritidae). *ZooKeys* (540): 95.

- Hess, H., Messing, C.G. 2011. Comatulida. Treatise on Invertebrate Paleontology, Part T, Echinodermata 2, Revised, Crinoidea. H. Hess, Messing, C.G., Ausich, W.I. Lawrence, Kansas, University of Kansas Press. 3: 127-145.
- Kendall, D. G. 1989. A survey of the statistical theory of shape. *Statistical Science* 87-99.
- Klingenberg, C. P., and McIntyre, G. S. 1998. Geometric morphometrics of developmental instability: analyzing patterns of fluctuating asymmetry with Procrustes methods. *Evolution* 1363-1375.
- Klingenberg, C.P. 2008. Novelty and 'Homology-free' Morphometrics: What's in a Name? *Evolutionary Biology* 35(3): 186-190.
- Ling, F., Tu, X., Huang, A., and Wang, G. 2016. Morphometric and molecular characterization of *Dactylogyrus vastator* and *D. intermedius* in goldfish (*Carassius auratus*). *Parasitology research*, 1-11.
- Liu, M., Ma, N., and Hua, B. Z. 2016. Intraspecific morphological variation of the scorpionfly *Dicerapanorpa magna* (Chou) (Mecoptera: Panorpidae) based on geometric morphometric analysis of wings. *Contributions to Zoology* 85(1): 1-11.
- Messing, C. G. 1981. Reclassification and Redescription of the Comatulid *Comatonia cristata* (Hartlaub) (Echinodermata: Crinoidea). *Proceedings of the Biological Society of Washington* 94(1): 240-253.
- Messing, C. G. 1984. Brooding and paedomorphosis in the deep-water feather star *Comatilia iridometrifomis* (Echinodermata: Crinoidea). *Marine Biology* 80(1): 83-91.
- Messing, C. G. and Dearborn, J. H. 1990. Marine Flora and Fauna of the Northeastern United States Echinodermata: Crinoidea. NOAA Technical Report NMFS 91: 1-30.
- Messing, C.G. 1997. Living comatulids.
- Messing, C. G. and White, C. M. 2001. A revision of the Zenometridae (new rank) (Echinodermata, Crinoidea, Comatulidina). *Zoologica Scripta* 30(3): 159-180.
- Messing, C. G. 2003. Unique morphology in the living bathyal feather star, *Atelecrinus* (Echinodermata: Crinoidea). *Invertebrate Biology* 122(3): 280-292.

- Messing, C. G. 2012. World Register of Marine Species (WoRMS). 2014.
- Messing, C.G. 2013. A revision of the genus *Atelecrinus* PH Carpenter (Echinodermata: Crinoidea). *Zootaxa* 3681(1): 001-043.
- Meyer, D.L. 1972. *Ctenantedon*, a new antedonid crinoid convergent with comasterids. *Bulletin of Marine Science* 22(1): 53-66.
- Meyer, D. L. and Macurda, D. B. 1977. Adaptive radiation of the comatulid crinoids. *Paleobiology* 3(01): 74-82.
- Meyer, D. L. and Oji, T. 1993. Eocene crinoids from Seymour Island, Antarctic Peninsula: paleobiogeographic and paleoecologic implications. *Journal of Paleontology* 250-257.
- Milson, C. V., Simms, M. J., and Gale, A. S. 1994. Phylogeny and palaeobiology of *Marsupites* and *Uintacrinus*. *Palaeontology* 37(3): 595-608.
- Mironov, A.N. and Pawson, D.L. 2014. A new species of Western Atlantic sea lily in the family Bathycrinidae (Echinodermata: Crinoidea), with a discussion of relationships between crinoids with xenomorphic stalks. *Zootaxa* 3873(3): 259-274.
- Mitteroecker, P. and Gunz, P. 2009. Advances in geometric morphometrics. *Evolutionary Biology* 36(2): 235-247.
- Mitteroecker, P. and Bookstein, F. 2011. Linear Discrimination, Ordination, and the Visualization of Selection Gradients in Modern Morphometrics. *Evolutionary Biology* 38: 100-114.
- Pawson, D. L. 2007. Phylum Echinodermata. *Zootaxa*, 1668: 749-764.
- Purens, K.J.S. 2016. Detecting comatulid crinoid cryptic species in the fossil record. *Palaeogeography, Palaeoclimatology, Palaeoecology* 446: 195-204.
- R Core Team. 2014. R: A language and environment for statistical computing. R Foundation for Statistical Computing, Vienna, Austria. URL <http://www.R-project.org/>.
- Ramirez-Sanchez, M.M., De Luna, E., and Cramer, C. 2016. Geometric and traditional morphometrics for the assessment of character state identity: multivariate statistical analyses of character variation in the genus *Arrenurus* (Acari, Hydrachnidia, Arrenuridae). *Zoological Journal of the Linnean Society*.

- Rankin, D. L. and Messing, C. G. 2008. A revision of the comatulid genus *Stephanometra* AH Clark with a rediagnosis of the genus *Lamprometra* AH Clark (Echinodermata: Crinoidea). *Zootaxa* 1888: 1-35.
- Rasmussen H.W. 1978. Evolution of articulate crinoids. Part T. Echinodermata. In: *Treatise on Invertebrate Paleontology* (R.C. Moore & C. Teichert eds), 2: T302-T316. Geological Society of America: Boulder.
- Renaud, S., Dufour, A-B., Hardouin, E.A., Ledevin, R., and Auffray, J-C. 2015. Once upon Multivariate Analyses: When They Tell Several Stories about Biological Evolution. *PLoS ONE* 10(7): e0132801.doi:10.1371/journal.pone.0132801.
- Rohlf, F. J., and Slice, D. 1990. Extensions of the Procrustes method for the optimal superimposition of landmarks. *Systematic Biology* 39(1): 40-59.
- Rohlf, F. J. and Marcus, L. F. 1993. A revolution morphometrics. *Trends in Ecology & Evolution* 8(4): 129-132.
- Rohlf, F.J. 1999. Shape Statistics: Procrustes Superimpositions and Tangent Spaces. *Journal of Classification* 16: 197-223.
- Rohlf, F. J. 2000. On the use of shape spaces to compare morphometric methods. *Hystrix, the Italian Journal of Mammalogy* 11(1).
- Rohlf, F.J. 2006. Tps series. Department of Ecology and Evolution, State University of New York at Stony Brook, New York, USA.
- Rohlf, F.J. 2015. Morphometrics. 2015. <http://life.bio.sunysb.edu/morph/index.html>.
- Rouse, G. W., Jermin, L.S., Wilson, N.G., Eeckhaut, I., Lanterbecq, D., Oji, T., Young, C.M., Browning, T., Cisternas, P., Helgen, L.E., Stuckey, M., and Messing, C.G. 2013. Fixed, free, and fixed: The fickle phylogeny of extant Crinoidea (Echinodermata) and their Permian-Triassic origin. *Molecular Phylogenetics and Evolution*. 66: 161-181.
- Rouse, et al. in prep.
- Roux, M., Messing, C.G., and Améziane, N. 2002. Artificial keys to the genera of living stalked crinoids (Echinodermata). *Bulletin of Marine Science* 70: 799-830.
- Roux, M., Eléaume, M., Hemery, L. G., and Améziane, N. 2013. When morphology meets molecular data in crinoid phylogeny: a challenge. *Cahiers de Biologie Marine* 54(4): 541-548.

- Sayers EW, Barrett T, Benson DA, Bryant SH, Canese K, Chetvernin V, Church DM, DiCuccio M, Edgar R, Federhen S, Feolo M, Geer LY, Helmberg W, Kapustin Y, Landsman D, Lipman DJ, Madden TL, Maglott DR, Miller V, Mizrachi I, Ostell J, Pruitt KD, Schuler GD, Sequeira E, Sherry ST, Shumway M, Sirotkin K, Souvorov A, Starchenko G, Tatusova TA, Wagner L, Yaschenko E, and Ye J. 2009. Database resources of the National Center for Biotechnology Information. *Nucleic Acids Res.* 2009 Jan; 37(Database issue): D5-15. Epub 2008 Oct 21.
- Sheets, H. D., Covino, K. M., Panasiewicz, J. M., and Morris, S. R. 2006. Comparison of geometric morphometric outline methods in the discrimination of age-related differences in feather shape. *Frontiers in zoology* 3(1): 1.
- Sherratt, E. (2014, June, 28). Morphometrics – Goal: Gathering two-dimensional landmark coordinates to describe the shape of my favorite structure. <http://www.emmasherratt.com/morphometrics>.
- Sherratt, E. (2015, April 4). Tips & Tricks 8: Examining Replicate Error. <http://www.r-bloggers.com/tips-tricks-8-examining-replicate-error/>.
- Simms, M.J. 1988. The phylogeny of post-Paleozoic crinoids. In: *Echinoderm Phylogeny and Evolutionary Biology* (C.R.C. Paul & A.B. Smith eds), pp.269-284. Clarendon Press: Oxford.
- Smith, A. B. 1997. Echinoderm Phylogeny: How Congruent are Morphological and Molecular Estimates? *Paleontological Society Papers* 3: 337-355.
- The Morphometrics Website: Morphomet. <http://www.morphometrics.org/home/morphmet>.
- Torrence, K. G., Correia, M. D., and Hoffman, E. A. 2012. Divergent sympatric lineages of the Atlantic and Indian Ocean crinoid *Tropiometra carinata*. *Invertebrate Biology* 131(4): 355-365.
- Ubaghs, G., Moore, R.C., Wienberg Rasmussen, H., Gary Lane, N., Breimer, A., Strimple, H.L., Brower, J.C., Jeffords, R.M., Sprinkle, J., Peck, R.E., Macurda, Jr, D.B., Meyer, D.L., Roux, M., Sieverts-Doreck, H., Fay, R.O., and Robison, R.A. 1978. Echinodermata 2, Crinoidea. *Treatise on Invertebrate Paleontology, Part T, Echinodermata 2, Crinoidea*. R. C. Moore, Teichert, C., University of Kansas Paleontological Institute: T9-T1003.
- Zelditch, M. L., Fink, W. L., and Swiderski, D. L. 1995. Morphometrics, homology, and phylogenetics: quantified characters as synapomorphies. *Systematic Biology* 44(2): 179-189.

Zelditch, M.L., Swiderski, D.L., Sheets, H.D. (2012). “Geometric Morphometrics for Biologists: A Primer.” Second Ed. Academic Press.

Zelditch, M.L., Li, J., Tran, L.A.P., and Swiderski, D.L. 2015. Relationships of diversity, disparity, and their evolutionary rates in squirrels (Sciuridae). *Evolution* 69(5): 1284-1300.